Holistic approach to designing hybrid assembly lines

Jonathan Oesterle

Thèse
de doctorat
de l'UTT

Jonathan OESTERLE

Holistic Approach to Designing Hybrid Assembly Lines

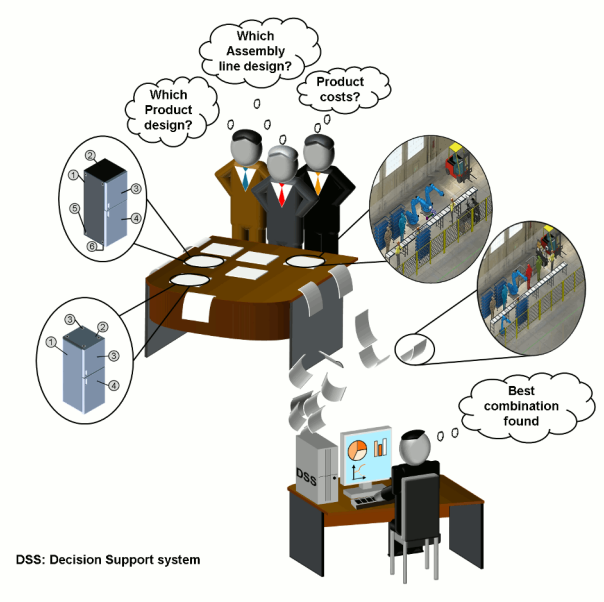

Spécialité :
Optimisation et Sûreté des Systèmes

2017TROY0012 **Année 2017**

utt
UNIVERSITÉ DE TECHNOLOGIE
TROYES

THESE

pour l'obtention du grade de

DOCTEUR de l'UNIVERSITE DE TECHNOLOGIE DE TROYES

Spécialité : OPTIMISATION ET SURETE DES SYSTEMES

présentée et soutenue par

Jonathan OESTERLE

le 3 avril 2017

Holistic Approach to Designing Hybrid Assembly Lines

JURY

M. N. REZG	PROFESSEUR DES UNIVERSITES	Président
M. L. AMODEO	PROFESSEUR DES UNIVERSITES	Directeur de thèse
M. A. DOLGUI	PROFESSEUR ENSM NANTES	Rapporteur
M. E.-G. TALBI	PROFESSEUR DES UNIVERSITES	Rapporteur
M. C. VARNIER	MAITRE DE CONFERENCES - HDR	Examinateur
M. F. YALAOUI	PROFESSEUR DES UNIVERSITES	Examinteur

Preface

The journey towards this thesis began four years ago when I started to work as a full-time research associate and consultant at the Fraunhofer Institute for Manufacturing Engineering and Automation in Stuttgart, Germany in the Factory and Manufacturing Management department. With experience in many industrial projects of different natures and purposes, including factory assembly planning and simulation of production operations combined with various national and international research projects, I have come to realise how great the gap between academia and industry was and remains. This divergence motivated the work proposed in this thesis.

Doing PhD research outside of conventional academic settings and entirely during my free time has been a real challenge with an unclear end. However, it has also provided opportunities, such as an improvement of my time management skills that would not have been expected otherwise.

This work is to the best of my knowledge original, except where acknowledgements and references are made to previous work.

Abstract

The collaborative design of products and assembly lines is a requirement that has been rooted in academia for many years. My original contribution to knowledge is the formulation of the problem associated with selecting the best product and assembly line configuration from a set of products, processes, and resource alternatives. An extended version which takes buffer sizing into consideration is also proposed. In both problems, the obtained solutions are optimal considering capacity and cost-oriented objectives. Concerning both problem formulations, a cost model was developed to translate the complex interdependencies between the selection of specific product designs, processes, and resources characteristics. For the first problem, the development of an empirical study aiming at comparing, based on several quality indicators, various multi-objective algorithms of several natures represent a novelty. Among these algorithms, various including evolutionary algorithms, ant colony optimisation, particle swarm optimisation, bat algorithm, cuckoo search algorithm, and flower pollination algorithm are proposed. In addition, several dominance rules have been tested and compared. Among them, the classical Pareto, Lorenz, and S-CDAS dominance rules and the best-performing algorithms were extended with a local search. For the second problem, which also considers the buffer sizing, the developed algorithms were enhanced with a generic discrete-event simulation model, which has a primary function of collecting the required information to evaluate the value of the objective functions. The diverse algorithms, including the presence of a local search, were compared based on fifty problem instances. For the first problem, the evolutionary algorithm obtained positive results for all quality indicators when considering all problem instances. However, when considering complex and small problems, different variants of multi-objective ant colony optimisation algorithms provided better results. For the second problem, the hybridisation of the NSGA-II and SPEA2 improved the results obtained for most of the quality indicators. These results were validated through the application of nonparametric statistical tests.

The demonstration of the developed resolution frameworks for both problems was validated through two industrial cases.

The principal contributions of this thesis are as follows:

— Formulation of two problems associated with the selection of the most suitable assembly line design while considering the product design, processes, and resource alternatives
— Development of a cost model with an objective of translating the complex interdependencies between the selection of specific product designs, processes, and resource characteristics
— Empirical study comparing several quality indicators and various multi-objective algorithms, including evolutionary algorithms, ant colony optimisation, particle swarm optimisation, bat algorithms, cuckoo search algorithms, and flower pollination algorithms.
— Analysis of the influence of local search and dominance rules on the performance of several algorithms
— Combination of optimisation methods with a generic discrete-simulation model for the second problem

Acknowledgments

Doing this thesis outside of a conventional academic setting has been a truly challenging experience, and it would not have been possible without the support and guidance of many people. I would like to express my deep gratitude to my advisor Mr. Lionel Amodeo for his availability, support, and encouragement over the last years. I cannot thank enough Mr. Farouk Yalaoui, Director of the Laboratory of Industrial Systems Optimisation, and Mr. Hicham Chehade, President of Opta LP for their kindness and support.

I express my gratitude to the members of the jury who give me the honour of participating in the examination of this thesis: Mr. Alexandre Dolgui, Professor at Institut Mines Télécom Atlantique, Mr. El Ghazali Talbi, Professor at Université Lille, Mr. Nidhal Rezg, Professor at Université Lorraine, Mr. Christophe Varnier, Lecturer at École Nationale Supérieure De Mécanique et des Microtechniques, and Mr. Farouk Yalaoui, Professor at Université de Technologie de Troyes.

My time at the Fraunhofer Institute for Manufacturing Engineering and Automation in Stuttgart, Germany was made enjoyable by many colleagues that became part of my life. Among them, I am especially grateful to my office mates Viktor B., David G., and Roman U. Many thanks also goes to the support I received from many friends, particularly from Oliver G. and Philipp H., who understood the conditions of a free-time PhD project.

I would also like to thank my parents and my sister. They were always supporting and encouraging me with their best wishes. Finally, I would like to thank Beatriz Meza who has always been there to encourage me and let me work on this thesis.

I dedicate this work to my father, who passed away recently, in May 2017.

Confidential Information

The presented use-cases in this thesis are not explicitly described since confidential information would have to be revealed and confidential agreements prohibit any detailed information from being published in this thesis. Thus, only general results are discussed.

Contents

List of Figures

List of Tables

List of Acronyms

ABC Artificial Bee Colony

ACO Ant Colony Optimisation

ALBP Assembly Line Balancing Problem

ALWABP Assembly Line Worker Assignment and Balancing Problem

APP Assembly Process Planning

ASA Assembly Sequence Analysis

ASP Assembly Sequence Planning

BA Bat Algorithm

BAP Buffer Allocation Problem

CSA Cuckoo Search Algorithm

DES Discrete-Event Simulation

DOE Design of Experiments

DMOABC Discrete Multi-Objective Artificial Bee Colony

DMOBAT Discrete Multi-Objective Bat Algorithm

DMOCSA Discrete Multi-Objective Cuckoo Search Algorithm

DMOFPA Discrete Multi-Objective Flower Pollination Algorithm

DMOPSO Discrete Multi-Objective Particle Swarm Optimisation

EA Evolutionary Algorithm

EAF Empirical Attainment Function

FPA Flower Pollination Algorithm

GA Genetic Algorithm

GALBP Generalised Assembly Line Balancing Problem

HV Hypervolume

IQR Interquartile Range

MALBP Mixed-Model Assembly Line Balancing Problem

MMALBP Multi-Manned Assembly Line Balancing Problem

MOACO Multi-Objective Ant Colony Optimisation

MOBA Multi-Objective Bat Algorithm

MOCSA Cuckoo Search Algorithm

MOO Multi-Objective Optimisation

MOP Multi-Objective Problem

MOPSO Multi-Objective Particle Swarm Optimisation

MOSA Multi-Objective Simulated Annealing

MTTF Mean Time To Failure

MTTR Mean Time To Repair

NSGA-II Non-dominated Sorted Genetic Algorithm-II

SPEA2 Strength Pareto Evolutionary Algorithm 2

OS Order Strength

PSO Particle Swarm Optimisation

SA Simulated Annealing

SALBP Simple Assembly Line Balancing Problem

TALBP Two-sided Assembly Line Balancing Problem

TPM Two-Phase Method

TSALBP Time and Space Assembly Line Balancing Problem

List of Notations

Association	Symbol	Unit	Explanation
Product	PDA	[-]	Number of considered product design alternatives
	G	[-]	Combined precedence Graph $G = (V, E)$ containing the all the single precedence graphs related to the PDA product alternatives
	V	[-]	Set of nodes contained in the precedence graph G
	E	[-]	Set of arcs contained in the precedence graph G
	N	[-]	Number of tasks in the precedence graph G, $N = \|V\|$
	Vr	[-]	Set of real tasks in the precedence graph G
	Vt	[-]	Set of terminal nodes in the precedence graph G
	Vs	[-]	Set of entry nodes in the precedence graph G
	Vd	[-]	Set of dummy nodes in the precedence graph G
	P_i	[-]	Set of direct predecessors of task $i \in V$
	F_i	[-]	Set of direct successors of task $i \in V$
	P_i^*	[-]	Set of all predecessors of task $i \in V$
	F_i^*	[-]	Set of all successors of task $i \in V$
	c_j	[€]	Material costs associated to task j
	a_j	[m^2]	Required Material Floor space for task j

Association	Symbol	Unit	Explanation
	CT	[t]	Average product time needed to meet the customer's demand
	$CT(t)$	[t]	Average product time needed to meet the customer's demand during a period t
Factory	$WT(t)$	[t]	Available net working time during a period t
	$d_p(t)$	[-]	Demand of a given product p during period t
	P	[-]	Total number of products that need to be produced on an assembly line
	c_e	[€/KW]	Costs of energy
	CRF_j	[-]	Capital Recovery Factor of either building, tooling, equipment, or buffers
	l_b	[m]	Length of the building
	w_b	[m]	Width of the building

Association	Symbol	Unit	Explanation
	E_j	[-]	Set of available resources for performing task j, $E_j = R_j \cap W_j$
	R_j	[-]	Set of automatic resources for performing task j
	W_j	[-]	Set of manual resources for performing task j
	t_{jl}	[t]	Processing time of task j when being performed by resource l, $l \in E_j$
	r_{jl}	[%]	Scrap rate of task j when being performed by resource l, $l \in E_j$
	t_j	[t]	Processing time of task j when being performed by any resource $l \in E_j$
Resource	C_{T0_l}	[€]	Initial purchasing price for a resource $l \in E_j$
	L_{T_l}	[t]	Useful life of tools belong to a resource l
	p_{jl}	[-]	Probability of failure of resource l when performing task j
	D_{jl}	[t]	Average planned and unplanned downtime of resource l when performing task j
	e_{jl}	[KW/t]	Average energy consumption per time unit of resource l when performing task j
	C_{R0_l}	[€]	Initial purchasing price for a resource $l \in E_j$
	L_{R_l}	[t]	Useful life of a resource l
	L_l	[m]	Length of resource l
	W_l	[m]	Width of resource l
	w_l	[€/t]	Wage rate of a manual resource l
	λ_{jl}	[-]	Failure rate of a resource l when performing task j
	μ_{jl}	[-]	Repair rate of a resource l when being assigned to task j
	$e_{0_{jl}}$	[KW/t]	Average energy consumption per time unit of resource l when selected for task j and being in operating state
	$e_{1_{jl}}$	[KW/t]	Average energy consumption per time unit of resource l when selected for task j and being in idle, starvation or blockage state
	σ_{jl}	[-]	Standard deviation of the processing time of resource l when performing task j

Algorithm	Symbol	Unit	Explanation
EAs	T_{size}	[-]	Size of the tournament in the roulette wheel selection of the evolutionary algorithms
	p_c	[%]	Probability of crossover
	p_m	[%]	Probability of mutation
ALL	$PopSize$	[-]	Number of solutions being evaluated and optimised by a specific optimisers
Discrete Algorithms	gB_i^t	[-]	Best position in terms of fitness that the population has, so far, encountered until generation t
	τ	[t]	Total operation time required in a year to produce the V_net products
MOACOs	$\eta_{i,j}$	[-]	Heuristic information between nodes i and j used by the MOACOs
	$p_{i,j}^k$	[-]	Probability transition used by the MOACOs when moving from one node i to a node j
	$\tau_{i,j}$	[-]	Pheromone information used by the MOACOs when moving from one node i to a node j
	α, β	[-]	Pheromone, heuristics importance in the construction process of MOACOs
	ρ	[-]	Evaporation rate
	q_0	[-]	Probability for a normal selection process in the transition rule
	q_1	[-]	Probability for a random selection process in the transition rule
DMOABC	limit	[-]	Number of allowed iterations without changes
DMOCSA	p_a	[%]	Abandonment ratio of solutions
DMOBAT	V_i	[-]	Velocity of solution i
	f_i	[-]	Frequency of solution i
DMOPSO	C1, C2, C3	[%]	Probability of crossover/mutation
DMOFPA	p	[%]	Threshold between global and local pollination
DMOBAT	α_B	[-]	Adaptation parameter for the loudness
	γ	[-]	Adaptation parameter for the pulse rate

Chapter 1

Introduction

Abstract

The present chapter discusses the subject of investigation in this thesis. First, a general introduction is provided. Challenges of mass customisation and personalisation are reported, based on which, the problem addressed in this thesis is described. This is followed by the objective definition and the work structure.

1.1 Introduction

Since mass customisation became a viable strategy in the mid-1990s, there has been tremendous market pressure on companies to deliver personalised products [228] and services to customers with mass production efficiency, cost, quality, and flexibility. As shown in Figure 1.1, product variety and engendered process variety, which is observed as an exponentially increasing number of process variations through machines, tools, fixtures, and labour [410, 193], challenges the conventional product and process development approaches and supply chain management to move from mass production to high-variety-low-volume production [392]. To accomplish economics of scope and scale, mass customisation can be achieved by (i) developing product platforms that are characterised by modularity and standardisation across different products and (ii) reusing already existing production systems [98, 323]. The use of product platforms has been widely considered in the literature and opting for this strategy can reduce development costs and product reliability [44]. However, the enormous competitive pressure, which is even more shaped by the transformation of the mass customisation into a mass personalisation strategy, compels companies to regularly renew their product and process platforms with new production technologies and factory infrastructure. This results in shorter products, factory, and process life cycles, and increases the complexity of planning efficient and cost-effective production systems.

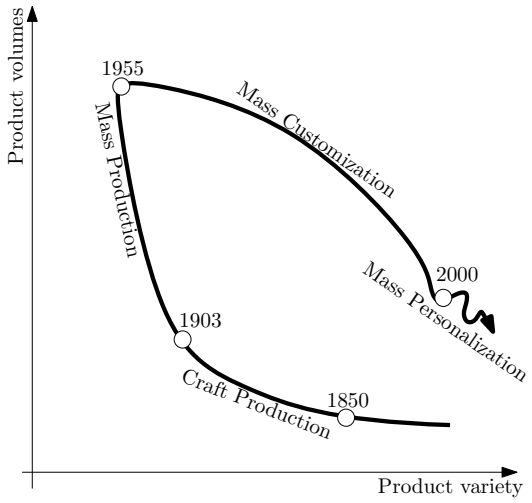

Figure 1.1: Evolution of manufacturing based on [220]

1.2 Problem definition

Assembly lines which meet these cost, quality, and efficiency requirements and are the most commonly used assembly systems, enable the assembly of products by workers with limited

training and by dedicated machines or robots. Because of the high investment and running costs involved, the correct design and redesign of such lines are fundamental. Some crucial decisions must be made in the design of assembly lines, including product design, process selection, line layout configuration, and line balancing [30]. Due to their complexity, these problems are usually not considered at once [394]. However, these design decisions are drastically influenced by the characteristic features of the markets, which are seen as increasingly difficult and doubtful. The associated uncertainty is mostly related to the choice of the right product design and the right level of automation (e.g. fully and semi-automatic or manual) concerning technical data and engendered product costs. This can be illustrated through a real industrial case, in which a company produces a given product in various plants around the world. It owns in its production network several components, suppliers, and dedicated plants for final assembly. Based on the geographical location of each plant, some specific characteristics may change (e.g. wage rate, raw material costs, the number of factor days, and the overhead ratio between direct and indirect workers). Figure 1.2 [1] presents the evolution of the product unit costs of manual and automated assembly lines regarding the annual demand for several plant locations [2]. As demonstrated in the figures below, the product unit costs of both manual and automated assembly lines have a wide range. Indeed, associated costs are based on plants' location characteristics. While for some scenarios manual assembly is always cheaper than automated (e.g. Scenarios 1 and 3), for other scenarios, automated assembly lines provide the cheapest unit costs.

While the majority of product cost is determined in the early product design stage, many decisions about product designs are made during this stage with little or no knowledge [68] of the effect on downstream cost centres (e.g. assembly). They usually rely on qualitative descriptions and subjective judgements in which experts and their knowledge are utilised [436]. The implication is that design decisions are more significant than subsequent manufacturing decisions [27]. Some authors (e.g. [395]) state that design decisions determine 70–75% or more of product costs and manufacturing decisions can only affect 10–25 % of product costs. However, compared to the cost responsibility, as shown in Figure 1.3, manufacturing costs represent about 70% of product costs [17] and design costs represent between 6 and 12% [366]. Thus, if any wrong decision is made in the early stages of the product design, engineering changes will be required.

1. The product unit costs are function of investment and running costs. The various cost elements can be represented, among others, by e.g. the material costs, personal costs, investment costs

2. The reader will note that the required investments for automated assembly lines are constant over the plant locations. Also, while automation can have following reasons: (i) increase productivity, (ii) reduce labour costs, (iii) improve worker safety and (iv) improve product quality, the automated assembly lines under consideration are identical in the different plants and are mostly related to increasing productivity and reduce labour costs.

Late product changes, especially with complex designs, can lead to alterations in other parts of the product and can consequently be costly [209] in terms of scraps, wasted inventory, and disruption. Furthermore, the cost of change increases drastically as the product progresses toward production. Thus, the earlier that changes and improvements are made, the lower the product costs. There is a consensus in the literature that the successful implementation of mass customisation requires a holistic approach taking both product and process design on board [192]. This induces the need to consider product design, process selection, and assembly line balancing together. In order to provide an effective and objective approach to systematically evaluate design concepts and their influence on upstream processes in the early stage of the design process, many methodologies such as Design for Manufacturing, Design for Assembly, Design for Environment, Design for Safety, Design for reliability, Design for Maintenance, Design for aesthetic features, Design for Economy and Design for Ergonomics, have been proposed by academia and industry. All of these methodologies were extensively

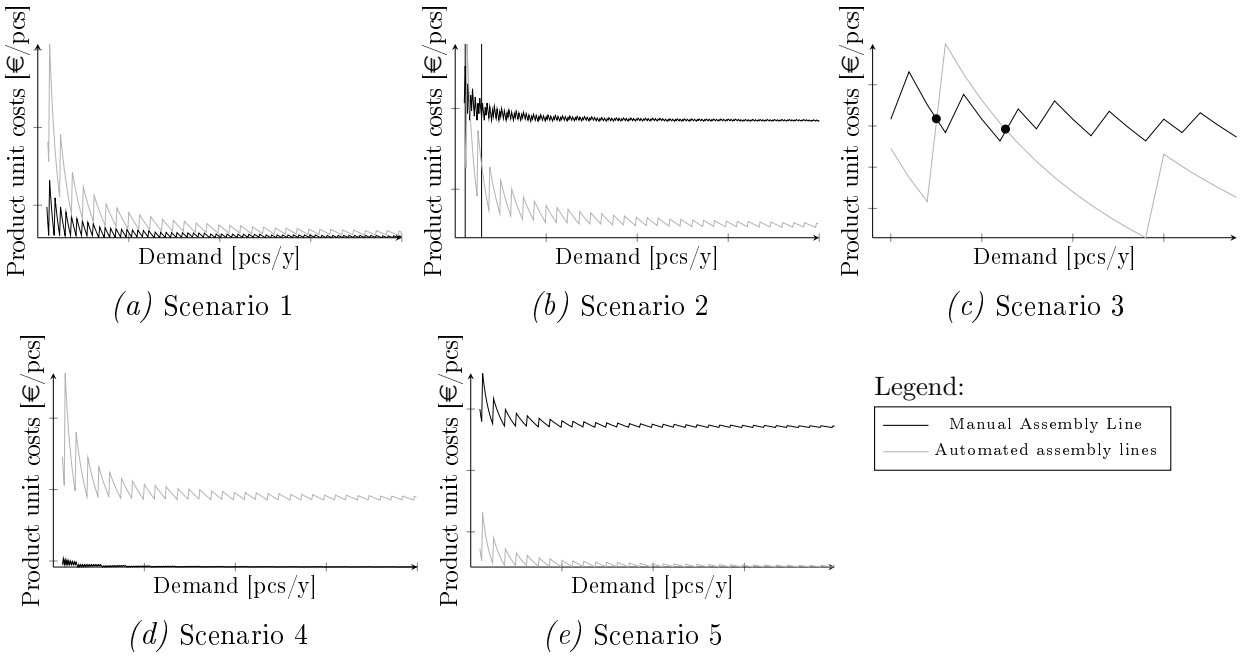

Figure 1.2: Illustration of the evolution of the product costs associated with manual and automatic assembly lines based on the annual demand for five scenarios

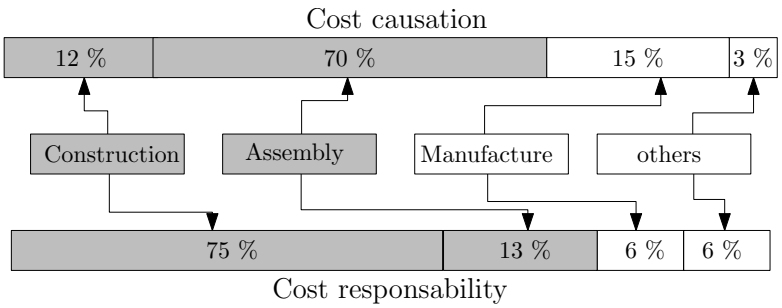

Figure 1.3: Causation and responsibility of final product costs [386]

described by Paramasivam and Senthil [314]. In these methodologies, evaluation metrics such as boolean, cost, time, quantitative, and abstract measure are used. In practice, there is often great flexibility in performing the manufacturing work for a given product alternative. This might concern a single operation (e.g. a part might be connected to the workpiece by gluing, screwing, riveting, or welding causing different execution times) and a complete set of operations [360]. The effects of product alternatives and greater flexibility in performing tasks associated with these designs in an assembly line are currently not being taken into consideration by any of these methodologies. Indeed, the iterative evaluation of product and process designs is time consuming and laborious since many factors must be examined. Furthermore, the evolution of product and process designs also requires decision-making tools that can consider large numbers of evaluation criteria that are too complex for a human decision maker [314].

1.3 Objective definition

In this global and competitive marketplace, companies must excel at various subjects, including product costs, design functionality, and product quality [345]. Developing a new product is an insecure and uncertain process [314]. In order to reduce the risks and uncertainties associated with the product and process design and to ensure the competitiveness of manufacturing firms, new planning methods that support decisionmakers during the design phases of an assembly line under consideration of product design, processes, and resource alternatives, aiming at both optimising capacity and cost-oriented objectives are required. Consequently, the lack of analytically based methods for addressing these drawbacks motivated this work.

The research objective of the present thesis is to address this point by developing a decision support method that can select the best product and assembly line configuration with the least resulting costs. As shown in Figure 1.4, another objective is to decrease the planning changes of the product and the process and thus the engendered planning and operation costs.

To deal with this, the following sub-objectives need to be addressed:

— Analysis of the interdependencies between the product designs, processes, and product design alternatives, and development of a cost model that can translate all these interdependencies between the various products, processes, and resource alternatives into one single metric

— Development and comparison of various optimisation methods and fine-tuning of the most promising one
— Incorporation of evaluation methods to analyse the influence of buffers in the efficiency of the assembly line

The following research questions can be derived from the objectives of this thesis:

— Which cost elements have a significant influence on the selection of the best product and assembly design?
— Which optimisation method(s) is/are the most suitable for selecting the best product and assembly line configuration?
— Does the proposed method decrease the number of design changes, planning costs, and product costs?

These research questions represent the guidelines for the present work and form the basis for the structure of this thesis.

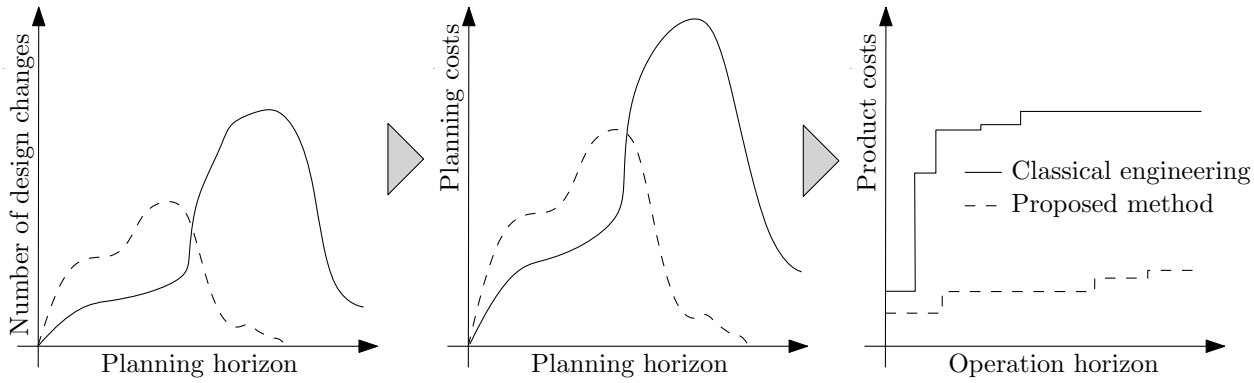

Figure 1.4: Objective definition of the proposed work

1.4 Research methodology and work structure

There are two approaches in research that may result in the acquisition of new knowledge: inductive and deductive approaches [185, 372, 223]. These approaches may differ in the way existing knowledge is used to draw a conclusion, make predictions, or construct explanations. In the deductive approach, the argumentation line follows the path of a general law or theory to a specific case, and the inductive approach can be described as the mirror image of the deductive process [194, 372]. The argumentation line moves from a specific empirical case or a collection of observation to a general law or theory.

The structure of this thesis, which is represented in Figure 1.5 mainly reflects the inductive-

deductive reasoning approach, which was used in the development and refinement of the decision support method.

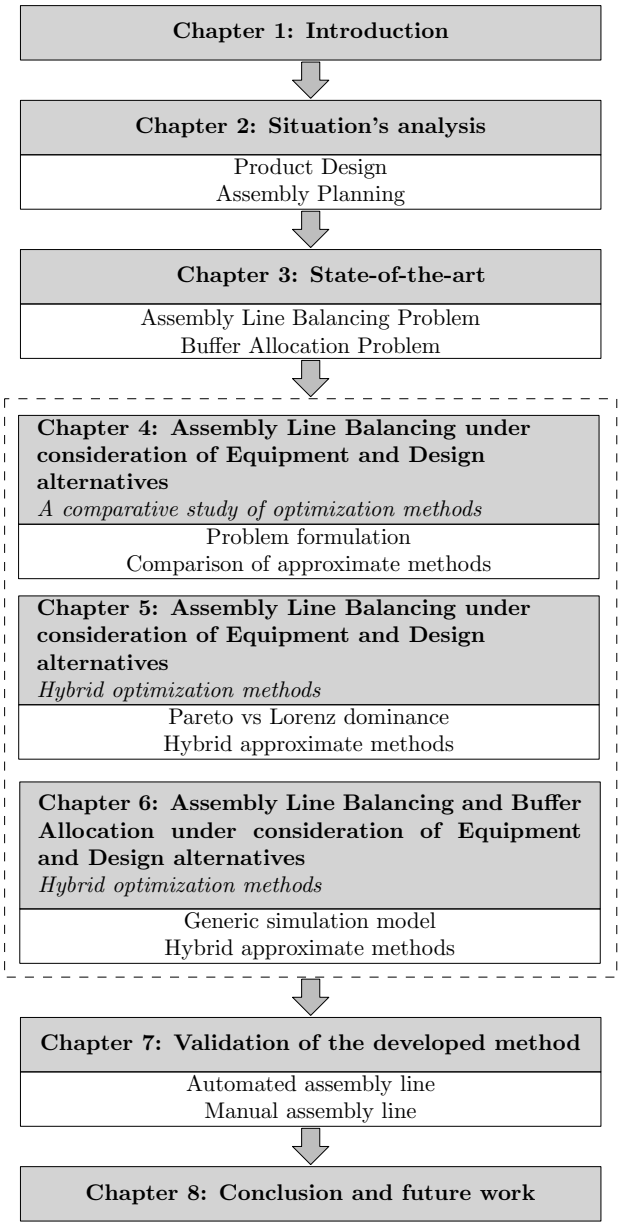

Figure 1.5: Structure of the work

Chapter 2 explains important fundamentals and provides a generalised description of the design phases of products and assembly lines, which are central subjects in this thesis. Current limitations are identified, leading to the definition of the scope of this thesis, and the requirements that must be considered in the development of the decision support method.

In Chapter 3, the state-of-the-art will be tackled by presenting optimisation methods, which are a core element of this thesis. In addition, the focus of this chapter relies on the reflection of existing models and problems related to the selection of the best product design

and assembly design. The identified drawbacks related to the assembly line balancing problem and buffer allocation problem will allow the definition of the research need. Based on this research need, two models and several different optimisation methods to tackle these models are presented in Chapters 4 to 6. Among these algorithms, several variants of evolutionary algorithms, artificial bee colony algorithms, cuckoo search optimisation algorithms, flower pollination algorithms, bat algorithms, particle swarm optimisation algorithms, and ant colony optimisation algorithms are proposed in Chapter 4 to tackle the first problem. Following the inductive-deductive approach, an empirical study was performed to accept or reject hypotheses that were defined based on several patterns discovered through the data analysis or defined based on the state-of-the-art. The combination of these hypotheses allow for the identification of the most suitable optimisation methods. In Chapter 5, the influence of dominance rules and local search on the most promising algorithms is analysed. In Chapter 6, the second problem is presented, and various resolution methods are introduced and compared. The decision support method is validated in Chapter 7 with two industrial use-cases. Finally, the work addressed is reflected and possible future work is identified.

Chapter 2

Situation's Analysis

Abstract

This chapter introduces the situation's analysis. First, basic concepts and common criteria used in the literature to classify assembly lines are presented. This is followed by the description of conventional methods for designing products and assembly lines. The concurrent product design approach, the method on which this thesis relies, is then introduced. Finally, general drawbacks that have been identified during four years of industrial consulting projects related to the design of products and assembly lines are listed, based on which the requirements for the approach that has to be developed in this thesis are defined.

2.1 Introduction

Assembly, which is one of the most cost-effective approaches to high product variety [182], is considered as an important and crucial stage in the product lifecycle. Therefore, the task of planning an efficient assembly system is of high importance for every producing company. The design of assembly lines requires a number of crucial decisions related to product design, process selection, line layout configuration, line balancing, and buffer sizing. However, due to their complexity, these problems are usually considered separately [337, 30]. Product design and process selection are steps that provide information about the work that must be performed in the assembly line and the set of constraints between these tasks. These constraints can be technological, economical, environmental, or ergonomic. In the step related to the line configuration, the choice of the line layout (e.g. straight, U-shaped, circular) that defines the flow directions of the material, must be made. Finally, the last two and probably the most crucial steps are line balancing and buffer sizing. In these steps, the tasks and their respective equipment are first assigned to workstations and then, the buffer sizes between these workstations are defined.

2.2 Basic concepts

The assembly planning has the task of developing an assembly system, in which it is possible, under given restrictions to bring together individual parts or assemblies. This can be done through the assembly processes described by the DIN 8580 [112] and shown in Figure 2.1. Bringing together individual parts is accomplished through one or several joining elements (e.g. screws) or joining techniques (e.g. welding or gluing). Figure 2.2 represents the various connection possibilities of two sheet-metal parts, which can be respectively realised by a bolt and nut, a screw, a rivet, press fitting, and welding. The primary difference between these techniques are the required tasks and their processing time. While the first technique necessitates four operations, the second only calls for two operations. In addition, these various designs may need different tools and resources. While the first design can hardly be automated due to the required exact position of the nut when inserting the bolt, the second design can be more easily be automated.

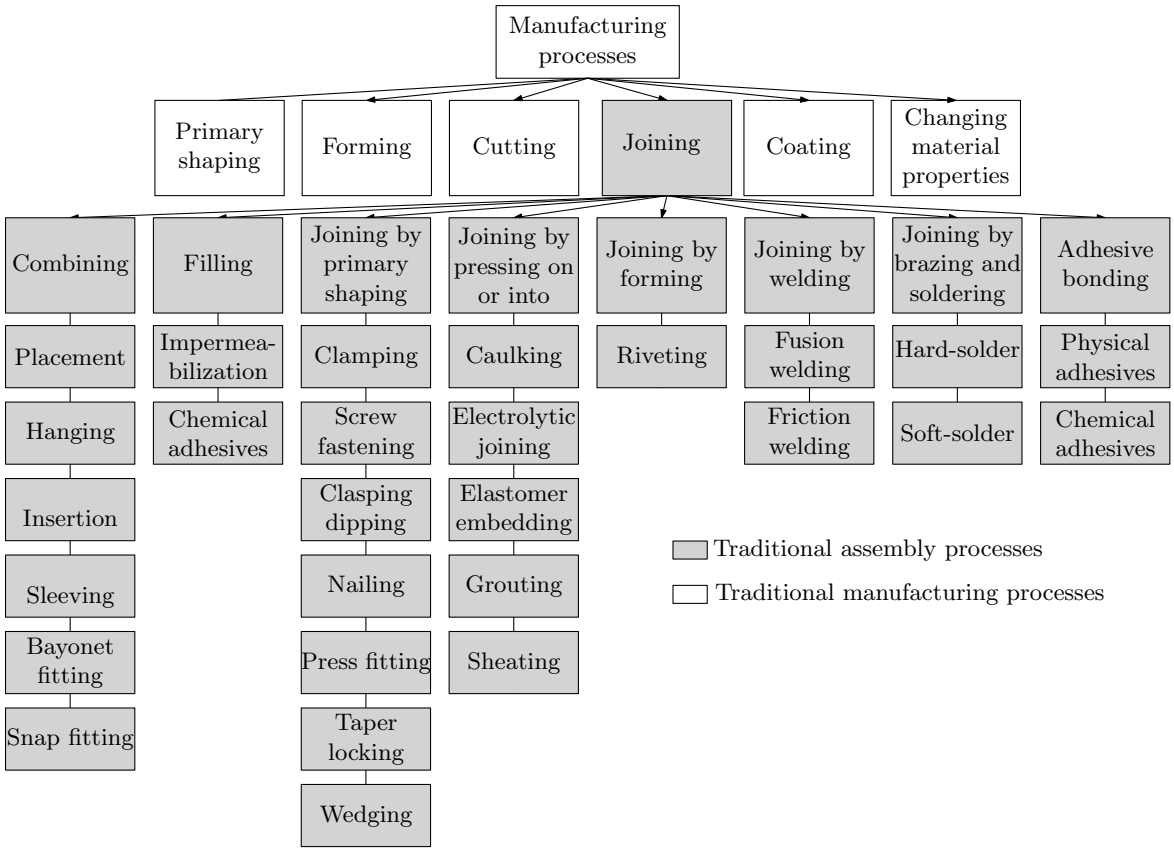

Figure 2.1: Traditional manufacturing and assembly processes

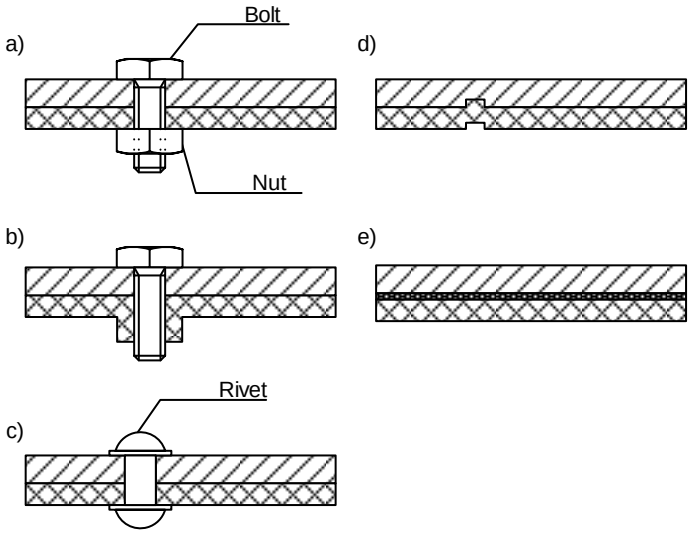

Figure 2.2: Assembly of two sheet-metal parts using different assembly processes

Assembly systems can be modeled as a sequence of M workstations and $M-1$ intermediate buffers. The size of the buffer between station m and $m+1$ is provided by B_m. In an assembly line, the M workstations are usually connected by a transportation mechanism such as a conveyor belt. Among these M workstations, N tasks are performed. Each task j,

$j = 1, ..., N$, requires a task processing time t_j, which can either be performed by a machine, a robot, a human worker or a combination of them. The total work required to manufacture a product is given by $\sum_{j=1}^{N} t_j$. Each station m, $m = 1, ..., M$, has a specific set of tasks called the station load S_m. The station time of a given station m is given by $t(S_m)$ and is calculated as follows:

$$t(S_m) = \sum_{j \in S_m} t_j \tag{2.1}$$

Definition 2.1 Product

A product is a composition of interconnected parts forming a stable unit realised through one or several joining elements (e.g. screws) or techniques (e.g. welding, glueing).

Definition 2.2 Part(Component)

A part (or a component) is a solid objective whose shape remains unchanged throughout the assembly process.

Definition 2.3 Task

A given product is subdivided into N indivisible working units, later on task. Each task $j, j = 1, ..., N$ requires a processing time t_j.

Definition 2.4 Cycle Time

The cycle time is the time available in each workstation to complete all assigned tasks and it represents the average time between the start of assembly of one unit and the start of the next one.

There is a great variety of assembly line configurations. This diversity is engendered by the layout and shape of the line, the number of products and models being assembled on the line, and the types of workstations that can be automated, hybrid, or manual.

Definition 2.5 Manual Assembly Line [408]

Assembly systems in which all operations are carried out manually, or that consist entirely of manual workstations.

Definition 2.6 Automated Assembly Line [408]

Assembly systems in which all operations are carried out automatically, or that consist entirely of automated workstations.

Definition 2.7 Hybrid Assembly Line [408]

Assembly systems composed of a combination of manual and automated workstations.

2.2.1 Classification of assembly lines

Assembly lines can be classified according to the following characteristics [30, 350]: (i) the number of products or models produced, (ii) the task duration, (iii) the layout or shape of the line, and (iv) the level of automation of the line.

According to the number of products or models, assembly lines can be classified into: (i) single model, (ii) multi-model, and (iii) mixed-model assembly lines.

- In a single model assembly line, only a unique product type is produced on the same line.
- In a mixed model assembly line, several variants of a basic product, referred to as models, are produced simultaneously on the line. The production process does not involve significant setup times since these models require similar manufacturing tasks and materials. These models are produced in a mixed-model sequence.
- In a multi-model assembly line, different models with significant differences are produced on the same line. These differences can be identified as different sequences in assembly tasks or different materials. Units of different models are processed in a sequence of batches, containing either the same model or a group of similar models.

According to the task duration, which can be referred to the level of automation, assembly lines can also be classified regarding the nature of the task duration and if they are: (i) deterministic or (ii) stochastic. In deterministic lines, all processing times are fixed and known with certainty, whereas in stochastic lines, task processing times may be significantly affected by the learning effect of workers and the availability of resources.

According to the line shape and layout, assembly lines can also be classified according to the shape of the line, which can be straight, U-shaped, or circle/closed.

- In a straight line, products are processed throughout a group of workstations arranged in a straight line.
- In a U-shaped line, which is commonly manual and allows workers to work on two or more workpieces at different stations across both legs of the line during the same cycle, the workstations are arranged in a U-shape. The U-shaped line allows the forward and backward assignment of tasks to stations [329] in contrast to a typical forward movement in a straight line [347].
- In a circle/closed line, the workstations are arranged around a circular conveyor.

While U-shaped assembly lines help to reduce the number of stations, they can also improve the efficiency of the assembly line by allowing workers to work on two or more workstations. Indeed, compared to straight lines, tasks can be grouped into a station by moving forward

and backwards or simultaneously in both directions through the precedence network [256]. Furthermore, Miltenburg [265] shows through an empirical study that the effectiveness of U-shaped lines are at least as good as that of straight lines when buffers are located between each workstation. Finally, the U-shaped line can also decrease work in progress, increase productivity, reduce material handling [330], and improve visibility and communication between workers [444]. However, to use all benefits of a U-shape line, multi-skilled workers must be hired [266]. These differences in the line and work assignment are shown in Figure 2.3.

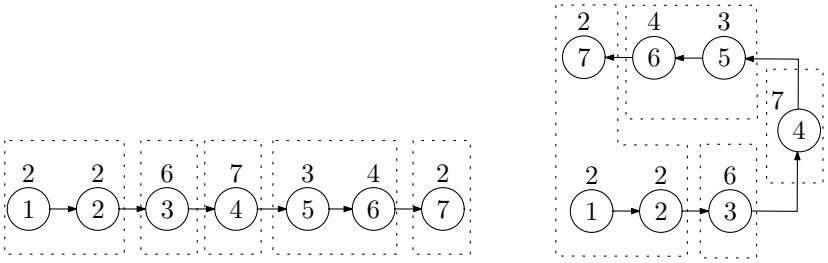

(a) Straight Line *(b)* U-shaped Line

Figure 2.3: Comparison of the layout of a straight and U-shaped line

Assembly lines can also be classified according to the layout of the line. Several layouts can be identified as: (i) parallel lines, (ii) parallel workstations, (iii) two-sided lines, and (iv) fishbone flow.

— Parallel lines are often used when several product types are assembled. Each of these lines is designed for a specific product type or family.
— Assembly lines with parallel stations are often used when either the net processing time or the gross processing time of equipment performing specific tasks exceeds the cycle time.
— In two-sided assembly lines, tasks can be performed on both sides of the line. This configuration is commonly used in the industry (e.g. automotive).
— Fishbone assembly lines consist of a main line, the spine, where the final assembly is performed and several smaller lines, and the bones, which produce subassemblies and deliver them to the final assembly line. The fishbone assembly lines are mostly suitable for modular products with sub-assemblies. In such a configuration, since each of the modules are fed by a rather long assembly line, the main assembly line is shorter.

According to the flow of workpieces, assembly lines can either be synchronous lines, asynchronous lines, or continuous lines.

— In synchronous lines, all workstations have a common cycle time CT and therefore all workstations start processing at the same time, and the workpieces move simultaneously at the end of each cycle time. Some workstations may finish their station loads

before the end of the cycle time CT but the workpieces need to wait until CT has passed. For this type of assembly line, the difference between the station time is used to compensate stochastic variations in the task time (e.g. equipment breakdown).

— In asynchronous lines, the workstations have different cycle times, and workpieces are transferred whenever the required tasks are completed. The workstations are linked by buffers to minimise the difference of cycle times. Asynchronous lines are often implemented due to temporary stochastic variations due to the model mix or if non-deterministic events such as machine breakdowns affect the station time. Taking the station time of stations m and $m+1$, respectively $t(S_m)$ and $t(S_{m+1})$, the difference between them may determine whether there will be blockage or starvation. If $t(S_m) < t(S_{m+1})$, the workpieces will move from station m to the buffer B_m. However, if the number of workpieces in the buffer between m and $m+1$ is equal to its storage capacity, the station m will be blocked since the workpiece cannot leave the workstation. If $t(S_m) > t(S_{m+1})$ and the buffer between m and $m+1$ is empty, the station $m+1$ will be in starvation. Starvation or blockage can also be ensured by machine breakdowns on either upstream or downstream workstations.

— In continuous lines, the workpieces continuously cross the various workstations at a constant speed. This type of line is often used for manual operations with high cycle times.

Synchronous assembly lines can also be paced or unpaced. The difference between a paced and unpaced synchronous assembly line is that an unpaced line moves only when all stations have completed their tasks[397].

Figure 2.4 shows a combination of possible line configurations based on a real industrial case study. In this example, several areas can be identified. Two parallel lines are used to produce two product families. The assembly of gas and electric ovens is respectively done on the first and second lines. In Area 1, the chassis are assembled on a circular line. After completion, the chassis are moved with a lift to the main straight line, where the following operations are done: (i) isolation of the chassis, (ii) assembly of sides and bottom panels, (iii) assembly of cooktops, (iv) assembly of drawers, (v) assembly of doors, and (vi) testing operations. After completion, both lines are merged before the packaging area. While most of these operations are realised on the main line, the pre-assembly of cooktops and doors is respectively done on separate lines, represented by Areas 2 and 3. Due to the high-processing times of the testing equipment, several ovens are simultaneously tested in a u-shape in the first line or in a circular line in the second line.

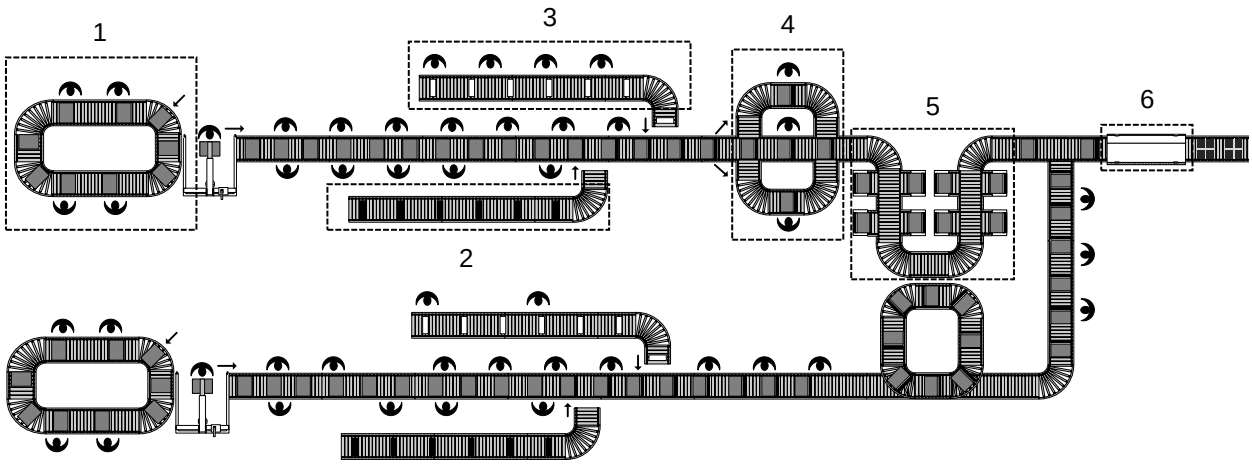

Figure 2.4: Industrial example of a complex assembly system

2.2.2 Conventional methods for product design

Several methodologies and models for the product design process have been developed and are found in the literature (e.g. [342, 143]). Designing a product requires finding and defining the geometry and materials in such a manner that the prescribed requirements are met in the most effective and efficient way. These methods may differ in their granularity, but they have the same sequence of tasks. Pahl and Beitz's method [178] is one of the most famous methods. They divided the design process into four distinct phases. In the first phase - clarification of the task - based on the information handed over by a client or the department responsible for the product planning, a program of requirements is drawn. These specifications define the functions, the properties, and the constraints that are required for the new product. In the second phase - conceptual design - broad solutions are generated and evaluated regarding the specifications defined in the first phase. In the third phase - embodiment design - the chosen concept is elaborated into a definitive layout. In the last phase - detail design - the geometrical shapes, dimensions, tolerance, surface properties, and materials are fully specified and the part lists, the production, and assembly instructions are generated and documented.

2.2.3 Conventional methods for assembly planning

In the literature, there are several conventional methods for planning assembly systems (e.g. [135, 59, 162]). They may differ in their granularity, but they all have similar steps. Bullinger's method [59], which is divided into six planning phases is shown in Figure 2.5.

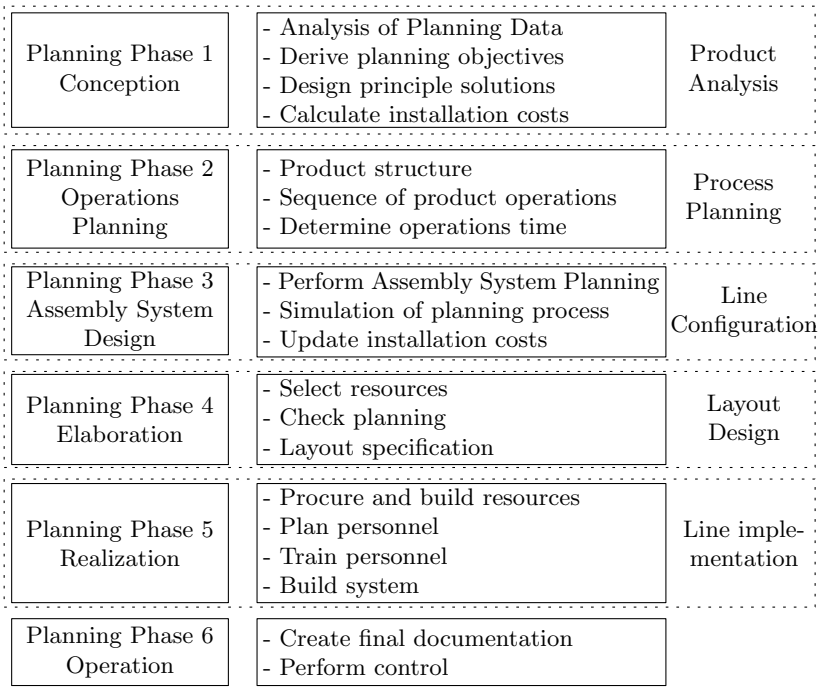

Figure 2.5: Main steps in the assembly line planning based on [59]

The first phase aims at analysing the products and their variants, the production strategy (e.g. number of products to be produced within a given time period, decision about make or buy strategy), and the specific personal data. Based on this analysis, planning objectives are defined, analysed, and weighted. These steps allow the definition of a takt time, CT, metric which gives the average unit production time needed to meet the customers' demands. CT defines the boundary for each station time $t(S_m)$, $m = 1, \ldots, M$. The cycle time for a given period t, denoted as $CT(t)$ can be calculated as follows:

$$CT(t) = \frac{WT(t)}{\sum_{p=1}^{P} d_p(t)} \tag{2.2}$$

where $WT(t)$ represents the available working time during period t and $d_p(t)$ represents the demand for a given product p during this period. P represents the total number of products or variants that need to be produced on the assembly line.

The second phase has the purpose of defining and determining all necessary tasks N for the assembly of the products and the various technological constraints, their sequential relationship, and all the tasks processing times. Classically, the resulting information of this phase is represented in a precedence diagram.

The third phase aims at determining the assignment of tasks to the workstations with respect to the objective(s) defined in the first phase. In this phase, several solutions are generated regarding various criteria (e.g. idle time on the assembly line and capital expenditures) and

different organisational systems (e.g. parallel stations and buffers). These solutions are then compared and put into different layouts (rough and detailed layouts) and their concepts are verified through simulation. This can be addressed by solving various problems, such as the Assembly Line Balancing Problem (ALBP), the equipment selection problem and the buffer sizing problem. The ALBP arises whenever an assembly line is configured, redesigned, or adjusted and distributes the total workload for manufacturing any unit of the products that will be assembled among the workstations [359]. The Buffer Sizing Problem is also known as the Buffer Allocation Problem (BAP). This problem aims at finding the optimal buffer sizes between workstations [107].

In the fourth phase, the resources for the execution of each task are selected and a final review of the different task processing times and investment costs is done. In addition, the material handling system is selected and the layout of the assembly system is designed in detail.

In the last two steps, the resources are designed and procured. After staff planning and staff training, the production system is set up and evaluated to check if the objective(s) defined in the first phase is/are reached.

The following sections present the various steps involved in the assembly planning in detail.

2.2.3.1 Assembly process planning

Assembly Process Planning (APP), which is an important stage in product design and manufacturing, considers two tasks, the Assembly Sequence Analysis (ASA) and Assembly Sequence Planning (ASP). The results of APP are the definition of all assembly process constraints, including the precedence relationships of parts or subassemblies and other assembly process constraints, such as assembly directions and tools [435]. To generate all possible assembly sequences, the ASA problem must be addressed. The ASA aims at defining the feasible assembly sequences for a product with a defined architecture by analysing possible assembly combinations. The objective is to find one possible and feasible sequence or all sequences. ASP considers the results of ASA and aims at finding the possible sequence of tasks, the assembly tools, and fixture planning [407]. Taking into consideration that defining the assembly sequence can be addressed through a combinatorial approach based on the total number of parts n, the maximum number of feasible solutions C can be expressed as follows:

$$C = n! \tag{2.3}$$

In their literature review, Klindworth *et al.* [217] classified the concepts associated with

finding assembly sequences or precedence restrictions into two main classes: (i) manual and automated approaches that are intended to detect all feasible sequences and (ii) genetic algorithms and case-based reasoning procedures applied to search for good sequences.

Once the various possible assembly sequences have been identified, they need to be represented in a precedence graph. Several methods have been proposed in the literature for the transformation of a set of assembly sequences into precedence graphs (e.g. [207, 267, 177, 217, 301]).

2.2.3.1.1 Method for representing precedence information for a single product

The precedence graph has been widely adopted in assembly planning to describe the sequential relationship and all the task processing times involved during the product analysis and process planning.

Definition 2.8 Precedence Graph
A precedence graph $G = (V, E, t)$ is a network plan, which represents the order in which tasks must be performed (e.g. due to zoning, technical or resource restrictions). The set of nodes $V = \{1, ..., N\}$ represents the different tasks and the set of arcs E represents the precedence relations (i, j) between tasks $i, j \in V$. The vector t contains the operation times t_j, $j = 1, ..., N$.

The precedence graph enables the identification of which tasks take precedence over other tasks and which tasks can be executed in parallel. Indeed, if there is an arc $(i, j) \in V$, i is an immediate predecessor of j. A given task may have more than one immediate predecessor and can only be started as soon as all its predecessors have been completed. In the example provided in Figure 2.6, $V = \{1, 2, 3, 4, 5, 6, 7, 8, 9, 10, 11\}$, $E = \{\{1, 2\}, \{2, 3\}, \{3, 4\}, \{4, 5\}, \{4, 6\}, \{6, 7\}, \{6, 8\}, \{7, 9\}, \{8, 9\}, \{9, 10\}, \{10, 11\}\}$ and
$t = 2, 5, 4, 6, 3, 2, 10, 1, 11, 12, 11$.

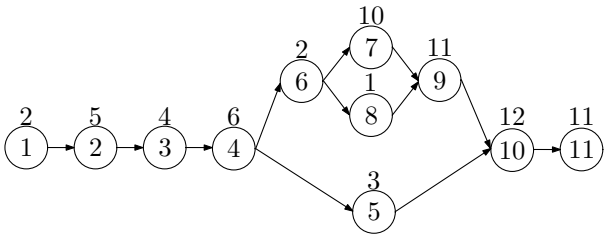

Figure 2.6: Example of a precedence graph

Braun [53] defines a precedence graph by the following properties:

— A precedence graph must be acyclic

— A precedence graph must not have any circuit
— A precedence graph must not have any transitive relations

An important measure characterising a precedence graph G is its order strength $OS(G)$ [301], which is defined as:

$$OS(G) = \frac{2 \cdot |E^T|}{N \cdot (N-1)} \tag{2.4}$$

The order strength Order Strength (OS) represents the ratio of the number of all (indirect and direct) precedence relations in G and the maximal number of precedence relations in G. In other words, it refers to the degrees of freedom for the assembly planning task. If $OS(G) = 1$, a graph is highly restricted and only one assembly sequence can be generated. The calculation of the order strength requires the transitive closure of the precedence graph G.

Definition 2.9 Transitive closure
A precedence graph $G = (V, E, t)$, $G^T = (V, E^T, t)$ is called the transitive closure of its original graph G iff there is a directed path from i to j (i.e. there is a sequence of vertices $a_1, ..., a_t$ with $t > 0$, $i = a_1 (a_r, a_{r+1}) \in E$, $\forall r < t$, and $a_t = j$)

One precedence graph typically corresponds to multiple possible assembly sequences [450]. To create the precedence graph of a given product, the possible assembly sequences must be analysed first. While the precedence graph represents a partial order of the assembly tasks, the assembly sequence represents a total order.

To define the task processing times, various methods covered by the term 'work measurement' can be used. Different research activities have been done in recent years to integrate methods and techniques from engineering and ergonomics with the intention of estimating the time needed to perform a specific task [114]. Several factors are involved in the decision process of selecting a specific evaluation method. Engineering methods known in the literature as predetermined motion time systems (PMTS) are usually used for short-cycle work (minute range). The methods-time measurement (MTM) [260], with the aim of analysing a task into its fundamental human activities to assess the complete time required for all these activities, is the first and one of the most widespread PMTS methods. One major drawback of MTM is the amount of time needed to analyse all tasks. For this reason, several variants have been developed during the last decades. Among them, the following methods can be identified: (i) Sequence-based Activity and Method analysis (SAM) [85], (ii) the Maynard Operation Sequence Technique (MOST) [60], and the Universal Analysing System. For long-cycle work, estimation methods relying on the experience of the estimator and require in-depth knowledge. Similar to MTM, the Robot Time and Motion (RTM) method [286] for

predetermining the robot cycle time based on standard elements of fundamental robot work motions was also developed.

2.2.3.1.2 Methods for representing precedence information for multiple products

When different variants and products are produced on one assembly line, the precedence graph has to include the relations between all tasks of all products or variants P. Usually, the generation of a joint precedence graph requires the information about the individual precedence graph $G_p = (V_p, E_p, t_p)$ for each model p, $p = 1, ..., P$. The node set V_p contains the model specific tasks, the arc set E_p reflects the precedence relations (i, j) between tasks $i, j \in V_p$, and the vector of node weights t_p contains the processing times t_{ip} of tasks $i \in V_p$. Using the demand d_p of model p and the various nodes and arc sets V_p and E_p, it is possible to create a joint precedence graph $G = (V, E, \bar{t})$ from the following definitions [254, 401]:

$$V = \bigcup_{p=1,...,P} V_p \tag{2.5}$$

$$\bar{t_i} = \bigcup_{p=1,...,P} \frac{d_p}{\sum_{p=1}^{P} d_p} \cdot t_{ip} \tag{2.6}$$

$$E = \bigcup_{p=1,...,P} E_p \setminus \text{redudant arcs} \tag{2.7}$$

In equation (2.5), each task that is common to different models receives a model wide consistent number. This allows common tasks to be assigned over different models to the same workstation [1]. If a specific task $i \in V$ is not required by a model p, its operation time $t_{ip} = 0$. In equation (2.6) the weighted operation time $\bar{t_i}$ is calculated. Equation (2.7) determines the joint precedence constraints by joining the model-specific arc sets. This can lead to redundant arcs (i, j) which represent transitive precedence relations. A redundant arc from i to j can be removed without any loss of information if there is another path from node i to j with more than one arc. An example of a joint precedence procedure, based on model-mix prognosis is shown in Figure 2.7.

Due to the increasing number of models and to reduce the processing time for generating a precedence graph, Boysen *et al.* [52] propose the option-based precedence graph. The main difference between the approach described before relies on the determination of the joint task times based on the estimated fraction of product units containing certain options instead of

1. Assigning model wide consistent numbers to common tasks is a requirement for a mixed-model line, but not necessarily for a multi-model line. This is induced since in a mixed-model line no setup times are taken into consideration and assigning similar model wide tasks to different stations would engender setup times.

respective forecasts for the large number of individual models. In their approach, the risk of systematically overvaluing task times and resource utilisation is reduced.

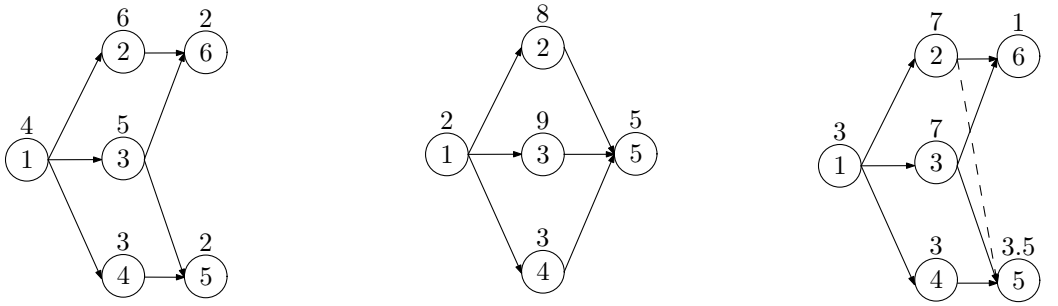

(a) Model 1 with $d_1 = 0.5$

(b) Model 2 with $d_2 = 0.5$

(c) Joint precedence graph

Figure 2.7: Creation process of a combined precedence graph

2.2.3.2 Line configuration

The line configuration determines the assignment of tasks to workstations and dimensioning buffers between workstations with respect to the objective(s) defined in the first phase of the conventional assembly planning process. Two main problems can be identified here: (i) the ALBP and (ii) the BAP. This is done considering what has been achieved in the process planning. The solution methods applied during this step can be summarised into two categories: (i) traditional methods or (ii) methods combined with optimisation algorithms. Process planners usually use the traditional manual trial-and-error techniques to solve these two problems. Even if they can reach a good solution, this process is relatively time-consuming and not adequate for complex products since it is impossible to explore all the solution space. It has been reported in the literature that this technique generally results in an estimated four to ten percent of operator's time losses through unequal work assignments [240]. Methods of Operations Research, which can be defined as follows, are often used to assist the decision maker to reach a better solution faster.

Definition 2.10 Operations Research [2]

Application of scientific principles to business management providing a quantitative basis for complex decisions

A detailed overview of these two problems with their respective solution methods is provided in the next chapter.

2. http://www.oxforddictionaries.com

2.2.3.3 Layout design

Based on the results of the line configuration, with an objective is to provide an assignment of tasks to workstations and a dimensioning of buffers between them, the detailed design of the manual and automatic stations occurs in Phase 4. In this phase, several alternatives are usually developed regarding various criteria, such as material handling systems, ergonomics concerns, and space utilisation [420]. The design of workstations under consideration of ergonomics is described by standards (e.g. [113]). The objective when designing a workplace is to accommodate a wide range of heights, from 1.54 to 1.87m, so that the largest percentage of the population is covered. In addition to the height of the workplace, the gripping area is also an important design criterion. The geometry of the work area should not cross a maximum depth of 40-60 cm and a width of 120 cm. When planning the material disposition on the line, the following criteria should also be taken into account: (i) accessibility, (ii) inclination, and (iii) consideration of the symmetrical movement sequence.

2.2.4 Concurrent engineering

The current high-variety-low-volume ratio and engendered short product life cycle requirements have forced product designers and manufacturing engineers to change the way products are designed [414]. In conventional product development, the following steps are considered in a sequential process: (i) conceptual design, (ii) preliminary design, (iii) detailed design, and (iv) prototyping verification. These steps occur before the process development. Since many departments are involved in the product and process development, and there is no interface between them, several iterations and changes are required both on the product and process side to achieve an ideal solution. In concurrent engineering, which is a systematic approach to integrating the concurrent design of products and processes, product designers are stimulated to consider all elements of the product lifecycle in the first stages of product development. To improve the quality and cost of planned products and fulfil customer requirements in the early stage of the design process, many methodologies such as design for manufacturing, design for assembly, design for environment, design for safety, and design for economy and design for ergonomics have been proposed by academia and industry. The previous terms starting with 'Design for ...' are often simplified using the acronym DFX, Design for X [131]. Common to all DFX methods are their two approaches for the evaluation process of a specific product design: (i) qualitative and (ii) quantitative. Examples of suitable qualitative evaluation criteria are the weight, number of parts, size, required assembly directions, and joining method. Examples of quantitative methods are costs and assembly

time.

2.3 Industrial context

Over the experience gathered through multiple industrial projects and seminars in different companies, from SMEs to multinational companies, working as a research engineer and consultant, the following gaps between academia and industry have been identified:

— Even if concurrent engineering is not a new concept in the industry and academia, current practice in the industry is still to develop products with a traditional engineering approach. Considering this, there are some information exchange barriers between stakeholders of the first activities of the product life cycle. This prevents to decrease time-to-market since many design changes, both on product and process sides, are needed. Furthermore, prototyping verification often fails due to the absence of a required manufacturing process.
— Product designs are usually based on the experience of designers and old designs may be reused without being changed and improved through time. Thus, most of the designs, which are obsolete and not updated, are not adequate for an efficient manufacture and assembly.
— As stated earlier, to achieve economics of scope and scale, mass customisation and personalisation can be achieved by developing product and process platforms that are characterised by modularity and standardisation across different platforms. A common phenomenon in the industry is to see different product variants, sharing the same skeleton, being differently designed.
— Process planners habitually do not use their full potential when it comes to designing a new assembly line and do not explore the entire solution space. Instead of employing any decision support tool, planners usually perform the design of assembly systems in workshops, without using a precedence graph of the product under study.
— Usually the determination of operation time in process planning is based on experience and is not close to the real processing times.
— Most of the companies do not have a clear overview of unit product costs when designing products and processes.
— Assembly lines are characterised by a medium capacity utilisation of workers and by the unnecessary material or material in a disproportional amount. Due to historically grown structures, the floor space available for new assembly lines and the expansion of existing assembly lines is often limited.

2.4 Conclusion

To address the problem identified in this thesis and the industrial drawbacks, a qualitative and quantitative method in the form of a support decision tool that evaluates products, processes, and resource alternatives is required. This method, which should support planners during the early stages of the product life cycles, has the following properties to cope with industrial needs:

— Generic - to enable its instantiation in several industrial sectors.
— Modular - to allow an easy adaptation of its components for any further industrial need.
— Realistic - to achieve a detailed approximation of the future product unit costs.
— Performant - to explore a highly constrained solution space, comprised of several restrictions and assignments (e.g. precedence constraints, resource allocation, and design alternatives).
— Environment specific - to represent various products alternatives, associated processes, and resource alternatives for each task. With the intention of decreasing the material space area on the assembly line and the used floor space, the required material space for each task and the total necessary floor space should also be considered. The developed method should provide a decision-support system regarding the decision of whether to automate specific tasks.

The scope of the thesis and subject refinement is represented in Figures 2.8 and 2.9. While the process planning and layout design are partially examined, the main core of the thesis relies, as stated earlier, on the line configuration and more precisely on the assembly system planning step. While the variety of decisions made during the product's and production system's life cycles can be classified into strategic, tactical, or operational groups, this thesis only focuses on tactical decisions [3]. Figure 2.9 shows a schematic representation of the objective of this thesis. Given several products and resource alternatives, which may engender different line configurations, the objective is to select the most suitable combination of product, process, and resource alternatives.

3. Strategic decisions related to what types of products will be manufactured/assembled will not be considered, but rather how the products can be assembled.

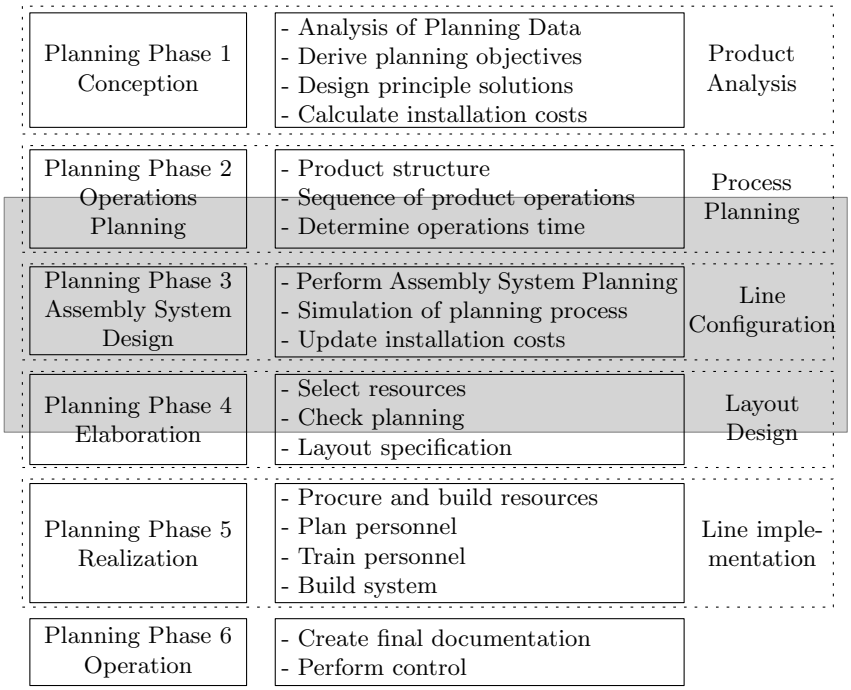

Figure 2.8: Scope of this thesis

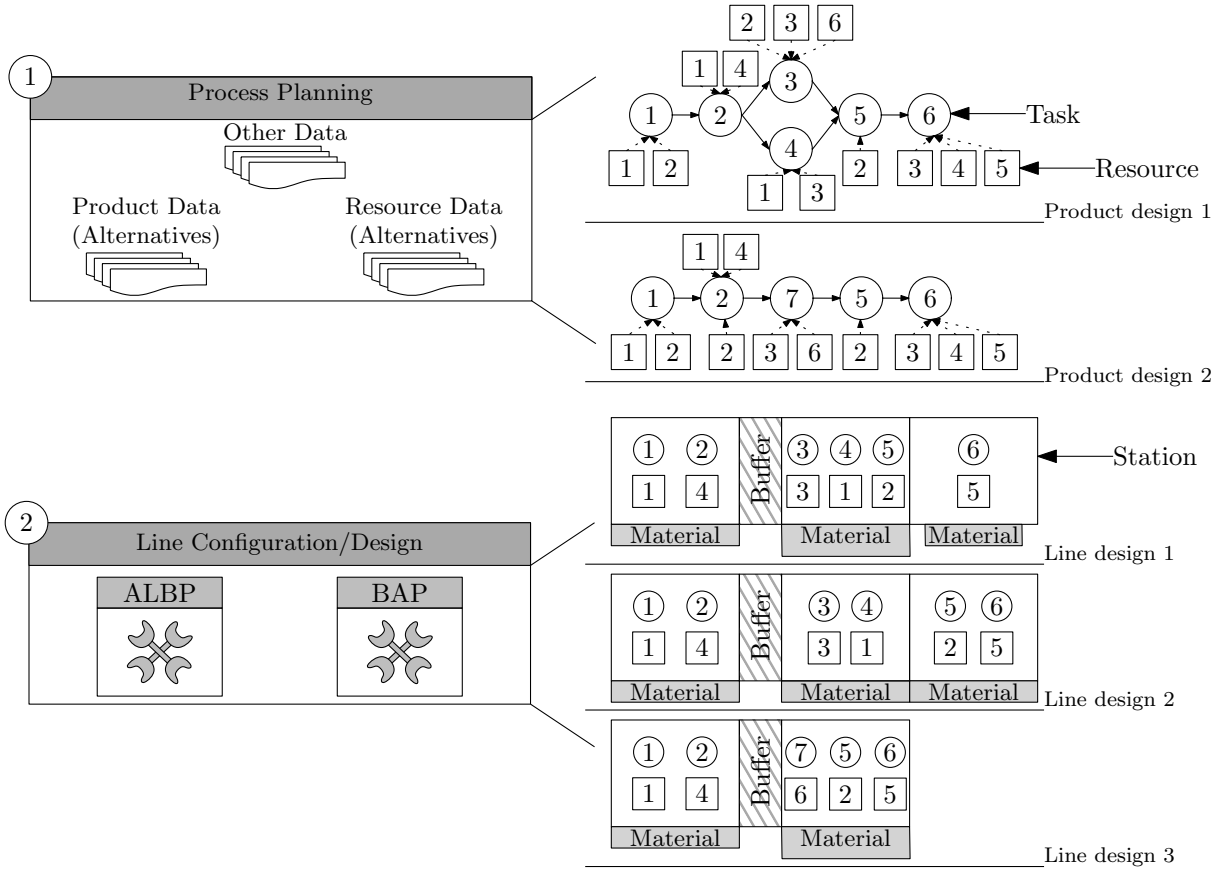

Figure 2.9: Schematical representation of the problem investigated in this thesis

Chapter 3

State-of-the-art

Abstract

The problem investigated in this thesis can be related to an optimisation problem. This chapter provides an introduction to multi-objective optimisation problems. This introduction offers insight into the two main classes of resolution methods and the various quality indicators used to compare them. Second, a detailed overview of models and methods for solving the assembly line balancing problem and buffer allocation problem is provided with the objective of identifying drawbacks of both models and methods that are addressed in the next chapters.

3.1 Introduction

Optimisation problems arise in almost all branches of industry, including product and process design, production, logistics, traffic control, and strategic planning [198]. These optimisation problems can be either mono-objective or multi-objective, depending on the number of objective functions taken into consideration. However, most real-life decision and planning situations involve multiple conflicting criteria that should be considered simultaneously. For these problems, no unique solution exists, but there is a set of mathematical equally good solutions [382, 459] that are optimal regarding some dominance rules. There has been a growing interest over the last years in multi-objective optimisation methods. By mid-2016, more than 21800 [1] publications had been published on multi-objective optimisation. The evolution of the number of papers related to Multi-Objective Problem (MOP) between 2000 and 2016 is shown in Figure 3.1.

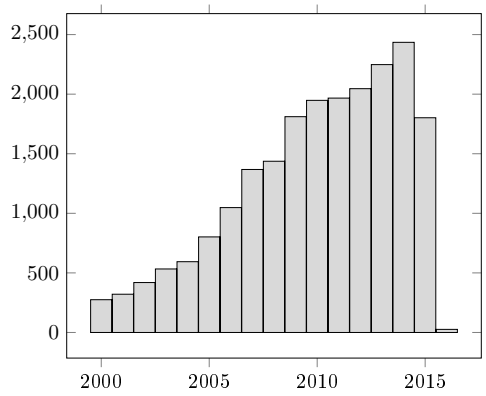

Figure 3.1: Evolution of the number of publications related to multi-objective optimisation between 2000 and 2016

The present chapter is organised as follows. First, an insight into optimisation problems and resolution methods is given. This is followed by an analysis of the literature on the assembly line balancing problem and the buffer allocation problem. Indeed, these two problems can be related to optimisation problems, making an introduction into optimisation problems and methods necessary.

1. The statistical data is based on the paper repository of Microsoft Academic, available at following address `http://academic.research.microsoft.com/` and by using following keywords: *multi-objective*, *MOEA*, *MOACO*, *DMOPSO*

3.2 Optimisation problem

In optimisation problems, the objective is to find the best solutions to mathematically defined problems, which are usually models of manufacturing and management systems [16]. This section first introduces the notations usually used to describe optimisation problems and present the best-known dominance relations used in multi-objective optimisation.

3.2.1 Introduction and notations

Without loss of generality, an optimisation problem involves a number of objective function(s) M, $(M \geq 1)$ which is/are to be minimised or maximised and may contain a number of constraints (J inequality constraints and K equality constraints) that any feasible solution must satisfy. Mathematically speaking, an optimisation problem has the following form:

$$\begin{array}{lll} \text{Min/Max} & f_m(x) & m = 1, ..., M \\ \text{s.t.} & g_j(x) \geq 0 & j = 1, ..., J \\ & h_k = 0 & k = 1, ..., K \\ & x_j^{(L)} \leq x_i \leq x^{(U)} & i = 1, ..., N \end{array} \tag{3.1}$$

A solution $x \in R^N$, called a decision vector, is a vector of n decision variables: $x = (x_1, ..., x_N)^T$. The sets of J and K constraints are called the inequality and equality constraints respectively. The last set of constraints is called variable bounds. These bounds restrict each decision variable x_i to take values within a lower and upper bound, respectively $x_j^{(L)}$ and $x^{(U)}$, $\forall i = 1, ..., n$. The solution satisfying the $J+K$ constraints and variable bounds constitutes a feasible solution. The set of all feasible solutions S is called the feasible region. S can be defined as follows:

$$S = \{x \in R^N : h(x) = 0, g(x) \geq 0, x_j^{(L)} \leq x \leq x^{(U)}\} \tag{3.2}$$

For each solution $x \in S$ in the solution space, there is a point $z \in R^M$, denoted objective vector, in the objective space $Z \subset R^M$, denoted by $z = (z_1, ..., z_M)^T = F(x) = (f_1, ..., f_M(x))^T$, that evaluates the quality of x. Z can be defined as:

$$Z = \{z \in R^N : z = F(x), x \in S\} \tag{3.3}$$

The mapping occurs between an M-dimensional solution vector and an N-dimensional objective vector. While in the case of a single-objective optimisation problem, $M = 1$, in the case of a multi-objective optimisation problem, $M \geq 2$.

3.2.2 Dominance relation

The objective functions of a MOP are generally in conflict, implying that by improving one objective, another objective will become worse. MOPs with such conflicting objectives will provide many optimal solutions instead of only one. The reason for the optimality of more than one solution is that no one can be considered better than any other with respect to all objectives [326]. An important concept of Multi-Objective Optimisation (MOO) is that of domination, a concept based on dominance rules, which provide conditions under which certain potential solutions can be ignored [21].

The most commonly accepted dominance rule is the Pareto dominance rule [234]. The Pareto concept has widely been used to establish superiority between solutions in MOP. Two types of solutions can be distinguished: weak Pareto optimum solutions and strict Pareto optimum solutions, also respectively defined as loose Pareto optimum solutions and strong Pareto optimum solutions. An example of this classification for a bi-objective minimisation problem is provided in Figure 3.2. In this figure, strict Pareto solutions are marked in white, while dominated and weak Pareto solutions are marked in grey and black, respectively.

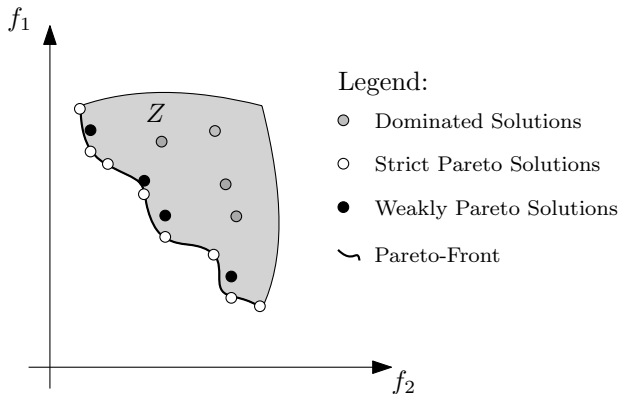

Figure 3.2: Example of the classification of Pareto solutions based on a bi-objective minimisation problem

Definition 3.1 Pareto Optimality [88]
A decision vector $x \in S$ is said to be Pareto optimal (also known as non-dominated) with respect to the feasible region S if and only if there is no decision vector $x' \in S$ for which $v = F(x') = (f_1(x'), ..., f_M(x'))$ dominates $u = F(x) = (f_1(x), ..., f_M(x))$.

Definition 3.2 Pareto Dominance [88]
A vector $u = (u_1, ..., u_M)$ is said to dominate another vector $v = (v_1, ..., v_M)$, denoted as $u \preceq_P v$, if and only if u is partial to v, in other words if $u_i \leq v_i \wedge \exists i \in \{1, ..., M\} : u_i < v_i$.

Definition 3.3 Weak Pareto Optimality [88]

A decision vector $x^* \in S$ is said to be weak Pareto optimal (denoted $x^* \preceq_P x$) if there is no decision vector $x \in S$, such that $f_i(x) < f_i(x^*), \quad \forall i = 1, ..., M$.

Definition 3.4 Strict Pareto Optimality [88]
A decision vector $x^* \in S$ is said to be strict Pareto optimal (denoted $x^* \prec_P x$) if there is no decision vector $x \in S$, such that $f_i(x) \leq f_i(x^*), \quad \forall i = 1, ..., M$.

The purpose of a MOP is to obtain solutions on or near the Pareto optimal front. The Pareto optimal front represents the image in the objective space of the set of strict Pareto optimal solutions.

Definition 3.5 Pareto Optimal Set [88]
The Pareto optimal set, P^*, is the set of all Pareto optimal solutions and is defined as:

$$P^* := \{x \in S | \nexists x' \in S : F(x') \preceq_P F(x)\} \tag{3.4}$$

Definition 3.6 Pareto Optimal Front [88]
The Pareto optimal front, PF^*, is the set of all objective vectors corresponding to all decision vectors in P'

$$PF^* := \{u = F(x) | x \in P^*\} \tag{3.5}$$

Several additional points, especially the ideal and nadir points, provide useful information when solving a MOP. Indeed, for a decision maker facing a multi-optimisation problem, both values show the possible range of the objective values over the Pareto set. Furthermore, they are often used by different algorithms as exact upper and lower bounds for the set of efficient solutions.

Definition 3.7 Ideal Point
The ideal point (denoted p^I) is the vector composed of the best objective values over the search space. Analytically, $p_j^I = \min_{x \in S} f_j(x)$, $j = 1, ..., M$.

Definition 3.8 Max point
The max point (denoted p^I) is the vector composed with the worst objective values over the search space. Analytically, $p_j^M = \max_{x \in S} f_j(x)$, $j = 1, ..., M$.

Definition 3.9 Nadir point
The nadir point (denoted p^N) is the vector composed with the worst objective values over the Pareto set. Analytically, $p_j^N = \max_{x \in P^*} f_j(x)$, $j = 1, ..., M$.

These three points are graphically represented for a minimisation problem with two objective functions in Figure 3.3

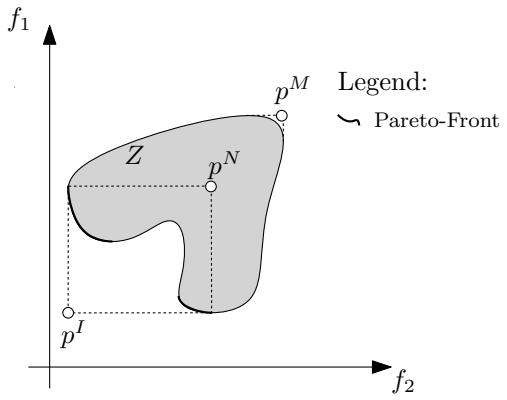

Figure 3.3: Ideal, max, and nadir points in a multi-objective space

3.2.2.1 Other types of dominance rules

Several other forms of dominance have been proposed recently. Relaxing the conventional Pareto dominance can improve the performance of MOO algorithms and reduce the set of optimal solutions. Indeed, for some problems, the set of optimal solutions can be large, such that the decision maker cannot evaluate all the optimal solutions. This is often the case for many NP-hard multi-objective combinatorial optimisation problems. Some of these relaxed forms of Pareto dominance are more effective at finding solutions in the extremes of the feasible region S and in tackling optimisation problems with irregular Pareto optimal fronts or problems for which it is difficult to generate feasible solutions [234]. Indeed, a Pareto front may, as shown in Figure 3.4, be divided into three regions. Regions 2 and 3 represent extremes of the Pareto front. These regions can be reached by minimising or maximising each objective function separately. Region 1, which represents the middle part of the Pareto front is more likely to be of interest to the decision maker. In general, relaxed forms of Pareto dominance allow a solution $x \in S$ to dominate another solution $x^* \in S$ for which x does not Pareto-dominate x^*. Relaxed forms of Pareto dominance include: ε-dominance [230], extended Pareto dominance [184], Lorenz-dominance which is also called equitable dominance relationship [222], and volume dominance [234, 233].

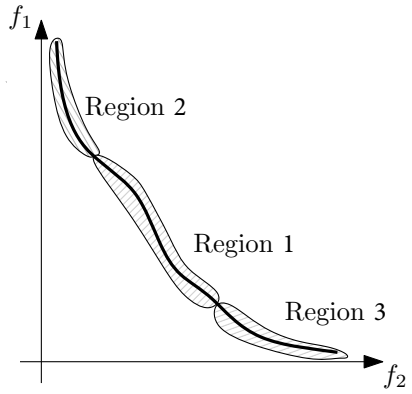

Figure 3.4: Classification of the Pareto front into three regions

The Lorenz dominance concept and rules are defined as follows:

Definition 3.10 Lorenz Optimality [122, 245, 269]
A decision vector $x \in S$ is said to be Lorenz optimal with respect to the feasible region S if and only if there is no decision vector $x' \in S$ for which $v = F(x') = (f_1(x'), ..., f_M(x'))$ dominates $u = F(x) = (f_1(x), ..., f_M(x))$.

Definition 3.11 Lorenz Dominance [122, 245, 269]
A vector $u = (u_1, ..., u_M)$ is said to dominate another vector $v = (v_1, ..., v_M)$, denoted as $u \preceq_L v$, if and only if the generalised Lorenz-vector of u, $L(u)$, Pareto dominates the generalised Lorenz vector of v, $L(v)$, in other words if $L(u) \preceq_P L(v)$.

The generalised Lorenz-vector of solution x, for a bi-objective function, $L(x)$ is given by:

$$L(x) = (max(f_1(x), f_2(x), f_1(x) + f_2(x)). \tag{3.6}$$

Definition 3.12 Lorenz Optimal Set [88]
The Lorenz optimal set, P_L^*, is the set of all Lorenz optimal solutions and is defined as:

$$P_L^* := \{x \in S | \nexists x^{'} \in S : F(x^{'}) \preceq_L F(x)\}. \tag{3.7}$$

Definition 3.13 Lorenz Optimal Front [88]
The Lorenz optimal front, PF_L^*, is the set of all objective vectors corresponding to all decision vectors in P'

$$PF_L^* := \{u = F(x) | x \in P_L^*\}. \tag{3.8}$$

The Controlling Dominance Area of Solutions (CDAS) [355] also relaxes the concept of Pareto dominance by controlling dominance areas of solutions using a user-defined parameter S to induce appropriate selection pressure in MOEA. However, to obtain a desirable search performance, S must be experimentally identified. Sato *et al.* [356] propose the

Self-Controlling Dominance Area of Solutions (S-CDAS), which reclassifies solutions in each front F_j to realise a fine-grained ranking that is different from CDAS. The S-CADS works as follows:

Step 1: Considering a set of solutions $X = \{X_1, ..., X_k\}$ of F_j, an origin point O is defined as follows:

$$O = \{O_1, ..., O_M\} = \{f_1^{max} + \delta, ..., f_M^{max} + \delta\} \tag{3.9}$$

where f_i^{max} is the maximum value of the i-th objective function in the set X and δ is a tiny constant. Also P_i Points, representing respectively the optimum solution of objective function i, $\forall i = 1, ..., M$, are defined as follows:

$$P_i = \{O_1, ..., f_i^{min} + \delta, O_{i+1}, ..., O_M\} \tag{3.10}$$

Step 2: For each point $X_j, \forall j = 1, ..., k$, the following steps are repeated:

(a) Based on sine theorem, the angles $\varphi_i(X_j)$, $\forall i = 1, ..., m$, and are calculated as follows:

$$\varphi_i(X_j))sin^{-1}\{\frac{r(X_j) \cdot sin(\omega_i(X_j))}{l_i(X_j)}\} \tag{3.11}$$

where $r(X_j)$ is the Euclidean distance between X_j and O, and $l_i(X_j)$ is the Euclidean distance between X_j and P_i,

(b) The fitness values of all other solutions $Y \in X$ are modified by following equation:

$$f_i'(Y)) = \{\frac{r(Y) \cdot sin(\omega_i(Y) + \varphi_i(X_j))}{sin(\varphi(X_j))}\} \tag{3.12}$$

(c) The Pareto-dominance is used to re-rank the solutions Y if they are dominated by any solution $X_j \in X$

3.2.2.2 Synthesis

The following properties are common to all dominance relations:

— *Symmetric*: the dominance relationship is not symmetric, because $u \preceq u'$ does not imply $u' \preceq u$.

— *Antisymmetric*: since the dominance relationship is not symmetric, it cannot be asymmetric.

— *Transitive*: the dominance relationship is transitive, because if $u' \preceq u'', u'' \preceq u'''$, it implies that $u' \preceq u'''$.

— *Reflexive*: the dominance relationship is not reflexive, since $u' \npreceq u'$.

For some problems the Pareto dominance rules seeks to its limits and other dominance rules,

e.g. Lorenz, S-CDAS, are more powerful [270]. As shown in Figure 3.5, the main difference between all of them is the guidance of the search agents toward different regions of the Pareto front.

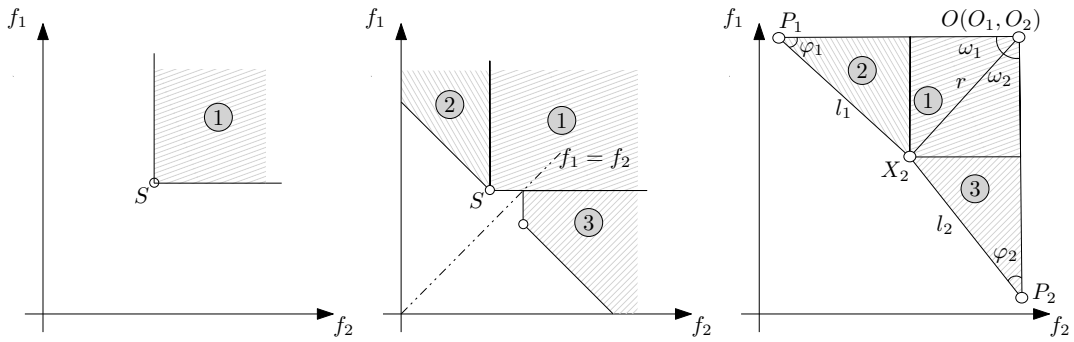

(a) Pareto Dominance *(b)* Lorenz Dominance *(c)* S-CDAS Dominance

Figure 3.5: Comparison of the Pareto, Lorenz, and S-CDAS dominance rules

3.3 Resolution methods

The optimisation methods for MOP can be classified into two main categories: exact methods and approximate methods. Since the Pareto curves cannot be computed efficiently in most cases - even if it is theoretically possible to find all these points exactly - and because most of the optimisation problems belong to the NP problem class, approximation methods are often used.

Definition 3.14 P **Problem [377]**
An optimisation problem belongs to P problems if there exists an algorithm that can solve the problem in polynomial time.

Definition 3.15 NP **Problem [377]**
An optimisation problem belongs to NP problems only if there is an algorithm that can solve the problem in non-deterministic polynomial-time.

The next sections provide an overview of both classes of optimisation methods.

3.3.1 Exact methods

A large number of exact methods for solving MOP essentially attempts to scalarise multiple objectives and perform repeated applications to find a set of Pareto-optimal solutions. Here, methods such as the weighted-sum method or scalarisation method [433], ϵ-constraints method [167], and goal programming [70] can be found. Ehrgott *et al.* [125] and Eichfelder

[126, 127] provide a review of some of these methods. Some of these techniques may be sensitive to the shape of the Pareto-optimal front. As the solution mainly depends on parameters such as weights and upper/lower bounds, these methods also require certain knowledge to find Pareto-optimal solutions. These methods are attractive popular because a wide range of well-studied algorithms for single optimisation problems can be used. The main criticism of most of these methods is that, although they may converge to one Pareto-optimal solution, they must be applied many times to obtain more than one optimal solution. This implies a systematic variation of weight vectors or ϵ parameters that does not guarantee diversity in the set of solutions and is thus an inefficient search. In this iterative process, the systematic variation of parameters may also lead to an important CPU time. Moreover, some of these techniques may be sensitive to the shape of the Pareto-optimal front. Indeed, non-convex parts of the Pareto set cannot be reached by optimising convex combinations of the objective functions [67]. Thus, most of these methods are not capable of finding non-supported solutions. Furthermore, as the solutions mainly depend on parameters such as weights and upper or lower bounds, these methods also required certain knowledge to find Pareto-optimal solutions.

3.3.1.1 Two-Phase Method

The Two-Phase Method (TPM), which was proposed by Ulungu and Teghem [396], proceeds in two phases and proposes a general scheme that can be adapted to any specific problem. The first phase consists of finding all supported solutions using a scalarisation method, which enables the transformation of a bi-objective problem into a single objective problem. The TPM starts by determining the extreme points of the Pareto front. Then, supported solutions are found by recursively searching between two already identified supported solutions z^r and z^s according to a direction λ perpendicular to the line (z^r, z^s), with $z_1^s < z_1^r$ and $z_2^s > z_2^r$ (see Figure 3.6 a)). $\lambda = (\lambda_1, \lambda_2)$ defines the normal to the line segment connecting z^r and z^s. λ_1 and λ_2 are defined as follows: $\lambda_1 = z_2^s - z_2^r$, and $\lambda_2 = z_1^r - z_1^s$. Each supported solution generates two searches, as shown in Figure 3.6 b. Once all supported solutions have been found, the second phase, which aims at finding any other efficient solutions, begins. It has been shown that this search can be reduced to the exploration of all the triangles underlying each pair of adjacent supported solutions. Each triangle is defined by z^r, z^s, and $z^N = [z_1^r, z_2^s]$. Figure 3.6 c) and d) show all supported and non-supported solutions.

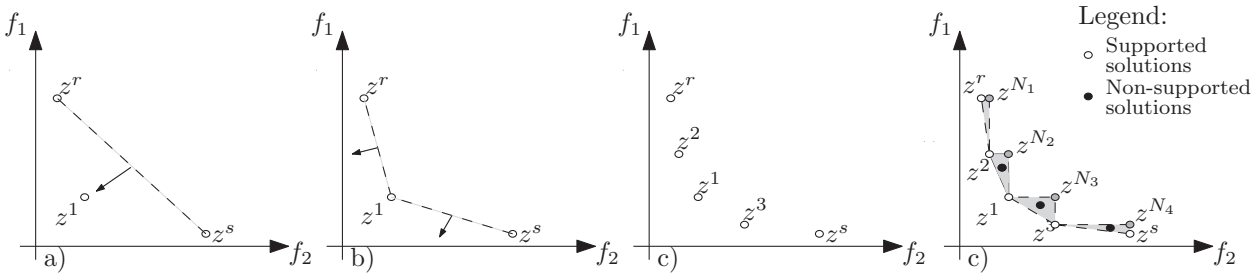

Figure 3.6: Illustration of the various steps involved in the Two-Phase Method

The advantage of the TPM is that all non-dominated solutions are found without exploring the entire search space. However, the efficiency of the TPM is based on the size of the generated triangles, which depends on the number of supported solutions in the Pareto set and on their distribution along the front. The TPM has been applied efficiently to bi-objective assignment problems (e.g. Moghaddam *et al.* [269] solved the single machine scheduling problem with rejection).

3.3.1.2 Parallel Partitioning Method

Other methods, such as the Parallel Partitioning Method (PPM) [237], can find the true Pareto front. The PPM can determine the efficient set of solutions in three stages. In the first stage, the ideal and nadir points are computed to limit the search space. In the second stage, the extremes found in the first search are used to equally split, according to one specific objective, the search space. During this stage, supported and non-supported solutions can be found. The third stage, which is similar to the second phase of TPM, consists of finding all remaining Pareto solutions.

3.3.2 Approximate methods

A plethora of methods exists for solving MOP. Several surveys of multi-objective approximate methods have been proposed in the literature (e.g. [87, 89, 375, 91, 235, 380, 447]). These methods can be categorised as follows: (i) classical methods which use direct or gradient-based methods following some mathematical principles and (ii) non-traditional and population-based methods following some natural or physical principles. Figure 3.7 shows a classification of multi-objective approaches.

Classical methods, also known as aggregating approaches, mostly attempt to scalarise multiple objectives and perform repeated applications to find a set of Pareto-optimal solutions.

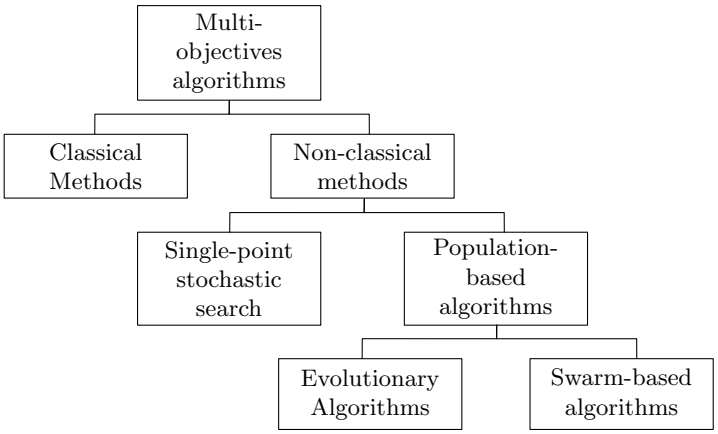

Figure 3.7: Classification of multi-objectives approaches

Several methods are identified, including the weighted sum approach, goal programming-based approach, goal attainment-based approach, and ϵ-constraint approach. In the weighted sum approach, the different objectives are combined using weights and merged to obtain one single function. In goal programming-based approaches, a target vector is defined for each objective and the deviation from the targets to the objectives is minimised. In the goal attainment-based approach, apart from the target vector, a weight vector representing the relative under- or over-attainment of the desired goals, is used. In the ϵ-constraint, one of the objectives is transformed into a constraint and the Pareto front is determined by systematically decreasing the parameter ϵ. First, one extreme with the best value for the objective f_1 is computed. This solution determines a bound on the other objective f_2 and the best solution regarding f_1 must be searched for below this bound. These methods are attractive and popular because a wide range of well-studied algorithms for single optimisation problems can be used. The main criticism of most of these methods is that, although they may converge to one Pareto-optimal solution, these methods must be applied many times to obtain more than one optimal solution. This implies a systematic variation of weight vectors or ϵ parameters that does not guarantee diversity in the set of solutions. Thus, it is an inefficient search. In this iterative process, the systematic variation of parameters may also lead to an important CPU time. Moreover, some of these techniques may be sensitive to the shape of the Pareto-optimal front. Indeed, non-convex parts of the Pareto set cannot be reached by optimising convex combinations of the objective functions [67]. Thus, most of these methods are not capable of finding non-supported solutions. Furthermore, as the solutions mainly depend on parameters, such as weights and upper/lower bounds, these methods also required certain knowledge to find Pareto-optimal solutions.

To solve MOP, numerous nature-inspired algorithms have been proposed to locate their Pareto fronts. These algorithms can be classified into two main categories: evolutionary

algorithms and swarm intelligence based algorithms. The vast majority of algorithms have been suggested depending on different intelligent behaviours of a swarm or by mimicking the behaviours of biological systems in nature [351]. The first category can be subdivided into: (i) genetic algorithm, (ii) evolutionary strategy, (iii) evolutionary programming, (iv) genetic programming, and (v) differential evolution. The second category can be divided into: (i) ant colony optimisation, (ii) particle swarm optimisation, (iii) bee colony optimisation-based algorithms, (iv) bat algorithms, and (v) cuckoo search algorithms (refer to Appendix B.1 for more information about resolution methods in multi-objective optimisation problems).

3.4 Comparison of resolution methods

During optimisation, algorithms must overcome many difficulties, such as infeasible regions, local optimal solutions, flat regions of objective functions, and isolation of optimums to converge to the global optimal solution(s). Moreover, since most of the real-life optimisation problems are NP-hard and due to practical limitations, an optimisation task must also be completed in a reasonable computation time [104]. Therefore, the quality of an algorithm not only depends on its effectiveness, defined as its spread, distribution, and convergence of obtained solutions [252], but also by its computation effort to obtain these solutions (i.e. CPU time, the number of evaluations/iterations, and use of spatial and temporal resources). The concepts of spread, distribution, and convergence are shown in Figure 3.8. While the upper left figure represents an ideal distribution of the Pareto solution with a poor spread, the upper right figure accounts for an ideal spread with a poor distribution. The figure in the bottom left corner represents poor convergence. Ideally, the Pareto solution should have a good spread, distribution, and convergence, as shown in the bottom right.

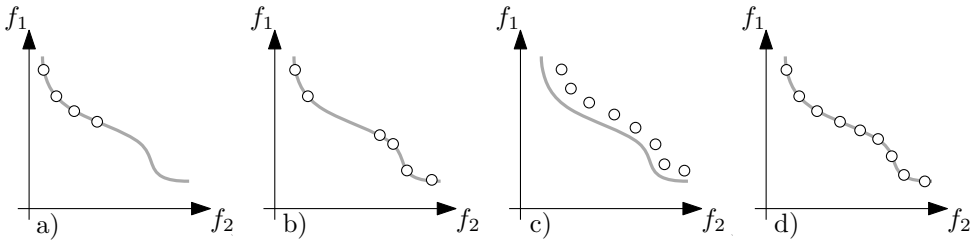

Figure 3.8: Concepts of spread, distribution, and convergence

To assess the performance of an algorithm and the quality of its approximation of the Pareto front, many quality indicators or metrics have been developed over the past two decades [45]. These metrics permit the comparison of algorithms and improve their performance [104].

A major focus has been on developing different metrics that can be classified as follows [191, 297]:

— Metrics evaluating capacity and cardinality of the approximate Pareto fronts
— Metrics evaluating the convergence of the approximate Pareto front to the true one
— Metrics evaluating the spread of solutions of the approximate Pareto front
— Metrics evaluating the convergence and diversity of solutions of the approximate Pareto front

3.4.1 Comparison indicators and metrics

To prevent possible inconsistencies and confusion when identifying or using dominance concepts, Van Veldhuizen [398] developed the following terminology. $P_{current}(t)$ represents the set of non-dominated solutions found by an optimisation algorithm at a given generation t. Since many population-based algorithms use a secondary population, referred to as an archive of non-dominated solutions, $P_{known}(t)$ is used to represent the set of optimal solutions currently known at generation t. In comparison, P_{known} represents the set of non-dominated solutions delivered by the optimisation algorithm. The true Pareto solution set, P^* is defined as P_{true}. Thus, when using an approximate method, the implicit assumption is that one of the following holds: $PF_{known} = PF_{true}$ or $PF_{known} \subset PF_{true}$. However, the true Pareto front is not always known. In this case, PF_{ref} is used to represent a known set of dominated solutions to which any approximate method should converge.

3.4.1.1 Capacity and cardinality metrics

The capacity and cardinality metrics quantify the number or ratio of dominated solutions PF_{known} obtained during the evolution process or after optimisation against either the true Pareto front PF_{true} or a reference set PF_{ref} [2], represented here by the set R. Among these metrics are the Overall Non-dominated Vector Generation (OVNG) [402], the Overall Generational Non-dominated Vector Generation Ratio (ONVGR) [402], the Error Ratio (ER) [398], the Non-dominated Points by Reference Set [457], and the C-metric [456, 457]. The ONVG metric provides the number of non-dominated solutions in PF_{known}. The ER metric gives the ratio of the number of solutions in PF_{true} or PF_{ref} that were not found by an optimiser. In comparison, ONVGR supplies the ratio of the number of optimal solutions that are present in PF_{true} or PF_{ref}. In order to compare the number of solutions of PF_{known} that are dominated by R, the Non-dominated Points by Reference Set, $C2_R$, which is formulated

2. It should be noted that the metrics may be sensitive to the choice of the reference set [271]

as follows, can be used:

$$C2_R(PF_{known}, R) = \frac{|x \in PF_{known}; \nexists y \in R : y \prec x|}{R|} \tag{3.13}$$

In reference to $C2_R$, the coverage metric, C, concentrates on the overlaps between two sets of optimal solutions. If $C(PF_{known1}, PF_{known2}) = 1$, then PF_{known1} dominates all solutions of S_2 and if $C(PF_{known1}, PF_{known2}) = 0$, none of the solutions from S_2 are dominated by S_1.

$$\mathrm{C}(PF_{known1}, PF_{known2}) = \frac{|x \in PF_{known2}; \exists y \in PF_{known1} : y \prec x|}{|PF_{known2}|} \tag{3.14}$$

As depicted by Okabe *et al.* [297], the metrics of this category provide no information about the accuracy and distribution of the solutions.

3.4.1.2 Convergence metrics

The metrics of this category measure the degree of proximity based on the distance between the solutions in PF_{known} and R. Among these metrics, the Generational Distance (GD) [400, 399], measures the Euclidean distance of points in S and to those in R.

$$GD(S, R) = \frac{\sum_{x \in PF_{known}} d(x, R)}{|PF_{known}|} \tag{3.15}$$

where $d(x, R)$ is the closest Euclidean distance from point x to a point in R. Zitzler *et al.* [458] proposed the commonly used ϵ-indicator, which measures the smallest distance necessary to translate every solution of the S, such that it dominates that of R. I_ϵ is calculated as follows:

$$I_\epsilon = max_{z \in PF_{known}} min_{y \in PF_{true}} max_{1 \leq i \leq n} \frac{y_i}{z_i} \tag{3.16}$$

3.4.1.3 Diversity metrics

Metrics belonging to this category indicate the distribution and spread of solutions in PF_{known}. Different distributions are identified: (i) distribution metrics, (ii) spread metrics, and (iii) distribution and spread metrics. In the distribution metrics category, Deb *et al.* [105] proposed a metric Δ' that compares all the solutions' consecutive distances with the average distance between the point in PF_{known}. Similar metrics have been proposed by Zitzler *et al.* [453]. The M_3^* uses the maximum distance instead of the average distance. The spread metrics quantify how much of the extreme regions are covered by PF_{known}. The Overall Pareto Spread (OS) quantifies how widely PF_{known} spreads over the objective space when the design objective functions are considered together. The distribution and spread

metrics consider the distribution and spread of optimal solutions set simultaneously.

3.4.1.4 Convergence and diversity metrics

In this category, the metrics measure the quality of a set of optimal solutions PF_{known} in terms of convergence and diversity on a single scale. Zitzler and Thiele [456, 457] proposed the Hypervolume (HV) metric, also known as the S metric [452], or the Lebesque measure [231, 139]. The HV metric is one of the most frequently applied measures for comparing the results of multi-objective approximate methods [54]. This metric is generally favoured since it captures in a single scalar both the closeness of the solutions of PF_{known} to R, and to some extent, the spread of the solutions across the objective space. HV considers the volume of the objective space covered or dominated by PF_{known}. Mathematically, for each solution $x \in PF_{known}$ a hypercube v_x is constructed with a reference point W. Figure 3.9 shows an example of the hypervolume measure.

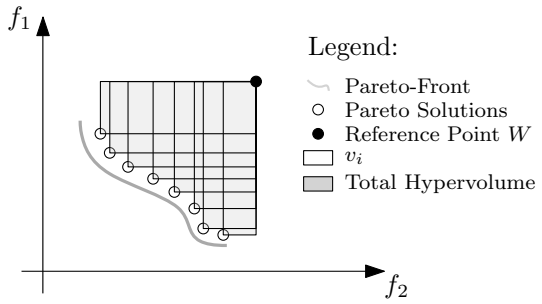

Figure 3.9: Example of the calculation of the Hypervolume measure

The Inverted Generational Distance (IGD, [458]) is an improved version of the GD metric and takes both diversity and convergence information into consideration. In opposition to GD, IGD calculates the closest average distance of solutions to R.

$$IGD(PF_{known}, R) = \frac{\sum_{x \in R} d(x, PF_{known})}{|R|} \tag{3.17}$$

3.4.1.5 Conclusion

Jiang *et al.* [191] highlighted and analysed the inadequacies of MOO metrics. While capacity metrics focus on the number of solutions in the set PF_{known}, they are not designed to provide convergence and diversity information. Taking the convergence metrics into consideration, two critical issues were identified by Okabe *et al.* [297]. First, most of them require PF_{true} to be known. In practice, it is almost impossible to know the true PF, since most of the problems are NP-hard. Second, convergence metrics often omit the diversity of PF_{known}.

Jiang *et al.* show that on convex PFs, two metrics, I_ϵ and IGD, show high consistency to the HV metric, meaning that these metrics can jointly be used to assess solution sets optimality on the convex PFs. On concave PFs, only I_ϵ is consistent with HV.

3.4.2 Attainment-function

While in the literature, many attempts have been made to describe the quality of a set of non-dominated solutions PF_{known} through the use of summary measures or quality indicators, the stochastic nature of such outcomes is usually averaged over several optimisation runs. The attainment approach is formulated on a functional basis and it recognises the set distribution of optimiser outcomes as a whole [141]. For visualisation purposes, the boundaries of regions of the objective space attained by a given percentage of the optimisation runs can also provide insight into the optimiser performance [219, 251]. When comparing two algorithms, it is possible to use the attainment function surfaces. In the next figure, the union of the output sets obtained by several runs of two algorithms are computed first. Then, for each point in the objective space where the value changes, the number of runs obtaining this point is counted. This computes the value of the attainment function of the first algorithm at that point minus the value of the attainment function of the second algorithm. The positive and negative difference at the points previously examined, encoding the magnitude of the differences using shades of grey, are plotted. The darker a point is, the larger the difference between these two algorithms. Figure 3.10 shows an example of the Empirical Attainment Function (EAF) obtained for two algorithms. The lower line on both plots connects the best set of points obtained over all runs of both algorithms. The dashed line corresponds with the median attainment surface of each algorithm. The bottom side-by-side plots show the location of the differences between EAFs of the two algorithms. On the left, points denote positive differences between the EAF of algorithm 1 over that of algorithm 2. In comparison, the right figure shows the difference in favour of Algorithm 2 over Algorithm 1. Only differences larger than 20 % are shown. These plots illustrate that algorithm 2 performs better at extremes of the nondominated sets, whereas there is a small difference in favour of Algorithm 1 at the centre of the nondominated sets. Such a fine-grained analysis would be impossible with most scalar quality indicators. The examination of the EAF differences reveals the magnitude of the differences between algorithms and where these differences are located in the objective space. Therefore, it is particularly helpful to identify problems with attaining certain regions of the objective space.

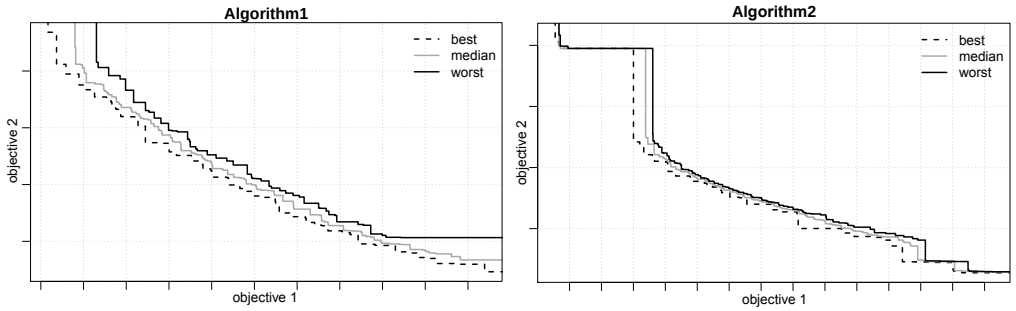

(a) Union of the output sets obtained by several runs of Algorithm 1

(b) Union of the output sets obtained by several runs of Algorithm 2

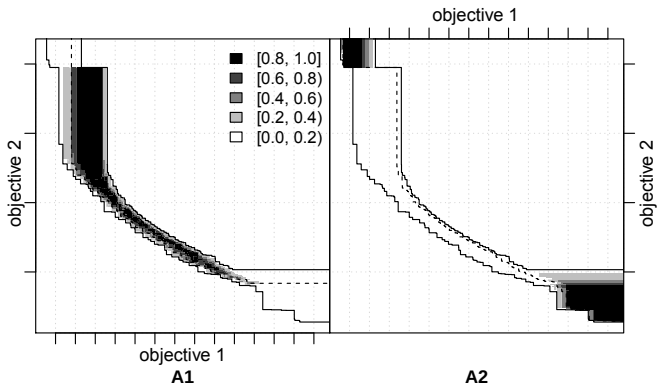

(c) Comparaison of Algorithm 1 and Algorithm 2

Figure 3.10: Comparison of the performances of two algorithms based on the attainment function

3.5 Assembly Line Balancing Problem

This section describes the classical line balancing problems and presents a classification scheme that has been proposed for problem identification. With the help of this classification, an overview of the problems and solution procedures is presented. Finally, some optimisation problems considering alternative configurations of assembly lines through either products or processes alternatives are presented to outline the problem under study in this thesis and identify the gaps between what has been proposed by academia and what is required by the industry.

3.5.1 Introduction and notations

The problem of assigning tasks to stations of an assembly line by optimising one or more specific objectives (e.g. minimising the number of stations for a given cycle time or minimising the cycle time for a given number of stations) under consideration of precedence constraints and possible further restrictions, is known as the ALBP.

The following sets are useful to describe the precedence relations:

$$\begin{aligned} P_i &:= \{h|(h,i) \in E\} && \text{Set of direct predecessors of task } i \in V \\ F_i &:= \{j|(i,j) \in E\} && \text{Set of direct successors of task } i \in V \\ P_i^* &:= \{h|(h,i) \in E\} && \text{Set of all predecessors of task } i \in V \\ F_i^* &:= \{j|(i,j) \in E\} && \text{Set of all successors of task } i \in V \end{aligned} \tag{3.18}$$

The general objective associated with any ALBP is to minimise the sum of the idle time at each station m, I_m, which is represented as the difference between the given cycle time CT and the station time $t(S_m)$ and can be expressed as: $I_m = CT - t(S_m)$, where S_m represents the station load of a station m and the cumulated task time $t(S_m) = \sum_{j \in S_m} t_j$ is called the station time. Since the tasks are indivisible work elements, the task processing times of a given task j, t_j, cannot be greater than CT, and CT is always greater than the greatest station workload time $CT \geq \max_{m=1,\ldots,M} t(S_m)$. Thus, the cycle time is bounded by following relation:

$$\max_{j=1,\ldots,N} t_j \leq \max_{m=1,\ldots,M} t(S_m) \leq CT \leq \sum_{j=1,\ldots,N} t_j \tag{3.19}$$

These notations are illustrated in Figure 3.11. In this figure, the gray area represents the idle time for each station. The darker line represents the cycle time and the white squares represent the processing time of the various tasks assigned to the different stations.

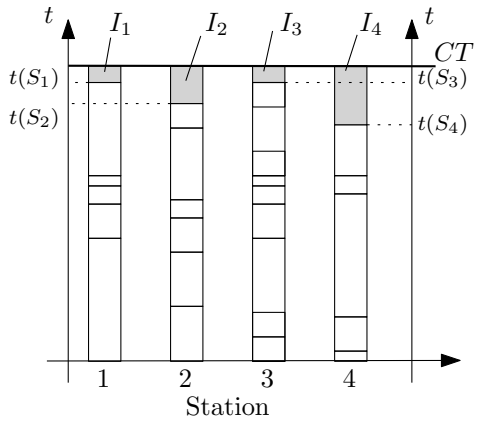

Figure 3.11: Visualisation of the notation for the ALBPs

The LE metric shows the percentage utilisation of the line and is expressed as follows:

$$LE = \frac{\sum_{m=1,\ldots,M} t(S_m)}{M \cdot C}. \tag{3.20}$$

The SI metric describes the relative smoothness for a given assembly line balance and an index of 0 indicates a perfect balance. Several SI metrics have been proposed in the literature.

The most common representation of the SI metric is:

$$SI = \sqrt{\sum_{m=1}^{M} (\max_{m=1,\ldots,M} t(S_m) - t(S_m))^2} \tag{3.21}$$

The LT metric describes the period of time required to produce a specific product on the assembly line and is calculated as follows:

$$LT = CT \cdot (M-1) + t(S_M) \tag{3.22}$$

The balance delay, which is represented by the sum of all idle times, can be computed as:

$$BD = M \cdot CT \sum_{m=1}^{M} t(S_m) \tag{3.23}$$

In the case of a mixed-model line and to eliminate operating inefficiencies such as work, overload, or idle time, the station times according to different models must be smoothed [257]. The horizontal smoothness index, with the objective of balancing workload for different models in each station, can be calculated as follows:

$$HSI = \sum_{p=1}^{P} \sum_{m=1}^{M} \Phi_p |t(S_{pm}) - C| \tag{3.24}$$

where $t(S_{pm})$ represents the total operation time of model p in station m and Φ_p is the overall proportion of units of model p, d_p being assembled and is given by:

$$\Phi_p = \frac{d_p}{\sum_{p=1}^{P}} \tag{3.25}$$

The vertical smoothness index, whose objective is to reduce the deviation of workload on a station from the average workload of all stations can be calculated using (3.21).

3.5.2 Classification of Assembly Line Balancing Problem

Since the first mathematical formalisation of ALBP by Salveson [353], ALBPs have been widely extended and studied, and different schemes and states-of-the-art have been proposed in the literature. The most well-known are those provided by Baybars [38], Gosh and Gagnon [154], Erel and Sarin [130], Becker and Scholl [41], Scholl and Becker [358], Boysen *et al.* [51], Saif *et al.* [350], Battaia and Dolgui [30], and Sivasankaran and Shahabudeen [370]. The high number of classification schemes and state-of-the-art can be explained by the different conditions in industrial manufacturing since assembly line systems and corresponding ALBPs are multifaceted [41]. Figure 3.12 [3] shows the evolution of the number of publications related

3. The statistical data is based on the paper repository of Microsoft Academic, available at following address `http://academic.research.microsoft.com/` and by using following keywords: *multiobjective*, *line*

to ALBPs between 2000 and 2016.

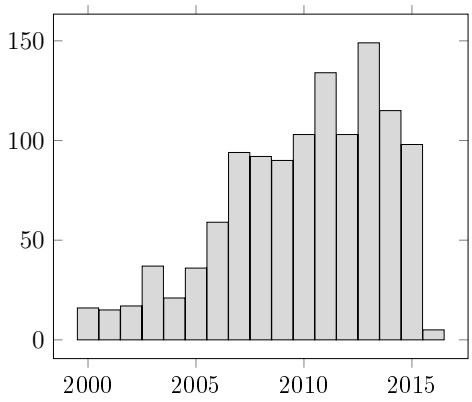

Figure 3.12: Evolution of the number of publications associated with ALBPs between 2000 and 2016

A well-known classification of ALBPs is proposed by Baybars [38], which distinguishes between two classic problems: Simple Assembly Line Balancing Problem (SALBP) and Generalised Assembly Line Balancing Problem (GALBP). In the former case, only a single product is processed and the problem is restricted by precedence relations and cycle time constraints. When other considerations are added to those of the SALBP family, the problems are known as GALBP. Gosh and Gognon [154] extended Baybars classification by considering the number of products being processed on the line and the variability of the task processing times. However, these classifications are too general and restricted to reflect the increasing variety of real-world balancing problems. Thus, more detailed classification schemes have been intended to ease communication between researchers and practitioners. Boysen *et al.* [51] used a triple-notation $[\alpha, \beta, \gamma]$ to classify ALBPs. In their classification, α represents the precedence graph characteristics, β represents the station and line characteristics, and γ represents the objectives. Battaia and Dolgui [30] provided a taxonomy based on the following points: (i) number of lines to be balanced, (ii) task attributes, (iii) workstation attributes, (iv) constraints to be respected by a feasible solution, and (v) criteria used to distinguish the best solutions. While the first elements have a significant impact on the number of decision variables, the last two elements principally designate the type of problem to be solved. Furthermore, the last point determines the nature of the optimisation problem, in other words, if it is a single-optimisation or multi-optimisation problem. Hazir *et al.* extended the classification of Boysen *et al.* by incorporating cost and profit aspects [174, 173].

The current section presents the various ALBPs that are found in the literature.

balancing, balancing problem

3.5.2.1 Simple Assembly Line Balancing Problem

The SALBP family presents four variants: (i) SALBP-1: which aims to minimise the number of stations M given a fixed value of the cycle time CT, (ii) SALBP-2: which aims to minimise the cycle time CT given a fixed number of stations M, (iii) SALBP-E: which aims to simultaneously minimise CT and M considering their relation with the total idle time or the inefficiency of the line, (iv) SALBP-F: whose aim is to determine the feasibility of the problem and find a solution given CT and M. Common to all four types of SALBP are the set of constraints and assumptions: (i) all tasks are processed in a predetermined mode (no processing alternatives), (ii) they all aim at balancing a paced line with a fixed common cycle, (iii) the line is considered serial with no parallel elements, (iv) the task processing times are deterministic, (v) all stations are equally equipped with respect to machines and workers [51].

There are several mathematical formulations for the SALBP such as White [409], Scholl [357], Pastor and Ferrer [316], and Ritt and Costa [340].

3.5.2.2 Generalised Assembly Line Balancing Problem

As stated earlier, the assumptions of SALBP are restrictive considering the nature of real-world assembly line systems. To better cope with the needs of the industry, researchers have focused on identifying and modelling more realistic situations in assembly lines, resulting in problems such as the Generalised Assembly Line Balancing Problem (GALBP). GALBPs take additional restrictions into consideration, including, parallel workstations, not equally equipped workstations, U-shaped assembly lines, two-sided assembly lines or problems involving sequence dependent or stochastic processing times and problems considering mixed models and multi-product lines.To highlight the increasing number of GALBPs and their variety, the tuple-notation of Boysen *et al.* [51] was used. Appendix B.2 shows the ALBPs under study over the last years. In their classification, α, which represents the precedence graph characteristics, is composed of six attributes, $\alpha_1, ..., \alpha_6$. According to the number of products or models to be balanced, α_1 can take the following values: (i) α_1=mix, (ii) α_1=mult, and (iii) α_1=° if a multi, mixed, or a single assembly line needs to be balanced, respectively. α_2 represents the structure of the precedence graph. If the precedence graph contains special structures, such as linear, diverging or converging graphs, α_2=spec; otherwise, α_2=°. The nature of the task processing times is represented by α_3, which can take three values, respectively, t^{sto}, t^{dy}, and ° for stochastic processing times, dynamic variations of processing times, or static and deterministic processing times. Indeed, production envir-

onments in the real world are subject to many sources of uncertainty and randomness, which may have a major impact on the efficiency of the line. When using stochastic processing times, the probability of time completion of all tasks is usually maximised [14]. This is especially useful in case of manual lines, in which the effectiveness of workers varies with work rate, skill level, and motivation, which in turn may affect the processing times [432]. Task processing times may follow a random distribution due to poorly maintained equipment or defects in raw materials. [368]. Stochastic processing times are usually generated using known distributions of probabilities with their parameters (e.g. [349, 384]). Other methods can be found in the taxonomy of Battaia and Dolgui [30]. Dynamic variations are often used for the formalisation of learning (e.g. [168, 387]) and deterioration effects of workers (e.g. [387]). α_4 represents the sequence-dependent task time, which can take three values depending on the influence of specific tasks on the processing time or setup time of any successor, $\alpha_4 = \Delta t^{dir}$, $\alpha_4 = \Delta t^{ind}$, $\alpha_4 = °$, respectively representing a direct influence from any assignment of a task to its successor, and indirect influence, or no influence. Examples of direct influence can be the processing time of a specific task assigned to a specific station that depends on the set of tasks already assigned, e.g. [381, 5, 428, 2, 3, 387]. α_5 represents assignment restrictions and can be classified as follows [362, 257]:

— Zoning restrictions - zoning restrictions can be negative or positive. In the former case, a set of tasks must be assigned to the same workstation (α_5=link), while in the latter case a set of tasks must be assigned to a different workstation (α_5=inc). These restrictions usually represent technological restrictions, such as a set of tasks requiring an expensive resource or a set of tasks requiring different equipment (e.g. [4, 5, 257, 2, 3, 332]).

— Distance restrictions - there are two types of distance restrictions: minimum and maximum distance between tasks. This distance can be measured in time, space, sequence, or workstation positions. An example of minimum distance is the case where colour has to dry before further tasks can be performed and an example of maximum distance is the case where melted metal must be prevented from cooling down before a specific task is performed [362]. Depending on the nature of this constraint, α_5=max if the distance has an upper bound and α_5=min if it has a lower bound [30].

— Resource restriction (α_5=cum) - the assignment of tasks to the station might be subject to the value of particular task attributes such as the size of equipment [331, 390], or the available area for materials and tools at workstations [77, 36, 83]. Otto and Scholl [300] and Bautista *et al.* [34, 35, 33] presented an extended version of the SALBP, in which the ergonomic risk associated with each workstation should not exceed a specific limit. Mutlu and Özgörmüş [277] consider the physical workload of operators. Furthermore,

Zah and Yu [434] consider walking time for each worker at each station.

— Station restriction - representing the need for assignment into specific workstations, a specific set of tasks, such as a task that needs to undergo position changes during the assembly [229], (α_5=type), or specific tasks must be performed on a specific side of the product [343]. In addition, some tasks have to be assigned to a specific type of workstation (α_5=fix), which can be seen as a fixed point for any further reconfiguration of the line (e.g. [215]). In other cases, stations might have conditions that prevent a task from being performed at this station (α_5=excl).

$\alpha_5 = \circ$ if no restrictions are considered. Processing alternatives are represented by α_6. If processing alternatives, either through resources or completely different tasks, are present, $\alpha_6 = pa$. Three cases are distinguished here. The processing alternative affects task specific attributes, such as processing times and operation costs, as well as precedence relationships between tasks, $\alpha_6 = pa$ (e.g. [331, 213, 47, 391, 273]). If processing alternatives alter the tasks, e.g. gluing instead of welding, $\alpha_6 = pa^{sg}$ (e.g. [66, 62, 64, 65, 360]). If neither of these two cases occur, $\alpha_6 = res$. If no processing alternatives are present, $\alpha_6 = \circ$.

β, which represents the stations and line characteristics, is composed of six attributes, $\beta_1, ..., \beta_6$. The first attribute, β_1 represents the flow of workpieces. To simplify the notations, β_1=$\circ$ will be used in case of a paced line, and $\beta_1 = unpac$ in case of a synchronous and asynchronous unpaced line. According to the line shape, β_2=$\circ$ means the stations are ordered in a straight line and u is ordered in a U-shaped line. While most of the studies aim at configuring a straight line, some also address the u-shaped line [206, 256, 330, 444, 415, 329, 347]. According to the layout of the line, $\beta_3 = pline$, when multiple lines need to be balanced (e.g. [332, 305]), $\beta_3 = pstat$ when stations are parallelised (e.g. [4, 256, 2, 3, 5]), $\beta_3 = ptask$ when tasks are parallelised and assigned to more than one station (e.g. [256, 221, 384]), and $\beta_3 = pwork$ when several workers are working on the same workpiece and do not obstruct each other (e.g. [344, 134, 306, 343]). According to the resource assignment, β_4 can take three values. Namely, $\beta_4 = equip$ if for each station one equipment must be chosen out of a set of equipment alternatives, and $\beta_4 = res$ when the tasks assigned to a station determine the set of resources which need to be allocated. β_5 represents the station-dependent time increments, and can take two values. $\beta_5 = \Delta t_{unp}$ when some part of the station time is consumed by unproductive activities, such as transportation of workpieces or walking time of workers in u-shaped lines (e.g. [329, 434]), otherwise $\beta_5 = \circ$. β_6 represents additional aspects such as $\beta_6 = buffer$ or $\beta_6 = mat$ if respective buffer sizing or material dimensioning and position are also part of the line balancing problem.

γ represents the objective functions, which have been used in ALBPs as shown in Table B.1.

In this table, the following abbreviations are used:

— Co: Optimisation of any cost elements
— m: Optimisation of the number of stations
— TP: Optimisation of the throughput of the line
— A: Optimisation of the total space area
— HSI: Optimisation of the horizontal smoothness index
— VSI: Optimisation of the vertical smoothness index
— BD: Optimisation of the balancing delay
— CT: Optimisation of the cycle time
— LE: Optimisation of the line efficiency
— ER: Optimisation of the ergonomic risks
— BS: Optimisation of the buffer size
— Pr: Optimisation of the probability that tasks can be accomplished before the cycle time
— FT: Optimisation of the flow time
— ARP: Optimisation of the accumulated risk of body postures
— WRI: Optimisation of the work related injuries
— W: Optimisation of the number of required workers
— ESI: Optimisation of the energy smoothness index
— $MMST$: Optimisation of the min-max station time
— $MMET$: Optimisation of the min-max station energy
— WIT: Optimisation of the weighted idle time
— WR: Optimisation of the work-relatedness
— S: Aggregation of the various optimisation functions

Figure 3.13 shows the frequency of the objective functions that were used. The optimisation of the number of stations remains the most used objective in the ALBPs field, followed by the cycle time. As demonstrated by the work of Hazir *et al.* [173, 174], the attention given to optimising cost elements in assembly line balancing has grown over the last years.

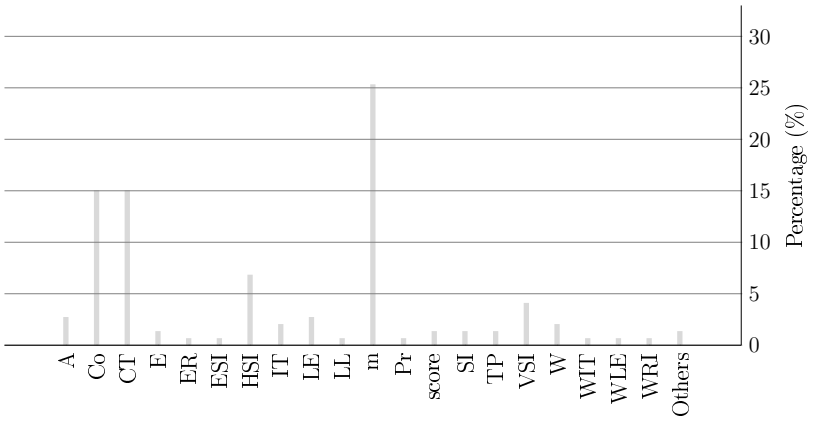

Figure 3.13: Frequency of used objective criteria in ALBPs

Table 3.1 shows a classification of the previously cited works regarding several cost components used in order to plan the most efficient production system. These cost components can be divided into short-term and long-term operating costs, considerinng operating costs, including wage, floor space, and capital investment costs. This table shows that existing studies treat the various costs elements heterogeneously. While some models only take station operating costs into consideration by implicitly considering resource costs, others only consider fixed costs associated with the various costs elements, denoted by (FC).

From Table B.1, the most frequent problems that have been addressed in the literature are identified and explained in the next paragraphs.

3.5.2.2.1 Mixed-model Assembly Line Balancing Problem

The Mixed-Model Assembly Line Balancing Problem, introduced by Thomopoulos [383], is abbreviated by some authors as Mixed-Model Assembly Line Balancing Problem (MALBP) (e.g. [416, 439], and [206]) is sometimes abbreviated by others as MMALBP (e.g. [4, 206]). The MALBP mirrors modern assembly line systems, for which the demand is much more variable among the models but the amount in demand of each model is relatively small. This condition can be seen in many car companies (e.g. BMW), TV companies (e.g. Samsung), laptop companies (e.g. Dell), and other industries [332].

Several adaptations of the classical mathematical model and resolution methods have been proposed in the literature. Among them are the consideration of sequence-dependent setup times with parallel workstations and zoning constraints [2, 3, 4] for a straight line, the consideration of task duplication costs in a U-shape line [206], and the consideration of different worker types with different costs and processing times [439]. Rabbani *et al.* [331] proposed a model for solving the robotic mixed-model assembly line balancing problem under

Table 3.1: Comparison of used cost components for evaluation equipment alternatives

	Investment costs		Operating costs		
Authors	R	S	R	T	W
Nicosia *et al.* [285]		(X)			
Bukchin and Tzur [57]	X				
Kazemi *et al.* [206]	X	X			
Rabbani *et al.* [331]	X		X		
Kim *et al.* [213]	X		(X)	(X)	(X)
Roshani *et al.* [343]		X			X
Yoosefelahi *et al.* [429]	X		X		
Hager *et al.* [390]			X		
Graves and Whitney [159]			X	X	
Pinto *et al.* [320]			X(FC)		X
Pinto *et al.* [321]			X(FC)		X
Graves and Lamar [160]			X(FC)	X(FC)	
Graves and Redfield [161]	X	X			
Rubinovitz *et al.* [346]		X		X	
Padron *et al.* [309]		X		X	
Ogan and Azizoglu [296]			X		
Zhang *et al.* [440]				X	
Kara *et al.* [201]		(X)		X	X
Bukchin and Rubinovitz [56]		X	(X)		
Levitin *et al.* [239]					
Khouja *et al.* [210]					
Cakir *et al.* [61]			X		X
Hamta *et al.* [170]		X			
Hamta *et al.* [169]		X			
Pekin and Azizoglu [317]	X	X			
Corominas *et al.* [93]		X	X		
Oesterle and Amodeo [289]	X		X		

* Following notations are used in this table:
R: Resources, S: Station, T: Task, W: Worker

consideration of non-overlapping constraints due to the allocation of multiple robots at each station.

3.5.2.2.2 Two-sided Assembly Line Balancing Problem

Two-sided assembly lines, which are considered more practical for the assembly of large products (e.g. trucks) than small ones (e.g. electrical drills) [227], were studied by Bartholdi, who introduced the Two-sided Assembly Line Balancing Problem (TALBP) [26]. Since then, this problem has been addressed by e.g. [411, 330, 226, 86, 427]

3.5.2.2.3 Assembly Line Worker Assignment and Balancing Problem

Motivated by the desire to incorporate disabled individuals into the active workforce, Miralles *et al.* [268] introduced the Assembly Line Worker Assignment and Balancing Problem (ALWABP), which is an extension of the SALBP. In this given problem, task processing times are worker-dependent. This occurs when balancing assembly lines with disabled workers, because a given worker might be efficient on a certain subset of the task while being inefficient on another subset [273]. Each worker is associated with an infeasible set of tasks. Similar to SALBP, ALWABP can also be classified as ALWABP-1 and ALWABP-2. Blum and Miralles [47] addressed this problem by minimising the cycle time and using a beam search algorithm to solve it. Other examples include following works: [278, 48, 404, 322]. Ramezanian *et al.* [336] extended this work for mixed-model lines by proposing a model aiming at both minimising the cycle time and the total operating costs. A model was proposed by Ritt *et al.* [341] to take high levels of absenteeism into consideration during the line balancing problem.

3.5.2.2.4 Multi-Manned Assembly Line Balancing Problem

Multi-manned assembly lines have specific advantages over simple assembly lines such as reducing the length of the line, the amount of throughput, the cost of tools and fixtures, the material handling, worker movement, and setup time [134]. This type of assembly line is often used for the assembly of large products, such as busses and trucks, in which tasks must be performed on a specific side of the product [343]. The associated problem, Multi-Manned Assembly Line Balancing Problem (MMALBP), has been addressed in the recent years by [208, 134, 344, 205].

3.5.2.2.5 Time and Space Assembly Line Balancing Problem

Bautista and Peireira [36] proposes the Time and Space Assembly Line Balancing Problem (TSALBP), problem in which each task j has a spatial attribute a_j and each station m has an available area A_m. Each space requirement for each station m , $a(S_m)$ cannot exceed A_m. Indeed, in classical industrial problems, the length of the workstation is limited due to required tools and components that must be assembled. They propose an ant algorithm to solve this problem. This problem has also been considered by several other authors, e.g. [78, 79, 81]. Ruda-Vilela *et al.* [333] propose a comparison of multi-objective ant colony optimisation algorithms for the TSALBP.

3.5.2.2.6 Alternative Subgraph Assembly Line Balancing Problem

The Alternative Subgraphs Assembly Line Balancing Problem (ASALBP), defined by Capacho and Pastor [64], considers alternative variants that an assembly process may admit and thus overcomes a risk of loss in efficiency. Each assembly variant is represented by a subgraph, which determines the tasks required to assemble a part of a particular product. This problem has been defined and modelled in a restricted version and an extended version [64, 63]. The ASALBP definition considers alternative assembly precedence subgraphs that involve either the same or different sets of tasks. In their representation, task processing times and/or precedence relations can depend on the selected subgraph. It is here assumed that assembly alternatives do not overlap with each other. Thus, each alternative of each subassembly is represented by a unique and independent precedence subgraph [63]. Constructed heuristic methods have been developed and tested comprehensively by Capacho *et al.* [66, 65]. Scholl *et al.* [360] proposed a mathematical formulation of the ASALBP to solve it optimally.

3.5.2.2.7 Other approaches to dealing with processing and resources alternatives

Two different approaches have been proposed to incorporate processing alternatives into ALBP [50]. The equipment selection problem is based on the assumption that there is a fixed set of equipment that has to be selected and assigned to a workstation. The latter consists of assigning processes to tasks. For each task, exactly one processing alternative must be selected. These alternatives can be engendered through technological reasons (e.g. gluing or clinching) or resources (e.g. machines or manpower).

Graves and Whitney [159] are two of the first people to address the problem of line balancing and equipment selection together. The objective is to select equipment and assign tasks to workstations, such that total costs, composed of capital and operating costs, are minimised. Each workstation is labelled by an annual capital cost and each task is labelled by an annual operation cost, which can also be avoided by assigning another specific task to the same workstation.

Pinto *et al.* [320] combined the line balancing problem with the decision of parallel workstations. The proposed model dealt with the trade-off between the cost of additional parallel workstations and savings in labour costs. Later on, Pinto *et al.* [321] presented a model that considers the choice of manufacturing alternatives and the assignment of tasks to minimise the total costs, defined as the sum of the labour cost and fixed expenses. A similar model was proposed by Graves and Lamar [160] for the automated system design problem. The

objective was to determine the type and number of workstations and to assign the operations to them.

Graves and Holmes [161] address the assembly line design problem (ALDP) with several equipment alternatives for the mixed-model assembly line. The proposed method aims at both assigning tasks to workstations and selecting equipment for each of them by minimising the total cost of the assembly line.

Buckin and Tzur [57] proposed a model in which the total equipment costs are minimised for a given cycle time. In their model, each equipment has individual costs and has an influence on the task processing times. Buckhin and Rubinovitz [56] later extended this model by considering parallel workstations.

Hamta *et al.* [170] present an approach to dealing with the Flexible task Time Assembly Line Balancing Problem (FTALBP). In their problem, the operation time of each task can be between a lower and upper bound. The equipment, in this case, the machines, can compress the processing time of tasks, leading to higher costs. In their approach, they proposed a bi-criterion non-linear integer programming model, which comprises two objective functions: minimising the cycle time and minimising the machine total costs. Hamta *et al.* [169] extended the previous work by adding the smoothness index as a third objective function. They proposed a method based on the combination of a particle swarm optimisation algorithm with a variable neighbourhood search.

Pekin and Azizoglu [317] address the ALDP, a problem in which each task can be performed through several equipment alternatives. In the proposed method, the total equipment cost and the number of workstations are minimised. For this, they proposed a branch and bound procedure with powerful reduction and bounding mechanisms. The proposed algorithm is capable of solving the problem instances with up to 25 tasks and five pieces of equipment.

Agpak and Gökcen [13] present an industrial ALBP, in which equipment and tasks are simultaneously assigned to workstations. In this problem, which is similar to the ALDP, a limited number of specific machines and a limited number of workers that can use these machines must be balanced. Agpak and Gökcen did not explicitly use any costs. Corominas *et al.* [93] extended this problem by formulating the general resource-constrained ALBP, which aims at minimising the total costs, namely the fixed station costs and the unit cost of different resource types. Finally, Oesterle and Amodeo [289] address the ALDP for a mixed-model line under consideration of equipment alternatives for each task. In the proposed model, each equipment has different processing times and different operation costs.

3.5.2.2.8 Other problems

Tuncel *et al.* [393] proposed an assembly line balancing model with positional constraints, task assignment restrictions, and station parallelling. Indeed, while some tasks must be mounted on the back, others can be mounted on the front of the workpiece.

Other researchers have also proposed simultaneously solving the sequencing and balancing of a mixed-model assembly line, e.g. [348, 307, 274, 246, 361, 226].

3.5.2.2.9 Synthesis of the models

In addition to the identified drawbacks associated with the absence of any cost model, the purpose of each problem type is compared with the requirements fixed earlier. The fulfillment (○: no fulfillment, ●: complete fulfilment) of each problem type is shown in Table 3.2. There is no existing model that can address the defined requirements, which include evaluating product and process alternatives, resource alternatives, and space requirements.

Table 3.2: Fulfillment of the requirements for each classical ALBP

	TSALBP	ALWABP	TALBP	ASALBP	ALDP	FTALBP	MMALBP
Product/Process Alternatives	○	○	○	●	○	○	○
Manual resources Alternatives	○	●	○	◔	◔	○	○
Automatic resources Alternatives	○	○	○	◔	◓	◓	○
Space Requirement	●	○	○	○	○	○	○

3.5.3 Resolution methods

The solution approaches used in ALBPs can be classified into two main groups [389]: exact methods and approximate methods. Detailed reviews of resolution methods are provided by Scholl and Becker [358] and Battaia and Dolgui [30] .

3.5.3.1 Exact methods

ALBPs can be solved by formulating a mathematical model that can be optimally solved through a general solver (e.g. ILOG Cplex and LINGO) or by developing a dedicated solution method. Over the last 60 years [353], several mathematical models have been described and solved with various solvers:

— for the SALBP-E and solved with CPLEX, e.g. [132] or with Lingo [443]

— for the RSALBP-2 and solved with CPLEX, e.g. [175]
— for the MALBP with setup times and solved with CPLEX, e.g. [2]
— for the transfer line balancing problem [165]
— for the TALBP and solved with CPLEX, e.g. [118]
— for the UALBP and fuzzy UALBP and respectively solved with Lingo by [441] and [442]
— assembly line balancing with positional constraints, task assignment restrictions and station parallelling [393] with CPLEX
— multi-objective assembly line balancing problem with bounded processing times, learning effect, and sequence-dependent setup times [168] with Lingo

However, for some extensions of the SALBP and real-world scale problems, the solvers may reach their limits and thus may be inefficient [359]. For this reason, dynamic programming or branch and bound procedures are often used. In the first case, the problem is divided into subproblems and several stage decision processes are made to identify the optimal solutions of the sub-problems (e.g. [25, 176, 188]), which are used to construct the optimal solution of the original problem. Examples of resolution methods using dynamic programming include Nicosia *et al.* [285], and Bautista and Pereira [37]. One major drawback of dynamic programming is the required computational effort. The 'branch and bound' is an enumeration method exploring the subset of feasible solutions to find an optimal solution. Branch and bound has been principally used for solving SALBP (e.g. Fast Algorithm for Balancing Lines Effectively (FABLE) [196], EUREKA [180], SALOME [363] and ABSALOM [362]). Other Branch and Bound procedures have been developed for the ALWABP [268, 48, 404], for the MALBP [58], the SALBP [373, 249, 365], the two sided ALBP [411], the PM-ALBP [208], ALBP with parallelling stations [319, 320], and the UALBP [296].

Battaia and Dolgui [29] presented reduction approaches to reducing the size of the initial problem associated with an ALBP in order to optimally solve ALBP faster than with exact methods.

3.5.3.2 Heuristics

For ALBPs, many heuristics have been proposed in the literature. Heuristics vary from simple list processing procedures to optimal-seeking procedures [22]. Most of the heuristics are based on priority rules, which are obtained considering e.g. the number of predecessors and successors or the task processing times. Erel and Sarin [130] classify heuristics according to three categories: (i) single-pass decision rule, (ii) multiple single-pass solutions, and (iii) backtracking methods. Single list processing procedures, referred as single-pass decision

rules by Talbot *et al.* [379], can be maximum ranking position weight, maximum number of followers, maximum task time first, minimum lower bound, and minimum upper bound. Single-pass decision rules are described by Ponnambalam *et al.* and Talbot *et al.* [324, 379] for the SALBP, by Balakrishnan *et al.* [22] for the UALBP and by Capacho *et al.* [65] for the ASALBP. In the second category, multiple single-pass procedures produce several solutions, and the most attractive solution is selected. The Computed Method of Sequencing Operations for Assembly Lines (COMSOAL) [15] is a well-known method in this category. The COMSOAL method is based on the list of each available task, representing tasks with various assignment constraints at each step during the exploration process. At each step, a task is randomly chosen from this list, and a new list is generated. A multiple single-pass procedure was proposed by Gamberini *et al.* [148] to solve the stochastic assembly line rebalancing problem, Yegul *et al.* [427] to solve the u-shaped two-sided assembly line balancing problem. In backtracking methods, solutions are incrementally built and abandoned as soon as it cannot be completed to a valid solution. Examples of backtracking methods can be found in Finel et al [137] and Kilincii [212].

3.5.3.3 Single-Objective Metaheuristics

Various surveys and classifications of metaheuristics have been proposed in the literature. The most recent ones are by Talbi [376], Bianci *et al.* [46], Boussaïd *et al.* [49], and Mahdavi *et al.* [255]. Metaheuristics can be classified according to various schemas. Using the number of solutions simultaneously manipulated during the search process, two classes can be identified: single-solutions and population-based metaheuristics. This classification is often taken as a fundamental distinction in the literature [49]. Single-solution-based methods usually manipulate a wide gamut of various neighbourhoods. In addition, they also incorporate several forms of strategies - from randomised to thoroughly deterministic - to explore the solution space. In comparison, population-based procedures aim to replace components of solutions with those of others by variously choosing exchange rules.

3.5.3.3.1 Single-solution based metaheuristics

Several metaheuristics have been applied to solve ALBPS, such as GRASP, Simulated Annealing, Tabu Search, Guided Local Search, and Iterative Local Search. GRASP, proposed by Feo and Resende [92], is a multi-start metaheuristic which involves two steps: constructing a solution and improving it through a local search. The construction process is achieved through a randomised, greedy heuristic. The obtained solution is then used as an initial solution of a local search procedure. This method has been applied by Andrés *et al.* [10],

Chica *et al.* [80], and Guschinskaya *et al.* [166]. Simulated Annealing, a probabilistic method proposed by Kirkpatrick *et al.* [216], simulates the physical cooling process of a solid. The algorithm starts with an initial solution and generates through neighbourhood procedures new solutions that may be accepted, even if they are worse than the initial solution. The probability of acceptance decreases during the search procedure. Simulated annealing has been proposed to solve ALBPs by Roshani *et al.* [344, 343], and Manavizadeh *et al.* [256]. Tabu search, which was proposed by Glover [155, 156], starts with an initial solution and iteratively moves to a new solution through a local or neighbourhood search procedure until some stopping criteria are met. The exploration procedures use a memory structure, known as the tabu list containing a set of rules and forbidden solutions used as a filter, to explore the neighbourhood of a solution. Tabu Search has been proposed by Chiang *et al.*[76], Özcan and Toklu [308, 133]. Moreover, the Guided Local Search, proposed by Voudouris and Tsang [406], utilises a utility function which penalises unwanted solution features during the local search iteration. An example of the application of a Guided Local Search can be found in the work of Daoud *et al.* [100].

3.5.3.3.2 Population based metaheuristics

Various population- based metaheuristics have been proposed in the literature to either deal with a single objective optimisation problem or with a scalarized multi objective optimisation problem. Examples include a genetic algorithm proposed by [206, 215, 329, 384]. Other authors tackled the ALBP by using Swarm Optimisation, e.g. [36, 99, 39, 273, 305] or Ant Colony Optimisation e.g. [445, 347, 134, 39]. Figure 3.14 shows the frequency of the algorithms used to solve the line balancing problem [4].

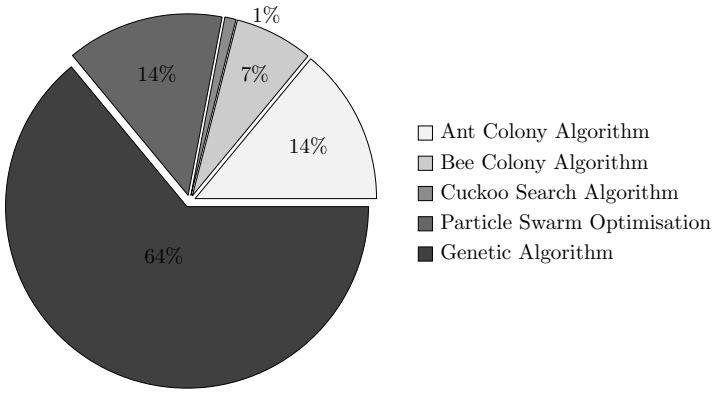

Figure 3.14: Pie diagram representing the frequency of used algorithms in ALBPs

4. The statistical analysis is based on the paper repository of Microsoft Academic, available at following address `http://academic.research.microsoft.com/` and by using following keywords: *Ant Colony Algorithm*, *Bee Colony Algorithm*, *Cuckoo Search Algorithm*, *Particle Swarm Optimisation*, *Genetic Algorithm*, Line Balancing Problem, Line Design Problem

3.5.3.4 Multi-Objective Metaheuristics

Chica *et al.* [79] proposed an advanced NSGA-II with some problem-specific encoding schemes and crossover schemes. In their work, they compared the proposed NSGA-II with the basic NSGA-II and a MOACO algorithm. Chutima and Chimklai [86] proposed a DMOPSO to solve the two-sided mixed-model assembly line balancing. The proposed algorithm was, among others, compared to a NSGA-II. Hamta *et al.* [169] proposed a hybrid DMOPSO to solve the single-model assembly line balancing problem. Furthermore, Zhang and Chen [440] proposed a hybrid MOEA, which has some features of the VEGA algorithms. They compared their hMOEA to a NSGA-II and SPEA2. Cakir *et al.* [61] proposed a simulated annealing-based algorithm, which is compared to a classical simulated annealing with a weighted-sum approach in order to solve the single-model stochastic assembly line balancing problem with parallel stations. Yagmahan [416] addressed the MALBP with a MOACO, which was compared to the ranked positional weight method, an Artificial Immune Algorithm, and a Genetic Algorithm. Saif *et al.* [348] propose a MOABC for simultaneously solving the sequencing and balancing of mixed model assembly lines. The MOABC is compared to a NSGA-II in their approach. Rabbani *et al.* [331] developed several multi-objective approximate methods, including a NSGA-II and DMOPSO, to solve the robotic mixed-model assembly line balancing problem. A hybrid PSO was proposed [169] to to solve an ALBP with flexible operation times, sequence-dependent setup times, and learning effects to minimise the cycle time, the total equipment costs, and the smoothness index. Rada-Vilela *et al.* [333] proposed an empirical comparison of various MOACO to solve the TSALBP.

3.5.4 Synthesis

Despite the large amount of research done over the last years to describe and solve GALBP, there is still a gap between the methods provided by the literature and the current industrial problems, making the practical use of these methods most difficult. These gaps are found in the following points:

— Objective function - As shown earlier, the classical objectives are to minimise the cycle time or the number of stations. While the cycle time is almost always given by the sales department, depending on the forecast, it is useless to reduce the line's cycle time below that value. Furthermore, the current practice in ALBP is to optimise specific metrics that indirectly or directly optimise other metrics that may be more usable for practitioners. An example would be to optimise the number of stations instead of the idle time on the line. In addition, though the proposed models incorporating cost

elements have increased over the last years, the absence of a unified and detailed cost model enabling an accurate estimation of the future product costs can be outlined.

— Despite the direct simplicity of the available models, some recent characteristic features of the present-day situation engendered shortcomings of the current methods. The first characteristic feature engendered by the pressure of globalisation and the increasing concurrence is uncertainty. This uncertainty is related to the following points: (i) which level of automation is useful? Which resources (fully automatic, semi-automatic, or manual) should be used? This uncertainty can only be countered by iteratively analysing the developed assembly system's solutions. In the traditional methods, these features are strongly defined in the earliest step of the production planning project. Thus, a wrong decision at this earliest step could have an important issue in the planned production system. This requires addressing both the assembly line balancing problem and the equipment selection problem. The second characteristic feature is the complexity of the products and their requirements for quality and prices. These requirements engender the need to select and plan the most reliable system, with low maintenance effort, low material waste, a low number of defective products, and the best price. While in the literature, few studies have addressed both problems simultaneously, common drawbacks are the absence of consideration of relevant resource properties that may affect the efficiency of the final assembly line, such as the availability of machines and scrap rates.

— The prediction of unit product costs requires a cost model. As stated in the previous section, no cost model uses all cost elements that may influence the design of an assembly line.

— The design of assembly lines can impact energy efficiency in two ways [397]. First, through the size of the assembly line. As noted by Despeisse *et al.* [111], for some manufacturing industries (e.g. automotive), building-related energy (e.g. space heating and lighting) contributes to approximately 40-60 percent of the overall energy consumption. Second, the productive and idle time also influences the energy consumption. As stated by Smith and Ball [371], the energy consumption cannot be influenced in operational mode since it is governed by the machine design and machining requirements. However, the energy consumption due to idle time can be influenced.

— Several optimisation algorithms of different natures have been proposed to solve ALBPs. However, the performance of algorithms is drastically influenced by the nature of the problem under study and to author's knowledge, no study has compared various optimisation algorithms of different natures.

3.6 Buffer Allocation Problem

To limit the effects of the unreliability of machines and robots (e.g. starvation and blockage on down or upstream stations and disruption of the material flow in the assembly line) buffer stations are often included in the assembly line. Buffers can help to smooth and balance the material flow between stations. One major drawback of buffer stations is that they require additional capital investment, floor space of the line, in-process inventory, and increases in the lead time [367, 107].

3.6.1 Introduction and notation

The BAP aims at allocating a certain amount of buffer among intermediate buffer locations of a production line to optimise a specific objective (e.g. throughput of the assembly line, minimum total buffer size). Given an assembly line with M unreliable stations, the problem is to optimally allocate a given number of buffer places amongst the $M-1$ buffer emplacement in order to, depending on the objective function, maximise the throughput rate for a given fixed number of buffers (problem BAP-1), achieve the desired throughput rate with the minimum total buffer size (BAP-2) or minimise the average work-in-process inventory (BAP-3). Other variants related to the minimisation of costs or maximisation of profit may be found [244]. A comprehensive survey of the BAP has been provided by Demir *et al.* [107].

An illustration definition of the utility of buffer is shown in Figure 3.15. Either through different station loads or due to machine breakdowns, Station 1 is blocked and the Station 3 is starved. However, due to the existence of buffers, the starvation and blockage are moving forward in the spatial time and thus, an increase in the throughput can be achieved.

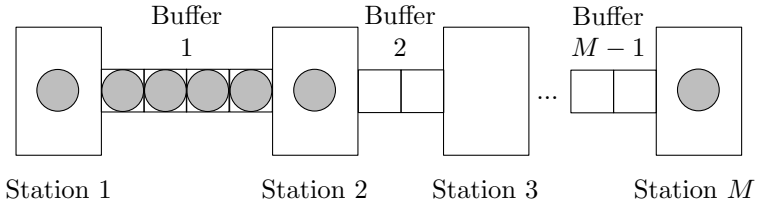

Figure 3.15: Example of a production line with M stations, in which Station 1 is blocked and Station 3 is starved

Taking the BAP-1, problem for which the throughput must be maximised given a fixed number of buffers BS that need to be dispatched between M stations, the possible buffer

configurations can be calculated as follows:

$$\binom{BS+M-2}{M-2} = \frac{(BS+1)(BS+2)...(BS+M-2)}{(M-2)!} \tag{3.26}$$

For instance, if a given assembly line involves 10 stations and 30 buffers need to be allocated, the total number of feasible buffer allocations is equal to 2.08381E+18. Figure 3.16 shows the influence of the capacity of two buffers on the throughput rate of an assembly line with three stations. Adding some buffers to the initial assembly line may, depending on the capacity of each buffer, increase the throughput rate of the assembly line by a maximum of 25 %

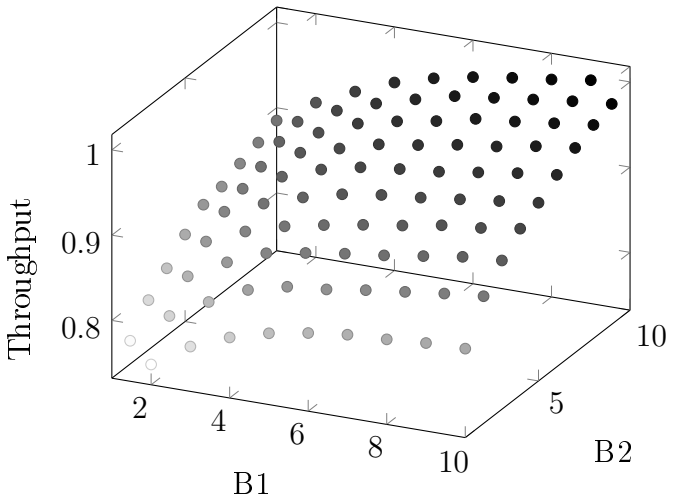

Figure 3.16: Example of throughput rate changes obtained with different buffer capacities in a three machine system

In a mathematical formulation, the three main BAPs can be summarized as follows:

— BAP-1

$$\begin{aligned} \text{Max} \quad & f(B) \\ \text{s.t.} \quad & \\ & \sum_{m=1}^{M-1} B_m = B_T \quad k = 1, ..., K \\ & B_m \in \mathbb{N}^*, \qquad m = 1, ..., M-1 \end{aligned} \tag{3.27}$$

— BAP-2

$$\begin{aligned} \text{Min} \quad & \min_{m=1}^{M-1} B_m \\ \text{s.t.} \quad & \\ & f(B) \geq f^* \\ & B_m \in \mathbb{N}^*, \quad m = 1, ..., M-1 \end{aligned} \tag{3.28}$$

— BAP-3

$$\begin{aligned} \text{Min} \quad & Q(B) \\ \text{s.t.} \quad & \\ & \sum_{m=1}^{M-1} B_m \leq B_T \quad k = 1, ..., K \\ & f(B) \geq f^* \\ & B_m \in \mathbb{N}^*, \qquad m = 1, ..., M-1 \end{aligned} \tag{3.29}$$

where $Q(B)$ represents the average work-in-process inventory as a function of buffer size , $f(B)$ represents the throughput rate as a function of the buffer allocation and $f*$ denotes the desired throughput rate

3.6.2 Resolution methods

The solution approaches used to solve the BAP involve generative and evaluative methods, as shown in Figure 3.17. While the former aims at searching for an optimal solution, the latter aims at evaluating various performance measures by means of analytical methods and simulation [116].

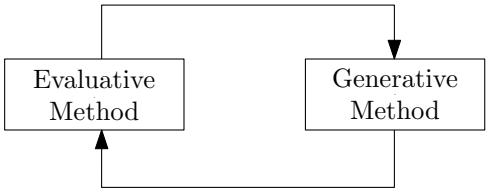

Figure 3.17: Solution approaches used in the BAP

3.6.2.1 Evaluative methods

To estimate the performances of an assembly system, two types of models can be used: (i) analytical models and (ii) simulation models. While analytical models can be described as a set of equations characterising a system, simulation models mimic the dynamic behaviour of the system. Analytical models tend to be more accurate whereas simulation models provide approximate and dynamic information about the system [388]. Compared to analytical models, simulation models offer more flexibility and can take a wide set of system characteristics into consideration [92].

The performance analysis of assembly lines has been extensively studied in the literature and several surveys have been proposed (e.g. [242, 241, 158]). The proposed methods for analysing the performance of assembly lines can be categorised according to several attributes

and line configuration, such as: (i) reliable and unreliable machines, (ii) finite and infinite buffers, and (iii) constant and random processing times. While constant processing times are applicable for automated production lines, a random distribution is often used for manual tasks. In addition, the methods can be further divided into homogeneous and inhomogeneous assembly lines if the machines have similar or different processing times.

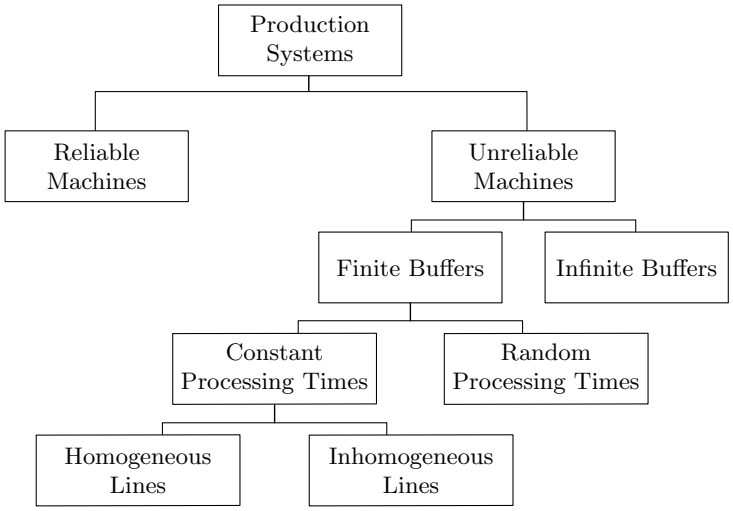

Figure 3.18: Categorisation of production systems in performance analysis of assembly lines [242, 241]

The classification shown in Figure 3.18 can be further developed regarding discrete and continuous models. The discrete models consist of using either the Bernoulli machine reliability model or the geometric reliability model, while the continuous models use exponential or non-exponential models.

The two reliability models for discrete event systems are defined as follows:

— Bernoulli reliability model [438, 74]: Assuming that the status of a machine can be modelled using a Bernoulli random variable, the probabilities of being up or down are given by p and $1 - p$, respectively, and are independent of the status of that machine in the previous time slots. The Bernoulli reliability model is often used for very short downtimes that are comparable with the cycle time of the machine.
— Geometric reliability model [438, 74]: In the geometric reliability model, the probability that a machine is in a specific state depends on its state in the previous time slots.

As stated above, to analyse the performance of assembly lines with the previously listed characteristics, either analytical or simulation models can be used. Analytical models can be further divided into exact and approximation models [190].

Analytical models

The behaviour of an unreliable station M_i in isolation can exist in two distinct states: operation or working and down or under repair. The status of the machine can be described by considering a discrete state Markov chain. In Markov chains [5], probabilities of moving from state to state are used in order to assess the probabilities that the process will be in a given state at a given time. Examples of approaches using the Markov chain as evaluation method are Zhou and Lian [449], and Papadopoulos and Vidas [313]. An example of the application of Markov chains to an unreliable machine in isolation and in a flow line can be found in Appendix B.3.1. However, Markov chains have limitations. As stated by Gershwin and Aziz *et al.* [152, 18], the challenge of treating large state spaces limits their use. For example, a system in which M stations are separated by a buffer B_m, $m = 1, ..., M-1$ of size N_m, the number of distinct Markov states M would be:

$$M = 2^M \prod_{m=1}^{M-1} (N_m + 1) \tag{3.30}$$

Gershwin [151] presented a decomposition technique for an approximate evaluation of tandem queues with finite storage. The common idea behind the decomposition methods is to decompose the original line, which consists of M stations, into a set of $M-1$ stations lines. Each of these lines consists of two fictive machines, which are separated by a buffer. Furthermore, each decomposition involves characterising the subsystems, deriving a set of equations that determines the unknown parameters of each subsystem, and developing an algorithm to solve these equations [412]. Each set of fictive machines is characterised by two types of failures, namely real and virtual [238]. While real failures represent real machine failures, virtual failures account for the starvation of machines. An additional example of the use of decomposition methods can be found in Massim *et al.* [259].

Another analytical method that can be used to evaluate the performance of an assembly line is the aggregation method, in which two principal components are used: backwards and forward aggregation. In the former case, the last two machines and the buffer between them are aggregated into a single equivalent station. Then, this equivalent station is combined with a buffer and the station from the original line to form a new aggregated station. This process is repeated until the first station is reached. In the latter case, the opposite process is repeated until the last station is reached. Examples of such analytical methods can be found in Dolgui *et al.* [115, 117]

5. One important property of the Markov chains is that the conditional probability of any state of the process at time $n+1$ is independent of its states at time $n-1, n-2, ---$ [243].

Simulation models

In addition to analytical models, simulation models have been developed to analyse the performance of an assembly line. Discrete-Event Simulation (DES) is often used, which is a computer evaluation of a discrete-event dynamic system model, where the operation of the system is represented as a chronological sequence of events [84].

Definition 3.16 System
Collection of entities (e.g. machines) that interact together over time to fulfil a specific objective.

These events may only change the state of the system under study at a discrete point in time.

Definition 3.17 System state
Collection of attributes or variables that contain all the necessary information to describe the entities of a system, enabling a description of the system at any time.

Definition 3.18 Entity
Any object or component in the system that requires explicit representation in the model (e.g. machines or workstations).

Definition 3.19 Event
An instantaneous occurrence in time that may change the state of the system (e.g. machine breakdowns).

Definition 3.20 Activity
A pair of events, where one initiates and the other completes an operation that alters the state of an entity.

Three types of DES have been identified: activity-based, event-based, and state-based. In the activity-based simulation, time advances in small steps and the alteration of the system state is checked. This type of simulation is inefficient and is only suitable for simple applications [325]. While in the event-based simulation, the system is modelled by defining the changes that occur at event times [84], in the state-based simulation, the dynamics of the system are described using the states of the resources in the system. An example of events modifying the state of a three-machine system is the arrival of workpieces at and the departure of workpieces from workstations. The various states of the associated model entities are shown in Appendix B.3.2.

Examples of the application of simulation models can be found in following papers [32, 9, 261, 42, 218].

Comparison of analytical and simulation models

While analytical methods have been extensively developed in the last 30-35 years, they are often meant to approximate the dynamic behaviour of manufacturing systems and they may pose restrictive assumptions [6]. In comparison, simulation models are often time-consuming and, due to available time for decision-making, they may not be adequate for industrial use. However, they offer a considerable advantage when the objective is to create a realistic model of a complex system [107]. Furthermore, most analytical models only measure a limited amount of performance criteria from the system, while the number of applicable criteria in simulation models is unlimited.

The fulfilment (○: no fulfilment, ●: complete fulfilment) of the analytical and simulation methods type is shown in Table 3.3. Comparing the performance by considering the required CPU time, analytical methods are more suitable than simulation models. However, this criterion is not important since the decision-making process should provide the optimal solution when planning activities, rather than provide fast, moderately accurate solutions. Since it is easier to adapt and extend simulation models to industrial use-cases, this method offers more advantages than analytical methods.

Table 3.3: Fulfillment of the requirements of each classical BAP resolution method

	Analytical	Simulation
Performance (CPU)	●	◓
Generic	●	●
Modular	◓	●

3.6.2.2 Generative models

Demir *et al.* [109] proposed a tabu search procedure to solve the BAP-1. Later, Demir *et al.* [106] extended the previous optimisation method by proposing an adaptive tabu search. Demir *et al.* [108] then extended these versions. Moreover, Massim *et al.* [259] proposed an artificial immune system to solve an extension of the BAP-1, which incorporates the product of the production rate, unit profit, and holding costs per unit for works in process. Dolgui *et al.* [117] also consider revenue for sold production units and incorporate buffer acquisition costs. To solve this problem, they propose a hybrid algorithm that is based on genetic and branch-and-bound approaches, which is an improvement of their earlier work [115]. Kose and Kilincci [221] proposed a hybrid simulated annealing and genetic algorithm

to solve the BAP-1. In addition, Costa *et al.* [94] proposed a parallel tabu search to solve the buffer allocation problem in reliable assembly systems with stochastic processing times. Chehade *et al.* [72, 73] presented a multi-objective problem in which the throughput of the line must be minimised in addition to the total number of buffers. They also used the Lorenz dominance and compared it with the Pareto dominance. The Lorenz dominance provided a better domination area in the central region of the Pareto front. Nahas *et al.* [280] proposed a model in which machines and buffers are selected to maximise the profit of the designed assembly system. The problem was solved using an Ant Colony Optimisation (ACO). Cruz *et al.* [96] proposed a multi-objective genetic algorithm to solve the problem of assigning a buffer to an assembly line by considering the throughput rate and the total cost of buffer allocation. Finally, Ouazene *et al.* [304] proposed a non-linear programming approach to address the BAP. The non-linear programming method is compared with six heuristic, neighbourhood searches.

3.6.3 Synthesis

In addition to the drawbacks of the ALBPs, which can be transferred to the BAP, the missing models that consider product design, processes, resources, and buffer alternatives can be identified. Indeed, the choice of the correct level of automation may have a strong influence on the buffer allocation and thus, the throughput rate of the assembly line. Finally, while a high number of papers have been published for the BAP, the number of multi-objective problems still remains low.

3.7 Conclusion

As stated above, the problem of this thesis can be related to an optimisation problem; given a set of product designs, processes, and resource alternatives, the best combination of product designs, processes, and resources must be selected to optimise specific criteria. In this chapter, insights into multi-objective optimisation are provided. In addition, an overview of models and resolution methods in the field of assembly line balancing and buffer allocation is provided. This information leads to the identification of drawbacks of models and methods that must be addressed in the upcoming chapters. The identification of these drawbacks relies on the definition of the requirements outlined in Chapter 2. One major drawback is related to the absence of any cost model that can translate all interdependencies between products, processes, and resource alternatives into one single metric. While

specific models have been developed to address product, process, or resources alternatives, none address them simultaneously, as demonstrated in Table 3.2. Further drawbacks can be identified when considering the resolution methods. While several optimisation algorithms of different natures have been proposed to solve the line balancing problems and buffer allocation problems, no study has compared them. By combining drawbacks from an industrial and research point of view, the following elements from this thesis can be characterised as a contribution to knowledge:

— Introduction of a model that enables a holistic approach to design assembly lines by considering product, processes, and resource alternatives (Chapter 4)
— Introduction of efficient optimization methods to solve the associated problem (Chapter 4)
— Introduction of combined algorithms to improve the obtained results (Chapter 5)
— Empirical study to compare various optimisation algorithms (Chapters 4, 5, and 6)
— Combination of optimization and simulation to evaluate the influence of buffers on the global performance of assembly lines (Chapter 6)

Chapter 4

Assembly Line Design Problem, Processing, and Resources Alternatives: Problem Formulation and Resolution

---

Abstract

In this chapter, identified drawbacks in the state-of-the-art models and methods are addressed and one of the problems investigated in this thesis is formulated. This problem involves simultaneously selecting product designs, processes, and resources alternatives in order to plan the most suitable assembly line for capacity and cost-oriented objectives. To address this problem, a detailed cost model was developed with the function of translating the complex interrelated consequences of choosing specific design alternatives with assembly technologies for a single cost metric. Thirty-four multi-objective algorithms were developed, including variants of evolutionary algorithms, an artificial bee colony, cuckoo search optimisation, a flower pollination algorithm, a bat algorithm, ant colony optimisation, and particle swarm optimisation. All the parameter values of these algorithms were analysed by means of a ANOVA and their performances were compared based on fifty well-known problem instances in accordance with four multi-objective quality indicators. Finally, the algorithms are ranked using a nonparametric statistical test.

4.1 Introduction

In the previous chapter, drawbacks of models and methods were identified by considering the requirements listed earlier in this thesis. Among these drawbacks, there is currently no available model that aims to support decision makers during the design phases of an assembly line by considering different product designs, processes, and resource alternatives. In addition, the absence of a unified and detailed cost model that enables accurate estimation of future product costs during the early planning tasks of an assembly line was identified. While different algorithms have been proposed to solve ALBPs, there is no study that compares the different optimisation algorithms. This chapter presents a resolution framework that aims to supporting decision makers during the design phases of an assembly line that addresses product designs, processes, and resources alternatives.

The formulation and resolution of the problem under investigation in this thesis requires the formulation of three research questions:

Research Question 1. *How can a problem be formulated that considers product designs, processes, and resource alternatives together?*

Research Question 2. *Since the performance of algorithms is influenced by the nature of the problem under study, which algorithm(s) perform the best?*

Research Question 3. *What is the most appropriate strategy for selecting the best solution(s) for swarm intelligence algorithms?*

This chapter is organised as follows: Section 4.2 presents the formulation of the problem and the mathematical model, including a detailed presentation of the cost model. To solve this problem, 34 multi-objective algorithms, including variants of evolutionary algorithms, an artificial bee colony, cuckoo search optimisation, flower pollination algorithm, bat algorithm and particle swarm optimisation were developed. The procedures of these algorithms are explained in Section 4.4; these algorithms are then compared with four quality indicators and the Friedman test is applied in Section 4.5. The conclusion and perspectives are drawn in Section 4.6.

4.2 Problem formulation and mathematical model

There is a set of process or design alternatives PDA, where each alternative $u \in PDA$ is represented by a precedence graph $G_u = (V_u, E_u)$. The node set V_u contains the product

design specific tasks, the arc set E_u reflects the precedence relations (i, j) between tasks $i, j \in V_u$. In order to represent a combined precedence graph of the various alternatives, the $(X)OR$-nodes representation proposed by Scholl *et al.* [360] can be used. In this graph, each assembly alternative is represented by a unique and independent subgraph g. This subgraph represents the tasks required to assemble parts of a particular product design alternative. In this representation, the combined precedence graph, which is represented by a set of nodes $V = 1, ..., N$ consists of four disjunctive subsets for different node types: (i) V_r the set of real tasks, (ii) V_s the set of entry nodes, (iii) V_t the set of terminal nodes and (iv) V_d the set of dummy tasks with duration 0. Each alternative g is represented between one node $i \in V_s$ and one node $j \in V_t$. A node $h \in V_d$ is used as a starting node for all alternative between two entry and terminal nodes. The various node sets are shown in Figure 4.1.

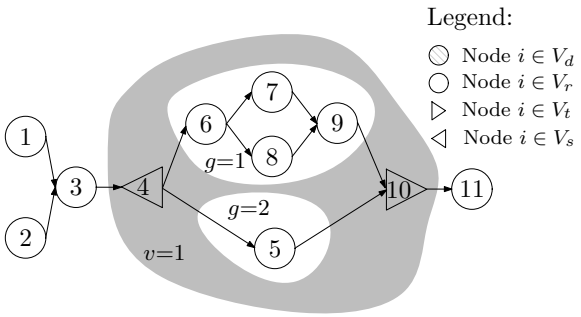

Figure 4.1: Example of the used sets of nodes in the ASALBP

In this example where $PDA = 2$, two designs or process alternatives are represented. The tasks 1, 2, 3, 11 are common to the two alternatives and the tasks 6, 7, 8, 9 represent the subgraph $g = 1$ and the task 5 the subgraph $g = 2$. $V(g)$ represents the set of nodes in the subgraph g. The two subgraph present between two entry and terminal nodes are represented by a subprocess v and $SG(v)$ is the number of subgraph for v. In the formulation, each task $j \in V - V_r$ does not have any processing times or costs. For each task $j \in V_r$, there is a set of available resources E_j with different properties, e.g. task processing times, costs and scrap rates. The problem under study is to simultaneously address three subproblems: (i) the product design problem, where for each subprocess a subgraph has to be selected, (ii) equipment selection problem, where the resources for each chosen subgraph have to be selected, and (iii) the assembly line balancing problem, where the tasks with their equipment of each chosen subgraph have to be assigned to workstations. The set of available resources $E_j = \{R_j \cup W_j\}$, $j \in V_r$, is represented by the set of respectively automatic and manual resources that can perform the task j. Each resource $l \in E_j$ has a task processing time for task j, t_{jl}, a scrap rate r_{jl} and C_{T0_l} and L_{T_l} respectively the initial purchasing price and useful life of tools. Each automatic resource $l \in R_j$ has a probability of failure p_{jl}, an average

planned and unplanned downtime D_{jl}, an average energy consumption e_{jl} per time unit, a useful life L_{R_l}, and C_{R0_l} the initial capital investment. Additionally, each automatic resource $l \in R_j$ has a maximum length and width L_l and W_l. Each manual resource $l \in W_j$ has a standard wage w_l, and one-time personal costs C_{L0_l}. To each task $j \in V_r$ are associated a wage rate ω_j, material costs c_j and required material floor space a_j. CRF_T, CRF_R and CRF_B represents the standard capital recovery factor for respectively tooling, automatic resources and building. Each station as a determined length of L and width W. The mathematical model requires one assignment variable, namely x_{jkl} (for $j \in V$, $k = 1, ..., \bar{m}$ and $l \in E_j$).

$$x_{jkl} = \begin{cases} 1, & \text{if the task } j \text{ is assigned to station } k \\ & \text{with equipment } l \\ 0, & \text{otherwise.} \end{cases} \tag{4.1}$$

Similarly to the approach of Scholl *et al.* [360], the number of variables of x_{jkl} can be reduced by defining the earliest and latest station, respectively E'_j and L'_j, to which a task j can be assigned. E'_j and L'_j can be calculated as follows:

$$E'_j = \lceil \tau_j + \sum_{h \in P^*(j)} \tau_h \rceil \tag{4.2}$$

$$L'_j = \bar{m} + 1 - \lceil \tau_j + \sum_{h \in F^*(j)} \tau_h \rceil \tag{4.3}$$

where $P^*(j)$ and $F^*(j)$ respectively represent the list of all predecessors and successors of a task j in a modified graph, in which all subprocesses $v \in PDA$ are replaced by a fictive task representing a lower bound on the total task time. The lower bound on the total task time is calculated as follows: $t(v) = \min_{g \in SG(v)}\{t(V(g)) | g \in SG(v)\}$. In order to simplify the formula, we set $t_j = min_{l \in E_j} t_{jl}$. $\tau_j = t_j / CT$ represents, based on the task time t_j and the cycle time, the earliest station in which the task j can be performed. This permits the identification of the subset $B_k = \{j \in V | k \in SI_j\}$, which represents potential tasks assignable to station k, where $SI_j = [E'_j, L'_j]$.

The mathematical model for the addressed problem is presented below.

$$\text{Min } Z_1 = \sum_{k=1}^{\bar{m}} [CT - \sum_{j \in B_k} \sum_{l \in E_j} x_{jkl} t_{jl}] \tag{4.4}$$

$$\text{Min } Z_2 = C_{part} \tag{4.5}$$

s.t.

$$\sum_{k \in SI_1} \sum_{l \in E_1} x_{1k1} = 1 \tag{4.6}$$

$$\sum_{k \in SI_j} \sum_{l \in E_j} x_{jkl} \leq 1, \quad \forall j \in V \setminus \{1\} \tag{4.7}$$

$$\sum_{j \in B_k} \sum_{l \in E_j} x_{jkl} t_{jl} \leq CT, \quad k = 1, ..., \bar{m} \tag{4.8}$$

$$\sum_{j \in B_k} x_{jkl} a_j \leq A, \quad \forall l \in E_j, \quad k = 1, ..., \bar{m} \tag{4.9}$$

$$\sum_{j \in B_k} \sum_{l \in R_j} x_{jkl} L_l \leq L, \quad k = 1, ..., \bar{m} \tag{4.10}$$

$$\sum_{j \in B_k} \sum_{l \in R_j} x_{jkl} W_l \leq W, \quad k = 1, ..., \bar{m} \tag{4.11}$$

$$\sum_{k \in SI_i} k x_{ikl_1} \leq \sum_{k \in SI_j} k x_{jkl_2}, \quad \forall i \in V \setminus V_s, \tag{4.12}$$

$$\forall l_1 \in E_i \quad j \in F_i | SI_i \cap SI_j \neq \emptyset, \quad \forall l_2 \in E_j$$

$$\sum_{k \in SI_i} x_{ikl_1} - \sum_{k \in SI_j} x_{jkl_2} \leq \bar{m}(1 - \sum_{k \in SI_j} x_{jkl_2}), \tag{4.13}$$

$$\forall i \in V_s, \quad \forall l_1 \in E_i, \quad \forall l_2 \in E_j,$$

$$\forall j \in F_i | SI_i \cap SI_j \neq \emptyset$$

$$\sum_{k \in SI_i} x_{ikl_1} \geq \sum_{k \in SI_j} x_{jkl_2}, \quad \forall l_1 \in E_i, \quad \forall i \in P_j \tag{4.14}$$

$$\forall j \in V \setminus V_t, \quad \forall l_2 \in E_j$$

$$\sum_{j \in F_i} \sum_{k \in SI_j} x_{ikl_1} - \sum_{k \in SI_i} x_{jkl_2} = 0, \quad \forall i \in V_s, \tag{4.15}$$

$$\forall l_1 \in E_i, \quad \forall l_2 \in E_j$$

$$\sum_{i \in P_j} \sum_{k \in SI_i} x_{ikl_1} - \sum_{k \in SI_j} x_{jkl_2} = 0, \quad \forall i \in V_t, \tag{4.16}$$

$$\forall l_1 \in E_i \quad \forall l_2 \in E_j$$

$$x_{jkl} \in \{0, 1\}, \quad \forall j \in V, \quad \forall k \in SI_j, \quad \forall l \in E_j \tag{4.17}$$

The two objective functions (4.4) and (4.5) aim at respectively optimising the idle time and the unit product costs. The module, which extracts the unit product costs denoted C_{Part} will be explained in the next section. Constraint (4.6) ensures that the first node of the precedence graph is assigned to any station. Constraint (4.7) verifies that any task is at most assigned once with one resource. Constraints (4.8)-(4.11) guarantee that the station load is not exceeding the cycle time CT. Additionally, they also verify that the material space or the machine floor space of the assigned tasks and resources at any station is less than the available floor space. The precedence constraints, except those emerging from any

node V_s are verified in (4.12). These precedence constraints only need to be activated for the selected subgraph/process or design alternative. This is done in (4.13). The same process is applied for any predecessors of the nodes in V_t in (4.14). Constraints (4.15)-(4.16) verify that only one process or design alternative is selected.

4.3 Unit product cost estimation

This section presents the cost model that was developed. First, various product cost estimation techniques are described. Regarding product cost calculation, three different types of methods can be distinguished [232]:

— Pre-calculation
— Intermediate calculation
— Post-calculation

For pre-calculation, the future costs are estimated before production. Alternatively, post-calculation determines the actual costs incurred after production begins. The intermediate calculation refines the cost elements when planning projects. Since the scope of this thesis is to develop a unit-product, cost-calculation model for the design phase, the pre-calculation method was used.

4.3.1 Product cost estimation techniques

The primary reason for developing a product cost model was to translate the complex and interrelated consequences of product design, manufacturing technologies, and process choices into a single cost metric [136]. This section provides a literature overview of manufacturing cost models. Product cost estimation covers a wide variety of issues, including manufacturing cost estimation for mechanical components, cost analysis of highly customised assembled products, unique approaches to estimation at the conceptual design stage, general costing rules designed for use at a later stage in the design cycle, and classical costing methods for highly novel cost estimation techniques [136].

Several different models and classification schemas have been developed for the purpose of assessing manufacturing costs. According to Tipnis *et al.* [385], these models can be divided into microeconomic and macroeconomic models. Asiedu and Gu [17] considered three quantitative methods: (i) analogy-based techniques, parametric methods and engineering approaches. Shehab and Abdalla [366] classified techniques into four categories: (i) knowledge-, (ii) feature-, (iii) function- and (iv) operation-based approaches. Ben-Arieh and

Qian [43] classified these techniques into four categories: (i) knowledge-based approaches, (ii) feature-based approaches, (iii) function-based approaches and (iv) operation-based approaches. In addition, Ben-Arieh and Qian [35] classified cost estimation methods into intuitive, analogical, parametric, and analytical methods. Niazi *et al.* [200] extended the previous classification and grouped product cost estimation techniques into qualitative and quantitative categories, as shown in Figure 4.2.

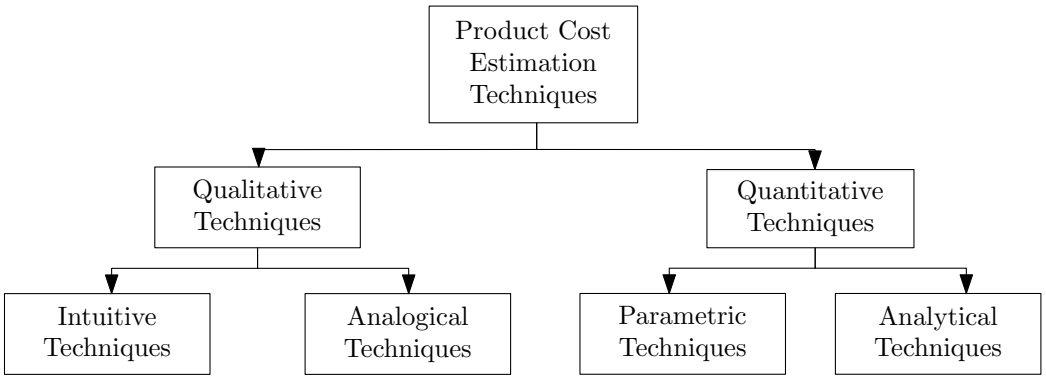

Figure 4.2: Cost estimation techniques

Qualitative cost estimation techniques are primarily based on comparison analyses of a new product with previously manufactured products. This comparison analysis enabled the use of past data to obtain the product cost of a new product. Compared to qualitative cost estimation techniques, quantitative techniques are based on detailed analyses of product design, including its features and corresponding manufacturing processes. Intuitive techniques are based on past experience and a domain expert's knowledge to systematically generate product costs for parts and assemblies. This knowledge may be stored in the form of rules or decision trees. Analogical techniques employ similarity criteria and assess, based on historical data for products with known costs, the cost of a new product. Parametric techniques are based on the analytical function of a set of parameters and variables, and they provide high-level characterisation of a product (top-down approach). In analytical techniques, detailed analysis of work is performed to identify elementary units, operations, and activities that represent different resources that are consumed during the production cycle and express the cost as a summation of all components. The difference between parametric and analytical techniques is their scale; while the former is used on high levels, the latter is used on a deeper level. Of the many methods for cost estimation, the most accurate method belongs to the analytical techniques [366]. In this category, methods such as: (i) operation-based cost models, (ii) break-down cost models, (iii) cost tolerance models, feature-based cost models, (iv) activity-based models, and process-based models can be found. A detailed review of the state of the art in the product cost estimation covering techniques listed below

is provided by [283]. Analytical methods evaluate the cost of a product through a decomposition of the required work into elementary tasks, operations, or activities with known or easily calculated costs. In these methods, the total cost associated with the manufacturing and assembly of a product is expressed as the summation of various cost components [199].

4.3.2 Process based cost model

The Process-based cost modelling [136] (PBCM) postulates that costs can be regarded as a function of technical factors and models for the material flow to and from each process step and calculates the cost of processing materials at each step. Since this method can project manufacturing or assembly costs based on part and process characteristics [95] and has been applied by researchers to compare several materials, processes, and product alternatives [138, 146, 195] it is suitable for evaluating different products, processes, and resources alternatives. The first sub-model of the PBCM relates the specification of the final product or part characteristics, such as size, shape, and material, to the technical parameters of the process of producing that product. These technical parameters can be associated with cycle time, downtime, reject rate, equipment and tooling requirements, and material [339]. The second sub-model uses the processing requirements and scales them to the total amount of equipment, labour, floor space, and energy consumption. The last sub-model projects prices of resource requirements and allocates costs over time and across products in order to develop a unit product [279].

The proposed product cost estimation module aims to dissect the costs associated with a solution to the mathematical problem presented earlier. The development of the PBCM starts with the decomposition of each elementary process into basic cost elements that result from the required resources. These cost elements can be divided into two major categories, namely fixed and variable costs. The difference between the former and the latter is based on whether the expense varies regarding the level of produced output. Fixed costs include the cost of the factory building, insurance, property taxes, and production equipment. Variable costs include labour, raw materials, and electrical power to operate the production machines. Assuming that only the costs differ between different products, processes, and resource alternatives, an estimation of production costs for the specific planning period must be determined for each possible combination of products, processes, and resources alternatives.

The basic cost elements that influence the product costs are: (i) C_M: raw material costs, (ii) C_L: labour costs, (iii) C_{OH}: overhead costs, (iv) C_E: energy consumption costs and (v) C_B, C_R, C_T : fix costs associated with respectively building, automatic resources and tools.

In order to assess the unit product costs C_{Part}, the total annual costs C_{tot} associated with the production of V_{net} non-defect goods will first be assessed. The relation between C_{tot}, C_{Part} and V_{net} is represented in following equation:

$$C_{Part} = \frac{C_{tot}}{V_{net}} \tag{4.18}$$

The total annual costs C_{tot} are calculated as following:

$$C_{tot} = C_M + C_L + C_{OH} + C_E + C_B + C_R + C_T \tag{4.19}$$

The reader will note that all these cost elements are considered over a time period of one year before breaking them down to product unit costs.

Since C_{tot} represents the total annual cost of non-defect goods, the gross number of products V_{gross} that needs to be produced to satisfy the demand V_{net} has to be introduced ($V_{gross} \geq V_{net}$). V_{gross} is calculated based on the quotient of V_{net} and the rejection rate of the assembly line, which is expressed as the product of the rejection rate r_k of each station $k = 1, ..., \bar{m}$.

$$V_{gross} = \frac{V_{net}}{\prod_{k=1}^{\bar{m}}(1 - r_k)} \tag{4.20}$$

The rejection rate r_k of a station k is calculated based on the rejection rates of the single resources assigned to station k. r_k is expressed as follows:

$$r_k = 1 - \prod_{j \in B_k} \sum_{l \in E_j} x_{jkl}(1 - r_{jl}) \tag{4.21}$$

The total annual material costs, C_M, are provided by the sum of the material costs of all parts, C_{M_k}, used at each station k:

$$C_M = V_{gross} \sum_{k=1}^{\bar{m}} C_{M_k} \tag{4.22}$$

The annual material costs C_{M_k} at station $k = 1, ..., \bar{m}$, depend on which task j, with its associated material cost c_j, is assigned to station k. C_{M_k} is calculated as follows:

$$C_{M_k} = \sum_{j \in B_k} c_j x_{jkl}, \quad \forall l \in E_j \tag{4.23}$$

In opposition to these cost elements, C_L, C_{OH} and C_E not only depend on the number of pieces produced but also on the required operation time to produce them. By extension, the total operation time τ required in a year for producing the V_{net} units, and respectively the V_{gross} units when considering scrap rates, is given by:

$$\tau = CT \cdot V_{gross} \tag{4.24}$$

Taking the average planned and unplanned downtime D_{jl} and the probability of failure p_{jl} of automatic resources assigned to the assembly line, the real cycle time of the assembly

line may slightly be different from the one planned and the equation (4.24) thus needs to be replaced by the following one:

$$\tau = \max(CT; CT_2) \cdot V_{gross} \tag{4.25}$$

where CT_2 represents the real cycle time of the line when considering machine breakdowns and is expressed as follows:

$$CT_2 = \max_{k=1,\ldots,\bar{m}} \Big(\sum_{j \in B_k} \big(\sum_{l \in R_j} x_{jkl}(t_{jl} + p_{jl} D_{jl}) + \sum_{l \in W_j} x_{jkl}(t_{jl}) \big) \Big) \tag{4.26}$$

The wage rate of a worker is determined according to the most difficult part that has to be performed on station k [8]. Since wage rate is also paid for downtime, the total annual labour costs C_L are calculated as follows:

$$C_L = \tau \cdot \max_{k=1,\ldots,\bar{m}} \Big(\sum_{l \in E_j} w_l [\max_{j \in B_k} \omega_j \cdot x_{jkl}] \Big) \tag{4.27}$$

The reader will note that one-time personal costs (e.g. recruitment and training costs) could also be taken into consideration by distributing them over the contract length and adding these costs to C_L.

Overhead costs C_{OH} are related to indirect labour required to maintain production, which is modelled by a ratio of the number of indirect workers r_{ind}. Each indirect worker is paid at wage rate w_{ind}. Since the overhead costs depend on the number of direct workers $M(x_{jkl})$ assigned to the assembly line, it can be calculated as follows:

$$C_{OH} = r_{ind} \cdot M(x_{jkl}) \cdot w_{ind} \cdot \tau \tag{4.28}$$

The total annual energy costs C_E depend on the energy consumption of automatic equipment. Here, we simplified the energy consumption model and only used the average energy consumption per time unit e_{jl} of equipment l when performing task j. The reader is referred to Zhou *et al.* [448] for more details about the decomposition of energy consumption of automatic equipment. The average annual energy consumption of the whole assembly line can be calculated as follows:

$$C_E = \tau \cdot c_E \cdot \sum_{k=1}^{\bar{m}} \sum_{l \in E_j} x_{jkl} e_{jl} \tag{4.29}$$

where c_E represents the costs of energy.

A key element of any cost forecast is the method used to allocate cash flows to appropriate activities. Here, the investment costs for buildings, equipment and tools are assumed to be distributed evenly in time over the usable lifetime of a resource. The opportunity cost associated with tying up these funds in a long-term investment is incorporated using the

standard capital recovery factor CRF_j. Since building, tooling, and equipment are considered to be capital investments, CRF_j is used to determine annual payment and is calculated as follows:

$$CRF_j = \frac{r(1+r)^{L_j}}{r(1+r)^{L_j} - 1} \tag{4.30}$$

where r is the periodic discount rate, L_j is representing the useful life in number of years over which the investment is distributed. The annual costs of automatic resources and tools are given by respectively multiplying the initial purchasing price (C_{R0_l},C_{T0_l}) by the capital recovery factor. The annual building cost C_B is computed given one-off costs, the initial building C_{B0} of size l_B and width w_B and running costs, e.g. cost of energy for lighting, heating, air conditioning, which can be calculated by multiplying the space occupied by the assembly line with a factor E, representing the annual energy cost for each m^2.

$$C_B = K(x_{jkl}) \cdot L \cdot W[C_{B0} \cdot CRF_B/(l_b \cdot w_b) + E] \tag{4.31}$$

where $K(x_{jkl})$ represents the number of workstations assigned to the assembly line.

The objective function (4.5) and constraints associated with cost estimation are non-linear. For accuracy, no approximation in the form of a linear optimisation model is proposed.

4.4 Resolution methods

In recent years, nature-inspired meta-heuristic algorithms have gained huge popularity, because they have demonstrated some promising results in solving optimisation problems [424]. As depicted in Figure 3.14, among utilised multi-objective optimisation algorithms, following were identified: Ant Colony Algorithms, Genetic Algorithms, Bee Colony Algorithms, Particle Swarm Optimisation, and Cuckoo Search Algorithm.

While some work has been done to empirically compare Multi-Objective Ant Colony Optimisation algorithm by Rada-Vilela [333], to the best known of the author, the previous approximate methods have never been compared to each other for the ALBPs. In order to address this gap and solve the problem stated earlier, the algorithms present in Table 4.1 were developed.

Table 4.1: List of developed algorithms and their abbreviations

Algorithm's family	Name
Multi-Objective Ant Colony	BIANT-1
	BIANT-2
	CHAC-1
	CHAC-2
	MOACS-1
	MOACS-2
Discrete Multi-Objective Artificial Bee Colony	DMOABC
Discrete Multi-Objective Cuckoo Search Optimisation	DMOCSA-1-1
	DMOCSA-1-2
	DMOCSA-1-3
	DMOCSA-1-4
	DMOCSA-1-5
	DMOCSA-2-1
	DMOCSA-2-2
	DMOCSA-2-3
	DMOCSA-2-4
	DMOCSA-2-5
Discrete Multi-Objective Flower Pollination Algorithm	DMOFPA-1
	DMOFPA-2
	DMOFPA-3
	DMOFPA-4
	DMOFPA-5
Discrete Multi-Objective Bat Algorithm	MOBAT-1
	MOBAT-2
	MOBAT-3
	MOBAT-4
	MOBAT-5
Discrete Multi-Objective Particle Swarm Optimisation	MOPSO-1
	MOPSO-2
	MOPSO-3
	MOPSO-4
	MOPSO-5
Evolutionary Algorithm	NSGA-II
	SPEA2

Since the Bat Algorithm (BA), Artificial Bee Colony (ABC), Particle Swarm Optimisation (PSO), Flower Pollination Algorithm (FPA) algorithms were developed for continuous functions, in which bats, bees, particles and pollen move in the search space toward continuous position, it is impossible to directly exploit them and it requires an adaptation of their continuous encoding scheme. In order to use these algorithms, either their original form can be used by constructing a direct mapping relationship between the discrete variables and the vector of individuals or a discrete encoding scheme must be adapted. Krause *et al.* [225] proposed a survey of swarm algorithms applied to discrete optimisation problems and

presented several discretisation methods.

The general discrete encoding scheme that was used for all algorithms is presented in the next section.

4.4.1 General discrete encoding scheme

The general encoding scheme, which is common to all algorithms, can be summarised by their solution encoding, the initialisation of the population, the parent selection, the recombination and the mutation procedures. To simplify the notations in the upcoming section, the vocabulary is generalised; instead of using specific vocabulary for each algorithm, such as bats, swarms, or bees, the terms solutions, populations, and archives are used.

4.4.1.1 Solution Encoding

The individuals of a population represent a possible solution to optimisation problems. To evaluate the effectiveness of different solution representations, several critical issues are summarised by Gen et al [247], including: are:

1. Space - The solution encoding should not require extravagant amounts of memory
2. Time - The time required to evaluate, recombine, and mutate should be small
3. Heritability - Offspring of simple crossover should represent solutions that combine substructures of their parental solutions
4. Locality - A mutated solution should usually represent a solution similar to its parent
5. Uniqueness - The solution encoding scheme represents exactly one solution

In the field of ALBP, several encoding schemes can be found. Three encoding methods are introduced by Guo *et al.* [164], namely: (i) the workstation-oriented representation, (ii) the sequence-oriented representation and (iii) the operation-oriented representation. Other representations are the random key-based genetic representation used e.g. by Zhang and Gen [439] or by Nearchou [282]. Hamta *et al.* [170] propose an encoding scheme where individuals are represented by a permutation of tasks, and some negative integers, which show the assignment of tasks to workstations. Chica *et al.* [78] propose a similar encoding scheme, in which, real integers are used instead of negative integers. For both methods, the maximum number of separators is $N-1$. Kim *et al.* [215], Simaria and Vilarinho [369], Yu and Yin [431] use a workstation-oriented scheme of length N, where each element i represents the task i and its value j represents the workstation j to which the task will be assigned. Chen *et al.* [75] propose a solution encoding scheme composed of three vectors: (i) the first

part indicates the assignment of task i to workstation j, (ii) the second the assignment of operators type to the workstation j and the last part (iii) the number of operators assigned to workstation j.

The proposed solution encoding scheme is workstation-based. Since the solutions to the addressed problem are a list of tasks, equipment and station assignment, each solution has three vectors representing respectively: (i) the task number, TN, its equipment assignment, EA, and (ii) its station assignment, SA. The length of each vector is represented by N, the number of tasks. Depending on the number of alternative tasks, the used length of each vector may be less than N. An example of the solution encoding for the precedence graph shown in Figure 4.4 is represented in Figure 4.5. In this example, the tasks 5 and 6 represent precedence alternatives, and the tasks 4 and 7 are fictive nodes. In the provided example, the task 6 is selected and will be performed by the equipment 3 at station 2. The separators '-' and '*' represent dummy elements which do not represent any specific task, equipment or station assignment.

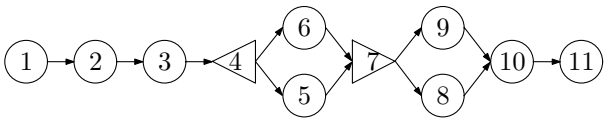

Figure 4.4: Example of precedence graph

Tasks	1	2	3	4	6	7	8	9	10	11	*
Equipment	1	2	1	-	3	-	2	1	10	2	*
Station	1	1	2	-	2	-	2	3	3	3	*

Figure 4.5: Example of the used solution encoding schema

4.4.1.2 Initial Solution

The population initialisation is a crucial task in optimisation since it directly affects the convergence speed and also the quality of the final solution. If no information about the solution is available, the most commonly used method to generate the initial population is random initialisation [312, 334]. In the proposed approach, a combination of 19 heuristics and a pseudo-random initialisation is used. Due to the existence of precedence relations among the tasks, it is not possible to generate populations in a random manner and eliminating infeasible solutions or replacing them with new solutions is time-consuming. Here, a constructive method satisfying the precedence relations and the choice of equipment is applied. The initialisation mechanism is as follows. First, a task from the ones without any predecessors is selected and assigned to the first position of the vector TN. In parallel, a

resource is selected out of the available resource set of this task and assigned to the first position of the vector EA. Afterwards, the set of tasks without any predecessors is updated and the next task and respective equipment are chosen. As soon as the station load exceeds the cycle time or the station space is reached, the workstation number is increased. This mechanism continues until no tasks can be assigned anymore.

4.4.1.3 Guide Selection

The selection of suitable solutions for recombination plays an important role in distinguishing between individuals based on their quality, such that the best individuals share their solution characteristics. For the EAs, a standard tournament method was used, choosing T_{size} individuals randomly from the population and selecting the best individual from this group as a parent. For the DMOCSA, DMOFPA, DMOBAT and DMOPS, several strategies that have been developed in the past are used. Examples of these strategies are: (i) the random strategy, which chooses an archive member randomly, (ii) the sigma method, introduced by Mostaghim and Teich [275], (iii) the minimum particle angle proposed by Gong *et al.* [157], (iv) the k-means strategy, proposed by Qiu *et al.* [328], and (v) the strip strategy [405]. These strategies were described in Chapter 3 and their differences are represented in Figure B.2. To differentiate the various strategies, following integers are used:

— *Name of the algorithm*-1: Random strategy
— *Name of the algorithm*-2: Sigmoid strategy
— *Name of the algorithm*-3: Minimum particle angle strategy
— *Name of the algorithm*-4: K-means strategy
— *Name of the algorithm*-5: Strip strategy

4.4.1.4 Recombination

The role of recombination is to generate new solutions from the selected solutions, in preference such that the offspring contains the desirable features of both parents. As stated by Yu and Yin [431], traditional two-point crossover or multi-point crossover are not suitable for combinatorial optimisation problems. The recombination step is carried out with a probability p_c, otherwise the individual with the best fitness value is copied into the offspring population. The recombination process between two solutions X and Y contains one component, F, and is formulated as follows:

$$F = p_c \otimes f(X,Y) = \begin{cases} f(X,Y), & \text{if } r < p_c \\ X, & \text{otherwise.} \end{cases} \tag{4.32}$$

where f represents a single-point crossover using a similarity vector $VS(X,Y)$ between the task assignments of two solutions X and Y, where an element $i, i = 1, ..., N$, of VS is given by:

$$VS_i(X_i, Y_i) = \begin{cases} i, & \text{if } X_{TN_i} = Y_{TN_i} \\ \emptyset, & \text{otherwise.} \end{cases} \tag{4.33}$$

The position of the crossover point c_p is randomly chosen out of VS. Figure 4.6 shows an example of crossover operation, where the similarity vector $VS = 1, 2, 3, 4, 5, 6, 9, 10$. From the two parents X and Y, the elements i of the offspring Z are generated as follows:

$$Z_i = \begin{cases} X_i, & \text{if } i \leq c_p \\ Y_i, & \text{otherwise.} \end{cases} \tag{4.34}$$

In other words, the offspring takes the element of the Parent X until the cutting point and in the same sequence order. The remaining elements are taken from the Parent Y.

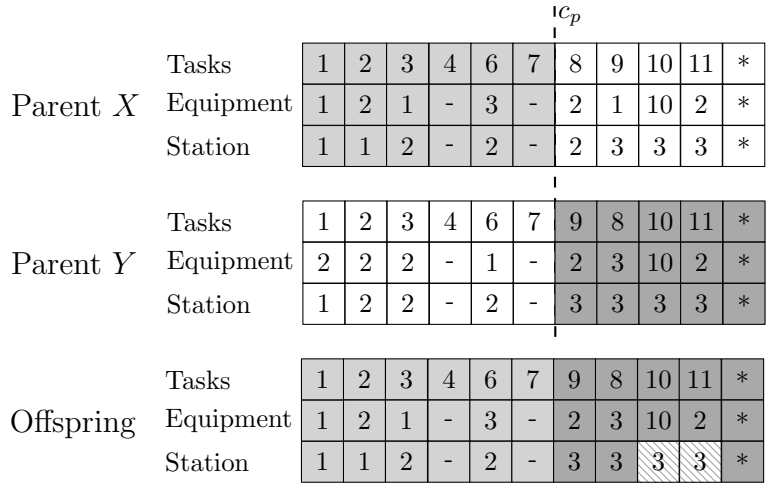

Figure 4.6: Example of recombination between two solutions

As represented with dashed lines in Figure 4.6, due to the verification of the preservation of the various constraints (e.g. cycle time and precedence constraints), some tasks and their respective resources have no valid workstation after the crossover process. In order to produce feasible individuals, these tasks must be reassigned. The reassignment procedure allocates the tasks to workstations, such that all the previously defined constraints are respected. For each task j to be reassigned, the procedure computes the earliest station M_E and the latest station M_L to which it can be assigned. When it is not possible to find a feasible workstation within $[M_E; M_L]$, a new workstation is opened and all successors of j will be reassigned.

4.4.1.5 Mutation

Once an offspring has been generated, another stochastic change is applied with probability p_m to enhance the diversity in the population and prevent the population to converge prematurely at local minima. The mutation process Z of one solution X, which contains four neighbourhood searches is formulated as follows:

$$Z = p_m \otimes X = \begin{cases} f(X), & \text{if } r < p_m \\ X, & \text{otherwise.} \end{cases} \tag{4.35}$$

If a random number is smaller than the mutation rate p_m, one of following mutation operator is randomly selected:

— Swap tasks: For a specific solution X, an element i is randomly selected, $i = rand(1, N-1)$. Let $F^*_{X_{TN_i}} := \{j|(i,j) \in E^*\}$ be the set of all successors of task X_{TN_i} and $P^*_{X_{TN_i}} := \{h|(h,i) \in E^*\}$ the set of all predecessors of task X_{TN_i}, where E^* represents the transitive closure of the set of arcs E. The set $NPT = V - X_{TN_i} - F^*_{X_{TN_i}} - P^*_{X_{TN_i}}$ represents the set of potential tasks that can be swapped with the task X_{TN_i}. A task j is randomly chosen out of NPT. If the task $j \in X_{TN}$, the elements of X_i and X_j are swapped, otherwise, $X_{TN_i} = j$ and an equipment is randomly selected for j. This allows not only to swap already assigned tasks, but also, in case of tasks alternatives, to replace a specific task by another alternative.

— Insert task: For a specific solution X, an element i is randomly generated, $i = rand(1, N-1)$. Let $BST = \{X_{TN_1}, ..., X_{TN_i-1}\}$ be the set of tasks already assigned before X_{TN_i}. The set $NPT = V - X_{TN_i} - F^*_{X_{TN_i}} - P^*_{X_{TN_i}} + F_{X_{TN_i}}$ represents the set of potential tasks before which the task X_{TN_i} can be inserted. A task j is randomly chosen as follows out of $NPT \cap BST$. The elements X_{TN_i}, X_{EA_i} and X_{SA_i} are inserted before the element h, s.t., $X_{TN_h} = j$.

— Change equipment: For a specific solution X, and a randomly selected element i, $i = rand(1, N-1)$, the current equipment assignment is replaced by a new one, randomly selected.

— Change station: For a specific solution X, and a randomly generated element i, $i = rand(1, N)$, the current workstation assignment is replaced by a new one, such that $X_{SA_i} = SI_{rand(1, L'_{X_{TN_i}})}$, where $L'_{X_{TN_i}}$ represents the latest workstation to which the task X_{TN_i} can be assigned. $L'_{X_{TN_i}} = min(L_{X_{TN_i}}; min_{j \in F^*_{X_{TN_i}}} X_{SA_j})$

In the case one of the selected mutation operators cannot change a given solution X, another mutation operator is randomly selected. The advantage of the proposed mutation operators is that they do not generate infeasible solutions regarding precedence constraints and only

the cycle time constraint or the station space need to be verified.

4.4.2 Evolutionary Algorithms

Among the EAs, the NSGA-II and SPEA2 are the two most widely used Multi-Objective algorithms in the literature [187]. This can be explained by their good results in various applications. Both algorithms use the framework previously described. The main differences between these algorithms are the diversity assignment and the replacement and archiving strategy. In the NSGA-II algorithm, the crowding-distance is used to maintain well spread non-dominated solutions, while in the SPEA2, the k-nearest neighbour approach is used. In addition, the NSGA-II uses elitist replacement, while the SPEA2 applies a general replacement strategy. Finally, the SPEA2 uses an archive set whereas the NSGA-II does not.

4.4.3 Multi-Objective Ant Colony Optimisation

An important number of proposals of ACO algorithms have shown their applicability to Multi-Objective optimization problems, especially for the line balancing problem, and they have generally provided good results. Examples of the application of ACO to solve ALBPs can be found in following works: [416, 434, 333, 83]. Rada-Vilela *et al.* [333] propose a comparative study of MOACO algorithm for the Time and Space Assembly Line Balancing Problem, in which they compare the influence of different components, such as the number of pheromone matrices and the number of heuristic functions. García-Martinez *et al.* [149] propose a taxonomy for MOPs based on two criteria: (i) number of structures to store the pheromone trail and (ii) the number of heuristic functions. Angus and Woodward [11] presented an alternative and extended study, which included five components used to classify MOACO.

Among the existing algorithms, this study focuses on those which utilise one or more pheromone matrix and multiple heuristic functions. Since the two objective functions being minimised are different, algorithms using single heuristic information were not considered in the present study. The following MOACOs were adapted (their differences are shown in Table 4.2).

— Bi-Criterion Ant - 1 (BIANT - 1)
— Bi-Criterion Ant - 1 (BIANT - 2)
— Multi-Objective Ant Colony System - 1 (MOACS -1)
— Multi-Objective Ant Colony System - 1 (MOACS -2)

— CHAC - 1
— CHAC - 2

Table 4.2: Taxonomy of MOACO and classification of proposed algorithms

Pheromone matrices	Heuristic Information Single	Multiple
Single	X	MOACS
Multiple	X	BIANT, CHAC

As demonstrated in Table 4.2, all the proposed algorithms use multiple heuristic information, which provides guidance about the preference of assigning a task with a specific equipment to an open workstation. Here, following heuristic information for respectively each objective function $\eta_{1_{i,j}}$ and $\eta_{2_{i,j}}$ [1] were used. The heuristics are computed as follows:

$$\begin{aligned} \eta_{1_{i,j}} &= \frac{t_j}{\bar{t}_{\sum}} \cdot \frac{|F_j|+1}{max_{u \in N_i^k} |F_u|+1} \\ \eta_{2_{i,j}} &= \frac{c_j}{\bar{c}_{\sum}} \cdot \frac{|F_j|+1}{max_{u \in N_i^k} |F_u|+1} \end{aligned} \tag{4.36}$$

where $\bar{t}_{\sum}$ and $\bar{c}_{\sum}$ represents the sum of the average task processing time and costs for each task, respectively. $\mid F_j \mid$ is the number of available tasks from j, and $max_{u \in N_i^k} \mid F_u \mid$ is the maximum number of tasks available from any task following j.

One major risk with ACO is the possibility of premature convergence during the search procedure leading to suboptimal solutions. To avoid this, the transition rule of all proposed algorithms will be extended with random selection, which is incorporated in all second variants of the proposed algorithms.

4.4.3.1 BIANT

The Bicriterion Ant (BIANT), which was proposed by Iredi *et al.* [186], uses two pheromone matrices and two heuristic functions, respectively one for each objective function. Through this, the search was conducted in different regions of the Pareto front.

BIANT-1

The pheromone update and evaporation were implemented for each matrix and only the Δ ants finding non-dominated solutions could update the pheromone matrices. The adapted

1. In the case of a MOACO algorithm uses a single heuristic $\eta_{i,j}$, the two previous heuristics are merged such as $\eta_{i,j} = \eta_{1_{i,j}} \eta_{2_{i,j}}$.

BIANT uses following transition rule:

$$p_{i,j}^k = \begin{cases} \frac{\tau_{1_{i,j}}^{\lambda_k \alpha} \cdot \tau_{2_{i,j}}^{(1-\lambda_k)\alpha} \cdot \eta_{1_{i,j}}^{\lambda_k \beta} \cdot \eta_{2_{i,j}}^{(1-\lambda_k)\beta}}{\sum_{u \in N_i^k} \tau_{1_{i,u}}^{\lambda_k \alpha} \cdot \tau_{2_{i,u}}^{(1-\lambda_k)\alpha} \cdot \eta_{1_{i,u}}^{\lambda_k \beta} \cdot \eta_{2_{i,u}}^{(1-\lambda_k)\beta}}, & \text{if } j \in N_i^k \\ 0, & \text{otherwise.} \end{cases} \tag{4.37}$$

where α and β are positive parameters whose values determine the relative importance of pheromones versus heuristic information. To regulate the weight of the various objectives in the search, $\lambda_k = \frac{k-1}{\Gamma-1}$, where Γ is the number of ants. The BIANT uses a roulette wheel to choose the next node in the solution path and performs a global pheromone updating strategy that includes evaporation in all nodes and contribution at the edges of non-dominated solutions in the current iteration. The evaporation is conducted as follows:

$$\begin{aligned} \tau_{1_{i,j}} &= (1-\rho) \cdot \tau_{1_{i,j}} \\ \tau_{2_{i,j}} &= (1-\rho) \cdot \tau_{2_{i,j}} \end{aligned} \tag{4.38}$$

and for the contribution:

$$\begin{aligned} \tau_{1_{i,j}} &= \tau_{1_{i,j}} + \tfrac{1}{f_1}, \forall (i,j) \in S_\Delta \\ \tau_{2_{i,j}} &= \tau_{2_{i,j}} + \tfrac{1}{f_2}, \forall (i,j) \in S_\Delta \end{aligned} \tag{4.39}$$

The definition of the contribution of the BIANT in (4.39) and the transition rule in (4.37) demonstrate that if the ranges of objective functions' values are different, the solutions will converge near one of the objective functions. To find better distributed solutions, a normalised schema is inevitable. The initial amount of deposed pheromone is calculated according to following expressions:

$$\begin{aligned} \tau_{1_{i,j}} &= \tfrac{1}{C_1} \\ \tau_{2_{i,j}} &= \tfrac{1}{C_2} \end{aligned} \tag{4.40}$$

where C_1 and C_2 represent the objective function value obtained using a greedy algorithm for solving the problem.

BIANT-2

In order to avoid early convergence, the transition rule of the BIANT-1 is extended with a random selection process as follows:

If $q > q_1$:

$$p_{i,j}^k = \begin{cases} \frac{\tau_{1_{i,j}}^{\lambda_k \alpha} \cdot \tau_{2_{i,j}}^{(1-\lambda_k)\alpha} \cdot \eta_{1_{i,j}}^{\lambda_k \beta} \cdot \eta_{2_{i,j}}^{(1-\lambda_k)\beta}}{\sum_{u \in N_i^k} \tau_{1_{i,u}}^{\lambda_k \alpha} \cdot \tau_{2_{i,u}}^{(1-\lambda_k)\alpha} \cdot \eta_{1_{i,u}}^{\lambda_k \beta} \cdot \eta_{2_{i,u}}^{(1-\lambda_k)\beta}}, \text{if } j \in N_i^k \\ 0, \text{ otherwise.} \end{cases} \tag{4.41}$$

Else :

$$p_{i,j}^k = \text{random selection of } j \in N_i^k$$

where $q_1 \in [0,1]$ is a pre-defined constant.

4.4.3.2 MOACS

Baran *et al.* [24] proposed the MOACS, which uses a single pheromone matrix for both objectives.

MOACS-1

The transition rule works as follows:

$$\begin{aligned} &\text{If } q \leq q_0: \\ &\qquad p_{i,j}^k = \begin{cases} 1 & \text{if } j = max_{u \in N_i^k}\{\tau_{i,u} \cdot \eta_{1_{i,u}}^{\beta\lambda} \cdot \eta_{2_{i,u}}^{\beta(1-\lambda)}\} \\ 0, & \text{otherwise.} \end{cases} \\ &\text{Else}: \\ &\qquad p_{i,j}^k = \begin{cases} \frac{\tau_{i,j} \cdot \eta_{1_{i,j}}^{\beta\lambda} \cdot \eta_{2_{i,j}}^{\beta(1-\lambda)}}{\sum_{u \in N_i^k} \tau_{i,u} \cdot \eta_{1_{i,u}}^{\beta\lambda} \cdot \eta_{2_{i,u}}^{\beta(1-\lambda)}}, & \text{if } j \in N_i^k \\ 0, & \text{otherwise.} \end{cases} \end{aligned} \tag{4.42}$$

When an ant k is building a solution path and is placed at one node i, a random number $q \in [0,1]$ is generated and if $q \leq q_0$, the best neighbour j is selected as the next node in the path. Otherwise, the algorithm decides which node is the next by using a roulette wheel considering $p_{i,j}^k$ as probability of every feasible neighbour $j \in N_i^k$. Since the MOACS is an ACS, there are two levels of pheromone update: local and global. The local pheromone update is given by:

$$\tau_{i,j} = (1-\rho) \cdot \tau_{i,j} + \rho \cdot \tau_0, \text{ with } \tau_0 = \frac{1}{C_1 \cdot C_2} \tag{4.43}$$

The MOACS uses a reinitialisation pheromone mechanism. Every time an ant k builds a solution, it is compared to the current Pareto front PF to determine whether it is a non-dominated solution. At the end of each iteration, $\tau_0^{'}$ is calculated as follows:

$$\tau_0^{'} = \frac{1}{\bar{f}_1 \cdot \bar{f}_2} \tag{4.44}$$

where $\bar{f}_1$ and $\bar{f}_2$ represent the average costs in each objective for the solution paths currently included in the current archive. If $\tau_0^{'} > \tau_0$, the pheromone trails are reinitialised considering $\tau_0 \leftarrow \tau_0^{'}$. Otherwise, the global pheromone updating is performed for all Δ solutions in the Pareto set, as follows:

$$\tau_{i,j} = (1-\rho) \cdot \tau_{i,j} + \frac{\rho}{f_1 \cdot f_2}, \forall (i,j) \in S_\Delta \tag{4.45}$$

MOACS-2

Similar to the BIANT, the transition rule of the MOACS is also extended with a random selection process to avoid early convergence as follows:

$$\begin{aligned}
&\text{If } q_1 < q \leq q_0: \\
&\qquad p_{i,j}^k = \begin{cases} 1 & \text{if } j = max_{u \in N_i^k}\{\tau_{i,u} \cdot \eta_{1_{i,u}}^{\beta\lambda} \cdot \eta_{2_{i,u}}^{\beta(1-\lambda)}\} \\ 0, & \text{otherwise.} \end{cases} \\
&\text{If } q > q_0: \\
&\qquad p_{i,j}^k = \begin{cases} \frac{\tau_{i,j} \cdot \eta_{1_{i,j}}^{\beta\lambda} \cdot \eta_{2_{i,j}}^{\beta(1-\lambda)}}{\sum_{u \in N_i^k} \tau_{i,u} \cdot \eta_{1_{i,u}}^{\beta\lambda} \cdot \eta_{2_{i,u}}^{\beta(1-\lambda)}}, & \text{if } j \in N_i^k \\ 0, & \text{otherwise.} \end{cases} \\
&\text{If } q \leq q_1: \\
&\qquad p_{i,j}^k = \text{random selection of } j \in N_i^k
\end{aligned} \tag{4.46}$$

4.4.3.3 CHAC

Mora *et al.* [272] proposed the so-called CHAC, which is an ACS with some features of both BIANT (same combined state transition rule) and MOACS (local and global pheromone update with no reinitialisation of the pheromone matrices) using a combined heuristic and pheromone information of both objectives.

CHAC-1

The transition rule is as follows:

$$\begin{aligned}
&\text{If } q \leq q_0: \\
&\qquad p_{i,j}^k = \begin{cases} 1 & \text{if } j = max_{u \in N_i^k}\{\tau_{1_{i,u}}^{\alpha\lambda_k} \cdot \tau_{2_{i,u}}^{\alpha(1-\lambda_k)} \cdot \eta_{1_{i,u}}^{\beta\lambda_k} \cdot \eta_{2_{i,u}}^{\beta\cdot(1-\lambda_k)}\} \\ 0, & \text{otherwise.} \end{cases} \\
&\text{If } q > q_0: \\
&\qquad p_{i,j}^k = \begin{cases} \frac{\tau_{1_{i,j}}^{\alpha\lambda_k} \cdot \tau_{2_{i,j}}^{\alpha(1-\lambda_k)} \cdot \eta_{1_{i,j}}^{\beta\lambda_k} \cdot \eta_{2_{i,j}}^{\beta\cdot(1-\lambda_k)}}{\sum_{u \in N_i^k} \tau_{1_{i,u}}^{\alpha\lambda_k} \cdot \tau_{2_{i,u}}^{\alpha(1-\lambda_k)} \cdot \eta_{1_{i,u}}^{\beta\lambda_k} \cdot \eta_{2_{i,u}}^{\beta\cdot(1-\lambda_k)}}, & \text{if } j \in N_i^k \\ 0, & \text{otherwise.} \end{cases}
\end{aligned} \tag{4.47}$$

The local pheromone update is calculated as follows:

$$\begin{aligned}
\tau_{1_{i,j}} &= (1-\rho) \cdot \tau_{1_{i,j}} + \rho \cdot \tfrac{1}{C_1} \\
\tau_{2_{i,j}} &= (1-\rho) \cdot \tau_{2_{i,j}} + \rho \cdot \tfrac{1}{C_2}
\end{aligned} \tag{4.48}$$

and the global pheromone is determined by the following equations:

$$\begin{aligned} \tau_{1_{i,j}} &= (1-\rho)\cdot\tau_{1_{i,j}} + \frac{\rho}{f_1} \\ \tau_{2_{i,j}} &= (1-\rho)\cdot\tau_{2_{i,j}} + \frac{\rho}{f_2} \end{aligned} \tag{4.49}$$

where, f_1 and f_2 are the objective function values of all members in the current archive.

CHAC-2

The CHAC-2 uses following transition rule:

$$\begin{aligned} &\text{If } q_1 < q \leq q_0: \\ &\qquad p_{i,j}^k = \begin{cases} 1 & \text{if } j = max_{u\in N_i^k}\{\tau_{1_{i,u}}^{\alpha\lambda_k}\cdot\tau_{2_{i,u}}^{\alpha(1-\lambda_k)}\cdot\eta_{1_{i,u}}^{\beta\lambda_k}\cdot\eta_{2_{i,u}}^{\beta\cdot(1-\lambda_k)}\} \\ 0, & \text{otherwise.} \end{cases} \\ &\text{If } q > q_0: \\ &\qquad p_{i,j}^k = \begin{cases} \frac{\tau_{1_{i,j}}^{\alpha\lambda_k}\cdot\tau_{2_{i,j}}^{\alpha(1-\lambda_k)}\cdot\eta_{1_{i,j}}^{\beta\lambda_k}\cdot\eta_{2_{i,j}}^{\beta\cdot(1-\lambda_k)}}{\sum_{u\in N_i^k}\tau_{1_{i,u}}^{\alpha\lambda_k}\cdot\tau_{2_{i,u}}^{\alpha(1-\lambda_k)}\cdot\eta_{1_{i,u}}^{\beta\lambda_k}\cdot\eta_{2_{i,u}}^{\beta\cdot(1-\lambda_k)}}, & \text{if } j\in N_i^k \\ 0, & \text{otherwise.} \end{cases} \\ &\text{If } q \leq q_1: \\ &\qquad p_{i,j}^k = \text{random selection of } j\in N_i^k \end{aligned} \tag{4.50}$$

4.4.4 Discrete Multi-Objective Artificial Bee Colony Optimisation

Similar to all meta-heuristics presented in this section, the basic ABC algorithm was originally designed for continuous function. In order to apply it here, a novel discrete variant of the ABC algorithm is proposed in this section. Different discrete ABCs have been proposed in the literature to solve different problems, particularly for flow shop scheduling problem [311, 250, 97]. In the basic ABC, a fitness value is assigned to each solution, which is used in a stochastic selection strategy to select individuals for mutation. Given that a multi-objective problem must be solved, another fitness assignment strategy is required. The following fitness assignment technique proposed by Zou *et al.* [413] and used by Akay [1], is used:

$$f_i = R(i) - TS(i) - d(i) \tag{4.51}$$

where $R(i)$ is the Pareto rank value of an individual i, which is represented by the number of solutions n_i that dominate this solution. The second term $S(i) = -p_T(i)log(p_T(i))$, where $T > 0$ is the temperature. $p_T(i) = (1/Z)exp^{-R(i)/T)}$ is the Gibbs distribution, $Z = \sum_{i=1}^{PopSize} exp^{(-R(i)/T)}$ is called the partition function and $d(i)$ is the crowding distance calculated by a density estimation technique similar to the one used in the proposed NSGA-II [105]. Since the best individuals will have low values of f_i, the fitness of an individual i,

f_i will be calculated as follows:

$$fitness_i = 1/f_i \tag{4.52}$$

Furthermore, the onlooker bee will choose a food source depending on the probability value associated with that food source, which is given by:

$$p_i = \frac{fitness_i}{\max_{j=1,...,PopSize}(fitness_j)} \tag{4.53}$$

The various steps of the proposed Discrete Multi-Objective Artificial Bee Colony (DMOABC), which are similar to the classical ABC, are summarised in the Algorithm 1. At each generation t, for each solution X_i^t, $i = 1, ..., PopSize$, a new solution $X_i'^t$ is generated using the equation (4.35). If the new solution $X_i'^t$ dominates the old solution, then the new solution is accepted. Otherwise, the old solution is kept and the number of trials, $trial(i)$, is updated. This process represents the employed bees. After this process, the onlookers obtain the information of the food sources from all employed bees and choose a food source depending on the probability value associated with that food source, which is defined by (4.53). Each time a new solution $X_i'^t$ is accepted during this process, the archive is updated and the number of trials is set to 0. After this process, the sources are checked to determine whether they will be abandoned. When a source is abandoned, a new solution is generated randomly.

Algorithm 1 Discrete Multi-Objective Artificial Bee Colony

Objective function $f(X), X = (X_1, ..., X_{PopSize})^T$
Initialise the X_i food sources, $\forall i = 1, ..., PopSize$
Evaluation the Fitness f_i of each solution i, $\forall i = 1, ..., PopSize$
while $t < Iteration_{max}$ or (Stop Criterion) **do**
    for i=1:PopSize **do**
        Generate a new solution X'_i with equation (4.35)
        Evaluate the fitness values of X'_i
        if $X' \preceq X$ **then**
            Replace X_i by X'_i and respective fitness values
        else
            $trial(i) = trial(i) + 1$
        Assign fitness values f_i using (4.51) and (4.52)
        Calculate probabilities for onlookers using (4.53)
    $s = 0, t = 0$
    while $t < PopSize/2$ **do**
        if $rand < p_s$ **then**
            $t = t + 1$
            Generate a new solution $X'(s)$ with equation (4.35)
            Evaluate the fitness values of $X'(s)$
            if $X' \preceq X$ **then**
                Replace $X(s)$ by $X'(s)$ and respective fitness values
                $trial(s) = 0$
                Update Archive Ar
            else
                $trial(s) = trial(s) + 1$
        $s = (s + 1) mod(PopSize - 1)$
    for i=1:PopSize **do**
        if $trial(i) > limit$ and $X_i \notin Ar$ **then**
            Generate a random solution $X(s)$
            $trial(i) = 0$

4.4.5 Discrete Multi-Objective Cuckoo Search Algorithm

Different discrete cuckoo search algorithms have recently been proposed for solving the 0-1 knapsack problem [153], job-shop scheduling problem [303], flow-shop scheduling problem [163], and the travelling salesman problem [302]. Since the Lévy flights have the characteristics of an intensive search around the solution, but also of big steps in the long run, its generated value was associated to the developed Discrete Multi-Objective Cuckoo Search Algorithm (DMOCSA) in order to select the choice of perturbation operators. Any move in the search space can be realised through a small change, a number of k successive changes and a big move. In order to facilitate the control of these moves via Lévy flights, they are

associated with an interval between 0 and 1. According to the value given by the Lévy flight in this interval, the appropriate change operator can be chosen (presented in Section 4.4.1.4 and 4.4.1.5). The interval is divided into the following five parts:

— Value of Lévy flight in $[0, 0.2[\rightarrow$ one change through the mutation operator explained earlier in Section 4.4.1.5
— Value of Lévy flight in $[0.2, 0.4[\rightarrow$ two changes through the mutation operator explained earlier in Section 4.4.1.5
— Value of Lévy flight in $[0.4, 0.6[\rightarrow$ three changes through the mutation operator explained earlier in Section 4.4.1.5
— Value of Lévy flight in $[0.6, 0.8[\rightarrow$ four changes through the mutation operator explained earlier in Section 4.4.1.5
— Value of Lévy flight in $[0.8, 1[\rightarrow$ Big change through the crossover operator between selected solution and one solution of the current archive explained earlier in Section 4.4.1.4 using the selection strategies explained in Section 4.4.1.3

Two main variants proposed are as follows:

— DMOCSA-1
— DMOCSA-2

While the DMOCSA-1 uses a static parameter control to abandon and create new solutions, the DMOCSA-2 uses a dominance ratio (DR) to control the creation of new solutions. For a given solution i, the number of solutions it is dominated by is given by s_i. The dominance ratio DR_i for this solution i is calculated as follows:

$$DR_i = \frac{s_i}{\sum_{j=1}^{PopSize} s_j} \tag{4.54}$$

Thus, instead of abandoning a fraction p_a at each iteration, the solutions with the highest dominance ratio will be stochastically abandoned. The advantage of this threshold is that until convergence, this threshold will decrease as the population is converging toward the Pareto front. Thus, at each iteration, a solution i is replaced by a new one if $rand > DR_i$.

The main steps of the proposed algorithm are depicted in Algorithm 2.

Algorithm 2 Discrete Multi-Objective Cuckoo Search Algorithm

Objective function $f(X), X = (X_1, ..., X_{PopSize})^T$
Initialise the X_i host nest, $\forall i = 1, ..., PopSize$
Evaluation the fitness $f(X_i)$ of each solution X_i, $\forall i = 1, ..., PopSize$
while $t < Iteration_{max}$ or (Stop Criterion) **do**
    Start searching with a fraction (p_c) of solution
    Get a new cuckoo X_i using the Lévy flight's value
    Evaluate the fitness $f(X_i)$
    Choose a nest among j randomly
    if $f(X_i) \preceq f(X_j)$ **then**
        Replace j by the new solution
    A fraction p_a of worse nests are abandoned and new ones are created
    Sort and find optimal solutions and update archive

4.4.6 Discrete Multi-Objective Flower Pollination Algorithm

As with the previous algorithms, the FPA cannot be used for discrete optimisation. The principle of the proposed discrete multi-objective flower pollination algorithm is similar to the discrete CSA. In the Discrete Multi-Objective Flower Pollination Algorithm (DMOFPA), any move in the search space can be realised through a global or a local pollination. In order to facilitate the control of the global pollination via Lévy flights, an identical interface to that of the DMOCSA is used. According to the value obtained by the Lévy flights, the right operator is chosen (as presented in Section 4.4.1.5 and 4.4.1.4). For the global pollination, a solution gB_i^t is selected out of the archive and a crossover is applied. For the local pollination, as illustrated in Figure 4.7, a Euclidean distance between a specific solution i and all others is used. The two neighbours j and k that are the closest neighbours of the solution i will be used for the local pollination update as follows:

$$X_i^{t+1} = f_2\{[X_i^t, (f_1(X_j^t, X_k^t)]\} \tag{4.55}$$

First a crossover f_1 is applied between both solution X_j and X_k, then a second crossover f_2 is applied between the obtained solution and X_i. Both crossovers are explained in Section 4.4.1.4.

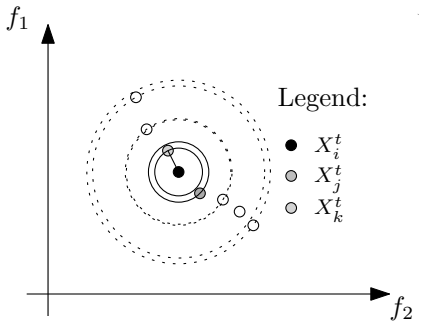

Figure 4.7: Illustration of the selection of the two solutions in the DMOFPA for the local pollination

Algorithm 3 Discrete Multi-Objective Flower Pollination Algorithm

```
Objective function f(X), X = (X_1, ..., X_PopSize)^T
Initialise the X_i flowers/pollen, ∀i = 1, ..., PopSize
Evaluation the Fitness f(X_i) of each solution i, ∀i = 1, ..., PopSize
while t < Iteration_max or (Stop Criterion) do
    for i=1:PopSize do
        if rand < p then
            Perform Global Pollination X_i using the Lévy flight's value
        else
            Choose j and k among closest solutions to i
            Perform Local Pollination
        Evaluate the fitness f(X_i)
        Update archive
    Sort and find optimal solutions and update archive
```

4.4.7 Discrete Multi-Objective Bat Algorithm

Different discrete bat algorithms have been proposed lately for e.g. solving the travelling salesman problem[352, 351] or the flowshop scheduling problem [253]. Similar to Hassan *et al.* [172], a difference operator d_i between the bat position X_i and the best bat position gB_i was used to generate new solutions in the proposed Discrete Multi-Objective Bat Algorithm (DMOBAT).

$$d_i = (X_i^t - gB_i^t) = \begin{cases} 1 & \text{if } X_i^t \neq gB_i^t \\ -1, & \text{otherwise.} \end{cases} \tag{4.56}$$

Using the velocity vector V_i^t of a solution i, and the difference operator, the new position value will be updated using following equation:

$$X_i^t = V_i^t \otimes f_2(X_i^{t-1}, gB_i^{t-1}) = \begin{cases} f_2(X_i^{t-1}, gB_i^{t-1}), & \text{if } V_i^t \geq 1 \\ X_i^{t-1}, & \text{otherwise.} \end{cases} \tag{4.57}$$

where f_2 uses the crossover mechanism explained earlier in section 4.4.1.4. The velocity and frequency vectors V_i^t and f_i are updated as follows:

$$f_i = f_{min} + (f_{max} - f_{min}) \cdot \beta \tag{4.58}$$

$$V_i^t = V_i^{t-1} + d_i \cdot f_i \tag{4.59}$$

Additionally, the local solution around a best solution gB_i^t is achieved through the mutation mechanism also explained earlier in section 4.4.1.5. The steps of the algorithm, which are presented below, are summarised in Algorithm 4.

Algorithm 4 Discrete Multi-Objective Bat Algorithm

Objective function $f(x), x = (X_1, ..., X_{PopSize})^T$
Initialise the bat population X_i and V_i, $, \forall i = 1, ..., PopSize$
Define pulse frequency f_i at X_i
Initialise pulse rates r_i and the loudness A_i
while $t < Iteration_{max} or (Stop\ Criterion)$ **do**
    Generate new solutions by adjusting frequency, and updating velocities and locations according to equations (4.58)-(4.59) and (4.56)-(4.57)
    if $rand > r_i$ **then**
        Select a best solution out of the archive
        Generate a local solution around the selected best solution
    Generate a new solution by flying randomly
    if $rand < A_i$ and $\nexists X_j \in Ar,\ f(X_i) \preceq fX_j$ **then**
        Accept the new solutions and update Archive
        Increase r_i and reduce A_i

The loudness A_i and pulse rate r_i are updated using the original equations, as follows:

$$A_i^{t+1} = \alpha_B \cdot A_i^t \tag{4.60}$$

$$r_i^{t+1} = r_i^0 \cdot [1 - e^{-\gamma \cdot t}] \tag{4.61}$$

4.4.8 Discrete Multi-Objective Particle Swarm

The global search of the proposed discrete Multi-Objective Particle Swarm Optimisation algorithm is conducted by updating the position of particles of the Discrete Multi-Objective Particle Swarm Optimisation (DMOPSO) as successfully proposed by Pan *et al.* [310] to solve a flow shop scheduling problem and by Zhang *et al.* [437] to solve a job shop scheduling problem. The position of a particle is updated as follows:

$$X_i^{t+1} = C_2 \otimes f_3\{[C_1 \otimes f_2(C_3 \otimes f_1(X_i^t), pB_i^t], gB^t\} \tag{4.62}$$

Where, X_i^t is the i-th particle at the t-th generation, C_3 is the inertia weight, C_1 and C_2 are acceleration coefficients between $[0, 1]$. pB_i^t and gB_i^t are respectively the best personal and

global best position of the swarm population at t-th generation, f_1, f_2 and f_3 are operations. The updating process contains three components, E_i^t, F_i^t and X_i^t and are formulated as follows:

$$E_i^t = C_3 \otimes f_1(X_i^t) = \begin{cases} f_1(X_i^t), & \text{if } r < C_3 \\ X_i^t, & \text{otherwise.} \end{cases} \tag{4.63}$$

where $r \in [0, 1]$ is a uniform random number, and $\otimes$ represent the crossover operation. According to (4.63), if $r < C_3$, then $f_1(X_i^t)$, which represents some neighbourhood search used to enhance the quality of the solution is carried out.

$$F_i^t = C_1 \otimes f_2(E_i^t, X_i^t) = \begin{cases} f_2(E_i^t, X_i^t), & \text{if } r < C_1 \\ E_i^t, & \text{otherwise.} \end{cases} \tag{4.64}$$

f_2 is applied between a given solution X_i^t and its current best position, pB_i^t, if $r < C_1$. The same mechanism is applied in f_3 between a given solution X_i^t and one global best position gB_i^t, when $r < C_2$. The operator f_1 uses the mutation mechanism explained earlier in section 4.4.1.5. The operators f_2 and f_3 uses the crossover mechanism explained earlier in section 4.4.1.4. The selection of the best particle gB_i^t is based on the strategies explained earlier in Section 4.4.1.3.

4.5 Computational results

In this section, various approximate methods are compared. Approximate algorithms are often used in optimisation due to a lack of knowledge about the fitness landscapes of the optimisation problem. However, the parameter setting of these approximate algorithms can greatly influence their performances [223]. The sensitivity of the parameter values to a specific problem explains why approximate algorithms can perform well on one type of problem and poorly on another. Thus, the success of approximate algorithms depends on adequate parameter settings. The present section is organised as follows: First the problem instances under consideration are presented. Then, the quality indicators and the various approximate methods that were used are compared based on the presented problem instances and the quality indicators.

4.5.1 Problem instances

Several experiments have been conducted to test the proposed model and algorithms. These experiments use different well-known problem instances that are available at www.assembly-

line-balancing.de. These instances include *Arc111*, *Buxey*, *Gunther*, *Hahn*, *Jackson*, *Kilbrid*, *Lutz1*, *Mitchell*, *Mukherje*, *Roszieg*, and *Sawyer*. All these instances, which belong to the ASALBP formulation, were adapted to the problem of this study. The problem instances and their characteristics are summarised in Table 4.3. Due to their different problem characteristics, these instances provide sufficient diversity to compare the algorithms. These characteristics are represented by (i) the mean order strength of the precedence graph (OS represents the mean order strength of the product design alternatives), (ii) the number of tasks (N), (iii) the number of subgraph or product design alternatives (PDA) and (iv) the total number of available resources E_{tot} (Table 4.3). Problems marked with an asterix (*) are solved with the TPM method. Therefore, they are are problems for which the true Pareto front is also known. For the remaining problems, a pseudo-optimal Pareto front was constructed, which combines all of the solutions that the algorithms identify and removes the dominated solutions. The process of constructing the pseudo-optimal Pareto front is shown in Figure 4.8. In this figure, the Pareto front obtained by the DMOABC, DMOBAT-1, BIANT, MOACS-1 and NSGA-II are respectively represented in red, blue, green, orange and yellow. Out of these sets of non-dominated solutions, the pseudo-optimal Pareto front is extracted and is represented by the black points.

The required processing time to obtain the true Pareto front for the problems marked with an asterix (*) are shown in Table 4.4. The time to obtain the real Pareto front is growing exponentially, indicating that the TPM is not suitable for large problem instances.

Figure 4.9 provides an example of the true Pareto front obtained through TPM and the approximate Pareto front for the Lutz1-4 and Arc111-1 problems, respectively. Some of the obtained Pareto fronts are shown in Appendix C.1.

Table 4.3: Problem characteristics of the various instances

Problem	N	OS	PDA	E_{tot}	Problem	N	OS	PDA	E_{tot}
Arc111-1	125	0.181	6	636	Gunther-1	41	0.378	2	220
Arc111-2	125	0.181	6	578	Gunther-2	41	0.378	2	209
Arc111-3	125	0.181	6	555	Gunther-3	41	0.364	2	209
Arc111-4	125	0.185	6	555	Gunther-4	41	0.353	2	209
Arc111-5	125	0.178	6	505	Gunther-5	41	0.353	2	194
Buxey-1	32	0.334	2	166	Hahn-1	68	0.348	5	363
Buxey-2	32	0.330	2	154	Hahn-2	68	0.348	5	339
Buxey-3	32	0.322	2	152	Hahn-3	68	0.343	5	339
Buxey-4	32	0.322	2	138	Hahn-4	68	0.345	5	339
Buxey-5	32	0.333	2	138	Hahn-5	68	0.345	5	304
Jackson-1*	15	0.442	2	28	Lutz1-1*	37	0.570	2	48
Jackson-2*	15	0.442	2	30	Lutz1-2*	37	0.553	2	47
Jackson-3*	15	0.442	2	37	Lutz1-3*	37	0.524	2	49
Jackson-4*	15	0.442	2	29	Lutz1-4*	37	0.530	2	51
Jackson-5*	15	0.442	2	31	Lutz1-5*	37	0.530	2	50
Kilbrid-1	50	0.641	2	70	Mitchell-1*	27	0.579	2	52
Kilbrid-2	50	0.641	2	76	Mitchell-2*	27	0.579	2	46
Kilbrid-3	50	0.641	2	87	Mitchell-3*	27	0.432	3	71
Kilbrid-4	50	0.622	2	87	Mitchell-4*	27	0.579	2	50
Kilbrid-5	50	0.600	2	87	Roszieg-1*	28	0.504	2	46
Mukherje-1	105	0.124	5	547	Roszieg-2*	28	0.547	2	42
Mukherje-2	105	0.124	5	517	Roszieg-3*	28	0.610	2	47
Mukherje-3	105	0.124	5	507	Roszieg-4*	28	0.605	2	39
Sawyer-1*	33	0.539	2	40	Sawyer-3*	33	0.539	2	45
Sawyer-2*	33	0.539	2	39	Sawyer-4*	33	0.539	2	44

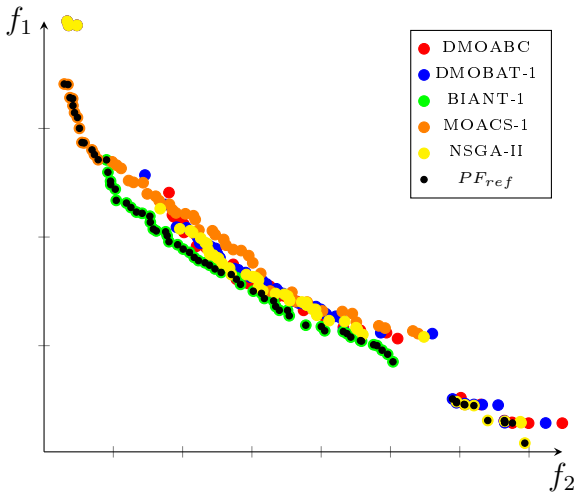

Figure 4.8: Extraction of the Reference-Pareto front for the Arc111-1 problem

Table 4.4: Results of the TPM method

Problem	PS	t (hh:mm:ss)	Problem	PS	t (hh:mm:ss)
Jackson-1	8	00:00:09	Mitchell-2	16	10:45:13
Jackson-2	8	00:00:10	Mitchell-3	5	03:50:11
Jackson-3	5	00:01:51	Mitchell-4	11	06:56:43
Jackson-4	13	00:01:16	Roszieg-1	9	19:04:02
Jackson-5	13	00:01:10	Roszieg-2	10	16:51:20
Kilbrid-1	27	11:46:50	Roszieg-3	15	19:46:50
Lutz1-1	10	01:37:56	Roszieg-4	2	00:08:36
Lutz1-2	19	01:58:33	Sawyer-1	2	00:05:08
Lutz1-3	14	10:11:32	Sawyer-2	5	01:04:21
Lutz1-4	34	21:42:04	Sawyer-3	11	00:34:23
Lutz1-5	33	19:56:47	Sawyer-4	22	07:16:54

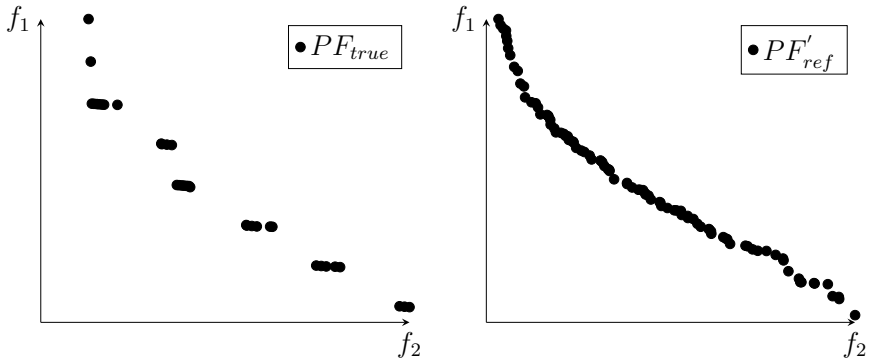

(a) True Pareto front for the Lutz1-4 Problem

(b) Approximate Pareto front for the Arc111-1 Problem

Figure 4.9: Comparison of the true and approximate Pareto front for two problem instances

4.5.2 Parameter settings

The parameter space can be explored before or during the search [224, 377, 102]. These two cases are respectively classified as parameter tuning and parameter control [203]. Several methods, which are shown in Figure 4.10, can be used when tuning parameters, including: (i) by hand, (ii) Design of Experiments (DOE), and (iii) meta-evolution. In the first case, parameters are defined based on the decision makers' experience. In the second case, statistical tools such as the Design of Experiments are used to choose the best parameter values. Bartz-Beielstein [28] discusses the role of experimental research in evolutionary computation. DOE is a systematic method for determining the relationship between factors that affect a process and its output by deliberately changing one or more factors to observe the effects on the process's output. In the last case, the evolutionary optimisation process occurs on two levels. On the first level, an outer optimisation algorithm tunes the parameters of an

embedded algorithm. On the second level, the parameter values are changed during optimisation; deterministic, adaptive, and self-adaptive methods can be found in this category. In the former case , the parameters are adjusted according to a fixed scheme, depending on e.g. the number of generations. In the second case, the parameters are changed according to predefined rules. In the last case , the parameter changes according to pre-defined functions.

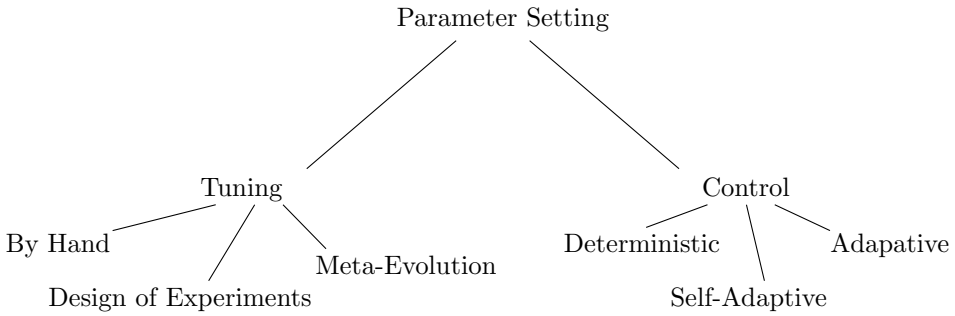

Figure 4.10: Parameter setting in EA cf. [224, 377]

To compare all the developed approximate methods efficiently, an the parameter space was explored before the search procedure. The parameters and their range, and the levels for each approximate method are respectively shown in Tables 4.5 to 4.17[2]. The assessment of the parameter values is based on the *Arc111-1* problem of Table 4.3. This problem, with its low order strength, high number of product design alternatives and high number of resources, is the most complicated problem over all tested problems instances.

Table 4.5: Factors and their levels for the DMOABC

Factor	Levels	Values
A PopSize (population size)	3	100, 150, 200
B *limit* (trials limit)	5	25, 50, 75, 100, 125

Table 4.6: Factors and their levels for the DMOBAT

Factor	Levels	Values
A PopSize (population size)	3	100, 150, 200
B (γ) (Adaptation parameter for pulse rate)	9	0.8, 0.85, 0.9, 0.92, 0.94, 0.96, 0.97, 0.98, 0.99
C (α_B) (Adaptation parameter for loudness)	9	0.1, 0.2, 0.3, 0.4, 0.5, 0.6, 0.7, 0.8, 0.9

2. The reader will note that the size of the archive for all the approximate methods was fixed to 50

Table 4.7: Factors and their levels for the BIANT-1

Factor	Levels	Values
A PopSize (population size)	3	100, 150, 200
B α (pheromone importance)	3	1, 2, 3
C β (heuristics importance)	3	1, 3, 5
D ρ (evaporation rate)	9	0.1, 0.2, 0.3, 0.4, 0.5, 0.6, 0.7, 0.8, 0.9

Table 4.8: Factors and their levels for the BIANT-2

Factor	Levels	Values
A PopSize (population size)	3	100, 150, 200
B α (pheromone importance)	3	1, 2, 3
C β (heuristics importance)	3	1, 3, 5
D ρ (evaporation rate)	9	0.1, 0.2, 0.3, 0.4, 0.5, 0.6, 0.7, 0.8, 0.9
E q_1 (Transition rule rate)	3	0.1, 0.2, 0.3

Table 4.9: Factors and their levels for the CHAC-1

Factor	Levels	Values
A PopSize (population size)	3	100, 150, 200
B α (pheromone importance)	3	1, 2, 3
C β (heuristics importance)	3	1, 3, 5
D q_0 (Transition rule rate)	9	0.1, 0.2, 0.3, 0.4, 0.5, 0.6, 0.7, 0.8, 0.9
E ρ (evaporation rate)	5	0.1, 0.2, 0.3, 0.4, 0.5

Table 4.10: Factors and their levels for the CHAC-2

Factor	Levels	Values
A PopSize (population size)	3	100, 150, 200
B α (pheromone importance)	3	1, 2, 3
C β (heuristics importance)	3	1, 3, 5
D q_0 (Transition rule rate)	8	0.1, 0.2, 0.3, 0.4, 0.5, 0.6, 0.7, 0.8
E ρ (evaporation rate)	4	0.1, 0.2, 0.3, 0.4
F q_1 (Transition rule rate)	3	0.1, 0.2, 0.3

Table 4.11: Factors and their levels for the DMOCSA

Factor	Levels	Values
A PopSize (population size)	3	100, 150, 200
B p_c (Crossover rate)	9	0.5, 0.55, 0.60, 0.65, 0.70, 0.75, 0.80, 0.85, 0.90
C p_a (Abandonment rate)	5	0.05, 0.10, 0.15, 0.20, 0.25

Table 4.12: Factors and their levels for the DMOFPA

Factor	Levels	Values
A PopSize (population size)	3	100, 150, 200
B p (Threshole global/local pollination)	9	0.50, 0.55, 0.60, 0.65, 0.70, 0.75, 0.80, 0.85, 0.90

Table 4.13: Factors and their levels for the MOACS-1

Factor	Levels	Values
A (population size)	3	100, 150, 200
B β (heuristics importance)	5	1, 2, 3, 4, 5
C q_0 (Transition rule rate)	9	0.1, 0.2, 0.3, 0.4, 0.5, 0.6, 0.7, 0.8, 0.9
D ρ (evaporation rate)	5	0.1, 0.3, 0.5, 0.7, 0.9

Table 4.14: Factors and their levels for the MOACS-2

Factor	Levels	Values
A PopSize (population size)	3	100, 150, 200
B β (heuristics importance)	5	1, 2, 3, 4
C q_0 (Transition rule rate)	6	0.1, 0.2, 0.3, 0.4, 0.5, 0.6
D ρ (evaporation rate)	5	0.1, 0.3, 0.5, 0.7, 0.9
E q_1 (Transition rule rate)	3	0.1, 0.2, 0.3

Table 4.15: Factors and their levels for the DMOPSO

Factor	Levels	Values
A (population size)	3	100, 150, 200
B C_1 (Crossover rate with current best)	5	70, 75, 80, 85, 90
C C_2 (Crossover rate with global best)	5	70, 75, 80, 85, 90
D C_3 (Mutation rate)	5	10, 15, 20, 25, 30

Table 4.16: Factors and their levels for the NSGA-II

Factor	Levels	Values
A PopSize (population size)	3	100, 150, 200
B HS (initialization with heuristics)	2	0,1
C p_c (Crossover percentage)	5	55, 60, 65, 70, 65
D p_m (Mutation percentage)	4	1, 2, 3, 4
E TS (Tournament size)	2	2, 4

Table 4.17: Factors and their levels for the SPEA2

Factor	Levels	Values
A PopSize (population size)	3	100, 150, 200
B HS (initialization with heuristics)	2	0,1
C p_c (Crossover percentage)	5	55, 60, 65, 70, 65
D p_m (Mutation percentage)	4	1, 2, 3, 4
E TS (Tournament size)	2	2, 4

The objective of a DOE is to understand which set of variables in a process has the strongest influence on the performance and then determine the best levels for these variables to obtain the optimal performance [12]. Several authors have also applied DOE to tuning the parameters of their optimisation algorithms, (e.g. [428, 20, 262, 310]). The following terminology is used in this section:

— Response variable - This variable represents the measured variable of interest. For the analysis of optimisation algorithms, commonly used measures include the solution quality, which can be expressed by the objective function value, and the computation time required for a specific algorithm to converge.
— Factors and levels - A factor is an independent variable that is manipulated in an experiment. The levels of a factor represent the values considered in the DOE.
— Effects - An effect is a change in the response variable due to a change in one or more factors. Here we can consider the main effect, which is the effect of one factor alone averaged across the levels of other factors, and the interaction, which is the variation among the differences between means for different levels of one factor over different levels of other factors.

A multi-factor analysis of variance (ANOVA) was used to assess the statistical significance of the factors and define the most optimal parameter values for each algorithm. First, for each algorithm class, the main effects and their interactions were analysed. In all analyses the p-value indicates whether its value is less than a specific parameter α_{lim}, that there is a significant difference between the analysed levels of the factor and the response variable. A confidence level of %95 ($\alpha_{lim} = 0.05$) was selected. Since many quality indicators can be used to assess the optimality of specific parameter values and only one can be used, the hypervolume indicator was selected. The advantage of this metric is that it encapsulates a measure of spread of the solutions along the Pareto front in a single value, in addition to the closeness of obtained solutions to the Pareto-optimal front.

The parameter definition process of the evolutionary algorithms is described. A detailed analysis of the other algorithms is presented in Appendix C.2.

4.5.2.1 Analysis of variance: NSGA-II and SPEA2

The various factors of interest for the NSGA-II and SPEA2, along with their levels and values, are shown in Tables 4.16 and 4.17. These factors result in $3 \times 2 \times 5 \times 4 \times 2 = 240$ possible combinations. Each combination represents an experiment, which was run three times to calculate the HV metric. The ANOVA results for the NSGA-II and SPEA2 are shown in Table 4.18. This table demonstrates that the population size, the initialisation of the population with heuristics, and the crossover have a significant effect on the response variable of the NSGA-II. In order to set the value of the parameters, the F-value is used. The F-value represents the ratio between the explained and unexplained variance. The greater this value is, the more effect on the response variable has a factor. Considering the F-value, it can be stated that A, B and C have the most effect on the variable response. Considering

these F-value in descending order, the values of B, A, and C can be fixed to 1, 200, and 55, respectively, in accordance with the main effect plots represented in Figure 4.11. Since the remaining factors do not have a significant influence on the hypervolume or computation time, as shown in Table 4.19, they can be fined as follows: A=200, B=1, C=55, D=3, E=2.

Table 4.18 also shows that the population size, crossover, and mutation rate have a significant effect on the response variable of the SPEA2. Figures 4.12 and 4.13 represent the significant main effects and interaction plots. The values of A, C, and D can respectively be fixed to 200, 65, and 2. The interaction between factors B and C is relevant and since the value of C is already defined, the value of B, for which the interaction BC maximises the response variable, is 1. Since factor E does not have a significant influence on the results, the chosen parameters for the proposed SPEA2 are as follows: A=200, B=1, C=65, D=2, and E=2.

Table 4.18: Analysis of variance for the NSGA-II and SPEA2 with HV as response value

		NSGA-II				SPEA2			
Factor	DF	SS	MS	F-value	p-value	SS	MS	F-value	p-value
A	2	0.002	0.001	24.820	0.000	0.006	0.003	18.700	0.000
B	1	0.005	0.005	105.700	0.000	0.000	0.000	1.270	0.261
C	4	0.001	0.000	3.700	0.010	0.002	0.001	3.630	0.006
D	3	0.000	0.000	0.880	0.450	0.001	0.000	2.770	0.042
BC	4	0.000	0.000	0.660	0.620	0.002	0.001	3.380	0.010

* Only factors/interactions with a significant influence ($\alpha_{lim} = 0.05$) are shown.

Table 4.19: Analysis of variance for the NSGA-II and SPEA2 with the computation time as response value

		NSGA-II				SPEA2			
Factor	DF	SS	MS	F-value	p-value	SS	MS	F-value	p-value
A	2	>500	>500	>500	0	>500	>500	>500	0.000

* Only factors/interactions with a significant influence ($\alpha_{lim} = 0.05$) are shown.

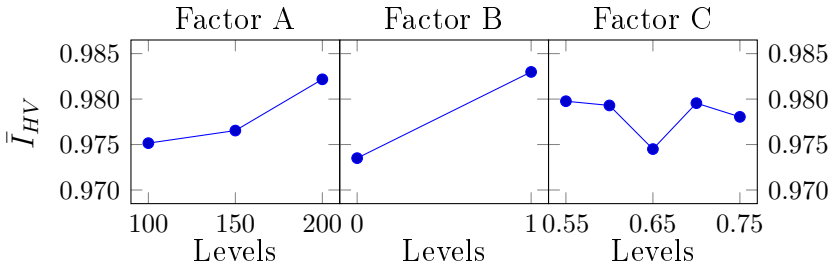

Figure 4.11: Main effects plot (fitted means) obtained for the NSGA-II with HV as response value

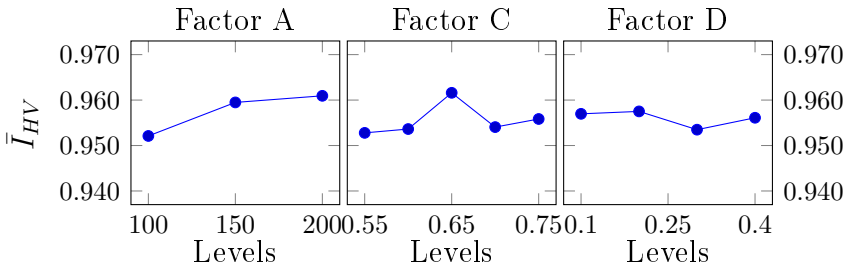

Figure 4.12: Main effects plot (fitted means) obtained for the SPEA2 with HV as response value

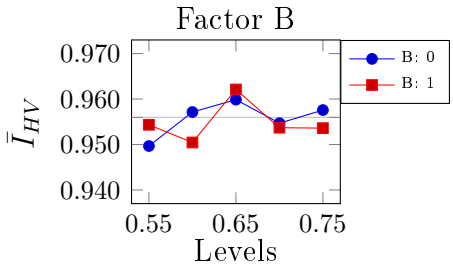

Figure 4.13: Interaction plot (fitted means) obtained for the SPEA2 with HV as response value

4.5.2.2 Summarised results for the parameter definitions

The previously defined parameter values are summarised for each algorithm in the following tables. The results of the other algorithms, which were obtained following the same reasoning, are shown in Table 4.20-4.26.

Table 4.20: Parameter settings for the NSGA-II and SPEA2 algorithms

Parameters	NSGA-II	SPEA2
Population size	200	
Initialisation with heuristics	Yes	
p_c	55	65
p_m	3	2
T_{size}	2	2

Table 4.21: Parameter settings for the MOACO algorithms

Parameters	BIANT-1	BIANT-2	MOACS-1	MOACS-2	CHAC-1	CHAC-2
Population size	200	200	100	200	200	200
Initialisation with heuristics	Yes	Yes	Yes	Yes	Yes	Yes
α	3	3	-		2	2
β	1	5	2	2	3	3
ρ	0,9	0,6	0,5	0,6	0,3	0,3
q0	-	0,1	0,8	0,6	0,6	0,6
q1	-	0.1	-	0,1	-	0,3

Table 4.22: Parameter settings for the DMOPSO algorithms

Parameters	DMOPSO-R	DMOPSO-S1	DMOPSO-S2	DMOPSO-KM	DMOPSO-S3
Population size			200		
Initialisation with heuristics			Yes		
C1			0,75		
C2			0,7		
C3			0,15		

Table 4.23: Parameter settings for the DMOBAT algorithms

Parameters	DMOBAT-R	DMOBAT-S1	DMOBAT-S2	DMOBAT-KM	DMOBAT-S3
Population size			200		
Initialisation with heuristics			Yes		
γ			0,75		
α			0,7		

Table 4.24: Parameter settings for the DMOCSA algorithms

Parameters	DMOCSA-1	DMOCSA-2
Population size	200	
Initialisation with heuristics	Yes	
p_c	0,8	
p_a	0.2	-

Table 4.25: Parameter settings for the DMOFPA algorithms

Parameters	DMOFPA-R	DMOFPA-S1	DMOFPA-S2	DMOFPA-KM	DMOFPA-S3
Population size			200		
Initialisation with heuristics			Yes		
p			0,8		

Table 4.26: Parameter settings for the DMOABC algorithms

Parameters	DMOABC
Population size	200
Initialisation with heuristics	Yes
limit	50

4.5.3 Quality indicators

In order to compare the developed approximate algorithms, the following indicators (explaiend in Section 3.4.1) were used: (i) I_{HV} (previously denoted HV), (ii) I_{ϵ}, (iii) I_{IGD} previously denoted IGD), and (iv) I_{Δ} previously denoted $Delta$). The choice of these indicators was motivated by their different objectives: (i) I_{ϵ} measures the convergence ability, (ii) I_{Δ} measures the distribution of the solutions and (iii) I_{IGD} and I_{HV} combine both of these components. The higher the values of I_{HV} and the lower the values of I_{IGD}, I_{Δ} and I_{ϵ} the better a specific algorithm will perform.

4.5.4 Comparison of approximate methods

This section presents a comparison of approximate methods performed through a statistical analysis. To compare the various approximate algorithms and due to the stochastic nature of these optimisers [142], several runs were performed. As a stopping criterion the MGBM criterion [258], which combines a local improvement metric and a global evidence accumulation criterion that decides when an algorithm should stop, was used. This metric is based on the set of non-dominated solutions for two consecutive iterations: ND_t and ND_{t-1}. The progress indicator $s_t \in [0, 1]$ represents how many elements of ND_t dominated ND_{t-1}. If the progress indicator $s_t = 1$, the population of iteration t is completely better than the precedent one of $t - 1$. If $s_t = 0$, there has not been any substantial progress. Thus, if no non-dominated solution has changed after a pre-specified number of generations, L_{iter}, the algorithm is stopped. Here L_{iter} is equal to 150.

4.5.4.1 Statistical analysis

Tables 4.27 to 4.31 show the median and IQR obtained through several experiments for the problems of the Arc111 family. The interquartile range measures the statistical dispersion obtained through several experiments. In addition, a statistical visualisation by means of a box plot that graphically depicts various statistics such as the median, variance, min, and max of a given data set, is available for the problems in Appendix C.3. The relationships between the statistics provided in Tables 4.27 to 4.31 and those provided in Appendix C.3 are presented in Figure 4.14. Promising results are coloured in gray and three different gray levels were used; the darker level indicates that the algorithm is obtaining the best rank of an indicator, the lighter levels represent the algorithms with ranks that belong to the $10^{th} - \%$ or $20^{th} - \%$ best algorithms. In Tables 4.27 to 4.31 only the best algorithms are shown.

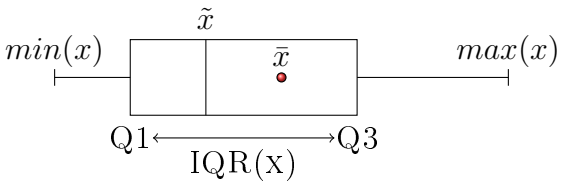

Figure 4.14: Relationship between $\tilde{x}$ and $IQR(x)$

As represented in Tables 4.27 to 4.31 the MOACS-2 obtained the best median values for the I_{HV}, I_{IGD} and I_{Δ} indicators. Regarding I_{ϵ}, the NSGA-II and SPEA2 obtained the best median values. According to the computation time required until convergence, it seems clear that the SPEA2 converges faster. While the MOACS-2 and the other MOACO algorithms performed better in the Arc111 family of problems regarding the obtained medians, which are higher, the obtained IQR values are not small enough to directly conclude that MOACO algorithms are better than the other algorithms.

Table 4.27: Median and interquartile range of I_{HV} obtained by the optimisers for the Arc111 problems

	Arc111-1 $\tilde{x} \pm IQR(x)$		Arc111-2 $\tilde{x} \pm IQR(x)$		Arc111-3 $\tilde{x} \pm IQR(x)$		Arc111-4 $\tilde{x} \pm IQR(x)$		Arc111-5 $\tilde{x} \pm IQR(x)$	
BIANT-1	0.87	0.02	0.89	0.04	0.86	0.06	0.90	0.03	0.85	0.04
BIANT-2	0.90	0.01	0.89	0.04	0.87	0.04	0.86	0.03	0.90	0.03
CHAC-2	0.87	0.01	0.85	0.01	0.84	0.00	0.85	0.01	0.86	0.01
DMOCSA-1-1	0.87	0.01	0.85	0.01	0.84	0.03	0.85	0.03	0.85	0.01
DMOCSA-1-2	0.86	0.01	0.85	0.01	0.85	0.00	0.84	0.01	0.86	0.02
DMOCSA-1-4	0.86	0.01	0.86	0.01	0.84	0.01	0.84	0.01	0.84	0.01
DMOCSA-1-5	0.86	0.01	0.85	0.02	0.84	0.02	0.85	0.02	0.85	0.00
DMOCSA-2-5	0.87	0.01	0.85	0.03	0.85	0.01	0.85	0.00	0.85	0.01
DMOFPA-2	0.86	0.01	0.86	0.02	0.85	0.00	0.85	0.01	0.85	0.01
DMOFPA-3	0.87	0.01	0.85	0.01	0.84	0.01	0.85	0.01	0.85	0.02
DMOFPA-4	0.86	0.01	0.85	0.00	0.85	0.02	0.84	0.02	0.85	0.03
DMOFPA-5	0.86	0.02	0.85	0.01	0.85	0.01	0.85	0.00	0.85	0.02
MOACS-1	0.84	0.01	0.87	0.01	0.87	0.01	0.87	0.01	0.87	0.00
MOACS-2	0.90	0.01	0.92	0.01	0.92	0.02	0.92	0.00	0.91	0.01
MOBAT-5	0.86	0.01	0.85	0.01	0.84	0.01	0.85	0.01	0.85	0.00
SPEA2	0.87	0.01	0.86	0.01	0.85	0.02	0.86	0.02	0.86	0.01

Table 4.28: Median and interquartile range of I_{IGD} obtained by the optimisers for the Arc111 problems

	Arc111-1 $\tilde{x} \pm IQR(x)$		Arc111-2 $\tilde{x} \pm IQR(x)$		Arc111-3 $\tilde{x} \pm IQR(x)$		Arc111-4 $\tilde{x} \pm IQR(x)$		Arc111-5 $\tilde{x} \pm IQR(x)$	
BIANT-1	0.68	0.06	0.78	0.08	0.88	0.24	0.64	0.11	0.84	0.18
BIANT-2	0.64	0.06	0.66	0.14	0.83	0.12	0.83	0.04	0.85	0.15
CHAC-2	0.78	0.00	0.87	0.04	0.78	0.03	0.86	0.07	0.78	0.03
DMOABC	0.81	0.03	0.91	0.11	0.78	0.04	0.88	0.01	0.79	0.03
DMOCSA-1-2	0.82	0.02	0.81	0.03	0.73	0.02	0.89	0.10	0.80	0.10
DMOCSA-1-4	0.80	0.05	0.84	0.03	0.77	0.03	0.88	0.01	0.84	0.03
DMOCSA-1-5	0.79	0.04	0.85	0.01	0.81	0.11	0.85	0.04	0.84	0.03
DMOCSA-2-4	0.77	0.04	0.84	0.06	0.77	0.02	0.86	0.04	0.75	0.08
DMOFPA-2	0.78	0.04	0.86	0.13	0.76	0.02	0.89	0.01	0.80	0.01
DMOFPA-4	0.79	0.02	0.87	0.01	0.80	0.09	0.89	0.02	0.82	0.08
DMOFPA-5	0.82	0.03	0.85	0.01	0.79	0.00	0.87	0.02	0.82	0.09
MOACS-1	0.94	0.12	0.74	0.05	0.57	0.02	0.60	0.07	0.58	0.04
MOACS-2	0.55	0.04	0.47	0.01	0.39	0.01	0.44	0.01	0.47	0.00
MOBAT-1	0.78	0.01	0.88	0.06	0.82	0.07	0.89	0.05	0.76	0.06
DMOPSO-2	0.78	0.01	0.88	0.05	0.78	0.06	0.86	0.03	0.81	0.06
DMOPSO-3	0.81	0.03	0.86	0.01	0.83	0.02	0.90	0.02	0.79	0.01
DMOPSO-4	0.80	0.03	0.85	0.02	0.82	0.02	0.89	0.02	0.81	0.02

Table 4.29: Median and interquartile range of I_ϵ obtained by the optimisers for the Arc111 problems

	Arc111-1 $\tilde{x} \pm IQR(x)$		Arc111-2 $\tilde{x} \pm IQR(x)$		Arc111-3 $\tilde{x} \pm IQR(x)$		Arc111-4 $\tilde{x} \pm IQR(x)$		Arc111-5 $\tilde{x} \pm IQR(x)$	
CHAC-2	0.24	0.00	0.31	0.00	0.36	0.00	0.36	0.01	0.37	0.00
DMOABC	0.24	0.00	0.31	0.01	0.35	0.01	0.36	0.00	0.38	0.00
DMOCSA-1-1	0.24	0.00	0.32	0.00	0.36	0.00	0.36	0.00	0.38	0.00
DMOCSA-1-5	0.24	0.00	0.31	0.00	0.35	0.00	0.36	0.00	0.38	0.01
DMOCSA-2-2	0.24	0.00	0.31	0.00	0.35	0.00	0.36	0.00	0.38	0.00
DMOCSA-2-5	0.24	0.01	0.32	0.01	0.36	0.00	0.36	0.00	0.38	0.00
DMOFPA-1	0.24	0.00	0.31	0.01	0.35	0.00	0.35	0.01	0.38	0.01
MOBAT-1	0.24	0.00	0.31	0.00	0.36	0.00	0.36	0.00	0.37	0.01
MOBAT-2	0.24	0.00	0.31	0.00	0.36	0.00	0.36	0.01	0.38	0.00
DMOPSO-1	0.24	0.00	0.31	0.00	0.35	0.00	0.36	0.00	0.38	0.00
DMOPSO-3	0.24	0.01	0.32	0.00	0.35	0.00	0.36	0.01	0.38	0.01
NSGA-II	0.14	0.00	0.18	0.00	0.22	0.00	0.22	0.01	0.32	0.00
SPEA2	0.15	0.00	0.18	0.00	0.22	0.00	0.23	0.00	0.32	0.00

Table 4.30: Median and interquartile range of I_Δ obtained by the optimisers for the Arc111 problems

	Arc111-1 $\tilde{x} \pm IQR(x)$		Arc111-2 $\tilde{x} \pm IQR(x)$		Arc111-3 $\tilde{x} \pm IQR(x)$		Arc111-4 $\tilde{x} \pm IQR(x)$		Arc111-5 $\tilde{x} \pm IQR(x)$	
BIANT-1	0.53	0.02	0.61	0.01	0.62	0.09	0.56	0.01	0.65	0.06
BIANT-2	0.54	0.02	0.57	0.11	0.65	0.07	0.66	0.07	0.63	0.03
CHAC-2	0.83	0.06	0.79	0.03	0.81	0.01	0.82	0.05	0.75	0.07
DMOCSA-2-1	0.91	0.01	0.85	0.07	0.82	0.03	0.84	0.04	0.79	0.07
DMOCSA-2-2	0.84	0.01	0.81	0.01	0.82	0.01	0.91	0.07	0.83	0.07
DMOCSA-2-3	0.86	0.03	0.84	0.06	0.78	0.06	0.87	0.02	0.82	0.01
DMOCSA-2-4	0.87	0.02	0.85	0.11	0.86	0.01	0.84	0.07	0.78	0.04
DMOFPA-1	0.86	0.01	0.86	0.04	0.87	0.07	0.88	0.01	0.87	0.10
DMOFPA-3	0.88	0.09	0.84	0.04	0.81	0.03	0.86	0.00	0.77	0.06
DMOFPA-4	0.82	0.01	0.90	0.10	0.86	0.12	0.92	0.03	0.84	0.06
MOACS-1	0.61	0.06	0.57	0.05	0.56	0.02	0.59	0.06	0.61	0.01
MOACS-2	0.44	0.03	0.52	0.09	0.40	0.05	0.48	0.07	0.49	0.17
MOBAT-1	0.87	0.05	0.85	0.01	0.82	0.10	0.88	0.07	0.80	0.03
DMOPSO-1	0.92	0.07	0.82	0.02	0.84	0.01	0.88	0.01	0.82	0.05
SPEA2	0.90	0.02	0.85	0.05	0.85	0.02	0.91	0.07	0.80	0.01

Table 4.31: Median and interquartile range of the computation time required by the optimisers for the Arc111 problems

	Arc111-1 $\tilde{x} \pm IQR(x)$		Arc111-2 $\tilde{x} \pm IQR(x)$		Arc111-3 $\tilde{x} \pm IQR(x)$		Arc111-4 $\tilde{x} \pm IQR(x)$		Arc111-5 $\tilde{x} \pm IQR(x)$	
BIANT-2	1.00	0.00	0.64	0.47	0.54	0.18	0.40	0.14	0.68	0.13
DMOCSA-1-1	0.34	0.07	0.34	0.06	0.26	0.30	0.37	0.17	0.42	0.20
DMOCSA-1-4	0.26	0.07	0.26	0.06	0.51	0.07	0.37	0.26	0.26	0.03
DMOCSA-1-5	0.32	0.14	0.33	0.03	0.41	0.23	0.35	0.14	0.44	0.21
DMOFPA-1	0.26	0.06	0.35	0.16	0.42	0.13	0.38	0.06	0.32	0.05
DMOFPA-4	0.26	0.03	0.30	0.04	0.35	0.05	0.26	0.12	0.31	0.16
DMOFPA-5	0.23	0.18	0.47	0.05	0.58	0.34	0.33	0.14	0.34	0.05
MOACS-1	0.20	0.08	0.32	0.05	0.25	0.04	0.19	0.04	0.28	0.13
MOACS-2	0.22	0.04	0.25	0.05	0.27	0.10	0.20	0.02	0.42	0.19
MOBAT-1	0.24	0.08	0.26	0.16	0.44	0.01	0.30	0.10	0.40	0.20
MOBAT-2	0.31	0.06	0.35	0.02	0.39	0.09	0.30	0.05	0.37	0.13
MOBAT-5	0.29	0.08	0.28	0.17	0.28	0.12	0.32	0.04	0.41	0.17
DMOPSO-2	0.21	0.23	0.27	0.05	0.42	0.23	0.18	0.12	0.33	0.26
SPEA2	0.14	0.03	0.17	0.07	0.17	0.13	0.16	0.08	0.20	0.08

Figure 4.15 shows the evolution of I_{HV} using a box plot for the BIANT-1, BIANT-2, MOACS-2, NSGA-II, and DMOFPA-1 for the Arc111-1 problem. This figure demonstrates that the average performance of the MOACS-2 is better than the other algorithms due to its small variance and high mean value. However, difficulties can arise when trying to compare the other algorithms, which have similar distributions. For this type of comparison, a statistical visualisation is not suitable. Therefore, to address this point, a nonparametric statistical test was used and is discussed in the next section.

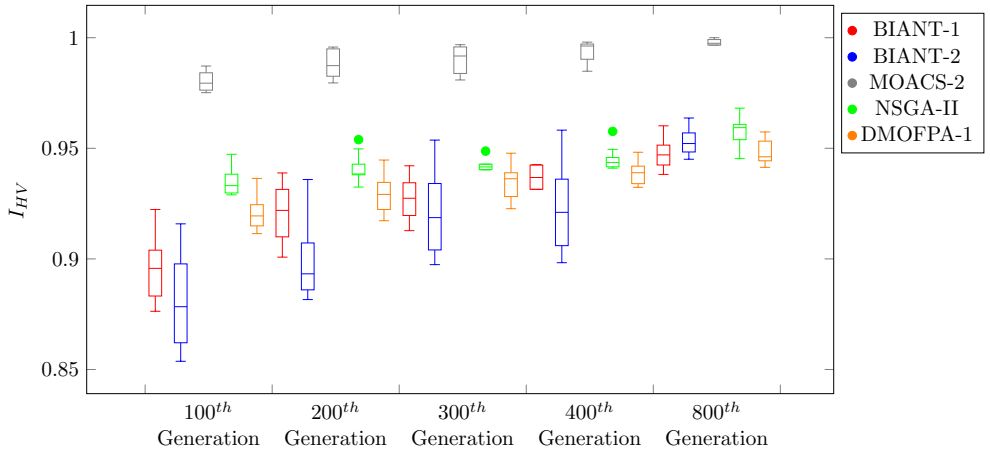

Figure 4.15: Evolution of the I_{HV} through the iterations for the BIANT-1, BIANT-2, MOACS-2, NSGA-II and DMOFPA-1 for the Arc111-1 problem

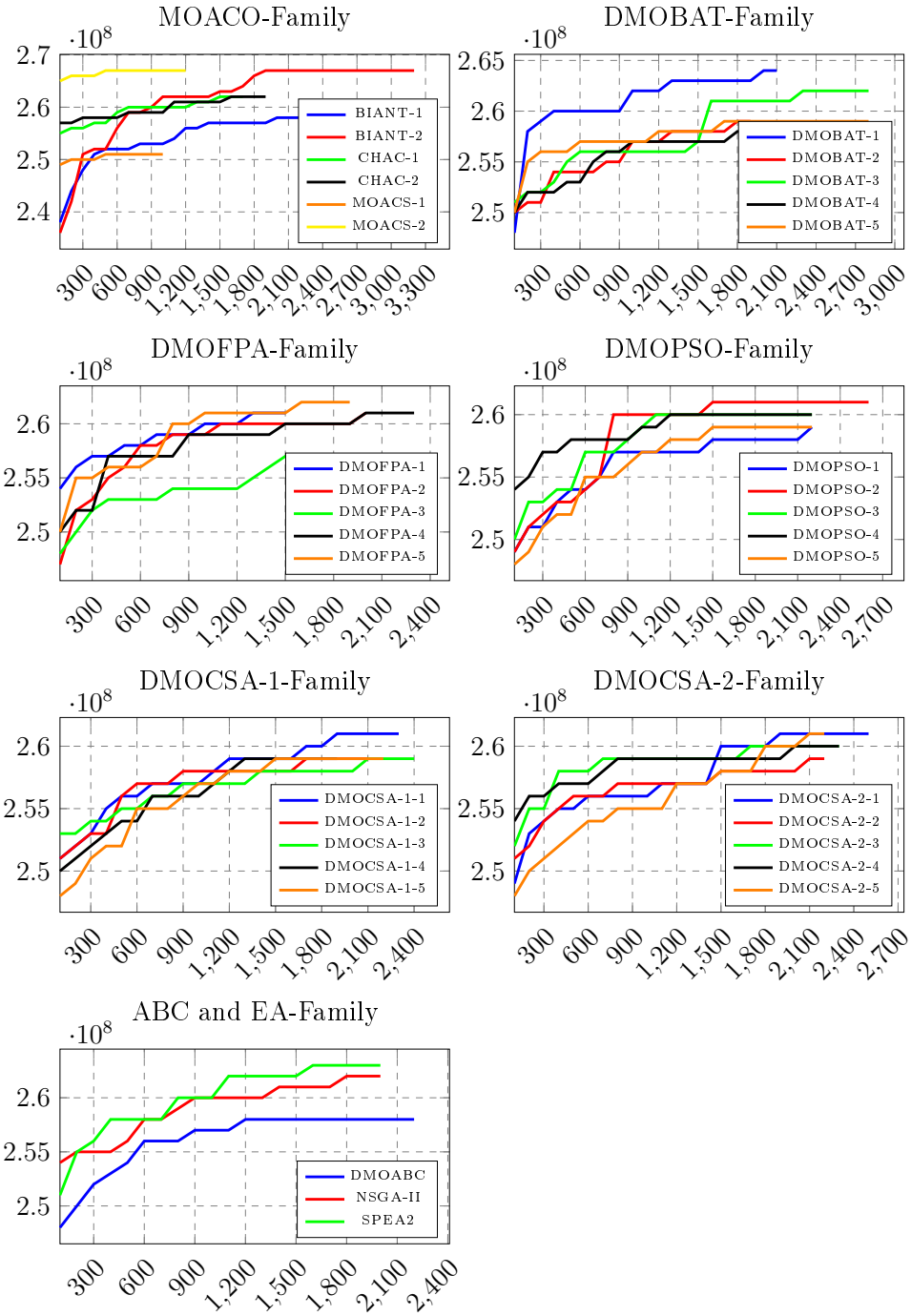

Figure 4.16: Best Evolution of the I_{HV} through the iterations obtained by all approximate methods for the Arc111-1 problem

Figure 4.16 shows the evolution of the best runs obtained by all approximate methods in accordance with I_{HV}. In this figure, the algorithms are grouped according to their family. The MOACS-1 and MOACS-2 are the algorithms that stop the earliest to converge toward the Pareto front. While the other algorithms stop at 2100 or more generations, they stop between 900 and 1200 iterations. Comparing the convergence speed of the MOACO-family with other families, it seems that the MOACOs converge slower. However, the BIANT,

DMOPSO, and EA families have a fast convergence speed in the earliest iterations of the optimisation process. Compared to the DMOCSA family, which reached a covered hypervolume of 2.6E8 after approximately 1,500 iterations, these algorithms reached this value after approximately 900 iterations.

4.5.4.2 Nonparametric statistical test

In order to identify the algorithm that performs better than others and similarly determine whether the differences between algorithms regarding the indicators listed above are significant or not, hypothesis testing can be used to identify differences or similarities between algorithms. Two hypotheses are used, including the null hypothesis (H_0) which states that there is no difference between two algorithms, and (H_1), which states that there is a significant difference between two algorithms. The $p-$value, which provides information about whether a statistical hypothesis test is significant or not, will reject H_0 for a small value. Moreover, nonparametric tests can be divided into pairwise or multiple comparison tests [263]. The former type detects significant differences between two samples of data (e.g. algorithms), and the latter type detects significant differences between multiple algorithms. Multiple comparison tests can be further subdivided into situations where one control algorithm is compared to all others, and situations where all algorithms are compared will all others and all pairwise differences between all algorithms must be detected. Derrac *et al.* [110] proposed a tutorial to use various pairwise and multiple comparison procedures.

In this section, multiple comparisons using the Friedman test [3], which is a commonly used nonparametric statistical test procedures [446] that allows for multiple comparison procedures with and without a control algorithm, are presented. The Friedman test [144, 145], which is a nonparametric analogue of the parametric two-way analysis of variance, was applied several times to determine whether there is a significant difference between algorithms (e.g. [299, 251, 446]).

The guideline provided by Derrac *et al.* [110] was followed to perform the nonparametric statistical analysis. The Friedman test has been applied to all problems according to all performance indicators used in the previous section. The obtained Friedman statistics for all problems and algorithms considered together in accordance with I_{HV}, I_{IGD}, I_{ϵ}, I_{Δ}, and the computation time and respective computed p-values are shown in Table 4.32. Given that $\chi^2_{0.0001} = 72$ with a 99.99% confidence level and 33 degrees of freedom, there are significant differences among the algorithms for all quality indicators.

3. The choice of nonparametric statistical analysis is explain in Appendix B.4.

Table 4.32: Friedman's statistic and computed p-value in accordance with I_{HV}, I_{IGD}, I_ϵ, I_Δ, and the computation time

Indicators	Friedman statistic	Computed p-values
I_{HV}	1035.35	0
I_{IGD}	803.43	2.87E-10
I_ϵ	834.81	2.99E-10
I_Δ	826.73	2.44E-10
Time	2923.22	0

Table 4.33: Average rankings returned by Friedman's nonparametric test for all problems according to the various quality indicators

Algorithm	I_{HV}	I_{IGD}	I_ϵ	I_Δ	Time
DMOABC	15.60	19.31	20.11	14.96	6.00
DMOBAT-1	16.48	18.74	19.09	16.11	21.94
DMOBAT-2	16.04	19.83	18.78	17.03	20.09
DMOBAT-3	15.11	20.03	19.56	16.95	17.43
DMOBAT-4	25.52	10.26	14.16	17.60	20.84
DMOBAT-5	16.10	19.73	18.60	15.75	18.64
BIANT-1	17.55	17.90	9.81	26.11	6.38
BIANT-2	17.35	17.32	9.59	24.91	5.97
CHAC-1	13.77	20.68	19.41	19.68	12.33
CHAC-2	13.82	20.57	19.48	19.05	13.83
DMOCSA-1-1	16.62	18.47	18.30	15.19	20.59
DMOCSA-1-2	16.41	18.45	18.28	15.38	20.54
DMOCSA-2-1	16.46	18.77	18.58	15.65	13.15
DMOCSA-2-2	16.11	18.81	18.25	15.97	14.88
DMOCSA-2-3	16.76	18.82	18.87	15.91	10.19
DMOCSA-2-4	24.80	10.92	14.78	18.15	14.97
DMOCSA-2-5	16.41	19.10	18.42	16.30	11.60
DMOCSA-1-3	17.57	18.18	17.84	15.72	20.25
DMOCSA-1-4	27.17	8.84	13.91	18.19	23.87
DMOCSA-1-5	17.29	18.28	18.58	15.46	22.74
DMOFPA-1	17.10	17.97	18.36	16.64	21.83
DMOFPA-2	17.22	18.44	18.27	16.64	18.11
DMOFPA-3	16.90	18.22	17.98	15.96	17.94
DMOFPA-4	27.03	9.05	13.32	16.99	28.75
DMOFPA-5	17.31	18.28	18.28	15.24	18.61
MOACS-1	19.85	15.03	11.26	26.10	10.50
MOACS-2	17.86	15.37	11.77	25.52	10.04
DMOPSO-1	15.47	19.83	20.36	17.53	23.62
DMOPSO-2	16.03	19.80	18.94	16.42	24.71
DMOPSO-3	16.19	19.23	19.54	16.63	22.78
DMOPSO-4	22.61	13.21	16.20	16.90	15.63
DMOPSO-5	14.98	19.37	20.06	17.31	20.31
NSGA-II	11.22	19.55	23.32	13.05	14.52
SPEA2	12.29	18.64	22.92	14.00	31.40

The Friedman rank defines a classification between algorithms and can be employed to measure their performance differences. The ranks obtained for each quality indicators are

shown in Table 4.33; outperforming results are coloured in gray. Three different gray levels were used. The darker level indicates the algorithm with the best indicator rank, and the lighter levels represent the algorithms with ranks that belong to the $10^{th} - \%$ or $20^{th} - \%$ best algorithms. The NSGA-II, followed by the SPEA2, CHAC-1, CHAC-2, and DMOPSO-5 obtained the best values on average for all problems. The CHAC-1 followed by the CHAC-2, DMOBAT-3, DMOBAT-2 and DMOPSO-1 obtained the best values of I_{IGD}. Regarding the I_ϵ values, again the NSGA-II obtained the best results, followed by the SPEA2, DMOPSO-1, DMOPSO-5, and DMOABC. For the I_Δ, the MOACO family outperformed the other algorithms. Regarding the computation time, the SPEA2, followed by the DMOPSO-2, DMOFPA-4, and DMOCSA-1-4 were the algorithms that converged the fastest to a non-dominated solution set.

To evaluate statistical significance of the better performance of a specific algorithm, the algoritm must be compared to other algorithms. In other words, all equal hypotheses between the algorithm that obtained the best rank, can be tested by applying a set of post-hoc procedures using Holm's post hoc test. The unadjusted and adjusted p-values obtained through the applications of Holm's post hoc procedures are shown in Tables 4.34 to 4.38. Regarding the adjusted p-value, (with a confidence level of 95%), it can be stated that, on average and for all the problem test:

— In accordance with I_{HV}:

  — The NSGA-II is significantly better than 96 % of the algorithms. It is only better than the SPEA2 but not significantly. It can also be stated that all approximate methods using the strategy of selection of g_{best} are significantly outperformed.

— In accordance with I_{IGD}:

  — the CHAC-1 is only significantly better than 24% of the algorithms. All approximate methods using the following strategies of selection of g_{best} are significantly outperformed: (i) random, (ii) sigmoid, (iii) minimum particle angle and (iv) strip. For the fourth g_{best} selection strategy, K-means, the CHAC-1 is improved, but the improvement is not significant.

— In accordance with I_ϵ:

  — Similar to the HV metric, the NSGA-II is significantly better than most of the algorithms. Compared to the SPEA2, it is improved, but the improvement is not significant.

— In accordance with I_Δ:

  — The BIANT-1 is better than 91% of the algorithms. The BIANT-1 is only bet-

ter than following algorithms, but not significantly: BIANT-2, MOACS-1 and MOACS-2.

— In accordance with the computation time:

  — The SPEA2 is significantly better than all other algorithms.

Table 4.34: Unadjusted and adjusted p-values obtained for all problems through the application of Holm's post hoc procedure, using the NSGA-II as control algorithm in accordance with I_{HV}

Algorithm	Unadjusted p-value	Adjusted p-value
Others	<5.6E-03	<1.7E-02
SPEA2	2.6E-01	2.6E-01

Table 4.35: Unadjusted and adjusted p-values obtained for the Arc111 family problem through the application of Holm's post hoc procedure, using the CHAC-1 as control algorithm in accordance with I_{IGD}

Algorithm	Unadjusted p-value	Adjusted p-value
Others	<3.0E-04	<7.9E-03
BIANT-1	2.8E-03	7.1E-02
DMOFPA-1	3.6E-03	8.6E-02
DMOCSA-1-3	7.3E-03	1.7E-01
DMOFPA-3	8.4E-03	1.8E-01
DMOCSA-1-5	9.9E-03	2.1E-01
DMOFPA-5	9.9E-03	2.1E-01
DMOCSA-1-1	1.7E-02	3.1E-01
DMOCSA-1-2	1.7E-02	3.1E-01
DMOFPA-2	1.6E-02	3.1E-01
SPEA2	2.9E-02	4.6E-01
DMOBAT-1	3.7E-02	5.5E-01
DMOCSA-2-1	4.0E-02	5.6E-01
DMOCSA-2-2	4.4E-02	5.7E-01
DMOCSA-2-3	4.5E-02	5.7E-01
DMOCSA-2-5	9.1E-02	1.0E+00
DMOPSO-3	1.2E-01	1.2E+00
DMOABC	1.4E-01	1.3E+00
DMOPSO-5	1.6E-01	1.3E+00
NSGA-II	2.3E-01	1.6E+00
CHAC-2	9.1E-01	1.9E+00
DMOBAT-2	3.6E-01	1.9E+00
DMOBAT-3	4.9E-01	1.9E+00
DMOBAT-5	3.1E-01	1.9E+00
DMOPSO-1	3.6E-01	1.9E+00
DMOPSO-2	3.4E-01	1.9E+00

Table 4.36: Unadjusted and adjusted p-values obtained for the Arc111 family problem through the application of Holm's post hoc procedure, using the NSGA-II as control algorithm in accordance with I_ϵ

Algorithm	Unadjusted p-value	Adjusted p-value
Others	<1.5E-03	<3.0E-03
SPEA2	6.7E-01	6.7E-01

Table 4.37: Unadjusted and adjusted p-values obtained for the Arc111 family problem through the application of Holm's post hoc procedure, using the BIANT-1 as control algorithm in accordance with I_Δ

Algorithm	Unadjusted p-value	Adjusted p-value
Others	<5.0E-12	< 2.0E-11
BIANT-2	2.0E-01	6.0E-01
MOACS-1	9.9E-01	1.1E+00
MOACS-2	5.3E-01	1.1E+00

Table 4.38: Unadjusted and adjusted p-values obtained for the Arc111 family problem through the application of Holm's post hoc procedure, using the SPEA2 as control algorithm in accordance with the computation time

Algorithm	Unadjusted p-value	Adjusted p-value
All	<4.3E-03	<4.3E-03

However, since this analysis was done taking into consideration all tested problems at once, the results may vary depending on the problem characteristics.

Since this analysis considered all tested problems at once, the results may vary depending on the problem characteristics. The Friedman statistics for all of the problems considered separately and the indicators are shown in Table 4.39. Given $\chi^2_{0.05} = 47.399$ with a 95% confidence level and 33 degrees of freedom, there are significant differences among the algorithm in accordance with all quality indicators despite the Mitchell's Problem, in which there are no significant differences for I_Δ. Regarding Friedman's test, the computed p-values are also shown in Table 4.39.

Table 4.40 shows the algorithms that performed the best for each problem family in accordance with all quality indicator and their score. The score represents how many algorithms are significantly outperformed by the best algorithm. The detailed results for each family of problems can be found in Appendix C.4. Comparing the results obtained with the characteristics of the tested problems shown in Table 4.3, , the MOACS and the BIANT outperform 90 of the algorithms on average for complex problems that are represented by a low order

strength[4] with the following indicators: I_{HV}, I_{IGD}, I_ϵ, and I_Δ. In addition, when the order strength is growing, ACO algorithms are outperformed by other algorithms. However, for small instances, the best algorithm that was obtained is only significantly better than, depending on the instances, 10-20 % of the algorithms.

Table 4.39: Friedman's statistic and computed p-value for all problems in accordance with I_{HV}, I_{IGD}, I_ϵ, I_Δ, and the computation time

	I_{HV}		I_{IGD}		I_ϵ		I_Δ		Time	
Problem	Friedman statistic	Computed p-values	Friedman statistic	Computed p-values	Friedman statistic	Computed p-values	Friedman statistic	Computed p-values	Friedman statistic	Computed p-values
Arc111	217.50	4.22E-06	132.07	9.53E-11	368.67	1.54E-10	325.05	1.51E-10	330.65	1.21E-10
Buxey	427.80	1.65E-10	366.93	1.49E-10	83.66	2.78E-06	256.65	1.39E-10	315.51	1.53E-10
Gunther	360.80	1.63E-10	303.75	1.30E-10	216.76	9.35E-11	261.87	1.63E-10	289.03	1.15E-10
Hahn	347.40	1.45E-10	273.55	1.25E-10	178.38	7.53E-11	278.80	1.46E-10	279.71	1.20E-10
Jackson	414.51	1.59E-10	164.59	1.14E-10	277.29	1.49E-10	94.50	7.67E-08	696.17	2.68E-10
Kilbrid	385.88	1.95E-10	387.65	2.02E-10	381.17	1.35E-10	112.50	1.86E-10	239.97	9.73E-11
Lutz1	311.52	1.23E-10	316.18	1.19E-10	303.65	1.27E-10	105.86	1.51E-09	571.23	2.34E-10
Mitchell	203.05	9.36E-11	252.45	9.92E-11	123.26	8.70E-11	42.35	1.28E-01	274.85	1.15E-10
Mukherje	197.60	1.17E-10	176.72	1.25E-10	241.34	1.52E-10	241.22	1.45E-10	194.81	1.27E-10
Roszieg	243.48	1.11E-10	214.94	1.43E-10	225.56	1.37E-10	48.64	3.88E-02	357.87	1.77E-10
Sawyer	160.54	7.37E-11	70.56	1.53E-04	160.25	1.19E-10	63.44	1.12E-03	467.11	2.21E-10

Table 4.40: Best algorithms regarding their average rankings returned by Friedman's nonparametric test according to the various quality indicators

	I_{HV}		I_{IGD}		I_ϵ		I_Δ		Time	
Problem	Best algorithm	Score [%]	Best algorithm	Score [%]	Best algorithm	Score [%]	Best algorithm	Score [%]	Best algorithm	Score [%]
Arc111	MOACS-2	97	MOACS-2	100	NSGA-II	97	MOACS-2	91	SPEA2	91
Buxey	MOACS-2	85	MOACS-1	91	MOACS-1	94	MOACS-1	91	SPEA2	94
Gunther	BIANT-1	91	BIANT-1	97	MOACS-2	91	MOACS-2	91	SPEA2	88
Hahn	BIANT-2	91	BIANT-1	97	NSGA-II	91	BIANT-1	91	SPEA2	100
Jackson	DMOBAT-2	27	DMOBAT-2	24	DMOCSA-2	18	BIANT-1	85	DMOFPA-4	82
Kilbrid	CHAC-1	24	CHAC-1	27	DMOPSO-1	24	DMOBAT-4	12	SPEA2	97
Lutz1	DMOPSO-1	24	DMOABC	24	CHAC-1, DMOABC	24	MOACS-1	36	DMOFPA-4	79
Mitchell	DMOCSA-1	24	DMOBAT-3	27	DMOPSO-5	21	DMOCSA-4	18	DMOFPA-4	76
Mukherje	BIANT-2	91	BIANT-1	91	NSGA-II	97	MOACS-2	85	SPEA2	76
Roszieg	CHAC-2	27	CHAC-2	27	DMOFPA-2	97	DMOCSA-4	3	DMOFPA-4	82
Sawyer	DMOPSO-2	12	DMOBAT-3	9	DMOPSO-2	12	BIANT-1	36	DMOCSA-1-4	76

By grouping the problems with low and high order strength values as shown in Table 4.41 and performing the same analysis again, the Friedmans average ranking can be recalculated. The results are shown in Table 4.42. These tables show that for the first group that represents complex problems, the MOACS-1, MOACS-2, BIANT-1, and BIANT-2 performed better than all other algorithms for I_{HV}, I_{IGD}, I_Δ. For I_ϵ, the MOACS-2 is in the third position, crossed by the NSGA-II and SPEA2. Taking the covered hypervolume, the MOACS-2 provides significantly better results than all other algorithms, despite the MOACS-1, BIANT-

4. The lower the order strength OS, the harder is the problem of finding optimal solutions

1, and BIANT-2, for which the improvement is not necessarily significant. Regarding the values of I_{IGD}, the BIANT-2 is significantly better than all algorithms despite the MOACS-2 and BIANT-1. Regarding the values of I_ϵ, the NSGA-II is, despite the SPEA2, significantly better than all algorithms. For the values of I_Δ, the MOACS-2 is, despite the BIANT-1, BIANT-2, and MOACS-1, significantly better than all algorithms. For the second group, the significant difference between algorithms is not as great as that of the first group. For the values of I_{HV}, the CHAC-2 is better than 28 % of the algorithms, including the MOACS-1, MOACS-2, BIANT-1, and BIANT-2. Regarding the I_{IGD}, the DMOPSO-1 is significantly better than 28 % of the algorithms. The similar observation as before can be done for I_ϵ. For the values of I_Δ, the DMOCSA-1-4 is significantly better than 42 % of the algorithms. However, it is not significantly better than the BIANT-2, BIANT-1, MOACS-2, and MOACS-1. The unadjusted and adjusted p-values obtained through the applications of Holm's post hoc procedures for the first and second groups are shown in Tables C.138 to C.141 and Tables C.143 to C.146.

Table 4.41: Grouping of problems according to the order strength

Problem	Group 1	Group 2
Arc111	X	
Buxey	X	
Gunther	X	
Hahn	X	
Jackson		X
Kilbrid		X
Lutz1		X
Mitchell		X
Mukherje	X	
Roszieg		X
Sawyer		X

When considering the problem characteristics expressed as the number of potential assignable tasks (N), the order strength (OS) and the total number of equipment available (E), it seems that the computation time required by the various optimisers is also function of them. This is shown through two bubble charts in Figure 4.17. Regarding the required computation for the problem instances from Group 1 and Group 2, the computation time stays balanced and small for problem instances of Group 1, and it explodes when considering the problem instances of Group 2. This phenomenon is shown in Figure 4.18.

Table 4.42: Average rankings returned by Friedman's nonparametric test for both groups, Group 1 and Group 2

	Group 1					Group 2				
Algorithm	I_{HV}	I_{IGD}	I_ϵ	I_Δ	Time	I_{HV}	I_{IGD}	I_ϵ	I_Δ	Time
DMOABC	18.52	17.24	17.75	11.85	7.05	12.78	21.23	22.29	17.83	5.04
DMOBAT-1	19.29	16.29	16.99	15.05	21.87	13.77	21.00	21.03	17.09	22.01
DMOBAT-3	17.85	17.99	17.00	16.90	19.80	12.46	21.92	21.94	17.00	15.24
DMOBAT-4	26.44	8.95	16.38	14.56	21.21	24.63	11.47	12.11	20.41	20.50
DMOBAT-5	19.05	17.26	16.39	15.06	19.74	13.25	22.01	20.64	16.38	17.61
BIANT-1	4.69	29.07	14.43	31.73	5.15	29.96	7.57	5.53	20.91	7.50
BIANT-2	3.55	29.19	15.07	31.85	5.11	30.66	6.34	4.52	18.50	6.75
CHAC-1	15.05	18.94	17.70	20.99	14.75	12.54	22.29	21.00	18.47	10.09
CHAC-2	15.46	19.03	17.00	19.95	16.28	12.24	22.00	21.77	18.22	11.57
DMOCSA-2-4	25.09	10.91	17.35	16.60	16.09	24.53	10.92	12.40	19.58	13.94
DMOCSA-1-4	27.58	7.98	17.01	14.08	23.46	26.76	9.63	11.05	21.99	24.26
DMOFPA-4	27.25	8.39	15.86	14.59	24.64	26.82	9.67	10.97	19.20	32.54
MOACS-1	7.47	24.69	19.36	32.44	13.36	31.80	6.09	3.78	20.24	7.85
MOACS-2	3.15	26.77	20.64	32.46	15.58	32.05	4.83	3.58	19.11	4.92
DMOPSO-5	17.41	18.39	18.05	17.70	19.60	12.64	20.27	21.91	16.95	20.97
DMOPSO-1	18.69	17.24	17.88	16.47	19.96	12.36	22.22	22.66	18.51	27.01
DMOPSO-2	18.98	17.94	16.29	16.19	23.82	13.18	21.52	21.39	16.64	25.54
DMOPSO-3	19.15	16.91	17.05	15.81	16.22	13.33	21.37	21.84	17.39	28.85
NSGA-II	9.74	17.58	25.54	8.75	19.00	12.64	21.37	21.26	17.03	10.39
SPEA2	11.61	15.51	24.50	11.34	31.95	12.94	21.54	21.46	16.46	30.90

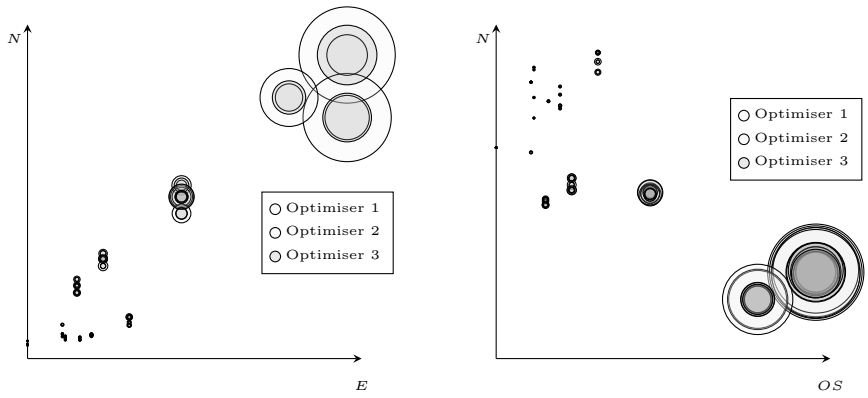

(a) Computation time depending on N and E

(b) Computation time depending on N and OS

Figure 4.17: Evolution of the computation time required by the various optimisers based on the problem characteristics

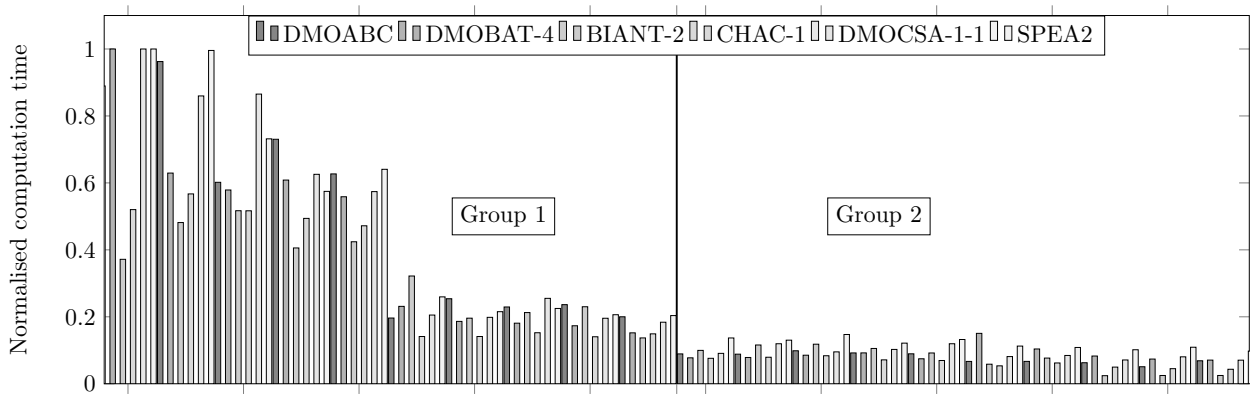

Figure 4.18: Evolution of the computation time based on the grouping of problem characteristics

For complex problems, it seems that the MOACS-2 offers more advantages regarding Friedman's test. Figures 4.19 to 4.21, which were created using the eaf-package available at `www.lopez-ibanez.eu/eaftools`, show the comparison of the attainment surface of the BIANT-1, BIANT-2, and MOACS-2 respectively for the following problems: Arc111-3, Mukherje-3, and Arc111-5. The examination of the differences between the obtained attainment surfaces reveals that the MOACS-2 is better at the extremes of the Pareto front, whereas the BIANT-1 and BIANT-2 are better in the middle of the true Pareto front. A Pareto front can be split into three main regions; two regions represent the extremums that can be reached by minimising each objective function separately. The region that represents the middle part of the Pareto front is more likely to be of interest to the decision maker. Thus, even if the MOACS-2 demonstrates slightly better results in the Friedman's test, the BIANT-1 and BIANT-2 are more suitable for industrial applications since they outperform the MOACS-2 in the central region of the Pareto front.

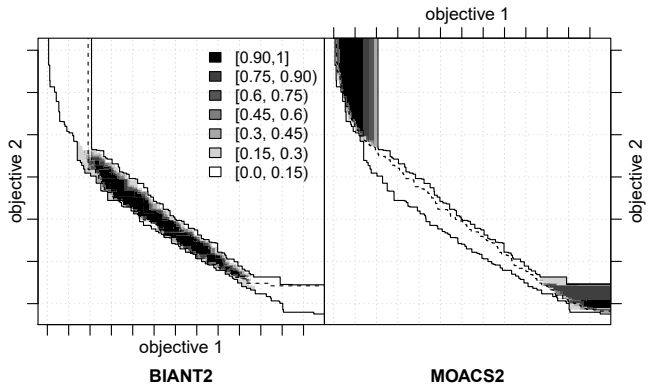

Figure 4.19: Differences in the attainment function between the BIANT-2 and MOACS-2 for Mukherje-3

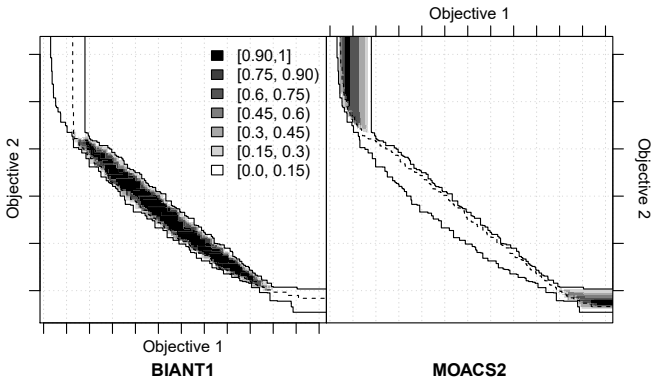

Figure 4.20: Differences in the attainment function between the BIANT-1 and MOACS-2 for Buxey-1

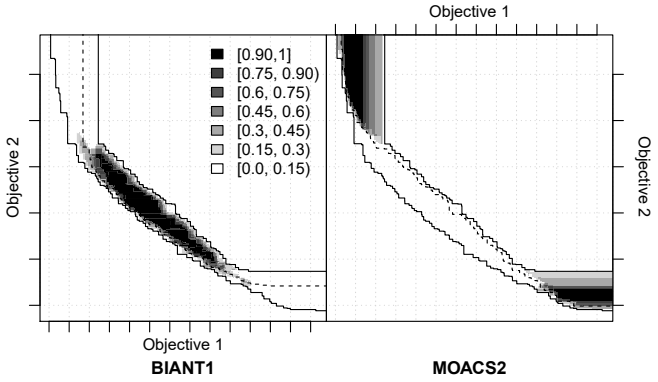

Figure 4.21: Differences in the attainment function between the BIANT-2 and MOACS-2 for Arc111-5

Regarding the strategies used for finding the best global solution in the discrete swarm intelligence algorithms, namely the DMOFPA, DMOCSA, DMOPSO, and DMOBAT, heterogeneous results were found. For the DMOBAT, it seems that the third strategy is, on average with all problems together, the most suitable strategy for the following metrics: I_{HV}, I_{IGD} and I_ϵ. Regarding the obtained p-values, the fourth strategy significantly outperformed the others for these three quality indicators. Moreover, the grouping of problem instances do not have any influence on the selection strategy, which remains the best for both groups. For the DMOCSA, the dynamic parameter control for abandoning and creating solutions offers advantages for the covered hypervolume compared to the static parameter control. Regarding the I_{IGD} and I_ϵ, the forth strategy obtained the best results with the static and dynamic parameter control, respectively and in decreasing order. Concerning the last indicator, I_Δ, the best results were obtained with the first strategy and also respectively with the static and dynamic parameter control. For the DMOFPA, the first, second, and third strategies obtained the best results for the first three quality indicators. The forth strategy, which significantly outperformed the others regarding I_{HV}, I_{IGD} and I_ϵ, is the best strategy in accordance with the obtained spread. Again for the DMOPSO, the fourth strategy significantly

outperformed the others regarding all quality indicators. The first and second strategies were the most effective for the first three quality indicators. The fifth strategy performed optimally for the spread indicator. These results are summarized in Table 4.43. The detailed results of this analysis, including the Friedman's average ranking and the unadjusted and adjusted p-values are presented in Appendix C.4.13.

Table 4.43: Synthesis of the best strategy for each class of algorithm and quality indicator

	Best Strategies			
Algorithm	I_{HV}	I_{IGD}	I_{ϵ}	I_{Δ}
DMOBAT	3	4	3	5
DMOCSA	2-2	2-5	1-4	1-1
DMOFPA	3	2	1	4
DMOPSO	1	2	1	5

4.6 Conclusion

In this chapter, a resolution framework is presented that aims to supporting decision makers during the design phases of an assembly line, while considering product designs, processes, and resource alternatives. In other words, this framework aims to simultaneously select product designs, processes, and resource alternatives in order to plan the most suitable assembly line regarding capacity and cost-oriented objectives. This problem was formulated and a mathematical model was proposed with a detailed cost model. The function of this model is to translate the complex and interrelated consequences of choosing specific design alternatives with manufacturing technologies into one single cost metric. To solve this problem, 34 state-of-the-art approximate methods were developed. All these methods were compared with each other based on fifty problem instances. Four multi-objective quality indicators were used and a nonparametric statistical test was applied to judge the performances of the algorithms. While the NSGA-II and SPEA2 demonstrate the best results, on average and considering all problem instances together, regarding I_{HV} and I_{ϵ}, the CHAC-1 and BIANT-1 obtain the best values for I_{IGD} and I_{Δ}, respectively. However, classifying the problem instances according to their order strengths shows that the proposed MOACS-1, MOACS-2, BIANT-1, and BIANT-2 are more suitable for complex problems. Comparing them graphically using the attainment function showed that the proposed BIANT-1 and BIANT-2 are better in the central region of the Pareto front, which implies that these two algorithms are more suitable for an industrial application. In order to answer the defined Research Question 3, the same procedure was applied to the various swarm intelligence al-

gorithms, including the DMOBAT, DMOCSA, DMOFPA, and DMOPSO. As stated earlier, the results are heterogeneous and the selection strategies seem to perform equally when considering all quality indicators together.

The proposed work in this chapter has partially been the subject to several publications: one accepted submission to an international journal [293], one accepted submission to a national journal [295], three communications at conferences [289, 290, 291].

Chapter 5

Assembly Line Design Problem, Processing, and Resources Alternatives: Influence of Dominance Rules and Local Search

---

Abstract

In the previous chapter, the various algorithms are compared and it is demonstrated that the MOACS-1, MOACS-2, BIANT-1, and BIANT-2 provide good solutions for complex problems regarding the various quality indicators. However, the BIANT-1 and BIANT-2 require the highest computation time to move forward to a set of non-dominated solutions, which is a considerable drawback. In addition, it is illustrated through graphical comparison that the BIANT-1 and BIANT-2 perform better in the central region of the Pareto front. Alternatively, the MOACS-1 and MOACS-2 are better in the extreme regions. In this chapter, the influence of different dominance rules and a local search is analysed in order to improve the performance of the MOACS-1 and MOACS-2 when applied to complex problems and of the CHAC-1 and CHAC-2 when applied to small problems.

5.1 Introduction

The previous chapter shows that the MOACS-1, MOACS-2, BIANT-1, and BIANT-2 are most suitable for complex problems. A graphical comparison by means of the attainment function illustrated that the BIANT-1 and BIANT-2 are better in the central region of the Pareto front. However, the BIANT-1 and BIANT-2 are the two algorithms that perform worse regarding the convergence speed. Furthermore, the NSGA-II and SPEA2 have on average a good performance when taking all the problems into consideration. In addition, CHAC-1 and CHAC-2 have good results for small problems. The objective of this chapter is to improve these algorithms by analysing the influence of other dominance rules and incorporating a local search.

5.2 Comparison of dominance rules

In the present section, the influence of the Lorenz and S-CDAS dominance rules is analysed and compared to the Pareto dominance rule. Since these three various dominance rules have different guidance for the search agents toward different regions of the Pareto front, using I_{HV} as a quality indicator may not completely highlight their strengths and weaknesses. In addition to the I_{HV}, the C metric, denoted as I_C, is also used to compare the number of solutions provided by an algorithm A1 that is dominated by another algorithm A2.

Table 5.1: List of algorithms and their abbreviations

	Dominance Rule				Dominance Rule	
Name	Pareto	Lorenz	S-CDAS	Name	Pareto	Lorenz
CHAC-1	X			DMOPSO-1	X	
CHAC-1-L		X		DMOPSO-1-L		X
CHAC-2	X			DMOPSO-2	X	
CHAC-2-L		X		DMOPSO-3	X	
MOACS-1	X			DMOPSO-4	X	
MOACS-1-L		X		DMOPSO-5	X	
MOACS-1-S-CDAS			X	NSGA-II	X	
MOACS-2	X			NSGA-II-L		X
MOACS-2-L		X		SPEA2	X	
MOACS-2-S-CDAS			X	SPEA2-L		X

The computation experiments were performed in the same configuration as the previous chapter. In order to ease the readiness of the algorithms' name, the abbreviations shown in Table 5.1, will be used in this chapter.

Since the true Pareto front is not known for all the problems, the approximate Pareto

front (computed as in the previous chapter) is used for these problem instances. Since the approximate Pareto front may change, as shown in Figure 5.1, it was recomputed for all problems for which the true Pareto front is not know.

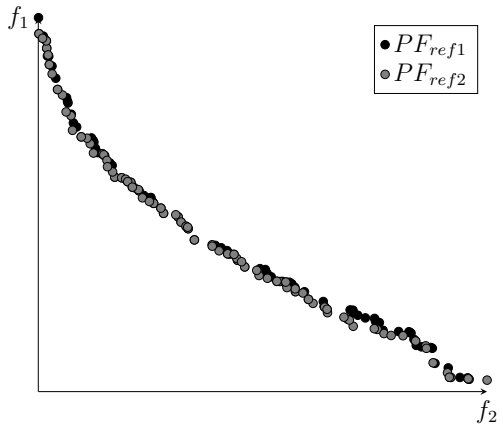

Figure 5.1: Differences between the two approximate Pareto fronts

5.2.1 Statistical analysis

Out of a statistical analysis, whose results are shown in Appendix D.1, the following research questions were identified:

Research Question 4. *Does the dominance rule significantly affect the various quality indicators?*

Research Question 5. *Which dominance rule is more suitable for the research problem of this thesis?*

Research Question 6. *Can the combination of a different dominance rule and an algorithm from chapter Chapter 4 improve the results obtained with the BIANT-1 or BIANT-2?*

In order to answer these research questions, the strengths and weaknesses of the various dominance rules must be identified by evaluating their influence on the quality indicators. As in the previous chapter, a nonparametric statistical test is used.

5.2.2 Nonparametric statistical test

In order to answer the Research Question 4, Research Question 5, and Research Question 6, the Friedman statistical test was applied. The obtained Friedman statistics for all problems and algorithms considered together in accordance with I_{HV}, I_{IGD}, I_ϵ, I_Δ, and the computation time and their respective computed p-values are shown in Table 5.2. Given $\chi^2_{0.05} = 32.7$

with a 95% confidence level and 21 degrees of freedom, it can be concluded that there are significant differences among the algorithms for all quality indicators.

Table 5.2: Friedman's statistic and computed p-value in accordance with I_{HV}, I_{IGD}, I_ϵ, I_Δ, and the computation time

Indicators	Friedman statistic	Computed p-values
I_{HV}	259.770	1.38E−10
I_{IGD}	152.060	8.39E−11
I_ϵ	679.250	2.04E−10
I_Δ	1193.530	0
Time	2216.600	0

Table 5.3: Average rankings returned by Friedman's nonparametric test for all problems according to the various quality indicators

	Ranking				
Algorithm	I_{HV}	I_{IGD}	I_ϵ	I_Δ	Time
BIANT-1	11.22	12.18	7.50	15.69	6.18
BIANT-2	11.21	12.06	7.38	14.87	5.75
CHAC-1	10.68	12.52	12.61	10.58	10.57
CHAC-1-L	10.76	12.77	12.74	10.25	11.21
CHAC-2	10.82	12.45	12.61	10.31	11.35
CHAC-2-L	10.36	12.97	13.13	10.24	10.24
MOACS-1	13.47	10.34	8.46	15.52	9.15
MOACS-1-S-CDAS	14.61	9.05	8.31	15.73	4.63
MOACS-1-L	13.12	10.40	8.86	15.82	8.50
MOACS-2	11.76	10.78	9.33	15.74	7.99
MOACS-2-S-CDAS	12.09	10.49	9.43	15.39	5.98
MOACS-2-L	11.82	10.94	9.27	15.72	8.13
DMOPSO-5	11.67	11.84	12.91	9.44	13.47
DMOPSO-1	11.35	12.40	13.23	9.61	14.80
DMOPSO-2	11.78	12.25	12.44	8.97	15.44
DMOPSO-3	11.86	11.77	12.63	9.27	15.07
DMOPSO-4	14.69	8.57	11.06	9.35	11.10
DMOPSO-1-L	11.77	11.56	12.93	8.91	14.68
NSGA-II	9.15	12.34	14.73	7.39	11.21
NSGA-II-L	9.18	11.91	14.83	8.38	17.76
SPEA2	9.76	11.76	14.31	7.97	19.96
SPEA2-L	9.83	11.65	14.31	7.87	19.84

Table 5.3 shows the average ranking returned by Friedman's nonparametric test for all problems considered at once and given all various quality indicators. If the obtained rankings are compared to those obtained in Table 4.33 of Chapter 4, it can be stated that, according to the new reference sets of the approximate Pareto front an improvement has been made regarding I_Δ. This indicator was maximised in the precedent chapter by the BIANT-1 and BIANT-2. Now, it is maximised by MOACS-1-L. In addition, on average, an improvement was made regarding I_{IGD} for the CHAC-1-L and CHAC-2-L. The adjusted and unadjusted

p-values are shown for each quality indicator respectively in Tables 5.4 to 5.8. Furthermore, a slight improvement was observed for the I_ϵ indicator with a value that is maximised by the NSGA-II-L.

Table 5.4: Unadjusted and adjusted p-values obtained for all problems through the application of Holm's post hoc procedure, using the NSGA-II as control algorithm according to I_{HV}

Algorithm	Unadjusted p-value	Adjusted p-value
Others	0.008	<0.046
CHAC-1	0.011	0.055
CHAC-2-L	0.045	0.180
SPEA2-L	0.260	0.779
SPEA2	0.311	0.779
NSGA-II-L	0.960	0.960

Table 5.5: Unadjusted and adjusted p-values obtained for Sawyer through the application of Holm's post hoc procedure, using the CHAC-2-L as control algorithm according to I_{IGD}

Algorithm	Unadjusted p-value	Adjusted p-value
Others	0.001	<0.017
BIANT-2	0.061	0.847
SPEA2	0.198	2.580
BIANT-1	0.216	2.586
DMOPSO-L	0.248	2.728
SPEA2-L	0.288	2.883
NSGA-II-L	0.315	2.883
DMOPSO	0.334	2.883
DMOPSO-3	0.540	3.777
DMOPSO-2	0.596	3.777
CHAC-1	0.613	3.777
NSGA-II	0.662	3.777
DMOPSO-1	0.708	3.777
CHAC-2	0.764	3.777
CHAC-1-L	0.918	3.777

Table 5.6: Unadjusted and adjusted p-values obtained for Sawyer through the application of Holm's post hoc procedure, using the NSGA-II-L as control algorithm according to I_ϵ

Algorithm	Unadjusted p-value	Adjusted p-value
Others	0.009	<0.035
SPEA2	0.387	1.160
SPEA2-L	0.389	1.160
NSGA-II	0.862	1.160

Table 5.7: Unadjusted and adjusted p-values obtained for Sawyer through the application of Holm's post hoc procedure, using the MOACS-1-L as control algorithm according to I_Δ

Algorithm	Unadjusted p-value	Adjusted p-value
Others	0.000	<5.460E-17
BIANT-2	0.119	0.835
MOACS-2-S-CDAS	0.477	2.865
MOACS-1	0.626	3.132
BIANT-1	0.829	3.315
MOACS-2-L	0.871	3.315
MOACS-1-S-CDAS	0.888	3.315
MOACS-2	0.897	3.315

Table 5.8: Unadjusted and adjusted p-values obtained for Mukherje through the application of Holm's post hoc procedure, using the SPEA2 as control algorithm in accordance with the computation time

Algorithm	Unadjusted p-value	Adjusted p-value
Others	0.022	<0.044
SPEA2-L	0.886	0.886

As discussed in the previous chapter, there are significant differences between problems with small and large order strengths. Using the same grouping as in the previous chapter and by performing the same analysis again, the results in Table 5.9 were obtained. As shown in this table, the MOACS-2-L obtained the best results for problems from Group 1 for I_{HV} and I_Δ. The NSGA-II-L reached the best value of I_ϵ, and the MOACS-2-L obtained the second best value. Even if the MOACS-2 family of algorithms demonstrates good results for I_{IGD}, the BIANT-1 and BIANT-2 still have the best values. For problems from Group 2, the CHAC-2-L demonstrated the best values of I_{HV}, I_{IGD}, and I_ϵ. In the classification of algorithms performing well on these quality indicators, the CHAC-2-L is followed by the DMOPSO-1. While the MOACS-1-S-CDAS cannot perform well regarding these quality indicators, it is the best algorithm when considering I_Δ, followed by the BIANT-1. For both groups, the SPEA2 and SPEA2-L converged the fastest toward a set of non-dominated solutions.

Table 5.9: Average rankings returned by Friedman's nonparametric test for both groups, Group 1 and Group 2

	Group 1					Group 2				
Algorithm	I_{HV}	I_{IGD}	I_ϵ	I_Δ	Time	I_{HV}	I_{IGD}	I_ϵ	I_Δ	Time
BIANT-1	5.29	17.70	8.67	17.64	4.15	16.71	6.89	6.43	13.89	8.14
BIANT-2	4.41	18.03	9.44	17.69	4.06	17.51	6.35	5.50	12.29	7.37
CHAC-1	14.23	9.79	10.46	9.81	10.29	7.40	15.14	14.58	11.28	10.84
CHAC-1-L	14.46	10.39	9.93	10.13	9.49	7.33	15.04	15.32	10.36	12.87
CHAC-2	14.69	9.68	9.90	9.36	11.33	7.25	15.10	15.09	11.18	11.36
CHAC-2-L	14.30	10.25	10.25	9.65	9.76	6.71	15.56	15.77	10.77	10.71
MOACS-1	8.38	14.85	11.85	18.36	9.66	18.18	6.02	5.36	12.92	8.67
MOACS-1-S-CDAS	11.23	12.09	10.70	17.55	7.71	17.74	6.15	6.12	14.07	1.66
MOACS-1-L	8.05	14.79	12.00	18.28	9.93	17.82	6.20	5.98	13.57	7.12
MOACS-2	4.45	16.20	14.10	19.27	10.73	18.52	5.60	4.96	12.51	5.33
MOACS-2-S-CDAS	4.87	15.70	14.17	18.82	10.23	18.77	5.51	5.08	12.24	1.87
MOACS-2-L	3.99	16.64	14.39	19.40	10.92	19.06	5.48	4.58	12.34	5.43
DMOPSO-5	15.31	9.85	10.47	8.24	13.00	8.30	13.74	15.15	10.54	13.93
DMOPSO-1	15.82	9.50	10.63	7.75	12.93	7.22	15.19	15.61	11.31	16.60
DMOPSO-2	16.18	9.51	9.92	7.50	15.43	7.71	14.88	14.75	10.32	15.45
DMOPSO-3	16.30	8.71	10.02	7.40	11.40	7.75	14.69	15.02	10.98	18.60
DMOPSO-4	18.81	5.18	9.43	7.32	8.07	10.88	11.81	12.55	11.21	14.03
DMOPSO-1-L	16.19	8.88	10.45	7.88	14.20	7.69	14.12	15.19	9.86	15.14
NSGA-II	10.94	9.37	14.22	4.04	12.34	7.50	15.18	15.19	10.46	10.11
NSGA-II-L	11.06	9.19	14.56	5.95	16.55	7.45	14.52	15.08	10.59	18.93
SPEA2	12.06	8.18	13.54	5.43	20.32	7.64	15.18	15.00	10.29	19.62
SPEA2-L	11.97	8.53	13.91	5.54	20.50	7.85	14.64	14.67	10.01	19.21

The unadjusted and adjusted p-values obtained through the applications of Holm's post hoc procedures for Group 1 and Group 2 are respectively shown in Tables D.85 to D.89 and Tables D.90 to D.94. The unadjusted and adjusted p-values show that, even if the MOACS-2-L is better than the BIANT-1 and BIANT-2 regarding I_{HV}, I_ϵ, and I_Δ for Group 1, it is not significantly better. However, the CHAC-2-L is significantly better that those algorithms for the problem instances of Group 2 for I_{HV}, I_{IGD} and I_ϵ. If the obtained results are compared to those of the Chapter 4, the MOACS-2-L optimises the value of I_ϵ for problem instances of Group 1. This quality indicator was previously being optimised by the NSGA-II. In addition, the gap between the BIANT and MOACS families of algorithms was increased for I_Δ. Considering problem instances of Group 2, the results became more homogeneous and the CHAC-2-L is the algorithm that obtained the best results for following quality indicators: I_{HV}, I_{IGD}, and I_ϵ. In summary, the results got harmonised for each group of problem instances and two algorithms can be identified that perform better on almost all quality indicators, namely, the MOACS-2-L and the CHAC-2-L. For the results obtained by considering all problem instances, the NSGA-II-L and the SPEA2 are also candidates for further improvements.

In order to further investigate the Research Question 4, Research Question 5, and Research

Question 6, the average value of I_C obtained when applying the Pareto dominance rule, the Lorenz and S-CDAS can be examined for each algorithm. The results are shown for each group of problems in Table 5.10. When applying the Lorenz dominance rule to the problems from Group 1, the obtained solutions are less dominated by the Pareto dominance rule than the opposite. For the S-CDAS dominance rule, it seems that regarding I_C, it is better than the Pareto dominance rule for the MOACS-1; the Pareto dominance rule is more suitable for the MOACS-2. More heterogeneous results are obtained when comparing the dominance rules when applied to problems from Group 2. For the CHAC-2 and MOACS-1, the Lorenz dominance rule is, regarding I_C better, than the Pareto dominance rule, but the opposite is true for the CHAC-1 and MOACS-2. It also seems that the S-CDAS is more suitable when applied in combination with the MOACS-2 for problems from Group 1.

Table 5.10: Evolution of the value of I_C based on the dominance rule and grouping of problem instances

Algorithm	Dominance Rule	Group 1	Group 2
CHAC-1	$I_C(L,P)$	0.39	0.11
	$I_C(P,L)$	0.39	0.10
CHAC-2	$I_C(L,P)$	0.39	0.10
	$I_C(P,L)$	0.39	0.11
MOACS-1	$I_C(L,P)$	0.39	0.19
	$I_C(P,L)$	0.42	0.23
MOACS-2	$I_C(L,P)$	0.38	0.20
	$I_C(P,L)$	0.42	0.14
MOACS-1	$I_C(S-CDAS,P)$	0.38	0.20
	$I_C(P,S-CDAS)$	0.42	0.14
MOACS-2	$I_C(S-CDAS,P)$	0.42	0.19
	$I_C(P,S-CDAS)$	0.38	0.22

The obtained I_C values for all of the problems and instances are provided in Appendix D.1.12. The I_C values obtained by the MOACS-2, MOACS-2-S-CDAS, MOACS-2-L and BIANT-2 are shown in Table 5.11 in the form of a box plot. According to this figure, the BIANT-2 is the algorithm that is less dominated by any other algorithm. Comparing the MOACS-2-S-CDAS and the MOACS-2-L, it seems that the former algorithm is more dominated by the second one. The obtained values of the C metric, I_C, for the other problems are present in Appendix D.1. According to them, the MOACS-2-S-CDAS is often more dominated by the MOACS-2-L than vice versa.

Table 5.11: C-metric for the Arc111-1 problem instance

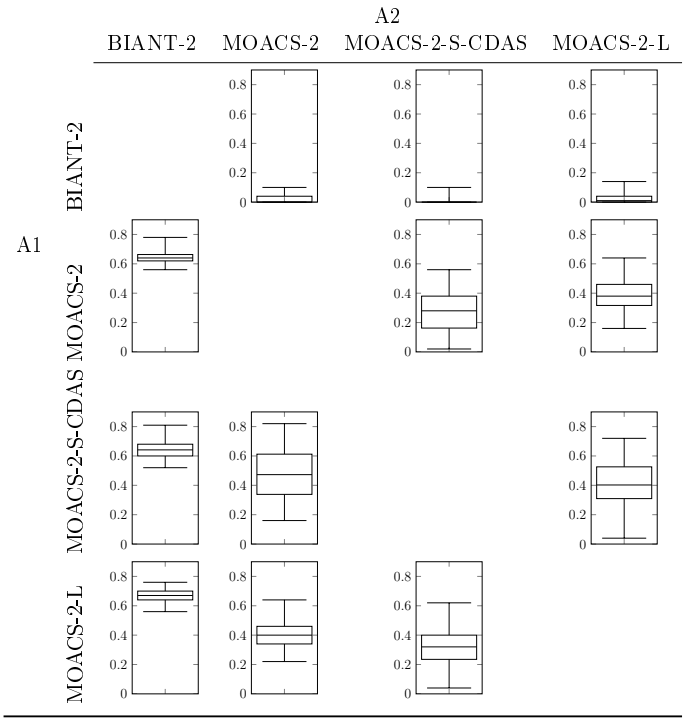

Figure 5.2 shows the evolution of the number of non-dominated solutions when applying the various dominance rules to specific algorithms and problems. As illustrated, on average, the number of non-dominated solutions is lower when applying the Lorenz dominance rule than when applying the Pareto dominance rule. In addition to the Friedman test, a multiple pairwise comparison of the dominance rules using Nemenyi's procedure was applied to the various quality indicators for each algorithm. The results are represented in Table 5.12-5.14. In these tables, "Yes"/"No" respectively represents whether there is significant differences between the dominance rules. As demonstrated by these tables, there is mostly no significant differences (alpha level set to 0.05) between the various dominance rules when considering following quality indicators: (i) I_{HV}, (ii) I_{IGD}, (iii) I_{ϵ}, (iv) I_{Δ}, (v) the computation time until convergence, (vi) I_C, and (vii) the number of non-dominated solutions (NDS). While the performance of the CHAC-1 and CHAC-2 is not significantly sensitive to the chosen dominance rule, the difference between the dominance rules is significant for MOACS-1 and MOACS-2 when they are applied to complex problems. The S-CDAS dominance rule performs worse than the Pareto and Lorenz dominance rules on complex problems. Indeed, compared to the Pareto dominance rule, the S-CDAS engenders a deterioration of the following quality indicators: (i) I_{HV}, (ii) I_{IGD}, (iii) I_{ϵ}, (iv) I_{Δ} and (v) the computation time required until convergence. If this deterioration is quantified, the value of these indicators will decrease respectively by 1.7%, 6.6 %, 19%, 2.7, and 23% for the MOACS-1. However, the S-CDAS, which is more aggressive in the middle region of the Pareto front, allows improving

I_C by 2 %. The same conclusion can be made for MOACS-2, for which all the previous indicators, except I_Δ, are deteriorated as follows: (i) I_{HV} by 4%, (ii) I_{IGD} by 5%, and (iii) I_ϵ by 3.5%, (iv) the computation time until convergence by 26%. Similar to the previous case, the MOACS-2 allows an improvement of I_C by 1%. When comparing the significant differences between the dominance rules, it seems that the effect of dominance rules is bigger when problem instances remain less complex.

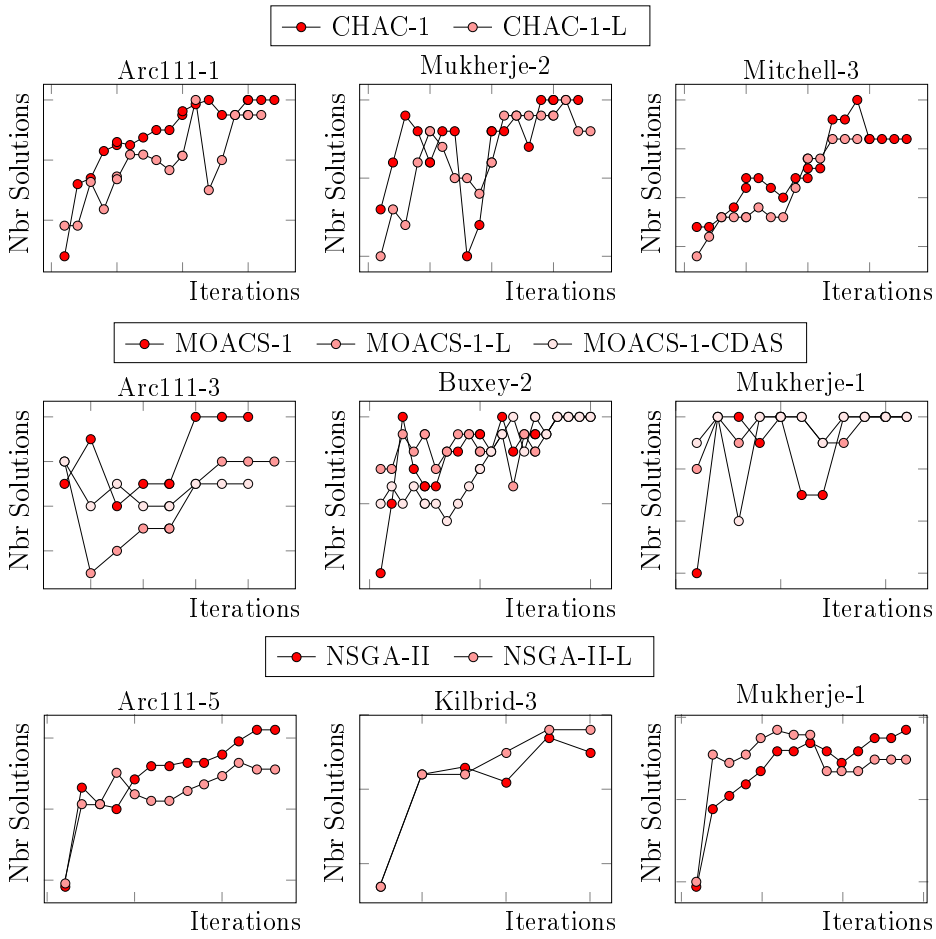

Figure 5.2: Comparison of the set of non-dominated solutions obtained by the various dominance rules

Table 5.12: Differences between the dominance rules based on a comparison with all problem instances

Algorithm	Dominance rules	I_{HV}	I_{IGD}	I_ϵ	I_Δ	Time	I_C	NDS
CHAC-1	Pareto / Lorenz	No	No	No	No	No	Yes	No
CHAC-2	Pareto / Lorenz	No	No	No	No	No	Yes	No
	Pareto / Lorenz	No	No	No	No	Yes	Yes	No
MOACS-1	Pareto / S-CDAS	Yes	No	No	No	Yes	No	No
	Lorenz / S-CDAS	No	No	Yes	No	Yes	Yes	No
	Pareto / Lorenz	No	No	No	No	No	Yes	No
MOACS-2	Pareto / S-CDAS	No	Yes	No	Yes	Yes	No	No
	Lorenz / S-CDAS	No	No	No	No	Yes	No	No
NSGA-II	Pareto / Lorenz	No	No	No	No	Yes	Yes	Yes
SPEA2	Pareto / Lorenz	No	No	No	No	Yes	No	No

Table 5.13: Differences between the dominance rules based on a comparison with problem instances of Group 1

Algorithm	Dominance rules	I_{HV}	I_{IGD}	I_ϵ	I_Δ	Time	I_C	NDS
CHAC-1	Pareto / Lorenz	No	No	No	No	No	Yes	No
CHAC-2	Pareto / Lorenz	No	No	No	No	No	No	No
	Pareto / Lorenz	No	No	No	No	No	Yes	No
MOACS-1	Pareto / S-CDAS	Yes	Yes	Yes	Yes	Yes	No	No
	Lorenz / S-CDAS	Yes	Yes	Yes	No	Yes	No	No
	Pareto / Lorenz	No	No	No	No	No	No	No
MOACS-2	Pareto / S-CDAS	No	Yes	No	Yes	Yes	No	No
	Lorenz / S-CDAS	No	No	No	No	Yes	No	No
NSGA-II	Pareto / Lorenz	No	No	No	No	Yes	Yes	Yes
SPEA2	Pareto / Lorenz	No	No	No	No	Yes	No	No

Table 5.14: Differences between the dominance rules based on a comparison with problem instances of Group 2

Algorithm	Dominance rules	I_{HV}	I_{IGD}	I_ϵ	I_Δ	Time	I_C	NDS
CHAC-1	Pareto / Lorenz	No	No	No	No	Yes	Yes	No
CHAC-2	Pareto / Lorenz	No	No	No	No	No	Yes	No
	Pareto / Lorenz	No	No	No	No	Yes	Yes	No
MOACS-1	Pareto / S-CDAS	No	No	No	No	Yes	No	No
	Lorenz / S-CDAS	No	No	No	No	Yes	Yes	No
	Pareto / Lorenz	No	No	No	No	No	Yes	No
MOACS-2	Pareto / S-CDAS	No	No	No	No	Yes	No	No
	Lorenz / S-CDAS	No	No	No	Yes	No	Yes	No
NSGA-II	Pareto / Lorenz	No	No	No	No	Yes	No	Yes
SPEA2	Pareto / Lorenz	No	No	No	No	Yes	Yes	No

5.2.3 Attainment-function

In the previous section, the various dominance rules were compared according to the various quality indicators. In order to highlight the difference between the dominance rules, the present section is based on the attainment functions obtained by these rules. Figures 5.3 to 5.5 show some examples of the obtained attainment functions by the various algorithms and dominance rules. The Lorenz dominance seems to be better than the S-CDAS in the extreme regions of the Pareto front. In comparison, it seems that the S-CDAS dominance rule is restrictive and it only enables a slight improvement in the central region. Comparing the Lorenz dominance rule with the Pareto dominance rule, a general observation can be made for all algorithms that the Lorenz dominance is better in the central region.

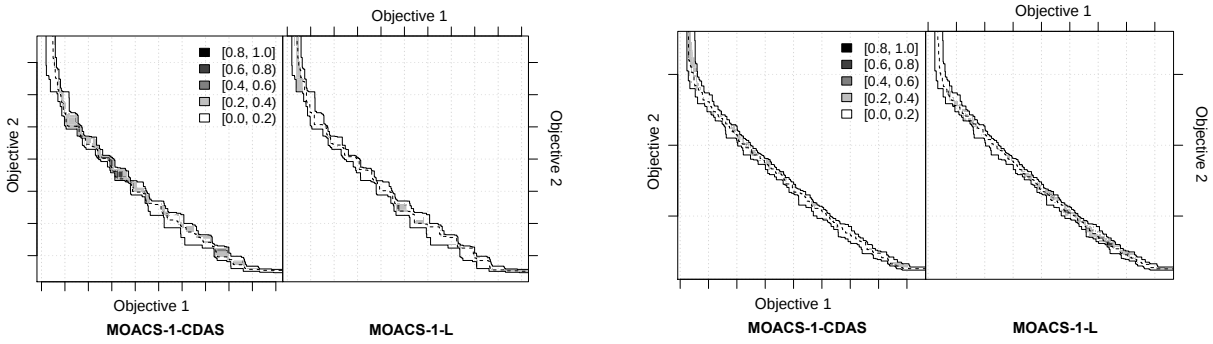

(a) Buxey-4 *(b)* Hahn-2

Figure 5.3: Differences in the attainment function between the MOACS-1-S-CDAS and MOACS-1-L

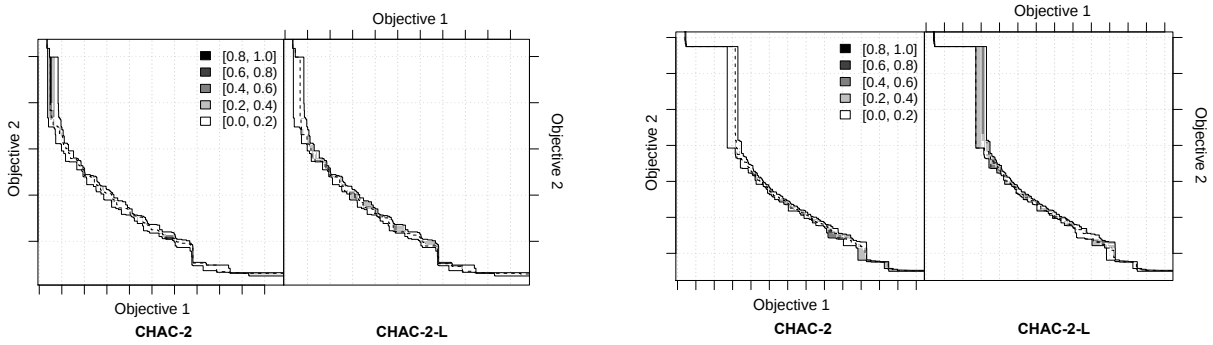

(a) CHAC-2: Buxey-1 *(b)* CHAC-1: Mukherje-3

Figure 5.4: Differences in the attainment function between the Pareto and Lorenz dominance rules for the CHAC-1 and CHAC-2

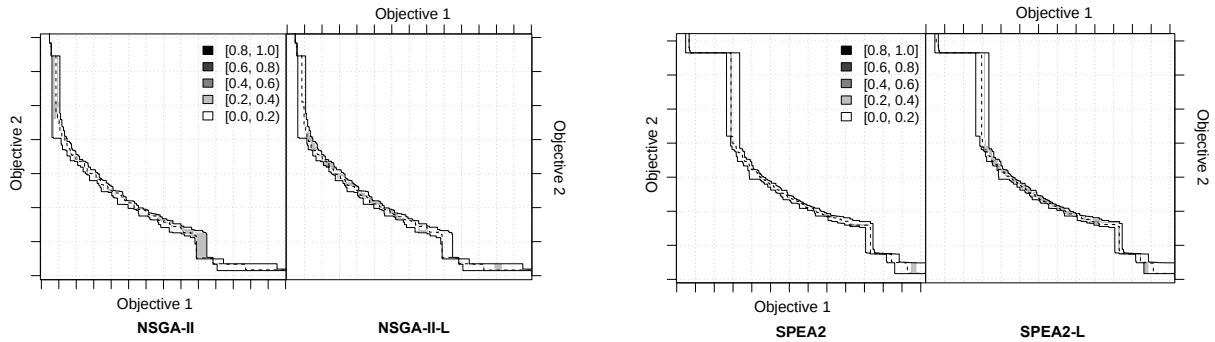

(a) NSGA-II: Gunther-4 *(b)* SPEA2: Mukherje-2

Figure 5.5: Differences in the attainment function between the Pareto and Lorenz dominance rules for EAs

5.2.4 Synthesis

The various dominance rules offer several advantages and disadvantages depending on the algorithm. The S-CDAS dominance rule did not show any improvements compared to the two other dominance rules. Although it may be more efficient in the central region of the Pareto front, its required time to convergence is much longer than that of the Pareto and Lorenz dominance rules. Therefore, it is not an appropriate choice for further investigation. Regarding the Lorenz and Pareto dominance rules, it seems that the impact of the Lorenz dominance rule is clear when it is used in combination with MOACOs. As previously demonstrated, the comparisons of these two rules are heterogeneous and the Lorenz dominance rule offers many more advantages than the Pareto dominance rule when it is combined with the MOACS-1. Alternatively, for the MOACS-2, even if the required time for converging toward a set of non-dominated solutions is better when applying the Lorenz dominance rule than the one of the Pareto dominance rule, it does not make hit a suitable candidate since the value of the other quality indicators are mostly all being worse than those obtained with the Pareto dominance rule. For the CHAC family of algorithms, the ranking of both dominance rules differ according to the quality indicator considered. Considering the Friedman's statistic and computed p-values, it seems that the Pareto dominance rule is being a better alternative. For the NSGA-II, the results are similar despite for the required computation time and I_{Δ}. This makes the Lorenz dominance a better candidate for further investigations. For the SPEA2, only the value of one quality indicator is better when using the Lorenz dominance rule. The computation time, which plays an important role when applying local search techniques, is here a crucial criterion. The same reasoning is used for the DMOPSO, for which the Lorenz dominance rule allows a faster convergence toward a set of non-dominated solutions.

5.3 Improvement through local search

Based on the analyses presented above, three algorithms were identified as suitable candidates for further improvement: the MOACS-2-L, NSGA-II-L, and SPEA2. The choice of the MOACS-2-L is based on its performances for complex problems, which are appropriate for industrial needs. The NSGA-II-L and SPEA2 were selected due to their general performances when considering all problems together. Although the DMOPSO-1 and CHAC-2-L perform well when considering the I_{HV}, I_{IGD} and I_{ϵ} for small problems, they are not considered future candidates for improvement since the related problem configurations are not appropriate for industrial needs.

When incorporating a local search procedure into multi-objective algorithms, the main issue is related to the fact that more than one objective must be optimised simultaneously. This section is organised as follows: First the general local search procedure is presented and then its integration with the four algorithms is outlined.

5.3.1 General local search procedure

Let LS_{set} denote the set of solutions that are candidates for the local search. First, the neighbourhood of any solution $s \in LS_{set}$ needs to be explored through the application of mutation operators. Any generated solution $s^{'}$ that is not dominated by the original solution s will be accepted. The improvement process of each solution $s \in LS_{set}$ is repeated a number of iterations, MAX_{LS}. This general procedure is depicted in Algorithm 5. Here, in order to vary the number of iterations MAX_{LS} during the iterations based on the convergence of the algorithm and in order to save on computation time, the number is increased in accordance with the stopping criteria MGBM used. Since the algorithm stops if no non-dominated solution has changed after a pre-specified number of generations L_{iter}, MAX_{LS} is increased when the number of iterations before iteration t, $L(t)$, for which no improvement has been observed, is getting closer to L_{iter}. $MAX_{LS}(t)$ at each generation t is calculated as follows:

$$MAX_{LS}(t) = e^{L(t)/30} + 4 \tag{5.1}$$

Algorithm 5 General procedure of the local search

```
1: procedure MyProcedure(LS_set)
2:     Output: s'
3:     for s ∈ LS_set do
4:         n=1
5:         while n < MAX_LS do
6:             s' ← Neighbourhood(s)
7:             if s ⊀ s' then
8:                 s ← s'
9:             n=n+1
```

The general neighbourhood search is working as follows. According to $p_{rand} \in [0, 1]$, which aims at choosing which objective function should be optimised. Here, the probability of optimising each objective is equal to 0.5. If $p_{rand} < 0.5$, the unit product cost will be optimised. A station m is randomly selected and the costs associated with each task $j \in S_m$ will be computed. The task $j_{c_{max}}$, which is responsible for the highest costs will be selected. The potential costs associated with each equipment $l \in E_{j_{c_{max}}}$ will be analysed and the equipment $l_{c_{min}}$ with the least associated costs will be assigned instead of the old one. If $p_{rand} \geq 0.5$, the idle time will be optimised. A station m is randomly selected and the idle time I_m is calculated. A task $j \in S_m$ is randomly selected. The potential idle time $I_{m,l}$ associated with the replacement of the resource to perform j is calculated, $\forall l \in S_m$. The old resource is replaced by the new one that minimises the idle time I_m.

5.3.1.1 NSGA-II-L-LS

In this section, the design of the combination of NSGA-II-L and the local search, denoted NSGA-II-L-LS will be explained. After a population P_{t+1} is created, the solutions are subject to the local search procedure, which is applied once. The solutions selected for the local search are the least crowded solutions, which means those with the greatest crowding distance value. If the number of solutions in the first Front is not enough to fill LS_{set}, the second and third are considered. Once the local search has been applied, the population P_{t+1} is combined with LS_{set}, $P_{t+1} \leftarrow P_{t+1} \cup LS_{set}$ and the crowding distance and sorting procedures are applied.

5.3.1.2 SPEA2-LS

In this section, the design of the combination of the SPEA2 and the local search, denoted as SPEA2-LS is presented. After the fitness of each individual in the population P_t and archive

A_t during the iteration t have been evaluated, all nondominated individuals in P_t and A_t are copied to A_{t+1}. The best solutions in the archive A_{t+1} are selected according to their fitness values, represented by low fitness values. If the number of solutions in the first Front is not enough to fill LS_{set}, solutions from the population P_t are taken. Once the local search has been applied, the archive A_{t+1} is combined with LS_{set}, $A_{t+1} \leftarrow A_{t+1} \cup LS_{set}$ and dominated solutions in A_{t+1} are removed.

5.3.1.3 MOACS-2-L-LS

Similar to the procedure of the SPEA2, after the fitness of each individual in the population P_t and archive A_{t-1} have been evaluated and all non-dominated solutions are copied to A_t, the best solutions in the archive, represented by a great crowding distance value are selected and copied to LS_{set}. Once the local search has been applied and the archive A_t and the set LS_{set} are combined and non-dominated solutions are removed, the global pheromone update is performed.

5.3.2 Evaluation of the influence of the local search

In this section the influence of the local search on the various algorithms will be studied. An identical statistical analysis as the one proposed in Section 4.5.4.1 was performed. The obtained results for all problems and the various combinations of algorithms and local search are shown in Appendix E.1. This analysis allowed to identified following research questions:

Research Question 7. *Does the local search significantly affect the various quality indicators?*

Research Question 8. *Does the local search make it possible to converge faster to non-dominated solutions?*

Research Question 9. *Considering the local search and dominance rule, which algorithm is the best regarding all problems together and the two groups of problem instances?*

In order to answer these research questions, the strengths and weaknesses of the local search must be identified by evaluating its influence on the various quality indicators. As described in the previous chapter, a nonparametric statistical test was used.

5.3.3 Nonparametric statistical test

In this section, nonparametric statistical tests are applied to highlight the strengths and weaknesses of the local search combined with the MOACS-2-L, NSGA-II-L, and SPEA2. Since the number of data samples does not meet the requirements to directly employ the Friedman test, the Wilcoxon signed rank test is used to answer the question of whether there are differences between the algorithms with and without a local search. This test is analogous to the paired t-test in nonparametric statistical procedures and aims to detect significant differences between two data samples. The obtained p-values for all problems and each family of algorithm under study in this section, which means the previous listed ones with and without local search, considering together I_{HV}, I_{IGD}, I_ϵ, I_Δ, and the computation time and respective computed $p-$ values are shown in Tables 5.15 to 5.17. These values demonstrate that, for the MOACS-2-L, there is a significant difference in all quality indicators. Furthermore, there is a significant difference between the NSGA-II-L and NSGA-II-L-LS for all quality indicators except I_Δ. For the SPEA2-based algorithms, there is only one significant difference between the SPEA2 and the SPEA2-LS for computation time and I_ϵ.

Table 5.15: Computed p-value with the Wilcoxon signed-rank test in accordance with I_{HV}, I_{IGD}, I_ϵ, I_Δ and the computation time for the MOACS-2-L and MOACS-2-L-LS algorithms

Indicators	Computed p-values
I_{HV}	<0.001
I_{IGD}	<0.001
I_ϵ	<0.001
I_Δ	<0.001
Time	<0.001

Table 5.16: Computed p-value with the Wilcoxon signed-rank test in accordance with I_{HV}, I_{IGD}, I_ϵ, I_Δ and the computation time for the NSGA-II-L and NSGA-II-L-LS algorithms

Indicators	Computed p-values
I_{HV}	<0.000
I_{IGD}	<0.000
I_ϵ	<0.000
I_Δ	0.118
Time	<0.000

Table 5.17: Computed p-value with the Wilcoxon signed-rank test in accordance with I_{HV}, I_{IGD}, I_ϵ, I_Δ and the computation time for the SPEA2 and SPEA2-LS algorithms

Indicators	Computed p-values
I_{HV}	0.169
I_{IGD}	0.347
I_ϵ	0.021
I_Δ	0.236
Time	<0.000

Table 5.18: Computed p-value with the Wilcoxon signed-rank test in accordance with I_{HV}, I_{IGD}, I_ϵ, I_Δ and the computation time to test the superiority/inferiority of the the local search

Algorithm 1	Algorithm 2	I_{HV}	I_{IGD}	I_ϵ	I_Δ	Time
MOACS-2-L	MOACS-2-L-LS	$<$ 0.0001	$<$ 0.0001	$<$ 0,0001	1.000	0.010
NSGA-II-L	NSGA-II-LS	1.000	1.000	1.000	-	0.010
SPEA2	SPEA2-LS	-	-	-	0.010	0.010

Table 5.18 shows the p-values of the Wilcoxon signed-rank test, applied in order to identify whether the local search improves the quality of specific indicators. If the computed p-value is less than 0.05, the local search has significantly improved the results of a specific quality indicator. In the opposite case, it represents a significant deterioration of the value of the quality indicator. As shown in this table, the MOACS-2-L-LS improves all quality indicators except I_Δ. The NSGA-II-L-LS only improved the time required to converge toward a set of non-dominated solutions. Furthermore, the SPEA2-LS improved all quality indicators, except the covered hypervolume. However, these improvements are not significant, despite for I_Δ. The values of I_C between the NSGA-II-L and NSGA-II-L-LS shown in Table 5.19, illustrate that the proposed NSGA-II-L-LS also has a large ratio of non-dominated solutions that are dominated by the NSGA-II-L. Thus, the NSGA-II-L-LS is definitely worse than the NSGA-II-L. An explanation for the poor results obtained by the NSGA-II-L-LS could be the nature of the solutions considered in the local search. While solutions from an external archive were used in the SPEA2-LS, solutions from the first front in the NSGA-II were used and may have engendered an early convergence toward local optima. This could explain why there is only a significant difference between the NSGA-II with and without the local search when considering the computation time. In order to avoid this problem, a different crowding distance should be used to sort solutions based on their fitness value and in the solution space. This phenomenon is shown in Figure 5.6, in which the evolution of the density of the non-dominated solutions is shown after 50, 100 and 150 iterations for both the NSGA-II-L-

LS and MOACS-II-L-LS. This figure shows that there is only an evolution of the solution in the central region. However, this evolution is much slower than that of the MOACS-II-L-LS.

Table 5.19: Evolution of the value of I_C between the NSGA-II-L and NSGA-II-L-LS for each group of problems

Algorithm	Dominance Rule	Group 1	Group 2
NSGA-II	$I_C(L,P)$	0.54	0.28
	$I_C(P,L)$	0.15	0.07

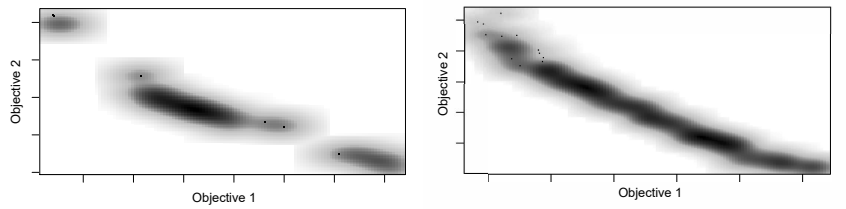

(a) After 50 iterations

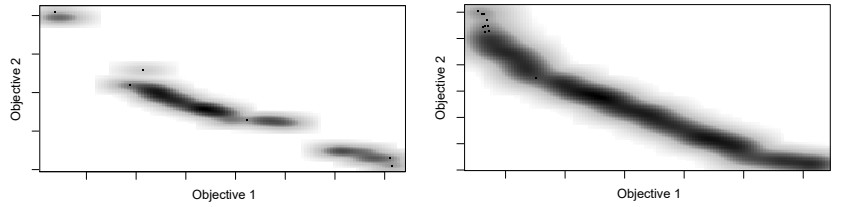

(b) After 100 iterations

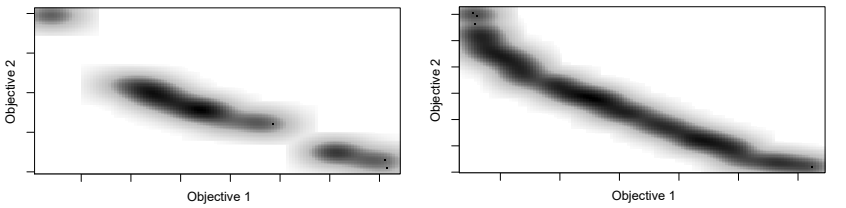

(c) After 150 iterations

Figure 5.6: Evolution of the density of non-dominated solutions through the iterations for the NSGA-II-L-LS on the left side and the MOACS-2-L-LS on the right side

In order to answer to Research Question 9, the Friedman test was applied to all algorithms and problem instances together and then grouped by order strength. Table 5.20 shows the Friedman's statistic and competed $p-$ value in accordance with the quality indicators, algorithms, and problems together. This table outlines the significant differences between all algorithms regarding all quality indicators. Table 5.21 shows the average ranking returned by Friedman's nonparametric test for all problems according to the various quality indicators. If these results are compared with the results obtained earlier in this section (shown in Table 5.3), while the NSGA-II and NSGA-II-L were obtaining the best results for I_{HV} and

I_Δ on average, by combining the MOACS-2-L with the local search, these two algorithms now dominate all other algorithms for I_{HV}. In addition, the MOACS-2-L-LS becomes the best algorithm for I_{IGD}. While the MOACS were not performing well for I_ϵ, the MOACS-2-L-LS has better values than all MOACS algorithms. For this indicator, the NSGA-II-L and SPEA2-LS have the best rankings. According to I_Δ, the introduction of the local search decreased the obtained value. Regarding the computation time, the MOACS-2-L-LS becomes one of the best algorithm regarding convergence time. The adjusted and unadjusted $p-$ values are respectively shown in Tables 5.22 to 5.26 for all quality indicators.

Table 5.20: Friedman's statistic and computed p-value in accordance with I_{HV}, I_{IGD}, I_ϵ, I_Δ and the computation time

Indicators	Friedman statistic	Computed p-values
I_{HV}	309.420	1.67E−10
I_{IGD}	259.080	1.12E−10
I_ϵ	744.420	2.74E−10
I_Δ	1279.150	0.000
Time	2879.220	0

Table 5.21: Average rankings returned by Friedman's nonparametric test for all problems according to the various quality indicators

Algorithm	Ranking I_{HV}	I_{IGD}	I_ϵ	I_Δ	Time
BIANT-1	11.27	10.12	6.13	12.17	4.25
BIANT-1	10.50	10.63	6.80	13.70	6.05
BIANT-2	10.39	10.49	6.65	12.93	5.56
CHAC-1	10.24	11.28	11.61	9.15	9.89
CHAC-1-L	10.27	11.46	11.87	8.94	10.27
CHAC-2	10.26	11.33	11.69	8.86	10.68
CHAC-2-L	10.01	11.59	12.03	8.86	9.49
MOACS-1	12.69	9.32	7.53	13.64	8.48
MOACS-1-S-CDAS	13.83	8.28	7.43	13.74	4.25
MOACS-1-L	12.36	9.38	7.96	13.86	7.88
MOACS-2	11.00	9.70	8.56	13.97	7.27
MOACS-2-S-CDAS	11.07	9.43	8.63	13.58	5.34
MOACS-2-L	11.12	9.76	8.51	13.90	7.39
MOACS-2-L-LS	7.82	12.68	10.59	12.60	12.14
NSGA-II	8.97	10.92	13.28	7.06	10.42
NSGA-II-L	9.48	11.04	13.46	7.47	15.09
NSGA-II-L-LS	11.08	9.17	12.42	7.03	17.89
SPEA2	9.27	10.71	13.16	7.12	17.01
SPEA2-LS	9.33	10.89	13.34	7.62	18.63
SPEA2-L	9.52	10.88	12.98	7.34	16.96

As demonstrated in these tables, the MOACS-2-LS is significantly better than all algorithms for I_{HV} and I_{IGD}. For I_ϵ, the SPEA2-LS is, however, significantly better than the MOACS-

2-L-LS. The same conclusion can be made for the computation time. For I_{Δ}, the MOACS-1-S-CDAS is significantly better than the MOACS-2-L-LS and all algorithms, except the MOACS family of algorithms.

Table 5.22: Unadjusted and adjusted p-values obtained for all problem instances through the application of Holm's post hoc procedure, using the MOACS-2-L-LS as control algorithm according to I_{HV}

Algorithm	Unadjusted p-value	Adjusted p-value
All	0.037	<0.037

Table 5.23: Unadjusted and adjusted p-values obtained for all problem instances through the application of Holm's post hoc procedure, using the MOACS-2-L-LS as control algorithm according to I_{IGD}

Algorithm	Unadjusted p-value	Adjusted p-value
Others	0.004	<0.019
CHAC-1	0.012	0.047
CHAC-2	0.015	0.047
CHAC-1-L	0.029	0.057
CHAC-2-L	0.050	0.057

Table 5.24: Unadjusted and adjusted p-values obtained for all problem instances through the application of Holm's post hoc procedure, using the NSGA-II-L as control algorithm according to I_{ϵ}

Algorithm	Unadjusted p-value	Adjusted p-value
Others	9.93E−03	<5.96E−02
NSGA-II-L-LS	0.061	0.303
SPEA2-L	0.387	1.549
SPEA2	0.584	1.752
NSGA-II	0.739	1.752
SPEA2-LS	0.821	1.752

Table 5.25: Unadjusted and adjusted p-values obtained for all problem instances through the application of Holm's post hoc procedure, using the MOACS-2 as control algorithm according to I_Δ

Algorithm	Unadjusted p-value	Adjusted p-value
Others	5.17E−18	<4.66E−17
MOACS-2-L-LS	1.37E−02	0.109
BIANT-2	6.11E−02	0.428
MOACS-2-S-CDAS	4.83E−01	2.899
MOACS-1	0.550	2.899
BIANT-1	0.618	2.899
MOACS-1-S-CDAS	0.676	2.899
MOACS-1-L	0.836	2.899
MOACS-2-L	0.892	2.899

Table 5.26: Unadjusted and adjusted p-values obtained for all problem instances through the application of Holm's post hoc procedure, using the SPEA2-LS as control algorithm according to the computation time

Algorithm	Unadjusted p-value	Adjusted p-value
Others	0.003	<0.008
NSGA-II-L-LS	0.180	0.180

The average rankings returned by the Friedman test for complex and less complex problems are shown in Table 5.27. The MOACS-2-L-LS obtained the best results for I_{HV} and I_{IGD} and belongs to the best algorithms for I_Δ and I_ϵ for all problem instances of Group 1. For problems belonging to Group 2, the CHAC-2-L still performs the best regarding I_{HV}, I_{IGD} and I_ϵ. The unadjusted and adjusted p-values obtained through the applications of Holm's post hoc procedures for the Group 1 and Group 2 are respectively shown in Tables E.56 to E.60 and Tables E.61 to E.65. Examining the unadjusted and adjusted p-values and taking a confidence value of 88%, the MOACS-2-L-LS is better than the BIANT-1 and BIANT-2 when considering I_{HV}, I_{IGD}, I_ϵ and the computation time for Group 1. For Group 2, the SPEA2-LS and the CHAC-1-L are provide better results than other algorithms. Regarding the p-values, there is no significant difference between them for the various quality indicators.

If the results of tihs chapter are compared to the results of the Chapter 4, it can be affirmed that the change of dominance rule and the use of the local search allowed to improve the performance of the basic MOACS-2. In addition, the MOACS-2-L-LS provides good results for problems from Group 2.

Table 5.27: Average rankings returned by Friedman's nonparametric test for both groups, Group 1 and Group 2

	Group 1					Group 2				
Algorithm	I_{HV}	I_{IGD}	I_ϵ	I_Δ	Time	I_{HV}	I_{IGD}	I_ϵ	I_Δ	Time
BIANT-1	5.71	15.00	7.40	14.95	4.08	14.97	6.78	6.26	12.57	7.85
BIANT-2	4.89	15.33	7.95	15.03	3.85	15.51	6.15	5.47	11.05	7.12
CHAC-1	14.47	8.43	9.06	7.87	9.20	6.30	13.90	13.92	10.26	10.52
CHAC-1-L	14.85	9.00	8.89	8.33	8.65	6.00	13.94	14.57	9.45	11.76
CHAC-2	14.80	8.24	8.79	7.44	10.10	6.03	14.00	14.33	10.10	11.22
CHAC-2-L	14.77	8.25	8.92	7.69	8.82	5.57	14.34	14.85	9.88	10.11
MOACS-1	9.04	12.86	10.05	15.78	8.56	16.09	6.19	5.24	11.76	8.40
MOACS-1-S-CDAS	11.42	10.41	9.04	15.03	7.08	16.08	6.33	5.98	12.66	1.66
MOACS-1-L	8.65	12.71	10.27	15.68	8.96	15.83	6.43	5.87	12.28	6.89
MOACS-2	5.05	14.03	12.68	16.88	9.63	16.55	5.87	4.82	11.34	5.11
MOACS-2-S-CDAS	5.35	13.72	12.67	16.31	9.15	16.42	5.59	4.97	11.13	1.84
MOACS-2-L	4.60	14.36	13.00	16.88	9.73	17.20	5.67	4.45	11.24	5.25
MOACS-2-L-LS	3.95	16.75	10.79	16.62	9.84	11.42	8.97	10.41	8.98	14.24
NSGA-II	11.44	7.86	12.26	3.95	11.15	6.68	13.61	14.20	9.85	9.75
NSGA-II-L	12.85	8.06	12.56	5.08	14.05	6.34	13.68	14.28	9.58	16.05
NSGA-II-L-LS	14.59	5.08	11.64	3.98	16.90	7.81	12.82	13.13	9.77	18.79
SPEA2	12.48	7.09	11.91	4.72	17.67	6.28	14.00	14.29	9.25	16.40
SPEA2-LS	12.75	7.58	11.77	4.96	17.93	6.15	13.89	14.76	10.03	19.27
SPEA2-L	12.88	7.61	11.79	5.25	17.79	6.39	13.75	14.07	9.23	16.20

5.3.4 Synthesis

In this section, the influence of the proposed local search is quantified. While the local search can improve several quality indicators for the SPEA2 and MOACS-2-L, it can only significantly improve the results of MOACS-2-L . The improvement of the MOACS-2-L through the application of a local search made it the best algorithm when considering all quality indicators together computed for all problems and for all problems from Group 1. As shown in Chapter 4, the BIANT-1 and BIANT-2 generally performed better in the central region of the Pareto front. Figure 5.7 shows values of I_C between the BIANT-2 and MOACS-2 in the left figure and between the BIANT-2 and MOACS-2-L-LS in the right figure for some problem instances of Group 1. This figure demonstrates that for most of the problem, the BIANT-2 dominates more solutions of the MOACS-2-L-LS than the opposite. Thus, even if the BIANT-2 is outperformed on most of the quality indicators, it still performs slightly better than the MOACS-2. However, the MOACS-2-L-LS is still a good candidate for further improvement since some companies prefer solutions present in the extreme regions of the Pareto front. In order to improve the performance of the MOACS-2-L-LS in the central region of the Pareto front, either another local search could be used (e.g. simulated annealing) or the frequency of the local search, which was set low to avoid increasing the

computation time of the algorithm, could be changed.

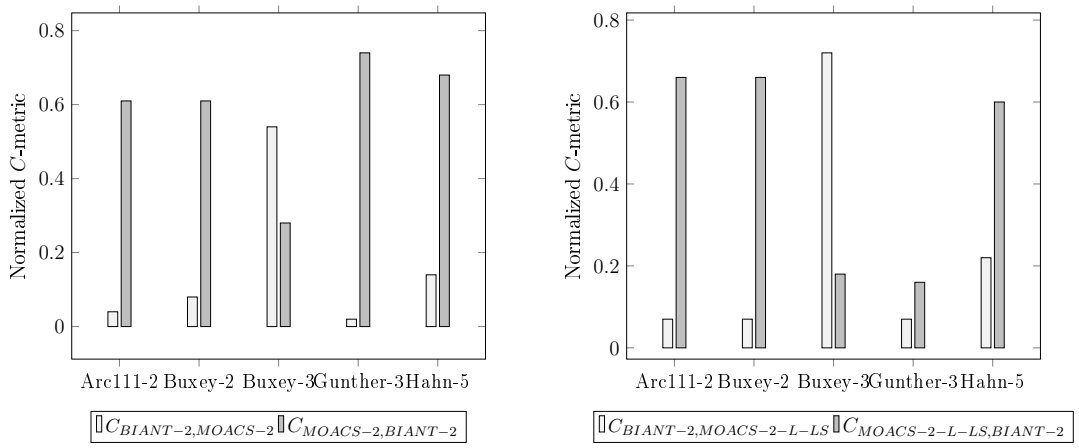

(a) BIANT-2 vs MOACS-2 *(b)* BIANT-2 vs MOACS-2-L-LS

Figure 5.7: C-metric between the BIANT-2 and the MOACS-2 with and without a local search

The ratio of non-dominated solutions has also been slightly decreased through the application of the Lorenz dominance rules and the local search to the MOACS-2, as shown in Figure 5.8.

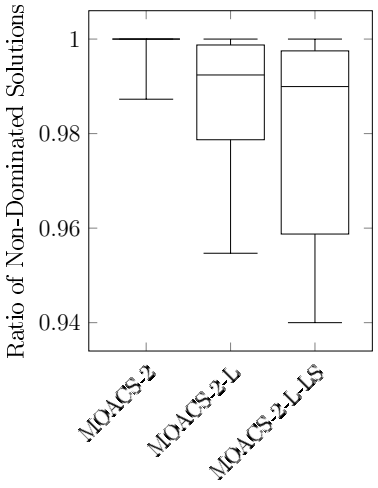

Figure 5.8: Ratio of Non-Dominated Solutions of the MOACS-2, MOACS-2-L, MOACS-2-L-LS for complex problems

5.4 Conclusion

In this chapter, various dominance rules were tested for the MOACS-1, MOACS-2, CHAC-1, CHAC-2, NSGA-II, SPEA2, and DMOPSO. CHAC-2, NSGA-II, SPEA2, and DMOPSO. The dominance rules were compared to each other based on Friedman's nonparametric test and depending on the algorithm, the Lorenz dominance rule improved its performance for

several quality indicators. While this dominance rule may be better for specific algorithms and problems, its difference with the Pareto dominance rule was not significant. Moreover, the MOACS-2-L, SPEA2, and NSGA-II-L were combined with a local search. For the former algorithm, its combination with a local search improved its performance on all quality indicators except for . Results of the SPEA2 were slightly improved, mostly for problems from Group 2. The results are completely different for the NSGA-II-L-LS, which could only improve its convergence time without improving other quality indicators. An explanation of these results may be that the local search was applied to the non-dominated solutions of the current population, which may have engendered an early convergence toward the local optima. To avoid getting stuck in local optima, a different crowding distance based on the solution space should also be used or a different local search (e.g. simulated annealing). Finally, the MOACS-2-L-LS provides good results since it improves almost all quality indicators and reduces the ratio of non-dominated solutions that are dominated by the classical MOACS-2 and the number of non-dominated solutions for complex problems, which are similar to real industrial needs.

The proposed work in this chapter has partially been the subject of one publication in an international journal [288].

Chapter 6

Assembly Line Design Problem, Processing, and Resources Alternatives, and Buffer Sizing: Problem Formulation and Resolution

---

Abstract

In this chapter, a new problem is introduced, which is an extension of the previous problem, of selecting the buffer sizes between workstations. The associated mathematical model is presented. As shown in the previous chapters, evolutionary EAs can obtain good results when considering problem instances of small and large sizes. Alternatively, the BIANT-1, BIANT-2, MOACS-1, and MOACS-2 demonstrated better results for complex problems. In this chapter, the strengths of EA and MOACO are combined into a hybrid form to improve the results for the various quality indicators. To assess the efficiency of the assembly line when using buffers, a generic simulation model, which provides necessary information to the product cost estimation module, was created and is presented. The different algorithms are compared to each other, as in the previous chapters, through nonparametric statistical tests.

6.1 Introduction

In the previous chapters, the objective was to present a new problem and new resolution methods for selecting the best product, processes, and resource alternatives that enable the most suitable assembly line. In this chapter, the definition of the buffer size between workstations is also considered. In order to evaluate the influence of the various buffers on the overall efficiency of the line, a generic simulation module was developed. This module aims to assess the various KPIs required by the product cost estimation module and evaluate the idle time in an assembly line.

As explained in the previous chapters, NSGA-II and SPEA2 obtained good results regarding the various multi-objective quality indicators when considering all problem instances. However, when considering complex problems, the BIANT and MOACS family of algorithms outperformed all other algorithms. While the problem under study in these chapters was a simplified version of the current problem, a similar behaviour of these algorithms is expected when they are applied to the problem under study in this chapter. In this chapter, the strengths of Evolutionary Algorithm (EA)s and Multi-Objective Ant Colony Optimisation (MOACO) will be combined in a hybridised form to improve the overall performance of the two original algorithms. Much work has been proposed to hybridise EAs and they are often combined with either a MOACO or a MOSA. For this reason, the EA was also coupled with a MOSA. The various hybrid forms are compared to each other using the multi-objective quality indicators that were used previously and nonparametric statistical tests.

The present chapter is organised as follows. Section 6.2 presents the problem in detail and Section 6.3 introduces the resolution framework, which includes the various hybrid multi-objective algorithms, the simulation model, and the process cost estimation module. In Section 6.4, the different algorithms are compared with the previously used multi-objective quality indicators and nonparametric Friedman tests.

6.2 Problem formulation and mathematical model

In addition to the problem defined in Chapter 4, this problem involves simultaneously addressing the product design problem, where a subgraph must be selected for each subprocess; the equipment selection problem, where the resources for each chosen subgraph must be selected; and the assembly line balancing problem, where the tasks with their equipment must be assigned to workstations, while solving the buffer allocation problem, where buffers must

be allocated between the workstations.

The set of available resources $E_j = \{R_j \cup W_j\}$, $j \in V_r$, is represented by the set of automatic and manual resources that can perform the task j. Each resource $l \in E_j$ has a task processing time for task j, t_{jl}, a scrap rate r_{jl} and C_{T0_l} and L_{T_l} respectively the initial purchasing price and useful life of tools. Each automatic resource $l \in R_j$ has a critical failure rate λ_{jl}, a critical repair rate μ_{jl}, an average energy consumption $e_{0_{jl}}$ per time unit when performing a task and an average energy consumption $e_{1_{jl}}$ per time unit when being idle, starved, blocked or down, a useful life L_{R_l}, and C_{R0_l} the initial capital investment. In addition, each automatic resource $l \in R_j$ has a maximum length and width L_l and W_l. Each manual resource $l \in W_j$ has a standard wage w_l, one-time personal costs C_{L0_l}, and a standard deviation σ_{jl} when performing task j. To each task $j \in V_r$ are associated a wage rate ω_j, material costs c_j and required material floor space a_j. CRF_T, CRF_R and CRF_B represent the standard capital recovery factors for tooling, automatic resources and building, respectively. Each station has a determined length L and width W. Buffers of length L_b must be assigned after each workstation. Here, these buffers can have a maximum size of B. The standard capital recovery factor for buffers is given by CRF_{Bu} and their initial capital investment is given by C_{Bu0}. The mathematical model requires two assignment variables: x_{jkl} (for $j \in V$, $k = 1, ..., \bar{m}$ and $l \in E_j$), and Y_{pq} (for $q = 1, ..., \bar{m} - 1$).

$$x_{jkl} = \begin{cases} 1, & \text{if the task } j \text{ is assigned to station } k \\ & \text{with equipment } l \\ 0, & \text{otherwise.} \end{cases} \tag{6.1}$$

$$Y_{pq} = \begin{cases} 1, & \text{if the buffer of size } p \text{ is assigned to buffer } q \\ 0, & \text{otherwise.} \end{cases} \tag{6.2}$$

Assuming that each task processing time t_{jl} ($j = 1, ..., N$ and $l \in W_j$) when performed by a manual resource follows a normal distribution $t_{jl} \sim N(t_{jl}, \sigma_{jl}^2)$ and that the processing times are independent, then the probability that a manual or hybrid workstation finishes one time should be considered.

In order to incorporate this , the approach generally used in the stochastic line balancing problem is used, in which various distributions represent the stochastic nature of resources performing specific tasks. As described by Agpak and Gökcen [14], when assuming that all tasks $j = 1, .., N$ follow a normal distribution $t'_j \sim N(t_j, \sigma_j^2)$ and considering the independ-

ency between the tasks processing times[1], if the station load of a given station k is given by $t(S_k) = \sum_{j \in S_k} t_j$ and we set $Y = \sum_{j \in S_k} t_j$, then $Y \sim N(\sum_{j \in S_k} t_j, \sum_{j \in S_k} \sigma_j^2)$. Using the transformation Z defined as,

$$Z = \frac{Y - \sum_{j \in S_k} t_j}{\sum_{j \in S_k} \sigma_j^2} \tag{6.3}$$

then $Z \sim N(0,1)$. Thus, the probability that a given station exceeds the cycle time CT is given by $P\Big(t(S_k) > CT\Big)$. Since this probability should stay under a specific limit α:

$$P\Big(t(S_k) > CT\Big) \leq \alpha \tag{6.4}$$

$$\equiv P\Big(\sum_{j \in S_k} t_j > CT\Big) \leq \alpha \tag{6.5}$$

$$\equiv P\Big(Y \leq CT\Big) \geq 1 - \alpha \tag{6.6}$$

Using the transformation Z:

$$\equiv P\Big(Y \leq CT\Big) \geq 1 - \alpha \tag{6.7}$$

$$\equiv \Big(Z \leq \frac{CT - \sum_{j \in S_k} t_j}{\sum_{j \in S_k} \sigma_j^2}\Big) \geq 1 - \alpha \tag{6.8}$$

$$\equiv z_{1-\alpha} \leq \frac{CT - \sum_{j \in S_k} t_j}{\sum_{j \in S_k} \sigma_j^2} \leq \alpha \tag{6.9}$$

$$\equiv \sum_{j \in S_k} t_j + z_{1-\alpha} \sum_{j \in S_k} \sigma_j^2 \leq CT \tag{6.10}$$

When considering the assignment variables and the more complex problem addressed here, in which only the processing time of manual resources may vary, the deterministic constraint of Chapter 4 represented in (6.11) has to be replaced by Equation (6.12).

$$\sum_{j \in B_k} \sum_{l \in E_j} x_{jkl} t_{jl} \leq CT, \quad k = 1, ..., \bar{m} \tag{6.11}$$

$$\sum_{j \in B_k} \Big(\sum_{l \in R_j} x_{jkl} t_{jl} + \sum_{l \in W_j} x_{jkl} t_{jl} \Big) + z_{1-\alpha} \sqrt{\sum_{j \in B_k} \sum_{l \in W_j} x_{jkl} \sigma_{jl}^2} \leq CT, \quad k = 1, ..., \bar{m} \tag{6.12}$$

The mathematical model for the addressed problem is presented below.

$$\text{Min } Z_1 = C_{idle}(x_{jkl}) \tag{6.13}$$

$$\text{Min } Z_2 = C_{part}(x_{jkl,Y_{bq}}) \tag{6.14}$$

s.t.

1. The order/sequence of the tasks on the workstation does not affect the total station time

$$\sum_{k\in SI_1}\sum_{l\in E_1} x_{1k1} = 1 \tag{6.15}$$

$$\sum_{k\in SI_j}\sum_{l\in E_j} x_{jkl} \leq 1, \quad \forall j \in V \setminus \{1\} \tag{6.16}$$

$$\sum_{j\in B_k}\Big(\sum_{l\in R_j} x_{jkl}t_{jl} + \sum_{l\in W_j} x_{jkl}t_{jl}\Big) + z_{1-\alpha}\sqrt{\sum_{j\in B_k}\sum_{l\in W_j} x_{jkl}\sigma_{jl}^2} \leq CT, \quad k = 1, ..., \bar{m} \tag{6.17}$$

$$\sum_{j\in B_k} x_{jkl}a_j \leq A, \quad \forall l \in E_j, \quad k = 1, ..., \bar{m} \tag{6.18}$$

$$\sum_{j\in B_k}\sum_{l\in R_j} x_{jkl}L_l \leq L, \quad k = 1, ..., \bar{m} \tag{6.19}$$

$$\sum_{j\in B_k}\sum_{l\in R_j} x_{jkl}W_l \leq W, \quad k = 1, ..., \bar{m} \tag{6.20}$$

$$\sum_{k\in SI_i} kx_{ikl_1} \leq \sum_{k\in SI_j} kx_{jkl_2}, \quad \forall i \in V \setminus V_s, \tag{6.21}$$

$$\forall l_1 \in E_i \quad j \in F_i | SI_i \cap SI_j \neq \emptyset, \quad \forall l_2 \in E_j$$

$$\sum_{k\in SI_i} x_{ikl_1} - \sum_{k\in SI_j} x_{jkl_2} \leq \bar{m}(1 - \sum_{k\in SI_j} x_{jkl_2}), \tag{6.22}$$

$$\forall i \in V_s, \quad \forall l_1 \in E_i, \quad \forall l_2 \in E_j,$$

$$\forall j \in F_i | SI_i \cap SI_j \neq \emptyset$$

$$\sum_{k\in SI_i} x_{ikl_1} \geq \sum_{k\in SI_j} x_{jkl_2}, \quad \forall l_1 \in E_i, \quad \forall i \in P_j \tag{6.23}$$

$$\forall j \in V \setminus V_t, \quad \forall l_2 \in E_j$$

$$\sum_{j\in F_i}\sum_{k\in SI_j} x_{ikl_1} - \sum_{k\in SI_i} x_{jkl_2} = 0, \quad \forall i \in V_s, \tag{6.24}$$

$$\forall l_1 \in E_i, \quad \forall l_2 \in E_j$$

$$\sum_{i\in P_j}\sum_{k\in SI_i} x_{ikl_1} - \sum_{k\in SI_j} x_{jkl_2} = 0, \quad \forall i \in V_t, \tag{6.25}$$

$$\forall l_1 \in E_i \quad \forall l_2 \in E_j$$

$$\sum_{p=1}^{B} Y_{pq} = 1, \quad q = 1, ..., \bar{m} - 1, \tag{6.26}$$

$$L_b\sum_{p=1}^{B}\sum_{q=1}^{\bar{m}-1} Y_{pq}b_{pq} + L\sum_{k=1}^{\bar{m}} x_{Nkl} \leq L_{max}, \qquad \forall l \in E_j \tag{6.27}$$

$$x_{jkl} \in \{0, 1\}, \quad \forall j \in V, \quad \forall k \in SI_j, \quad \forall l \in E_j$$

$$Y_{pq} \in \{0, 1\}, \quad p = 1, ..., B \quad q = 1, ..., \bar{m} - 1 \tag{6.28}$$

The two objective functions (6.13) and (6.14) aim at respectively optimising the idle time

and the unit product costs. The modules, which extract the unit product costs and the idle time in the assembly line are functions of the simulation model that is explained in the next chapter. The calculation of the unit product cost is mainly based on the cost model presented in Chapter 4. The slightly required adaptations of the cost model are presented in the next section. Constraint (6.15) ensures that the first node of the precedence graph is assigned to any station. Constraint (6.16)verifies that any task is at most assigned once with a single resource. Constraints (6.17)-(6.20) guarantee that the station load does not exceed the cycle time CT and that the material space or the machine floor space of the assigned tasks and resources at any station are not greater than the available floor space. The precedence constraints, except those emerging from any node V_s are verified in (6.21). These precedence constraints only need to be activated for the selected subgraph/process or design alternative, which is done in (6.22). The same process is applied to any predecessors of the nodes in V_t in (6.23). Furthermore, constraints (6.24)-(6.25) verify that only one process or design alternative is selected. Constraints (6.26)-(6.27) ensure that buffers are only assigned once after each workstation and that the total length of the assembly line does not exceed the total length L_{max} at disposition.

6.3 Resolution method

The resolution framework used in this chapter is shown Figure 6.1.

Compared to the resolution framework presented in the previous chapters, here, the proposed resolution framework is extended with a simulation module that evaluates the unit product cost and the idle time in the assembly line through a discrete event simulation. The procedure is as follows: first solutions for the assembly line balancing, resource allocation and buffer allocation problems must be generated and then these solutions must be evaluated. The characteristics of each solution are used as input for the generic simulation models, which mainly assesses different KPIs that are required by the product cost estimation module.

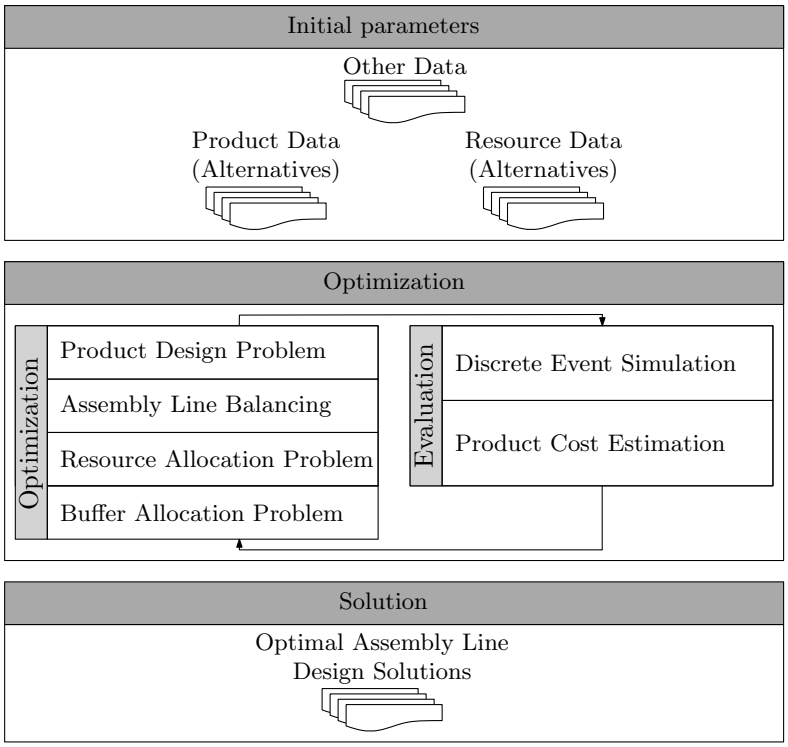

Figure 6.1: Resolution Framework: Evaluation of the product cost through simulation

6.3.1 General discrete encoding scheme

Compared to the Discrete Encoding Scheme used in Chapter 4, the encoding scheme used in this chapter is slightly different. These differences are clarified in the following sections.

6.3.1.1 Solution Encoding

The current solution encoding scheme uses two chromosomes of different sizes. While the first chromosome, which represents the assignment of tasks, and resources to workstations is identical to the previous chapters, the second chromosome represents the size of the buffers between workstations. This second chromosome is represented by two vectors: the BP vector representing the position of the buffer in the assembly line and the BS vector representing the size of the buffers. The length of the second chromosome is defined by the upper bound of the number of workstations, $\bar{m} - 1$, that any solution of the line and equipment selection problem cannot cross.

An example of the new solution encoding is provided in Figure 6.2. In this example, three workstations are required to assemble a given product. The size of the buffers between Stations 1 and 2 and Stations 2 and 3 are respectively 4 and 6.

Tasks	1	2	3	4	6	7	8	9	10	11	*
Equipment	1	2	1	-	3	-	2	1	10	2	*
Station	1	1	2	-	2	-	2	3	3	3	*

Buffer	1	2	*	*	*	*	*	*	*
Size	4	6	*	*	*	*	*	*	*

Figure 6.2: Example of solution encoding using a double chromosome

6.3.1.2 Initial Solution

Since the two vectors that are related to buffer sizing (second chromosome) depend on the line balancing and equipment selection result, the tasks are first assigned to workstations with their respective equipment. As in Chapter 4, a task from the set of tasks without any predecessors is selected first and assigned to the first position of the vector TN. In parallel, a resource is selected from the available resource set for this task and assigned to the first position of the vector EA. Subsequently, the set of tasks without any predecessors is updated and the next task and respective equipment are chosen. As soon as the station load exceeds the cycle time or the station space is reached, the workstation number is increased. This mechanism continues until no more tasks can be assigned. The production rate p_m of a station m in isolation is given by:

$$pr_m = \frac{\overline{\sum_{j \in B_m} \sum_{l \in E_j} x_{jml} t_{jl}}^{r_m}}{\mu_m + r_m} \tag{6.29}$$

where, r_m represents the average repair rate and μ_m represents its average failure. In order to avoid the effects of starvation and blockage, stations with a poor production rate and a greater chance of breakdown should have a larger buffer. The relative criticality CR_q of a buffer q can be determined by:

$$CR_q = \frac{\min\{pr_q, pr_{q+1}\}^{-1}}{\sum_{q=1}^{\bar{m}-1} \min\{pr_q, pr_{q+1}\}^{-1}} \tag{6.30}$$

The initial buffer allocation is provided by multiplying CR_q by the maximum buffer size B at each location q for $q = 1, ..., \bar{m} - 1$.

6.3.1.3 Recombination

Since two chromosomes are present in the solution encoding scheme, the recombination procedure requires minor adaptations. To ease the readiness, X_1 denotes the first part of the chromosome, which is the result of the line balancing and equipment selection; and X_2 represents the second part of the chromosome, which is the results of the buffer allocation.

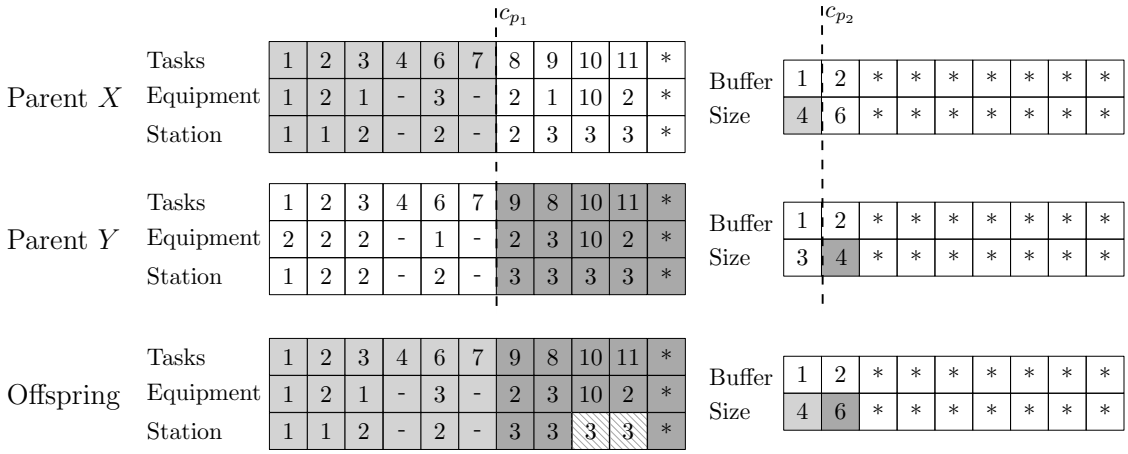

Figure 6.3: Example of recombination between two solutions

The recombination process between two solutions X and Y is defined as follows:

$$F = p_c \otimes f(X,Y) = \begin{cases} f(X,Y), & \text{if } r < p_c \\ X, & \text{otherwise.} \end{cases} \tag{6.31}$$

where f represents a single-point crossover using a similarity vector $VS(X,Y)$ between the task assignments of two solutions X and Y, where an element $i, i = 1, ..., N$, of VS is given by:

$$VS_i(X_i,Y_i) = \begin{cases} i, & \text{if } X_{TN_i} = Y_{TN_i} \\ \emptyset, & \text{otherwise.} \end{cases} \tag{6.32}$$

The recombination process uses two crossover-points, for the first and second chromosomes, respectively. The position of the crossover-point c_{p_1} is randomly chosen from the vector VS. The position of the second crossover point, c_{p_2} is chosen from $X_{BP} \cap Y_{BP}$. From the two parents X and Y, the elements i and j of the offspring Z, represented by Z_1 and Z_2, are generated as follows:

$$Z_{1_i} = \begin{cases} X_{1_i}, & \text{if } i \leq c_{p_1} \\ Y_{1_i}, & \text{otherwise.} \end{cases} \tag{6.33}$$

$$Z_{2_j} = \begin{cases} X_{2_j}, & \text{if } j \leq c_{p_2} \\ Y_{2_j}, & \text{otherwise.} \end{cases} \tag{6.34}$$

An example of the crossover operator is shown in Figure 6.3.

As explained in Chapter 4, due to the verification of the preservation of the different constraints, some tasks and their respective resources do not have a valid workstation after the crossover process. In addition, the total number of buffers in the assembly line may exceed the defined limit. In order to produce feasible individuals, tasks, resources, and buffers may

have to be reassigned. The reassignment is similar to the process used in Chapter 4. If buffers have to be reassigned, the initialization process explained earlier in this section is applied.

6.3.1.4 Mutation

Once an offspring has been generated, another stochastic change is applied with the probability p_m to enhance the diversity in the population and prevent the population from converging prematurely at local minima. The mutation process Z of one solution X, which contains four neighbourhood searches is formulated as follows:

$$Z = p_m \otimes X = \begin{cases} f(X), & \text{if } r < p_m \\ X, & \text{otherwise.} \end{cases} \tag{6.35}$$

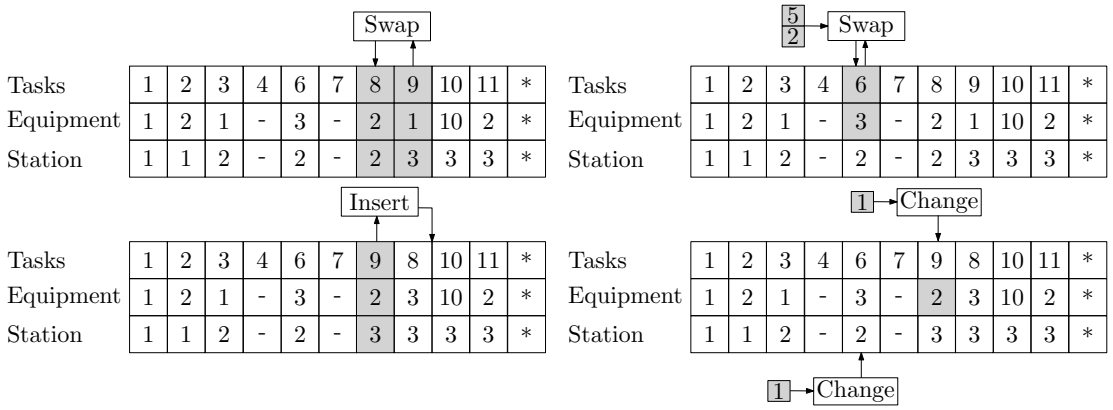

(a) Mutation operator on the first chromosome

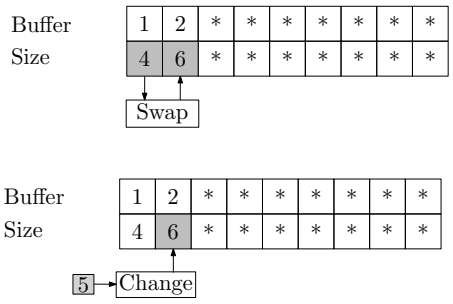

(b) Mutation operator on the second chromosome

Figure 6.4: Illustration of the mutation operators on both chromosomes

If a random number is smaller than the mutation rate p_m, in addition to the previous

mutation tasks explained in Chapter 4, two mutations are implemented on the second chromosome:

1. Swap buffers - For a specific solution X, a workstation q is randomly selected and its buffer size is swapped with the previous buffer or the next buffer.
2. Change buffer size - For a specific solution X, a buffer q is randomly selected and its size is either increased or decreased.

An example of the mutation operators is shown Figure 6.4.

6.3.2 Approximate methods

As shown in the previous chapters, while the evolutionary algorithms represented by the NSGA-II and SPEA2 obtained good results when considering all problem instances together, the MOACOs, represented by the BIANT, MOACS, and CHAC, obtained good results for complex or less complex problems. As stated above, since the problem under investigation in the previous chapters was a simplification of the current problem, similar behaviour of the resolution methods is expected. Due to the nature of this problem, directly using MOACOs to a solution may not be adequate for following reasons:

— The two chromosomes used in the solution encoding do not require the exploration of the same graph; they require exploration of two slightly different graphs. The first graph is represented by an exploration of the possible assignment of tasks and resources to workstations, and the second graph is represented by the exploration of the the possible assignment of buffers to workstations, which is indirectly related to the first graph.

— The assignment of the buffers to workstations requires a complete assignment of tasks and resources to workstations, such that the relative criticality CR_q can be calculated, $q = 1, ..., \bar{m} - 1$

In order to address this problem, the MOACO cannot be used alone for these two chromosomes, and a hybridization approach is required. The main idea behind the proposed hybridization is to combine several algorithms to exploit their strengths. As demonstrated in the previous chapter, the search capability of the NSGA-II identifies relative good solutions in a short time, but it often becomes stuck in local optima and is outperformed by MOACOs algorithms. Conversely, MOACS performance better than the NSGA-II regarding the quality of the obtained non-dominated set of solutions, have a poor convergence speed, and are mostly engendered by the initial pheromone matrices. The BIANT and CHAC have not been considered since the former requires a long time to convergence and the second can

only perform well for small problems.

Previous taxonomy or work based on the hybridization of Genetic Algorithm (GA) with ACO and Simulated Annealing (SA) have been proposed in the literature (e.g. [248, 264, 119, 264, 430, 128, 197, 327, 378]). The next sections present the hybridization of the NSGA-II with a MOACO and the NSGA-II and SPEA2 with a MOSA. This choice is motivated by the positive results of the NSGA-II obtained in average considering all problems for I_{HV}, I_{IGD} and I_{ϵ}. The SPEA2 has also been considered due to its average performance and its ability to converge faster than all algorithms.

6.3.2.1 Hybrid Genetic Ant Colony Algorithm

Two variants of the hybrid algorithm were developed. The utilisation sequence of the NSGA-II and MOACO is common to both. This sequence is shown in Figure 6.5. First, the NSGA-II is performed until there is no improvement after I_{iter_1}. The notion of improvement is related to the MGBM stopping criterion, used earlier in Chapter 4. If no improvement has been observed, the MOACO algorithm is started. Due to the positive results of the MOACS in the previous chapters, its main characteristics were used. In the first variant of the hybrid form, denoted as NSGA-II-ACO-1, the MOACO only creates solutions for the second chromosome, while in the second variant, the MOACO only creates solutions for the first chromosome.

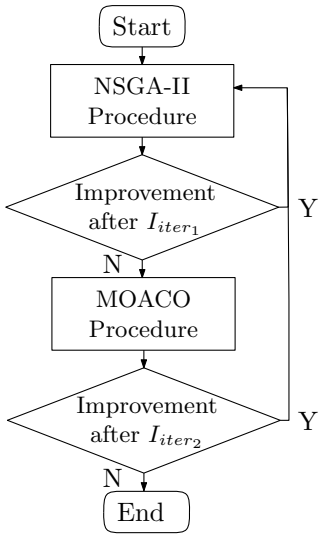

Figure 6.5: Utilisation sequence of the NSGA-II and MOACO in the hybrid algorithm

As a reminder, the transition rule of the MOACS works as follows:

$$\begin{aligned} &\text{If } q \leq q_0: \\ &\qquad p_{i,j}^k = \begin{cases} 1 & \text{if } j = max_{u \in N_i^k}\{\tau_{i,u} \cdot \eta_{1_{i,u}}^{\beta\lambda} \cdot \eta_{2_{i,u}}^{\beta(1-\lambda)}\} \\ 0, & \text{otherwise.} \end{cases} \\ &\text{Else}: \\ &\qquad p_{i,j}^k = \begin{cases} \frac{\tau_{i,j} \cdot \eta_{1_{i,j}}^{\beta\lambda} \cdot \eta_{2_{i,j}}^{\beta(1-\lambda)}}{\sum_{u \in N_i^k} \tau_{i,u} \cdot \eta_{1_{i,u}}^{\beta\lambda} \cdot \eta_{2_{i,u}}^{\beta(1-\lambda)}}, & \text{if } j \in N_i^k \\ 0, & \text{otherwise.} \end{cases} \end{aligned} \tag{6.36}$$

When an ant k is building a solution path and is placed at one node i, a random number $q \in [0,1]$ is generated and $q \leq q_0$, the best neighbour j is selected as the next node in the path. Otherwise, the algorithm decides which node is the next by using a roulette wheel considering $p_{i,j}^k$ as probability of every feasible neighbour $j \in N_i^k$. Due to its nature, the MOACS uses two levels of pheromone update, including, a local and global pheromone update. The local pheromone is given by:

$$\tau_{i,j} = (1-\rho) \cdot \tau_{i,j} + \rho \cdot \tau_0, \text{ with } \tau_0 = \frac{1}{C_1 \cdot C_2} \tag{6.37}$$

Every time an ant k builds a solution, it is compared to the set of non-dominated solutions to determine whether it is a non-dominated solution. At the end of each iteration, $\tau_0^{'}$ is calculated as follows:

$$\tau_0^{'} = \frac{1}{\bar{f}_1 \cdot \bar{f}_2} \tag{6.38}$$

where $\bar{f}_1$ and $\bar{f}_2$ respectively represent the average costs of each objective for the solution paths included in the current archive. If $\tau_0^{'} > \tau_0$, the pheromone trails are reinitialised considering $\tau_0 \leftarrow \tau_0^{'}$. Otherwise, the global pheromone updating is performed for all Δ solutions in the Pareto set, as follows:

$$\tau_{i,j} = (1-\rho) \cdot \tau_{i,j} + \frac{\rho}{f_1 \cdot f_2}, \forall (i,j) \in S_\Delta \tag{6.39}$$

Depending on the variant of the hybridised form, small differences are noticed and explained in the next paragraphs. These differences are mainly related to the pheromone matrix and the heuristics information. Another significant difference is that the MOACO procedure of the NSGA-II-ACO-1 only works on the second chromosome, while the NSGA-II-ACO-2 only works on the first chromosome. The procedure of the MOACO is as follows: For each solution x_i, $i = 1, ..., popsize$, the following procedure is applied: *popsize* ants are created using the solution x_i and the evolution process starts until no convergence is observed.

NSGA-II-ACO-1

During the construction of each solution by an ant k and the exploration of the graph shown Figure 6.6, two heuristic information values, $\eta_{1_{i,j}}$ and $\eta_{2_{i,j}}$, are used. The explored graph contains $B \cdot \bar{m} - 1$ nodes and two fictive nodes denoted as S and F, and $B \cdot B \cdot \bar{m} - 1$ arcs.

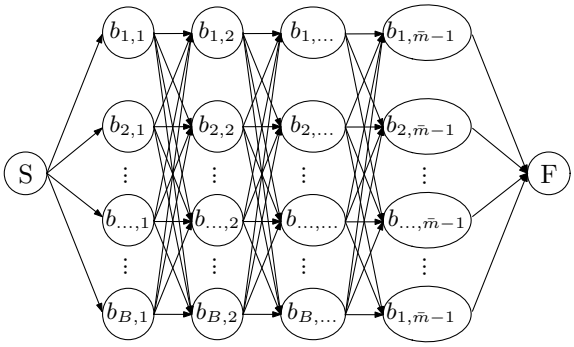

Figure 6.6: Exploration graph used by the NSGA-II-ACO-1 during the construction of solutions

Similar to Yalaoui *et al.* [417], the maximum performance rate of the line was used. The heuristic information use the maximum performance rate of the line, E_{max} when to each buffer is assigned the maximum capacity. In addition, the costs of buffer $c_{bu} = CRF_{Bu} \cdot C_{Bu_0}$ are also considered.

$$\begin{aligned} \eta_{1_{i,j}} &= \frac{b_j \cdot c_{bu}}{B} \\ \eta_{2_{i,j}} &= \frac{b_j}{B} \cdot \frac{1}{E_{max}} \end{aligned} \tag{6.40}$$

where b_j represents the capacity of node j during the exploration of the graph. This capacity is bounded by 1 and B.

In order to not provide preference to a particular heuristic information, they are normalised.

NSGA-II-ACO-2

In this variant of the hybridised form, the MOACO procedure only works on the first chromosome and the problem can be summarised by the problem previously studied in Chapters 4 and 5. Thus, no differences can be outlined with the procedure explained in Chapter 5.

6.3.2.2 Local Search with Simulated Annealing

The basic idea behind SA is to imitate the physical process of annealing. SA is a stochastic search technique that can escape local optima using a probability function. Starting from an

initial solution s, a new solution $s^{'}$ is generated in the neighbourhood of the original solution s. If the amount of change in the objective function value, denoted as $\Delta = f(s^{'}) - f(s)$, is less than 0 [2], then the new solution $s^{'}$ is accepted. If Δ is greater than 0 [2], then the solution is accepted with a specified probability, usually denoted as $P = \exp^{-\frac{\Delta}{T}}$, where T corresponds to a control parameter which is decreased during the search procedure. However, in the case of MOP, choosing a proper transition probability is difficult [281]. Several MOSAs, (general pseudo-code is shown Algorithm 6), have been proposed in the literature with different transition probabilities. For example, Huang and Chow [183] use the fitness value of the generated and current solution, represented by the number of solutions dominating them. Sankararao *et al.* [354] use the following transition probability P:

$$P = \prod_{m=1}^{M} \exp\{\frac{-\Delta_m}{T}\} \tag{6.41}$$

where M represents the number of objectives. Duh and Brown [123] use a slightly different probability transition:

$$P = \exp\Big(\sum_{m=1}^{M} \frac{\omega_m(f_m(s') - f_m(s))}{T}\Big) \tag{6.42}$$

where ω_m represents random weights such that $\omega_m \geq 0, m = 1, ..., M$ and $\sum_{m=1}^{M} \omega_m = 1$.

Algorithm 6 General procedure of the Multi-Objective Simulated Annealing

```
1:  procedure MyProcedure(LS_set)
2:      repeat
3:          s' ← Neighbourhood(s)
4:          if s' ⪯ s then
5:              s ← s'
6:          else if s' ⋠ s then
7:              s ← s'
8:          else
9:              if rand < P then
10:                 s' ⪯ s
11:     until Termination Criterion met
```

Other authors have also proposed slightly different probability transition rules. The most common rules are summarised by Zidi et al., Nam and Park, and Suman and Kumar [451, 281, 375].

Similar to the local search in Chapter 5, a set of solutions LS_{set} that are candidates for the local search is extracted. First, the neighbourhood of any solution $s \in LS_{set}$ needs to be explored through the application of mutation operators. If the new generation solution

2. In the minimisation case of a single-objective optimisation problem

$s^{'}$ dominates s or is not dominated by s, it is accepted. However, if s dominates $s^{'}$, it is accepted with the associated probability T_k. The subsequent geometric cooling, which is widely employed for the annealing scheme, was used:

$$T_k = \alpha^k T_0 \tag{6.43}$$

where T_k represents the used temperature at a given iteration. For each temperature, the neighbourhood is explored a specific number of times L_{iter}. The procedure stops when a number of iterations have been reached.

Since various acceptance criteria have been proposed in the literature, two research questions were formulated:

Research Question 10. *Is there any significant difference between the acceptance criteria?*

Research Question 11. *Independent from the previous research question, which acceptance criterion is the most appropriate?*

In the next sections, these two research questions are answered.

6.3.2.2.1 Choice of the acceptance criterion

Since the probability transition may play a major role in the algorithm and may influence its ability to move forward to the true Pareto front, various criteria were tested on the Arc111-1 problem instance, which is, as stated earlier, the most complex problem investigated in this thesis. The various criteria are listed in Table 6.1. The difference between the criteria C1-C4 and C5-C8 is the use of the range R of the solutions found thus far in the current set of non-dominated solutions.

Table 6.1: List of probability transitions for the MOSA

	Criterion	
Abbrevation	Transition probability	Δ
C1	$\exp\{\frac{-\Delta}{T}\}$	$\Delta = \min_{m=1}^{M}\{f_m(s') - f_m(s)\}$
C2	$\exp\{\frac{-\Delta}{T}\}$	$\Delta = \max_{m=1}^{M}\{f_m(s') - f_m(s)\}$
C3	$\prod_{m=1}^{M}\exp\{\frac{-\Delta_m}{T}\}$	$\Delta_m = f_m(s^{'}) - f_m(s)$
C4	$\exp\{\frac{-\Delta}{T}\}$	$\Delta = \sum_{m=1}^{M}\omega_m\Big(f_m(s') - f_m(s)\Big)$
C5	$\exp\{\frac{-\Delta}{T}\}$	$\Delta = \frac{\min_{m=1}^{M}\{f_m(s')-f_m(s)\}}{R}$
C6	$\exp\{\frac{-\Delta}{T}\}$	$\Delta = \frac{\max_{m=1}^{M}\{f_m(s')-f_m(s)\}}{R}$
C7	$\prod_{m=1}^{M}\exp\{\frac{-\Delta_m}{T}\}$	$\Delta_m = \frac{f_m(s^{'})-f_m(s)}{R}$
C8	$\exp\{\frac{-\Delta}{T}\}$	$\Delta = \frac{\sum_{m=1}^{M}\omega_m\Big(f_m(s')-f_m(s)\Big)}{R}$

The performance of each criterion combined with its transition probability is shown in Table 6.2. In addition, a graphical visualisation in the form of a boxplot is available in Appendix F.2.

Table 6.2: Influence of the various transition criteria on the quality indicators

		Used Criterion							
		C-1	C-2	C-3	C-4	C-5	C-6	C-7	C-8
I_{HV}	$\bar{x}$	0.97	0.97	0.97	0.97	0.98	0.97	0.97	0.97
	IQR(x)	0.00	0.02	0.01	0.02	0.01	0.01	0.01	0.01
I_{IGD}	$\bar{x}$	0.52	0.52	0.56	0.59	0.51	0.55	0.61	0.56
	IQR(x)	0.05	0.09	0.05	0.08	0.11	0.05	0.06	0.02
I_ϵ	$\bar{x}$	0.91	0.91	0.90	0.92	0.88	0.90	0.95	0.91
	IQR(x)	0.04	0.07	0.06	0.09	0.08	0.06	0.05	0.04
I_Δ	$\bar{x}$	0.84	0.81	0.81	0.80	0.79	0.84	0.87	0.84
	IQR(x)	0.09	0.07	0.10	0.04	0.09	0.09	0.19	0.08
Time	$\bar{x}$	0.46	0.51	0.43	0.36	0.32	0.34	0.37	0.45
	IQR(x)	0.21	0.27	0.26	0.13	0.27	0.12	0.14	0.32

The obtained Friedman's statistic and the associated computed p-value is shown in Table 6.3. Given that $\chi^2_{0.05} = 14.1$ with a 95% confidence level and seven degrees of freedom, it can be concluded that there are not significant differences among the transition criteria. However, taking I_{IGD} into consideration, a significant difference between the transition criteria could be observed by choosing a confidence level of 91%. The average rankings returned by Friedman's nonparametric test are shown in Table 6.4. The adjusted and unadjusted $p-$ values are shown in Appendix F.2. While the fifth transition criterion performs better for most of the quality indicators, the difference is not significant. However, since it can perform slightly better, it is an ideal candidate for further experiments.

Table 6.3: Friedman's statistic and computed p-value in accordance with I_{HV}, I_{IGD}, I_ϵ, I_Δ and the computation time

Indicators	Friedman statistic	Computed p-values
I_{HV}	6.23	0.51
I_{IGD}	12.37	0.09
I_ϵ	4.07	0.77
I_Δ	5.63	0.58
Time	7.41	0.39

Table 6.4: Average rankings returned by Friedman's nonparametric test for all probability transitions

	Ranking				
Algorithm	I_{HV}	I_{IGD}	I_{ϵ}	I_{Δ}	Time
C1	4.60	5.70	4.40	4.30	3.70
C2	4.00	6.00	4.90	4.60	3.60
C3	4.80	4.20	4.45	4.40	3.80
C4	4.80	3.80	4.80	5.30	5.30
C5	3.40	5.00	5.25	5.60	4.70
C6	4.30	4.60	4.05	3.40	5.25
C7	5.90	3.00	3.35	4.00	5.55
C8	4.20	3.70	4.80	4.40	4.10

6.3.3 Simulation model

In the developed simulation model, any given workstation can be in one of the following possible states:

— busy and assembling a product
— blocked when the buffer/queue after the station is full
— starved if the buffer/queue before the station is empty and the previous station has not performed its task yet
— down when a breakdown occurs, and the machine is being repaired

Likewise, any of the product units in the system can be in following states:

— blocked at a specific workstation if the next queue/buffer is already full
— served in a specific workstation
— waiting in queue

Thus, if an assembly line with M workstations is considered. Considering that the last workstation is never blocked, any unit has the possibility of passing $3M - 1$ states.

In the developed simulation model, two types of machine failures are considered: (i) operation-dependent failures and (ii) time-dependent failures. While in the first case, the failures can only occur during the processing state of a machine, in the second case, the machine breakdowns can also occur when a station is not busy.

Furthermore, the following assumptions were made during the creation of the simulation model:

— Automatic resources on each station are unreliable, and each station is separated by an intermediate finite buffer

— When a breakdown occurs and the machine is operating the unit being processed is considered scrap
— The last workstation is never blocked
— Workpieces move through buffers with zero transit time and follow the First-In-First-Out strategy
— The time between failures and repair time between failures are exponentially distributed
— The setup time is included in the task processing time
— No workstation is never lacking raw material
— Manual resources have an availability of 100 %
— All resources assigned to a specific station are statistically independent

The main steps of the simulation module are shown Figure 6.7. First the system is initialised with the results of the optimisation, in other words, with the five vectors from the solution encoding, which provide the station time $t(S_m)$, $m = 1, ..., \bar{m}$, the breakdowns and scrape rates of each station. This is followed by the initialisation of the system state, in which, every station has one workpiece in its buffer that is ready to be assembled. The *Main Program*, which is iteratively repeated until reaching the stopping criterion of the simulation, aims at managing and generating the events. In the *Event Manager*, every event modifying the system is managed and actualised. After the simulation is stopped, the results are sent to the product cost estimation module.

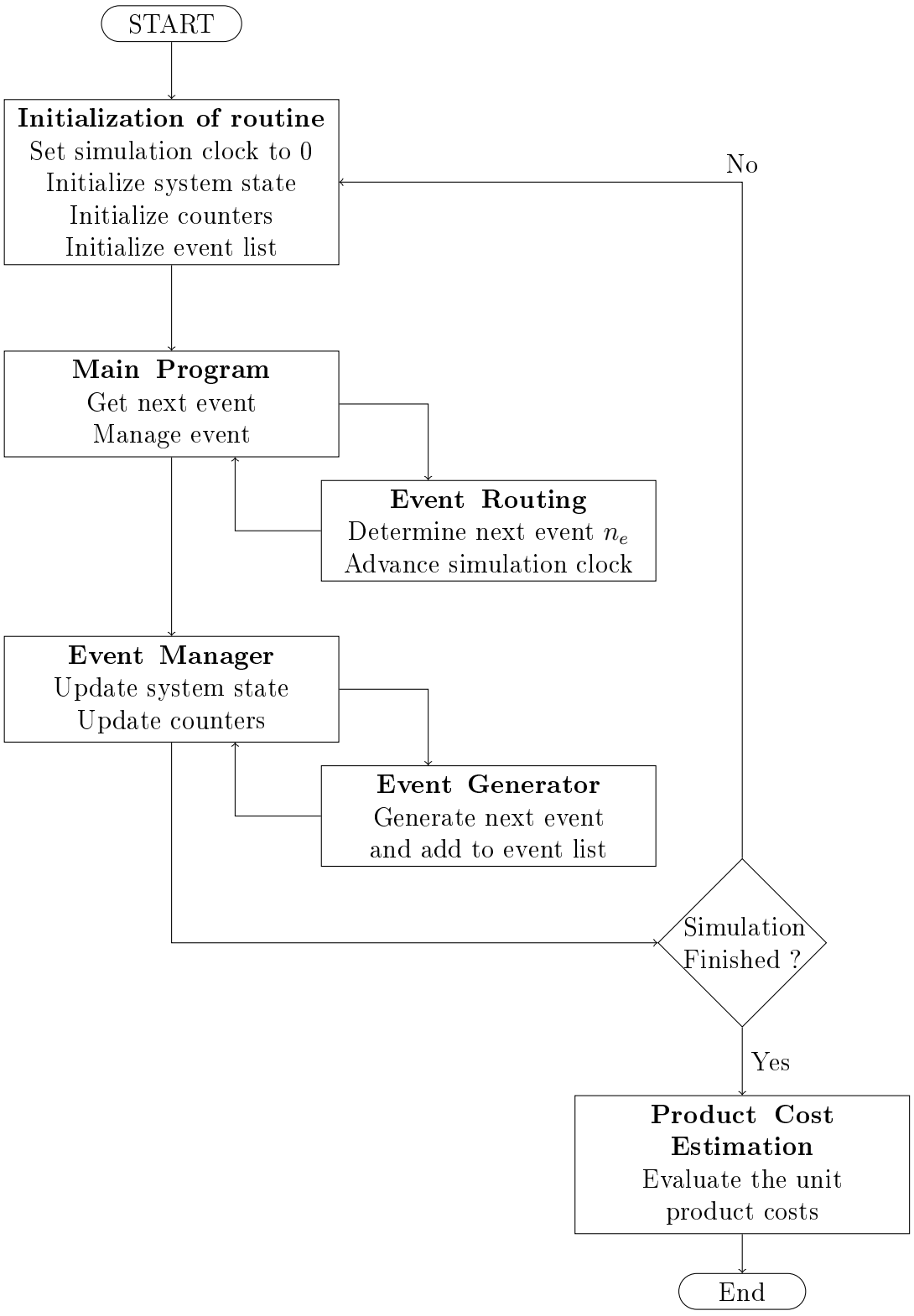

Figure 6.7: Main steps of the simulation module

6.3.4 Initialisation of the simulation model

Given a solution represented by its double chromosome as shown in Figure 6.2, the objective of the initialization of the simulation model, is to transform this representation and the implied tasks and resources characteristics into station characteristics. The required information for simulation model is shown in Table 6.5.

Table 6.5: Required information by the simulation model

Station characteristics				
Station #	Processing Time	MTBF	MTTR	Scrap rate
1	$t(S_1)$	$\frac{1}{\lambda_1}$	$\frac{1}{\mu_1}$	r_1
$\vdots$	$\vdots$	$\vdots$	$\vdots$	$\vdots$
M	$t(S_M)$	$\frac{1}{\lambda_M}$	$\frac{1}{\mu_M}$	r_M

For any station k, $k = 1, ..., M$, its processing time is required. Here, the various resources assigned to each station operate in series and not in parallel. The station time is calculated as follows:

$$t(S_k) = \sum_{j \in B_k} \Big(\sum_{l \in R_j} x_{jkl} t_{jl} + \sum_{l \in W_j} x_{jkl} t_{jl} \Big) + z_{1-\alpha} \sqrt{\sum_{j \in B_k} \sum_{l \in W_j} x_{jkl} \sigma_{jl}^2} \tag{6.44}$$

In order to ease the readiness and simplify the notation, the vector AF_m denotes the critical failure rate of automated resources assigned to station m, the vector AR_m denotes the critical repair rate of automated resources assigned to station m and AV_m denotes the availability of each resources assigned to station m when considering it in insolation. Figure 6.8 shows an example of the first part of the chromosome representing the task, and equipment assignments. Automatic resources are represented in gray. In this example, three assembly stations are required in this configuration and $AF_1 = \{\lambda_{1,2}\}$, $AF_2 = \{\lambda_{3,3}, \lambda_{6,4}, \lambda_{8,2}\}$ and $AF_3 = \{\lambda_{11,4}\}$. The same principles are followed for AR_m. For each automatic resource l, $l = 1, ..., |AF_m|$ assigned to station m the availability of a resource is defined by its critical failure and repair rates as $AV_{m_l} = \frac{AR_{m_l}}{AF_{m_l} + AV_{m_l}}$.

Tasks	1	2	3	4	6	7	8	9	10	11	*
Equipment	1	2	3	-	4	-	2	1	10	4	*
Station	1	1	2	-	2	-	2	3	3	3	*

Figure 6.8: Example of the first part of the chromosome encoding to generating AF_k

Since operating time and repair time between failures are exponentially distributed, the $MTBF(m)$ and $MTTR(m)$ are calculated as follows. Given the critical failure rate of a resource λ, its probability distribution function $F'(\lambda, t)$, which characterises its probability

to fail within time t, is expressed as:

$$F'(\lambda,t) = P(T \leq t) = \begin{cases} 1 - e^{-\lambda t} & \text{for } t \geq 0 \\ 0, & \text{for } t < 0 \end{cases} \tag{6.45}$$

Its reliability function $R'(\lambda,t)$, which represents the probability it will not fail during time t is expressed as:

$$R'(\lambda,t) = P(T > t) = \begin{cases} e^{-\lambda t} & \text{for } t \geq 0 \\ 1, & \text{for } t < 0 \end{cases} \tag{6.46}$$

Since the various resources assigned to a specific station m may have different reliabilities, the reliability $R'_m(t)$ of a specific station m is given by:

$$R'_k(\lambda_m,t) = \prod_{j=1}^{|AF_m|} R'(AF_{m_j},t) = \prod_{j=1}^{|AF_m|} e^{-AF_{m_j}t} = e^{-\sum_{j=1}^{|AF_m|} AF_{m_j}t} = e^{-\lambda_m t} \tag{6.47}$$

The associated $MTBF(m)$ of a station m can be calculated as follows:

$$MTBF(m) = \int_0^\infty R(\lambda_m,t)dt = \frac{1}{\lambda_m} = \frac{1}{\sum_{j=1}^{|AF_m|} AF_{m_j}} \tag{6.48}$$

In addition, the availability $A(m)$ of station m depends on $MTBF(m)$ and $MTTR(m)$ and is calculated as follows:

$$A(m) = \frac{MTBF(m)}{MTBF(m) + MTTR(m)} = \prod_{j=1}^{|AV_m|} AV_{m_j} \tag{6.49}$$

Thus, the MTTR of station m, $MTTR(m)$ is calculated by:

$$MTTR(m) = \frac{MTBF(m)(1 - \prod_{j=1}^{|AV_m|} AV_{m_j})}{\prod_{j=1}^{|AV_m|} AV_{m_j}} \tag{6.50}$$

For the scrap rate of each station, the same formula as in Chapter 4 is used.

6.3.5 Event management

Once the simulation model has been initialized with the previous values and the states of the various machines, the *Event Manager* manages all events influencing the global state of the system. For a better understanding of the *Event Manager* module, the system composed of $\bar{m}$ workstations and $\bar{m} - 1$ buffers is simplified into $\bar{m}$ subsystems. The decomposition is shown in Figure 6.9. In order to respect the assumptions made earlier, the buffer 0 and M both have an unlimited capacity. If the first subsystem is used as an example to

describe the events that influence its level, the arrival and departure of workpieces and the start and end of a breakdown can be identified. A rough description of these events is presented in Appendix F.1. Here, the arrival events of the first subsystem shown Figure 6.10 are explained. In this subsystem, every time a workpiece arrives, only one condition must be verified, namely, whether the server is busy. This determines whether the workpiece is directly processed or sent to the queue. If the workpiece is going to be processed, then the departure event for this given workpiece is scheduled. When a workpiece leaves the subsystem, it is checked to determine whether it is scrap. If the workpieces are not considered scrap and the next queue is not full, then the workpiece moves to the next subsystem. Otherwise, either the server is blocked if the next queue is full or a new workpiece is processed if any workpiece is waiting in the queue of the given subsystem. When a breakdown occurs, and the server is busy, then the workpiece being processed is considered scrap. Independent of the state of the server, the end of the repairing event is scheduled. After a station is repaired, the next breakdown for the subsystem is scheduled. Depending on whether the queue is empty or not, the station will either be starved or produce a new workpiece.

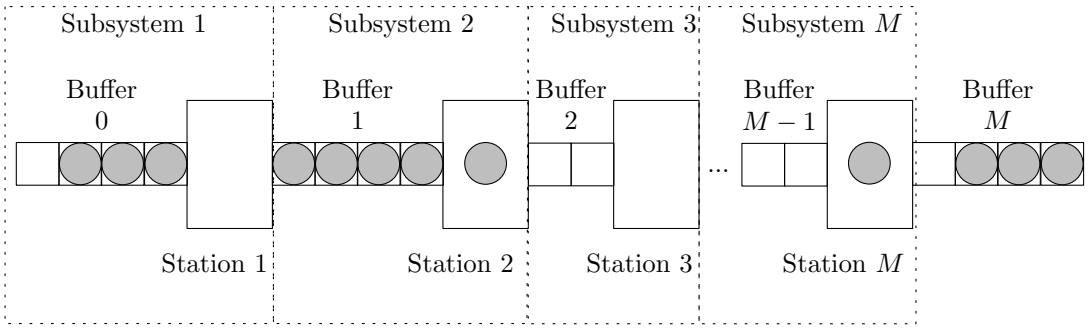

Figure 6.9: Decomposition of the assembly line into subsystems

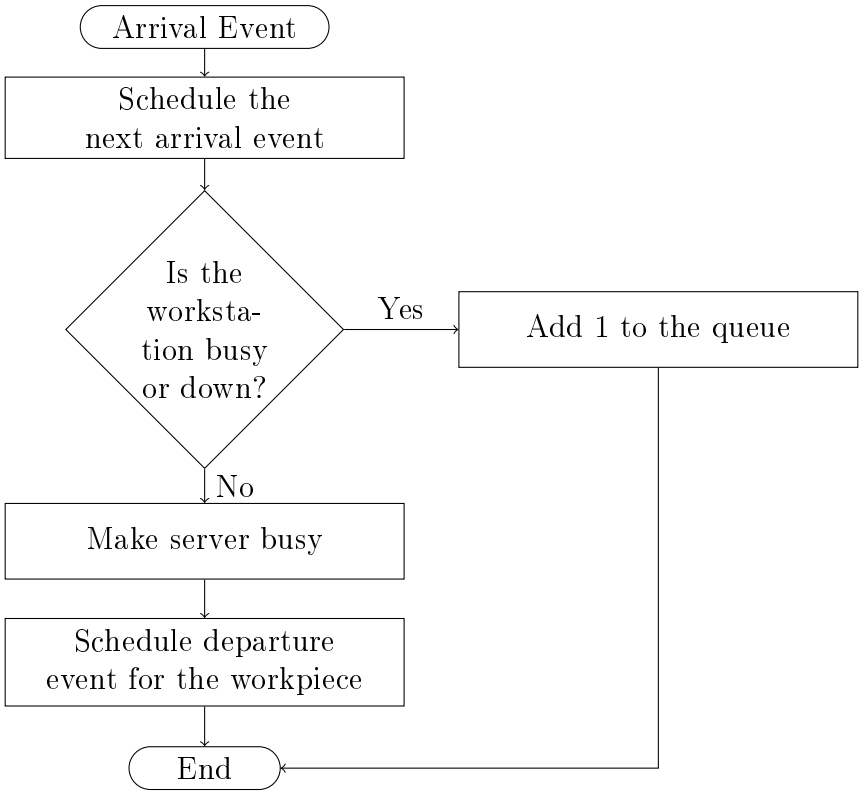

Figure 6.10: Description of the arrival event of the first subsystem

After the events have been generated and managed and updated as shown Figure 6.11, the various counters required for providing useful information to the decision maker after the optimisation or transferring the required information to the product cost estimation module are updated.

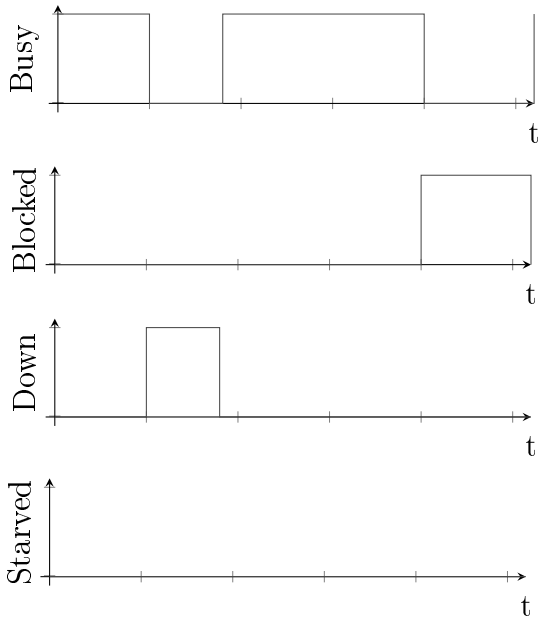

Figure 6.11: System state update

6.3.6 Process cost estimation module

The same decomposition of the total costs C_{tot} as in Chapter 4 is used here and is given by following equation:

$$C_{tot} = C_M + C_L + C_{OH} + C_E + C_B + C_{Eq} + C_T + C_{Bu} \tag{6.51}$$

where C_{Bu} additionnally represent the initial purchasing of buffers. In order to assess V_{gross}, the quotient of V_{net} and the rejection rate of the assembly line $RR(x_{jkl})$, which is evaluated through simulation, needs to be calculated as follows:

$$V_{gross} = \frac{V_{net}}{RR(x_{jkl})} \tag{6.52}$$

The total operating time τ required in a year for producing the V_{net} units is given by:

$$\tau = \frac{Sim_{time}}{V_{sim_{tot}}} \cdot V_{gross} \tag{6.53}$$

where $V_{sim_{tot}}$ is the total number of pieces that should have left the last station after Sim_{time} time units.

The total annual material costs C_M, the total annual labour costs C_L, the total overhead costs C_{OH} are calculated as in Chapter 4. The total annual energy costs C_E are provided by the sum of all energy costs C_{E_k} of each station k. The energy consumption for automatic equipment can be decomposed into various categories. The reader is referred to Zhou *et al.* [448] for more details. Here, the energy consumption model is simplified and only use the average energy consumption of equipment to get the average energy consumption of station k per time unit, C_{E_k}. The average annual energy costs can be calculated as follows:

$$C_E = \tau \cdot c_E \cdot \sum_{k=1}^{\bar{m}} \frac{Time_{busy}(k)}{Sim_{time}} \left(C_{E_{0_k}} + \left(\frac{Sim_{time}}{Time_{busy}(k)} - 1 \right) C_{E_{1_k}} \right) \tag{6.54}$$

where c_E represents the costs of energy per time unit. $C_{E_{0_k}}$ and $C_{E_{1_k}}$ represents the annual energy consumption in respectively producing mode and not producing mode. These two associated values are calculated as follows:

$$C_{E_{0_k}} = \sum_{j \in B_k} \sum_{l \in E_j} x_{jkl} e_{0_{jl}}, \quad C_{E_{1_k}} = \sum_{j \in B_k} \sum_{l \in E_j} x_{jkl} e_{1_{jl}} \tag{6.55}$$

The even distribution in time over the usable lifetime of tools, automatic resources, building and buffers are calculated using the method provided in Chapter 4. The annual building cost is computed using equation (6.56) instead of (6.57), where $B(y_{pq})$ represents the number of buffers assigned to the assembly line.

$$C_B = (K(x_{jkl}) \cdot L + B(y_{pq}) \cdot L_b) \cdot W[C_{B0} \cdot CRF_B/(l_b \cdot w_b) + E] \tag{6.56}$$

$$C_B = K(x_{jkl}) \cdot L \cdot W[C_{B0} \cdot CRF_B/(l_b \cdot w_b) + E] \tag{6.57}$$

Finally, these annual costs can be used to compute a unit cost per part C_{Part} as follows:

$$C_{Part} = \frac{C_{tot}}{V_{net}} \tag{6.58}$$

6.4 Computational experiments

The computational experiments in this chapter were performed with the same configuration as in the previous chapters.

6.4.1 Statistical analysis

Tables 6.6 to 6.10 respectively show the median and Interquartile Range (IQR) obtained through several experiments for the problems of the Arc111 family. Again, promising results are coloured in grey. Three different levels are used: (i) dark grey, (ii) grey and (iii) light grey for the best, second-best and third-best algorithms, respectively. As demonstrated in these tables, the results are heterogeneous, and it seems that SPEA2-LS shows good results on average when considering all the quality indicators. The obtained results for all problems and the various combinations of algorithms and local search are shown Appendix F.3.

Table 6.6: Median and interquartile range of I_{HV} obtained by the optimisers for the Arc111 problems

	Arc111-1		Arc111-2		Arc111-3		Arc111-4		Arc111-5	
	$\tilde{x}$	$IQR(x)$	$\tilde{x}$	$IQR(x)$	$\tilde{x}$	$IQR(x)$	$\tilde{x}$	$IQR(x)$	$\tilde{x}$	$IQR(x)$
NSGA-II	0.95	0.01	0.95	0.01	0.93	0.01	0.95	0.00	0.94	0.01
NSGA-II-ACO-1	0.95	0.01	0.94	0.01	0.93	0.01	0.95	0.01	0.94	0.01
NSGA-II-ACO-2	0.95	0.01	0.94	0.01	0.94	0.02	0.95	0.01	0.94	0.00
NSGA-II-LS	0.94	0.01	0.94	0.01	0.93	0.02	0.95	0.01	0.94	0.00
SPEA2	0.95	0.01	0.95	0.01	0.94	0.01	0.95	0.01	0.95	0.01
SPEA2-LS	0.95	0.01	0.95	0.01	0.94	0.00	0.96	0.01	0.96	0.01

Table 6.7: Median and interquartile range of I_{IGD} obtained by the optimisers for the Arc111 problems

	Arc111-1 $\tilde{x} \pm IQR(x)$		Arc111-2 $\tilde{x} \pm IQR(x)$		Arc111-3 $\tilde{x} \pm IQR(x)$		Arc111-4 $\tilde{x} \pm IQR(x)$		Arc111-5 $\tilde{x} \pm IQR(x)$	
NSGA-II	0.74	0.15	0.78	0.13	0.78	0.21	0.86	0.06	0.72	0.12
NSGA-II-ACO-1	0.77	0.04	0.85	0.08	0.86	0.13	0.91	0.07	0.74	0.19
NSGA-II-ACO-2	0.73	0.07	0.86	0.13	0.78	0.13	0.88	0.06	0.72	0.14
NSGA-II-LS	0.76	0.04	0.92	0.10	0.90	0.13	0.88	0.10	0.72	0.05
SPEA2	0.66	0.06	0.67	0.07	0.71	0.11	0.74	0.07	0.61	0.08
SPEA2-LS	0.72	0.07	0.77	0.15	0.71	0.07	0.74	0.05	0.68	0.06

Table 6.8: Median and interquartile range of I_ϵ obtained by the optimisers for the Arc111 problems

	Arc111-1 $\tilde{x} \pm IQR(x)$		Arc111-2 $\tilde{x} \pm IQR(x)$		Arc111-3 $\tilde{x} \pm IQR(x)$		Arc111-4 $\tilde{x} \pm IQR(x)$		Arc111-5 $\tilde{x} \pm IQR(x)$	
NSGA-II	0.97	0.02	0.94	0.02	0.93	0.03	0.93	0.01	0.92	0.02
NSGA-II-ACO-1	0.96	0.01	0.94	0.04	0.95	0.04	0.94	0.03	0.96	0.09
NSGA-II-ACO-2	0.97	0.01	0.96	0.04	0.91	0.05	0.95	0.03	0.92	0.04
NSGA-II-LS	0.98	0.04	0.96	0.05	0.93	0.06	0.94	0.03	0.92	0.02
SPEA2	0.95	0.03	0.94	0.01	0.91	0.05	0.92	0.04	0.91	0.04
SPEA2-LS	0.95	0.03	0.94	0.04	0.91	0.07	0.91	0.02	0.87	0.06

Table 6.9: Median and interquartile range of I_Δ obtained by the optimisers for the Arc111 problems

	Arc111-1 $\tilde{x} \pm IQR(x)$		Arc111-2 $\tilde{x} \pm IQR(x)$		Arc111-3 $\tilde{x} \pm IQR(x)$		Arc111-4 $\tilde{x} \pm IQR(x)$		Arc111-5 $\tilde{x} \pm IQR(x)$	
NSGA-II	0.83	0.13	0.84	0.07	0.81	0.10	0.79	0.13	0.89	0.07
NSGA-II-ACO-1	0.80	0.09	0.86	0.08	0.79	0.05	0.82	0.08	0.95	0.03
NSGA-II-ACO-2	0.77	0.11	0.81	0.04	0.83	0.02	0.85	0.12	0.90	0.02
NSGA-II-LS	0.81	0.07	0.82	0.06	0.77	0.07	0.86	0.08	0.90	0.11
SPEA2	0.80	0.08	0.78	0.07	0.78	0.12	0.76	0.05	0.87	0.06
SPEA2-LS	0.78	0.06	0.84	0.10	0.77	0.07	0.76	0.09	0.89	0.05

Table 6.10: Median and interquartile range of the computation time required by the optimisers for the Arc111 problems

	Arc111-1 $\tilde{x} \pm IQR(x)$		Arc111-2 $\tilde{x} \pm IQR(x)$		Arc111-3 $\tilde{x} \pm IQR(x)$		Arc111-4 $\tilde{x} \pm IQR(x)$		Arc111-5 $\tilde{x} \pm IQR(x)$	
NSGA-II	0.02	0.00	0.02	0.00	0.02	0.00	0.03	0.00	0.04	0.00
NSGA-II-ACO-1	0.49	0.20	0.30	0.19	0.35	0.16	0.56	0.17	0.76	0.15
NSGA-II-ACO-2	0.44	0.24	0.62	0.23	0.77	0.34	0.67	0.34	0.93	0.15
NSGA-II-LS	0.12	0.01	0.14	0.00	0.14	0.00	0.18	0.00	0.22	0.00
SPEA2	0.12	0.09	0.13	0.11	0.11	0.11	0.15	0.14	0.23	0.17
SPEA2-LS	0.03	0.00	0.04	0.00	0.03	0.00	0.05	0.00	0.06	0.01

6.4.2 Nonparametric statistical test

In this section, nonparametric statistical tests are applied to highlight the strengths and weaknesses of each algorithm. The obtained Friedman statistics for all problems and each family of algorithms, considering together the I_{HV}, I_{IGD}, I_ϵ, I_Δ and the computation time and respective computed p-values are shown in Table 6.11. Taking into consideration $\chi^2_{0.05} = 11.1$ with a 95.00% confidence level and five degrees of freedom, it can be concluded that there is a significant difference between the algorithms for the following indicators: I_{HV}, I_{IGD}, I_ϵ, and the computation time. However, for the spread indicator, I_Δ, there is no significant difference between the algorithms when considering all problem instances together.

Table 6.11: Friedman's statistic and computed p-value in accordance with I_{HV}, I_{IGD}, I_ϵ, I_Δ and the computation time for the various algorithms

Indicators	Friedman statistic	Computed p-values
I_{HV}	291.243	0.000
I_{IGD}	221.310	0.000
I_ϵ	110.326	0.000
I_Δ	6.351	0.274
Time	829.249	0.000

The Friedman ranks obtained for each quality indicator by considering all problem instances together are shown in Table 6.12. This table reveals that the SPEA2-LS is the algorithm that demonstrates the best Friedman rankings for I_{HV}, I_{IGD} and I_ϵ. The algorithm with the best spread, represented by the obtained Friedman ranks for I_Δ, is the SPEA2. Regarding the computation time, the algorithm that converged the fastest was the NSGA-II, followed by the SPEA2 and SPEA2-LS. Regarding the NSGA-II family of algorithms, in general, the covered hypervolume is improved when either applying the simulated annealing or the ant colony optimisation algorithm as a hybridised form. An improvement of I_ϵ was also observed when using the NSGA-II-ACO-1 and NSGA-II-ACO-2. The deterioration of the value of I_Δ is common to all of the hybridised forms. However, as illustrated in Table 6.11, this deterioration is not significant. The unadjusted and adjusted p-values obtained through the applications of Holm's post hoc procedures are shown in Tables 6.13 to 6.17. As these tables show, while the SPEA2-LS obtains the best results for most of the quality indicators, it is never significantly better than the SPEA2.

Table 6.12: Average rankings returned by Friedman's nonparametric test for all problems according to the various quality indicators

Algorithm	I_{HV}	I_{IGD}	I_ϵ	I_Δ	Time
NSGA-II	4.29	3.04	3.13	3.68	5.84
NSGA-II-LS	4.17	2.93	3.03	3.38	3.28
NSGA-II-ACO-1	3.99	2.85	3.18	3.49	1.89
NSGA-II-ACO-2	3.98	3.04	3.18	3.36	1.60
SPEA2	2.37	4.52	4.07	3.66	4.53
SPEA2-LS	2.20	4.61	4.41	3.44	3.86

Table 6.13: Unadjusted and adjusted p-values obtained for all problems through the application of Holm's post hoc procedure, using the SPEA2-LS as control algorithm in accordance with I_{HV}

Algorithm	Unadjusted p-value	Adjusted p-value
NSGA-II	0.000	0.000
NSGA-II-LS	0.000	0.000
NSGA-II-ACO-1	0.000	0.000
NSGA-II-ACO-2	0.000	0.000
SPEA2	0.290	0.290

Table 6.14: Unadjusted and adjusted p-values obtained for the Arc111 family problem through the application of Holm's post hoc procedure, using the SPEA2-LS as control algorithm in accordance with I_{IGD}

Algorithm	Unadjusted p-value	Adjusted p-value
NSGA-II-ACO-1	0.000	0.000
NSGA-II-LS	0.000	0.000
NSGA-II	0.000	0.000
NSGA-II-ACO-2	0.000	0.000
SPEA2	0.485	0.485

Table 6.15: Unadjusted and adjusted p-values obtained for the Arc111 family problem through the application of Holm's post hoc procedure, using the SPEA2-LS as control algorithm in accordance with I_ϵ

Algorithm	Unadjusted p-value	Adjusted p-value
NSGA-II	0.000	0.000
NSGA-II-ACO-2	0.000	0.000
NSGA-II-LS	0.000	0.000
NSGA-II-ACO-1	0.000	0.000
SPEA2	0.175	0.175

Table 6.16: Unadjusted and adjusted p-values obtained for the Arc111 family problem through the application of Holm's post hoc procedure, using the NSGA-II as control algorithm in accordance with I_Δ

Algorithm	Unadjusted p-value	Adjusted p-value
NSGA-II-ACO-2	0.023	0.115
NSGA-II-LS	0.043	0.171
SPEA2-LS	0.074	0.223
NSGA-II-ACO-1	0.080	0.223
SPEA2	0.564	0.564

Table 6.17: Unadjusted and adjusted p-values obtained for the Arc111 family problem through the application of Holm's post hoc procedure, using the NSGA-II as control algorithm in accordance with the computation time

Algorithm	Unadjusted p-value	Adjusted p-value
NSGA-II-ACO-2	0.000	0.000
NSGA-II-ACO-1	0.000	0.000
NSGA-II-LS	0.000	0.000
SPEA2-LS	0.000	0.000
SPEA2	0.201	0.201

As discussed in the previous chapters, the results may vary depending on the problem characteristics. Similar to the previous analysis and chapters, the obtained Friedman statistics for all the problems are considered separately and the various indicators are shown Table 6.18. There are significant differences between algorithms for all problem instances when considering I_{HV} and I_{IGD}. However, these differences are not necessarily significant for I_ϵ and I_Δ. Table 6.19 shows the algorithms that performed the best for each problem family in accordance with all quality indicators and their scores, which represents the percentage of algorithms for which the best one is significantly better. In opposition to Chapter 4, no noticeable difference between the performances of the algorithms were noticed when solving problem instances belonging to Group 1 or Group 2.

Table 6.18: Friedman's statistic and computed p-value for all problems in accordance to I_{HV}, I_{IGD}, I_ϵ, I_Δ and the computation time

	I_{HV}		I_{IGD}		I_ϵ		I_Δ		Time	
Problem	Friedman statistic	Computed p-values	Friedman statistic	Computed p-values	Friedman statistic	Computed p-values	Friedman statistic	Computed p-values	Friedman statistic	Computed p-values
Arc111	26.58	0.00	42.81	0.00	15.78	0.01	6.35	0.27	136.80	0.00
Buxey	36.98	0.00	36.19	0.00	7.69	0.17	3.88	0.57	111.76	0.00
Gunther	49.71	0.00	40.75	0.00	7.57	0.18	2.74	0.74	116.59	0.00
Hahn	38.47	0.00	52.88	0.00	11.92	0.04	4.36	0.50	98.10	0.00
Jackson	25.80	0.00	10.54	0.06	6.53	0.26	6.40	0.27	25.79	0.00
Kilbrid	17.17	0.00	36.97	0.00	18.41	0.00	10.91	0.05	91.89	0.00
Lutz1	23.09	0.00	9.57	0.09	15.16	0.01	0.51	0.99	89.49	0.00
Mitchell	36.14	0.00	25.68	0.00	22.36	0.00	4.25	0.51	72.89	0.00
Mukherje	25.90	0.00	10.24	0.07	15.33	0.01	10.35	0.07	64.71	0.00
Roszieg	33.89	0.00	10.75	0.06	16.41	0.01	6.71	0.24	73.32	0.00
Sawyer	14.86	0.01	14.86	0.01	12.59	0.03	2.60	0.76	83.40	0.00

Table 6.19: Best algorithms regarding their average rankings returned by Friedman's nonparametric test according to the various quality indicators

	I_{HV}		I_{IGD}		I_{ϵ}		I_{Δ}		Time	
Problem	Best algorithm	Score [%]	Best algorithm	Score [%]	Best algorithm	Score [%]	Best algorithm	Score [%]	Best algorithm	Score [%]
Arc111	SPEA2	80.00	SPEA2	40.00	SPEA2-LS	40.00	SPEA2	-	NSGA-II	80.00
Buxey	SPEA2-LS	80.00	SPEA2	40.00	SPEA2-LS	20.00	NSGA-II	-	NSGA-II	60.00
Gunther	SPEA2	80.00	SPEA2	40.00	SPEA2	40.00	NSGA-II-LS	-	NSGA-II	80.00
Hahn	SPEA2-LS	80.00	SPEA2	40.00	SPEA2-LS	20.00	NSGA-II	-	NSGA-II	80.00
Jackson	SPEA2-LS	80.00	SPEA2-LS	-	SPEA2-LS	20.00	NSGA-II-ACO-1	-	NSGA-II	40.00
Kilbrid	SPEA2-LS	80.00	SPEA2-LS	40.00	SPEA2-LS	20.00	SPEA2	20.00	NSGA-II	60.00
Lutz1	SPEA2-LS	80.00	SPEA2-LS	-	SPEA2-LS	40.00	NSGA-II	-	NSGA-II	80.00
Mitchell	SPEA2	80.00	SPEA2-LS	40.00	SPEA2-LS	60.00	NSGA-II	20.00	NSGA-II	40.00
Mukherje	SPEA2-LS	80.00	SPEA2-LS	40.00	SPEA2-LS	40.00	NSGA-II-LS	20.00	NSGA-II	80.00
Roszieg	SPEA2-LS	80.00	SPEA2-LS	-	SPEA2	40.00	NSGA-II-ACO-1	-	NSGA-II	40.00
Sawyer	SPEA2-LS	60.00	NSGA-II-ACO-1	20.00	SPEA2-LS	20.00	NSGA-II	-	NSGA-II	60.00

Figure 6.12 shows the Friedman's ranking obtained when isolating the NSGA-II algorithms. A significant difference only exists when considering the time to convergence. Tables 6.20 to 6.24 show the unadjusted and adjusted p-values obtained for the quality indicators with the NSGA-II-ACO-2 and NSGA-II as control algorithm. As outlined in these tables, none of these algorithms are significantly better than the others. Even if the NSGA-II-ACO-2 is slightly better than all other algorithms for some quality indicator, it is not a good candidate for further investigation due to its relative high computation time.

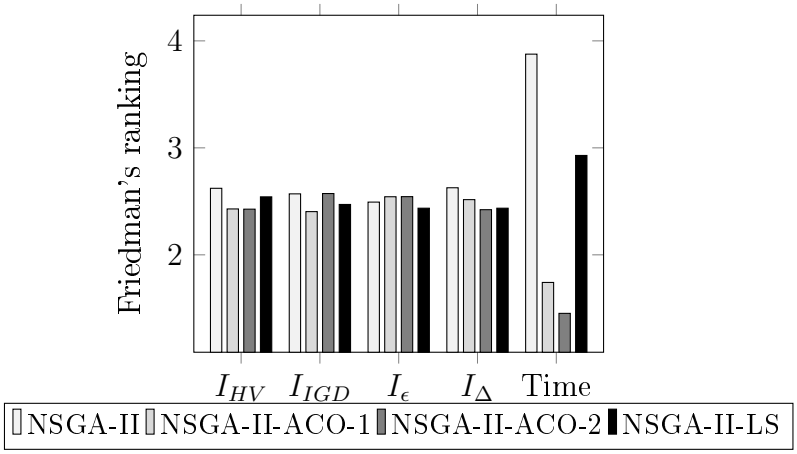

Figure 6.12: Friedman's ranking for the NSGA-II family of algorithm and all quality indicators

Table 6.20: Unadjusted and adjusted p-values obtained for I_{HV} through the application of Holm's post hoc procedure, using the NSGA-II-ACO-2 as control algorithm according to all problem instances

Algorithm	Unadjusted p-value	Adjusted p-value
NSGA-II	0.135	0.405
NSGA-II-LS	0.501	1.002
NSGA-II-ACO-1	0.813	1.002

Table 6.21: Unadjusted and adjusted p-values obtained for I_{IGD} through the application of Holm's post hoc procedure, using the NSGA-II-ACO-2 as control algorithm according to all problem instances

Algorithm	Unadjusted p-value	Adjusted p-value
NSGA-II-LS	0.234	0.702
NSGA-II-ACO-1	0.258	0.702
NSGA-II	0.698	0.702

Table 6.22: Unadjusted and adjusted p-values obtained for I_ϵ through the application of Holm's post hoc procedure, using the NSGA-II-ACO-2 as control algorithm according to all problem instances

Algorithm	Unadjusted p-value	Adjusted p-value
NSGA-II	0.377	1.131
NSGA-II-LS	0.490	1.131
NSGA-II-ACO-1	0.654	1.131

Table 6.23: Unadjusted and adjusted p-values obtained for I_Δ through the application of Holm's post hoc procedure, using the NSGA-II as control algorithm according to all problem instances

Algorithm	Unadjusted p-value	Adjusted p-value
NSGA-II-ACO-2	0.021	0.063
NSGA-II-LS	0.048	0.097
NSGA-II-ACO-1	0.060	0.097

Table 6.24: Unadjusted and adjusted p-values obtained for the computation time through the application of Holm's post hoc procedure, using the NSGA-II as control algorithm according to all problem instances

Algorithm	Unadjusted p-value	Adjusted p-value
NSGA-II-ACO-2	0.000	0.000
NSGA-II-ACO-1	0.000	0.000
NSGA-II-LS	0.000	0.000

6.5 Conclusion

In this chapter, the problem of selecting the best combination of products, processes, and resource alternatives in order to balance the most efficient assembly line by considering the buffer sizes was introduced. The associated mathematical model that aims to optimise capacity and cost-oriented criteria was presented. In order to assess the efficiency of the assembly line when using buffers, a generic simulation model, which provides necessary information to the product cost estimation module, was created and is presented. The different algorithms are compared to each other, as in the previous chapters, through nonparametric statistical tests. A list of optimisation algorithms, including evolutionary algorithms and memetic algorithms was proposed to solve this problem. The different algorithms were compared to each other based on a nonparametric statistical test. The nonparametric statistical test showed that a deterioration of I_Δ for all hybridised forms could be identified. Furthermore, it seems that the SPEA2 in combination with the proposed local search improves I_{HV}, I_{IGD}

and I_ϵ. When considering the computation time, the algorithm that was able to converge the fastest to a set of non-dominated solutions, was the NSGA-II. In addition, the NSGA-II-ACO-1 and NSGA-II-ACO-2 required the most computational effort to move forward to a set of non-dominated solutions.

The proposed work in this chapter has partially been the subject of several publications: one submission to an international journal [292], one submission to a national journal [181], and one communication at conference [294].

Chapter 7

Industrial application

Abstract

This chapter presents two industrial use-cases, in which the presented framework was used to assist product designers and process planers with planning the most suitable configuration of product and assembly design.

7.1 Introduction

The developed framework was used in two different use-cases to plan an automated assembly line in the first use-case and a manual assembly line in the second use-case.

7.2 Use-Case 1: Automated Assembly Line

In this use-case, given products were produced on a circle, automated, and synchronous assembly line (the layout is shown Figure 7.1). Different intermediate buffers were placed between all workstations to minimise starvation and blockage. In the last station, the workpieces are tested, and if they do not respond to quality requirements, they are sent to the repair station, which is represented by the dashed square. In this system, the products that will be assembled are positioned on a workpiece carrier and move from one station to another. In total, 100 workpiece carriers are present in the system. The automated circle line has a predefined cycle time of 4.9 seconds and follows a three-shift model. The operation of the line, which is characterised by 30 assembly tasks in 13 workstations, requires four operators which can be categorised into three wage groups according to their functions and qualifications. Two operators are associated with wage group 1, one operator and one shift supervisor are associated with wage group 2, and one technical supervisor is associated with wage group 3.

In this use-case, the challenge was to design a new assembly line for a new variant of the already existing product to optimise the overall efficiency of the new assembly line on the basis of the current one. In addition, the developed assembly line concept had to be compared to three already planned concepts.

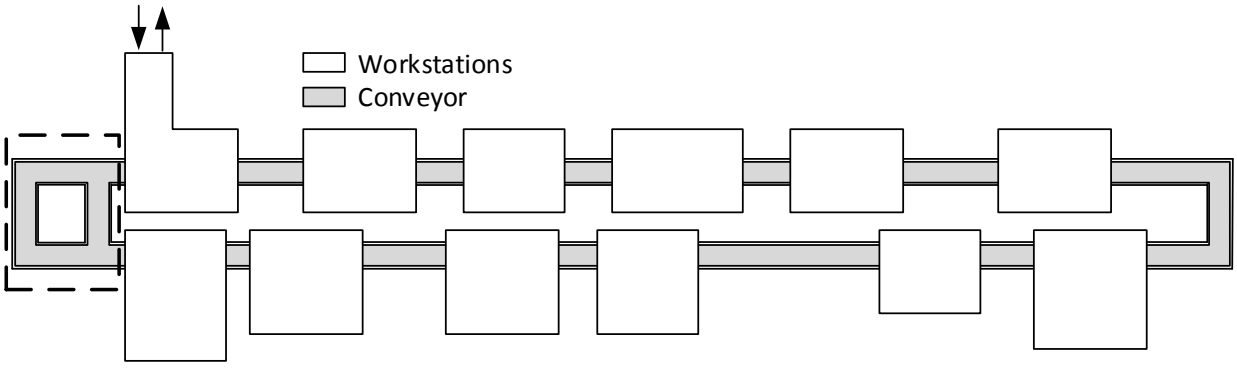

Figure 7.1: Circle assembly line in Use-Case 1

7.2.1 As-Is Situation

During this project, several activities were performed to assess and collect the required data and information.

7.2.1.1 Analysis of the current assembly line: Data Collection

The objective of this phase was the collection of the required data for machine cycle times and production disturbances. A sample of data was collected over one month through the machine data acquisition module of the existing assembly line. In this sample, only relevant and technical downtimes were considered. Organisational downtimes related to lack of material and cleaning were not considered in this study. From this data, the failures were classified according to their Mean Time To Failure (MTTF) and Mean Time To Repair (MTTR). The bar chart shown in Figure 7.2 represents an example of the classification of the MTTR. Furthermore, the scrap data was collected through a process control chart over several weeks.

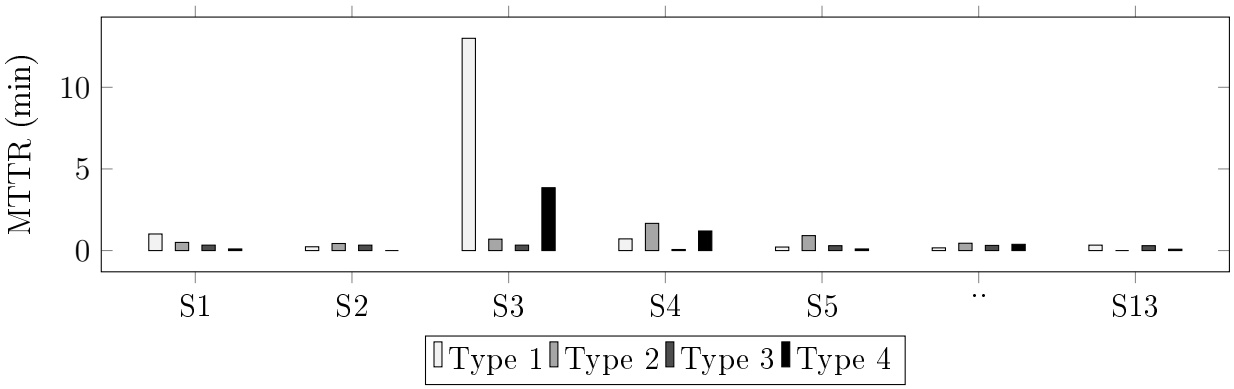

Figure 7.2: Classification of the various Mean Time to Repair for the different stations

7.2.1.2 Analysis of the current assembly line: Video analysis

Due to the small cycle time of the existing assembly line and to identify optimisation potential, a video analysis was performed.

7.2.1.3 Analysis of the current assembly line: Simulation model

To obtain highlights inside the current situation, the actual assembly line was simulated. Figure 7.3 shows the proportion of time workstations were starved or blocked. Due to the poor balance of the line and inadequate buffer sizes, the first workstations were always

blocked and the last workstations were always starved. A more detailed analysis is shown in Figure 7.4, where the average buffer content for the buffers 1 to 5 is represented.

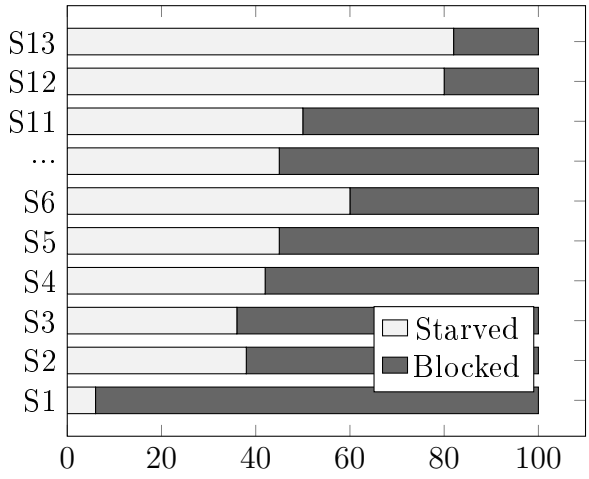

Figure 7.3: Percentage of blockage and starvation of each assembly station

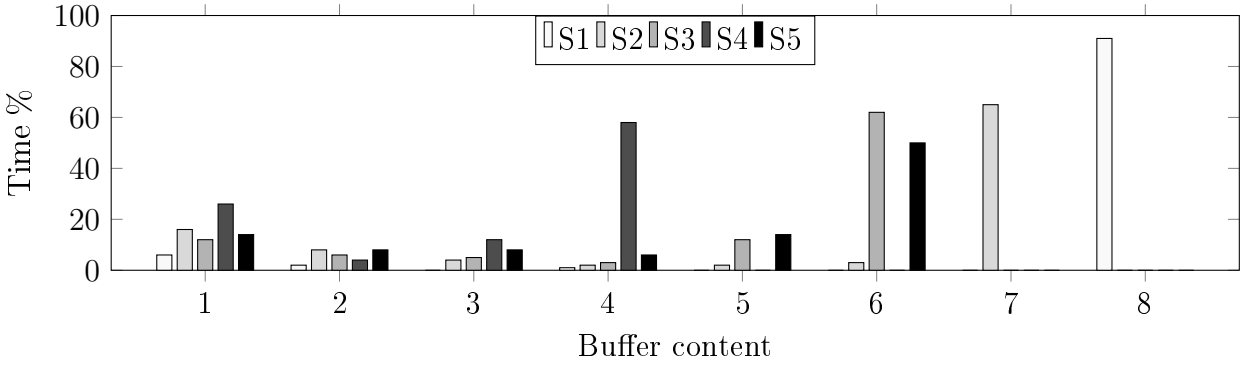

Figure 7.4: Average content of the buffers

7.2.1.4 Conclusion

The collection and analysis of the required data and the video analysis enabled the definition of process and resources alternatives. These alternatives were considered in the precedence graph.

7.2.2 To-Be Situation

Based on the previous analysis and identified process and resources alternatives, several solutions were computed. These solutions are shown in Figure 7.5, in which these solutions are compared to the concepts that were already planned. The optimised concepts found by

the algorithm dominate all three planned concepts. The chosen concept from these eight alternatives increases the throughput rate by 4 %. In comparison to the actual assembly lines, around 17 % of the buffer positions were modified and some were added.

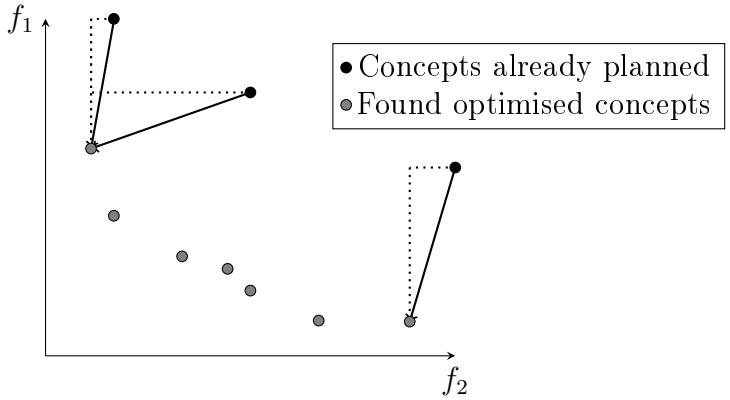

Figure 7.5: Comparison of the three already planned concepts and the generated concepts

In addition to the line balancing, the throughput was also increased by 3 % after changing the rework strategy. If a workpiece was defined as scrap during the assembly process, the workpiece carrier was still moving through all workstations. This strategy, which leads to unused capacity, was changed by extracting the workpiece carriers out of the line by a conveyor belt as soon as the workpiece was defined as scrap. After rework, the workpiece was, through the same system, entering the workstation it was supposed to visit before leaving the line.

7.3 Use-Case 2: Manual Assembly Line

In this use-case, several products with different functions were produced or were planned to be produced in the near future. The first product type that was produced comprised two main models that are denoted as P1 and P2. The other types are planned to be produced in the upcoming years in different volumes. These products are denoted as P3, P4, P5, and P6.

The forecast provided by the sales department for each product is shown in Figure 7.6. The demand is increasing drastically and sometimes exponentially. To ensure the ability of the production system to cope with new products and the increasing demand, the objective was to design an efficient production system that can address both requirements.

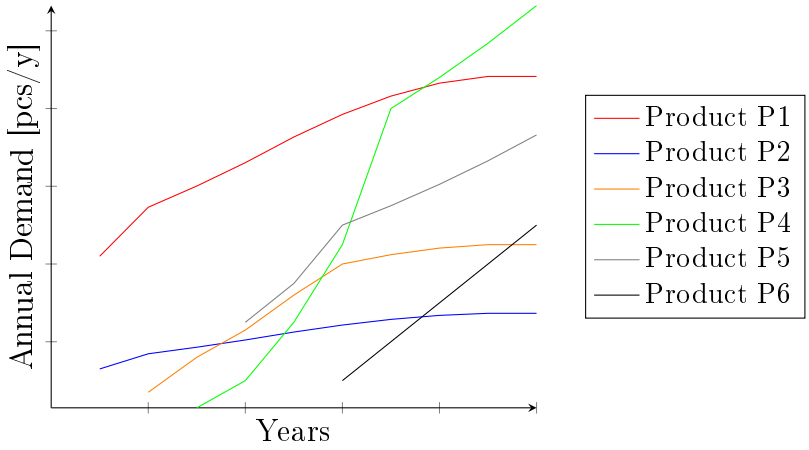

Figure 7.6: Evolution of the demand over the next years for each product

According to the similarities of tasks, their processing times, and the required equipment between these products, the product family clustering of Table 7.1 was obtained.

Table 7.1: Differences and similarities between the various products based on their required tasks and equipment

	Process															
	1	**2**	**3**	**4**	**5**	**6**	**7**	**8**	**9**	**10**	**11**	**12**	**13**	**14**	**15**	Product Family
P1	X	X	X	X	X		X	X			X	X		X	X	1
P2	X	X	X	X	X			X	X	X	X	X			X	1
P3		X	X	X	X			X	X				X	X	X	2
P4		X	X	X	X	X	X	X	X		X	X			X	3
P5		X	X	X	X	X	X	X	X		X	X		X	X	3
P6		X	X	X					X			X			X	4

Only products P1 and P2 were produced at the time of the application of the developed method. To create an efficient assembly system for upcoming products, for which no accurate data existed, products P1 and P2 were used as a reference in the as-is situation.

7.3.1 As-Is Situation

In the as-is situation, the products P1 and P2 were produced by two operators. In total, depending on the product configuration of P1 and P2 and the choice of the following modules and product specifications over 100 variants of P1 and 60 of P2 could be assembled: (i) probe length, (ii) process connection, (iii) display, (iv) house, and (v) switching output. In the first station, the electronic board was programmed and tested. The rejection rate at this station was around 25 %. At the second station, an impermeability test was performed. The rejection rate at this station was approximately 5 %. After this process, the second operator

was in charge of a final semi-automatic test. The first phase of the test is manual and requires the operator to visually check the sensor. During the second phase, which is automated and lasts four minutes, the operator cut the probe of the next order and packed the sensor of the previous order. Depending on the type of sensor, three packages were available.

To assess the degree of capacity utilisation of the two operators and identify optimisation potential, a video analysis was done. One result of this analysis is represented in Figure 7.7. The poor capacity utilisation of the two operators can be explained with the following reasons:

— unneeded motion due to the high material area on the assembly line
— waiting until various testing phases were finished to manually confirm the success of the test
— rework of specific components
— overprocessed tasks

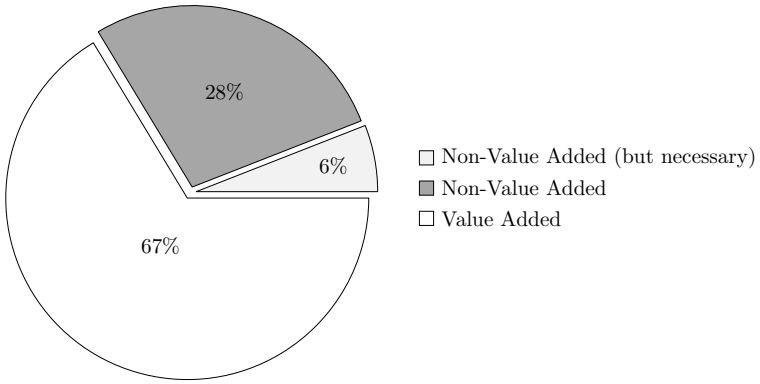

Figure 7.7: Pie diagram representing the ratio of non-value and value added tasks

To increase the throughput of the line and increase the capacity utilisation of the operators, the following product design and process alternatives were considered in this study:

— Outsourcing the board programming, which is responsible for high scrap rates in the early stages of the assembly
— Outsourcing the probe cutting process, which requires high material space and a stochastic processing time, making efficient balancing more difficult. Furthermore, this choice is motivated by the fact that, as shown in Figure 7.8 only eight lengths represent 80% of the annual demand
— Redesigning the house of the product to increase the process quantity during the final testing phase
— Redesign the packaging to decrease the current number of available packages

The required material space for each task was assessed after optimising the required material space on the line.

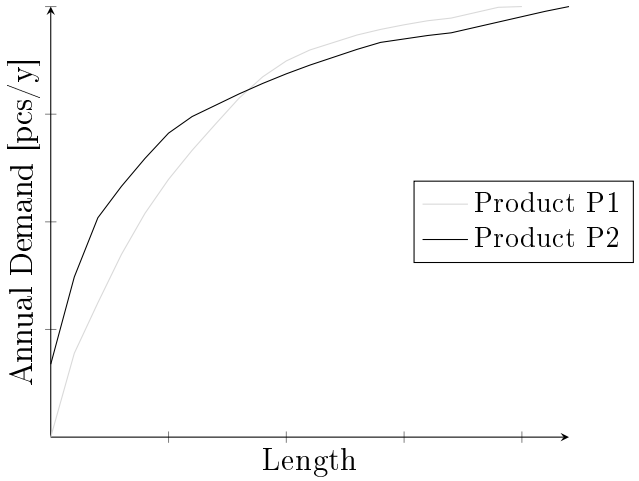

Figure 7.8: ABC-Analysis of the required probe length for products P1 and P2

A partial combined precedence graph comprising most of the design or process alternatives is presented in Figure 7.9. In this figure, the darker region represents a simplified subgraph associated with the decision of cutting the probe in-house or outsourcing it. Node 4, which represents the in-house cutting has only been simplified and replaced by one node to ease the interpretation of the figure. The less dark region represents the final testing with a maximum process quantity of either one or two products. The light gray region represents the two alternatives associated with programming the electronic board in-house or not. Finally, the dashed arrows represent two distances constrained and associated with the automatic processing time of programming or testing tasks.

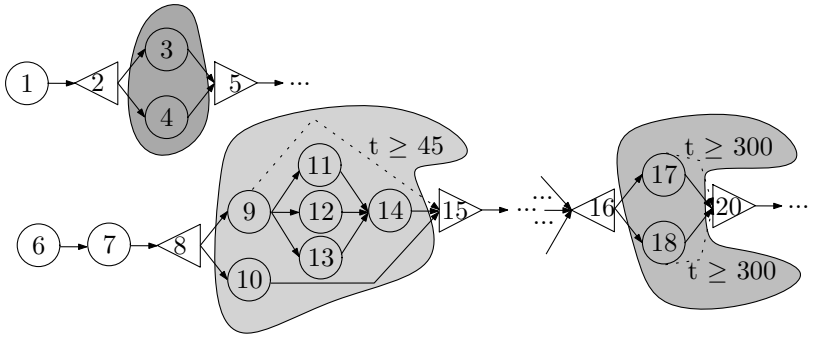

Figure 7.9: Partial representation of the developed precedence graph

7.3.2 To-Be Situation

Based on the product family shown in Table 7.1, Figure 7.10 shows the evolution of the required cycle time for each product family over the years.

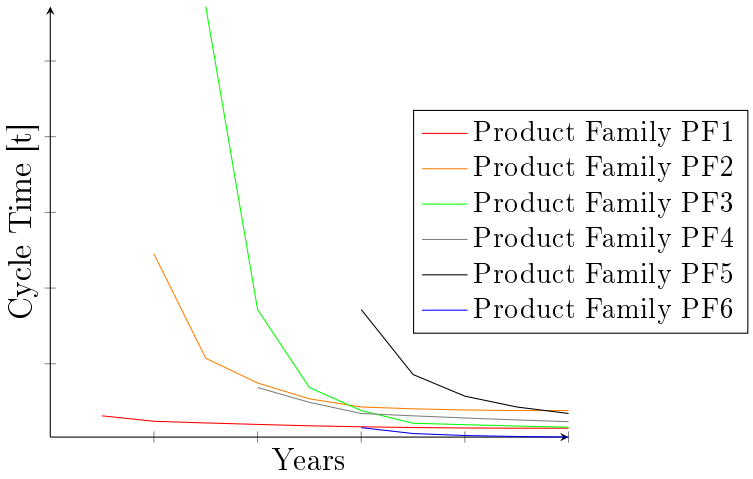

Figure 7.10: Evolution of required cycle time over the next years for each product family

In the first year, only the product family PF1 must be produced within a cycle time of 15 min. By applying the MOACS-2-L-LS, which provides better results in the extreme regions of the Pareto regions, the chosen solutions provide the improvement or deterioration shown in Table 7.2. In this solution, the redesign of the house of the product to increase the process quantity was not chosen since it would have decreased the savings associated with the unit product costs. Even if the costs associated with some raw materials increased, on average the total costs associated with raw material have decreased, and the chosen concept makes it possible to decrease the total unit cost by 17 %.

Table 7.2: Product costs when considering all products together

Cost elements	Improvement/Deterioration [%]
C_{M_1}	+29
C_{M_2}	-5
C_{M_3}	-1
C_{M_4}	+33
C_{M_Σ}	+3
C_L	+138
C_{OH}	+100
C_E	+11
C_B	+11
C_{Part}	117

In the second year, the new product family PF2 is introduced and the product P3 must be assembled within a cycle time of 21 min. In comparison, the required cycle time of the first

product family PF1 reaches 10 min. The production system developed thus far needs to be readjusted. In the solution chosen, insourcing the probe cutting was chosen again to increase the capacity utilisation of all workers. The ALBP was solved for the upcoming years and the probe cutting will only be outsourced in the fourth year.

To minimise the required effort of changing the production system, transformation scenarios were developed. Several line layouts were compared based on the characteristics of the line. To stay flexible, three main assembly lines are planned for the six product families. The evolution of the production systems over the time and the introduction of new product families is schematically represented in Figure 7.11. The reader will note that the third PF is not represented in Figure 7.11.

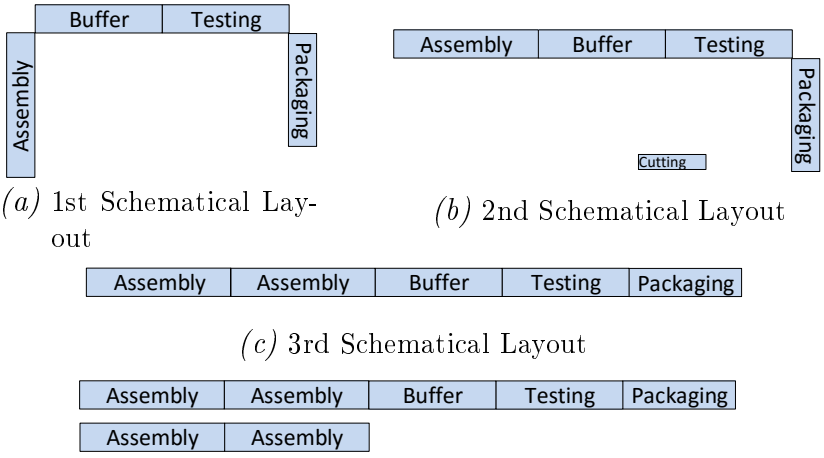

(a) 1st Schematical Layout

(b) 2nd Schematical Layout

(c) 3rd Schematical Layout

(d) 4th Schematical Layout

Figure 7.11: Evolution of the various layouts for the upcoming years

7.4 Conclusion

In this chapter, the previously developed methods are applied, considering products, processes, and resource alternatives in two different use-cases. In the first case, the objective was to design an automated assembly line with buffers and in the second case, a manual assembly line had to be designed.

Chapter 8

Conclusion

The holistic design of products and assembly lines is a requirement that has been established in academia for many years. In this thesis, two problems associated with the selection of the best product and assembly line configuration under consideration of a set of products, processes, and resource alternatives were formulated. In the first problem, the idea relies on analysing the interdependencies between the selection of specific products, processes, and resource characteristics, and their influence on the design of a straight assembly line. In the second problem, the buffer sizes are also considered. The evaluation of the capacity and cost-oriented objectives is done mathematically, through a discrete event simulation for these two problems.

This thesis consists of seven chapters. The first and second chapters discuss the subject of investigation in this thesis. A general introduction is provided and challenges faced by producing companies are presented. In the third chapter, a quick overview of optimisation problems and associated resolution methods is proposed. A detailed overview of models and methods used for solving similar sub-problems is alo presented based on which, the drawbacks of both models and methods are identified. Based on the identified drawbacks, a new problem with the objective of simultaneously selecting product designs, processes, and resource alternatives to plan the most suitable assembly line is presented in Chapter four. Several optimisation algorithms are compared, and the most promising ones are extended with a local search in Chapter five. The influence of the dominance rules is also quantified. In Chapter six, an extended version of the problem is proposed; its objective is to also select the buffer sizes between the workstations. Different hybridisation forms are proposed to solve this problem. In Chapter seven, two industrial use-cases, in which the present approach was used, are presented.

8.1 Synthesis of contributions

For the first problem, a list of 34 state-of-the-art approximate methods was developed. Among these algorithms, variants of swarm intelligence, such as ant colony optimisation, particle swarm optimisation, cuckoo search algorithms, flower pollination algorithms, bat algorithms, and evolutionary algorithms, can be found. These algorithms were compared through nonparametric statistical tests based on four multi-objective quality indicators according to fifty problem instances. Each problem instance is characterised by the order strength of the precedence graph, the number of subgraphs or product design alternatives, and the total number of available resources. The diversity of these instances enabled their classification into simple and complex problems. When considering all problem instances together, the proposed NSGA-II and SPEA2 had the best results on average, when considering the covered hypervolume and the distance required to translate every solution of the approximate Pareto front, such that it dominates the true Pareto front. When considering the spread of the solutions and the inverted general distance metric which measures how far the elements in the true Pareto front are from the solutions in the approximate Pareto front, the proposed CHAC-1 and BIANT-1 obtained the best results. However, when considering the problem instances according to their order strengths (i.e. their resolution complexity), the MOACS-1, MOACS-2, BIANT-1, and BIANT-2 were more suitable than the other algorithms. The significant difference between the MOACS and BIANT algorithms were identified using the attainment function, which showed that the former algorithms performed better in the extreme regions of the Pareto front and the latter algorithms preformed better in the central one.

By considering the computation required by each algorithm until convergence to an approximate Pareto front, it was identified that the BIANT-1 and BIANT-2 require the highest computation time. To improve the results of algorithms that were identified as promising due to their good results, the Lorenz and S-CDAS dominance rules were applied. The comparison of these dominance rules based on the Friedman's nonparametric test showed heterogeneous results and there was no significant difference between them. However, the application of the Lorenz dominance rule to the MOACS-2 improved the necessary distance to translate every solution of the approximate Pareto front, such that it dominates the true Pareto front. In addition, the gap between the MOACS and BIANT was also increased when considering the spread of the obtained solutions. In a second step, a local search procedure was combined with the MOACS-2-L, SPEA2, and NSGA-II-L. For the former algorithm, the application of the local procedure improved the performance of the algorithm on all quality indicators, except for the spread indicator which decreased. For the second algorithm, slight

improvements were observed, primarily on simple problems. The results are completely different for the NSGA-II-L, which only improve its convergence time without improving other quality indicators. An explanation for these results may be that the local search was applied to the non-dominated solutions of the current population. This may have engendered an early convergence toward local optima. To avoid getting stuck in local optima, a different crowding distance based on the solution space should be used or a different local search (e.g. simulated annealing). By combining the results obtained for the first problem, it can be affirmed that the MOACS-2-L-LS provides good results since it improved almost all quality indicators and reduced the ratio of non-dominated solutions that were dominated by the classical MOACS-2.

For the second problem, due to the nature of the proposed solution encoding, the direct application of MOACO was not possible. Due to the positive results obtained on average when considering all problem instances together, two hybridised forms of multi-objective resolution methods were proposed. In the former type, the NSGA-II and SPEA2 were extended with a simulated annealing, while in the latter type, the NSGA-II was extended with components of the MOACS. When considering the NSGA-II family of algorithms, the covered hypervolume improved with the hybridised forms. Given the drawbacks identified between the requirements of the industry and the recommendations that have been proposed in the literature, it can be affirmed that the problem under study in this thesis has been addressed since the proposed approach was successfully implemented in the two use-cases.

Thus, the principal contributions of this thesis are as follows:

— Formulation of two problems associated with the selection of the most suitable assembly line design under consideration of product design, processes, and resource alternatives
— Development of a cost model with the objective of translating the complex interdependencies between the selection of specific product designs, processes, and resource characteristics
— Empirical study comparing various multi-objective algorithms according to several quality indicators, including evolutionary algorithms, ant colony optimisation, particle swarm optimisation, bat algorithm, cuckoo search algorithm, and flower pollination algorithm.
— Analysis of the influence of local search and dominance rules on the performance of several algorithms
— Combination of optimisation methods with a generic discrete-event simulation model for the second problem

8.2 Perspectives and future work

Regarding the perspectives, it could be interesting to extend the proposed models by incorporating strategic decisions, such as:

— The number of products or models produced on the assembly line and the number of assembly lines - the number of products or models on each line, which is an indirect case of the number of assembly lines, is a topic that raises attention in the industry. While the cycle time is usually defined for the assembly process, depending on the type of products and resources, and other optimisation criteria (e.g. flexibility regarding variation in the demand), it may be more efficient to increase the number of lines in the assembly process and thus plan assembly lines with a higher takt time.

— Make-Or-Buy decision - an interesting question is also usually related to the decision of manufacturing a part in-house or purchasing it from an external supplier. The make-or-buy decision is usually made by considering the associated costs of production[1]. However, it might be interesting to also consider the required manufacturing capacity to produce the parts needed in the assembly process.

— The shape and layout of the assembly line - an interesting approach would also be to enrich the current work by solving a new problem, in which a decision regarding the line shape and layout would be taken. Indeed, the selected line design may increase or decrease the efficiency of a specific line shape (e.g. a straight or U-shaped line) or layout (e.g. parallel stations or two-sided assembly lines).

To stay as close as possible to reality, the proposed models could also be extended as follows:

— Characteristics of task duration - while both deterministic and stochastic processing times were taken into account, considering learning effect of workers, which is usually non-negligible in assembly lines, would enhance the proposed models. Also, given a set of tasks assigned to a station, the station time may depend on the sequence in which the tasks are performed. Thus, it would also be interesting to consider sequence-dependent processing time. This is especially true when the tasks are performed manually.

— Restrictions between specific resources could be modelled to incorporate zoning and distance constraints.

— Consider the lack and uncertainty of information and data: due to the lack of information in the early design process, problems may arise when information is fuzzy or uncertain which makes the design evaluation difficult. To fill this gap and decrease the sensitivity of the proposed approach to any uncertain information, approaches of

1. This condition can be modelled in the generic approach proposed in this thesis

robust optimisation could be used.

It would also be interesting to consider future demand scenarios in which the proposed models could be extended with rebalancing aspects. This would require to consider the associated costs of rebalancing the assembly line and would require using a dynamic cost model.

Regarding opportunities for resolution methods, it would also be interesting to analyse:

- the influence of different evolution processes and thus consider different optimisation metaheuristics, such as:
  - Imperialist Competitive Algorithm
  - Invasive Weed Optimization
  - Intelligent Water Drops Algorithm
  - the influence of other local searches.

Finally, it could be useful to also perform a sensitivity analysis of the various parameters on the performance of the algorithms when solving complex and less complex problems. Regarding the application, it would also be interesting to focus on the design of the product and restructure the proposed approach to use less information.

Annexe A

Résumé substantiel

Abstract

This section presents a french summary of the proposed study.

A.1 Introduction

Depuis que la personnalisation de masse est devenue une stratégie viable dans le milieu des années 1990, une énorme pression est exercée sur le marché industriel. Cette pression force les entreprises à fournir des produits ou services uniques [228] tout en respectant les contraintes d'efficacité, de coûts et de qualité de production en série. Pour répondre à ces exigences, il est possible d'envisager les solutions suivantes :

(a) de développer des plateformes de produits qui se caractérisent par une modularité et une standardisation des produits et procédés de fabrication
(b) de réutiliser les systèmes de production déjà existants.

Cette pression s'accentue avec l'adoption d'une stratégie de personnalisation des produits, contraignant les entreprises à renouveler régulièrement leurs produits et leurs procédés de fabrication et d'assemblage. Cela se traduit non seulement par une réduction des cycles de vie des produits et systèmes de production, mais également par une augmentation de la complexité associée à la planification de ces systèmes de production et d'assemblage, qui se doivent d'être efficaces et rentables.

Les chaînes d'assemblage qui répondent à ces exigences de coûts, de qualité et d'efficacité sont les systèmes d'assemblage les plus couramment utilisés. En raison des coûts d'investissement élevés, la conception et la re-conception de ces lignes sont très importantes. De nombreuses décisions doivent être prises durant les activités associées à la conception d'une chaîne d'assemblage. La plupart sont reliées à la conception du produit, à la sélection des procédés de fabrication et d'assemblage et à l'équilibrage de ligne [30, 338]. En général, ces décisions liées à de nombreux sous-problèmes ne sont pas prises en compte simultanément à cause de leurs complexités. Rekiek *et al.* [338] catégorisent la conception de chaîne d'assemblage en conception logique et physique. Durant la conception logique :

(a) les différentes tâches nécessaires à l'assemblage d'un produit sont attribuées aux stations de travail (Line Balancing) ;
(b) les équipements et ressources nécessaires sont distribués entre ces stations (Resource Planning) ;
(c) les stocks tampon sont distribués entre les stations de travail (Buffer Allocation).

Durant la conception physique, l'architecture de la ligne, le système de transfert et choisi et un schéma d'implantation sont définis.

Bien que la majorité des coûts du produit final soit déterminée durant le développement du produit, de nombreuses décisions liées au design d'un produit sont prises sans prendre

en compte les tâches d'assemblage requises [68]. Certains auteurs, par ex. Ullman [395], indiquent que les décisions prises lors de la conception d'un produit déterminent environ 70-75 % de son coût final et celles prises lors de la conception de la chaîne d'assemblage environ 10-25 %. Les coûts de production (fabrication et assemblage) représentent quant à eux environ 70 % du coût final alors que les coûts de développement du produit uniquement 6-12 % [366]. Cela signifie non seulement que si de mauvaises décisions sont prises durant les premières activités du cycle de vie d'un produit, des modifications techniques seront nécessaires par la suite, mais également que des changements tardifs du design du produit peuvent être très coûteux [209]. De plus, les coûts associés au développement d'un produit augmentent considérablement à mesure que le projet de conception avance. Cela signifie que, plus les changements et les améliorations sont effectués dans les premières étapes d'un projet de conception, plus le coût final du produit sera réduit. Ce qui induit la nécessité de paralléliser les activités nécessaires à la conception d'une chaîne d'assemblage en considérant simultanément la conception du produit, la sélection des procédés d'assemblage, l'équilibrage de ligne, le choix d'équipements/ressources et l'allocation des stocks tampon.

Le travail présenté dans cette thèse concerne la formulation et la résolution de deux problèmes d'optimisation multiobjectifs associés à une approche holistique d'ingénierie concourante. Ce sujet est basé sur l'expérience acquise à travers de multiples projets industriels dans différentes entreprises en tant qu'ingénieur de recherche et consultant.

A.2 Synthèse de l'état de l'art

Dans cette section, différentes méthodes permettant l'évaluation de solutions liées aux problèmes de conception de produits, du choix de procédés d'assemblage, d'équilibrage de ligne, de sélection d'équipement et d'allocation de stocks tampon seront présentées. L'objectif étant d'identifier les lacunes dans les approches et les méthodes actuelles. De plus amples informations se trouvent dans le chapitre 3.

A.2.1 Évaluation de différents designs d'un produit

Habituellement, le processus d'évaluation des différents designs d'un produit repose sur des descriptions qualitatives et des jugements subjectifs dans lesquels des experts et leurs connaissances personnelles sont sollicités [436]. De nombreuses méthodologies telles que Design for Manufacturing, Design for Assembly, Design for Environment, Design for Safety, Design for Maintenance, Design for Economy et Design for Ergonomics ont été proposées

par le monde universitaire et l'industrie afin d'évaluer de façon systématique les différents designs. Toutes ces méthodologies sont largement décrites par Paramasivam et Senthil [314].

A.2.2 Problème d'équilibrage de chaîne d'assemblage

Un problème d'équilibrage se pose chaque fois qu'une ligne d'assemblage doit être conçue, modifiée ou ajustée et consiste à affecter les tâches nécessaires à l'assemblage d'un produit spécifique aux différentes stations de travail d'une ligne d'assemblage. En raison de conditions différentes dans le domaine industriel, de nombreux problèmes d'équilibrage ont été étudiés et différents schémas de classification ont été proposés dans la littérature. L'un de ces schémas distingue : (i) le problème d'équilibrage de ligne d'assemblage simple (Simple Assembly Line Balancing Problem, SALBP), et (ii) le problème d'équilibrage de ligne d'assemblage généralisé (Generalized Assembly Line Balancing Problem, GALBP). Dans le premier cas, un seul produit est considéré et le problème est limité par les relations de précédences et les contraintes de temps de cycle. Dans le second cas, les problèmes sont plus complexes et prennent en considération des stations d'assemblage parallèles, des temps d'assemblage stochastiques, ou des problèmes avec des lignes mixtes. Afin de mieux cerner la variété croissante des problèmes d'équilibrage du monde réel, Boysen *et al.* [50] ont fourni un schéma de classification basé sur les caractéristiques : (i) du graphe de précédence, (ii) des stations d'assemblage et de la ligne d'assemblage et (iii) des objectifs à optimiser. Battaia et Dolgui [30] ont fourni une taxonomie permettant de classifier les problèmes d'équilibrage de ligne selon la nature de la fonction objectif. Hazir *et al.* [174, 173] ont étendu la classification de Boysen *et al.* en intégrant les aspects liés aux coûts et aux bénéfices. Plusieurs problèmes bien connus liés à ce sujet de thèse ont été abordés et seront détaillés dans cette section.

A.2.3 Problème d'équilibrage de ligne d'assemblage avec sous-graphes alternatifs

Le problème d'équilibrage de ligne d'assemblage avec sous-graphes alternatifs (Alternative Subgraph Assembly Line Balancing Problem, ASALBP), défini par Capacho et Pastor [64], considère différents types d'assemblage permettant une liaison entre deux pièces, comme l'assemblage direct (clinchage), l'assemblage permanent (soudage) et l'assemblage démontable (rivet, vis). Chacune de ses variantes d'assemblage est représentée par un sous-graphe qui détermine les tâches requises pour assembler une partie du produit et le temps de traitement. Le problème associé, qui a pour but de sélectionner les sous-graphes optimisant certains critères, a été défini et modélisé dans une version restreinte et une version plus étendue

[64, 63]. Dans leurs représentations, les temps de traitement des tâches et/ou les relations de précédence peuvent dépendre du sous-graphe sélectionné. Dans le modèle proposé, les différents types d'assemblage ne se chevauchent pas et chaque alternative est représentée par un sous-graphe unique et indépendant [63]. Des méthodes heuristiques ont été développées et testées de manière exhaustive par Capacho *et al.* [66, 65]. Scholl *et al.* [360] ont proposé une résolution exacte du problème.

A.2.4 Sélection des procédés d'assemblage et évaluation des ressources

Deux approches ou problèmes différents ont été proposés pour incorporer le choix d'équipements/ressources au problème d'équilibrage de ligne [50]. Le premier est connu comme le problème de sélection d'équipements/ressources et est basé sur l'hypothèse qu'il existe un ensemble fixe d'équipements/ressources qui doit être sélectionné et affecté à une station d'assemblage. Le dernier consiste à affecter un(e) équipement/ressource à chaque tâche. Le nombre d'équipements/ressources est défini en fonction de contraintes technologiques (par exemple collage ou clinchage) ou par rapport au niveau d'automatisation souhaité (manuel, semi-automatisé ou automatisé).

Graves et Whitney [159] font partie des premiers auteurs à avoir abordé le problème d'équilibrage de ligne et de choix d'équipements/ressources. Ils proposent un modèle dans lequel l'objectif est de sélectionner les équipements et d'assigner des tâches aux postes de travail afin que les coûts totaux, composés des coûts d'investissement et d'opération, soient minimisés.

Pinto *et al.* [320] ont combiné le problème d'équilibrage de ligne avec la décision liée à l'utilisation ou non de stations parallèles. Le modèle proposé permet d'analyser les compromis entre les coûts additionnels liés à l'utilisation de stations parallèles et l'économie réalisée sur la main-d'œuvre. Plus tard, Pinto *et al.* [321] ont présenté un modèle qui considère le choix des ressources d'assemblage et l'attribution des tâches de manière à minimiser les coûts totaux, définis comme la somme des coûts de main-d'œuvre et des dépenses fixes. Un modèle similaire a été proposé par Graves et Lamar [160] pour le problème de conception de ligne automatisée. L'objectif était de déterminer le type et le nombre de postes de travail et l'affectation d'opérations.

Graves et Holmes [161] abordent le problème de conception de ligne d'assemblage avec choix d'équipement pour une ligne de type mixte. La méthode proposée vise à la fois à assigner des tâches aux postes de travail et à sélectionner des équipements, en minimisant le coût total de la ligne d'assemblage.

Buckin et Tzur [57] proposent un modèle dans lequel les coûts totaux associés à la sélection des équipements sont minimisés pour un temps de cycle donné. Dans leur modèle, chaque équipement a un coût et un temps de traitement différents. Plus tard, Buckhin et Rubinovitz [56] ont étendu ce modèle en considérant des postes de travail parallèles.

Hamta *et al.* [170] présentent une approche pour traiter le problème d'équilibrage de ligne d'assemblage avec temps de tâche flexibles (Flexible Time Assembly Line Balancing Problem, FTALBP). Dans leur problème, le temps d'opération des tâches peut être défini entre une borne inférieure et une borne supérieure. Plus le temps de fonctionnement est faible, plus les coûts de traitement associés sont élevés. Dans leur approche, deux fonctions objectifs sont considérées : (i) minimiser le temps de cycle et (ii) minimiser les coûts totaux de la machine. Hamta *et al.* [169] ont étendu le travail précédent en ajoutant un indice de lissage de la charge de travail. Ils ont proposé une méthode basée sur la combinaison d'un algorithme d'optimisation par essaims particulaires avec une recherche locale.

Pekin et Azizoglu [317] proposent un Branch & Bound et des procédures de réduction pour un problème considérant l'équilibrage de ligne et le choix de ressources. L'algorithme proposé est capable de résoudre des problèmes comprenant jusqu'à 25 tâches et 5 équipements.

Agpak et Gökcen [13] présentent un cas industriel dans lequel des équipements et des tâches sont assignés simultanément aux postes de travail. Dans ce problème, un nombre limité de ressources automatisées et manuelles doit être associé aux stations de travail. Dans ce modèle, aucun coût n'est explicitement considéré. Corominas *et al.* [93] ont étendu ce problème en considérant des contraintes entre les différentes ressources.

Polat *et al.* [322] traitent le problème associé à l'allocation simultanée de tâches et de travailleurs aux stations de travail afin de minimiser le temps de cycle (Assembly Line Worker Assignment Problem, ALWABP). Ce problème a été largement abordé dans la littérature, par ex. Borba et Ritt [48] et Ritt *et al.* [341].

Le Tableau A.1 montre une classification des éléments de coûts utilisés lors de l'évaluation d'un ensemble de ressources qui peuvent être affectées à une tâche. Ces éléments peuvent être divisés en (i) coûts des opérations de fabrication et d'assemblage, qui comprennent par exemple les différents salaires ou le coût d'entretien des ressources automatisées, ou en (ii) coût d'investissement. Ce tableau montre que les études traitent de façon hétérogène les différents éléments. Bien que certains modèles prennent en compte les coûts des opérations, d'autres considèrent uniquement les coûts fixes, dénotés (FC).

Tableau A.1: Comparaison des éléments de coûts considérés lors de l'évaluation d'un ensemble de ressources

	Coût d'investissement		Coût d'opération		
Auteurs	R	S	R	T	W
Graves and Whitney [159]			X	X	
Pinto *et al.* [320]			X (FC)		X
Pinto *et al.* [321]			X (FC)		X
Graves and Lamar [160]			X (FC)	X (FC)	
Graves and Redfield [161]	X	X			
Rubinovitz *et al.* [346]		X		X	
Bukchin and Tzur [57]		X			
Bukchin and Rubinovitz [56]		X	(X)		
Levitin *et al.* [239]					
Khouja *et al.* [210]					
Nicosia *et al.* [285]		(X)			
Hamta *et al.* [170]		X			
Hamta *et al.* [169]		X			
Pekin and Azizoglu [317]	X	X			
Corominas *et al.* [93]		X	X		
Oesterle and Amodeo [289]	X		X		

* les notations suivantes sont utilisées : R : Ressource automatisée, S : Station, T : Tâche, W : Ressource manuelle

A.2.5 Allocation de stocks tampon

Afin de limiter les effets de famine et de blocage à cause de défaillances des ressources automatisées et afin d'augmenter la productivité d'une ligne d'assemblage, des stocks tampon sont souvent alloués entre les stations de travail. Le problème d'allocation de stocks tampon (Buffer Allocation Problem, BAP) vise à allouer les stocks tampon d'une ligne de production afin d'optimiser un/des objectif(s) spécifique(s). Une étude exhaustive des problèmes d'allocation de stocks tampon a été effectuée par Demir *et al.* [107]. Les approches utilisées pour résoudre le problème associé à l'allocation de stocks tampon impliquent à la fois une méthode générative et une méthode évaluative. Alors que dans le premier cas, une solution au problème est générée, dans le second, cette solution est évaluée en utilisant diverses mesures de performance au moyen de (i) méthodes analytiques et/ou (ii) simulation [116]. Alors que les modèles analytiques peuvent être décrits comme un ensemble d'équations caractérisant un système, les modèles de simulation imitent le comportement dynamique du système. Les modèles analytiques ont tendance à être plus précis alors que les modèles de simulation fournissent des informations approximatives et dynamiques sur le système [388]. Par rapport aux modèles analytiques, les modèles de simulation offrent plus de flexibilité

et peuvent prendre en considération un large ensemble de caractéristiques du système [92]. Des exemples d'application de modèles analytiques peuvent être trouvés dans les travaux suivants [449, 313, 151, 412, 259, 117]. Des exemples d'application de modèles de simulation peuvent être trouvés dans les travaux suivants [32, 9, 261, 42, 218].

A.2.6 Synthèse

Les lacunes dans les modèles et méthodes présentés précédemment peuvent être identifiées sur les plans :

(a) de l'évaluation d'un ensemble de solutions développées lors de la conception d'un produit,
(b) de la sélection des procédés d'assemblage et du choix de ressources,
(c) de l'équilibrage de ligne, et
(d) de l'allocation de stocks tampon.

Au niveau des méthodologies existantes permettant l'évaluation des solutions développées durant la conception de produits, un défaut majeur consiste en l'absence de considération lorsqu'il s'agit d'analyser l'influence et les effets du choix du design sur les procédés de fabrication et d'assemblage. Les travaux consacrés à l'évaluation des procédés d'assemblage et d'un ensemble de ressources sont principalement axés sur des objectifs de capacité, qui ne prennent pas en considération des notions de coûts de production ou de coûts du produit final. De plus, l'ensemble des modèles d'équilibrage de lignes d'assemblage qui traitent le choix de ressources manuelles ou automatisées ne considère pas certaines caractéristiques comme la disponibilité des ressources ou le taux de rebut. Par ailleurs, l'absence d'un modèle de coûts permettant une estimation précise du coût futur du produit peut être identifiée.

Bien que les méthodes analytiques aient été largement développées pour le problème de l'allocation de stocks tampon au cours des 30 à 35 dernières années, elles sont souvent destinées à estimer d'une façon approximative le comportement dynamique des systèmes d'assemblage et utilisent en général des hypothèses restrictives. En comparaison, les modèles de simulation requièrent souvent un temps de calcul non négligeable. Toutefois, ils offrent un avantage considérable lorsque l'objectif est de créer un modèle réaliste d'un système complexe [107]. En outre, les modèles analytiques ne mesurent généralement qu'un nombre limité de critères de performance du système, tandis que le nombre de critères applicables dans les modèles de simulation est illimité.

Considérant l'état de l'art, une méthode holistique permettant l'évaluation et la sélection simultanée des procédés d'assemblage, de ressources, l'équilibrage de ligne et l'allocation de

stocks tampon est proposée dans cette thèse.

A.3 Approche holistique pour la conception de lignes d'assemblage hybrides

Le travail présenté dans les chapitres 4 à 6 concerne la formulation et la résolution de deux problèmes d'optimisation multiobjectifs associés à une approche holistique d'ingénierie concourante. La différence entre les deux problèmes formulés est présentée dans le Tableau A.2.

Tableau A.2: Différences entre les deux problèmes traités

	Problème 1	Problème 2
Choix du design du produit	X	X
Choix procédés d'assemblage	X	X
Choix de ressources	X	X
Allocation de stocks tampon		X
Évaluation mathématique	X	
Evaluation par simulation		X

L'objectif principal, comme représenté dans la Figure A.1, est de diminuer les changements de design lors de la conception du produit et de la ligne d'assemblage en incluant dès les premières phases de conception le choix de procédés d'assemblage et de ressources. Cela permet l'obtention d'un système plus stable et avec des coûts de production diminués.

Pour supporter les travaux de recherche, les sous-objectifs suivants sont abordés dans cette thèse :

— Développement d'un modèle de coût qui peut traduire toutes les interdépendances entre les différents designs d'un produit, les différents processus d'assemblage et ressources en une seule métrique ;
— Développement et comparaison de différentes méthodes d'optimisation ;
— Incorporation de méthodes d'évaluation pour analyser l'influence des stocks tampon sur l'efficacité de la chaîne d'assemblage.

Les questions de recherche suivantes peuvent être tirées des objectifs de cette thèse :

— Quels éléments de coûts ont une influence significative sur le choix du meilleur produit et de la conception de l'assemblage (tâches, procédés d'assemblage, ressources) ?
— Quelles méthodes d'optimisation sont les mieux adaptées pour sélectionner la meilleure configuration de ligne d'assemblage ?

— Enfin, la méthode proposée permet-elle de diminuer le nombre de modifications de conception, de planification et de coûts ?

Ces questions de recherche représentent la ligne directrice et forment la base de la structure de cette thèse.

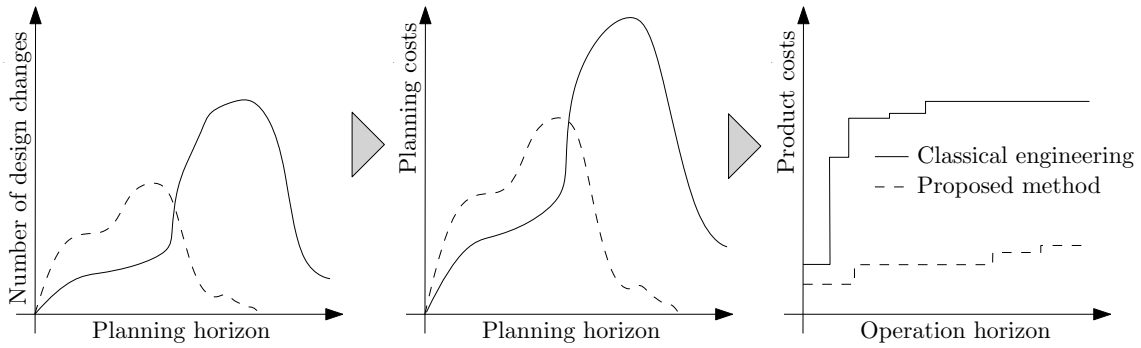

Figure A.1: Définition des objectifs du travail proposé

La méthode de résolution, dont les étapes sont représentées dans la Figure A.2, comprend une composante générative et évaluative. Dans le module génératif, qui est composé d'algorithmes d'optimisation multiobjectifs, les solutions aux différents problèmes représentés dans le Tableau A.2 sont générées. Dans le composant évaluatif, les solutions générées sont évaluées. Pour le premier problème, cette évaluation est purement mathématique alors que pour le second, un module de simulation à événements discrets est utilisé. Ce module fournit les informations nécessaires au module d'estimation du coût final du produit. L'objectif de ce dernier est de traduire les conséquences complexes et interreliées entre les procédés d'assemblage, les choix d'équipement et l'équilibrage de ligne en une seule métrique de coût.

A.3.1 Problème 1 : Étude numérique

Pour résoudre le premier problème, différents algorithmes de différentes familles ont été développés. Ces algorithmes et leurs abréviations sont listés dans le Tableau A.3. Plusieurs expériences ont été menées pour tester ces algorithmes. Ces tests sont basés sur les instances du Tableau A.4, qui ont été créées à partir d'une adaptation de problème disponible à l'adresse suivante : www.assembly-line-balancing.de. En raison de leurs caractéristiques différentes, ces instances fournissent une diversité suffisante pour comparer les différents algorithmes. Ces caractéristiques, représentées par :

(a) l'ordre moyen du graphe de précédence (OS, représente la complexité du problème) ;
(b) le nombre de tâches (N) ;
(c) le nombre de sous-graphes (PDA) ;

(d) le nombre total de ressources disponibles E_{tot} ;

sont indiquées dans le Tableau A.4. Les problèmes marqués avec * sont des problèmes qui ont également été résolus avec une méthode exacte (TPM) [396]. De par la nature du problème, toutes les instances ne peuvent être résolues de manière exacte. Pour le reste des problèmes, un front de Pareto pseudo-optimal combinant toutes les solutions trouvées par tous les algorithmes et supprimant les solutions dominées a été construit.

Afin de comparer efficacement toutes les méthodes d'optimisation, une définition de leurs paramètres a été effectuée à l'aide d'un plan d'expérience. Les détails de cette analyse se trouvent en Annexe C.2. Dans le chapitre 4, les différents algorithmes sont comparés grâce à : (i) l'indicateur d'hypervolume (I_{HV}) [457], (ii) l'indicateur ϵ (I_ϵ) [458], (iii) l'indicateur IGD (I_{IGD}) [90] et (iv) l'indicateur de dispersion (I_Δ) [103]. Le choix de ces indicateurs est motivé par leurs différents objectifs : (i) I_ϵ mesure la capacité de convergence, (ii) I_Δ mesure la distribution des solutions et (iii) I_{IGD} et I_{HV} combinent ces deux composantes. Plus les valeurs de I_{HV} sont élevées et les valeurs de I_{IGD}, I_Δ et I_ϵ faibles, meilleure sera la performance d'un algorithme.

Afin d'identifier les algorithmes qui ont une meilleure performance que d'autres et de déterminer si les différences entre eux sont significatives ou non, le test de Friedman peut être appliqué [144, 145]. Le test de Friedman est une des procédures d'analyse statistique non paramétrique couramment utilisées [446] pour analyser les différences entre les algorithmes [299, 251, 446].

La directive fournie par Derrac *et al.* [110] a été suivie pour effectuer l'analyse statistique.

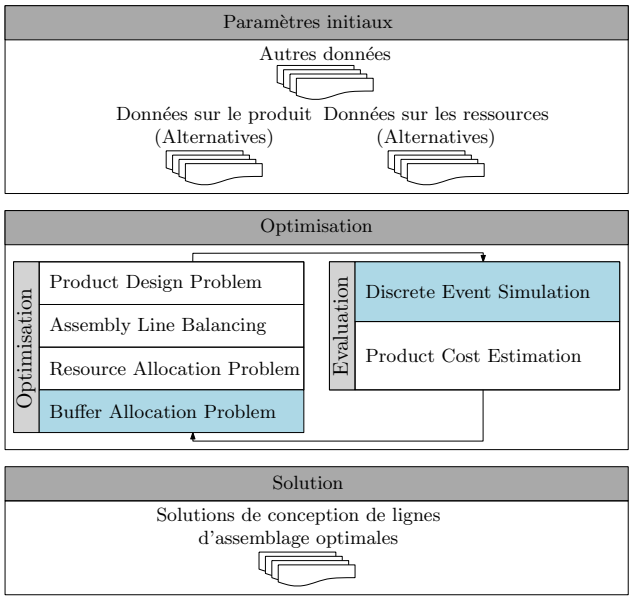

Figure A.2: Méthode de résolution

Tableau A.3: Liste d'algorithmes et leurs abréviations

Famille d'algorithmes	Noms
Optimisation par colonie de fourmis	BIANT-1
	BIANT-2
	CHAC-1
	CHAC-2
	MOACS-1
	MOACS-2
Optimisation par colonie d'abeilles artificielles	DMOABC
Recherche du coucou	DMOCSA-1-1
	DMOCSA-1-2
	DMOCSA-1-3
	DMOCSA-1-4
	DMOCSA-1-5
	DMOCSA-2-1
	DMOCSA-2-2
	DMOCSA-2-3
	DMOCSA-2-4
	DMOCSA-2-5
Algorithme de pollinisation des fleurs	DMOFPA-1
	DMOFPA-2
	DMOFPA-3
	DMOFPA-4
	DMOFPA-5
Chauve-souris	MOBAT-1
	MOBAT-2
	MOBAT-3
	MOBAT-4
	MOBAT-5
Optimisation par essaims particulaires	MOPSO-1
	MOPSO-2
	MOPSO-3
	MOPSO-4
	MOPSO-5
Algorithmes évolutionnaires	NSGA-II
	SPEA2

Les statistiques de Friedman obtenues pour tous les problèmes et les algorithmes considérés simultanément en fonction de I_{HV}, I_{IGD}, I_ϵ et I_Δ et les $p-$values respectives sont affichées dans le Tableau A.5. En considérant $\chi^2_{0.0001} = 72$ avec un niveau de confiance de 99.99 % et 33 degrés de liberté, on peut conclure qu'il existe des différences significatives entre les algorithmes pour tous les indicateurs de qualité.

L'utilisation des rangs de Friedman permet de définir une classification des algorithmes et peut être utilisée pour mesurer les différences entre algorithmes. Les rangs obtenus par les meilleurs algorithmes pour chaque indicateur sont présentés dans le Tableau A.6. Le NSGA-II, suivi du SPEA2, CHAC-1, CHAC-2 et DMOPSO-5 sont les algorithmes qui ont obtenu, en moyenne pour tous les problèmes, les meilleures valeurs pour I_{HV}. Le CHAC-1 suivi du CHAC-2, du DMOBAT-3, du DMOBAT-2 et du DMOPSO-1 ont obtenu les meilleures

Tableau A.4: Caractéristiques des différents problèmes

Problem	N	OS	PDA	E_{tot}	Problem	N	OS	PDA	E_{tot}
Arc111-1	125	0.181	6	636	Gunther-1	41	0.378	2	220
Arc111-2	125	0.181	6	578	Gunther-2	41	0.378	2	209
Arc111-3	125	0.181	6	555	Gunther-3	41	0.364	2	209
Arc111-4	125	0.185	6	555	Gunther-4	41	0.353	2	209
Arc111-5	125	0.178	6	505	Gunther-5	41	0.353	2	194
Buxey-1	32	0.334	2	166	Hahn-1	68	0.348	5	363
Buxey-2	32	0.330	2	154	Hahn-2	68	0.348	5	339
Buxey-3	32	0.322	2	152	Hahn-3	68	0.343	5	339
Buxey-4	32	0.322	2	138	Hahn-4	68	0.345	5	339
Buxey-5	32	0.333	2	138	Hahn-5	68	0.345	5	304
Jackson-1*	15	0.442	2	28	Lutz1-1*	37	0.570	2	48
Jackson-2*	15	0.442	2	30	Lutz1-2*	37	0.553	2	47
Jackson-3*	15	0.442	2	37	Lutz1-3*	37	0.524	2	49
Jackson-4*	15	0.442	2	29	Lutz1-4*	37	0.530	2	51
Jackson-5*	15	0.442	2	31	Lutz1-5*	37	0.530	2	50
Kilbrid-1*	50	0.641	2	70	Mitchell-1	27	0.579	2	52
Kilbrid-2	50	0.641	2	76	Mitchell-2*	27	0.579	2	46
Kilbrid-3	50	0.641	2	87	Mitchell-3*	27	0.432	3	71
Kilbrid-4	50	0.622	2	87	Mitchell-4*	27	0.579	2	50
Kilbrid-5	50	0.600	2	87	Roszieg-1*	28	0.504	2	46
Mukherje-1	105	0.124	5	547	Roszieg-2*	28	0.547	2	42
Mukherje-2	105	0.124	5	517	Roszieg-3*	28	0.610	2	47
Mukherje-3	105	0.124	5	507	Roszieg-4*	28	0.605	2	39
Sawyer-1*	33	0.539	2	40	Sawyer-3*	33	0.539	2	45
Sawyer-2*	33	0.539	2	39	Sawyer-4*	33	0.539	2	44

Tableau A.5: Statistique de Friedman et p-value conformément à I_{HV}, I_{IGD}, I_ϵ, I_Δ

Indicateur	Statistique de Friedman	$p-$values
I_{HV}	1035.35	0
I_{IGD}	803.43	2.87E-10
I_ϵ	834.81	2.99E-10
I_Δ	826.73	2.44E-10

valeurs pour I_{IGD}. En ce qui concerne I_ϵ, le NSGA-II, suivi par le SPEA2, le DMOPSO-1, le DMOPSO-5 et le DMOABC ont obtenu les meilleurs résultats. Pour I_Δ, la famille MOACO a surpassé les autres algorithmes. Une analyse identique a été effectuée pour le temps de calcul. Cette analyse a montré que le SPEA2, suivi par le DMOPSO-2, DMOFPA-4, DMOCSA-1-4 sont les algorithmes qui convergent le plus rapidement vers un ensemble de solutions non dominées. Afin d'évaluer si ces algorithmes sont significativement meilleurs que les autres, la procédure de Holm a été appliquée. En utilisant un intervalle de confiance de 95 %, le NSGA-II est significativement meilleur que 96 % des algorithmes pour I_{HV}. Cependant, il n'est pas significativement meilleur que le SPEA2. En considérant I_{IGD}, le CHAC-1 est uniquement significativement meilleur que 24 % des algorithmes. En ce qui concerne I_ϵ, la même conclusion que pour I_{HV} peut être faite. Pour I_Δ, le BIANT-1 est meilleur que 91 %

Tableau A.6: Rangs moyens retournés par le test non paramétrique de Friedman pour tous les problèmes selon les différents indicateurs de qualité

Algorithmes	I_{HV}	I_{IGD}	I_ϵ	I_Δ
DMOABC	15.6	19.3	20.1	15.0
DMOBAT-2	16.0	19.8	18.8	17.0
DMOBAT-3	15.1	20.0	19.6	17.0
BIANT-1	17.6	17.9	9.8	26.1
BIANT-2	17.4	17.3	9.6	24.9
CHAC-1	13.8	20.7	19.4	19.7
CHAC-2	13.9	20.6	19.5	19.1
DMOCSA-1-4	27.2	8.8	13.9	18.2
DMOFPA-4	27.0	9.1	13.3	17.0
MOACS-1	19.9	15.0	11.3	26.1
MOACS-2	17.9	15.4	11.8	25.5
DMOPSO-1	15.5	19.8	20.4	17.5
DMOPSO-2	16.0	19.8	18.9	16.4
DMOPSO-5	15.0	19.4	20.0	17.3
NSGA-II	11.2	19.6	23.3	13.1
SPEA2	12.3	18.6	23.0	14.0

des algorithmes. Pour le temps de calcul, le SPEA2 est significativement meilleur que tous les autres algorithmes.

Toutefois, étant donné que cette analyse a été effectuée en tenant compte de tous les problèmes, les résultats peuvent varier en fonction des caractéristiques du problème. Une analyse similaire a montré que, en considérant les différents problèmes séparément, ces résultats dépendent de la complexité du problème à résoudre. Les résultats du test de Friedman obtenus en considérant les problèmes complexes (groupe 1) et moins complexes (groupe 2) sont représentés dans le Tableau A.7. Ce tableau montre que pour les problèmes complexes, le MOACS-1, MOACS-2, BIANT-1 et BIANT-2 ont obtenu de meilleurs résultats que tous les autres algorithmes concernant I_{HV}, I_{IGD} , I_Δ. Pour I_ϵ, le MOACS-2 est en troisième position, et est dépassé par le NSGA-II et SPEA2. En considérant I_{HV}, le MOACS-2 est meilleur que tous les algorithmes sauf le MOACS-1, BIANT-1 et BIANT-2, pour lesquels l'amélioration n'est pas nécessairement significative. En ce qui concerne les valeurs de I_{IGD}, le BIANT-2 est significativement meilleur que tous les algorithmes sauf le MOACS-2 et BIANT-1. Pour I_ϵ, le NSGA-II est significativement meilleur que tous les algorithmes, sauf le SPEA2. En ce qui concerne les valeurs de I_Δ, le MOACS-2 est significativement meilleur que tous les algorithmes, exceptés pour les BIANT-1, BIANT-2 et MOACS-1. Pour les problèmes moins complexes, les différences entre les divers algorithmes ne sont pas forcément significatives. Pour les valeurs de I_{HV}, le CHAC-2 est significativement meilleur que 28 % des algorithmes uniquement. En ce qui concerne le I_{IGD}, le DMOPSO-1 est significativement meilleur que 28 % des algorithmes. Pour les valeurs de I_Δ, le DMOCSA-1-4 est significativement supérieur

Tableau A.7: Rangs moyens retournés par le test non paramétrique de Friedman pour les problèmes complexes et moins complexes

	Groupe 1				Groupe 2			
Algorithmes	I_{HV}	I_{IGD}	I_ϵ	I_Δ	I_{HV}	I_{IGD}	I_ϵ	I_Δ
BIANT-1	4.69	29.07	14.43	31.73	29.96	7.57	5.53	20.91
BIANT-2	3.55	29.19	15.07	31.85	30.66	6.34	4.52	18.5
CHAC-1	15.05	18.94	17.7	20.99	12.54	22.29	21	18.47
CHAC-2	15.46	19.03	17	19.95	12.24	22.00	21.77	18.22
DMOABC	18.52	17.24	17.75	11.85	12.78	21.23	22.29	17.83
DMOBAT-1	19.29	16.29	16.99	15.05	13.77	21	21.03	17.09
DMOBAT-3	17.85	17.99	17	16.9	12.46	21.92	21.94	17
DMOBAT-4	26.44	8.95	16.38	14.56	24.63	11.47	12.11	20.41
DMOBAT-5	19.05	17.26	16.39	15.06	13.25	22.01	20.64	16.38
DMOCSA-1-4	27.58	7.98	17.01	14.08	26.76	9.63	11.05	21.99
DMOCSA-2-4	25.09	10.91	17.35	16.6	24.53	10.92	12.4	19.58
DMOFPA-4	27.25	8.39	15.86	14.59	26.82	9.67	10.97	19.2
DMOPSO	17.41	18.39	18.05	17.7	12.64	20.27	21.91	16.95
DMOPSO-1	18.69	17.24	17.88	16.47	12.36	22.22	22.66	18.51
DMOPSO-2	18.98	17.94	16.29	16.19	13.18	21.52	21.39	16.64
DMOPSO-3	19.15	16.91	17.05	15.81	13.33	21.37	21.84	17.39
MOACS-1	7.47	24.69	19.36	32.44	31.8	6.09	3.78	20.24
MOACS-2	3.15	26.77	20.64	32.46	32.05	4.83	3.58	19.11
NSGA-II	9.74	17.58	25.54	8.75	12.64	21.37	21.26	17.03
SPEA2	11.61	15.51	24.50	11.34	12.94	21.54	21.46	16.46

à 42 % des algorithmes.

Afin d'améliorer les performances des algorithmes les plus performants, différentes règles de dominance ont été comparées les unes aux autres à l'aide du test de Friedman dans le chapitre 5. Les abréviations des algorithmes avec leurs règles de dominance sont représentées dans le Tableau A.8.

Tableau A.8: Liste d'algorithmes avec leurs règles de dominances

	Règle de dominance				Règle de dominance	
Nom	Pareto	Lorenz	S-CDAS	Name	Pareto	Lorenz
CHAC-1	X			DMOPSO-1	X	
CHAC-1-L		X		DMOPSO-1-L		X
CHAC-2	X			DMOPSO-2	X	
CHAC-2-L		X		DMOPSO-3	X	
MOACS-1	X			DMOPSO-4	X	
MOACS-1-L		X		DMOPSO-5	X	
MOACS-1-S-CDAS			X	NSGA-II	X	
MOACS-2	X			NSGA-II-L		X
MOACS-2-L		X		SPEA2	X	
MOACS-2-S-CDAS			X	SPEA2-L		X

Les statistiques de Friedman obtenues pour tous les problèmes et les algorithmes avec différentes règles de dominances et considérant les indicateurs de qualité suivant I_{HV}, I_{IGD}, I_ϵ et I_Δ ainsi que les $p-$value respectives sont affichées dans le Tableau A.9. En considérant

$\chi^2_{0.05} = 32.7$ avec un niveau de confiance de 95% et 21 degrés de liberté, on peut conclure que les différences entre les règles de dominance sont significatives pour tous les indicateurs de qualité.

Tableau A.9: Statistique de Friedman et p-value conformément à I_{HV}, I_{IGD}, I_ϵ, I_Δ

Indicators	Friedman statistic	Computed p-values
I_{HV}	259.770	1.38E−10
I_{IGD}	152.060	8.39E−11
I_ϵ	679.250	2.04E−10
I_Δ	1193.530	0
Time	2216.600	0

Les résultats du test de Friedman obtenus en considérant les problèmes complexes et moins complexes sont représentés dans le Tableau A.10. Comme l'indique ce tableau, le MOACS-2-L obtient les meilleurs résultats pour les problèmes du groupe 1 et pour I_{HV} et I_Δ. Alors que le NSGA-II-L atteint la meilleure valeur pour I_ϵ, le MOACS-2-L obtient le deuxième meilleur résultat. Même si la famille d'algorithmes MOACS-2 obtient de bons résultats pour I_{IGD}, les BIANT-1 et BIANT-2 ont toujours les meilleures valeurs. Pour les problèmes du groupe 2, le CHAC-2-L obtient les meilleures valeurs pour I_{HV}, I_{IGD} et I_ϵ. Bien que le MOACS-1-S-CDAS ne soit pas en mesure d'améliorer les résultats obtenus par le MOACS-1, il est suivi par le BIANT-1, meilleur algorithme considérant I_Δ. Pour les deux groupes, les SPEA2 et SPEA2-L sont les algorithmes qui convergent le plus rapidement vers un ensemble de solutions.

Sachant qu'une dégradation de certains indicateurs peut-être espérée lors de l'application de règles de dominance, qui sont par définition plus restrictives que celle de Pareto, l'indicateur I_C a été également utilisé. Cet indicateur permet de calculer le nombre de solutions obtenues par un algorithme qui sont dominées par celles obtenues par un autre algorithme. Les valeurs de I_C sont présentées pour chaque groupe de problèmes dans le Tableau A.11. Comme on peut le voir dans ce tableau, généralement, en appliquant la règle de dominance de Lorenz pour les problèmes du groupe 1, les solutions obtenues sont moins dominées par la règle de dominance de Pareto. Pour la règle de dominance S-CDAS, en ce qui concerne I_C, il semble qu'elle soit meilleure que la règle de dominance de Pareto pour le MOACS-1. Des résultats plus hétérogènes sont obtenus en comparant les règles de dominance appliquées aux problèmes du groupe 2. Alors que pour le CHAC-2 et le MOACS-1, la règle de dominance de Lorenz est, en ce qui concerne I_C supérieure à la règle de dominance de Pareto, le contraire peut être affirmé pour les algorithmes CHAC-1 et MOACS-2. Il semble également que la règle de dominance S-CDAS soit plus appropriée lorsqu'elle est appliquée en combinaison avec le MOACS-2 pour les problèmes du groupe 1.

La Figure A.3 montre l'évolution du nombre de solutions non dominées obtenu lors de l'application des différentes règles de dominance pour différents algorithmes et problèmes.

Tableau A.10: Rangs moyens retournés par le test non paramétrique de Friedman pour les problèmes complexes et moins complexes

	Groupe 1					Groupe 2				
Algorithm	I_{HV}	I_{IGD}	I_ϵ	I_Δ	Time	I_{HV}	I_{IGD}	I_ϵ	I_Δ	Time
BIANT-1	5.29	17.70	8.67	17.64	4.15	16.71	6.89	6.43	13.89	8.14
BIANT-2	4.41	18.03	9.44	17.69	4.06	17.51	6.35	5.50	12.29	7.37
CHAC-1	14.23	9.79	10.46	9.81	10.29	7.40	15.14	14.58	11.28	10.84
CHAC-1-L	14.46	10.39	9.93	10.13	9.49	7.33	15.04	15.32	10.36	12.87
CHAC-2	14.69	9.68	9.90	9.36	11.33	7.25	15.10	15.09	11.18	11.36
CHAC-2-L	14.30	10.25	10.25	9.65	9.76	6.71	15.56	15.77	10.77	10.71
MOACS-1	8.38	14.85	11.85	18.36	9.66	18.18	6.02	5.36	12.92	8.67
MOACS-1-S-CDAS	11.23	12.09	10.70	17.55	7.71	17.74	6.15	6.12	14.07	1.66
MOACS-1-L	8.05	14.79	12.00	18.28	9.93	17.82	6.20	5.98	13.57	7.12
MOACS-2	4.45	16.20	14.10	19.27	10.73	18.52	5.60	4.96	12.51	5.33
MOACS-2-S-CDAS	4.87	15.70	14.17	18.82	10.23	18.77	5.51	5.08	12.24	1.87
MOACS-2-L	3.99	16.64	14.39	19.40	10.92	19.06	5.48	4.58	12.34	5.43
DMOPSO-5	15.31	9.85	10.47	8.24	13.00	8.30	13.74	15.15	10.54	13.93
DMOPSO-1	15.82	9.50	10.63	7.75	12.93	7.22	15.19	15.61	11.31	16.60
DMOPSO-2	16.18	9.51	9.92	7.50	15.43	7.71	14.88	14.75	10.32	15.45
DMOPSO-3	16.30	8.71	10.02	7.40	11.40	7.75	14.69	15.02	10.98	18.60
DMOPSO-4	18.81	5.18	9.43	7.32	8.07	10.88	11.81	12.55	11.21	14.03
DMOPSO-1-L	16.19	8.88	10.45	7.88	14.20	7.69	14.12	15.19	9.86	15.14
NSGA-II	10.94	9.37	14.22	4.04	12.34	7.50	15.18	15.19	10.46	10.11
NSGA-II-L	11.06	9.19	14.56	5.95	16.55	7.45	14.52	15.08	10.59	18.93
SPEA2	12.06	8.18	13.54	5.43	20.32	7.64	15.18	15.00	10.29	19.62
SPEA2-L	11.97	8.53	13.91	5.54	20.50	7.85	14.64	14.67	10.01	19.21

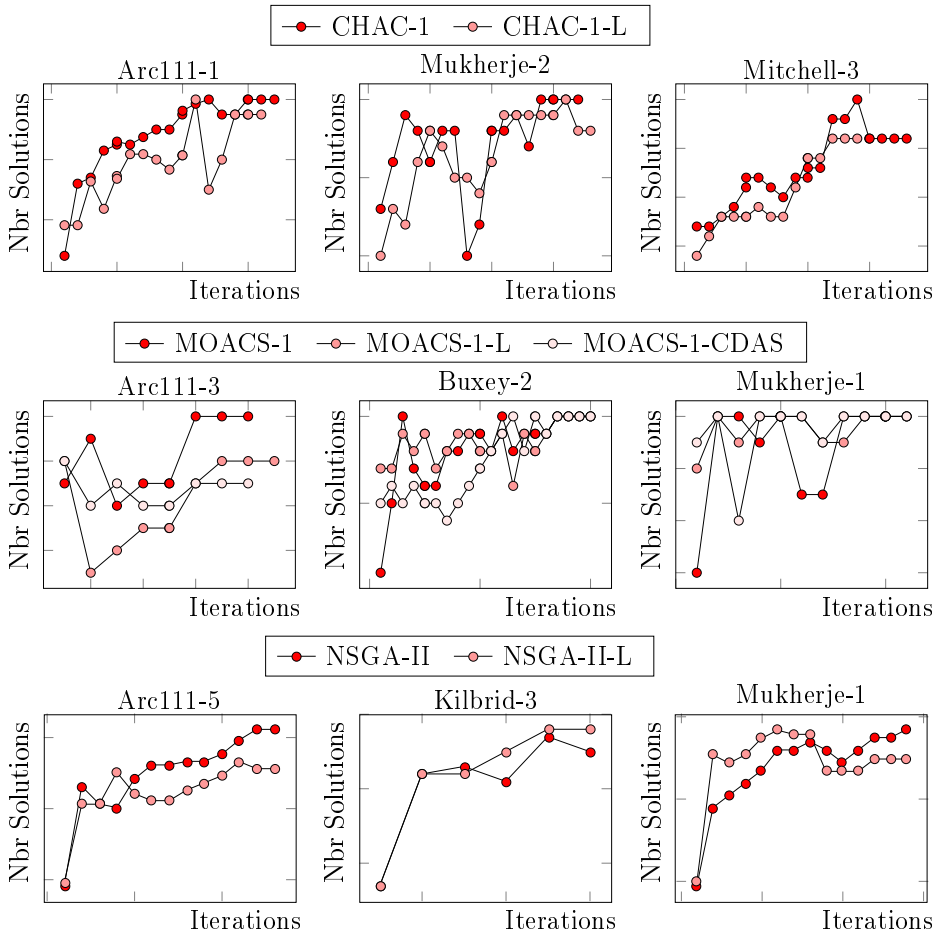

Figure A.3: Comparaison de l'ensemble des solutions non dominées obtenues par les différentes règles de dominance

Comme on peut le voir, en moyenne, le nombre de solutions non dominées est plus faible lorsque l'on applique la règle de dominance de Lorenz. En plus du test de Friedman, une com-

Tableau A.11: Évolution de la valeur moyenne de I_C entre l'utilisation des différentes règles de dominance

Algorithm	Dominance Rule	Group 1	Group 2
CHAC-1	$I_C(L,P)$	0.39	0.11
	$I_C(P,L)$	0.39	0.10
CHAC-2	$I_C(L,P)$	0.39	0.10
	$I_C(P,L)$	0.39	0.11
MOACS-1	$I_C(L,P)$	0.39	0.19
	$I_C(P,L)$	0.42	0.23
MOACS-2	$I_C(L,P)$	0.38	0.20
	$I_C(P,L)$	0.42	0.14
MOACS-1	$I_C(S-CDAS,P)$	0.38	0.20
	$I_C(P,S-CDAS)$	0.42	0.14
MOACS-2	$I_C(S-CDAS,P)$	0.42	0.19
	$I_C(P,S-CDAS)$	0.38	0.22

paraison des règles de dominance par paires multiples en utilisant la procédure de Nemenyi a été appliquée sur les différents indicateurs de qualité pour chaque algorithme. L'analyse des p-values montre qu'il n'existe pratiquement aucune différence significative (niveau alpha à 0.05) entre les différentes règles de dominance quand on considère les indicateurs de qualité suivants : (i) I_{HV}, (ii) I_{IGD}, (iii) I_ϵ, (iv) I_Δ, (v) le temps nécessaire jusqu'à convergence, (vi) I_C et (vii) le nombre de solutions non-dominées obtenu, dénoté NDS. Bien que la performance du CHAC-1 et CHAC-2 ne soit pas sensible à la règle de dominance choisie, la différence entre les règles de dominance est significative pour le MOACS-1 et MOACS-2 lorsqu'elle est appliquée à des problèmes complexes. Ce que l'on peut remarquer, c'est que la règle de dominance du S-CDAS est plus mauvaise que les règles de dominance de Pareto et Lorenz sur des problèmes complexes. En effet, par rapport à la règle de la domination de Pareto, le S-CDAS engendre une détérioration des indicateurs de qualité suivants : (i) I_{HV}, (ii) I_{IGD}, (iii) I_ϵ, (iv) I_Δ et (v) le temps nécessaire à la convergence de l'algorithme. Si cette détérioration est quantifiée, la valeur de ces indicateurs diminuera respectivement de 1.7 %, 6.6 %, 19 %, 2.7 %, et 23 % pour le MOACS-1. Cependant, le CDAS, qui est plus agressif dans la région moyenne du front de Pareto, permet d'améliorer I_C de 2 %. La même conclusion peut être obtenue pour le MOACS-2, pour lequel tous les indicateurs précédents, à l'exception de I_Δ, sont détériorés comme suit : i) I_{HV} de 4 %, (ii) I_ϵ de 3.5 %, (iii) le temps de calcul jusqu'à convergence de 26 %. Comme dans le cas précédent, le MOACS-2 permet une amélioration de I_C de 1 %. En comparant les différences significatives entre les règles de dominance, il semble que l'effet des règles de dominance soit plus grand lorsque les instances de problème restent moins complexes.

En plus des règles de dominance, une recherche locale a été appliquée au MOACS-2-L, SPEA2 et NSGA-II-L. Pour le premier algorithme, la combinaison avec une recherche locale a permis d'améliorer sa performance en considérant tous les indicateurs de qualité, à l'exception de I_Δ. Les résultats du SPEA2 ont été légèrement améliorés, principalement pour les problèmes du groupe 2. Les résultats sont complètement différents pour le NSGA-II-L-LS, qui n'a pu qu'améliorer son temps de convergence sans améliorer d'autres indicateurs de qualité. Une explication de ces résultats peut être liée au fait que la recherche locale a été appliquée aux solutions non dominées de la population actuelle pouvant ainsi enregistrer une convergence précoce.

A.3.2 Problème 2 : Étude numérique

Comme indiqué précédemment, les différences entre les deux problèmes traités dans ce rapport de thèse se rapportent à l'ajout de l'allocation de stocks tampon entre les stations de

travail.

Lors de la résolution du premier problème, les algorithmes évolutionnaires ont obtenu, en considérant tous les problèmes, de bons résultats. Cependant, les MOACO représentés par le BIANT, MOACS et CHAC, obtiennent de meilleurs résultats pour respectivement les problèmes complexes et moins complexes. En raison de la nature du problème étudié, l'utilisation directe des MOACO pour résoudre ce problème ne peut être envisagée. Cela s'explique par les raisons suivantes :

— Les deux chromosomes utilisés dans l'encodage de la solution n'exigent pas exactement l'exploration du même graphe, mais plutôt de deux graphes légèrement différents. En effet, alors que le premier est représenté par une exploration de l'attribution possible de tâches et de ressources aux postes de travail, le second est représenté par l'exploration de l'affectation possible de stocks aux postes de travail, indirectement liée au premier graphe
— L'affectation des stocks aux postes de travail nécessite une affectation complète des tâches et des ressources aux postes de travail

Pour y remédier, les MOACO ne peuvent pas être utilisés seuls pour ces deux chromosomes, et une approche d'hybridation est nécessaire. L'idée principale derrière l'hybridation proposée est de combiner plusieurs algorithmes pour exploiter leurs forces. Sachant que les algorithmes évolutionnaires obtiennent de bons résultats, une hybridation est proposée avec des procédures du MOACS. Plusieurs types d'hybridation sont proposés pour résoudre le problème, entre autres une hybridation des algorithmes évolutionnaires avec un recuit simulé. Les statistiques de Friedman obtenues pour tous les problèmes et les algorithmes avec différentes règles de dominances et considérant les indicateurs de qualité suivants : I_{HV}, I_{IGD}, I_ϵ et I_Δ ainsi que les $p-$values respectives sont affichées dans le Tableau A.12. En considérant $\chi^2_{0.05} = 11.1$ avec un niveau de confiance de 95% et 5 degrés de liberté, on peut conclure qu'il existe des différences significatives entre les formes d'hybridation pour tous les indicateurs de qualité sauf pour I_Δ.

Tableau A.12: Statistique de Friedman et p-value conformément à I_{HV}, I_{IGD}, I_ϵ, I_Δ et au temps de calcul

Indicators	Friedman statistic	Computed p-values
I_{HV}	291.243	0.000
I_{IGD}	221.310	0.000
I_ϵ	110.326	0.000
I_Δ	6.351	0.274
Time	829.249	0.000

Les rangs de Friedman obtenus pour chaque indicateur de qualité en considérant tous les

problèmes sont représentés dans le Tableau A.13. Ce tableau révèle que le SPEA2-LS est l'algorithme qui obtient le meilleur rang pour respectivement I_{HV}, I_{IGD} et I_ϵ. L'algorithme obtenant la meilleure dispersion est le SPEA2. En ce qui concerne le temps de calcul, l'algorithme qui converge le plus rapidement était le NSGA-II, suivi du SPEA2 et du SPEA2-LS. En ce qui concerne la famille d'algorithmes NSGA-II, on peut affirmer que, en général, I_{HV} est amélioré soit en appliquant l'hybridation par recuit simulé ou par l'algorithme d'optimisation des colonies de fourmis. On remarque également l'amélioration de I_ϵ lors de l'utilisation du NSGA-II-ACO-1 et du NSGA-II-ACO-2. La dégradation de la valeur de I_Δ est commune à toutes les formes hybrides. L'analyse des p-values montre que le SPEA2-LS est significativement meilleur que les autres algorithmes, excepté le SPEA2, pour I_{HV}, I_ϵ, I_{IGD}.

Tableau A.13: Rangs moyens retournés par le test non paramétrique de Friedman pour tous les problèmes

Algorithm	I_{HV}	I_{IGD}	I_ϵ	I_Δ	Time
NSGA-II	4.29	3.04	3.13	3.68	5.84
NSGA-II-LS	4.17	2.93	3.03	3.38	3.28
NSGA-II-ACO-1	3.99	2.85	3.18	3.49	1.89
NSGA-II-ACO-2	3.98	3.04	3.18	3.36	1.60
SPEA2	2.37	4.52	4.07	3.66	4.53
SPEA2-LS	2.20	4.61	4.41	3.44	3.86

De plus amples informations se trouvent dans le chapitre 6.

A.4 Application de l'approche holistique

L'outil d'aide à la décision développé a été utilisé dans deux cas industriels avec pour objectif de concevoir une ligne d'assemblage automatisée et manuelle.

A.4.1 Cas industriel 1

À partir de l'analyse de la chaîne d'assemblage automatisée et de l'identification de nouveaux procédés d'assemblage et ressources, plusieurs solutions ont été trouvées. Ces solutions sont présentées dans la Figure A.4. Cette figure montre les différences entre les concepts trouvés et ceux déjà planifiés par les ingénieurs de l'entreprise en question (en suivant une approche classique). Comme on peut le voir, les concepts trouvés par l'approche holistique dominent les trois concepts planifiés. Le concept choisi a donné la possibilité d'augmenter l'efficacité de 4 %. De plus, environ 17 % des positions de stocks tampon ont été modifiées et certaines ont été ajoutées.

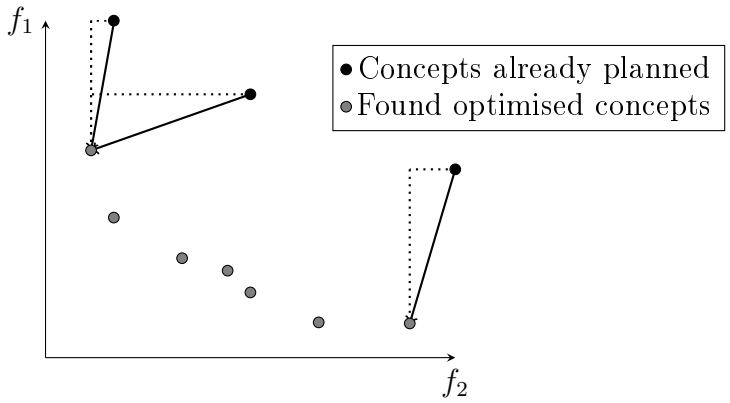

Figure A.4: Comparaison des résultats obtenus par l'approche holistique et ceux obtenus par l'approche classique

En plus de l'équilibrage de ligne, l'efficacité a également été augmentée de 3 % en modifiant la stratégie de retraitement.

A.4.2 Cas industriel 2

À partir de l'analyse de la chaîne d'assemblage manuelle et de l'identification de nouveaux designs produits et ressources, plusieurs solutions ont été trouvées. Les améliorations et détériorations obtenues lors de l'application de l'approche holistique se trouvent dans le Tableau A.14. Dans ce tableau, C_M représente les coûts de matériel, C_L les coûts de main-d'œuvre, C_{OH} les frais généreux, C_E les coûts liés aux équipements et C_B les coûts liés à la surface de production.

Tableau A.14: Amélioration/Détérioration des coûts après application de l'approche holistique

Coûts	Amélioration/Détérioration [%]
C_{M_1}	+29
C_{M_2}	-5
C_{M_3}	-1
C_{M_4}	+33
C_{M_Σ}	+3
C_L	+138
C_{OH}	+100
C_E	+11
C_B	+11
C_{Part}	117

A.4.3 Synthèse

La méthode holistique proposée a été appliquée dans deux cas industriels différents. Dans le premier cas, l'objectif était de concevoir une ligne d'assemblage automatisée avec des stocks tampon, dans le deuxième une ligne d'assemblage manuelle. Dans les deux cas, l'utilisation de la méthode a permis d'améliorer significativement les systèmes planifiés ou déjà en place.

A.5 Conclusion

Dans cette thèse, deux problèmes d'optimisation suivant une approche holistique ont été proposés.

A.5.1 Synthèse de la contribution

Cette thèse se compose de sept chapitres. Les premiers chapitres soulèvent le sujet étudié dans cette thèse. Une introduction générale est fournie, et les problèmes rencontrés dans le secteur industriel sont brièvement présentés. Dans le troisième chapitre, une vue d'ensemble sur des problèmes d'optimisation et des méthodes de résolution associées est proposée. De plus, un aperçu détaillé des modèles et des méthodes utilisés pour résoudre des sous-problèmes similaires est présenté. Cet aperçu permet d'identifier les inconvénients sur les modèles et les méthodes de résolutions actuels. Sur la base des inconvénients identifiés, deux nouveaux problèmes d'optimisation sont proposés. Pour résoudre le premier problème, plusieurs algorithmes d'optimisation sont comparés et les plus prometteurs sont combinés avec une recherche locale. De plus, l'influence des règles de dominance est également quantifiée. Dans le sixième chapitre, différentes formes d'hybridation sont proposées pour résoudre le second problème. Dans le chapitre sept, l'utilisation de l'approche holistique dans deux cas industriels est décrite.

Une liste de 34 algorithmes est présentée pour résoudre le premier problème. Ces algorithmes ont été comparés par rapport à quatre indicateurs de qualité et 50 problèmes. Cette comparaison est réalisée à travers une analyse non-paramétrique de Friedman. Lorsque tous les problèmes, indépendamment de leurs complexités, sont considérés, le NSGA-II et SPEA2 obtiennent - en moyenne - les meilleurs résultats quand on considère l'hypervolume couvert et la distance nécessaire pour translater le front de solutions obtenu de telle sorte qu'il domine le vrai front de Pareto. Si l'on considère la diversité des solutions et la métrique de distance générale inversée, le CHAC-1 et BIANT-1 ont obtenu les meilleurs résultats. Cepen-

dant, lorsqu'on considère la complexité des problèmes, on peut affirmer que le MOACS-1, MOACS-2, BIANT-1 et BIANT-2 sont plus performants que le reste des algorithmes pour des problèmes complexes. Dans un second temps, l'influence de différentes règles de dominance a été analysée. Le test de Friedman a montré que l'influence de ces règles de dominance est hétérogène et qu'il n'y a pas de différence significative entre elles. Cependant, l'application de la règle de dominance de Lorenz a permis d'améliorer significativement les performances du MOACS-2 pour un indicateur de qualité. Un test de Friedman a également été utilisé pour analyser l'influence d'une procédure de recherche locale sur le MOACS-2-L, SPEA2 et NSGA-II-L. Cette recherche locale a permis d'obtenir une amélioration significative pour le MOACS-2-L. Pour le second problème, différentes formes d'hybridation ont été proposées. Une étude statistique a montré que la combinaison entre un SPEA2 et un recuit simulé permet de surpasser les autres algorithmes.

Ainsi, les principales contributions de cette thèse sont les suivantes :

— Présentation de deux problèmes associés à la conception de lignes d'assemblage hybrides en considérant divers sous-problèmes à travers une approche holistique ;
— Élaboration d'un modèle de coût dont l'objectif est de traduire les interdépendances complexes entre la sélection des procédés d'assemblage, ressources, et l'équilibrage de ligne ;
— Étude empirique visant à comparer, selon plusieurs indicateurs de qualité, divers algorithmes multiobjectifs de nature différente ;
— Analyse de l'influence de règles de dominance et recherche locale sur divers algorithmes ;
— Combinaison de méthodes d'optimisation avec un modèle générique de simulation à événement discret pour le second problème.

A.5.2 Perspectives et travaux futurs

En ce qui concerne les perspectives, il pourrait être intéressant d'étendre les modèles proposés en intégrant des décisions stratégiques, telles que :

— Le nombre de produits sur la ligne d'assemblage et le nombre de lignes d'assemblage ;
— Make-or-Buy : une question intéressante est aussi généralement liée à la décision de Make-or-Buy, en tenant compte par exemple des problématiques capacitaires ou des coûts de revient ;
— La forme et la disposition des lignes : une approche intéressante serait également d'enrichir le travail actuel en considérant différentes formes et dispositions de la ligne.

En outre, pour rester aussi près que possible de la réalité, les modèles proposés pourraient

également être étendus comme suit :

— Considération des caractéristiques de la durée d'une tâche : alors que les temps de traitement déterministes et stochastiques ont été pris en compte, l'effet d'apprentissage, généralement non négligeable dans les chaînes d'assemblage, améliorerait les modèles proposés. De plus, compte tenu d'un ensemble de tâches assignées à une station, le temps de station peut dépendre de la séquence dans laquelle les tâches sont exécutées. Ainsi, il serait également intéressant de considérer le temps de traitement lié à la séquence d'exécution des tâches. Cela est particulièrement vrai lorsque les tâches sont effectuées manuellement.

— Considérer l'incertitude des informations ou des données : en raison du manque d'informations dans les premières phases de la conception de lignes d'assemblage, des problèmes peuvent survenir lorsque l'information est floue ou incertaine, rendant ainsi l'évaluation de solutions aux problèmes difficiles. Pour combler cette lacune et diminuer la sensibilité de l'approche proposée à toute information incertaine, des approches d'optimisation robustes pourraient être utilisées

De plus, il serait intéressant d'envisager des scénarios de demande futurs, dans lesquels les modèles proposés pourraient être étendus avec des aspects de rééquilibrage. Cela nécessiterait d'examiner les coûts associés au rééquilibrage de la chaîne d'assemblage en tenant compte des variations de la demande et nécessiterait l'utilisation d'un modèle de coût dynamique.

En ce qui concerne les opportunités sur les méthodes de résolution, il serait également intéressant d'analyser l'influence de différents processus d'évolution en considérant différentes méthodes de résolutions.

Enfin, il pourrait être intéressant d'effectuer également une analyse de sensibilité des différents paramètres sur la performance des algorithmes lors de la résolution de problèmes complexes et moins complexes.

En ce qui concerne la demande, il serait également intéressant de se concentrer davantage sur la conception du produit et d'essayer de restructurer l'approche proposée pour utiliser moins d'informations.

Appendix B

Further general information

Abstract

The present chapter presents further information about the state-of-the-art and namely (i) an explanation of the various resolution methods for a multi-objective optimisation, (ii) the complete problem characteristic extraction and resolution methods proposed in the last years in the field of ALBP, (iii) an example of the application of analytical and simulation models for the analysis of assembly lines, and (iv) further information about statistical comparison of stochastic optimisation algorithms.

B.1 Resolution methods for multi-objective problems

This section presents the various optimisation methods aiming at solving multi-objective problems.

B.1.1 Evolutionary Algorithms

EAs are optimisers based on Darwin's theory of evolution, where the fittest individuals survive and produce offspring to populate the next generation. A population $P(t) = \{X_1^t, ..., X_{PopSize}^t\}$ of $PopSize$ individuals is maintained, in which each individual X_i, $i = 1, ..., PopSize$, represents a solution to the problem under study and to which a fitness value is assigned, measuring how good an individual solution is. The operation of a particular EA is defined by a number of procedures or operators. Typically, the three major evolutionary operators can be identified, namely :(i) mutation, (ii) recombination and (iii) selection. The basic idea behind the evolutionary process is that, if only individuals, which meet certain selection criteria are allowed to reproduce and generate a new population $P(t+1)$, then the population will converge to those individuals that best meet the selection criteria.

The general process of MOEA is presented in the flowchart Figure B.1 and the specific features will be described below.

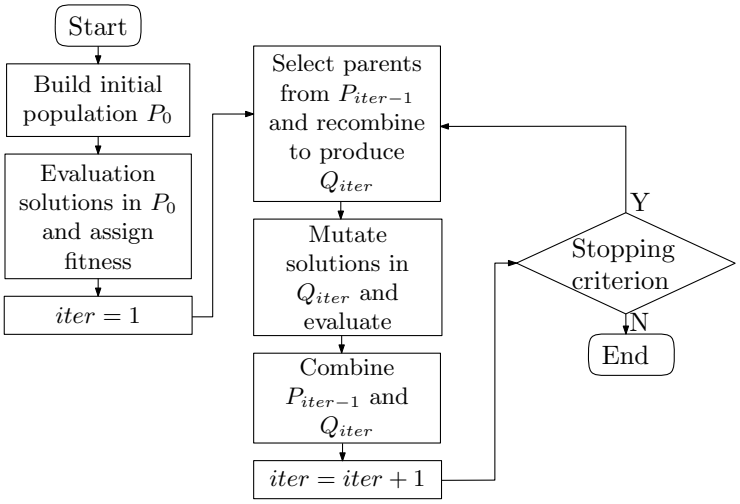

Figure B.1: Main steps of an evolutionary algorithm

During the evolution process, the objective functions are evaluated for every solution in the population, and to each individual is assigned a fitness value which drives the natural selection process [150] and represents the survival rate of this specific solution at the next generation. There are many methods to evaluate fitness and assign a real number to each

solution in the multiobjective case. Commonly used areq the Pareto dominance relation based fitness strategies. According to Zitzler *et al.* [454], these methods can be classified as follows: (i) dominance rank, representing the number of solutions in the population that dominate the solution under consideration, (ii) dominance count, representing the number of solutions in the population that are dominated by the solution under consideration, and (iii) dominance depth [105], representing the rank of the solution in the non-dominated sorted population, which is utilised by many successful algorithms, e.g. the Non-dominated Sorted Genetic Algorithm-II (NSGA-II). The dominance rank was first employed by Fonseca and Fleming [140]. Dominance depth and rank are successfully combined in the Strength Pareto Evolutionary Algorithm 2 (SPEA2) [455].

The parent selection or mating selection plays an important role in EAs and aims at distinguishing between individuals based on their quality to allow the best individuals to become the parents for the next generations. However, low-fitness individuals should also be given a small change to participate in the mating process. A standard tournament method, called Roulette Wheel Selection [101], achieves this by choosing the best individual from a group of T_{size} [1] individuals. This selection is done according to the probability of each individual to be selected, which is based on its current fitness value. The role of recombination is to generate new individuals from the selected parents, in preference such that the offspring contains the desirable features from both parents. This is achieved through crossover operations. Several crossover operations have been proposed in the literature, e.g. [189, 298, 204, 179]. The uniform crossover operator is known as one of the most effective crossovers in conventional genetic algorithms [364].

Once an offspring has been generated, another stochastic change, the mutation, is applied to enhance the diversity in the population and prevent the population to converge prematurely at local minima.

B.1.2 Swarm Intelligence Based Algorithms

As stated before, different optimisation methods are attached to swarm intelligence. The most famous algorithms will be detailed in the upcoming sections.

1. If the value of T_{size} is too large, only a small portion of the population will contribute to genetic diversity. Other selection mechanisms can be found in the literature, e.g. [19, 189].

B.1.2.1 Ant Colony Optimisation

ACO is a meta-heuristic search algorithm, which was first proposed by Dorigo *et al.* in the 1990s [121, 120]. Ant algorithms are inspired by the collective behaviour of ants on the survival of their colonies. While searching for food, they deposit on the ground a substance called pheromone, which helps other ants to follow the path leading to the food. The more ants follow the same path, the more it gets attractive for following ants. ACO is one of the most efficient meta-heuristic algorithms on combinatorial optimisation problem [305], and this is especially true if the problem has an inherently network structure [40]. Generally speaking, ACO algorithms can be classified into algorithms belonging to: (i) Ant System (AS) or (ii) Ant Colony System (ACS). All these algorithms follow two main parts:(i) solution construction and (ii) pheromone update and evaporation. In the former step, starting from the source node, ants select operations from a candidate list using a step-by-step decision policy, called transition rule, until reaching a complete solution. At each node, local information stored on the node itself or on its outgoing arcs is used in a stochastic way to decide which node to move next. An ant k uses both the attractiveness $\eta_{i,j}$, computed by some heuristics, which indicates the desirability of moving from node i to j, and the pheromone trail $\tau_{i,j}$, providing, out of experience, how proficient is has been to move from node i to j. Once reaching the destination node, the ant moves backwards to the source node. To avoid quick convergence of all ants toward a suboptimal path, the pheromone intensity is decreased during the evolution of the algorithm. The algorithms belonging to the class of AS are characterised by a pheromone update once all ants have completed their solutions and by a constant pheromone trails decrease. The algorithms belonging to the class of ACS are using a different transition rule, called the pseudo-random proportional rule. Compared to AS, at each step, an ant can choose randomly between exploitation and exploration.

B.1.2.2 Particle Swarm Optimisation

The PSO, initially proposed by Eberhart and Kennedy [124], is a population-based search algorithm based on the simulation of the social behaviour of birds within a flock. Similarly to EA, PSO exploits a population, called a swarm, of potential solutions, called particles, which are modified statistically at each iteration of the algorithm. One major difference with EA is the manipulation of the swarm as a cooperative model rather than a competitive one [315].

Each particle i is characterised by a position X_i^t, a velocity V_i^t and a vector pB_i^t that serves as

a memory of the best position in terms of fitness that the particle has, so far, encountered, where t represents the current iteration. Particles interact by communicating their best discovered positions to other particles within their neighbourhood. Particles move in the search space by stochastically updating their velocity and position, attached by their own best position pB_i^t as well as their neighbourhoods best position gB_i^t, as follows:

$$\begin{aligned} V_i^{t+1} &= w \cdot V_i^t + c_1 r_1 \cdot (pB_i^t - X_i^t) + c_2 r_2 \cdot (gB_i^t - X_i^t) \\ X_i^{t+1} &= X_i^t + V_i^{t+1} \end{aligned} \tag{B.1}$$

where w represents a positive parameter called inertia weight, c_1 and c_2 are two positive constraints called cognitive and social parameter that controls the magnitude of stochastic attraction towards pB_i^t and gB_i^t. r_1 and r_2 are realisations of two independent random variables that assume the uniform distribution in range $(0, 1)$. The best position of each particle is updated at each iteration by setting:

$$pB_i^t = X_i^t, \text{if } f(X_i^t) \preceq f(pB_i^t) \tag{B.2}$$

The inertia weight w plays a key role in the process of providing a good balance between exploration and exploitation. Bansal *et al.* [23] and Nickabadi *et al.* [284] proposed a review of inertia weight strategies [2].

One major difference between the PSO and Multi-Objective Particle Swarm Optimisation (MOPSO) is the number of suitable guide particles gB_i^t that can be chosen at an iteration t. Indeed, in MOP, a set of optimal particles are suitable candidates for the selection process of the guide particle. Several strategies have been developed in the past. The random strategy chooses an archive member randomly. However, if the chosen best solution is far from the particle, erratic oscillations could be caused, leading in turn to a chaotic search behaviour. The Sigma method, introduced by Mostaghim and Teich [275], involves choosing the guide particle $\vec{p_g}$ based on the similarity of the angular position in the objective space of an archive member and a particle in the swarm. A σ value is assigned to all particles in the archive and swarm, representing the gradient of the line connecting the location of the particle and the origin of the objective space. For each particle $i = 1, ..., N$, the particle from the archive with the closest σ is selected. For a 2-dimensional objective space, σ_i is defined as:

$$\sigma_i = \frac{f_1^2 - f_2^2}{f_1^2 + f_2^2} \tag{B.3}$$

However, a specific particle i may select the same global best for many iterations, which

2. In their review, the inertia weights are classified into three categories. In the first class, strategies using a constant and randomly generated inertia weight can be found. In the second class, the inertia weight is defined as a function of time or iteration number and the situation of the particles in the search space is not taken into consideration. The third class represents inertia weights using a feedback parameter to monitor the state of the algorithm and adjust the value of the inertia weight

would engender a premature convergence to a local optimum. Gong *et al.* [157] proposed a similar approach to the Sigma method. The selection of the best particle is based on the minimum particle angle δ_i^{min} of a particle in the swarm and an archive member. For the location of the minimum particle angle, particle angles $\delta_{i,j}$ between a particle i in the swarm and all the j archive members are computed. Considering i and j being two particles in the swarm, $\delta_{i,j}$ is calculated as follows:

$$\delta_{i,j} = cos^{-1} \frac{f(x_i) \cdot f(x_j)}{\|f(x_i)\|} \cdot \|f(x_j)\| \tag{B.4}$$

Alvarez-Benitez *et al.* [7] present three strategies for selecting the global guide: (i) rounds, a strategy which promotes diversity and assigns as a guide the particle in the archive that dominates the fewest x_n in the population. The guide is removed from consideration until all other particles in the swarm have been chosen as a guide. The random strategy chooses one particle randomly. The last strategy is a combination of the two previous ones, in which a leader is selected based on the probability that it dominates least particles. Qiu *et al.* [328] present a strategy based on a k-means algorithm and a proportional distribution approach. In their approach, the set of non-dominated solutions are clustered according to k clusters and the particle with the least distance to the centroid of its cluster is defined as a representative for this given cluster. The representative particle is chosen according to its probability represented by the number of solutions. The strip strategy [405] is based on the use of stripes uniformly distributed, to which belong non-dominated solutions. A stripe is randomly chosen and its leader represents the best swarm.

Some of these strategies are represented in Figure B.2. The sigma method is represented in Figure B.2-a, the minimum particle angle in Figure B.2-b, the stripe method in Figure B.2-c and the random selection in Figure B.2-d.

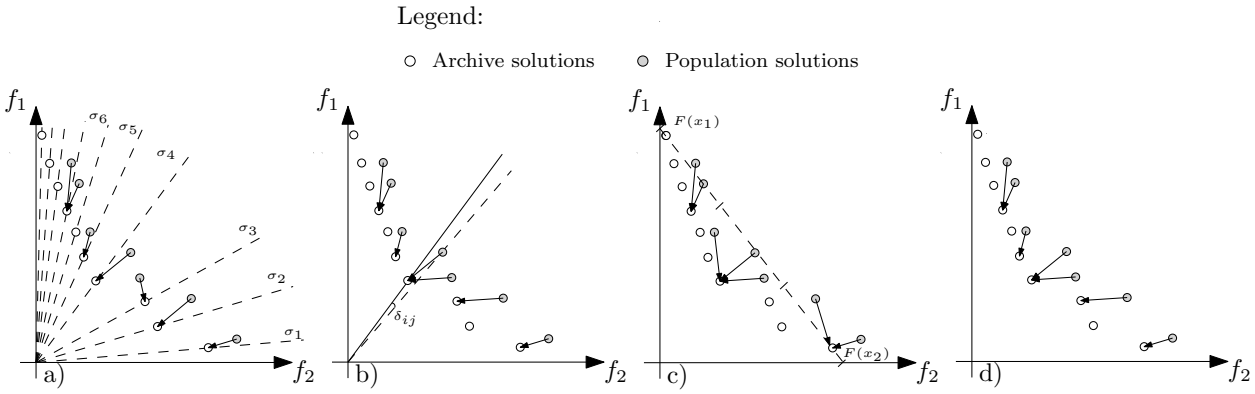

Figure B.2: Example of the selection processes for the best particle $\vec{p_g}$ in a Multi-Objective Particle Swarm Optimisation

B.1.2.3 Bat Algorithm

The BA, initially proposed by Yang [421], is based on bat's behaviour, which use echolocation to find their prey and discriminate different types of insects, even in complete darkness, by varying pulse rates of emission and loudness [351]. By emitting calls out to their environment and listening to the echoes that bounce back, they can identify the location of other objects and their position by following the delay of the returning sounds. These echolocation pulses are characterised by: (i) pulse frequency, which varies depending on the position of the target, (ii) pulse emission rate, which corresponds to the number of emitted emissions per seconds, (iii) and the loudness or intensity, which characterises the emitted pulse.

In the BA, a bat i and its respective position X_i^0, velocity V_i^0, and frequency F_i are initialised. The movement of the virtual bats is given by updating their frequency F_i, their velocity V_i^t using following equations:

$$F_i = F_{min} + (F_{max} - F_{min}) \cdot \beta \tag{B.5}$$

$$V_i^t = V_i^{t-1} + (X_i^{t-1} - gB_i^t) \cdot F_i \tag{B.6}$$

$$X_i^t = X_i^{t-1} + V_i^t \tag{B.7}$$

where $\beta \in [0, 1]$ represents a random generated vector from a uniform distribution. Secondly, new bats will be generated using a procedure that employs two probabilistic generation schemes referred to as random flying and local search [171]. While the former remote position in the search space, the latter enables a more exploitable search, where bats are perturbed in the close vicinity of its current solution to browse neighbours. The chance of generating a new micro-bat using either random flying or local search is respectively provided by R_i and $1 - R_i$, which represents the pulse rate of the i-th bat. Once generated, the objective function values are evaluated for each bat candidates. After the evaluation, the echolocation parameters are updated. A bat is only allowed to update its echolocation parameters if: (i) it produces a better solution and (ii) if a uniform random number $u \in [0, 1]$ is smaller than its loudness A_i. If it is the case, its loudness A_i and echolocation R_i will be updated using following equations:

$$A_i^{t+1} = \alpha_B \cdot A_i^t \tag{B.8}$$

$$R_i^{t+1} = R_i^0 \cdot [1 - e^{-\gamma t}] \tag{B.9}$$

where, $0 < \alpha_B < 1$ and $\gamma > 0$ are constants and represent the adaptation parameters for loudness and pulse rate respectively. In order to simplify the implementation of the algorithm, some authors e.g. [299] fix $\alpha_B = \gamma$.

Examples of the application of the BA to MOP, defined as Multi-Objective Bat Algorithm

(MOBA) can be found in following works: [419, 418, 129]

B.1.2.4 Cuckoo Search Algorithm

The Cuckoo Search Algorithm (CSA), proposed by Yang and Deb [426] is one of the latest nature-inspire metaheuristics. The CSA is inspired by the Cuckoo behaviour, A feature of cuckoos is that, to increase the probability of having new cuckoo, some species lay their eggs in the nests of other species to let host birds hatch and brood young cuckoo chicks. The CSA follows idea rules: (i) each cuckoo lays one egg at a time and selects a nest randomly, (ii) the best nest with the highest quality egg can pass onto the new generations, (iii) the number of host nests is fixed and the egg laid by a cuckoo can be discovered by the host bird with a probability of $p_a \in [0, 1]$.

When generating a new solution X_i^{t+1}, a Lévy Flight [3] is used, as follows:

$$X_i^{t+1} = X_i^t + \alpha \oplus \textit{Lévy}(\lambda) \tag{B.10}$$

where α ($\alpha > 0$) is the step size and is generally associated with the scales of the problem to be solved. The Lévy flight essentially provides a random walk and follows the Lévy distribution:

$$\textit{Lévy}(s, \lambda) \sim s^{-\lambda}, 1 \geq \lambda \geq 3 \tag{B.11}$$

which has an infinite variance with an infinite mean.

Examples of the application of the CSA to MOP, defined as Cuckoo Search Algorithm (MOCSA) can be found in following works: [423, 69].

B.1.2.5 Flower Pollination Algorithm

The FPA was introduced by Yang [422], and is inspired by the flow of pollination process of flowering plants. The pollination process can occur through two forms, (i) the pollen is transmitted by pollinators, or (ii) the pollination is assisted by wind and water [276]. The FPA uses four rules [422, 425]:

— The former pollination form can be considered as a process of global pollination, and pollen-carrying pollinators move in a way that obeys Lévy flights
— The second pollination case can be considered as a local pollination
— Pollinators such as insects can develop flower constancy, which is equivalent to a reproduction probability that is proportional to the similarity of two flowers involved

3. A Lévy Flight is a random walk using a step-length with a probability distribution that is heavy-tailed. More information can be found in following works: [71]

— The interaction or switching of local pollination and global pollination can be controlled by a switch probability $p \in [0, 1]$, slightly biased towards local pollination

The global pollination step, as mentioned earlier, is represented as follows:

$$X_i^{t+1} = X_i^t + L(X_i^t - gB_i^t) \tag{B.12}$$

where x_i^{t+1} is the pollen i and gB_i^t the best solution found so far. The parameter L represents the power of pollination, which is the step size.

The local pollination is represented as follows:

$$X_i^{t+1} = X_i^t + \epsilon(X_j^t - X_k^t) \tag{B.13}$$

where X_j^t and X_k^t is the pollen from the same type. ϵ enables a random step by providing a random value following a uniform distribution from 0 to 1. FPA has been extended to MOP by using a weighted sum to combine all multiple objectives into a composite single objective [425].

B.1.2.6 Bee Colony Algorithm

In the ABC, initially proposed by Karaboga and Basturk [202], each solution is called a food source and its fitness the nectar amount. The ABC contains three groups of bees: (i) the employed bees, which are sent to food sources and try to improve them by using neighbour information, (ii) onlookers, which choose one of these food sources based on the quality of food sources shared by employed bees, and try to improve them, (iii) scout bees, that find food sources that have not been optimised in a limited number of cycles so as to reinitialise them in order to get rid of poor solutions [446]. The number of employed bees or the onlooker bees is equal to the number of solutions in the population.

Let $X_i = \{X_{i,1}, X_{i,2}, ..., X_{i,n}\}$ represent the i-th solution in the population. Each solution is generated as follows:

$$X_{i,j} = LB_j + r(UB_j - LB_j) \tag{B.14}$$

where $i = 1, ..., SN$ and $j = 1, ..., n$; $r \in [0, 1]$ is a uniform random number; LB_j and UB_j are the lower and upper bounds for the dimension j. A new solution $Y_i = \{Y_{i,1}, Y_{i,2}, ..., Y_{i,n}\}$ is generated out of the neighbourhood of old solutions as follows:

$$Y_{i,j} = X_{i,j} + \phi(X_{i,j} - X_{k,j}) \tag{B.15}$$

where $k = 1, ..., SN$ and $j = 1, ..., n$ are randomly chosen indexes. k is different from i and ϕ is a random number between $[-1, 1]$. After having produced the new solution, it will be evaluated and compared to the old one. If the objective fitness of the new one is

better than the old one, the new solution will be accepted, otherwise, the old solution will be kept. When all employed bees have finished this process, an onlooker bee can obtain the information of the food sources from all employed bees and choose a food source depending on the probability value associated with that food source, using the following expression:

$$p_i = \frac{fitness_i}{\max_{i=1}^{PopSize}(fitness_i)} \tag{B.16}$$

where the $fitness_i$ is the fitness value of the solution i. The onlooker bee produces a new source in the selected food source site by using ((B.15)). Similar to the employed bees, the new source will be evaluated and compared to the primary food solution. If the new source has a better nectar amount that the primary food source, the new source will be accepted. After all onlookers have finished their process, the sources are checked to see if they will be abandoned or not. Every time a food source does not improve through determined number of the trails, then the food source is abandoned by its employed bee and then it becomes a scout.

B.2 Assembly Line Balancing Problem

This section presents the complete problem characteristic extraction and resolution methods proposed in the literature in the last years in the field of ALBP.

Table B.1: Extraction of problem characteristics and resolution methods proposed in the last years in the ALBP field

Authors	α_1	α_2	α_3	α_4	α_5	α_6	β_1	β_2	β_3	β_4	β_5	β_6	γ	Resolution method
[285]						pa				equip			Co	DP
[320]									pstat				Co	B&B, Heuristic
[321]						pa							Co	B&B
[56]						pa			pstat	equip			m	B&B
[57]						pa				equip			Co	B&B
[55]	Mix						unpac						TP	Heuristic
[66]						pa^{sg}							m	Heuristic
[62]						pa^{sg}							m	Solver
[64]						pa^{sg}							m	Solver
[65]						pa^{sg}							m	Heuristic
[360]						pa^{sg}							m	B&B
[36]					cum								m, C, A	ACO
[416]	Mix												HSI, VSI, BD	MOACO
[4]	Mix				inc; link				pstat				C(m, VSI, HSI)	hGA
[206]	Mix							u	ptask				Co	GA
[5]	Mix			Δ_{dir}	inc; link								C(m, VSI, HSI)	hACO-GA
[439]	Mix					pa				equip			CT, HSI, Co	MOGA

Continued on next page

Table B.1 – *Continued from previous page*

Authors	α_1	α_2	α_3	α_4	α_5	α_6	β_1	β_2	β_3	β_4	β_5	β_6	γ	Resolution method
[257]	Mix				inc; link								m, CT, HSI, VSI	PESA, NPGA, NPGA-II, MOGA, NSGA, PAES
[256]	Mix							u	pstat				C(WIT, WLE), Co, Others	SA
[214]					cum					equip			m	B&B
[215]					fix, type				pwork				m	GA
[239]						pa				equip			CT	GA
[318]						pa				equip			Co	B&B
[330]	Mix				type			u	pwork				CT, m	GA
[331]	Mix			Δ_{dir}	cum	pa				res			CT; Co	DMOPSO, NSGA-II
[300]					cum								C(m, ER)	Heuristic
[2, 3]	Mix			Δ_{ind}	inc; link				pstat				m	Solver,
[221]					inc; link				ptask				HSI; CT	MCHBA
[332]	Mix								pline				C(CT_1, CT_2)	hGA, GA, SA
[444]	Mix		t^{sto}					u					HSI	Heuristic

Continued on next page

Table B.1 – *Continued from previous page*

Authors	α_1	α_2	α_3	α_4	α_5	α_6	β_1	β_2	β_3	β_4	β_5	β_6	γ	Resolution method
[393]					type, link, fix				pstat				m	Solver
[213]						pa			pwork	equip			Co	Solver
[169]			t^{sto}	Δ_{dir}									CT; Co; HSI	hMOPSO
[168]			t^{dy}	Δ_{dir}									CT; Co; HSI	Solver
[387]			t^{dy}	Δ_{ind}								buffer	m	Heuristic
[394]			t^{sto}										TP, HSI, BS	-
[384]	Mix		t^{sto}						ptask			buffer	Normalized Design Cost	GA
[348]	Mix											seq	VSI; HSI; FT	MOABC, NSGA-II
[397]			t^{sto}				unpac						m	Heuristic
[374]				Δ_{ind}	cum, inc							mat	Co	Heuristic
[335]					cum							risk of posture	C(HSI, IT, ARP)	GA
[78]					cum								A, m	NSGA-II
[47]						pa				equip			CT	Beam Search
[329]	Mix							u			Δt_{unp}		C(m, HSI)	GA
[344]									pwork				C(LE, W, HSI)	SA

Continued on next page

Table B.1 – *Continued from previous page*

Authors	α_1	α_2	α_3	α_4	α_5	α_6	β_1	β_2	β_3	β_4	β_5	β_6	γ	Resolution method
[277]					cum								WRI	Solver
[211]													CT	Heuristics, Petri Nets
[391]					inc	pa				equip			CT, Co	hMOGA
[134]									pwork				C(m, W)	ACO
[445]													CT	ACO
[273]						pa				equip			CT	Heuristic
[305]									pline				C(LE, IT)	MCACO
[381]				Δ_{dir}	inc; link				pwork				LE	BA
[428]				Δ_{dir}									CT	hGA
[306]					inc; link				pwork				C(m, HSI)	BC
[343]					type				pwork				Co	SA
[432]			t^{dy}										E	GA
[37]					cum								m	DP
[347]								u					m	ACO
[429]						pa				equip			CT, Co	MOES
[390]					cum	pa				equip			CT, Co	MOGA
[31]												energy expenditure	C(SI, ESI), C(MMSE, MMST)	-

Continued on next page

Table B.1 – *Continued from previous page*

Authors	α_1	α_2	α_3	α_4	α_5	α_6	β_1	β_2	β_3	β_4	β_5	β_6	γ	Resolution method
[349]			t^{sto}										CT, Pr, HSI	MOABC
[441]													m	Solver
[39]								u,					m	ACO
[317]						pa				equip			C(m, Co)	B&B
[227]	Mix				inc; link; type				pline, pstat				C(m, LL)	ABACO
[226]	Mix				inc; link; type				pline, pstat				C(IT, m, LL)	ABACO
[309]									pstat				Co	Heuristic+Exact method
[82]					cum								M, A	MOACO
[336]	Mix					pa				equip			CT, Co	ICA
[404]						pa				equip			CT	B&B
[365]													M	B&B
[296]						pa				equip			Co	B&B
[322]						pa				equip			CT	VNS
[79]					cum								m, A	NSGA-II, MACS
[434]					cum			u			Δt_{unp}		Co, Others	hACO
[76]							unpac						m	TS
[99]						pa				equip			E	ACO, PSO, GA
[440]			t^{sto}										CT, Co	hMOEA

Continued on next page

Table B.1 – *Continued from previous page*

Authors	α_1	α_2	α_3	α_4	α_5	α_6	β_1	β_2	β_3	β_4	β_5	β_6	γ	Resolution method
[403]													m	B&B
[86]									pwork				M, W, WRI, HSI	DMOPSO
[75]						pa				res			HSI	GGA
[200]	Mix								ptask				C(m, CT, Co)	GP
[61]			t^{sto}						pstat				VSI, Co	MOSA+TS
[308]					inc; link; type				pwork				C(LE, SI)	TS
[133]	Mix								pline				CT	TS
[236]					type				pwork				CT	VNS
[80]					cum								A; m	GRASP

B.3 Buffer Allocation Problem

This section presents examples of the application of Markov chains or discrete event simulation for the evaluative procedure of the resolution methods for the BAP.

B.3.1 Example of the application of Markov chains

Assuming a transition rate of λ_i to move from the operating state to the down state, and μ_i from down state to operating state, the Markov chain representation for an isolated unreliable machine shown in Figure B.3 can be used. Thus, as stated by Gershwin [152], when $t \longrightarrow \infty$, the probability that a machine is either down or in operating state can be defined as follows:

$$\begin{aligned} P_i(Down) &= \frac{\lambda_i}{\mu_i + \lambda_i} \\ P_i(Up) &= \frac{\mu_i}{\mu_i + \lambda_i} \end{aligned} \tag{B.17}$$

The efficiency of M_i can be calculated as follows:

$$e_i = \frac{P_i(Up)}{P_i(Up) + P_i(Down)} = \frac{\mu_i}{\mu_i + \lambda_i} \tag{B.18}$$

and the production rate as follows:

$$q_i = \mu_i \cdot e_i \tag{B.19}$$

The balance equation is given as follows:

$$P_i(Down)\mu_i = P_i(Up)\lambda_i \tag{B.20}$$

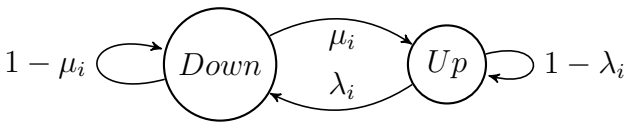

Figure B.3: Transition diagram of a Markov chain for an unreliable machine in isolation

However, unlike an isolated station, a station operating in an assembly line has a third state that is due to starvation or blockage phenomena. Indeed, due to the effects of machine breakdowns on up and downstream and the limited buffer capacity, a given station M_i can be in a forced idle time. Since the station M_i can be in three different states (down, operating and idle), the efficiency of a machine M_i when it operates in a flow line is given by:

$$e_i = \frac{P_i(Operating)}{P_i(Up) + P_i(Idle) + P_i(Down)} \tag{B.21}$$

The Markov chain representation for an unreliable machine in a flow line is represented in Figure B.4. Taking into consideration that a machine M_i cannot be both in idle and operating time, the probability of being up is given as follows:

$$P_i(Up) = P_i(Operating \cup Idle) = P_i(Operating) + P_i(Idle) \tag{B.22}$$

thus, the efficiency is given by:

$$P_i(Operating) = \frac{P_i(Up) - P_i(Idle)}{P_i(Up) + P_i(Down)} \tag{B.23}$$

Using $P_i(Operating)\lambda_i = P_i(Down)\mu_i$ and the propriety of the transition probabilities

$$\begin{aligned}
&P_i(Operating) + P_i(Down) + P_i(Idle) = 1 \\
\Leftrightarrow &P_i(Operating) + \frac{\lambda_i}{\mu_i} P_i(Operating) + P_i(Idle) = 1 \\
\Leftrightarrow &P_i(Operating)(1 + \frac{\lambda_i}{\mu_i} P) = 1 - P_i(Idle) \\
\Leftrightarrow &P_i(Operating)(\frac{\mu_i + \lambda_i}{\mu_i} P) = 1 - P_i(Idle) \\
\Leftrightarrow &P_i(Operating) = e_i(1 - P_i(Idle))
\end{aligned} \tag{B.24}$$

The previous equation shows the difference between the efficiency of a station M_i in isolation and in an assembly line. The throughput of a specific station M_i is given by:

$$TR = \mu_i \cdot P_i(Operating) = \mu_i \cdot e_i(1 - P_i(Idle)) \tag{B.25}$$

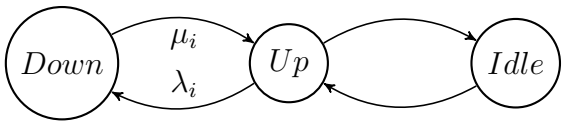

Figure B.4: Transition diagram of a Markov chain for an unreliable machine in a flow line

B.3.2 Example of the application of discrete event simulation

Taking the example provided in Figure 3.16, in which 3 workstations are separated by two finite buffers, the events modifying the state of the system are the arrival and departure of workpieces at/from workstations. The various states of the entities of the associated model are represented in Figure B.5.

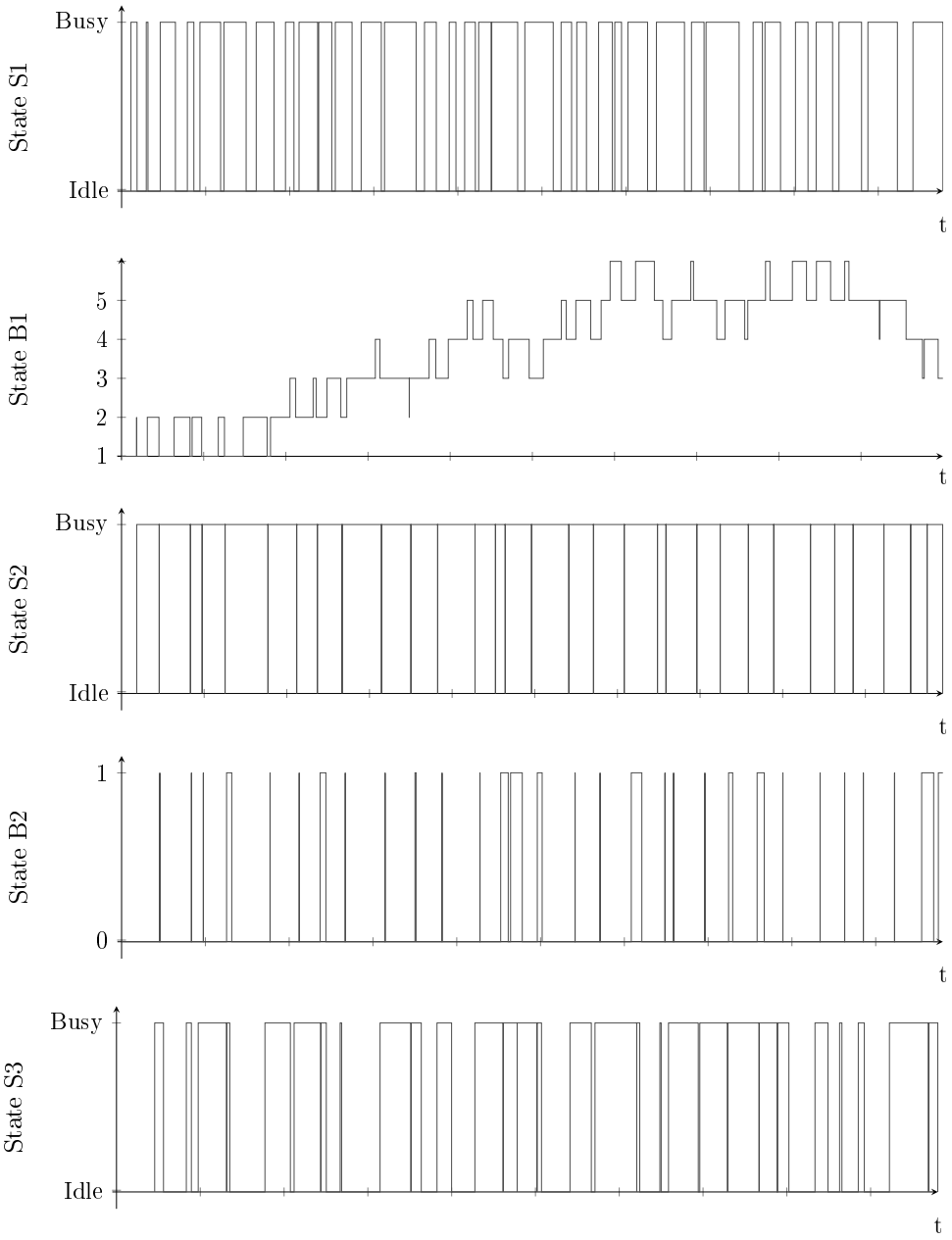

Figure B.5: Simulation model trajectory of an assembly system with 3 workstations and 2 finite buffers

B.4 Statistical comparison of stochastic optimisation algorithms

As seen in Chapter 3, many stochastic optimisation algorithms have been developed recently. When it comes to measuring the performance of an algorithm, it has to be decided if whether it is better than other ones. Usually, researchers use hypothesis testing, also called significance testing, which is a method of statistical inference that can be used for testing

a hypothesis about the relationship between two or more populations. In the first step, two hypotheses are defined. The null hypothesis, H_0 and the one opposite H_1 respectively state that there is or no difference/effect between two sample of data. In the second step, an appropriate test statistic is selected, which reduces the data-set to one value that can be used to perform the hypothesis test. In a third step, the level of significance α (also called significance level), which represents the probability threshold below which the null hypothesis will be rejected is computed. In the last step, a decision about whether the null hypothesis is rejected or not is taken. This decision can be based on two approaches, (i) the critical value approach or (ii) the p-value approach. In the former one, critical values define regions where the test statistic is unlikely to tend to H_1 if H_0 is true. In the second one, the p-value is calculated, which represents the probability of observing a more extreme test statistic in the direction of H_1. H_0 is rejected if the p.value is less than the selected significance level.

In order to perform a statistical comparison of stochastic optimisation algorithms, parametric and nonparametric statistical tests can be applied. In the former case, the application of parametric tests require some properties, such as: (i) independency, (ii) normality, (iii) and homoscedasticity of the variances of the data [287]. While the first one is always true, the second condition needs to be verified through e.g. a Kolmogorov-Smirnov, Shapiro-Wilk, D'Agostino-Pearson. These tests can verifiy if the data-sample follow a normal or Gaussian distribution. The validity of this condition can also be verified by graphical representation through a histogram representation and a Q-Q plot. The Q-Q plot is a probability plot, whose aim is to compare two probability distributions. If the two distributions are similar, than the points in the Q-Q plot will be approximately lie on the line. An example of a histogram and Q-Q plot is shown in Figure B.6. As it can be seen in this figure, it seems that the data sample, representing the achieved I_{HV}, does not necessarily follow a normal distribution. The same conclusion can be done when the Shapiro-Wilk test is applied, as shown in Table B.2.

Table B.2: Test of normality using the Shapiro-Wilk Test

Problem Instance	DMOBAT-3	DMOABC	DMOCSA-2-2	DMOFPA-1	DMOPSO-1
Arc111-1	0.023	0.632	0.408	0.933	0.341

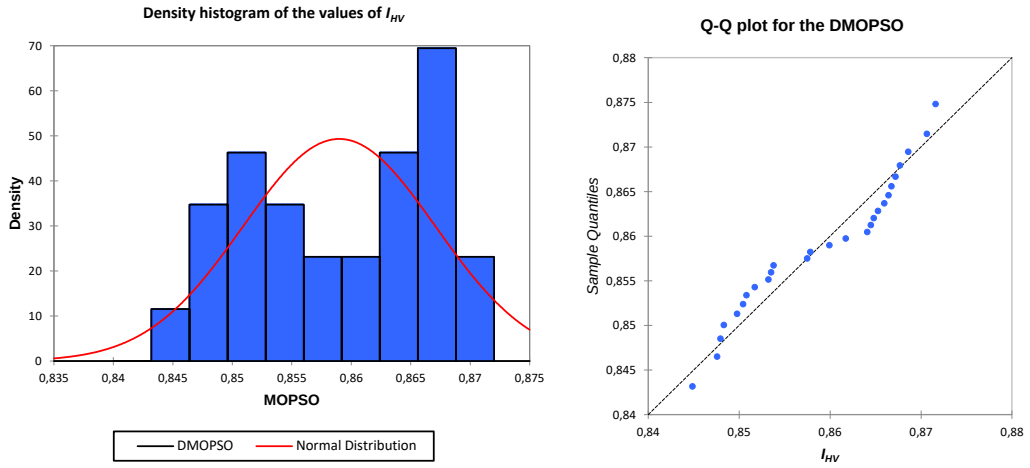

(a) Density Histogram *(b)* Q-Q Plot

Figure B.6: Graphical representation of the density function of I_{HV} and Q-Q plot obtained by the DMOPSO

Table B.3 shows the p-values from the Levene's Test in order to verify the homoscedasticity based on the average means obtained by the various algorithms for different metrics and problem instances. In order to ease the results, p-values less than the signifiance level are marked gray. This indicates that at least one variance of a specific algorithm is different from the other ones.

Table B.3: Test of homoscedasticity using the Levene's Test for an algorithm of Chapter 4

Problem Instance	I_{HV}	I_{IGD}	I_ϵ	I_Δ	Time
Arc111-1	0.037	0.049	0.000	0.078	0.070
Buxey-2	0.234	0.992	0.000	0.242	0.000
Gunther-2	0.010	0.009	0.000	0.310	0.906
Jackson-2	0.000	0.000	0.000	0.000	0.000
Kilbrid-3	0.000	0.036	0.000	0.637	0.000
Mukherje-3	0.612	0.135	0.000	0.217	0.000
Roszieg-4	0.000	0.000	0.000	0.000	0.000
Sawyer-4	0.000	0.000	0.000	0.000	0.000

Since not all the previous conditions are met for all quality indicators, algorithms and problem instances, parametric statistic test cannot be used. When parametric test cannot be properly applied to the data sample, for which mean and standard deviation are improper and misleading, nonparametric tests can be applied. The difference between parametric and nonparametric tests is that, the latter does not use the values of observations, but rather use rank tests involving ranking parametric data from lowest to highest [147]. Nonparametric tests, which do not require the probability distribution to be known, allow to determine if whether there: (i) is a relationship among two data samples, (ii) two data samples are

independent, (iii) there are significant differences among them. When it comes to comparing various algorithms, these tests can be classified into [110]:

— Pairwise comparisons (P), which allows to compare two algorithms over multiple cases of problems
— Multiple comparisons (1xN) with a control algorithm.
— Multiple comparisons (NxN)among all algorithms, which aims at detecting differences considering the global set of algorithms.

Table B.4 describes the use of some nonparametric tests and the type of comparisons made with them.

Table B.4: Differences between nonparametric statistical tests [287]

Statistical Test	Purpose	Type of comparison
Wilkcoxon signed-rank test	Tests if two samples are representing two different populations	P
U test	Defines whether a rate of success is really better than another	P
Multiple sign test	Serves as a filter to remove samples that are easily distinguishable as worse than the control method	1xN
Contrast Estimation test	Calculates the estimation of the difference among the performance of two algorithms	1xN
Friedman test	This test considers that all problems have equal importance	1xN,NxN
Friedman aligned ranks test	Makes comparisons between performances of algorithms as a single whole, without considering the interrelationships that exist between the sets of the complete test	1xN
Quade test	Defines whether the differences between the observation and recorded data are significantly larger or not	1xN

Appendix C

Detailed Analysis and Results of Chapter 4

Abstract

The present chapter presents a synthesis of the various analyses of Chapter 4, and (i) the true or reference Pareto front of the various problems, (ii) the parameter settings of the various optimisers, (iii) the values of the various quality indicators obtained by each optimisers for each problem instance, and (iv) the detailed values of the Friedman's test.

C.1 True and Reference Pareto front of the various problems

This section presents the true or reference Pareto front of some problem instance.

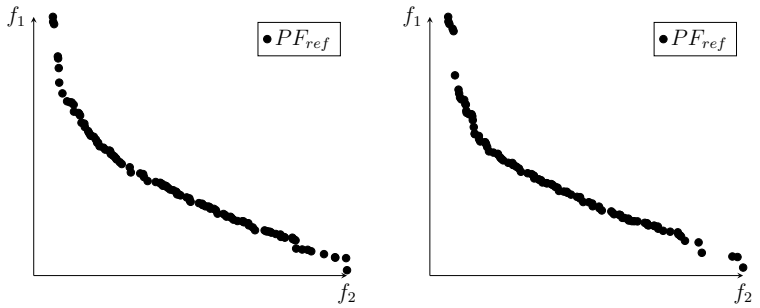

(a) Arc111-3 *(b)* Arc111-5

Figure C.1: Reference Pareto front for the Arc111 Problem

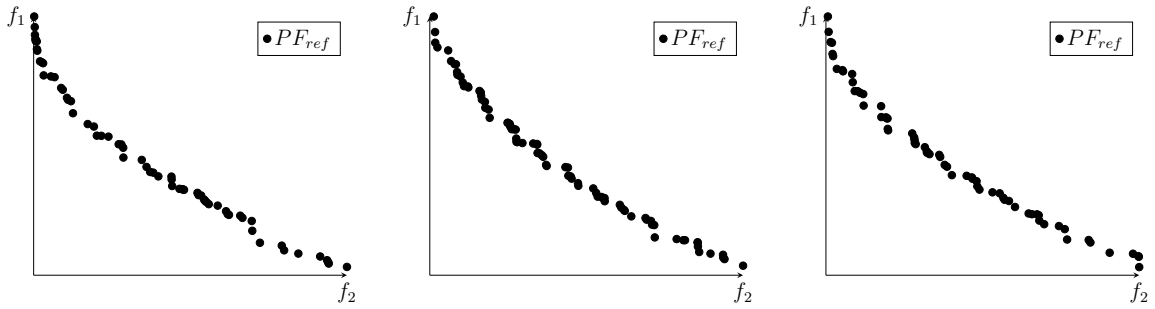

(a) Buxey-2 *(b)* Buxey-4 *(c)* Buxey-5

Figure C.2: Reference Pareto front for the Buxey Problem

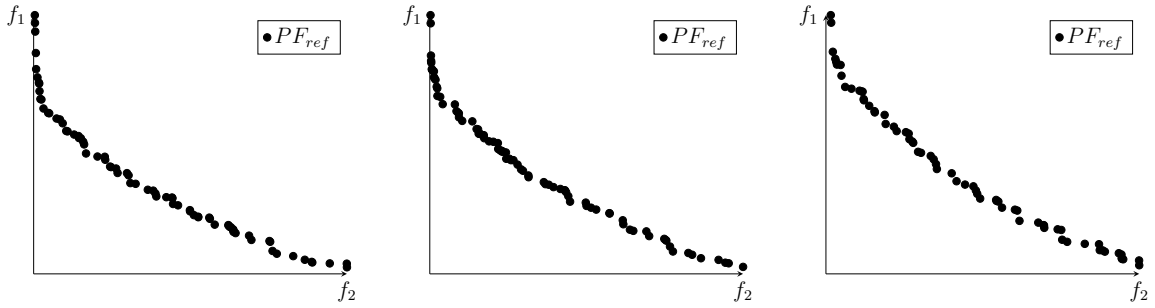

(a) Gunther-3 *(b)* Gunther-4 *(c)* Gunther-5

Figure C.3: Reference Pareto front for the Gunther Problem

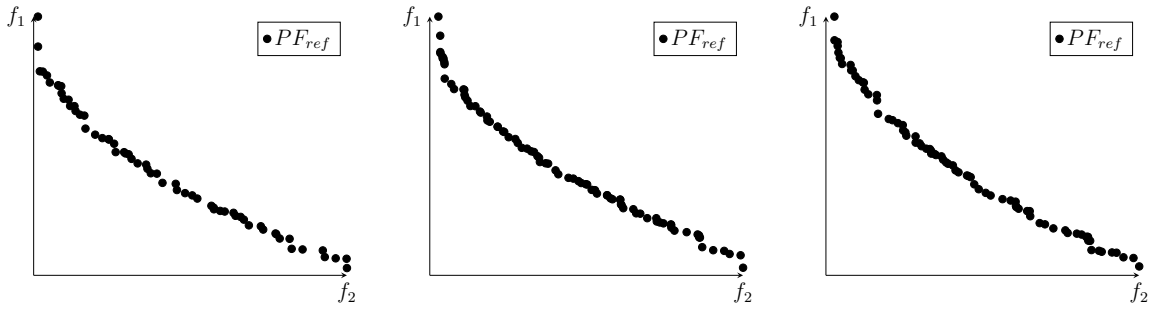

(a) Hahn-1 *(b)* Hahn-3 *(c)* Hahn-5

Figure C.4: Reference Pareto front for the Hahn problems

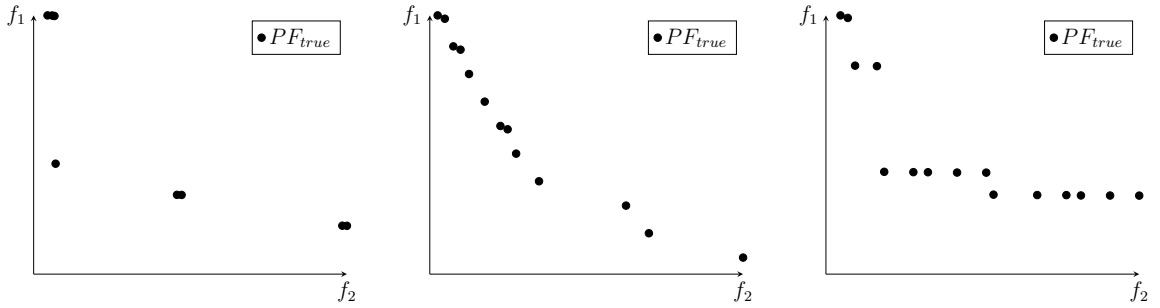

(a) Jackson-2 *(b)* Jackson-4 *(c)* Jackson-5

Figure C.5: True Pareto front for the Jackson problems

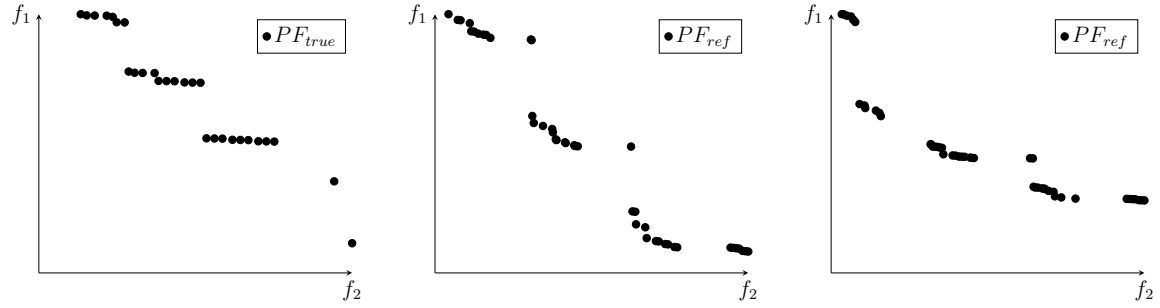

(a) Kilbrid-1 *(b)* Kilbrid-3 *(c)* Kilbrid-5

Figure C.6: Reference Pareto front for the Kilbrid problems

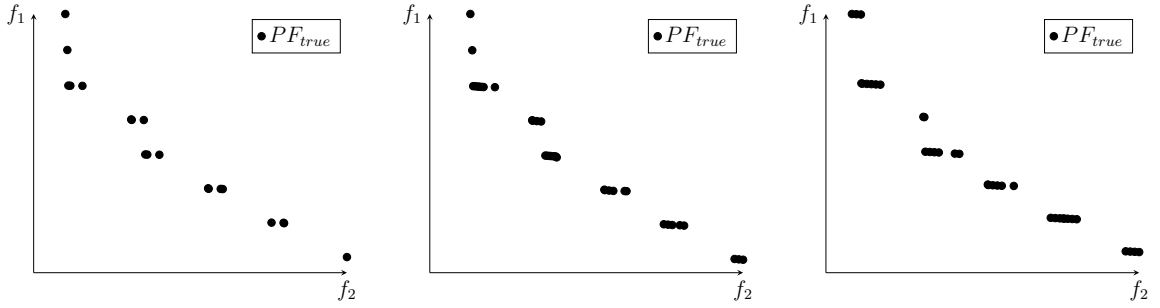

(a) Lutz1-2 *(b)* Lutz1-4 *(c)* Lutz1-5

Figure C.7: True Pareto front for the Lutz1 problems

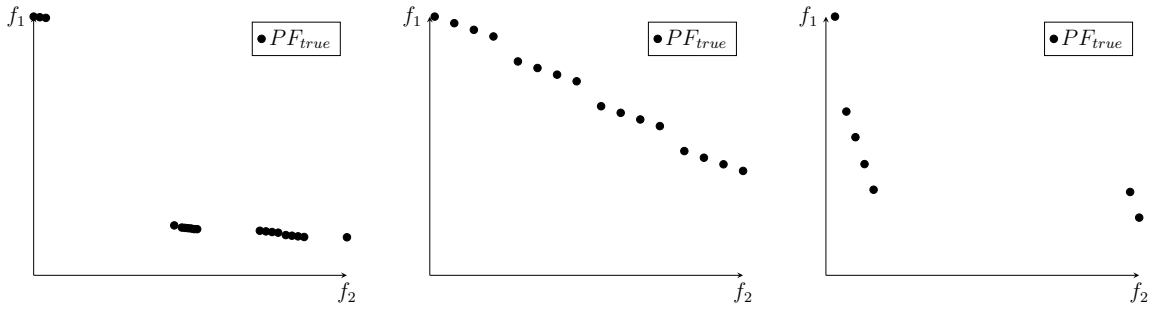

(a) Mitchell-1 *(b)* Mitchell-2 *(c)* Mitchell-4

Figure C.8: True Pareto front for the Mitchell problems

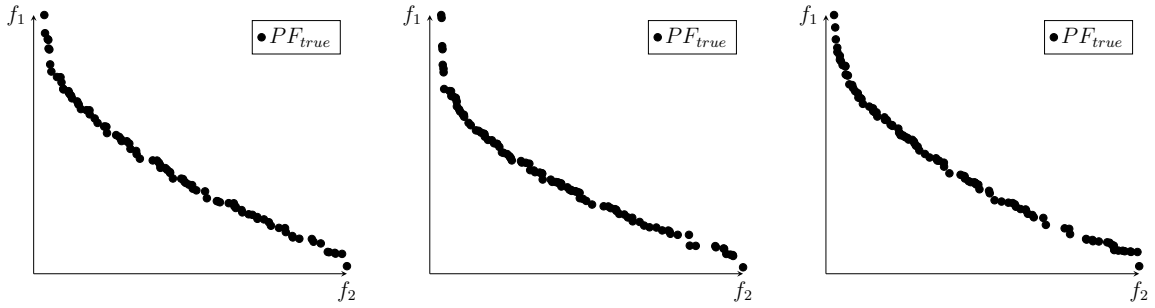

(a) Mukherje-1 *(b)* Mukherje-2 *(c)* Mukherje-3

Figure C.9: Reference Pareto front for the Mukherje problems

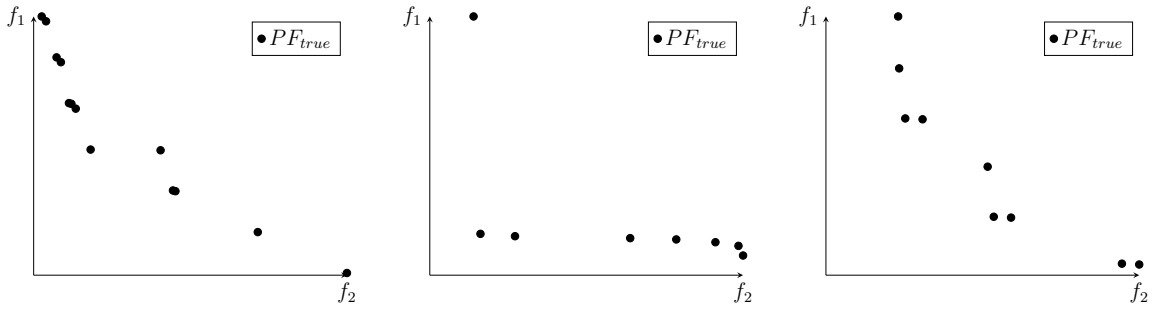

(a) Roszieg-1 *(b)* Roszieg-2 *(c)* Roszieg-3

Figure C.10: True Pareto front for the Roszieg problems

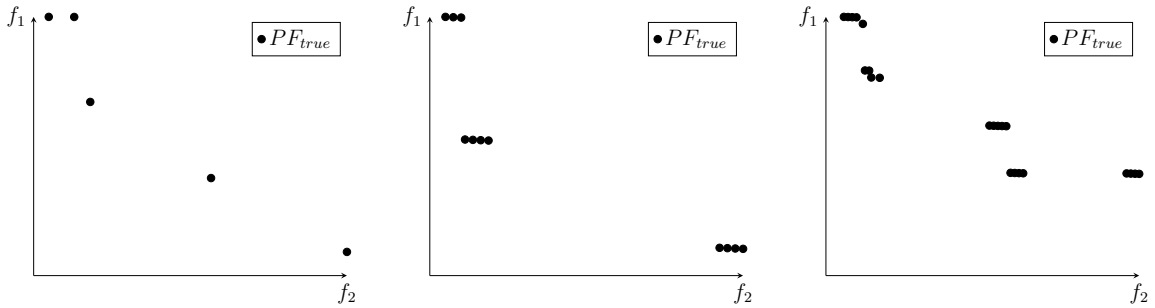

(a) Sawyer-2 *(b)* Sawyer-3 *(c)* Sawyer-4

Figure C.11: True Pareto front for the Sawyer problems

C.2 Parameter settings

This section presents the procedure used for the definition of the parameters of the various optimization algorithms.

C.2.1 ANOVA results: BIANT

The ANOVA results for the BIANT-1 and BIANT-2 are shown in Tables C.1 to C.3. Table C.1 shows that the population size, the pheromone importance, and the evaporation rate have a significant effect on the hypervolume when considering the BIANT-1. By considering successively the factors with a p-value less than α_{lim} in F-value descendent order and the main plot effects shown Figure C.12, the parameter values can be fixed as follows: population size to 200, pheromone rate 3 and evaporation rate to 0.9. For the heuristics importance β, represented by the factor C, since it does not have a significant influence on the hypervolume and does have an influence on the computation time as shown in Table C.2, it is fixed to 1. The value of 1 is the one minimising the computation time, as shown in Figure C.13.

Regarding the results obtained for the BIANT-2, which are shown in Table C.3, all factors have a significant influence on the response variable. Additionally, an interaction between the factors B and E, and C and D can be observed. The factor E, which has the strongest F-value can be fixed to 0.1. The population size to 200, the evaporation rate to 0.6, the pheromone rate and the heuristics importance are respectively fixed to 3 and 5.

Table C.1: Analysis of variance for the BIANT-1 with HV as response value

Factor	DF	SS	MS	F-value	p-value
A	2	0.753	0.376	>500	0.000
B	2	0.004	0.002	3.640	0.027
D	8	0.013	0.002	3.230	0.001

* Only factors/interactions with a significant influence ($\alpha_{lim} = 0.05$) are shown.

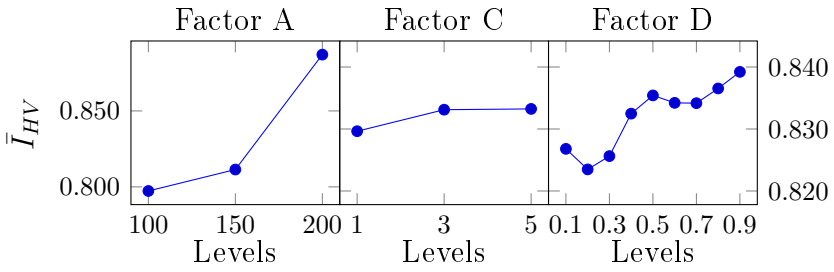

Figure C.12: Main effects plot (fitted means) obtained for the BIANT-1 with HV as response value

Table C.2: Analysis of variance for the BIANT-1 with the computation time as response value

Factor	DF	SS	MS	F-value	p-value
A	2	>500	>500	>500	0.000
B	2	0.233	0.117	>500	0.000
C	2	0.000	0.000	5.080	0.006
D	8	>500	0.143	>500	0.000
AB	4	0.017	0.004	111.920	0.000
AD	16	0.080	0.005	131.200	0.000
BD	16	0.199	0.012	325.450	0.000

* Only factors/interactions with a significant influence ($\alpha_{lim} = 0.05$) are shown.

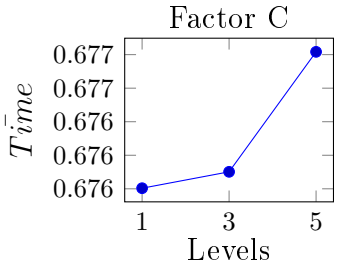

Figure C.13: Main effects plot (fitted means) obtained for the BIANT-1 with the computation as response variable

Table C.3: Analysis of variance for the BIANT-2 with HV as response value

Factor	DF	SS	MS	F-value	p-value
A	2	0.026	0.013	30.990	0.000
B	2	0.004	0.002	4.760	0.009
C	2	0.007	0.003	8.210	0.000
D	4	0.037	0.009	21.520	0.000
E	2	0.040	0.020	46.400	0.000
BE	4	0.005	0.001	2.890	0.022
CD	8	0.008	0.001	2.220	0.026

* Only factors/interactions with a significant influence ($\alpha_{lim} = 0.05$) are shown.

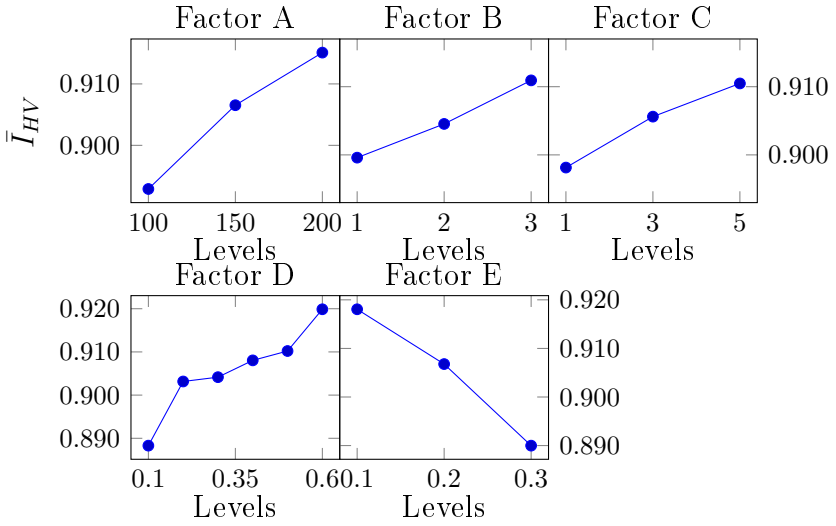

Figure C.14: Main effects plot (fitted means) obtained for the BIANT-2 with HV as response value

C.2.2 ANOVA results: MOACS

Tables C.4 and C.5 show the ANOVA results for the MOACS-1 and MOACS-2. For the MOACS-1, the factor C and D and the interactions AC, BC and BD are significant, when using the hypervolume as response variable. By considering successively the factors with a p-value less than α_{lim} and their F-value in a descendent order, following factors can be set to following values: q_0 to 0.8 and ρ to 0.1. The value of β maximising the hypervolume regarding its interaction with the factor C is 2. Since the population size does not have either a significant influence on the covered hypervolume or on the computation time (as shown Table C.6), it is not necessarily beneficial to choose the lowest value for the population size in order to decrease the running time, thus it was fixed to 200. Taking the results for the MOACS-2 into consideration, most of the factors and the interaction between factors of order 2 are significant. Using the F-value in descendent order, q_0 can be fixed to 0.6, the population size to 200, and q_1 to 0.1 and β to 2. Since the interaction BE is significant and E has already been defined, the value of B maximising the HV metric, under consideration of its interaction with E, is 2. Following the same reasoning, ρ is set to 0.6.

Table C.4: Analysis of variance for the MOACS-1 with HV as response variable

Factor	DF	SS	MS	F-value	p-value
C	8	>500	0.542	>500	0
D	4	0.002	0.001	4.130	0.003
AC	16	0.004	0.000	1.690	0.043
BC	32	0.010	0.000	2.420	0
BD	16	0.004	0.000	1.930	0.015

* Only factors/interactions with a significant influence ($\alpha_{lim} = 0.05$) are shown.

Table C.5: Analysis of variance for the MOACS-2 with HV as response variable

Factor	DF	SS	MS	F-value	p-value
A	2	0.031	0.016	84.870	0.000
B	4	0.002	0.001	2.760	0.027
C	5	>500	0.500	>500	0.000
E	2	0.006	0.003	17.130	0.000
AC	10	0.004	0.000	2.020	0.030
BC	20	0.007	0.000	1.860	0.014
BE	8	0.007	0.001	4.670	0.000
CD	20	0.008	0.000	2.100	0.004
CE	10	0.009	0.001	5.140	0.000

* Only factors/interactions with a significant influence ($\alpha_{lim} = 0.05$) are shown.

Table C.6: Analysis of variance for the MOACS-1 with the computation time as response value

Factor	DF	SS	MS	F-value	p-value
B	4	0.245	0.061	>500	0.000
C	8	0.073	0.009	161.800	0.000
BC	32	0.008	0.000	4.690	0.000
CD	32	0.005	0.000	2.720	0.000

* Only factors/interactions with a significant influence ($\alpha_{lim} = 0.05$) are shown.

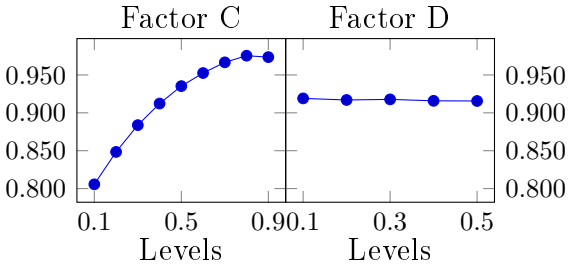

Figure C.15: Main effects plot (fitted means) obtained for the MOACS-1 with HV as response value

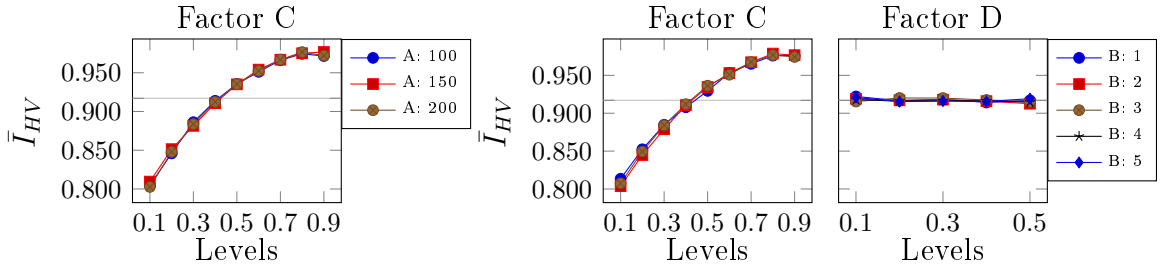

Figure C.16: Interaction plot (fitted means) obtained for the MOACS-1 with HV as response value

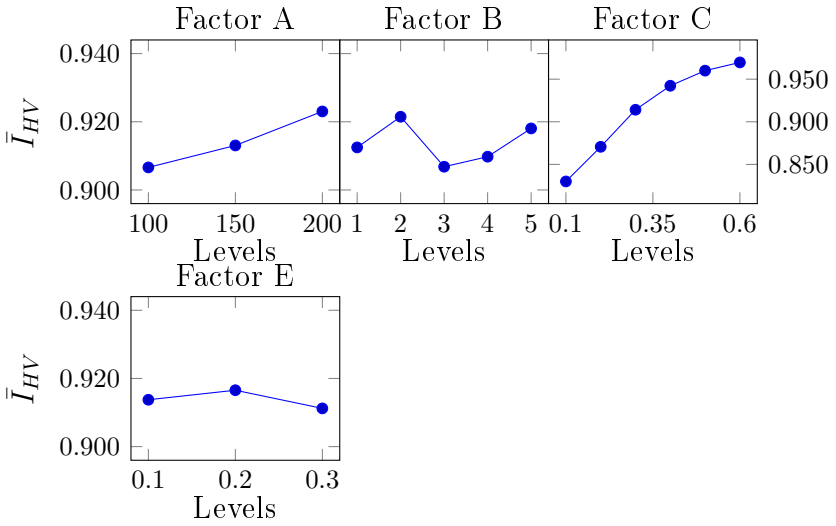

Figure C.17: Main effects plot (fitted means) obtained for the MOACS-2 with HV as response value

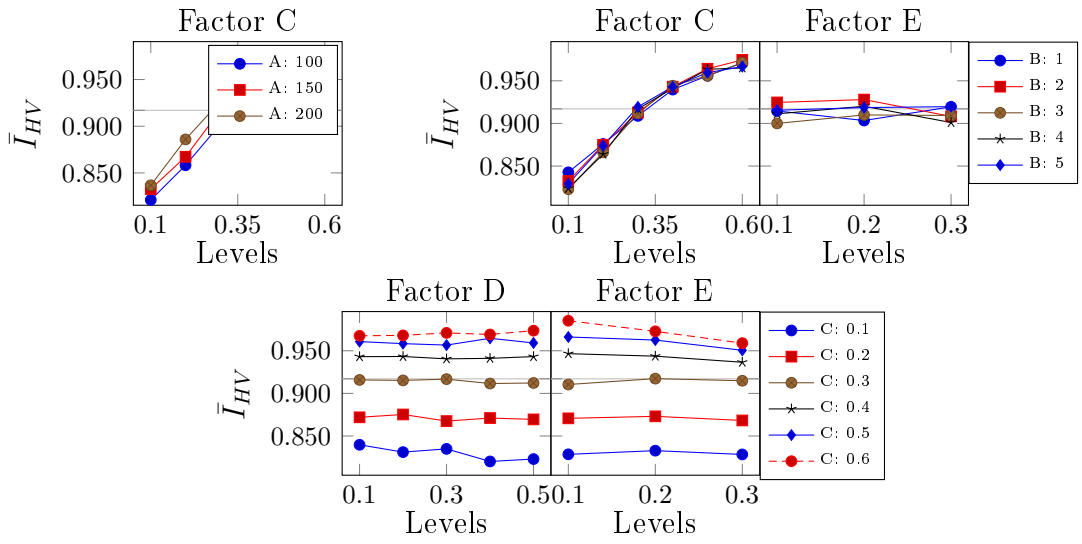

Figure C.18: Interaction plot (fitted means) obtained for the MOACS-2 with HV as response value

C.2.3 ANOVA results: CHAC-1 and CHAC-2

The results obtained for the ANOVA of the CHAC-1 and CHAC-2 are respectively shown in Tables C.7 and C.8. By considering successively the factors of CHAC-1 with a p-value less than α_{lim} and their F-value in a descendent order, q_0 is set to 0.6, the population size to 200, α to 2, β to 3. The interaction DE allows us to fix E to 0.3. Regarding the results of the CHAC-2, most of the factors and the interaction between factors of order 2 are significant. By considering successively the factors and their interactions with a p-value less than α and their F-value in a descendent order, while the values of all the common factors with the CHAC-1 stays unchanged, the value of q_1 is can be fixed to 0.3. Regarding the results of the CHAC-2, most of the factors and the interaction between factors of order 2 are significant. By considering successively the factors and their interactions with a p-value less than α and their F-value in a descendent order, while the values of all the common factors with the CHAC-1 stays unchanged, the value of q_1 is can be fixed to 0.3.

Table C.7: Analysis of variance for the CHAC-1

Factor	DF	SS	MS	F-value	p-value
A	2	0.002	0.001	64.070	0.000
B	2	0.001	0.000	16.040	0.000
C	2	0.000	0.000	11.330	0.000
D	6	0.027	0.005	242.890	0.000
AC	4	0.000	0.000	2.680	0.030
BD	12	0.001	0.000	3.190	0.000
CD	12	0.002	0.000	8.310	0.000
DE	18	0.001	0.000	1.760	0.030

* Only factors/interactions with a significant influence ($\alpha_{lim} = 0.05$) are shown.

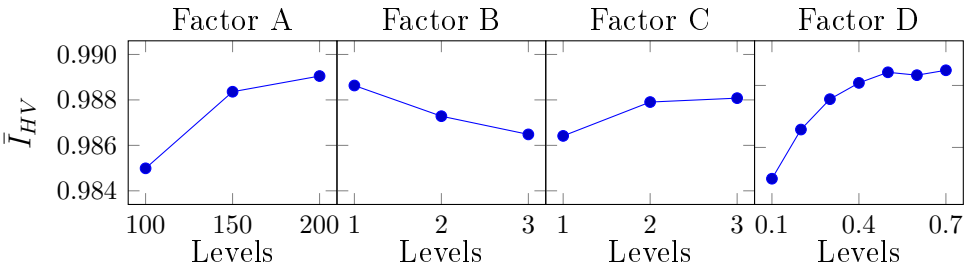

Figure C.19: Main effects plot (fitted means) obtained for the CHAC-1 with HV as response value

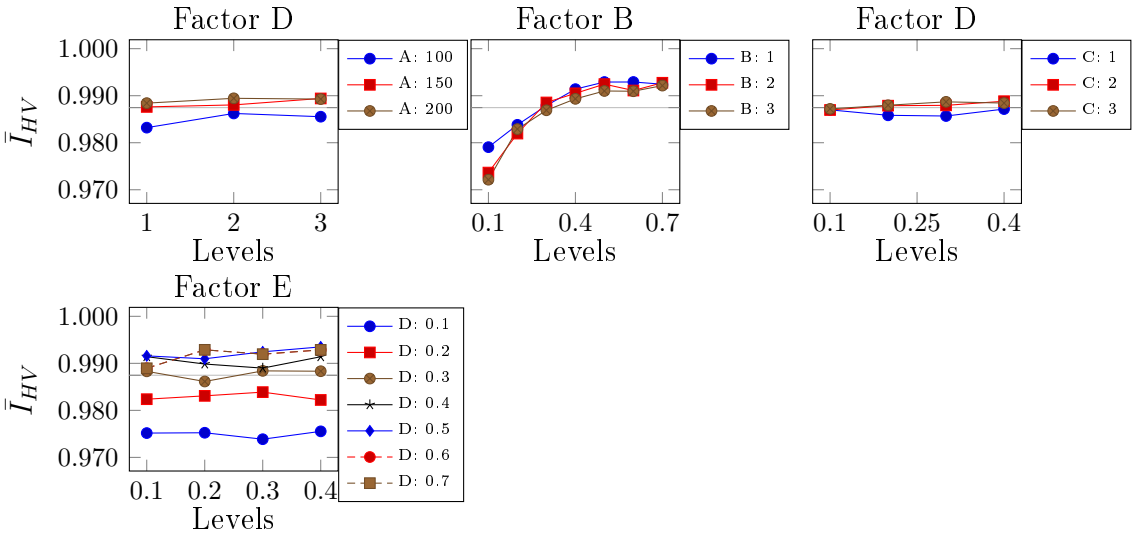

Figure C.20: Interaction plot (fitted means) obtained for the CHAC-1 with HV as response value

Table C.8: Analysis of variance for the CHAC-2

Factor	DF	SS	MS	F-value	p-value
A	2	0.016	0.008	194.430	0.000
B	2	0.001	0.000	7.260	0.000
C	2	0.007	0.003	81.820	0.000
D	5	0.214	0.043	1048.390	0.000
F	2	0.002	0.001	26.450	0.000
AD	10	0.002	0.000	5.410	0.000
BD	10	0.002	0.000	5.250	0.000
BF	4	0.001	0.000	3.920	0.000
CD	10	0.013	0.001	31.800	0.000
CE	6	0.001	0.000	2.540	0.020
CF	4	0.000	0.000	2.780	0.030
DE	15	0.002	0.000	3.040	0.000
DF	10	0.003	0.000	7.710	0.000

* Only factors/interactions with a significant influence ($\alpha_{lim} = 0.05$) are shown.

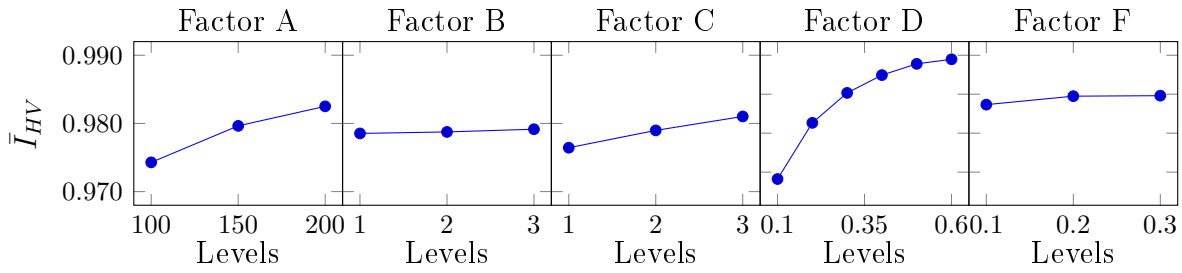

Figure C.21: Main effects plot (fitted means) obtained for the CHAC-2 with HV as response value

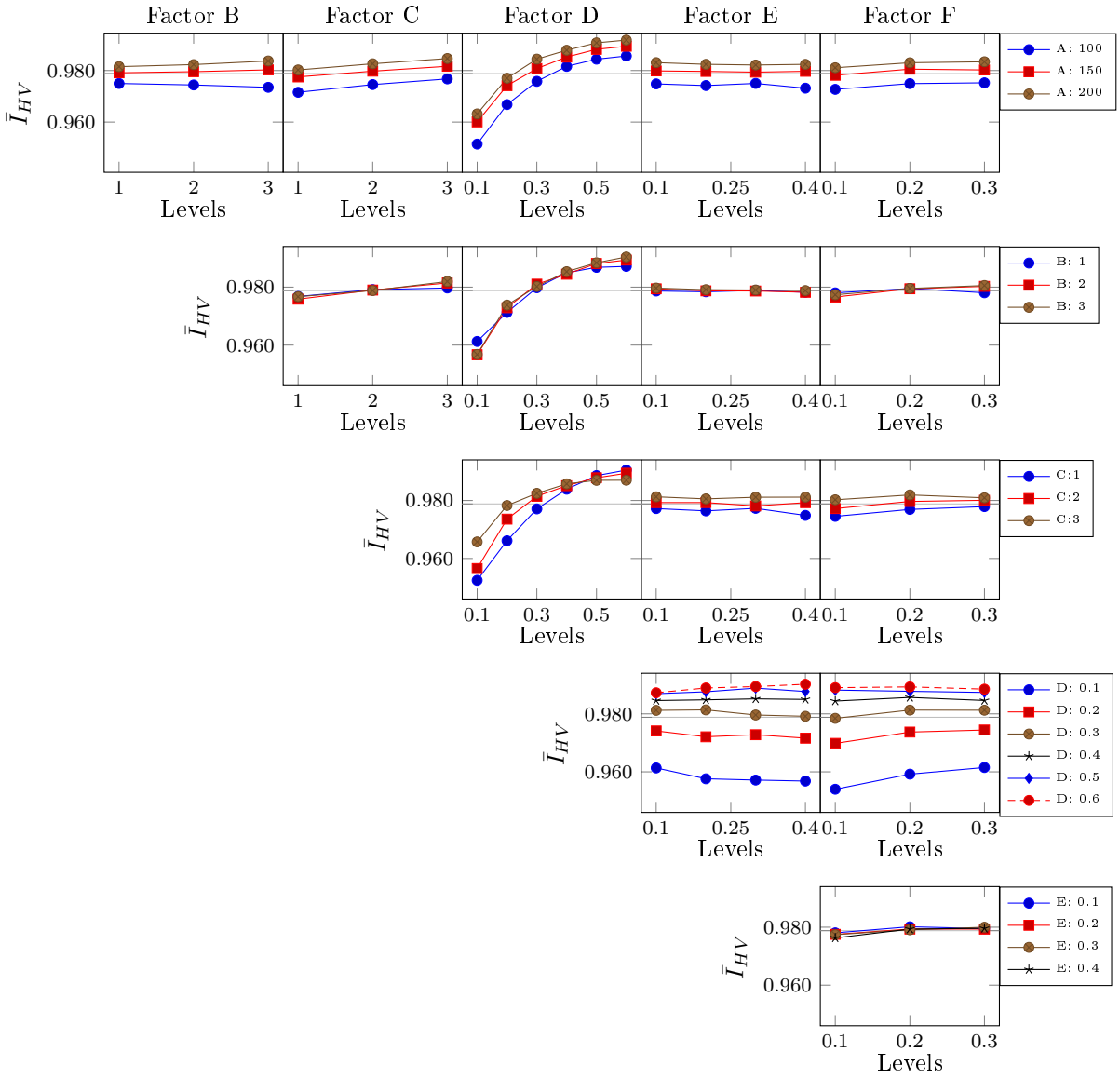

Figure C.22: Interaction plot (fitted means) obtained for the CHAC-2 with HV as response value

C.2.4 ANOVA results: DMOABC

The ANOVA results for the DMOABC are shown in Table C.9. This table shows that the factor A, which represents the size of the population, is the only factor having a significant influence on the hypervolume. The value of this factor which maximizes the response value, is 200, as shown in Figure C.23. Since neither the factor B nor the interaction between the factors A and B have a significant influence on the response variable considering separately the covered hypervolume and the computation time, shown in Table C.10, B is set to 50, value for which the covered hypervolume is maximized.

Table C.9: Analysis of variance for the DMOABC with HV as response variable

Factor	DF	SS	MS	F-value	p-value
A	2	0.001	0.000	10.200	0.000

* Only factors/interactions with a significant influence ($\alpha_{lim} = 0.05$) are shown.

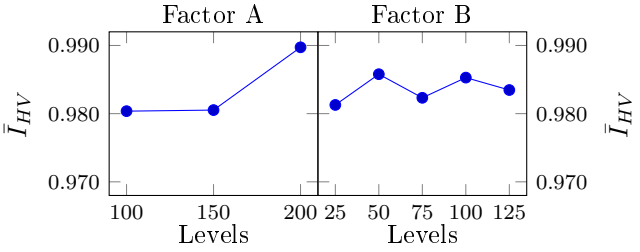

Figure C.23: Main effects plot (fitted means) obtained for the DMOABC with HV as response value

Table C.10: Analysis of variance for the DMOABC with the computation time as response variable

Factor	DF	SS	MS	F-value	p-value
A	2	0.943	0.471	191.340	0.000

* Only factors/interactions with a significant influence ($\alpha_{lim} = 0.05$) are shown.

C.2.5 ANOVA results: DMOCSA

The ANOVA results for the DMOCSA are shown in Table C.11. This table shows that, while the factor A has a significant influence on the response value, the factor B only has a significant influence when considering a confidence level of 92.3%. Thus, according to the main effects plot, the population size can be set to 200 and B to 0.9. Since the factor C does definitely not have any influence on either the covered hypervolume or the computation time, as shown in Table C.12, the interaction between A and C, which is significant for the hypervolume as response value, is used to set C to 0.20.

Table C.11: Analysis of variance for the DMOCSA with HV as response variable

Factor	DF	SS	MS	F-value	p-value
A	2	0.003	0.002	34.350	0.000
B	8	0.001	0.000	1.800	0.077

* Only factors/interactions with a significant influence ($\alpha_{lim} = 0.10$)are shown.

Table C.12: Analysis of variance for the DMOCSA with the computation time as response variable

Factor	DF	SS	MS	F-value	p-value
A	2	0.632	0.316	11.640	0.000
AC	8	0.453	0.057	2.090	0.038
BC	32	141.414	0.044	1.630	0.022

* Only factors/interactions with a significant influence ($\alpha_{lim} = 0.05$) are shown.

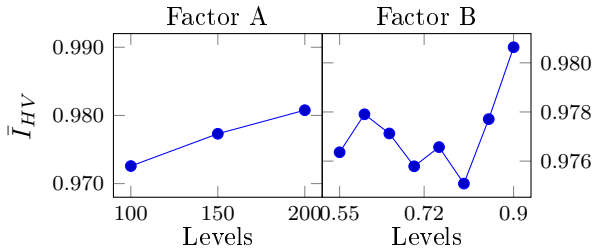

Figure C.24: Main effects plot (fitted means) obtained for the DMOCSA with HV as response value

C.2.6 ANOVA results: DMOFPA

The ANOVA results for the DMOFPA are shown in Table C.13. This table shows that the population size and the threshold between global and local pollination have a significant effect on the response variable (hypervolume). Taking the F-Value in descendent order and in accordance with the main effect and interaction plots shown in Figure C.25, the population size was set to 200 and the threshold rate, B, to 0.90

Table C.13: Analysis of variance for the DMOFPA with HV as response variable

Factor	DF	SS	MS	F-value	p-value
A	2	0.002	0.001	21.110	0.000
B	8	0.002	0.000	3.770	0.001

* Only factors/interactions with a significant influence ($\alpha_{lim} = 0.05$) are shown.

Figure C.25: Main effects plot (fitted means) obtained for the DMOFPA with HV as response value

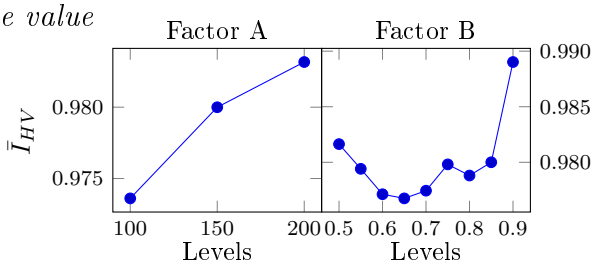

C.2.7 ANOVA results: DMOBAT

The ANOVA results obtained are shown in Table C.14. This table shows that the population size has a significant effect on the response variable (hypervolume). Considering the main effect plot shown in Figure C.26, the population size was set to 200.

Table C.14: Analysis of variance for the DMOBAT

Factor	DF	SS	MS	F-value	p-value
A	2	0.000	0.000	3.180	0.046

* Only factors/interactions with a significant influence ($\alpha_{lim} = 0.05$) are shown.

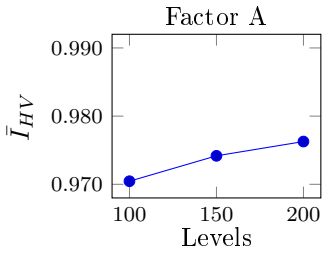

Figure C.26: Main effects plot (fitted means) obtained for the DMOBAT with HV as response value

C.2.8 ANOVA results: DMOPSO

The obtained ANOVA results are shown in Table C.15. This table shows that the population size, and the two crossover rates have a significant effect on the response variable (hypervolume). Taking the F-Value in descendent order, we fix the population size to 200, the crossover rate C_1 between a solution X_i^k and its best position pB_i^k to 0.75 and the crossover rate C_2 between a solution X_i^k and the best global position gB_i^k to 0.70. We fix arbitrary the mutation rate to 0.15. This is done taking the main effects plot and interaction plot shown in Figure C.27.

Table C.15: Analysis of variance for the DMOPSO with HV as response variable

Factor	DF	SS	MS	F-value	p-value
A	2	0.007	0.004	107.980	0.000
B	4	0.000	0.000	2.500	0.040
C	4	0.000	0.000	2.610	0.030

* Only factors/interactions with a significant influence ($\alpha_{lim} = 0.05$) are shown.

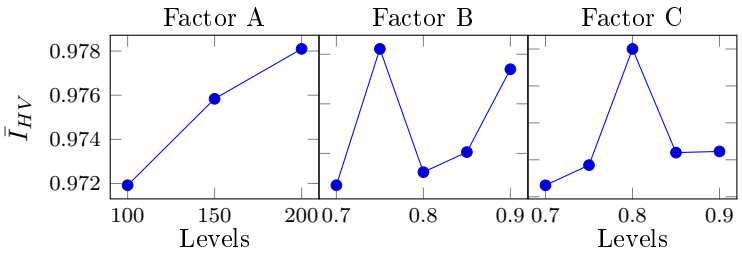

Figure C.27: Main effects plot (fitted means) obtained for the DMOPSO with HV as response value

C.3 Detailed values of the metrics

This section presents the detailed values of the metrics obtained by the different optimization algorithms for all problem instances.

C.3.1 Problem Family: Arc111

Table C.16: Median and interquartile range of I_{HV} obtained by the optimisers for the Arc111 problems

	Arc111-1 $\tilde{x} \pm IQR(x)$		Arc111-2 $\tilde{x} \pm IQR(x)$		Arc111-3 $\tilde{x} \pm IQR(x)$		Arc111-4 $\tilde{x} \pm IQR(x)$		Arc111-5 $\tilde{x} \pm IQR(x)$	
BIANT-1	0.87	0.02	0.89	0.04	0.86	0.06	0.90	0.03	0.85	0.04
BIANT-2	0.90	0.01	0.89	0.04	0.87	0.04	0.86	0.03	0.90	0.03
CHAC-1	0.87	0.01	0.85	0.01	0.84	0.01	0.84	0.01	0.85	0.03
CHAC-2	0.87	0.01	0.85	0.01	0.84	0.00	0.85	0.01	0.86	0.01
DMOABC	0.86	0.01	0.84	0.01	0.85	0.02	0.85	0.01	0.85	0.01
DMOCSA-1-1	0.87	0.01	0.85	0.01	0.84	0.03	0.85	0.03	0.85	0.01
DMOCSA-1-2	0.86	0.01	0.85	0.01	0.85	0.00	0.84	0.01	0.86	0.02
DMOCSA-1-3	0.86	0.01	0.85	0.01	0.85	0.01	0.85	0.01	0.85	0.02
DMOCSA-1-4	0.86	0.01	0.86	0.01	0.84	0.01	0.84	0.01	0.84	0.01
DMOCSA-1-5	0.86	0.01	0.85	0.02	0.84	0.02	0.85	0.02	0.85	0.00
DMOCSA-2-1	0.86	0.01	0.85	0.02	0.84	0.02	0.85	0.02	0.86	0.01
DMOCSA-2-2	0.86	0.01	0.86	0.01	0.84	0.02	0.85	0.01	0.85	0.02
DMOCSA-2-3	0.86	0.01	0.85	0.01	0.85	0.01	0.84	0.01	0.85	0.01
DMOCSA-2-4	0.87	0.01	0.85	0.02	0.85	0.01	0.85	0.01	0.85	0.01
DMOCSA-2-5	0.87	0.01	0.85	0.03	0.85	0.01	0.85	0.00	0.85	0.01
DMOFPA-1	0.86	0.01	0.85	0.02	0.85	0.02	0.85	0.02	0.85	0.03
DMOFPA-2	0.86	0.01	0.86	0.02	0.85	0.00	0.85	0.01	0.85	0.01
DMOFPA-3	0.87	0.01	0.85	0.01	0.84	0.01	0.85	0.01	0.85	0.02
DMOFPA-4	0.86	0.01	0.85	0.00	0.85	0.02	0.84	0.02	0.85	0.03
DMOFPA-5	0.86	0.02	0.85	0.01	0.85	0.01	0.85	0.00	0.85	0.02
MOACS-1	0.84	0.01	0.87	0.01	0.87	0.01	0.87	0.01	0.87	0.00
MOACS-2	0.90	0.01	0.92	0.01	0.92	0.02	0.92	0.00	0.91	0.01
DMOBAT-1	0.86	0.01	0.85	0.01	0.84	0.02	0.85	0.01	0.85	0.01
DMOBAT-2	0.86	0.01	0.85	0.01	0.84	0.00	0.85	0.01	0.85	0.01
DMOBAT-3	0.86	0.01	0.86	0.03	0.84	0.01	0.85	0.02	0.85	0.01
DMOBAT-4	0.86	0.01	0.85	0.01	0.85	0.01	0.84	0.01	0.85	0.02
DMOBAT-5	0.86	0.01	0.85	0.01	0.84	0.01	0.85	0.01	0.85	0.00
DMOPSO-1	0.87	0.02	0.85	0.01	0.85	0.01	0.85	0.01	0.86	0.01
DMOPSO-2	0.87	0.01	0.85	0.01	0.85	0.01	0.84	0.01	0.85	0.02
DMOPSO-3	0.86	0.01	0.85	0.01	0.84	0.02	0.84	0.02	0.85	0.01
DMOPSO-4	0.86	0.01	0.85	0.02	0.84	0.00	0.84	0.01	0.85	0.01
DMOPSO-5	0.86	0.01	0.85	0.01	0.85	0.01	0.85	0.01	0.85	0.02
NSGA-II	0.87	0.01	0.86	0.03	0.86	0.01	0.86	0.03	0.86	0.02
SPEA2	0.87	0.01	0.86	0.01	0.85	0.02	0.86	0.02	0.86	0.01

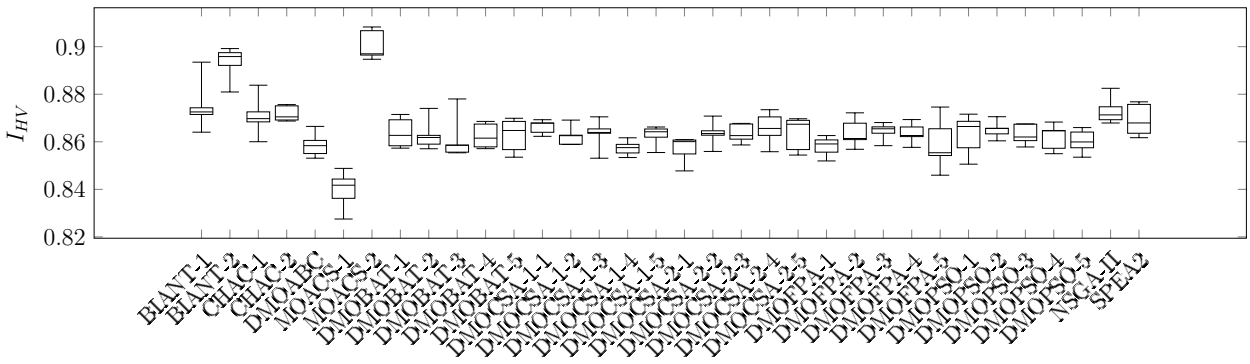

Figure C.28: Boxplot for I_{HV}: Arc111-1

Table C.17: Median and interquartile range of I_{IGD} obtained by the optimisers for the Arc111 problems

	Arc111-1 $\tilde{x} \pm IQR(x)$		Arc111-2 $\tilde{x} \pm IQR(x)$		Arc111-3 $\tilde{x} \pm IQR(x)$		Arc111-4 $\tilde{x} \pm IQR(x)$		Arc111-5 $\tilde{x} \pm IQR(x)$	
BIANT-1	0.68	0.06	0.78	0.08	0.88	0.24	0.64	0.11	0.84	0.18
BIANT-2	0.64	0.06	0.66	0.14	0.83	0.12	0.83	0.04	0.85	0.15
CHAC-1	0.76	0.03	0.83	0.07	0.84	0.03	0.86	0.06	0.78	0.06
CHAC-2	0.78	0.00	0.87	0.04	0.78	0.03	0.86	0.07	0.78	0.03
DMOABC	0.81	0.03	0.91	0.11	0.78	0.04	0.88	0.01	0.79	0.03
DMOCSA-1-1	0.78	0.01	0.88	0.02	0.78	0.09	0.90	0.07	0.84	0.02
DMOCSA-1-2	0.82	0.02	0.81	0.03	0.73	0.02	0.89	0.10	0.80	0.10
DMOCSA-1-3	0.78	0.01	0.85	0.07	0.80	0.07	0.88	0.03	0.82	0.06
DMOCSA-1-4	0.80	0.05	0.84	0.03	0.77	0.03	0.88	0.01	0.84	0.03
DMOCSA-1-5	0.79	0.04	0.85	0.01	0.81	0.11	0.85	0.04	0.84	0.03
DMOCSA-2-1	0.82	0.03	0.88	0.03	0.75	0.09	0.88	0.04	0.79	0.04
DMOCSA-2-2	0.78	0.01	0.82	0.01	0.80	0.06	0.88	0.07	0.79	0.02
DMOCSA-2-3	0.79	0.02	0.86	0.02	0.74	0.04	0.90	0.01	0.79	0.03
DMOCSA-2-4	0.77	0.04	0.84	0.06	0.77	0.02	0.86	0.04	0.75	0.08
DMOCSA-2-5	0.78	0.06	0.82	0.11	0.78	0.04	0.85	0.02	0.78	0.04
DMOFPA-1	0.81	0.02	0.86	0.04	0.77	0.05	0.89	0.05	0.84	0.11
DMOFPA-2	0.78	0.04	0.86	0.13	0.76	0.02	0.89	0.01	0.80	0.01
DMOFPA-3	0.78	0.02	0.83	0.03	0.78	0.03	0.86	0.06	0.79	0.05
DMOFPA-4	0.79	0.02	0.87	0.01	0.80	0.09	0.89	0.02	0.82	0.08
DMOFPA-5	0.82	0.03	0.85	0.01	0.79	0.00	0.87	0.02	0.82	0.09
MOACS-1	0.94	0.12	0.74	0.05	0.57	0.02	0.60	0.07	0.58	0.04
MOACS-2	0.55	0.04	0.47	0.01	0.39	0.01	0.44	0.01	0.47	0.00
DMOBAT-1	0.78	0.01	0.88	0.06	0.82	0.07	0.89	0.05	0.76	0.06
DMOBAT-2	0.82	0.03	0.86	0.04	0.79	0.03	0.87	0.02	0.78	0.09
DMOBAT-3	0.81	0.01	0.84	0.17	0.80	0.06	0.88	0.12	0.82	0.04
DMOBAT-4	0.80	0.05	0.88	0.06	0.78	0.05	0.90	0.08	0.82	0.06
DMOBAT-5	0.79	0.02	0.83	0.01	0.84	0.03	0.88	0.06	0.77	0.06
DMOPSO-1	0.82	0.05	0.84	0.03	0.76	0.06	0.89	0.03	0.76	0.06
DMOPSO-2	0.78	0.01	0.88	0.05	0.78	0.06	0.86	0.03	0.81	0.06
DMOPSO-3	0.81	0.03	0.86	0.01	0.83	0.02	0.90	0.02	0.79	0.01
DMOPSO-4	0.80	0.03	0.85	0.02	0.82	0.02	0.89	0.02	0.81	0.02
DMOPSO-5	0.81	0.02	0.84	0.04	0.77	0.05	0.87	0.03	0.79	0.07
NSGA-II	0.80	0.04	0.89	0.08	0.76	0.05	0.80	0.11	0.78	0.04
SPEA2	0.82	0.02	0.84	0.07	0.79	0.04	0.92	0.02	0.79	0.02

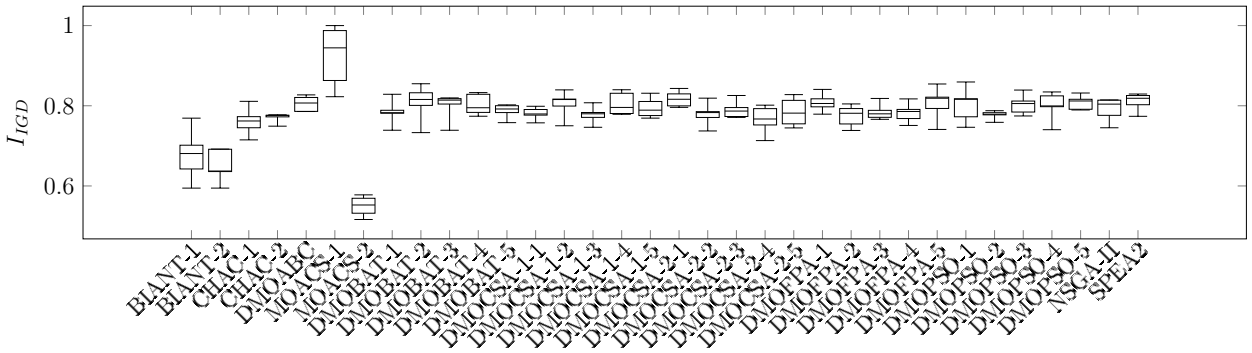

Figure C.29: Boxplot for I_{IGD}: Arc111-1

Table C.18: Median and interquartile range of I_ϵ obtained by the optimisers for the Arc111 problems

	Arc111-1 $\tilde{x} \pm IQR(x)$		Arc111-2 $\tilde{x} \pm IQR(x)$		Arc111-3 $\tilde{x} \pm IQR(x)$		Arc111-4 $\tilde{x} \pm IQR(x)$		Arc111-5 $\tilde{x} \pm IQR(x)$	
BIANT-1	0.74	0.03	0.81	0.12	0.76	0.02	0.73	0.02	0.91	0.16
BIANT-2	0.69	0.03	0.68	0.05	0.80	0.01	0.75	0.04	0.83	0.05
CHAC-1	0.24	0.01	0.31	0.01	0.36	0.01	0.36	0.01	0.37	0.00
CHAC-2	0.24	0.00	0.31	0.00	0.36	0.00	0.36	0.01	0.37	0.00
DMOABC	0.24	0.00	0.31	0.01	0.35	0.01	0.36	0.00	0.38	0.00
DMOCSA-1-1	0.24	0.00	0.32	0.00	0.36	0.00	0.36	0.00	0.38	0.00
DMOCSA-1-2	0.24	0.00	0.32	0.01	0.35	0.01	0.36	0.01	0.38	0.00
DMOCSA-1-3	0.24	0.00	0.32	0.00	0.35	0.00	0.36	0.01	0.38	0.00
DMOCSA-1-4	0.24	0.01	0.31	0.01	0.35	0.00	0.36	0.01	0.38	0.01
DMOCSA-1-5	0.24	0.00	0.31	0.00	0.35	0.00	0.36	0.00	0.38	0.01
DMOCSA-2-1	0.24	0.00	0.32	0.00	0.35	0.01	0.36	0.01	0.37	0.00
DMOCSA-2-2	0.24	0.00	0.31	0.00	0.35	0.00	0.36	0.00	0.38	0.00
DMOCSA-2-3	0.24	0.01	0.31	0.01	0.35	0.01	0.36	0.01	0.38	0.00
DMOCSA-2-4	0.24	0.00	0.31	0.00	0.35	0.00	0.36	0.00	0.38	0.01
DMOCSA-2-5	0.24	0.01	0.32	0.01	0.36	0.00	0.36	0.00	0.38	0.00
DMOFPA-1	0.24	0.00	0.31	0.01	0.35	0.00	0.35	0.01	0.38	0.01
DMOFPA-2	0.24	0.00	0.31	0.01	0.35	0.01	0.36	0.00	0.38	0.00
DMOFPA-3	0.24	0.00	0.31	0.00	0.36	0.00	0.36	0.00	0.38	0.01
DMOFPA-4	0.24	0.00	0.31	0.00	0.35	0.00	0.36	0.01	0.38	0.00
DMOFPA-5	0.24	0.00	0.31	0.00	0.36	0.00	0.36	0.00	0.38	0.01
MOACS-1	0.94	0.04	0.93	0.01	0.95	0.06	0.89	0.03	0.96	0.04
MOACS-2	0.50	0.04	0.49	0.02	0.45	0.01	0.48	0.03	0.56	0.04
DMOBAT-1	0.24	0.00	0.31	0.00	0.36	0.00	0.36	0.00	0.37	0.01
DMOBAT-2	0.24	0.00	0.31	0.00	0.36	0.00	0.36	0.01	0.38	0.00
DMOBAT-3	0.24	0.00	0.31	0.00	0.35	0.01	0.36	0.00	0.38	0.00
DMOBAT-4	0.24	0.01	0.32	0.01	0.36	0.00	0.36	0.01	0.38	0.00
DMOBAT-5	0.24	0.00	0.31	0.00	0.36	0.00	0.36	0.01	0.38	0.00
DMOPSO-1	0.24	0.00	0.31	0.00	0.35	0.00	0.36	0.00	0.38	0.00
DMOPSO-2	0.24	0.01	0.31	0.01	0.36	0.00	0.36	0.00	0.38	0.00
DMOPSO-3	0.24	0.01	0.32	0.00	0.35	0.00	0.36	0.01	0.38	0.01
DMOPSO-4	0.24	0.00	0.31	0.01	0.35	0.01	0.36	0.01	0.37	0.01
DMOPSO-5	0.24	0.00	0.31	0.01	0.35	0.00	0.36	0.00	0.38	0.00
NSGA-II	0.14	0.00	0.18	0.00	0.22	0.00	0.22	0.01	0.32	0.00
SPEA2	0.15	0.00	0.18	0.00	0.22	0.00	0.23	0.00	0.32	0.00

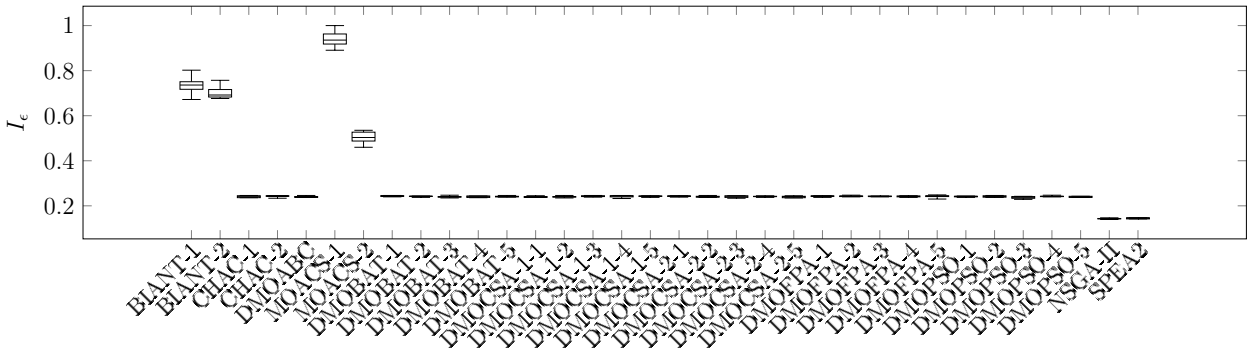

Figure C.30: Boxplot for I_ϵ: Arc111-1

Table C.19: Median and interquartile range of I_Δ obtained by the optimisers for the Arc111 problems

	Arc111-1 $\tilde{x} \pm IQR(x)$		Arc111-2 $\tilde{x} \pm IQR(x)$		Arc111-3 $\tilde{x} \pm IQR(x)$		Arc111-4 $\tilde{x} \pm IQR(x)$		Arc111-5 $\tilde{x} \pm IQR(x)$	
BIANT-1	0.53	0.02	0.61	0.01	0.62	0.09	0.56	0.01	0.65	0.06
BIANT-2	0.54	0.02	0.57	0.11	0.65	0.07	0.66	0.07	0.63	0.03
CHAC-1	0.78	0.03	0.84	0.03	0.83	0.09	0.86	0.03	0.71	0.05
CHAC-2	0.83	0.06	0.79	0.03	0.81	0.01	0.82	0.05	0.75	0.07
DMOABC	0.91	0.03	0.92	0.04	0.84	0.06	0.89	0.06	0.84	0.04
DMOCSA-1-1	0.84	0.02	0.89	0.07	0.85	0.02	0.90	0.03	0.89	0.05
DMOCSA-1-2	0.87	0.06	0.89	0.04	0.83	0.05	0.89	0.06	0.79	0.04
DMOCSA-1-3	0.84	0.03	0.84	0.08	0.84	0.03	0.87	0.04	0.87	0.04
DMOCSA-1-4	0.87	0.02	0.93	0.13	0.84	0.04	0.86	0.01	0.83	0.01
DMOCSA-1-5	0.89	0.02	0.82	0.04	0.89	0.10	0.84	0.02	0.85	0.06
DMOCSA-2-1	0.91	0.01	0.85	0.07	0.82	0.03	0.84	0.04	0.79	0.07
DMOCSA-2-2	0.84	0.01	0.81	0.01	0.82	0.01	0.91	0.07	0.83	0.07
DMOCSA-2-3	0.86	0.03	0.84	0.06	0.78	0.06	0.87	0.02	0.82	0.01
DMOCSA-2-4	0.87	0.02	0.85	0.11	0.86	0.01	0.84	0.07	0.78	0.04
DMOCSA-2-5	0.81	0.05	0.87	0.04	0.82	0.04	0.86	0.05	0.77	0.04
DMOFPA-1	0.86	0.01	0.86	0.04	0.87	0.07	0.88	0.01	0.87	0.10
DMOFPA-2	0.85	0.04	0.85	0.05	0.85	0.01	0.87	0.02	0.83	0.05
DMOFPA-3	0.88	0.09	0.84	0.04	0.81	0.03	0.86	0.00	0.77	0.06
DMOFPA-4	0.82	0.01	0.90	0.10	0.86	0.12	0.92	0.03	0.84	0.06
DMOFPA-5	0.91	0.03	0.82	0.07	0.83	0.01	0.83	0.09	0.85	0.04
MOACS-1	0.61	0.06	0.57	0.05	0.56	0.02	0.59	0.06	0.61	0.01
MOACS-2	0.44	0.03	0.52	0.09	0.40	0.05	0.48	0.07	0.49	0.17
MOBAT-1	0.87	0.05	0.85	0.01	0.82	0.10	0.88	0.07	0.80	0.03
MOBAT-2	0.85	0.02	0.88	0.05	0.84	0.05	0.90	0.04	0.85	0.04
MOBAT-3	0.85	0.05	0.92	0.21	0.85	0.03	0.86	0.02	0.79	0.07
MOBAT-4	0.86	0.02	0.84	0.11	0.85	0.06	0.86	0.14	0.86	0.01
MOBAT-5	0.85	0.10	0.88	0.10	0.86	0.04	0.86	0.06	0.84	0.07
DMOPSO-1	0.92	0.07	0.82	0.02	0.84	0.01	0.88	0.01	0.82	0.05
DMOPSO-2	0.87	0.08	0.86	0.04	0.80	0.05	0.85	0.08	0.80	0.06
DMOPSO-3	0.87	0.05	0.86	0.08	0.84	0.04	0.88	0.04	0.84	0.02
DMOPSO-4	0.87	0.04	0.81	0.06	0.83	0.06	0.89	0.04	0.82	0.02
DMOPSO-5	0.86	0.01	0.83	0.01	0.81	0.04	0.89	0.02	0.85	0.04
NSGA-II	0.87	0.06	0.90	0.07	0.89	0.02	0.94	0.02	0.84	0.07
SPEA2	0.90	0.02	0.85	0.05	0.85	0.02	0.91	0.07	0.80	0.01

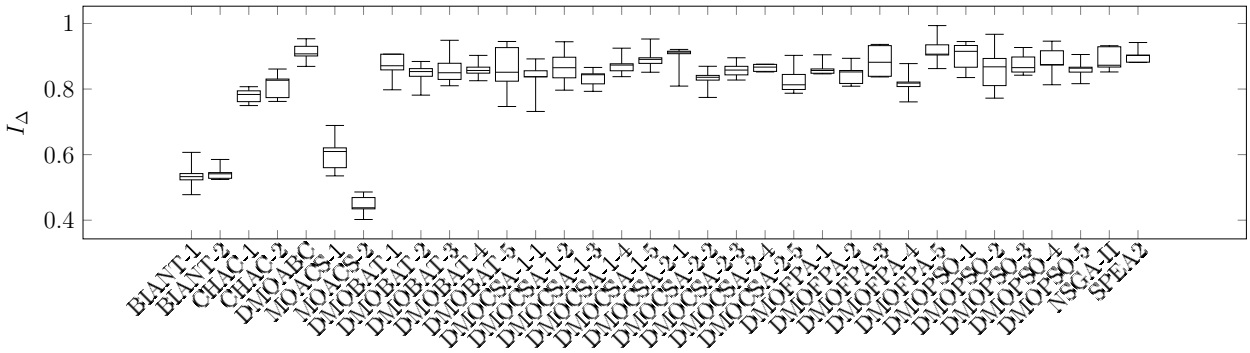

Figure C.31: Boxplot for I_Δ: Arc111-1

Table C.20: Median and interquartile range of the computation time required by the optimisers for the Arc111 problems

	Arc111-1 $\tilde{x} \pm IQR(x)$		Arc111-2 $\tilde{x} \pm IQR(x)$		Arc111-3 $\tilde{x} \pm IQR(x)$		Arc111-4 $\tilde{x} \pm IQR(x)$		Arc111-5 $\tilde{x} \pm IQR(x)$	
BIANT-1	0.54	0.17	0.80	0.21	0.83	0.12	0.79	0.25	0.50	0.36
BIANT-2	1.00	0.00	0.64	0.47	0.54	0.18	0.40	0.14	0.68	0.13
CHAC-1	0.43	0.04	0.40	0.07	0.44	0.10	0.30	0.18	0.38	0.25
CHAC-2	0.39	0.07	0.35	0.04	0.39	0.18	0.28	0.24	0.39	0.10
DMOABC	0.55	0.07	0.51	0.35	0.75	0.30	0.54	0.11	0.93	0.29
DMOCSA-1-1	0.34	0.07	0.34	0.06	0.26	0.30	0.37	0.17	0.42	0.20
DMOCSA-1-2	0.36	0.15	0.33	0.15	0.47	0.13	0.23	0.20	0.46	0.16
DMOCSA-1-3	0.37	0.16	0.31	0.13	0.44	0.16	0.45	0.11	0.30	0.22
DMOCSA-1-4	0.26	0.07	0.26	0.06	0.51	0.07	0.37	0.26	0.26	0.03
DMOCSA-1-5	0.32	0.14	0.33	0.03	0.41	0.23	0.35	0.14	0.44	0.21
DMOCSA-2-1	0.38	0.15	0.40	0.12	0.60	0.27	0.66	0.27	0.67	0.18
DMOCSA-2-2	0.53	0.12	0.63	0.13	0.71	0.12	0.57	0.28	0.52	0.22
DMOCSA-2-3	0.33	0.21	0.49	0.05	0.87	0.17	0.47	0.12	0.68	0.06
DMOCSA-2-4	0.52	0.15	0.46	0.09	0.58	0.24	0.57	0.12	0.80	0.30
DMOCSA-2-5	0.53	0.18	0.48	0.34	0.51	0.30	0.42	0.23	0.61	0.22
DMOFPA-1	0.26	0.06	0.35	0.16	0.42	0.13	0.38	0.06	0.32	0.05
DMOFPA-2	0.31	0.18	0.46	0.08	0.41	0.18	0.35	0.14	0.39	0.30
DMOFPA-3	0.32	0.08	0.43	0.04	0.55	0.18	0.29	0.17	0.43	0.10
DMOFPA-4	0.26	0.03	0.30	0.04	0.35	0.05	0.26	0.12	0.31	0.16
DMOFPA-5	0.23	0.18	0.47	0.05	0.58	0.34	0.33	0.14	0.34	0.05
MOACS-1	0.20	0.08	0.32	0.05	0.25	0.04	0.19	0.04	0.28	0.13
MOACS-2	0.22	0.04	0.25	0.05	0.27	0.10	0.20	0.02	0.42	0.19
DMOBAT-1	0.24	0.08	0.26	0.16	0.44	0.01	0.30	0.10	0.40	0.20
DMOBAT-2	0.31	0.06	0.35	0.02	0.39	0.09	0.30	0.05	0.37	0.13
DMOBAT-3	0.26	0.18	0.41	0.21	0.42	0.17	0.36	0.17	0.47	0.07
DMOBAT-4	0.32	0.14	0.36	0.12	0.30	0.07	0.32	0.14	0.41	0.06
DMOBAT-5	0.29	0.08	0.28	0.17	0.28	0.12	0.32	0.04	0.41	0.17
DMOPSO-1	0.37	0.14	0.41	0.26	0.43	0.10	0.41	0.06	0.35	0.07
DMOPSO-2	0.21	0.23	0.27	0.05	0.42	0.23	0.18	0.12	0.33	0.26
DMOPSO-3	0.46	0.21	0.38	0.28	0.44	0.12	0.29	0.13	0.31	0.13
DMOPSO-4	0.52	0.26	1.00	0.41	0.77	0.10	0.51	0.14	0.86	0.27
DMOPSO-5	0.38	0.05	0.39	0.25	0.39	0.22	0.45	0.04	0.39	0.17
NSGA-II	0.26	0.13	0.30	0.10	0.47	0.22	0.42	0.27	0.43	0.13
SPEA2	0.14	0.03	0.17	0.07	0.17	0.13	0.16	0.08	0.20	0.08

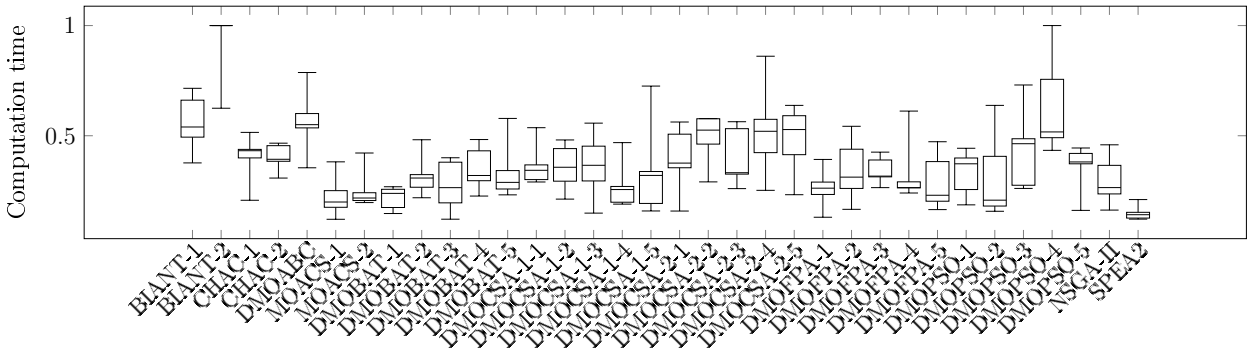

Figure C.32: Boxplot for the computation time: Arc111-1

C.3.2 Problem Family: Buxey

Table C.21: Median and interquartile range of I_{HV} obtained by the optimisers for the Buxey problems

	Buxey-1 $\tilde{x} \pm IQR(x)$		Buxey-2 $\tilde{x} \pm IQR(x)$		Buxey-3 $\tilde{x} \pm IQR(x)$		Buxey-4 $\tilde{x} \pm IQR(x)$		Buxey-5 $\tilde{x} \pm IQR(x)$	
BIANT-1	0.94	0.06	0.93	0.03	0.92	0.03	0.93	0.04	0.92	0.03
BIANT-2	0.95	0.02	0.93	0.03	0.91	0.05	0.94	0.03	0.93	0.03
CHAC-1	0.92	0.01	0.92	0.01	0.91	0.01	0.90	0.01	0.91	0.01
CHAC-2	0.93	0.01	0.92	0.01	0.91	0.00	0.90	0.02	0.91	0.01
DMOABC	0.92	0.01	0.92	0.01	0.91	0.00	0.91	0.01	0.90	0.02
DMOCSA-1-1	0.92	0.01	0.92	0.01	0.90	0.00	0.90	0.02	0.90	0.01
DMOCSA-1-2	0.93	0.01	0.92	0.01	0.91	0.01	0.90	0.01	0.91	0.01
DMOCSA-1-3	0.92	0.00	0.92	0.01	0.91	0.00	0.90	0.02	0.91	0.01
DMOCSA-1-4	0.90	0.02	0.89	0.01	0.88	0.01	0.88	0.01	0.87	0.00
DMOCSA-1-5	0.93	0.02	0.92	0.01	0.90	0.01	0.90	0.02	0.90	0.01
DMOCSA-2-1	0.92	0.00	0.92	0.01	0.91	0.01	0.90	0.01	0.91	0.00
DMOCSA-2-2	0.92	0.01	0.92	0.01	0.91	0.02	0.90	0.02	0.91	0.01
DMOCSA-2-3	0.93	0.01	0.92	0.01	0.91	0.01	0.90	0.01	0.90	0.01
DMOCSA-2-4	0.90	0.01	0.90	0.01	0.88	0.02	0.87	0.02	0.88	0.02
DMOCSA-2-5	0.92	0.01	0.92	0.01	0.90	0.02	0.91	0.01	0.90	0.01
DMOFPA-1	0.92	0.01	0.92	0.01	0.91	0.01	0.91	0.02	0.91	0.01
DMOFPA-2	0.92	0.01	0.92	0.00	0.90	0.01	0.90	0.01	0.90	0.00
DMOFPA-3	0.92	0.01	0.92	0.01	0.91	0.01	0.90	0.01	0.90	0.02
DMOFPA-4	0.90	0.02	0.90	0.01	0.89	0.02	0.88	0.04	0.88	0.01
DMOFPA-5	0.92	0.01	0.92	0.01	0.90	0.01	0.89	0.01	0.91	0.00
MOACS-1	0.94	0.01	0.94	0.01	0.93	0.01	0.94	0.01	0.95	0.01
MOACS-2	0.93	0.01	0.94	0.01	0.94	0.01	0.94	0.01	0.95	0.01
DMOBAT-1	0.91	0.01	0.92	0.01	0.90	0.01	0.90	0.01	0.91	0.01
DMOBAT-2	0.93	0.01	0.92	0.01	0.91	0.01	0.90	0.01	0.90	0.00
DMOBAT-3	0.93	0.01	0.92	0.01	0.91	0.01	0.90	0.03	0.91	0.01
DMOBAT-4	0.90	0.01	0.90	0.01	0.89	0.01	0.88	0.01	0.88	0.02
DMOBAT-5	0.92	0.01	0.92	0.01	0.91	0.00	0.90	0.02	0.91	0.00
DMOPSO-1	0.92	0.01	0.92	0.00	0.90	0.01	0.90	0.01	0.90	0.01
DMOPSO-2	0.93	0.01	0.92	0.01	0.90	0.01	0.90	0.01	0.91	0.01
DMOPSO-3	0.92	0.01	0.93	0.02	0.91	0.01	0.90	0.00	0.91	0.00
DMOPSO-4	0.91	0.03	0.91	0.02	0.88	0.05	0.89	0.04	0.89	0.03
DMOPSO-5	0.92	0.01	0.91	0.01	0.90	0.01	0.91	0.02	0.90	0.01
NSGA-II	0.94	0.01	0.92	0.01	0.92	0.01	0.91	0.02	0.91	0.02
SPEA2	0.93	0.00	0.93	0.01	0.91	0.01	0.92	0.01	0.91	0.02

Table C.22: Median and interquartile range of I_{IGD} obtained by the optimisers for the Buxey problems

	Buxey-1 $\tilde{x} \pm IQR(x)$		Buxey-2 $\tilde{x} \pm IQR(x)$		Buxey-3 $\tilde{x} \pm IQR(x)$		Buxey-4 $\tilde{x} \pm IQR(x)$		Buxey-5 $\tilde{x} \pm IQR(x)$	
BIANT-1	0.48	0.17	0.55	0.09	0.52	0.12	0.47	0.13	0.57	0.05
BIANT-2	0.44	0.16	0.50	0.09	0.58	0.09	0.55	0.17	0.46	0.06
CHAC-1	0.65	0.20	0.58	0.07	0.61	0.01	0.64	0.02	0.62	0.04
CHAC-2	0.60	0.07	0.63	0.06	0.64	0.05	0.64	0.08	0.64	0.11
DMOABC	0.60	0.04	0.60	0.04	0.64	0.03	0.56	0.07	0.58	0.11
DMOCSA-1-1	0.60	0.18	0.61	0.02	0.67	0.05	0.59	0.08	0.67	0.06
DMOCSA-1-2	0.61	0.03	0.60	0.06	0.67	0.03	0.66	0.06	0.65	0.06
DMOCSA-1-3	0.61	0.05	0.62	0.04	0.65	0.04	0.61	0.06	0.64	0.06
DMOCSA-1-4	0.80	0.11	0.86	0.03	0.91	0.05	0.86	0.04	0.88	0.02
DMOCSA-1-5	0.63	0.11	0.60	0.04	0.69	0.05	0.64	0.03	0.67	0.06
DMOCSA-2-1	0.66	0.14	0.64	0.05	0.66	0.05	0.65	0.06	0.63	0.03
DMOCSA-2-2	0.61	0.10	0.61	0.08	0.65	0.03	0.65	0.04	0.60	0.02
DMOCSA-2-3	0.60	0.06	0.61	0.06	0.68	0.09	0.64	0.04	0.65	0.06
DMOCSA-2-4	0.78	0.04	0.80	0.03	0.88	0.10	0.86	0.03	0.82	0.08
DMOCSA-2-5	0.61	0.07	0.60	0.01	0.65	0.02	0.59	0.03	0.69	0.06
DMOFPA-1	0.55	0.01	0.66	0.03	0.68	0.03	0.61	0.09	0.58	0.00
DMOFPA-2	0.59	0.04	0.63	0.05	0.67	0.03	0.62	0.02	0.67	0.05
DMOFPA-3	0.63	0.11	0.63	0.04	0.60	0.06	0.61	0.03	0.64	0.06
DMOFPA-4	0.77	0.04	0.79	0.02	0.80	0.11	0.75	0.05	0.84	0.04
DMOFPA-5	0.56	0.02	0.64	0.06	0.66	0.06	0.64	0.11	0.62	0.06
MOACS-1	0.53	0.05	0.50	0.04	0.47	0.06	0.48	0.04	0.32	0.06
MOACS-2	0.59	0.12	0.56	0.05	0.48	0.01	0.43	0.03	0.41	0.05
DMOBAT-1	0.63	0.03	0.63	0.10	0.67	0.05	0.61	0.04	0.62	0.08
DMOBAT-2	0.63	0.17	0.66	0.03	0.61	0.06	0.66	0.06	0.63	0.05
DMOBAT-3	0.57	0.06	0.64	0.07	0.65	0.08	0.63	0.02	0.62	0.05
DMOBAT-4	0.77	0.01	0.77	0.06	0.79	0.03	0.84	0.03	0.75	0.10
DMOBAT-5	0.61	0.16	0.62	0.07	0.64	0.06	0.64	0.05	0.65	0.03
DMOPSO-1	0.57	0.06	0.64	0.02	0.62	0.08	0.62	0.04	0.65	0.01
DMOPSO-2	0.58	0.09	0.60	0.01	0.66	0.02	0.63	0.04	0.62	0.04
DMOPSO-3	0.54	0.10	0.60	0.05	0.67	0.09	0.62	0.07	0.66	0.05
DMOPSO-4	0.71	0.14	0.78	0.14	0.81	0.25	0.79	0.16	0.79	0.12
DMOPSO-5	0.54	0.02	0.63	0.05	0.65	0.05	0.60	0.04	0.65	0.10
NSGA-II	0.66	0.05	0.63	0.01	0.63	0.06	0.62	0.06	0.62	0.10
SPEA2	0.60	0.04	0.63	0.08	0.66	0.06	0.61	0.03	0.64	0.07

Table C.23: Median and interquartile range of I_ϵ obtained by the optimisers for the Buxey problems

	Buxey-1 $\tilde{x} \pm IQR(x)$		Buxey-2 $\tilde{x} \pm IQR(x)$		Buxey-3 $\tilde{x} \pm IQR(x)$		Buxey-4 $\tilde{x} \pm IQR(x)$		Buxey-5 $\tilde{x} \pm IQR(x)$	
BIANT-1	0.42	0.41	0.39	0.20	0.62	0.48	0.59	0.34	0.65	0.01
BIANT-2	0.28	0.14	0.49	0.23	0.84	0.44	0.23	0.06	0.50	0.31
CHAC-1	0.87	0.00	1.00	0.00	0.65	0.00	0.26	0.00	0.77	0.00
CHAC-2	0.87	0.00	1.00	0.00	0.65	0.00	0.26	0.00	0.77	0.00
DMOABC	0.87	0.00	1.00	0.00	0.65	0.00	0.26	0.00	0.77	0.00
DMOCSA-1-1	0.87	0.00	1.00	0.00	0.65	0.00	0.26	0.00	0.77	0.00
DMOCSA-1-2	0.87	0.00	1.00	0.00	0.65	0.00	0.26	0.00	0.77	0.00
DMOCSA-1-3	0.87	0.00	1.00	0.00	0.65	0.00	0.26	0.00	0.77	0.00
DMOCSA-1-4	0.87	0.00	1.00	0.00	0.65	0.00	0.26	0.00	0.77	0.00
DMOCSA-1-5	0.87	0.00	1.00	0.00	0.65	0.00	0.26	0.00	0.77	0.00
DMOCSA-2-1	0.87	0.00	1.00	0.00	0.65	0.00	0.26	0.00	0.77	0.00
DMOCSA-2-2	0.87	0.00	1.00	0.00	0.65	0.00	0.26	0.00	0.77	0.00
DMOCSA-2-3	0.87	0.00	1.00	0.00	0.65	0.00	0.26	0.00	0.77	0.00
DMOCSA-2-4	0.87	0.00	1.00	0.00	0.65	0.00	0.26	0.00	0.77	0.00
DMOCSA-2-5	0.87	0.00	1.00	0.00	0.65	0.00	0.26	0.00	0.77	0.00
DMOFPA-1	0.87	0.00	1.00	0.00	0.65	0.00	0.26	0.00	0.77	0.00
DMOFPA-2	0.87	0.00	1.00	0.00	0.65	0.00	0.26	0.00	0.77	0.00
DMOFPA-3	0.87	0.00	1.00	0.00	0.65	0.00	0.26	0.00	0.77	0.00
DMOFPA-4	0.87	0.00	1.00	0.00	0.65	0.00	0.26	0.00	0.77	0.00
DMOFPA-5	0.87	0.00	1.00	0.00	0.65	0.00	0.26	0.00	0.77	0.00
MOACS-1	0.19	0.05	0.17	0.03	0.28	0.16	0.30	0.19	0.24	0.03
MOACS-2	0.20	0.06	0.09	0.07	0.26	0.18	0.42	0.11	0.22	0.04
DMOBAT-1	0.87	0.00	1.00	0.00	0.65	0.00	0.26	0.00	0.77	0.00
DMOBAT-2	0.87	0.00	1.00	0.00	0.65	0.00	0.26	0.00	0.77	0.00
DMOBAT-3	0.87	0.00	1.00	0.00	0.65	0.00	0.26	0.00	0.77	0.00
DMOBAT-4	0.87	0.00	1.00	0.00	0.65	0.00	0.26	0.00	0.77	0.00
DMOBAT-5	0.87	0.00	1.00	0.00	0.65	0.00	0.26	0.00	0.77	0.00
DMOPSO-1	0.87	0.00	1.00	0.00	0.65	0.00	0.26	0.00	0.77	0.00
DMOPSO-2	0.87	0.00	1.00	0.00	0.65	0.00	0.26	0.00	0.77	0.00
DMOPSO-3	0.87	0.00	1.00	0.00	0.65	0.00	0.26	0.00	0.77	0.00
DMOPSO-4	0.87	0.00	1.00	0.00	0.65	0.00	0.26	0.00	0.77	0.00
DMOPSO-5	0.87	0.00	1.00	0.00	0.65	0.00	0.26	0.00	0.77	0.00
NSGA-II	0.87	0.00	1.00	0.00	0.65	0.00	0.26	0.00	0.77	0.00
SPEA2	0.87	0.00	1.00	0.00	0.65	0.00	0.26	0.00	0.77	0.00

Table C.24: Median and interquartile range of I_Δ obtained by the optimisers for the Buxey problems

	Buxey-1 $\tilde{x} \pm IQR(x)$		Buxey-2 $\tilde{x} \pm IQR(x)$		Buxey-3 $\tilde{x} \pm IQR(x)$		Buxey-4 $\tilde{x} \pm IQR(x)$		Buxey-5 $\tilde{x} \pm IQR(x)$	
BIANT-1	0.67	0.06	0.64	0.09	0.68	0.10	0.62	0.04	0.66	0.10
BIANT-2	0.60	0.05	0.71	0.11	0.68	0.07	0.58	0.02	0.64	0.10
CHAC-1	0.82	0.01	0.82	0.04	0.87	0.03	0.85	0.01	0.78	0.09
CHAC-2	0.84	0.02	0.86	0.04	0.87	0.01	0.82	0.04	0.82	0.05
DMOABC	0.90	0.05	0.91	0.09	0.90	0.06	0.93	0.08	0.72	0.06
DMOCSA-1-1	0.84	0.03	0.87	0.08	0.82	0.05	0.82	0.00	0.85	0.09
DMOCSA-1-2	0.86	0.04	0.86	0.05	0.82	0.07	0.80	0.01	0.84	0.06
DMOCSA-1-3	0.85	0.06	0.84	0.04	0.91	0.11	0.85	0.05	0.83	0.05
DMOCSA-1-4	0.84	0.04	0.88	0.10	0.89	0.13	0.84	0.04	0.88	0.05
DMOCSA-1-5	0.83	0.06	0.82	0.00	0.87	0.05	0.87	0.10	0.77	0.07
DMOCSA-2-1	0.93	0.03	0.86	0.05	0.81	0.02	0.85	0.04	0.86	0.08
DMOCSA-2-2	0.90	0.13	0.86	0.05	0.87	0.05	0.87	0.06	0.84	0.07
DMOCSA-2-3	0.81	0.04	0.88	0.08	0.88	0.11	0.84	0.09	0.82	0.08
DMOCSA-2-4	0.84	0.07	0.80	0.08	0.81	0.04	0.84	0.09	0.84	0.07
DMOCSA-2-5	0.84	0.01	0.84	0.01	0.89	0.06	0.83	0.05	0.82	0.05
DMOFPA-1	0.84	0.07	0.80	0.01	0.86	0.07	0.79	0.04	0.82	0.08
DMOFPA-2	0.85	0.03	0.86	0.01	0.89	0.03	0.85	0.05	0.83	0.07
DMOFPA-3	0.88	0.04	0.86	0.09	0.83	0.11	0.85	0.03	0.76	0.04
DMOFPA-4	0.90	0.01	0.80	0.07	0.86	0.02	0.86	0.05	0.77	0.13
DMOFPA-5	0.80	0.07	0.90	0.09	0.84	0.09	0.88	0.03	0.85	0.04
MOACS-1	0.60	0.01	0.58	0.13	0.62	0.04	0.59	0.05	0.53	0.09
MOACS-2	0.58	0.15	0.50	0.02	0.69	0.20	0.69	0.12	0.53	0.10
DMOBAT-1	0.85	0.11	0.90	0.03	0.90	0.04	0.84	0.01	0.84	0.09
DMOBAT-2	0.86	0.06	0.84	0.02	0.80	0.09	0.85	0.04	0.76	0.05
DMOBAT-3	0.85	0.03	0.85	0.01	0.82	0.08	0.83	0.03	0.81	0.11
DMOBAT-4	0.90	0.05	0.83	0.04	0.83	0.03	0.84	0.03	0.79	0.05
DMOBAT-5	0.90	0.08	0.84	0.11	0.89	0.03	0.86	0.00	0.87	0.09
DMOPSO-1	0.83	0.10	0.86	0.04	0.83	0.06	0.83	0.03	0.82	0.04
DMOPSO-2	0.86	0.10	0.87	0.04	0.84	0.03	0.84	0.02	0.81	0.05
DMOPSO-3	0.82	0.05	0.88	0.04	0.84	0.06	0.88	0.07	0.86	0.02
DMOPSO-4	0.80	0.01	0.87	0.04	0.81	0.02	0.85	0.07	0.82	0.03
DMOPSO-5	0.87	0.05	0.84	0.07	0.80	0.08	0.83	0.03	0.81	0.10
NSGA-II	0.87	0.06	0.90	0.02	0.86	0.05	0.91	0.05	0.91	0.06
SPEA2	0.81	0.15	0.90	0.05	0.88	0.09	0.87	0.02	0.85	0.03

Table C.25: Median and interquartile range of the computation time required by the optimisers for the Buxey problems

	Buxey-1		Buxey-2		Buxey-3		Buxey-4		Buxey-5	
	$\tilde{x}$	$IQR(x)$	$\tilde{x}$	$IQR(x)$	$\tilde{x}$	$IQR(x)$	$\tilde{x}$	$IQR(x)$	$\tilde{x}$	$IQR(x)$
BIANT-1	0.79	0.42	0.59	0.34	0.66	0.43	0.94	0.37	0.55	0.24
BIANT-2	0.97	0.43	0.68	0.24	0.78	0.33	0.75	0.40	0.67	0.44
CHAC-1	0.44	0.26	0.51	0.24	0.60	0.04	0.39	0.28	0.41	0.27
CHAC-2	0.34	0.43	0.43	0.25	0.54	0.08	0.43	0.11	0.45	0.27
DMOABC	0.48	0.28	0.52	0.03	0.58	0.11	0.65	0.23	0.49	0.08
DMOCSA-1-1	0.32	0.09	0.39	0.19	0.34	0.08	0.31	0.06	0.40	0.14
DMOCSA-1-2	0.38	0.21	0.35	0.05	0.48	0.26	0.29	0.15	0.40	0.16
DMOCSA-1-3	0.30	0.22	0.37	0.21	0.49	0.26	0.33	0.17	0.47	0.05
DMOCSA-1-4	0.23	0.17	0.30	0.09	0.25	0.04	0.34	0.14	0.30	0.10
DMOCSA-1-5	0.37	0.26	0.32	0.18	0.28	0.08	0.20	0.38	0.33	0.14
DMOCSA-2-1	0.32	0.22	0.38	0.04	0.38	0.10	0.41	0.19	0.40	0.03
DMOCSA-2-2	0.40	0.13	0.46	0.07	0.47	0.17	0.34	0.04	0.37	0.40
DMOCSA-2-3	0.32	0.39	0.48	0.17	0.49	0.30	0.43	0.09	0.42	0.27
DMOCSA-2-4	0.36	0.24	0.39	0.05	0.33	0.10	0.30	0.15	0.40	0.06
DMOCSA-2-5	0.38	0.39	0.55	0.17	0.43	0.24	0.52	0.12	0.58	0.35
DMOFPA-1	0.25	0.28	0.34	0.04	0.40	0.09	0.39	0.27	0.55	0.06
DMOFPA-2	0.29	0.19	0.42	0.04	0.40	0.02	0.45	0.13	0.36	0.18
DMOFPA-3	0.29	0.28	0.44	0.15	0.45	0.02	0.43	0.08	0.35	0.19
DMOFPA-4	0.18	0.05	0.30	0.18	0.40	0.10	0.27	0.07	0.42	0.11
DMOFPA-5	0.33	0.09	0.44	0.25	0.34	0.20	0.34	0.03	0.36	0.26
MOACS-1	0.59	0.16	0.56	0.22	0.68	0.25	0.59	0.46	0.99	0.30
MOACS-2	0.45	0.15	0.49	0.29	0.51	0.41	0.45	0.07	0.59	0.04
DMOBAT-1	0.21	0.15	0.35	0.03	0.39	0.08	0.39	0.03	0.37	0.33
DMOBAT-2	0.29	0.11	0.42	0.17	0.42	0.17	0.22	0.08	0.39	0.14
DMOBAT-3	0.39	0.15	0.25	0.20	0.45	0.30	0.38	0.16	0.31	0.35
DMOBAT-4	0.30	0.15	0.45	0.12	0.40	0.30	0.32	0.18	0.43	0.13
DMOBAT-5	0.28	0.12	0.28	0.03	0.44	0.04	0.42	0.14	0.56	0.23
DMOPSO-1	0.19	0.16	0.33	0.03	0.42	0.07	0.36	0.02	0.33	0.15
DMOPSO-2	0.39	0.23	0.45	0.04	0.45	0.18	0.26	0.12	0.34	0.17
DMOPSO-3	0.39	0.21	0.45	0.21	0.60	0.38	0.40	0.07	0.57	0.26
DMOPSO-4	0.37	0.40	0.49	0.33	0.38	0.35	0.44	0.07	0.44	0.23
DMOPSO-5	0.25	0.27	0.46	0.26	0.33	0.05	0.35	0.09	0.36	0.37
NSGA-II	0.41	0.34	0.45	0.10	0.39	0.33	0.31	0.26	0.32	0.45
SPEA2	0.17	0.17	0.21	0.12	0.21	0.07	0.20	0.09	0.25	0.13

C.3.3 Problem Family: Gunther

Table C.26: Median and interquartile range of I_{HV} obtained by the optimisers for the Gunther problems

	Gunther-1 $\tilde{x} \pm IQR(x)$		Gunther-2 $\tilde{x} \pm IQR(x)$		Gunther-3 $\tilde{x} \pm IQR(x)$		Gunther-4 $\tilde{x} \pm IQR(x)$		Gunther-5 $\tilde{x} \pm IQR(x)$	
BIANT-1	0.95	0.02	0.95	0.02	0.94	0.02	0.93	0.02	0.93	0.01
BIANT-2	0.94	0.02	0.94	0.07	0.93	0.04	0.95	0.02	0.96	0.00
CHAC-1	0.91	0.02	0.91	0.01	0.91	0.00	0.92	0.01	0.90	0.01
CHAC-2	0.91	0.01	0.91	0.01	0.91	0.01	0.92	0.01	0.89	0.01
DMOABC	0.91	0.01	0.91	0.00	0.92	0.01	0.91	0.01	0.90	0.01
DMOCSA-1-1	0.92	0.01	0.91	0.00	0.91	0.01	0.92	0.01	0.90	0.02
DMOCSA-1-2	0.92	0.00	0.91	0.01	0.91	0.01	0.92	0.01	0.90	0.01
DMOCSA-1-3	0.91	0.01	0.91	0.02	0.91	0.01	0.92	0.01	0.90	0.00
DMOCSA-1-4	0.89	0.02	0.89	0.01	0.89	0.01	0.89	0.02	0.88	0.01
DMOCSA-1-5	0.91	0.01	0.92	0.01	0.91	0.01	0.91	0.02	0.90	0.01
DMOCSA-2-1	0.92	0.01	0.91	0.01	0.91	0.00	0.91	0.00	0.90	0.01
DMOCSA-2-2	0.91	0.01	0.91	0.01	0.91	0.02	0.92	0.02	0.90	0.00
DMOCSA-2-3	0.92	0.01	0.91	0.01	0.91	0.02	0.91	0.02	0.90	0.01
DMOCSA-2-4	0.90	0.01	0.89	0.01	0.89	0.01	0.90	0.01	0.88	0.03
DMOCSA-2-5	0.92	0.02	0.91	0.00	0.91	0.01	0.91	0.01	0.90	0.00
DMOFPA-1	0.91	0.00	0.91	0.01	0.92	0.00	0.91	0.00	0.89	0.01
DMOFPA-2	0.91	0.01	0.91	0.01	0.91	0.01	0.92	0.01	0.89	0.00
DMOFPA-3	0.92	0.01	0.91	0.00	0.91	0.01	0.91	0.01	0.90	0.00
DMOFPA-4	0.90	0.01	0.89	0.02	0.89	0.02	0.89	0.01	0.87	0.02
DMOFPA-5	0.91	0.01	0.90	0.01	0.91	0.01	0.92	0.02	0.90	0.02
MOACS-1	0.91	0.01	0.91	0.01	0.91	0.01	0.91	0.00	0.92	0.01
MOACS-2	0.92	0.01	0.91	0.01	0.92	0.01	0.94	0.02	0.93	0.01
DMOBAT-1	0.92	0.00	0.91	0.01	0.91	0.00	0.91	0.01	0.89	0.01
DMOBAT-2	0.92	0.01	0.91	0.01	0.91	0.01	0.91	0.00	0.90	0.01
DMOBAT-3	0.92	0.01	0.91	0.01	0.91	0.01	0.91	0.01	0.90	0.02
DMOBAT-4	0.90	0.01	0.89	0.02	0.89	0.01	0.89	0.01	0.87	0.02
DMOBAT-5	0.92	0.01	0.91	0.02	0.91	0.01	0.91	0.01	0.91	0.01
DMOPSO-1	0.92	0.01	0.91	0.01	0.91	0.01	0.92	0.00	0.89	0.03
DMOPSO-2	0.91	0.01	0.91	0.02	0.91	0.00	0.92	0.01	0.90	0.01
DMOPSO-3	0.92	0.01	0.91	0.01	0.90	0.01	0.91	0.02	0.90	0.02
DMOPSO-4	0.90	0.02	0.90	0.02	0.90	0.03	0.90	0.02	0.88	0.04
DMOPSO-5	0.91	0.01	0.92	0.01	0.91	0.01	0.92	0.01	0.89	0.03
NSGA-II	0.92	0.01	0.92	0.01	0.91	0.00	0.92	0.01	0.91	0.01
SPEA2	0.92	0.02	0.92	0.01	0.91	0.01	0.92	0.02	0.91	0.01

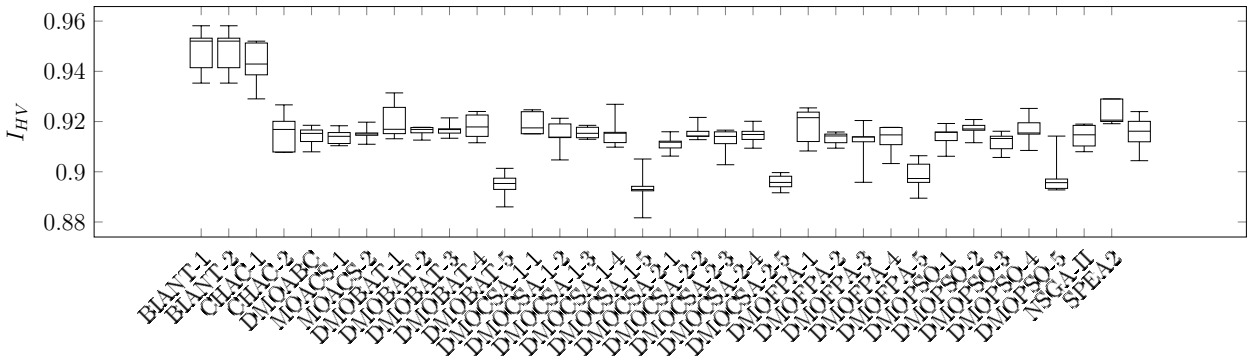

Figure C.33: Boxplot for I_{HV}: Gunther-1

Table C.27: Median and interquartile range of I_{IGD} obtained by the optimisers for the Gunther problems

	Gunther-1 $\tilde{x} \pm IQR(x)$		Gunther-2 $\tilde{x} \pm IQR(x)$		Gunther-3 $\tilde{x} \pm IQR(x)$		Gunther-4 $\tilde{x} \pm IQR(x)$		Gunther-5 $\tilde{x} \pm IQR(x)$	
BIANT-1	0.39	0.08	0.40	0.11	0.32	0.06	0.13	0.02	0.32	0.07
BIANT-2	0.48	0.22	0.35	0.05	0.34	0.05	0.15	0.00	0.30	0.08
CHAC-1	0.75	0.03	0.81	0.02	0.79	0.04	0.30	0.01	0.72	0.12
CHAC-2	0.77	0.02	0.80	0.02	0.81	0.12	0.31	0.02	0.83	0.10
DMOABC	0.82	0.06	0.80	0.04	0.74	0.10	0.33	0.01	0.77	0.01
DMOCSA-1-1	0.85	0.07	0.83	0.01	0.80	0.08	0.31	0.01	0.76	0.03
DMOCSA-1-2	0.84	0.04	0.82	0.11	0.82	0.05	0.30	0.04	0.74	0.08
DMOCSA-1-3	0.82	0.02	0.80	0.04	0.74	0.07	0.32	0.02	0.82	0.08
DMOCSA-1-4	0.89	0.05	0.89	0.04	0.91	0.01	0.35	0.02	0.82	0.07
DMOCSA-1-5	0.85	0.02	0.83	0.06	0.79	0.03	0.29	0.02	0.81	0.08
DMOCSA-2-1	0.82	0.03	0.82	0.03	0.74	0.09	0.31	0.02	0.84	0.04
DMOCSA-2-2	0.83	0.05	0.77	0.02	0.85	0.03	0.29	0.02	0.73	0.06
DMOCSA-2-3	0.84	0.03	0.81	0.06	0.79	0.14	0.31	0.03	0.77	0.03
DMOCSA-2-4	0.85	0.04	0.86	0.01	0.90	0.03	0.33	0.01	0.82	0.07
DMOCSA-2-5	0.85	0.05	0.83	0.06	0.76	0.05	0.31	0.01	0.83	0.07
DMOFPA-1	0.87	0.02	0.79	0.05	0.83	0.03	0.30	0.01	0.79	0.14
DMOFPA-2	0.86	0.02	0.80	0.02	0.82	0.05	0.31	0.01	0.77	0.08
DMOFPA-3	0.81	0.07	0.86	0.03	0.74	0.07	0.31	0.01	0.84	0.05
DMOFPA-4	0.96	0.06	0.85	0.05	0.95	0.03	0.32	0.01	0.86	0.05
DMOFPA-5	0.81	0.01	0.86	0.05	0.79	0.01	0.30	0.01	0.82	0.04
MOACS-1	0.78	0.07	0.91	0.05	0.62	0.03	0.27	0.01	0.56	0.02
MOACS-2	0.79	0.04	0.87	0.03	0.58	0.02	0.27	0.55	0.53	0.01
DMOBAT-1	0.83	0.04	0.79	0.03	0.82	0.06	0.32	0.02	0.77	0.10
DMOBAT-2	0.81	0.03	0.86	0.04	0.75	0.04	0.31	0.02	0.77	0.03
DMOBAT-3	0.82	0.03	0.85	0.03	0.77	0.08	0.29	0.03	0.76	0.04
DMOBAT-4	0.91	0.06	0.91	0.02	0.85	0.01	0.32	0.04	0.86	0.02
DMOBAT-5	0.81	0.01	0.83	0.03	0.81	0.03	0.30	0.01	0.79	0.06
DMOPSO-1	0.84	0.07	0.83	0.03	0.79	0.12	0.30	0.01	0.76	0.10
DMOPSO-2	0.80	0.02	0.79	0.03	0.81	0.04	0.31	0.01	0.75	0.05
DMOPSO-3	0.84	0.05	0.83	0.02	0.82	0.06	0.30	0.01	0.79	0.09
DMOPSO-4	0.91	0.12	0.85	0.06	0.82	0.07	0.32	0.02	0.86	0.10
DMOPSO-5	0.84	0.03	0.83	0.03	0.80	0.07	0.30	0.06	0.72	0.05
NSGA-II	0.81	0.04	0.83	0.01	0.74	0.03	0.29	0.04	0.79	0.04
SPEA2	0.84	0.11	0.83	0.01	0.85	0.02	0.30	0.00	0.79	0.04

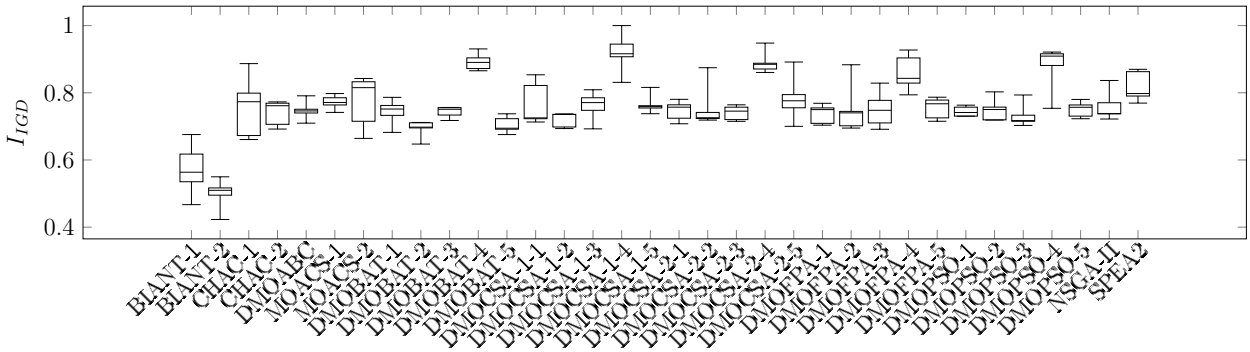

Figure C.34: Boxplot for I_{IGD}: Gunther-1

Table C.28: Median and interquartile range of I_ϵ obtained by the optimisers for the Gunther problems

	Gunther-1 $\tilde{x} \pm IQR(x)$		Gunther-2 $\tilde{x} \pm IQR(x)$		Gunther-3 $\tilde{x} \pm IQR(x)$		Gunther-4 $\tilde{x} \pm IQR(x)$		Gunther-5 $\tilde{x} \pm IQR(x)$	
BIANT-1	0.51	0.16	0.53	0.24	0.28	0.07	0.28	0.07	0.65	0.03
BIANT-2	0.60	0.12	0.45	0.07	0.26	0.19	0.26	0.19	0.49	0.09
CHAC-1	0.96	0.00	1.00	0.03	1.00	0.00	1.00	0.00	1.00	0.14
CHAC-2	0.96	0.00	1.00	0.00	1.00	0.00	1.00	0.00	1.00	0.00
DMOABC	0.96	0.00	1.00	0.03	1.00	0.00	1.00	0.00	1.00	0.00
DMOCSA-1-1	0.96	0.00	1.00	0.00	1.00	0.00	1.00	0.00	1.00	0.00
DMOCSA-1-2	0.96	0.00	1.00	0.00	1.00	0.00	1.00	0.00	1.00	0.00
DMOCSA-1-3	0.96	0.00	1.00	0.00	1.00	0.00	1.00	0.00	1.00	0.14
DMOCSA-1-4	0.96	0.00	1.00	0.00	1.00	0.00	1.00	0.00	1.00	0.00
DMOCSA-1-5	0.96	0.00	1.00	0.00	1.00	0.00	1.00	0.00	1.00	0.00
DMOCSA-2-1	0.96	0.00	1.00	0.00	1.00	0.00	1.00	0.00	1.00	0.00
DMOCSA-2-2	0.96	0.00	1.00	0.00	1.00	0.00	1.00	0.00	1.00	0.00
DMOCSA-2-3	0.96	0.00	1.00	0.00	1.00	0.00	1.00	0.00	1.00	0.00
DMOCSA-2-4	0.96	0.00	1.00	0.00	1.00	0.00	1.00	0.00	1.00	0.00
DMOCSA-2-5	0.96	0.00	1.00	0.00	1.00	0.00	1.00	0.00	1.00	0.00
DMOFPA-1	0.96	0.00	1.00	0.00	1.00	0.00	1.00	0.00	1.00	0.02
DMOFPA-2	0.96	0.00	1.00	0.00	1.00	0.00	1.00	0.00	1.00	0.00
DMOFPA-3	0.96	0.00	1.00	0.00	1.00	0.00	1.00	0.00	1.00	0.14
DMOFPA-4	0.96	0.00	1.00	0.00	1.00	0.00	1.00	0.00	1.00	0.00
DMOFPA-5	0.96	0.00	1.00	0.00	1.00	0.05	1.00	0.05	1.00	0.04
MOACS-1	0.21	0.01	0.21	0.02	0.20	0.02	0.20	0.02	0.48	0.02
MOACS-2	0.16	0.03	0.16	0.03	0.13	0.06	0.13	0.06	0.31	0.02
DMOBAT-1	0.96	0.00	1.00	0.00	1.00	0.02	1.00	0.02	1.00	0.01
DMOBAT-2	0.96	0.00	1.00	0.00	1.00	0.00	1.00	0.00	1.00	0.01
DMOBAT-3	0.96	0.00	1.00	0.00	1.00	0.00	1.00	0.00	0.73	0.53
DMOBAT-4	0.96	0.00	1.00	0.00	1.00	0.00	1.00	0.00	1.00	0.00
DMOBAT-5	0.96	0.00	1.00	0.00	1.00	0.00	1.00	0.00	1.00	0.04
DMOPSO-1	0.96	0.00	1.00	0.00	1.00	0.00	1.00	0.00	1.00	0.13
DMOPSO-2	0.96	0.00	1.00	0.00	0.99	0.02	0.99	0.02	1.00	0.00
DMOPSO-3	0.96	0.00	1.00	0.00	1.00	0.11	1.00	0.11	1.00	0.07
DMOPSO-4	0.96	0.00	1.00	0.00	1.00	0.00	1.00	0.00	1.00	0.00
DMOPSO-5	0.96	0.00	1.00	0.00	1.00	0.00	1.00	0.00	1.00	0.01
NSGA-II	0.96	0.00	1.00	0.00	1.00	0.00	1.00	0.00	1.00	0.00
SPEA2	0.96	0.00	1.00	0.00	1.00	0.00	1.00	0.00	1.00	0.00

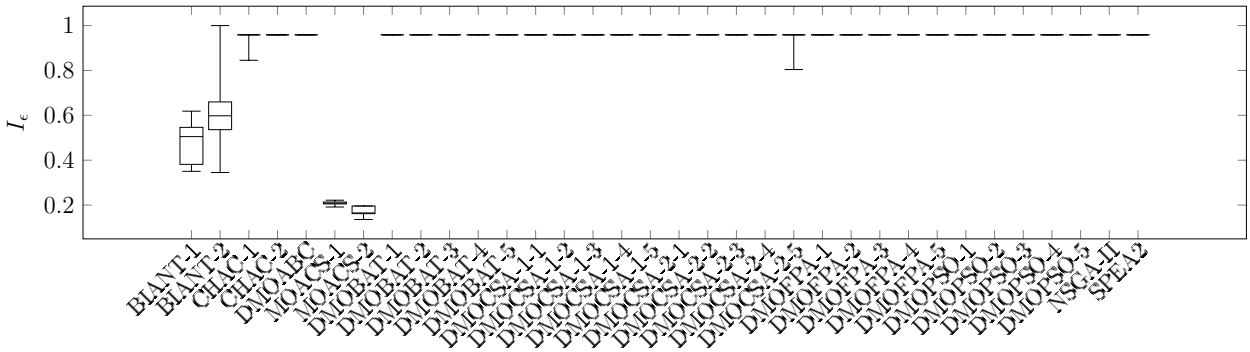

Figure C.35: Boxplot for I_ϵ: Gunther-1

Table C.29: Median and interquartile range of I_Δ obtained by the optimisers for the Gunther problems

	Gunther-1 $\tilde{x} \pm IQR(x)$		Gunther-2 $\tilde{x} \pm IQR(x)$		Gunther-3 $\tilde{x} \pm IQR(x)$		Gunther-4 $\tilde{x} \pm IQR(x)$		Gunther-5 $\tilde{x} \pm IQR(x)$	
BIANT-1	0.62	0.05	0.54	0.12	0.52	0.05	0.56	0.11	0.59	0.07
BIANT-2	0.63	0.14	0.66	0.12	0.66	0.04	0.58	0.09	0.53	0.07
CHAC-1	0.76	0.05	0.83	0.05	0.78	0.04	0.82	0.11	0.85	0.08
CHAC-2	0.74	0.06	0.83	0.08	0.81	0.07	0.81	0.07	0.90	0.01
DMOABC	0.79	0.08	0.84	0.06	0.83	0.14	0.86	0.07	0.89	0.01
DMOCSA-1-1	0.82	0.06	0.81	0.05	0.83	0.03	0.86	0.09	0.89	0.01
DMOCSA-1-2	0.74	0.03	0.83	0.07	0.79	0.01	0.89	0.08	0.90	0.03
DMOCSA-1-3	0.80	0.03	0.78	0.05	0.84	0.07	0.83	0.05	0.83	0.08
DMOCSA-1-4	0.79	0.03	0.84	0.10	0.84	0.04	0.83	0.08	0.90	0.02
DMOCSA-1-5	0.81	0.02	0.86	0.05	0.78	0.03	0.88	0.06	0.85	0.05
DMOCSA-2-1	0.81	0.05	0.79	0.13	0.80	0.04	0.85	0.03	0.88	0.03
DMOCSA-2-2	0.75	0.04	0.80	0.07	0.83	0.11	0.87	0.03	0.89	0.03
DMOCSA-2-3	0.80	0.06	0.81	0.06	0.78	0.08	0.83	0.05	0.87	0.04
DMOCSA-2-4	0.76	0.02	0.78	0.09	0.82	0.12	0.84	0.04	0.82	0.06
DMOCSA-2-5	0.74	0.06	0.82	0.05	0.81	0.04	0.88	0.06	0.89	0.06
DMOFPA-1	0.77	0.02	0.80	0.11	0.77	0.09	0.84	0.07	0.88	0.11
DMOFPA-2	0.75	0.03	0.79	0.02	0.85	0.06	0.86	0.01	0.85	0.02
DMOFPA-3	0.77	0.05	0.82	0.03	0.80	0.07	0.86	0.02	0.89	0.05
DMOFPA-4	0.74	0.07	0.87	0.03	0.79	0.10	0.79	0.03	0.86	0.07
DMOFPA-5	0.73	0.07	0.83	0.05	0.84	0.03	0.81	0.03	0.85	0.08
MOACS-1	0.54	0.02	0.54	0.15	0.56	0.11	0.49	0.02	0.60	0.06
MOACS-2	0.47	0.19	0.51	0.06	0.55	0.07	0.52	0.10	0.56	0.05
DMOBAT-1	0.81	0.11	0.85	0.02	0.82	0.04	0.76	0.06	0.86	0.06
DMOBAT-2	0.71	0.06	0.84	0.05	0.82	0.09	0.84	0.09	0.86	0.10
DMOBAT-3	0.79	0.04	0.84	0.10	0.76	0.04	0.87	0.08	0.87	0.07
DMOBAT-4	0.72	0.07	0.80	0.08	0.81	0.02	0.86	0.07	0.86	0.02
DMOBAT-5	0.82	0.07	0.77	0.07	0.89	0.11	0.82	0.07	0.79	0.05
DMOPSO-1	0.81	0.04	0.79	0.04	0.80	0.04	0.82	0.10	0.86	0.06
DMOPSO-2	0.77	0.09	0.85	0.14	0.84	0.03	0.80	0.04	0.88	0.03
DMOPSO-3	0.81	0.04	0.82	0.02	0.81	0.04	0.85	0.11	0.83	0.12
DMOPSO-4	0.79	0.06	0.80	0.04	0.82	0.08	0.80	0.03	0.84	0.05
DMOPSO-5	0.79	0.08	0.80	0.06	0.80	0.11	0.83	0.09	0.82	0.07
NSGA-II	0.86	0.01	0.87	0.04	0.90	0.05	0.89	0.02	0.88	0.04
SPEA2	0.85	0.08	0.85	0.01	0.85	0.04	0.91	0.03	0.86	0.07

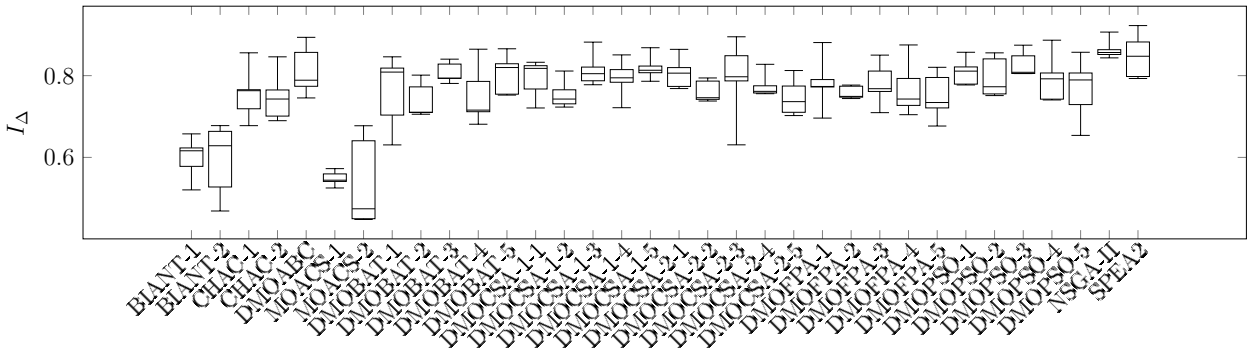

Figure C.36: Boxplot for I_Δ: Gunther-1

Table C.30: Median and interquartile range of the computation time required by the optimisers for the Gunther problems

	Gunther-1 $\tilde{x} \pm IQR(x)$		Gunther-2 $\tilde{x} \pm IQR(x)$		Gunther-3 $\tilde{x} \pm IQR(x)$		Gunther-4 $\tilde{x} \pm IQR(x)$		Gunther-5 $\tilde{x} \pm IQR(x)$	
BIANT-1	0.58	0.23	0.70	0.14	0.86	0.37	0.72	0.10	0.72	0.12
BIANT-2	0.87	0.40	0.92	0.22	0.93	0.22	1.00	0.14	1.00	0.00
CHAC-1	0.24	0.24	0.47	0.31	0.38	0.28	0.47	0.07	0.42	0.05
CHAC-2	0.28	0.04	0.54	0.40	0.36	0.05	0.44	0.14	0.33	0.03
DMOABC	0.34	0.26	0.50	0.07	0.54	0.16	0.50	0.34	0.56	0.27
DMOCSA-1-1	0.28	0.07	0.46	0.25	0.43	0.22	0.34	0.22	0.25	0.05
DMOCSA-1-2	0.25	0.11	0.34	0.02	0.36	0.22	0.35	0.14	0.32	0.12
DMOCSA-1-3	0.30	0.05	0.25	0.07	0.36	0.03	0.48	0.22	0.29	0.13
DMOCSA-1-4	0.24	0.06	0.28	0.12	0.23	0.09	0.25	0.21	0.28	0.16
DMOCSA-1-5	0.20	0.19	0.34	0.17	0.38	0.11	0.28	0.18	0.36	0.04
DMOCSA-2-1	0.34	0.13	0.43	0.26	0.28	0.13	0.48	0.19	0.46	0.09
DMOCSA-2-2	0.21	0.01	0.40	0.16	0.43	0.17	0.48	0.17	0.27	0.09
DMOCSA-2-3	0.34	0.15	0.49	0.15	0.58	0.36	0.49	0.21	0.40	0.12
DMOCSA-2-4	0.18	0.31	0.46	0.05	0.35	0.10	0.48	0.06	0.32	0.24
DMOCSA-2-5	0.28	0.20	0.56	0.47	0.50	0.07	0.51	0.24	0.40	0.04
DMOFPA-1	0.18	0.18	0.44	0.15	0.44	0.31	0.40	0.21	0.25	0.07
DMOFPA-2	0.29	0.12	0.43	0.13	0.35	0.29	0.39	0.03	0.32	0.06
DMOFPA-3	0.22	0.11	0.31	0.17	0.25	0.20	0.41	0.13	0.39	0.18
DMOFPA-4	0.17	0.13	0.26	0.15	0.28	0.09	0.25	0.11	0.17	0.16
DMOFPA-5	0.29	0.25	0.38	0.23	0.28	0.29	0.47	0.38	0.32	0.09
MOACS-1	0.47	0.43	0.41	0.21	0.57	0.21	0.48	0.31	0.32	0.13
MOACS-2	0.34	0.10	0.43	0.23	0.43	0.20	0.71	0.48	0.29	0.07
DMOBAT-1	0.28	0.22	0.47	0.29	0.29	0.03	0.38	0.08	0.25	0.10
DMOBAT-2	0.25	0.04	0.25	0.20	0.43	0.40	0.42	0.05	0.33	0.11
DMOBAT-3	0.33	0.19	0.40	0.21	0.32	0.09	0.31	0.08	0.31	0.18
DMOBAT-4	0.21	0.11	0.24	0.06	0.28	0.10	0.26	0.06	0.26	0.13
DMOBAT-5	0.28	0.21	0.29	0.05	0.33	0.16	0.30	0.15	0.49	0.08
DMOPSO-1	0.21	0.20	0.30	0.28	0.28	0.13	0.45	0.12	0.22	0.12
DMOPSO-2	0.22	0.23	0.33	0.28	0.28	0.05	0.37	0.16	0.18	0.06
DMOPSO-3	0.41	0.29	0.27	0.21	0.33	0.05	0.26	0.17	0.33	0.05
DMOPSO-4	0.23	0.08	0.71	0.49	0.46	0.09	0.42	0.09	0.39	0.17
DMOPSO-5	0.26	0.11	0.43	0.25	0.42	0.23	0.40	0.19	0.30	0.11
NSGA-II	0.23	0.21	0.37	0.11	0.39	0.18	0.43	0.14	0.31	0.11
SPEA2	0.10	0.19	0.20	0.07	0.17	0.04	0.22	0.03	0.21	0.08

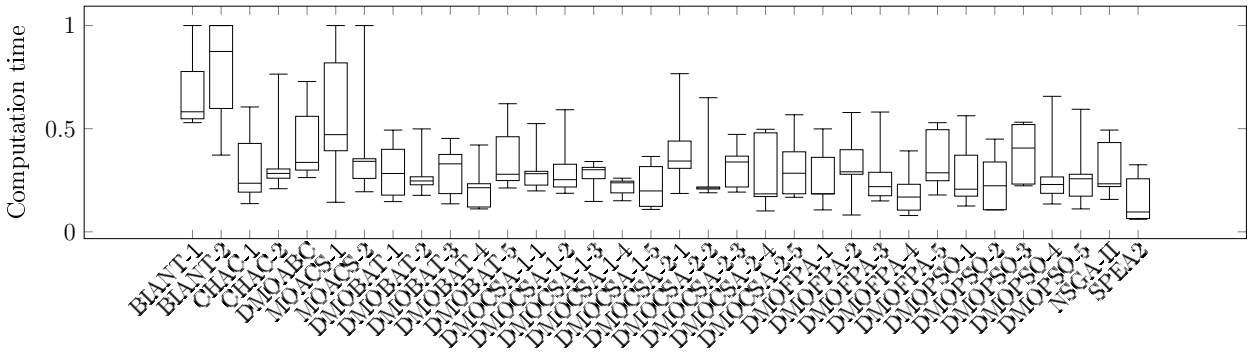

Figure C.37: Boxplot for the computation time: Gunther-1

C.3.4 Problem Family: Hahn

Table C.31: Median and interquartile range of I_{HV} obtained by the optimisers for the Hahn problems

	Hahn-1 $\tilde{x} \pm IQR(x)$		Hahn-2 $\tilde{x} \pm IQR(x)$		Hahn-3 $\tilde{x} \pm IQR(x)$		Hahn-4 $\tilde{x} \pm IQR(x)$		Hahn-5 $\tilde{x} \pm IQR(x)$	
BIANT-1	0.94	0.04	0.94	0.02	0.94	0.02	0.95	0.03	0.94	0.02
BIANT-2	0.94	0.06	0.94	0.02	0.96	0.02	0.95	0.02	0.95	0.03
CHAC-1	0.89	0.01	0.88	0.01	0.89	0.01	0.88	0.00	0.86	0.01
CHAC-2	0.88	0.01	0.88	0.00	0.88	0.01	0.87	0.00	0.85	0.01
DMOABC	0.88	0.01	0.88	0.02	0.89	0.02	0.87	0.02	0.86	0.02
DMOCSA-1-1	0.87	0.02	0.87	0.01	0.89	0.01	0.87	0.01	0.86	0.01
DMOCSA-1-2	0.87	0.01	0.87	0.02	0.88	0.02	0.88	0.01	0.86	0.02
DMOCSA-1-3	0.88	0.01	0.87	0.01	0.89	0.02	0.87	0.01	0.85	0.02
DMOCSA-1-4	0.87	0.00	0.86	0.02	0.86	0.02	0.86	0.01	0.85	0.01
DMOCSA-1-5	0.87	0.00	0.87	0.01	0.88	0.01	0.88	0.01	0.85	0.01
DMOCSA-2-1	0.88	0.01	0.88	0.00	0.89	0.02	0.87	0.00	0.86	0.01
DMOCSA-2-2	0.88	0.01	0.88	0.01	0.88	0.02	0.88	0.01	0.86	0.01
DMOCSA-2-3	0.88	0.01	0.88	0.01	0.88	0.02	0.88	0.00	0.86	0.01
DMOCSA-2-4	0.88	0.01	0.87	0.00	0.87	0.01	0.87	0.01	0.85	0.02
DMOCSA-2-5	0.87	0.01	0.87	0.00	0.89	0.01	0.87	0.00	0.86	0.03
DMOFPA-1	0.87	0.00	0.88	0.01	0.88	0.01	0.88	0.02	0.86	0.03
DMOFPA-2	0.87	0.01	0.89	0.02	0.88	0.01	0.88	0.01	0.86	0.02
DMOFPA-3	0.87	0.01	0.87	0.01	0.89	0.01	0.88	0.01	0.85	0.01
DMOFPA-4	0.86	0.02	0.87	0.01	0.86	0.01	0.87	0.01	0.84	0.01
DMOFPA-5	0.88	0.00	0.87	0.01	0.88	0.01	0.88	0.01	0.86	0.01
MOACS-1	0.90	0.01	0.91	0.01	0.91	0.01	0.91	0.01	0.91	0.02
MOACS-2	0.90	0.01	0.91	0.00	0.93	0.01	0.93	0.01	0.92	0.01
DMOBAT-1	0.88	0.01	0.88	0.02	0.88	0.02	0.87	0.01	0.86	0.02
DMOBAT-2	0.88	0.01	0.88	0.02	0.88	0.02	0.88	0.01	0.86	0.02
DMOBAT-3	0.88	0.00	0.87	0.01	0.89	0.01	0.89	0.02	0.86	0.01
DMOBAT-4	0.86	0.02	0.87	0.01	0.88	0.00	0.87	0.02	0.85	0.01
DMOBAT-5	0.88	0.01	0.87	0.01	0.88	0.02	0.88	0.00	0.87	0.02
DMOPSO-1	0.87	0.01	0.87	0.02	0.88	0.01	0.88	0.01	0.85	0.03
DMOPSO-2	0.88	0.00	0.88	0.00	0.88	0.01	0.88	0.01	0.86	0.01
DMOPSO-3	0.88	0.02	0.87	0.01	0.88	0.02	0.87	0.01	0.85	0.01
DMOPSO-4	0.86	0.03	0.88	0.02	0.87	0.02	0.87	0.02	0.84	0.01
DMOPSO-5	0.87	0.00	0.88	0.01	0.89	0.01	0.88	0.01	0.87	0.01
NSGA-II	0.88	0.01	0.89	0.02	0.89	0.02	0.89	0.01	0.86	0.01
SPEA2	0.88	0.03	0.88	0.01	0.89	0.01	0.89	0.01	0.87	0.01

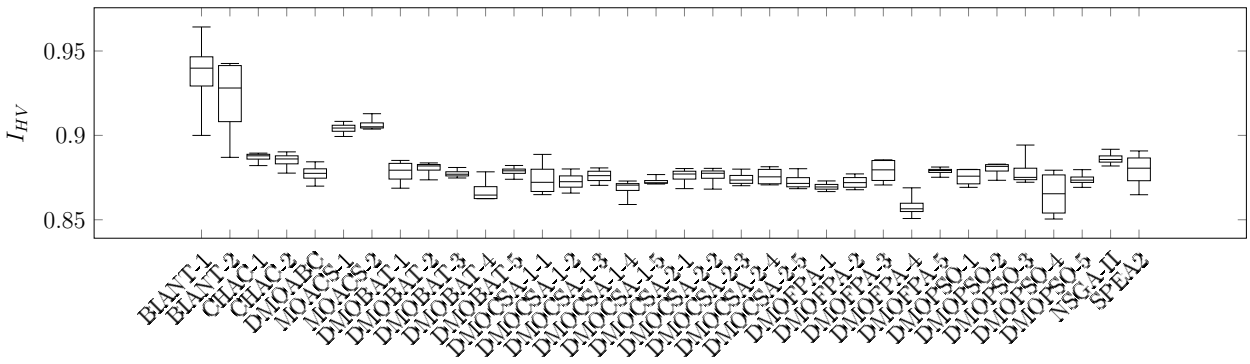

Figure C.38: Boxplot for I_{HV}: Hahn-1

Table C.32: Median and interquartile range of I_{IGD} obtained by the optimisers for the Hahn problems

	Hahn-1 $\tilde{x} \pm IQR(x)$		Hahn-2 $\tilde{x} \pm IQR(x)$		Hahn-3 $\tilde{x} \pm IQR(x)$		Hahn-4 $\tilde{x} \pm IQR(x)$		Hahn-5 $\tilde{x} \pm IQR(x)$	
BIANT-1	0.39	0.08	0.40	0.11	0.32	0.06	0.13	0.02	0.32	0.07
BIANT-2	0.48	0.22	0.35	0.05	0.34	0.05	0.15	0.00	0.30	0.08
CHAC-1	0.75	0.03	0.81	0.02	0.79	0.04	0.30	0.01	0.72	0.12
CHAC-2	0.77	0.02	0.80	0.02	0.81	0.12	0.31	0.02	0.83	0.10
DMOABC	0.82	0.06	0.80	0.04	0.74	0.10	0.33	0.01	0.77	0.01
DMOCSA-1-1	0.85	0.07	0.83	0.01	0.80	0.08	0.31	0.01	0.76	0.03
DMOCSA-1-2	0.84	0.04	0.82	0.11	0.82	0.05	0.30	0.04	0.74	0.08
DMOCSA-1-3	0.82	0.02	0.80	0.04	0.74	0.07	0.32	0.02	0.82	0.08
DMOCSA-1-4	0.89	0.05	0.89	0.04	0.91	0.01	0.35	0.02	0.82	0.07
DMOCSA-1-5	0.85	0.02	0.83	0.06	0.79	0.03	0.29	0.02	0.81	0.08
DMOCSA-2-1	0.82	0.03	0.82	0.03	0.74	0.09	0.31	0.02	0.84	0.04
DMOCSA-2-2	0.83	0.05	0.77	0.02	0.85	0.03	0.29	0.02	0.73	0.06
DMOCSA-2-3	0.84	0.03	0.81	0.06	0.79	0.14	0.31	0.03	0.77	0.03
DMOCSA-2-4	0.85	0.04	0.86	0.01	0.90	0.03	0.33	0.01	0.82	0.07
DMOCSA-2-5	0.85	0.05	0.83	0.06	0.76	0.05	0.31	0.01	0.83	0.07
DMOFPA-1	0.87	0.02	0.79	0.05	0.83	0.03	0.30	0.01	0.79	0.14
DMOFPA-2	0.86	0.02	0.80	0.02	0.82	0.05	0.31	0.01	0.77	0.08
DMOFPA-3	0.81	0.07	0.86	0.03	0.74	0.07	0.31	0.01	0.84	0.05
DMOFPA-4	0.96	0.06	0.85	0.05	0.95	0.03	0.32	0.01	0.86	0.05
DMOFPA-5	0.81	0.01	0.86	0.05	0.79	0.01	0.30	0.01	0.82	0.04
MOACS-1	0.78	0.07	0.91	0.05	0.62	0.03	0.27	0.01	0.56	0.02
MOACS-2	0.79	0.04	0.87	0.03	0.58	0.02	0.27	0.55	0.53	0.01
DMOBAT-1	0.83	0.04	0.79	0.03	0.82	0.06	0.32	0.02	0.77	0.10
DMOBAT-2	0.81	0.03	0.86	0.04	0.75	0.04	0.31	0.02	0.77	0.03
DMOBAT-3	0.82	0.03	0.85	0.03	0.77	0.08	0.29	0.03	0.76	0.04
DMOBAT-4	0.91	0.06	0.91	0.02	0.85	0.01	0.32	0.04	0.86	0.02
DMOBAT-5	0.81	0.01	0.83	0.03	0.81	0.03	0.30	0.01	0.79	0.06
DMOPSO-1	0.84	0.07	0.83	0.03	0.79	0.12	0.30	0.01	0.76	0.10
DMOPSO-2	0.80	0.02	0.79	0.03	0.81	0.04	0.31	0.01	0.75	0.05
DMOPSO-3	0.84	0.05	0.83	0.02	0.82	0.06	0.30	0.01	0.79	0.09
DMOPSO-4	0.91	0.12	0.85	0.06	0.82	0.07	0.32	0.02	0.86	0.10
DMOPSO-5	0.84	0.03	0.83	0.03	0.80	0.07	0.30	0.06	0.72	0.05
NSGA-II	0.81	0.04	0.83	0.01	0.74	0.03	0.29	0.04	0.79	0.04
SPEA2	0.84	0.11	0.83	0.01	0.85	0.02	0.30	0.00	0.79	0.04

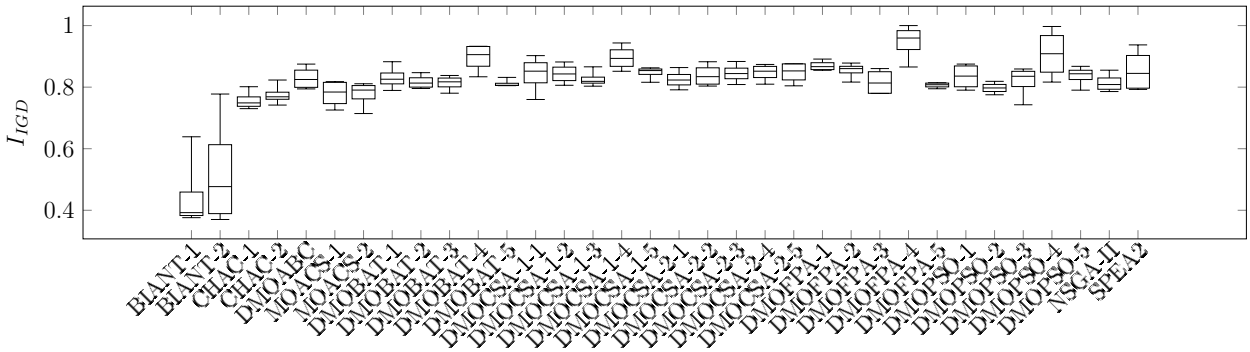

Figure C.39: Boxplot for I_{IGD}: Hahn-1

Table C.33: Median and interquartile range of I_ϵ obtained by the optimisers for the Hahn problems

	Hahn-1 $\tilde{x} \pm IQR(x)$		Hahn-2 $\tilde{x} \pm IQR(x)$		Hahn-3 $\tilde{x} \pm IQR(x)$		Hahn-4 $\tilde{x} \pm IQR(x)$		Hahn-5 $\tilde{x} \pm IQR(x)$	
BIANT-1	0.53	0.13	0.80	0.04	0.81	0.16	0.18	0.03	0.71	0.21
BIANT-2	0.66	0.43	0.84	0.14	0.69	0.05	0.16	0.05	0.56	0.21
CHAC-1	0.48	0.03	0.73	0.00	0.66	0.00	0.16	0.01	0.58	0.01
CHAC-2	0.54	0.12	0.72	0.00	0.67	0.01	0.17	0.00	0.59	0.00
DMOABC	0.61	0.03	0.72	0.01	0.66	0.00	0.17	0.00	0.57	0.01
DMOCSA-1-1	0.54	0.12	0.72	0.01	0.66	0.00	0.16	0.00	0.58	0.02
DMOCSA-1-2	0.61	0.03	0.71	0.01	0.67	0.01	0.16	0.00	0.59	0.02
DMOCSA-1-3	0.61	0.03	0.72	0.01	0.67	0.01	0.16	0.00	0.58	0.02
DMOCSA-1-4	0.61	0.03	0.73	0.02	0.67	0.01	0.16	0.00	0.58	0.00
DMOCSA-1-5	0.61	0.03	0.73	0.01	0.66	0.01	0.16	0.00	0.59	0.00
DMOCSA-2-1	0.61	0.03	0.72	0.01	0.66	0.01	0.16	0.01	0.58	0.01
DMOCSA-2-2	0.61	0.03	0.71	0.01	0.67	0.01	0.16	0.00	0.59	0.00
DMOCSA-2-3	0.61	0.00	0.72	0.00	0.65	0.01	0.16	0.00	0.58	0.01
DMOCSA-2-4	0.54	0.12	0.72	0.03	0.66	0.01	0.16	0.00	0.59	0.01
DMOCSA-2-5	0.61	0.03	0.73	0.02	0.66	0.01	0.16	0.00	0.58	0.02
DMOFPA-1	0.61	0.03	0.71	0.01	0.66	0.01	0.16	0.00	0.58	0.01
DMOFPA-2	0.61	0.03	0.72	0.00	0.66	0.00	0.16	0.01	0.58	0.00
DMOFPA-3	0.54	0.12	0.73	0.02	0.66	0.01	0.16	0.00	0.58	0.01
DMOFPA-4	0.61	0.03	0.72	0.01	0.67	0.01	0.16	0.00	0.58	0.01
DMOFPA-5	0.61	0.03	0.73	0.01	0.66	0.01	0.17	0.00	0.58	0.00
MOACS-1	0.36	0.04	0.68	0.04	0.59	0.07	0.15	0.01	0.53	0.02
MOACS-2	0.33	0.04	0.65	0.13	0.42	0.03	0.11	0.54	0.34	0.01
DMOBAT-1	0.54	0.12	0.72	0.01	0.67	0.03	0.16	0.00	0.59	0.00
DMOBAT-2	0.61	0.00	0.73	0.00	0.67	0.02	0.16	0.00	0.57	0.02
DMOBAT-3	0.61	0.00	0.73	0.01	0.66	0.01	0.16	0.00	0.59	0.00
DMOBAT-4	0.61	0.00	0.73	0.02	0.67	0.01	0.16	0.01	0.59	0.00
DMOBAT-5	0.54	0.12	0.73	0.02	0.67	0.01	0.16	0.00	0.58	0.02
DMOPSO-1	0.54	0.12	0.72	0.01	0.65	0.02	0.16	0.00	0.57	0.02
DMOPSO-2	0.61	0.03	0.72	0.02	0.66	0.01	0.16	0.01	0.58	0.00
DMOPSO-3	0.48	0.00	0.72	0.01	0.66	0.01	0.16	0.00	0.59	0.01
DMOPSO-4	0.61	0.03	0.73	0.02	0.67	0.00	0.16	0.00	0.59	0.01
DMOPSO-5	0.54	0.12	0.72	0.02	0.66	0.00	0.16	0.00	0.57	0.01
NSGA-II	0.48	0.00	0.56	0.00	0.44	0.10	0.11	0.00	0.40	0.01
SPEA2	0.61	0.00	0.62	0.13	0.44	0.00	0.11	0.00	0.40	0.00

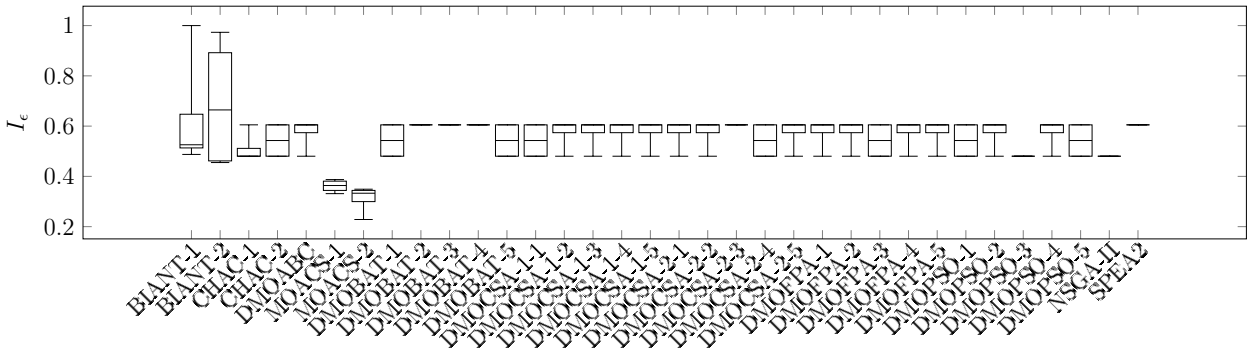

Figure C.40: Boxplot for I_ϵ: Hahn-1

Table C.34: Median and interquartile range of I_Δ obtained by the optimisers for the Hahn problems

	Hahn-1 $\tilde{x} \pm IQR(x)$		Hahn-2 $\tilde{x} \pm IQR(x)$		Hahn-3 $\tilde{x} \pm IQR(x)$		Hahn-4 $\tilde{x} \pm IQR(x)$		Hahn-5 $\tilde{x} \pm IQR(x)$	
BIANT-1	0.43	0.09	0.30	0.01	0.40	0.05	0.27	0.04	0.37	0.05
BIANT-2	0.43	0.11	0.30	0.05	0.44	0.01	0.31	0.11	0.33	0.08
CHAC-1	0.81	0.04	0.83	0.01	0.76	0.08	0.82	0.01	0.85	0.04
CHAC-2	0.69	0.04	0.83	0.05	0.82	0.03	0.87	0.06	0.85	0.09
DMOABC	0.81	0.07	0.86	0.06	0.87	0.07	0.89	0.07	0.86	0.06
DMOCSA-1-1	0.81	0.02	0.88	0.08	0.82	0.04	0.87	0.04	0.84	0.06
DMOCSA-1-2	0.79	0.07	0.87	0.04	0.86	0.03	0.84	0.03	0.85	0.05
DMOCSA-1-3	0.82	0.03	0.82	0.04	0.82	0.07	0.86	0.05	0.86	0.04
DMOCSA-1-4	0.83	0.06	0.82	0.02	0.85	0.08	0.86	0.04	0.85	0.03
DMOCSA-1-5	0.84	0.05	0.86	0.03	0.84	0.04	0.89	0.05	0.87	0.05
DMOCSA-2-1	0.82	0.08	0.82	0.02	0.79	0.01	0.90	0.06	0.90	0.03
DMOCSA-2-2	0.80	0.05	0.87	0.04	0.83	0.03	0.85	0.02	0.85	0.01
DMOCSA-2-3	0.82	0.05	0.82	0.06	0.83	0.13	0.87	0.06	0.87	0.09
DMOCSA-2-4	0.84	0.05	0.86	0.06	0.87	0.01	0.90	0.03	0.85	0.04
DMOCSA-2-5	0.84	0.05	0.85	0.10	0.76	0.05	0.88	0.04	0.89	0.04
DMOFPA-1	0.80	0.03	0.84	0.02	0.79	0.03	0.86	0.07	0.87	0.05
DMOFPA-2	0.82	0.06	0.85	0.07	0.85	0.06	0.88	0.10	0.89	0.05
DMOFPA-3	0.78	0.02	0.86	0.04	0.88	0.03	0.88	0.05	0.89	0.03
DMOFPA-4	0.84	0.07	0.90	0.04	0.86	0.02	0.90	0.03	0.87	0.03
DMOFPA-5	0.83	0.08	0.85	0.01	0.84	0.06	0.90	0.08	0.87	0.07
MOACS-1	0.36	0.03	0.42	0.05	0.41	0.04	0.39	0.03	0.32	0.03
MOACS-2	0.36	0.02	0.37	0.04	0.44	0.09	0.43	0.51	0.30	0.03
DMOBAT-1	0.85	0.06	0.85	0.05	0.84	0.03	0.89	0.05	0.87	0.06
DMOBAT-2	0.77	0.06	0.86	0.05	0.80	0.06	0.86	0.04	0.85	0.05
DMOBAT-3	0.83	0.02	0.82	0.07	0.79	0.05	0.86	0.09	0.83	0.04
DMOBAT-4	0.82	0.02	0.88	0.01	0.84	0.01	0.89	0.02	0.90	0.04
DMOBAT-5	0.84	0.05	0.89	0.03	0.84	0.03	0.86	0.03	0.84	0.03
DMOPSO-1	0.81	0.12	0.88	0.02	0.80	0.04	0.85	0.06	0.87	0.03
DMOPSO-2	0.81	0.05	0.85	0.02	0.82	0.04	0.87	0.08	0.87	0.04
DMOPSO-3	0.77	0.04	0.84	0.03	0.75	0.10	0.81	0.01	0.86	0.03
DMOPSO-4	0.81	0.05	0.84	0.03	0.84	0.06	0.91	0.03	0.88	0.05
DMOPSO-5	0.82	0.09	0.82	0.01	0.79	0.01	0.86	0.10	0.87	0.06
NSGA-II	0.88	0.11	0.88	0.02	0.85	0.02	0.90	0.03	0.89	0.04
SPEA2	0.87	0.07	0.87	0.04	0.87	0.03	0.88	0.03	0.86	0.03

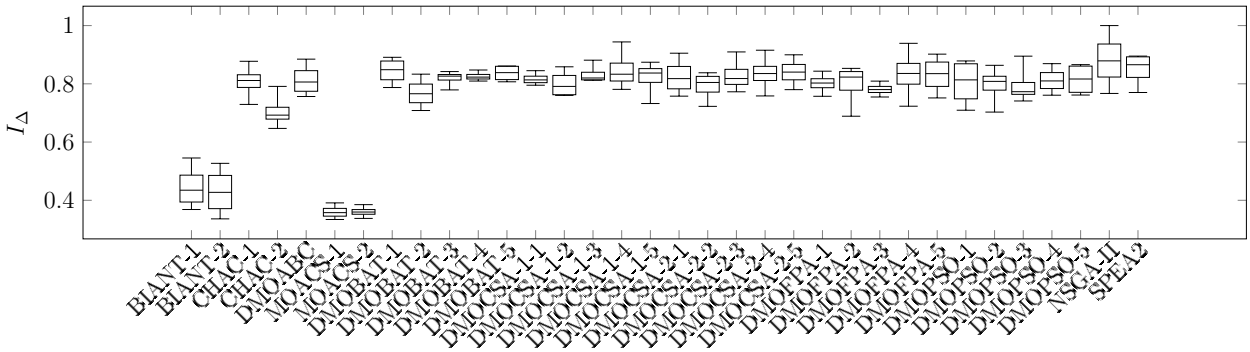

Figure C.41: Boxplot for I_Δ: Hahn-1

Table C.35: Median and interquartile range of the computation time required by the optimisers for the Hahn problems

	Hahn-1 $\tilde{x} \pm IQR(x)$		Hahn-2 $\tilde{x} \pm IQR(x)$		Hahn-3 $\tilde{x} \pm IQR(x)$		Hahn-4 $\tilde{x} \pm IQR(x)$		Hahn-5 $\tilde{x} \pm IQR(x)$	
BIANT-1	1.00	0.04	0.57	0.47	0.63	0.43	0.56	0.53	0.45	0.05
BIANT-2	0.56	0.06	0.60	0.41	1.00	0.08	1.00	0.15	0.98	0.14
CHAC-1	0.53	0.05	0.26	0.10	0.38	0.04	0.30	0.11	0.42	0.39
CHAC-2	0.56	0.12	0.32	0.11	0.27	0.08	0.26	0.05	0.31	0.12
DMOABC	0.65	0.25	0.80	0.46	0.48	0.12	0.29	0.20	0.31	0.42
DMOCSA-1-1	0.25	0.08	0.31	0.18	0.37	0.04	0.17	0.11	0.29	0.10
DMOCSA-1-2	0.31	0.13	0.32	0.23	0.27	0.06	0.27	0.08	0.34	0.22
DMOCSA-1-3	0.46	0.20	0.26	0.22	0.29	0.13	0.17	0.01	0.27	0.05
DMOCSA-1-4	0.42	0.08	0.32	0.11	0.20	0.02	0.22	0.12	0.36	0.15
DMOCSA-1-5	0.40	0.03	0.23	0.19	0.23	0.07	0.19	0.04	0.31	0.16
DMOCSA-2-1	0.47	0.11	0.36	0.31	0.43	0.19	0.20	0.09	0.53	0.24
DMOCSA-2-2	0.42	0.02	0.43	0.28	0.35	0.14	0.37	0.10	0.42	0.16
DMOCSA-2-3	0.44	0.18	0.34	0.31	0.45	0.09	0.35	0.09	0.40	0.31
DMOCSA-2-4	0.49	0.18	0.40	0.10	0.26	0.07	0.23	0.09	0.43	0.40
DMOCSA-2-5	0.46	0.46	0.30	0.20	0.34	0.16	0.29	0.11	0.45	0.51
DMOFPA-1	0.32	0.11	0.28	0.13	0.27	0.04	0.23	0.07	0.24	0.07
DMOFPA-2	0.33	0.10	0.26	0.14	0.28	0.09	0.21	0.19	0.38	0.16
DMOFPA-3	0.45	0.17	0.24	0.17	0.33	0.09	0.22	0.10	0.27	0.06
DMOFPA-4	0.26	0.08	0.23	0.14	0.15	0.08	0.26	0.16	0.21	0.09
DMOFPA-5	0.44	0.12	0.20	0.17	0.26	0.15	0.23	0.01	0.23	0.17
MOACS-1	0.55	0.03	0.30	0.12	0.31	0.06	0.31	0.08	0.59	0.37
MOACS-2	0.27	0.16	0.34	0.12	0.59	0.23	0.33	0.23	0.51	0.37
DMOBAT-1	0.34	0.15	0.33	0.09	0.30	0.02	0.16	0.10	0.29	0.03
DMOBAT-2	0.37	0.04	0.22	0.09	0.32	0.16	0.20	0.07	0.25	0.22
DMOBAT-3	0.42	0.12	0.20	0.11	0.31	0.09	0.29	0.12	0.54	0.29
DMOBAT-4	0.34	0.23	0.20	0.08	0.23	0.14	0.28	0.08	0.37	0.24
DMOBAT-5	0.45	0.13	0.26	0.18	0.23	0.07	0.20	0.12	0.35	0.23
DMOPSO-1	0.36	0.09	0.44	0.45	0.41	0.04	0.21	0.10	0.24	0.30
DMOPSO-2	0.39	0.13	0.27	0.18	0.22	0.04	0.18	0.09	0.27	0.06
DMOPSO-3	0.47	0.17	0.38	0.25	0.31	0.07	0.24	0.11	0.29	0.12
DMOPSO-4	0.30	0.23	0.43	0.13	0.31	0.48	0.32	0.15	0.48	0.38
DMOPSO-5	0.35	0.19	0.28	0.09	0.29	0.01	0.23	0.02	0.23	0.25
NSGA-II	0.43	0.14	0.29	0.09	0.22	0.05	0.29	0.07	0.25	0.17
SPEA2	0.16	0.07	0.12	0.04	0.13	0.07	0.11	0.03	0.14	0.04

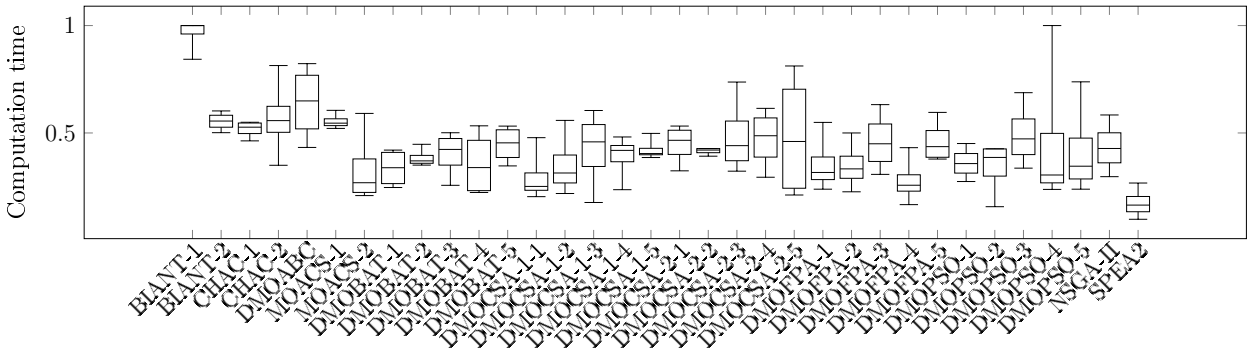

Figure C.42: Boxplot for the computation time: Hahn-1

C.3.5 Problem Family: Jackson

Table C.36: Median and interquartile range of I_{HV} obtained by the optimisers for the Jackson problems

	Jackson-1 $\tilde{x} \pm IQR(x)$		Jackson-2 $\tilde{x} \pm IQR(x)$		Jackson-3 $\tilde{x} \pm IQR(x)$		Jackson-4 $\tilde{x} \pm IQR(x)$		Jackson-5 $\tilde{x} \pm IQR(x)$	
BIANT-1	0.50	0.00	0.53	0.00	0.60	0.00	0.92	0.00	0.36	0.00
BIANT-2	0.50	0.00	0.54	0.00	0.63	0.00	0.89	0.00	0.36	0.00
CHAC-1	0.57	0.00	0.60	0.00	0.64	0.00	0.97	0.00	0.38	0.00
CHAC-2	0.57	0.00	0.60	0.00	0.64	0.00	1.00	0.00	0.38	0.00
DMOABC	0.57	0.00	0.60	0.00	0.64	0.00	0.97	0.00	0.38	0.00
DMOCSA-1-1	0.57	0.00	0.60	0.00	0.64	0.00	0.97	0.00	0.38	0.00
DMOCSA-1-2	0.57	0.00	0.60	0.00	0.64	0.00	1.00	0.00	0.38	0.00
DMOCSA-1-3	0.57	0.00	0.60	0.00	0.64	0.00	0.97	0.00	0.38	0.00
DMOCSA-1-4	0.57	0.00	0.59	0.00	0.63	0.00	0.96	0.00	0.37	0.00
DMOCSA-1-5	0.57	0.00	0.60	0.00	0.64	0.00	0.97	0.00	0.38	0.00
DMOCSA-2-1	0.57	0.00	0.60	0.00	0.64	0.00	0.99	0.00	0.38	0.00
DMOCSA-2-2	0.57	0.00	0.60	0.00	0.64	0.00	0.99	0.00	0.38	0.00
DMOCSA-2-3	0.57	0.00	0.60	0.00	0.64	0.00	0.99	0.00	0.38	0.00
DMOCSA-2-4	0.57	0.00	0.60	0.00	0.63	0.00	0.97	0.00	0.37	0.00
DMOCSA-2-5	0.57	0.00	0.60	0.00	0.64	0.00	0.98	0.00	0.38	0.00
DMOFPA-1	0.57	0.00	0.60	0.00	0.64	0.00	0.97	0.00	0.38	0.00
DMOFPA-2	0.57	0.00	0.60	0.00	0.64	0.00	0.98	0.00	0.38	0.00
DMOFPA-3	0.57	0.00	0.60	0.00	0.64	0.00	0.97	0.00	0.38	0.00
DMOFPA-4	0.57	0.00	0.60	0.00	0.63	0.00	0.97	0.00	0.37	0.00
DMOFPA-5	0.57	0.00	0.60	0.00	0.64	0.00	0.97	0.00	0.38	0.00
MOACS-1	0.52	0.00	0.55	0.00	0.62	0.00	0.92	0.00	0.36	0.00
MOACS-2	0.52	0.00	0.54	0.00	0.62	0.00	0.90	0.00	0.36	0.00
DMOBAT-1	0.57	0.00	0.60	0.00	0.64	0.00	0.99	0.00	0.38	0.00
DMOBAT-2	0.57	0.00	0.60	0.00	0.64	0.00	1.00	0.00	0.38	0.00
DMOBAT-3	0.57	0.00	0.60	0.00	0.64	0.00	1.00	0.00	0.38	0.00
DMOBAT-4	0.57	0.00	0.60	0.00	0.63	0.00	0.97	0.00	0.37	0.00
DMOBAT-5	0.57	0.00	0.60	0.00	0.64	0.00	1.00	0.00	0.38	0.00
DMOPSO-1	0.57	0.00	0.60	0.00	0.64	0.00	0.97	0.00	0.38	0.00
DMOPSO-2	0.57	0.00	0.60	0.00	0.64	0.00	0.98	0.00	0.38	0.00
DMOPSO-3	0.57	0.00	0.60	0.00	0.64	0.00	0.97	0.00	0.38	0.00
DMOPSO-4	0.57	0.00	0.60	0.00	0.63	0.00	0.97	0.00	0.37	0.00
DMOPSO-5	0.57	0.00	0.60	0.00	0.64	0.00	0.98	0.00	0.38	0.00
NSGA-II	0.57	0.00	0.60	0.00	0.64	0.00	0.97	0.00	0.38	0.00
SPEA2	0.57	0.00	0.60	0.00	0.64	0.00	0.97	0.00	0.38	0.00

Table C.37: Median and interquartile range of I_{IGD} obtained by the optimisers for the Jackson problems

	Jackson-1 $\tilde{x} \pm IQR(x)$		Jackson-2 $\tilde{x} \pm IQR(x)$		Jackson-3 $\tilde{x} \pm IQR(x)$		Jackson-4 $\tilde{x} \pm IQR(x)$		Jackson-5 $\tilde{x} \pm IQR(x)$	
BIANT-1	0.99	0.00	0.95	0.13	0.75	0.14	0.46	0.25	0.96	0.00
BIANT-2	0.99	0.00	0.81	0.17	0.74	0.00	0.65	0.20	0.96	0.00
CHAC-1	0.99	0.00	0.73	0.00	0.73	0.00	0.17	0.00	1.00	0.00
CHAC-2	0.99	0.00	0.73	0.00	0.73	0.00	0.03	0.00	1.00	0.00
DMOABC	0.99	0.00	0.73	0.00	0.73	0.00	0.17	0.01	1.00	0.00
DMOCSA-1-1	0.99	0.00	0.73	0.00	0.73	0.00	0.17	0.15	1.00	0.00
DMOCSA-1-2	0.99	0.00	0.73	0.00	0.73	0.00	0.02	0.02	1.00	0.00
DMOCSA-1-3	0.99	0.00	0.73	0.00	0.73	0.00	0.17	0.00	1.00	0.00
DMOCSA-1-4	0.99	0.00	0.73	0.00	0.73	0.00	0.18	0.06	1.00	0.00
DMOCSA-1-5	0.99	0.00	0.73	0.00	0.73	0.00	0.17	0.14	1.00	0.00
DMOCSA-2-1	0.99	0.00	0.73	0.00	0.73	0.00	0.17	0.14	1.00	0.00
DMOCSA-2-2	0.99	0.00	0.73	0.00	0.73	0.00	0.04	0.14	1.00	0.00
DMOCSA-2-3	0.99	0.00	0.73	0.00	0.73	0.00	0.17	0.14	1.00	0.00
DMOCSA-2-4	0.99	0.00	0.73	0.00	0.73	0.00	0.18	0.07	1.00	0.00
DMOCSA-2-5	0.99	0.00	0.73	0.00	0.73	0.00	0.17	0.00	1.00	0.00
DMOFPA-1	0.99	0.00	0.73	0.00	0.73	0.00	0.17	0.00	1.00	0.00
DMOFPA-2	0.99	0.00	0.73	0.00	0.73	0.00	0.17	0.14	1.00	0.00
DMOFPA-3	0.99	0.00	0.73	0.00	0.73	0.00	0.17	0.00	1.00	0.00
DMOFPA-4	0.99	0.00	0.73	0.00	0.73	0.00	0.18	0.06	1.00	0.00
DMOFPA-5	0.99	0.00	0.73	0.00	0.73	0.00	0.17	0.00	1.00	0.00
MOACS-1	0.99	0.00	0.78	0.00	0.75	0.00	0.30	0.14	0.96	0.00
MOACS-2	0.99	0.01	0.80	0.02	0.74	0.00	0.42	0.18	0.96	0.04
DMOBAT-1	0.99	0.00	0.73	0.00	0.73	0.00	0.04	0.14	1.00	0.00
DMOBAT-2	0.99	0.00	0.73	0.00	0.73	0.00	0.02	0.04	1.00	0.00
DMOBAT-3	0.99	0.00	0.73	0.00	0.73	0.00	0.04	0.17	1.00	0.00
DMOBAT-4	0.99	0.00	0.73	0.00	0.73	0.00	0.18	0.01	1.00	0.00
DMOBAT-5	0.99	0.00	0.73	0.00	0.73	0.00	0.02	0.01	1.00	0.00
DMOPSO-1	0.99	0.00	0.73	0.00	0.73	0.00	0.17	0.14	1.00	0.00
DMOPSO-2	0.99	0.00	0.73	0.00	0.73	0.00	0.17	0.01	1.00	0.00
DMOPSO-3	0.99	0.00	0.73	0.00	0.73	0.00	0.17	0.01	1.00	0.00
DMOPSO-4	0.99	0.00	0.73	0.00	0.73	0.00	0.18	0.00	1.00	0.00
DMOPSO-5	0.99	0.00	0.73	0.00	0.73	0.00	0.18	0.01	1.00	0.00
NSGA-II	0.99	0.00	0.73	0.00	0.73	0.00	0.17	0.00	1.00	0.00
SPEA2	0.99	0.00	0.73	0.00	0.73	0.00	0.17	0.01	1.00	0.00

Table C.38: Median and interquartile range of I_ϵ obtained by the optimisers for the Jackson problems

	Jackson-1 $\tilde{x} \pm IQR(x)$		Jackson-2 $\tilde{x} \pm IQR(x)$		Jackson-3 $\tilde{x} \pm IQR(x)$		Jackson-4 $\tilde{x} \pm IQR(x)$		Jackson-5 $\tilde{x} \pm IQR(x)$	
BIANT-1	0.93	0.05	0.90	0.76	0.53	0.00	0.38	0.37	0.76	0.00
BIANT-2	0.97	0.04	0.22	0.66	0.53	0.00	0.38	0.37	0.76	0.00
CHAC-1	0.17	0.00	0.19	0.00	0.44	0.00	0.17	0.00	0.76	0.00
CHAC-2	0.17	0.00	0.19	0.00	0.44	0.00	0.13	0.00	0.76	0.00
DMOABC	0.17	0.00	0.19	0.00	0.44	0.00	0.17	0.00	0.76	0.00
DMOCSA-1-1	0.17	0.00	0.19	0.00	0.44	0.00	0.17	0.04	0.76	0.00
DMOCSA-1-2	0.17	0.00	0.19	0.00	0.44	0.00	0.13	0.00	0.76	0.00
DMOCSA-1-3	0.17	0.00	0.19	0.00	0.44	0.00	0.17	0.00	0.76	0.00
DMOCSA-1-4	0.17	0.00	0.19	0.00	0.48	0.00	0.17	0.00	0.76	0.00
DMOCSA-1-5	0.17	0.00	0.19	0.00	0.44	0.00	0.17	0.04	0.76	0.00
DMOCSA-2-1	0.17	0.00	0.19	0.00	0.44	0.00	0.17	0.04	0.76	0.00
DMOCSA-2-2	0.17	0.00	0.19	0.00	0.44	0.00	0.13	0.04	0.76	0.00
DMOCSA-2-3	0.17	0.00	0.19	0.00	0.44	0.00	0.17	0.04	0.76	0.00
DMOCSA-2-4	0.17	0.00	0.19	0.00	0.48	0.03	0.17	0.00	0.76	0.00
DMOCSA-2-5	0.17	0.00	0.19	0.00	0.44	0.00	0.17	0.00	0.76	0.00
DMOFPA-1	0.17	0.00	0.19	0.00	0.44	0.00	0.17	0.00	0.76	0.00
DMOFPA-2	0.17	0.00	0.19	0.00	0.44	0.00	0.17	0.04	0.76	0.00
DMOFPA-3	0.17	0.00	0.19	0.00	0.44	0.00	0.17	0.00	0.76	0.00
DMOFPA-4	0.17	0.00	0.19	0.00	0.45	0.01	0.17	0.00	0.76	0.00
DMOFPA-5	0.17	0.00	0.19	0.00	0.44	0.00	0.17	0.00	0.76	0.00
MOACS-1	0.20	0.00	0.22	0.00	0.53	0.05	0.17	0.01	0.76	0.00
MOACS-2	0.20	0.02	0.22	0.00	0.73	0.27	0.18	0.02	0.86	0.00
DMOBAT-1	0.17	0.00	0.19	0.00	0.44	0.00	0.13	0.04	0.76	0.00
DMOBAT-2	0.17	0.00	0.19	0.00	0.44	0.00	0.13	0.00	0.76	0.00
DMOBAT-3	0.17	0.00	0.19	0.00	0.44	0.00	0.13	0.04	0.76	0.00
DMOBAT-4	0.17	0.00	0.19	0.00	0.48	0.04	0.17	0.00	0.76	0.00
DMOBAT-5	0.17	0.00	0.19	0.00	0.44	0.00	0.13	0.00	0.76	0.00
DMOPSO-1	0.17	0.00	0.19	0.00	0.44	0.00	0.17	0.04	0.76	0.00
DMOPSO-2	0.17	0.00	0.19	0.00	0.44	0.00	0.17	0.00	0.76	0.00
DMOPSO-3	0.17	0.00	0.19	0.00	0.44	0.00	0.17	0.00	0.76	0.00
DMOPSO-4	0.17	0.00	0.19	0.00	0.44	0.04	0.17	0.00	0.76	0.00
DMOPSO-5	0.17	0.00	0.19	0.00	0.44	0.00	0.17	0.00	0.76	0.00
NSGA-II	0.17	0.00	0.19	0.00	0.44	0.00	0.17	0.00	0.76	0.00
SPEA2	0.17	0.00	0.19	0.00	0.44	0.00	0.17	0.00	0.76	0.00

Table C.39: Median and interquartile range of I_Δ obtained by the optimisers for the Jackson problems

	Jackson-1 $\tilde{x} \pm IQR(x)$		Jackson-2 $\tilde{x} \pm IQR(x)$		Jackson-3 $\tilde{x} \pm IQR(x)$		Jackson-4 $\tilde{x} \pm IQR(x)$		Jackson-5 $\tilde{x} \pm IQR(x)$	
BIANT-1	0.92	0.00	0.89	0.05	0.78	0.04	0.76	0.07	0.87	0.00
BIANT-2	0.94	0.03	0.87	0.03	0.83	0.01	0.82	0.10	0.87	0.04
CHAC-1	1.00	0.00	0.99	0.00	0.85	0.01	0.84	0.07	0.66	0.00
CHAC-2	1.00	0.00	0.99	0.00	0.85	0.01	0.80	0.00	0.66	0.00
DMOABC	1.00	0.00	0.99	0.00	0.85	0.00	0.84	0.05	0.66	0.00
DMOCSA-1-1	1.00	0.00	0.99	0.00	0.86	0.01	0.86	0.01	0.66	0.00
DMOCSA-1-2	1.00	0.00	0.99	0.00	0.87	0.01	0.86	0.02	0.66	0.00
DMOCSA-1-3	1.00	0.00	0.99	0.00	0.85	0.00	0.87	0.01	0.66	0.00
DMOCSA-1-4	0.98	0.00	0.94	0.02	0.85	0.05	0.85	0.04	0.69	0.02
DMOCSA-1-5	1.00	0.00	0.99	0.00	0.86	0.02	0.87	0.10	0.66	0.00
DMOCSA-2-1	1.00	0.00	0.99	0.00	0.86	0.01	0.90	0.03	0.66	0.00
DMOCSA-2-2	1.00	0.00	0.99	0.00	0.86	0.02	0.87	0.03	0.66	0.00
DMOCSA-2-3	1.00	0.00	0.99	0.00	0.85	0.02	0.84	0.04	0.66	0.00
DMOCSA-2-4	0.99	0.01	0.99	0.02	0.82	0.00	0.85	0.04	0.70	0.06
DMOCSA-2-5	1.00	0.00	0.99	0.00	0.86	0.01	0.84	0.04	0.66	0.00
DMOFPA-1	1.00	0.00	0.99	0.00	0.86	0.01	0.86	0.03	0.66	0.00
DMOFPA-2	1.00	0.00	0.99	0.00	0.85	0.00	0.87	0.07	0.66	0.00
DMOFPA-3	1.00	0.00	0.99	0.00	0.87	0.02	0.87	0.03	0.66	0.00
DMOFPA-4	0.99	0.02	0.98	0.01	0.83	0.08	0.81	0.04	0.70	0.02
DMOFPA-5	1.00	0.00	0.99	0.00	0.86	0.01	0.87	0.00	0.66	0.00
MOACS-1	0.92	0.02	0.89	0.03	0.72	0.02	0.67	0.15	0.96	0.00
MOACS-2	0.89	0.05	0.86	0.05	0.70	0.07	0.83	0.18	0.95	0.01
DMOBAT-1	1.00	0.00	0.99	0.00	0.86	0.00	0.84	0.07	0.66	0.00
DMOBAT-2	1.00	0.00	0.99	0.00	0.86	0.01	0.80	0.07	0.66	0.00
DMOBAT-3	1.00	0.00	0.99	0.00	0.86	0.01	0.84	0.08	0.66	0.00
DMOBAT-4	1.00	0.00	0.98	0.04	0.85	0.01	0.81	0.04	0.66	0.02
DMOBAT-5	1.00	0.00	0.99	0.00	0.86	0.01	0.86	0.00	0.66	0.00
DMOPSO-1	1.00	0.00	0.99	0.00	0.85	0.00	0.87	0.10	0.66	0.00
DMOPSO-2	1.00	0.00	0.99	0.00	0.86	0.01	0.87	0.05	0.66	0.00
DMOPSO-3	1.00	0.00	0.99	0.00	0.86	0.01	0.87	0.03	0.66	0.00
DMOPSO-4	1.00	0.00	0.99	0.01	0.84	0.05	0.87	0.04	0.71	0.33
DMOPSO-5	1.00	0.00	0.99	0.00	0.87	0.01	0.84	0.03	0.66	0.00
NSGA-II	1.00	0.00	0.99	0.00	0.85	0.01	0.90	0.10	0.66	0.00
SPEA2	1.00	0.00	0.99	0.00	0.86	0.01	0.84	0.07	0.66	0.00

Table C.40: Median and interquartile range of the computation time required by the optimisers for the Jackson problems

	Jackson-1 $\tilde{x} \pm IQR(x)$		Jackson-2 $\tilde{x} \pm IQR(x)$		Jackson-3 $\tilde{x} \pm IQR(x)$		Jackson-4 $\tilde{x} \pm IQR(x)$		Jackson-5 $\tilde{x} \pm IQR(x)$	
BIANT-1	0.84	0.08	0.84	0.06	0.90	0.08	0.91	0.17	1.00	0.05
BIANT-2	0.78	0.13	0.83	0.05	0.91	0.09	0.95	0.04	0.97	0.05
CHAC-1	0.62	0.04	0.69	0.02	0.80	0.08	0.71	0.13	0.80	0.03
CHAC-2	0.61	0.03	0.66	0.02	0.80	0.10	0.70	0.12	0.80	0.04
DMOABC	0.71	0.02	0.76	0.03	0.89	0.11	0.82	0.13	0.91	0.03
DMOCSA-1-1	0.59	0.03	0.64	0.02	0.76	0.08	0.68	0.12	0.77	0.05
DMOCSA-1-2	0.59	0.01	0.64	0.01	0.77	0.08	0.68	0.12	0.75	0.02
DMOCSA-1-3	0.61	0.03	0.65	0.02	0.77	0.11	0.68	0.13	0.75	0.04
DMOCSA-1-4	0.59	0.04	0.62	0.02	0.76	0.00	0.66	0.13	0.73	0.03
DMOCSA-1-5	0.57	0.02	0.62	0.04	0.71	0.11	0.64	0.12	0.73	0.01
DMOCSA-2-1	0.61	0.03	0.66	0.01	0.79	0.08	0.71	0.14	0.79	0.04
DMOCSA-2-2	0.60	0.04	0.64	0.01	0.77	0.08	0.68	0.11	0.74	0.03
DMOCSA-2-3	0.65	0.03	0.69	0.01	0.83	0.10	0.72	0.13	0.79	0.05
DMOCSA-2-4	0.60	0.03	0.65	0.02	0.79	0.04	0.70	0.12	0.79	0.05
DMOCSA-2-5	0.62	0.03	0.67	0.03	0.81	0.08	0.72	0.13	0.80	0.04
DMOFPA-1	0.59	0.01	0.63	0.02	0.74	0.08	0.67	0.11	0.75	0.02
DMOFPA-2	0.60	0.03	0.64	0.02	0.79	0.08	0.70	0.10	0.80	0.08
DMOFPA-3	0.61	0.03	0.66	0.02	0.80	0.08	0.71	0.12	0.77	0.03
DMOFPA-4	0.30	0.06	0.34	0.01	0.37	0.37	0.33	0.04	0.35	0.02
DMOFPA-5	0.61	0.04	0.65	0.02	0.76	0.12	0.69	0.08	0.78	0.01
MOACS-1	0.82	0.06	0.87	0.08	0.91	0.00	0.83	0.14	0.91	0.04
MOACS-2	1.00	0.11	1.00	0.00	0.94	0.10	1.00	0.15	0.94	0.04
DMOBAT-1	0.58	0.04	0.63	0.01	0.74	0.08	0.66	0.12	0.74	0.02
DMOBAT-2	0.61	0.06	0.64	0.03	0.79	0.02	0.68	0.12	0.76	0.05
DMOBAT-3	0.62	0.04	0.67	0.01	0.80	0.08	0.71	0.12	0.77	0.03
DMOBAT-4	0.61	0.09	0.65	0.02	0.81	0.19	0.70	0.06	0.78	0.06
DMOBAT-5	0.60	0.02	0.65	0.01	0.79	0.09	0.70	0.11	0.78	0.04
DMOPSO-1	0.57	0.10	0.62	0.18	0.67	0.21	0.55	0.19	0.67	0.17
DMOPSO-2	0.58	0.03	0.62	0.01	0.74	0.09	0.67	0.12	0.75	0.05
DMOPSO-3	0.44	0.04	0.47	0.04	0.55	0.08	0.46	0.06	0.50	0.05
DMOPSO-4	0.51	0.02	0.56	0.09	0.76	0.13	0.54	0.05	0.60	0.01
DMOPSO-5	0.59	0.03	0.64	0.04	0.77	0.08	0.69	0.12	0.77	0.04
NSGA-II	0.83	0.04	0.91	0.03	0.97	0.13	0.91	0.16	0.91	0.04
SPEA2	0.53	0.03	0.56	0.01	0.69	0.07	0.62	0.10	0.73	0.03

C.3.6 Problem Family: Lutz1

Table C.41: Median and interquartile range of I_{HV} obtained by the optimisers for the Lutz1 problems

	Lutz1-1 $\tilde{x} \pm IQR(x)$		Lutz1-2 $\tilde{x} \pm IQR(x)$		Lutz1-3 $\tilde{x} \pm IQR(x)$		Lutz1-4 $\tilde{x} \pm IQR(x)$		Lutz1-5 $\tilde{x} \pm IQR(x)$	
BIANT-1	0.94	0.00	0.95	0.02	0.90	0.07	0.91	0.03	0.86	0.07
BIANT-2	0.94	0.00	0.94	0.15	0.86	0.03	0.87	0.14	0.88	0.04
CHAC-1	1.00	0.00	1.00	0.00	1.00	0.00	1.00	0.00	1.00	0.00
CHAC-2	1.00	0.00	1.00	0.00	1.00	0.00	1.00	0.00	1.00	0.00
DMOABC	1.00	0.00	1.00	0.00	1.00	0.00	1.00	0.00	1.00	0.00
DMOCSA-1-1	1.00	0.00	1.00	0.00	1.00	0.00	1.00	0.00	1.00	0.00
DMOCSA-1-2	1.00	0.00	1.00	0.00	1.00	0.00	1.00	0.00	1.00	0.00
DMOCSA-1-3	1.00	0.00	1.00	0.00	1.00	0.00	1.00	0.00	1.00	0.00
DMOCSA-1-4	1.00	0.00	1.00	0.00	0.99	0.01	1.00	0.00	0.99	0.01
DMOCSA-1-5	1.00	0.00	1.00	0.00	1.00	0.00	1.00	0.00	1.00	0.00
DMOCSA-2-1	1.00	0.00	1.00	0.00	1.00	0.00	1.00	0.00	1.00	0.00
DMOCSA-2-2	1.00	0.00	1.00	0.00	1.00	0.00	1.00	0.00	1.00	0.00
DMOCSA-2-3	1.00	0.00	1.00	0.00	1.00	0.00	1.00	0.00	1.00	0.00
DMOCSA-2-4	1.00	0.00	1.00	0.00	1.00	0.01	1.00	0.01	1.00	0.00
DMOCSA-2-5	1.00	0.00	1.00	0.00	1.00	0.00	1.00	0.00	1.00	0.00
DMOFPA-1	1.00	0.00	1.00	0.00	1.00	0.00	1.00	0.00	1.00	0.00
DMOFPA-2	1.00	0.00	1.00	0.00	1.00	0.00	1.00	0.00	1.00	0.00
DMOFPA-3	1.00	0.00	1.00	0.00	1.00	0.00	1.00	0.00	1.00	0.00
DMOFPA-4	1.00	0.00	1.00	0.00	0.98	0.02	1.00	0.00	1.00	0.00
DMOFPA-5	1.00	0.00	1.00	0.00	1.00	0.00	1.00	0.00	1.00	0.00
MOACS-1	0.94	0.00	0.85	0.05	0.87	0.17	0.76	0.22	0.70	0.09
MOACS-2	0.94	0.00	0.85	0.13	0.74	0.08	0.79	0.06	0.81	0.11
DMOBAT-1	1.00	0.00	1.00	0.00	1.00	0.00	1.00	0.00	1.00	0.00
DMOBAT-2	1.00	0.00	1.00	0.00	1.00	0.00	1.00	0.00	1.00	0.00
DMOBAT-3	1.00	0.00	1.00	0.00	1.00	0.00	1.00	0.00	1.00	0.00
DMOBAT-4	1.00	0.00	1.00	0.00	1.00	0.00	1.00	0.00	1.00	0.00
DMOBAT-5	1.00	0.00	1.00	0.00	1.00	0.00	1.00	0.00	1.00	0.00
DMOPSO-1	1.00	0.00	1.00	0.00	1.00	0.00	1.00	0.00	1.00	0.00
DMOPSO-2	1.00	0.00	1.00	0.00	1.00	0.00	1.00	0.00	1.00	0.00
DMOPSO-3	1.00	0.00	1.00	0.00	1.00	0.00	1.00	0.00	1.00	0.00
DMOPSO-4	1.00	0.00	1.00	0.00	1.00	0.00	1.00	0.01	1.00	0.00
DMOPSO-5	1.00	0.00	1.00	0.00	1.00	0.00	1.00	0.00	1.00	0.00
NSGA-II	1.00	0.00	1.00	0.00	1.00	0.00	1.00	0.00	1.00	0.00
SPEA2	1.00	0.00	1.00	0.00	1.00	0.00	1.00	0.00	1.00	0.00

Table C.42: Median and interquartile range of I_{IGD} obtained by the optimisers for the Lutz1 problems

	Lutz1-1 $\tilde{x} \pm IQR(x)$		Lutz1-2 $\tilde{x} \pm IQR(x)$		Lutz1-3 $\tilde{x} \pm IQR(x)$		Lutz1-4 $\tilde{x} \pm IQR(x)$		Lutz1-5 $\tilde{x} \pm IQR(x)$	
BIANT-1	1.00	0.00	0.41	0.13	0.45	0.05	0.48	0.01	0.52	0.07
BIANT-2	1.00	0.00	0.41	0.24	0.65	0.18	0.47	0.07	0.52	0.07
CHAC-1	0.00	0.00	0.00	0.00	0.00	0.00	0.01	0.00	0.05	0.00
CHAC-2	0.00	0.00	0.00	0.00	0.00	0.00	0.01	0.00	0.05	0.00
DMOABC	0.00	0.00	0.00	0.00	0.00	0.00	0.01	0.00	0.05	0.00
DMOCSA-1-1	0.00	0.00	0.00	0.00	0.06	0.10	0.08	0.00	0.05	0.00
DMOCSA-1-2	0.00	0.00	0.00	0.00	0.11	0.00	0.08	0.02	0.05	0.00
DMOCSA-1-3	0.00	0.00	0.00	0.00	0.00	0.03	0.08	0.00	0.05	0.00
DMOCSA-1-4	0.00	0.00	0.01	0.00	0.12	0.03	0.05	0.06	0.06	0.00
DMOCSA-1-5	0.00	0.00	0.00	0.00	0.11	0.00	0.08	0.00	0.05	0.00
DMOCSA-2-1	0.00	0.00	0.00	0.00	0.11	0.03	0.08	0.00	0.05	0.00
DMOCSA-2-2	0.00	0.00	0.00	0.00	0.01	0.03	0.08	0.00	0.05	0.00
DMOCSA-2-3	0.00	0.00	0.00	0.00	0.06	0.10	0.08	0.00	0.05	0.00
DMOCSA-2-4	0.00	0.00	0.00	0.00	0.11	0.00	0.02	0.02	0.05	0.02
DMOCSA-2-5	0.00	0.00	0.00	0.00	0.11	0.03	0.08	0.00	0.05	0.00
DMOFPA-1	0.00	0.00	0.00	0.00	0.11	0.03	0.08	0.02	0.05	0.01
DMOFPA-2	0.00	0.00	0.00	0.00	0.11	0.03	0.08	0.00	0.05	0.01
DMOFPA-3	0.00	0.00	0.00	0.00	0.11	0.03	0.08	0.00	0.05	0.00
DMOFPA-4	0.00	0.00	0.00	0.04	0.16	0.09	0.09	0.00	0.05	0.02
DMOFPA-5	0.00	0.00	0.00	0.00	0.06	0.10	0.08	0.00	0.05	0.00
MOACS-1	1.00	0.00	0.61	0.07	0.53	0.11	0.82	0.27	0.91	0.07
MOACS-2	1.00	0.00	0.57	0.16	0.89	0.11	0.70	0.16	0.60	0.11
DMOBAT-1	0.00	0.00	0.00	0.00	0.00	0.00	0.01	0.01	0.05	0.00
DMOBAT-2	0.00	0.00	0.00	0.00	0.00	0.00	0.01	0.02	0.05	0.00
DMOBAT-3	0.00	0.00	0.00	0.00	0.00	0.00	0.01	0.00	0.05	0.00
DMOBAT-4	0.00	0.00	0.00	0.00	0.04	0.03	0.09	0.00	0.05	0.01
DMOBAT-5	0.00	0.00	0.00	0.00	0.00	0.00	0.01	0.01	0.05	0.00
DMOPSO-1	0.00	0.00	0.00	0.00	0.00	0.00	0.01	0.00	0.05	0.00
DMOPSO-2	0.00	0.00	0.00	0.00	0.00	0.00	0.01	0.00	0.05	0.00
DMOPSO-3	0.00	0.00	0.00	0.00	0.00	0.00	0.01	0.00	0.05	0.00
DMOPSO-4	0.00	0.00	0.06	0.12	0.03	0.02	0.02	0.01	0.05	0.00
DMOPSO-5	0.00	0.00	0.00	0.00	0.00	0.00	0.01	0.00	0.05	0.00
NSGA-II	0.00	0.00	0.00	0.00	0.00	0.01	0.01	0.00	0.05	0.00
SPEA2	0.00	0.00	0.00	0.00	0.00	0.00	0.01	0.00	0.05	0.00

Table C.43: Median and interquartile range of I_ϵ obtained by the optimisers for the Lutz1 problems

	Lutz1-1 $\tilde{x} \pm IQR(x)$		Lutz1-2 $\tilde{x} \pm IQR(x)$		Lutz1-3 $\tilde{x} \pm IQR(x)$		Lutz1-4 $\tilde{x} \pm IQR(x)$		Lutz1-5 $\tilde{x} \pm IQR(x)$	
BIANT-1	1.00	0.00	0.87	0.02	0.88	0.02	0.72	0.00	0.58	0.19
BIANT-2	1.00	0.00	0.87	0.05	0.90	0.06	0.72	0.04	0.47	0.05
CHAC-1	0.89	0.00	0.79	0.00	0.76	0.00	0.63	0.00	0.42	0.00
CHAC-2	0.89	0.00	0.79	0.00	0.76	0.00	0.63	0.00	0.42	0.00
DMOABC	0.89	0.00	0.79	0.00	0.76	0.00	0.63	0.00	0.42	0.00
DMOCSA-1-1	0.89	0.00	0.79	0.00	0.76	0.00	0.63	0.00	0.42	0.01
DMOCSA-1-2	0.89	0.00	0.79	0.00	0.76	0.00	0.63	0.00	0.42	0.00
DMOCSA-1-3	0.89	0.00	0.79	0.00	0.76	0.00	0.63	0.00	0.43	0.01
DMOCSA-1-4	0.89	0.00	0.79	0.00	0.78	0.02	0.64	0.00	0.44	0.00
DMOCSA-1-5	0.89	0.00	0.79	0.00	0.76	0.00	0.63	0.00	0.42	0.00
DMOCSA-2-1	0.89	0.00	0.79	0.00	0.76	0.00	0.63	0.00	0.42	0.00
DMOCSA-2-2	0.89	0.00	0.79	0.00	0.76	0.00	0.63	0.00	0.42	0.00
DMOCSA-2-3	0.89	0.00	0.79	0.00	0.76	0.00	0.63	0.00	0.42	0.00
DMOCSA-2-4	0.89	0.00	0.79	0.00	0.76	0.01	0.63	0.00	0.44	0.00
DMOCSA-2-5	0.89	0.00	0.79	0.00	0.76	0.00	0.63	0.00	0.42	0.00
DMOFPA-1	0.89	0.00	0.79	0.00	0.76	0.00	0.63	0.00	0.42	0.00
DMOFPA-2	0.89	0.00	0.79	0.00	0.76	0.00	0.63	0.00	0.43	0.01
DMOFPA-3	0.89	0.00	0.79	0.00	0.76	0.00	0.63	0.00	0.42	0.00
DMOFPA-4	0.89	0.00	0.79	0.00	0.81	0.06	0.64	0.00	0.44	0.00
DMOFPA-5	0.89	0.00	0.79	0.00	0.76	0.00	0.63	0.00	0.42	0.00
MOACS-1	1.00	0.00	0.90	0.00	0.88	0.04	0.91	0.18	0.94	0.07
MOACS-2	1.00	0.00	0.90	0.03	0.99	0.03	0.85	0.04	0.71	0.14
DMOBAT-1	0.89	0.00	0.79	0.00	0.76	0.00	0.63	0.00	0.42	0.00
DMOBAT-2	0.89	0.00	0.79	0.00	0.76	0.00	0.63	0.00	0.42	0.00
DMOBAT-3	0.89	0.00	0.79	0.00	0.76	0.00	0.63	0.00	0.42	0.00
DMOBAT-4	0.89	0.00	0.79	0.00	0.76	0.00	0.64	0.01	0.43	0.00
DMOBAT-5	0.89	0.00	0.79	0.00	0.76	0.00	0.63	0.00	0.42	0.00
DMOPSO-1	0.89	0.00	0.79	0.00	0.76	0.00	0.63	0.00	0.42	0.00
DMOPSO-2	0.89	0.00	0.79	0.00	0.76	0.00	0.63	0.00	0.42	0.00
DMOPSO-3	0.89	0.00	0.79	0.00	0.76	0.00	0.63	0.00	0.42	0.00
DMOPSO-4	0.89	0.00	0.79	0.00	0.76	0.00	0.64	0.01	0.42	0.01
DMOPSO-5	0.89	0.00	0.79	0.00	0.76	0.00	0.63	0.00	0.42	0.00
NSGA-II	0.89	0.00	0.79	0.00	0.76	0.00	0.63	0.00	0.42	0.00
SPEA2	0.89	0.00	0.79	0.00	0.76	0.00	0.63	0.00	0.42	0.00

Table C.44: Median and interquartile range of I_Δ obtained by the optimisers for the Lutz1 problems

	Lutz1-1 $\tilde{x} \pm IQR(x)$		Lutz1-2 $\tilde{x} \pm IQR(x)$		Lutz1-3 $\tilde{x} \pm IQR(x)$		Lutz1-4 $\tilde{x} \pm IQR(x)$		Lutz1-5 $\tilde{x} \pm IQR(x)$	
BIANT-2	1.00	0.00	0.88	0.08	0.87	0.08	0.81	0.09	0.82	0.03
CHAC-1	0.83	0.00	0.93	0.00	0.88	0.00	0.93	0.01	0.95	0.00
CHAC-2	0.83	0.00	0.93	0.00	0.88	0.01	0.93	0.02	0.95	0.00
DMOABC	0.83	0.00	0.93	0.00	0.88	0.00	0.92	0.02	0.95	0.00
DMOCSA-1-1	0.83	0.00	0.93	0.00	0.92	0.06	0.96	0.00	0.95	0.00
DMOCSA-1-2	0.83	0.00	0.93	0.00	0.95	0.01	0.96	0.01	0.96	0.01
DMOCSA-1-3	0.83	0.00	0.93	0.00	0.88	0.02	0.97	0.00	0.95	0.00
DMOCSA-1-4	0.83	0.00	0.91	0.04	0.85	0.14	0.91	0.02	0.96	0.02
DMOCSA-1-5	0.83	0.00	0.93	0.00	0.95	0.00	0.96	0.00	0.96	0.01
DMOCSA-2-1	0.83	0.00	0.93	0.00	0.95	0.02	0.96	0.00	0.96	0.00
DMOCSA-2-2	0.83	0.00	0.93	0.00	0.89	0.02	0.96	0.01	0.95	0.00
DMOCSA-2-3	0.83	0.00	0.93	0.00	0.90	0.03	0.96	0.01	0.96	0.01
DMOCSA-2-4	0.83	0.00	0.93	0.00	0.92	0.03	0.93	0.02	0.92	0.01
DMOCSA-2-5	0.83	0.00	0.93	0.00	0.95	0.02	0.97	0.00	0.95	0.00
DMOFPA-1	0.83	0.00	0.93	0.00	0.95	0.02	0.96	0.01	0.95	0.01
DMOFPA-2	0.83	0.00	0.93	0.00	0.95	0.02	0.96	0.01	0.96	0.02
DMOFPA-3	0.83	0.00	0.93	0.00	0.95	0.02	0.96	0.00	0.96	0.01
DMOFPA-4	0.83	0.00	0.93	0.03	0.86	0.05	0.96	0.03	0.95	0.03
DMOFPA-5	0.83	0.00	0.93	0.00	0.92	0.07	0.96	0.01	0.95	0.02
MOACS-1	1.00	0.00	0.91	0.04	0.77	0.19	0.71	0.17	0.73	0.14
MOACS-2	1.00	0.00	0.89	0.02	0.80	0.13	0.74	0.17	0.81	0.04
DMOBAT-1	0.83	0.00	0.93	0.00	0.88	0.01	0.92	0.01	0.96	0.01
DMOBAT-2	0.83	0.00	0.93	0.00	0.88	0.01	0.94	0.03	0.96	0.01
DMOBAT-3	0.83	0.00	0.93	0.00	0.90	0.04	0.92	0.02	0.95	0.01
DMOBAT-4	0.83	0.00	0.90	0.05	0.85	0.04	0.97	0.04	0.96	0.02
DMOBAT-5	0.83	0.00	0.93	0.00	0.92	0.01	0.92	0.01	0.96	0.01
DMOPSO-1	0.83	0.00	0.93	0.00	0.88	0.00	0.92	0.01	0.95	0.00
DMOPSO-2	0.83	0.00	0.93	0.00	0.88	0.01	0.93	0.01	0.95	0.00
DMOPSO-3	0.83	0.00	0.93	0.00	0.86	0.04	0.92	0.01	0.95	0.00
DMOPSO-4	0.83	0.00	0.96	0.07	0.85	0.02	0.92	0.02	0.94	0.02
DMOPSO-5	0.83	0.00	0.93	0.00	0.88	0.01	0.93	0.00	0.95	0.00
NSGA-II	0.83	0.00	0.93	0.00	0.88	0.01	0.93	0.02	0.95	0.00
SPEA2	0.83	0.00	0.93	0.00	0.88	0.00	0.94	0.01	0.95	0.00

Table C.45: Median and interquartile range of the computation time required by the optimisers for the Lutz1 problems

	Lutz1-1 $\tilde{x} \pm IQR(x)$		Lutz1-2 $\tilde{x} \pm IQR(x)$		Lutz1-3 $\tilde{x} \pm IQR(x)$		Lutz1-4 $\tilde{x} \pm IQR(x)$		Lutz1-5 $\tilde{x} \pm IQR(x)$	
BIANT-1	0.65	0.01	0.73	0.04	0.79	0.02	0.78	0.17	0.78	0.05
BIANT-2	0.65	0.02	0.76	0.06	0.79	0.06	0.72	0.09	0.79	0.01
CHAC-1	0.59	0.00	0.65	0.04	0.69	0.01	0.55	0.09	0.71	0.03
CHAC-2	0.58	0.01	0.63	0.05	0.67	0.01	0.53	0.08	0.71	0.09
DMOABC	0.70	0.02	0.76	0.04	0.81	0.01	0.64	0.09	0.83	0.03
DMOCSA-1-1	0.49	0.00	0.54	0.04	0.59	0.02	0.46	0.07	0.60	0.02
DMOCSA-1-2	0.49	0.01	0.55	0.04	0.58	0.01	0.47	0.07	0.61	0.02
DMOCSA-1-3	0.49	0.02	0.55	0.03	0.58	0.02	0.49	0.07	0.62	0.03
DMOCSA-1-4	0.48	0.01	0.53	0.04	0.61	0.08	0.50	0.11	0.69	0.23
DMOCSA-1-5	0.48	0.01	0.54	0.05	0.57	0.01	0.45	0.08	0.61	0.02
DMOCSA-2-1	0.56	0.01	0.62	0.04	0.66	0.01	0.59	0.09	0.68	0.03
DMOCSA-2-2	0.54	0.00	0.61	0.05	0.64	0.01	0.51	0.11	0.67	0.06
DMOCSA-2-3	0.57	0.02	0.64	0.05	0.68	0.02	0.55	0.08	0.72	0.09
DMOCSA-2-4	0.57	0.02	0.61	0.05	0.65	0.02	0.54	0.06	0.82	0.12
DMOCSA-2-5	0.57	0.01	0.63	0.05	0.68	0.01	0.54	0.08	0.71	0.06
DMOFPA-1	0.48	0.01	0.54	0.04	0.57	0.01	0.46	0.07	0.61	0.02
DMOFPA-2	0.51	0.01	0.57	0.06	0.60	0.00	0.53	0.04	0.63	0.03
DMOFPA-3	0.50	0.01	0.57	0.05	0.60	0.01	0.53	0.15	0.63	0.05
DMOFPA-4	0.31	0.01	0.34	0.02	0.36	0.04	0.31	0.04	0.48	0.21
DMOFPA-5	0.51	0.00	0.56	0.04	0.60	0.01	0.47	0.10	0.67	0.13
MOACS-1	0.85	0.01	0.81	0.07	0.87	0.04	0.82	0.09	0.83	0.08
MOACS-2	1.00	0.00	1.00	0.00	1.00	0.00	0.91	0.19	1.00	0.02
DMOBAT-1	0.50	0.02	0.54	0.04	0.59	0.00	0.46	0.08	0.64	0.11
DMOBAT-2	0.50	0.01	0.56	0.04	0.60	0.01	0.46	0.06	0.61	0.06
DMOBAT-3	0.52	0.01	0.57	0.04	0.61	0.01	0.49	0.07	0.65	0.05
DMOBAT-4	0.50	0.01	0.55	0.04	0.59	0.03	0.46	0.05	0.66	0.10
DMOBAT-5	0.50	0.01	0.56	0.04	0.60	0.01	0.47	0.07	0.61	0.03
DMOPSO-1	0.45	0.03	0.51	0.06	0.54	0.03	0.43	0.05	0.53	0.09
DMOPSO-2	0.47	0.02	0.51	0.03	0.55	0.01	0.49	0.10	0.57	0.00
DMOPSO-3	0.42	0.07	0.47	0.03	0.50	0.10	0.45	0.01	0.51	0.05
DMOPSO-4	0.51	0.05	0.59	0.01	0.65	0.04	0.55	0.13	0.67	0.11
DMOPSO-5	0.48	0.04	0.51	0.06	0.58	0.02	0.44	0.05	0.59	0.03
NSGA-II	0.70	0.01	0.71	0.06	0.69	0.01	0.60	0.11	0.70	0.03
SPEA2	0.40	0.01	0.42	0.02	0.46	0.01	0.36	0.02	0.44	0.02

C.3.7 Problem Family: Kilbrid

Table C.46: Median and interquartile range of I_{HV} obtained by the optimisers for the Kilbrid problems

	Kilbrid-1 $\tilde{x} \pm IQR(x)$		Kilbrid-2 $\tilde{x} \pm IQR(x)$		Kilbrid-3 $\tilde{x} \pm IQR(x)$		Kilbrid-4 $\tilde{x} \pm IQR(x)$		Kilbrid-5 $\tilde{x} \pm IQR(x)$	
BIANT-1	0.44	0.10	0.90	0.15	0.84	0.10	0.83	0.10	0.89	0.08
BIANT-2	0.46	0.16	0.93	0.03	0.80	0.05	0.90	0.09	0.81	0.08
CHAC-1	0.74	0.01	0.97	0.00	0.94	0.03	0.93	0.02	0.95	0.02
CHAC-2	0.74	0.01	0.96	0.02	0.94	0.03	0.96	0.02	0.94	0.02
DMOABC	0.73	0.00	0.97	0.01	0.92	0.02	0.95	0.02	0.95	0.00
DMOCSA-1-1	0.74	0.01	0.95	0.04	0.94	0.01	0.95	0.00	0.94	0.00
DMOCSA-1-2	0.75	0.01	0.95	0.00	0.93	0.01	0.95	0.01	0.94	0.01
DMOCSA-1-3	0.74	0.01	0.95	0.03	0.93	0.00	0.95	0.00	0.94	0.02
DMOCSA-1-4	0.73	0.01	0.92	0.03	0.91	0.00	0.92	0.01	0.92	0.02
DMOCSA-1-5	0.74	0.01	0.96	0.02	0.94	0.01	0.95	0.01	0.94	0.01
DMOCSA-2-1	0.75	0.01	0.96	0.01	0.94	0.01	0.95	0.01	0.94	0.01
DMOCSA-2-2	0.74	0.01	0.96	0.03	0.93	0.01	0.94	0.02	0.94	0.01
DMOCSA-2-3	0.74	0.01	0.95	0.03	0.94	0.01	0.94	0.01	0.94	0.02
DMOCSA-2-4	0.73	0.02	0.92	0.03	0.91	0.02	0.92	0.01	0.92	0.01
DMOCSA-2-5	0.74	0.01	0.95	0.02	0.94	0.01	0.94	0.01	0.94	0.01
DMOFPA-1	0.74	0.01	0.96	0.01	0.93	0.01	0.95	0.00	0.94	0.01
DMOFPA-2	0.74	0.02	0.96	0.02	0.94	0.00	0.95	0.01	0.94	0.01
DMOFPA-3	0.74	0.00	0.96	0.02	0.94	0.00	0.95	0.01	0.94	0.00
DMOFPA-4	0.73	0.01	0.91	0.03	0.92	0.01	0.91	0.02	0.91	0.01
DMOFPA-5	0.74	0.02	0.96	0.03	0.94	0.01	0.94	0.01	0.94	0.01
MOACS-1	0.62	0.09	0.90	0.03	0.86	0.07	0.83	0.04	0.84	0.04
MOACS-2	0.62	0.08	0.92	0.04	0.82	0.04	0.83	0.02	0.85	0.03
DMOBAT-1	0.74	0.01	0.97	0.02	0.93	0.03	0.94	0.00	0.96	0.02
DMOBAT-2	0.73	0.01	0.96	0.04	0.93	0.02	0.94	0.00	0.95	0.02
DMOBAT-3	0.74	0.01	0.97	0.01	0.93	0.02	0.95	0.02	0.94	0.02
DMOBAT-4	0.72	0.01	0.92	0.02	0.90	0.04	0.91	0.01	0.93	0.02
DMOBAT-5	0.74	0.01	0.96	0.01	0.93	0.02	0.95	0.01	0.95	0.01
DMOPSO-1	0.74	0.02	0.97	0.02	0.93	0.01	0.94	0.01	0.95	0.02
DMOPSO-2	0.74	0.02	0.96	0.02	0.94	0.02	0.94	0.01	0.95	0.02
DMOPSO-3	0.73	0.01	0.96	0.03	0.93	0.03	0.96	0.02	0.95	0.02
DMOPSO-4	0.72	0.01	0.95	0.06	0.92	0.03	0.95	0.02	0.94	0.04
DMOPSO-5	0.73	0.01	0.96	0.03	0.93	0.02	0.95	0.03	0.95	0.01
NSGA-II	0.73	0.01	0.97	0.01	0.93	0.02	0.95	0.02	0.95	0.01
SPEA2	0.73	0.01	0.96	0.01	0.94	0.02	0.96	0.02	0.95	0.01

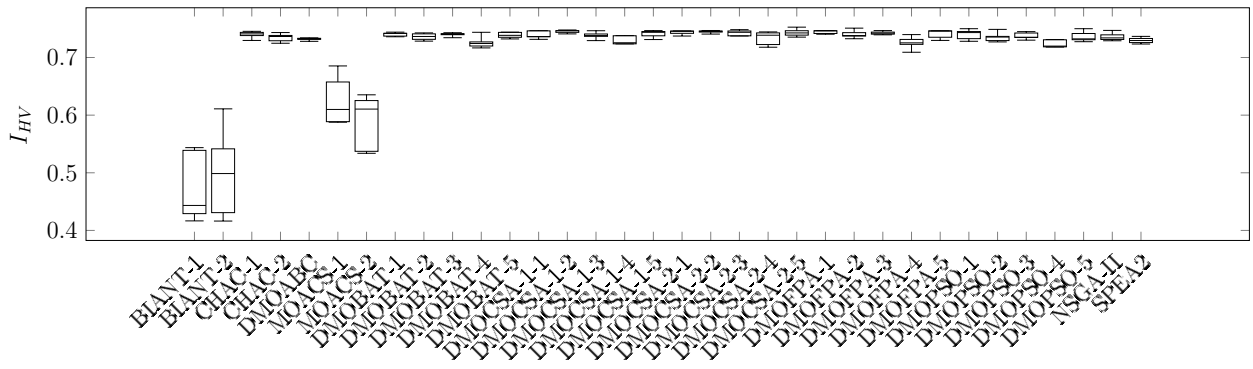

Figure C.43: Boxplot for I_{HV}: Kilbrid-1

Table C.47: Median and interquartile range of I_{IGD} obtained by the optimisers for the Kilbrid problems

	Kilbrid-1 $\tilde{x} \pm IQR(x)$		Kilbrid-2 $\tilde{x} \pm IQR(x)$		Kilbrid-3 $\tilde{x} \pm IQR(x)$		Kilbrid-4 $\tilde{x} \pm IQR(x)$		Kilbrid-5 $\tilde{x} \pm IQR(x)$	
BIANT-1	0.83	0.32	0.55	0.19	0.73	0.08	0.98	0.20	0.46	0.18
BIANT-2	0.66	0.37	0.56	0.02	0.84	0.10	0.70	0.15	0.60	0.25
CHAC-1	0.18	0.00	0.22	0.03	0.55	0.02	0.40	0.07	0.31	0.02
CHAC-2	0.18	0.01	0.26	0.11	0.54	0.06	0.39	0.04	0.30	0.06
DMOABC	0.18	0.00	0.25	0.04	0.57	0.05	0.38	0.01	0.31	0.02
DMOCSA-1-1	0.18	0.00	0.25	0.03	0.57	0.04	0.43	0.04	0.36	0.04
DMOCSA-1-2	0.18	0.00	0.26	0.02	0.61	0.03	0.40	0.03	0.36	0.02
DMOCSA-1-3	0.18	0.00	0.28	0.02	0.57	0.09	0.39	0.03	0.36	0.02
DMOCSA-1-4	0.18	0.00	0.43	0.08	0.73	0.14	0.51	0.08	0.46	0.05
DMOCSA-1-5	0.18	0.00	0.26	0.07	0.58	0.04	0.42	0.00	0.33	0.02
DMOCSA-2-1	0.18	0.00	0.23	0.03	0.59	0.05	0.42	0.02	0.36	0.03
DMOCSA-2-2	0.18	0.00	0.28	0.02	0.64	0.03	0.41	0.04	0.37	0.00
DMOCSA-2-3	0.18	0.00	0.28	0.08	0.57	0.01	0.42	0.02	0.35	0.05
DMOCSA-2-4	0.19	0.00	0.38	0.10	0.70	0.08	0.47	0.04	0.49	0.06
DMOCSA-2-5	0.18	0.00	0.31	0.08	0.59	0.02	0.37	0.04	0.35	0.06
DMOFPA-1	0.18	0.00	0.27	0.05	0.63	0.05	0.41	0.01	0.37	0.04
DMOFPA-2	0.18	0.00	0.26	0.02	0.58	0.01	0.39	0.02	0.39	0.04
DMOFPA-3	0.18	0.00	0.29	0.04	0.62	0.05	0.39	0.02	0.36	0.03
DMOFPA-4	0.19	0.00	0.48	0.00	0.70	0.07	0.57	0.03	0.53	0.10
DMOFPA-5	0.18	0.00	0.22	0.05	0.59	0.05	0.40	0.00	0.34	0.04
MOACS-1	0.35	0.11	0.58	0.04	0.72	0.09	0.75	0.13	0.63	0.26
MOACS-2	0.37	0.20	0.58	0.10	0.69	0.13	0.78	0.06	0.61	0.05
DMOBAT-1	0.18	0.00	0.25	0.12	0.59	0.02	0.40	0.02	0.35	0.00
DMOBAT-2	0.18	0.00	0.28	0.01	0.61	0.03	0.37	0.04	0.35	0.02
DMOBAT-3	0.18	0.00	0.28	0.04	0.59	0.04	0.40	0.08	0.37	0.01
DMOBAT-4	0.18	0.01	0.36	0.09	0.73	0.08	0.54	0.01	0.38	0.04
DMOBAT-5	0.18	0.00	0.25	0.02	0.59	0.02	0.38	0.02	0.35	0.03
DMOPSO-1	0.18	0.00	0.26	0.02	0.58	0.01	0.40	0.05	0.31	0.03
DMOPSO-2	0.18	0.01	0.24	0.03	0.56	0.04	0.40	0.02	0.31	0.01
DMOPSO-3	0.18	0.00	0.26	0.04	0.59	0.04	0.41	0.02	0.29	0.04
DMOPSO-4	0.19	0.00	0.24	0.08	0.70	0.11	0.40	0.08	0.33	0.07
DMOPSO-5	0.18	0.00	0.25	0.02	0.60	0.03	0.36	0.06	0.30	0.01
NSGA-II	0.18	0.00	0.25	0.04	0.60	0.06	0.40	0.07	0.30	0.03
SPEA2	0.18	0.00	0.23	0.01	0.56	0.03	0.38	0.07	0.29	0.01

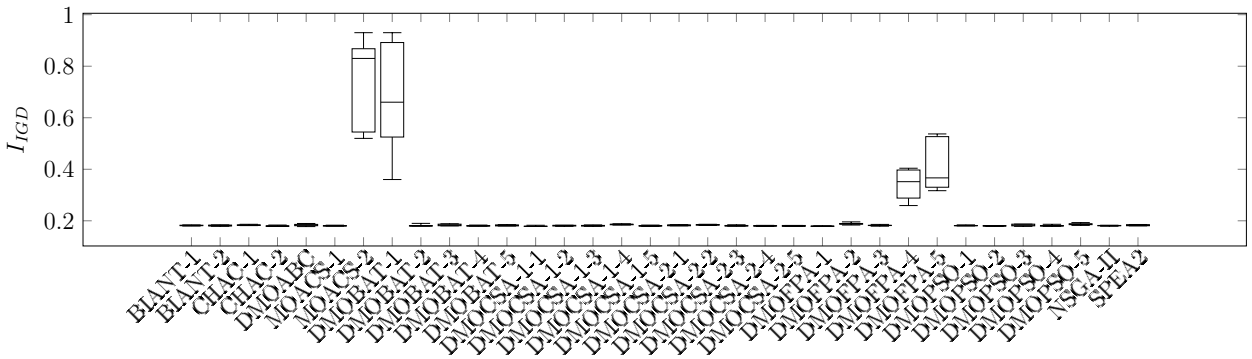

Figure C.44: Boxplot for I_{IGD}: Kilbrid-1

Table C.48: Median and interquartile range of I_ϵ obtained by the optimisers for the Kilbrid problems

	Kilbrid-1 $\tilde{x} \pm IQR(x)$		Kilbrid-2 $\tilde{x} \pm IQR(x)$		Kilbrid-3 $\tilde{x} \pm IQR(x)$		Kilbrid-4 $\tilde{x} \pm IQR(x)$		Kilbrid-5 $\tilde{x} \pm IQR(x)$	
BIANT-1	0.98	0.06	0.91	0.03	0.90	0.08	0.91	0.02	0.85	0.10
BIANT-2	0.95	0.06	0.91	0.01	0.95	0.07	0.82	0.05	0.94	0.11
CHAC-1	0.88	0.00	0.89	0.01	0.77	0.00	0.76	0.00	0.80	0.01
CHAC-2	0.88	0.00	0.91	0.01	0.77	0.00	0.75	0.00	0.80	0.01
DMOABC	0.88	0.00	0.90	0.01	0.78	0.01	0.75	0.01	0.80	0.00
DMOCSA-1-1	0.88	0.00	0.91	0.01	0.77	0.00	0.75	0.01	0.80	0.00
DMOCSA-1-2	0.88	0.00	0.91	0.00	0.77	0.00	0.75	0.01	0.80	0.00
DMOCSA-1-3	0.88	0.00	0.91	0.00	0.77	0.00	0.75	0.00	0.80	0.02
DMOCSA-1-4	0.88	0.00	0.92	0.01	0.79	0.01	0.76	0.00	0.81	0.01
DMOCSA-1-5	0.88	0.00	0.91	0.00	0.77	0.00	0.75	0.00	0.80	0.00
DMOCSA-2-1	0.88	0.00	0.91	0.00	0.77	0.00	0.75	0.00	0.80	0.00
DMOCSA-2-2	0.88	0.00	0.91	0.00	0.77	0.00	0.75	0.00	0.79	0.01
DMOCSA-2-3	0.88	0.00	0.91	0.00	0.77	0.00	0.75	0.01	0.80	0.01
DMOCSA-2-4	0.88	0.00	0.93	0.01	0.77	0.01	0.76	0.01	0.81	0.01
DMOCSA-2-5	0.88	0.00	0.91	0.00	0.77	0.00	0.75	0.01	0.79	0.02
DMOFPA-1	0.88	0.00	0.91	0.00	0.77	0.00	0.75	0.00	0.80	0.00
DMOFPA-2	0.88	0.00	0.91	0.00	0.77	0.00	0.75	0.00	0.80	0.01
DMOFPA-3	0.88	0.00	0.91	0.00	0.77	0.00	0.75	0.00	0.80	0.00
DMOFPA-4	0.88	0.00	0.93	0.01	0.77	0.00	0.77	0.02	0.81	0.01
DMOFPA-5	0.88	0.00	0.91	0.00	0.77	0.00	0.75	0.00	0.80	0.01
MOACS-1	0.89	0.02	0.92	0.02	0.90	0.05	0.91	0.03	0.96	0.06
MOACS-2	0.89	0.04	0.91	0.02	0.93	0.03	0.92	0.03	0.96	0.01
DMOBAT-1	0.88	0.00	0.90	0.01	0.77	0.00	0.75	0.00	0.80	0.00
DMOBAT-2	0.88	0.00	0.91	0.01	0.77	0.00	0.75	0.00	0.80	0.00
DMOBAT-3	0.88	0.00	0.91	0.00	0.77	0.00	0.75	0.00	0.80	0.00
DMOBAT-4	0.88	0.00	0.92	0.00	0.77	0.04	0.77	0.01	0.80	0.00
DMOBAT-5	0.88	0.00	0.91	0.00	0.77	0.00	0.75	0.00	0.80	0.00
DMOPSO-1	0.88	0.00	0.91	0.01	0.77	0.00	0.75	0.01	0.80	0.01
DMOPSO-2	0.88	0.00	0.91	0.00	0.77	0.00	0.75	0.00	0.80	0.00
DMOPSO-3	0.88	0.00	0.91	0.00	0.77	0.02	0.75	0.01	0.80	0.00
DMOPSO-4	0.88	0.00	0.90	0.01	0.79	0.01	0.76	0.00	0.80	0.01
DMOPSO-5	0.88	0.00	0.90	0.01	0.77	0.00	0.75	0.01	0.78	0.01
NSGA-II	0.88	0.00	0.90	0.00	0.77	0.01	0.75	0.00	0.80	0.01
SPEA2	0.88	0.00	0.90	0.01	0.77	0.00	0.75	0.00	0.78	0.02

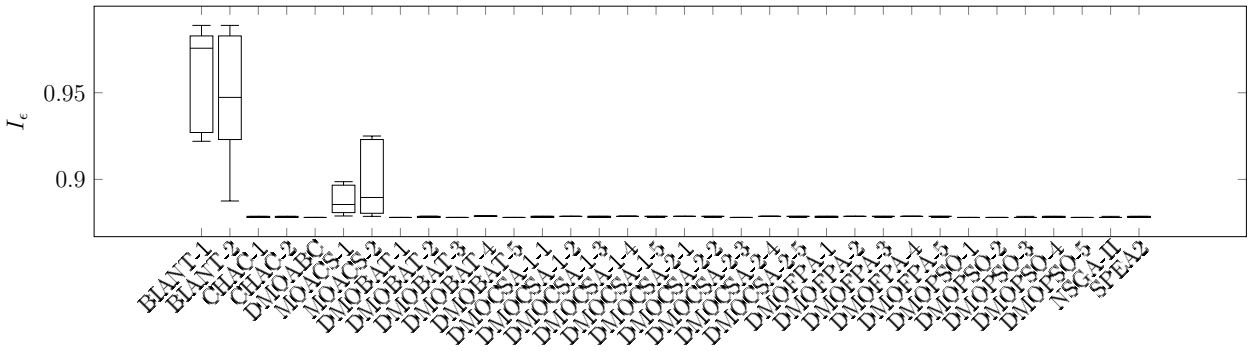

Figure C.45: Boxplot for I_ϵ: Kilbrid-1

Table C.49: Median and interquartile range of I_Δ obtained by the optimisers for the Kilbrid problems

	Kilbrid-1 $\tilde{x} \pm IQR(x)$		Kilbrid-2 $\tilde{x} \pm IQR(x)$		Kilbrid-3 $\tilde{x} \pm IQR(x)$		Kilbrid-4 $\tilde{x} \pm IQR(x)$		Kilbrid-5 $\tilde{x} \pm IQR(x)$	
BIANT-1	0.83	0.07	0.84	0.12	0.87	0.15	0.84	0.03	0.90	0.02
BIANT-2	0.85	0.10	0.96	0.09	0.86	0.03	0.86	0.09	0.98	0.02
CHAC-1	0.85	0.03	0.62	0.03	0.77	0.07	0.82	0.07	0.77	0.08
CHAC-2	0.86	0.05	0.72	0.14	0.78	0.05	0.80	0.12	0.72	0.10
DMOABC	0.86	0.04	0.62	0.12	0.78	0.02	0.75	0.05	0.75	0.04
DMOCSA-1-1	0.87	0.03	0.61	0.08	0.74	0.04	0.74	0.04	0.81	0.03
DMOCSA-1-2	0.87	0.01	0.60	0.04	0.77	0.12	0.76	0.10	0.86	0.11
DMOCSA-1-3	0.89	0.00	0.67	0.05	0.76	0.03	0.80	0.05	0.88	0.04
DMOCSA-1-4	0.86	0.02	0.66	0.05	0.75	0.07	0.69	0.02	0.82	0.03
DMOCSA-1-5	0.87	0.01	0.71	0.01	0.75	0.09	0.78	0.06	0.84	0.05
DMOCSA-2-1	0.85	0.03	0.57	0.13	0.75	0.11	0.78	0.09	0.84	0.07
DMOCSA-2-2	0.86	0.00	0.62	0.08	0.80	0.06	0.72	0.05	0.87	0.04
DMOCSA-2-3	0.86	0.03	0.70	0.05	0.75	0.02	0.79	0.04	0.80	0.04
DMOCSA-2-4	0.89	0.05	0.68	0.11	0.70	0.12	0.81	0.05	0.78	0.08
DMOCSA-2-5	0.88	0.02	0.73	0.11	0.75	0.06	0.70	0.05	0.81	0.14
DMOFPA-1	0.84	0.04	0.69	0.06	0.79	0.03	0.80	0.08	0.78	0.10
DMOFPA-2	0.85	0.01	0.62	0.01	0.79	0.08	0.72	0.02	0.83	0.03
DMOFPA-3	0.86	0.05	0.59	0.09	0.78	0.04	0.76	0.04	0.87	0.07
DMOFPA-4	0.85	0.07	0.77	0.14	0.78	0.03	0.71	0.10	0.83	0.10
DMOFPA-5	0.87	0.04	0.58	0.15	0.81	0.02	0.76	0.05	0.80	0.11
MOACS-1	0.91	0.04	0.86	0.08	0.80	0.11	0.80	0.03	0.85	0.01
MOACS-2	0.95	0.07	0.85	0.06	0.91	0.08	0.85	0.03	0.91	0.03
DMOBAT-1	0.88	0.04	0.67	0.15	0.72	0.09	0.77	0.05	0.84	0.06
DMOBAT-2	0.88	0.02	0.65	0.10	0.76	0.05	0.81	0.06	0.85	0.08
DMOBAT-3	0.88	0.01	0.65	0.11	0.77	0.03	0.78	0.03	0.87	0.05
DMOBAT-4	0.86	0.05	0.59	0.17	0.72	0.02	0.76	0.03	0.75	0.05
DMOBAT-5	0.89	0.03	0.65	0.04	0.84	0.07	0.77	0.05	0.83	0.01
DMOPSO-1	0.86	0.01	0.68	0.06	0.81	0.04	0.75	0.08	0.79	0.03
DMOPSO-2	0.87	0.02	0.62	0.03	0.74	0.05	0.82	0.07	0.78	0.02
DMOPSO-3	0.87	0.00	0.63	0.05	0.79	0.09	0.77	0.00	0.74	0.05
DMOPSO-4	0.89	0.03	0.60	0.17	0.74	0.08	0.72	0.09	0.76	0.04
DMOPSO-5	0.88	0.03	0.69	0.12	0.80	0.03	0.74	0.01	0.78	0.02
NSGA-II	0.87	0.01	0.70	0.18	0.77	0.04	0.77	0.07	0.78	0.11
SPEA2	0.86	0.03	0.66	0.05	0.80	0.06	0.78	0.06	0.81	0.04

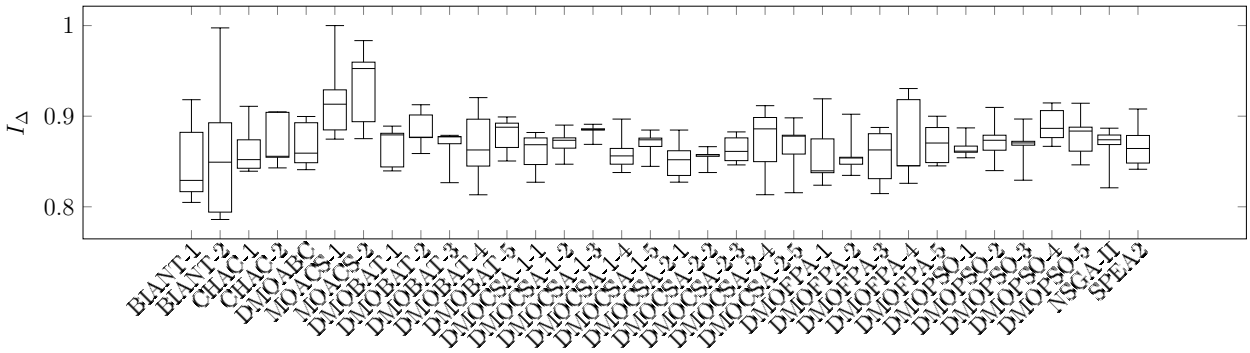

Figure C.46: Boxplot for I_Δ: Kilbrid-1

Table C.50: Median and interquartile range of the computation time required by the optimisers for the Kilbrid problems

	Kilbrid-1 $\tilde{x} \pm IQR(x)$		Kilbrid-2 $\tilde{x} \pm IQR(x)$		Kilbrid-3 $\tilde{x} \pm IQR(x)$		Kilbrid-4 $\tilde{x} \pm IQR(x)$		Kilbrid-5 $\tilde{x} \pm IQR(x)$	
BIANT-1	0.59	0.16	0.83	0.24	0.46	0.03	0.42	0.15	0.40	0.18
BIANT-2	0.60	0.18	0.83	0.23	0.46	0.06	0.45	0.18	0.41	0.15
CHAC-1	0.73	0.26	0.79	0.24	0.54	0.25	0.41	0.10	0.49	0.23
CHAC-2	0.57	0.13	0.77	0.24	0.65	0.29	0.51	0.16	0.38	0.19
DMOABC	0.89	0.22	0.99	0.29	0.60	0.22	0.89	0.31	0.64	0.42
DMOCSA-1-1	0.59	0.15	0.66	0.21	0.49	0.08	0.39	0.08	0.35	0.17
DMOCSA-1-2	0.48	0.14	0.65	0.19	0.49	0.33	0.66	0.41	0.36	0.17
DMOCSA-1-3	0.54	0.12	0.64	0.20	0.45	0.34	0.56	0.09	0.32	0.03
DMOCSA-1-4	0.57	0.10	0.64	0.21	0.36	0.06	0.38	0.17	0.40	0.31
DMOCSA-1-5	0.53	0.06	0.65	0.02	0.67	0.16	0.43	0.11	0.41	0.09
DMOCSA-2-1	0.79	0.26	0.79	0.24	0.75	0.25	0.47	0.14	0.64	0.33
DMOCSA-2-2	0.57	0.16	0.78	0.18	0.52	0.05	0.55	0.34	0.59	0.18
DMOCSA-2-3	0.66	0.14	0.80	0.24	0.57	0.42	0.55	0.06	0.52	0.12
DMOCSA-2-4	0.69	0.10	0.76	0.25	0.52	0.16	0.55	0.04	0.38	0.25
DMOCSA-2-5	0.57	0.33	0.81	0.25	0.72	0.36	0.53	0.13	0.50	0.27
DMOFPA-1	0.49	0.15	0.64	0.21	0.41	0.07	0.47	0.05	0.34	0.21
DMOFPA-2	0.61	0.20	0.67	0.19	0.50	0.32	0.50	0.28	0.50	0.24
DMOFPA-3	0.63	0.28	0.67	0.22	0.48	0.43	0.53	0.12	0.41	0.15
DMOFPA-4	0.37	0.32	0.45	0.14	0.44	0.27	0.28	0.05	0.22	0.02
DMOFPA-5	0.50	0.19	0.67	0.19	0.49	0.10	0.40	0.06	0.43	0.08
MOACS-1	0.58	0.20	0.81	0.24	0.48	0.09	0.41	0.13	0.38	0.15
MOACS-2	0.71	0.20	0.87	0.28	0.46	0.04	0.44	0.17	0.42	0.15
DMOBAT-1	0.53	0.11	0.67	0.02	0.53	0.17	0.38	0.07	0.49	0.16
DMOBAT-2	0.50	0.09	0.68	0.24	0.47	0.09	0.50	0.18	0.45	0.14
DMOBAT-3	0.56	0.08	0.69	0.21	0.60	0.14	0.50	0.14	0.36	0.08
DMOBAT-4	0.59	0.13	0.67	0.01	0.48	0.13	0.43	0.19	0.43	0.10
DMOBAT-5	0.59	0.27	0.69	0.09	0.59	0.12	0.44	0.06	0.45	0.06
DMOPSO-1	0.51	0.07	0.63	0.17	0.43	0.23	0.49	0.14	0.42	0.27
DMOPSO-2	0.50	0.11	0.63	0.19	0.55	0.06	0.33	0.07	0.43	0.14
DMOPSO-3	0.49	0.11	0.57	0.16	0.47	0.07	0.45	0.29	0.57	0.27
DMOPSO-4	0.73	0.03	0.75	0.14	0.59	0.09	0.65	0.36	0.45	0.46
DMOPSO-5	0.53	0.16	0.65	0.09	0.47	0.07	0.45	0.25	0.39	0.10
NSGA-II	0.49	0.19	0.70	0.23	0.40	0.18	0.49	0.17	0.33	0.10
SPEA2	0.33	0.12	0.49	0.15	0.35	0.08	0.31	0.05	0.34	0.13

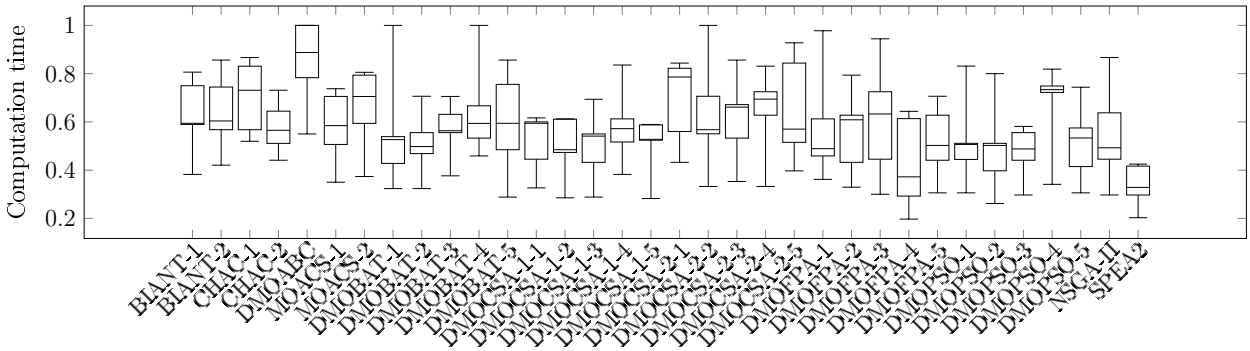

Figure C.47: Boxplot for the computation time: Kilbrid-1

C.3.8 Problem Family: Mitchell

Table C.51: Median and interquartile range of I_{HV} obtained by the optimisers for the Mitchell problems

	Mitchell-1 $\tilde{x} \pm IQR(x)$		Mitchell-2 $\tilde{x} \pm IQR(x)$		Mitchell-3 $\tilde{x} \pm IQR(x)$		Mitchell-4 $\tilde{x} \pm IQR(x)$	
BIANT-1	0.98	0.29	0.91	0.07	0.55	0.04	0.88	0.03
BIANT-2	0.77	0.30	0.91	0.03	0.54	0.04	0.87	0.01
CHAC-1	0.97	0.03	0.99	0.01	0.59	0.01	0.87	0.03
CHAC-2	0.97	0.01	0.99	0.01	0.59	0.01	0.86	0.03
DMOABC	0.97	0.04	0.98	0.02	0.59	0.01	0.87	0.04
DMOCSA-1-1	0.96	0.03	0.98	0.01	0.60	0.02	0.87	0.00
DMOCSA-1-2	0.96	0.06	0.98	0.01	0.59	0.00	0.86	0.01
DMOCSA-1-3	0.98	0.04	0.98	0.02	0.59	0.01	0.86	0.02
DMOCSA-1-4	0.87	0.06	0.95	0.01	0.56	0.00	0.80	0.06
DMOCSA-1-5	0.96	0.05	0.98	0.01	0.58	0.01	0.87	0.03
DMOCSA-2-1	0.96	0.02	0.99	0.01	0.59	0.01	0.87	0.01
DMOCSA-2-2	0.96	0.03	0.98	0.00	0.59	0.01	0.87	0.01
DMOCSA-2-3	0.96	0.03	0.98	0.01	0.59	0.01	0.87	0.03
DMOCSA-2-4	0.93	0.05	0.96	0.01	0.56	0.00	0.83	0.01
DMOCSA-2-5	0.99	0.03	0.98	0.01	0.58	0.00	0.87	0.01
DMOFPA-1	0.98	0.01	0.98	0.02	0.59	0.01	0.86	0.01
DMOFPA-2	0.93	0.02	0.97	0.01	0.59	0.02	0.87	0.02
DMOFPA-3	0.96	0.03	0.99	0.02	0.58	0.01	0.85	0.02
DMOFPA-4	0.89	0.01	0.95	0.01	0.56	0.01	0.81	0.02
DMOFPA-5	0.97	0.03	0.99	0.01	0.60	0.01	0.85	0.01
MOACS-1	0.97	0.16	0.87	0.06	0.57	0.02	0.84	0.03
MOACS-2	0.83	0.23	0.87	0.02	0.55	0.02	0.81	0.05
DMOBAT-1	0.96	0.02	0.99	0.02	0.58	0.01	0.86	0.03
DMOBAT-2	0.98	0.02	0.99	0.01	0.58	0.01	0.87	0.03
DMOBAT-3	0.98	0.03	1.00	0.02	0.59	0.02	0.87	0.01
DMOBAT-4	0.92	0.03	0.96	0.00	0.56	0.01	0.81	0.07
DMOBAT-5	0.97	0.03	0.99	0.01	0.59	0.01	0.85	0.03
DMOPSO-1	0.97	0.03	0.99	0.01	0.58	0.00	0.87	0.03
DMOPSO-2	0.97	0.02	0.99	0.03	0.59	0.00	0.87	0.02
DMOPSO-3	0.97	0.01	1.00	0.00	0.58	0.02	0.86	0.02
DMOPSO-4	0.97	0.06	0.97	0.04	0.56	0.04	0.79	0.09
DMOPSO-5	0.96	0.04	1.00	0.00	0.58	0.01	0.86	0.03
NSGA-II	0.99	0.02	0.98	0.03	0.59	0.01	0.86	0.01
SPEA2	0.97	0.06	1.00	0.01	0.59	0.01	0.85	0.03

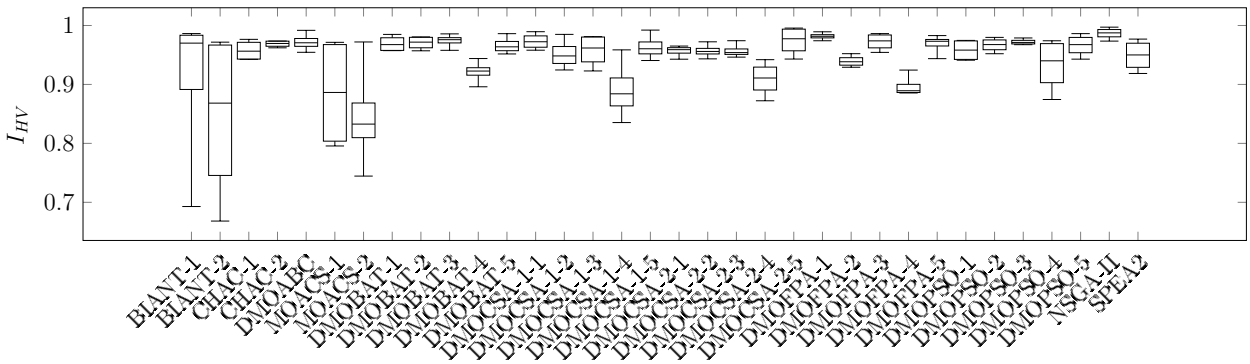

Figure C.48: Boxplot for I_{HV}: Mitchell-1

Table C.52: Median and interquartile range of I_{IGD} obtained by the optimisers for the Mitchell problems

	Mitchell-1 $\tilde{x} \pm IQR(x)$		Mitchell-2 $\tilde{x} \pm IQR(x)$		Mitchell-3 $\tilde{x} \pm IQR(x)$		Mitchell-4 $\tilde{x} \pm IQR(x)$	
BIANT-1	0.30	0.23	0.51	0.38	0.92	0.04	0.44	0.25
BIANT-2	0.34	0.35	0.49	0.20	0.94	0.02	0.35	0.08
CHAC-1	0.10	0.03	0.24	0.01	0.86	0.01	0.36	0.17
CHAC-2	0.10	0.01	0.24	0.06	0.87	0.00	0.38	0.10
DMOABC	0.09	0.04	0.24	0.06	0.88	0.01	0.31	0.19
DMOBAT-1	0.11	0.01	0.16	0.17	0.87	0.01	0.29	0.25
DMOBAT-2	0.11	0.02	0.11	0.09	0.87	0.00	0.39	0.09
DMOBAT-3	0.11	0.03	0.24	0.05	0.87	0.03	0.38	0.18
DMOBAT-4	0.20	0.08	0.29	0.14	0.97	0.03	0.80	0.30
DMOBAT-5	0.11	0.01	0.24	0.04	0.89	0.03	0.25	0.07
DMOCSA-1-1	0.12	0.01	0.06	0.06	0.87	0.01	0.40	0.08
DMOCSA-1-2	0.11	0.02	0.25	0.06	0.87	0.01	0.28	0.06
DMOCSA-1-3	0.11	0.01	0.25	0.06	0.87	0.01	0.40	0.10
DMOCSA-1-4	0.16	0.05	0.28	0.01	0.96	0.01	0.71	0.10
DMOCSA-1-5	0.10	0.04	0.16	0.16	0.87	0.02	0.26	0.07
DMOCSA-2-1	0.11	0.01	0.15	0.19	0.87	0.02	0.34	0.10
DMOCSA-2-2	0.13	0.02	0.25	0.05	0.87	0.04	0.43	0.09
DMOCSA-2-3	0.11	0.01	0.16	0.18	0.87	0.02	0.23	0.07
DMOCSA-2-4	0.21	0.06	0.54	0.06	0.93	0.05	0.91	0.04
DMOCSA-2-5	0.11	0.02	0.16	0.17	0.86	0.01	0.32	0.19
DMOFPA-1	0.32	0.04	0.74	0.31	0.94	0.01	0.65	0.30
DMOFPA-2	0.27	0.06	0.70	0.17	0.91	0.02	0.84	0.03
DMOFPA-3	0.08	0.06	0.15	0.17	0.88	0.05	0.44	0.12
DMOFPA-4	0.08	0.02	0.06	0.08	0.86	0.02	0.35	0.06
DMOFPA-5	0.08	0.02	0.24	0.05	0.85	0.03	0.35	0.23
DMOPSO	0.20	0.02	0.29	0.07	0.94	0.06	0.86	0.08
DMOPSO-1	0.10	0.03	0.17	0.15	0.86	0.00	0.25	0.04
DMOPSO-2	0.11	0.01	0.24	0.05	0.87	0.01	0.36	0.07
DMOPSO-3	0.11	0.02	0.18	0.14	0.88	0.02	0.27	0.06
DMOPSO-4	0.10	0.01	0.15	0.19	0.87	0.03	0.38	0.09
MOACS-1	0.12	0.06	0.29	0.12	0.96	0.03	0.69	0.10
MOACS-2	0.11	0.04	0.24	0.05	0.86	0.01	0.35	0.05
NSGA-II	0.10	0.02	0.24	0.05	0.85	0.01	0.34	0.07
SPEA2	0.12	0.04	0.24	0.01	0.85	0.01	0.37	0.03

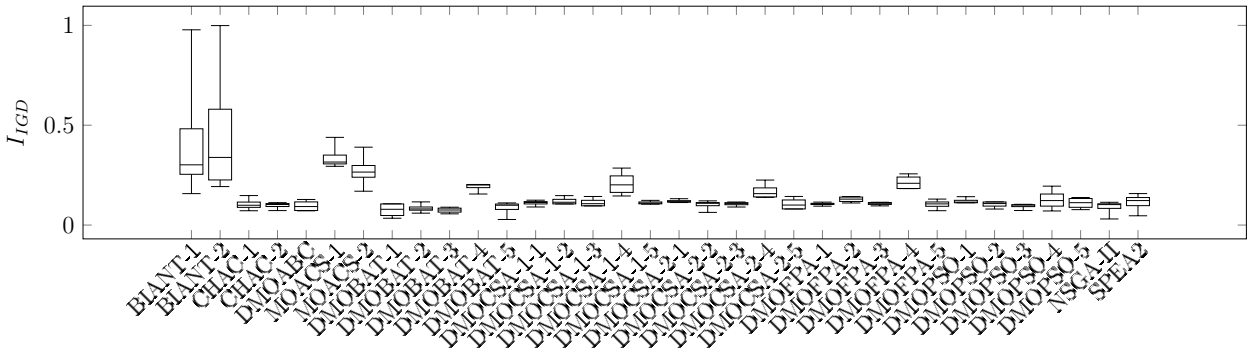

Figure C.49: Boxplot for I_{IGD}: Mitchell-1

,

Table C.53: Median and interquartile range of I_ϵ obtained by the optimisers for the Mitchell problems

	Mitchell-1 $\tilde{x} \pm IQR(x)$		Mitchell-2 $\tilde{x} \pm IQR(x)$		Mitchell-3 $\tilde{x} \pm IQR(x)$		Mitchell-4 $\tilde{x} \pm IQR(x)$	
BIANT-1	0.72	0.08	0.95	0.03	0.84	0.07	0.88	0.01
BIANT-2	0.82	0.20	0.94	0.01	0.85	0.01	0.90	0.02
CHAC-1	0.74	0.03	0.90	0.01	0.82	0.00	0.89	0.01
CHAC-2	0.72	0.01	0.89	0.01	0.82	0.00	0.90	0.03
DMOABC	0.72	0.01	0.90	0.01	0.82	0.00	0.89	0.03
DMOCSA-1-1	0.72	0.02	0.90	0.01	0.82	0.00	0.90	0.02
DMOCSA-1-2	0.75	0.03	0.91	0.01	0.82	0.00	0.90	0.00
DMOCSA-1-3	0.73	0.04	0.90	0.01	0.82	0.00	0.89	0.02
DMOCSA-1-4	0.80	0.05	0.92	0.01	0.82	0.00	0.94	0.03
DMOCSA-1-5	0.73	0.02	0.90	0.01	0.82	0.00	0.89	0.02
DMOCSA-2-1	0.73	0.01	0.90	0.01	0.82	0.00	0.89	0.00
DMOCSA-2-2	0.74	0.01	0.90	0.01	0.82	0.00	0.90	0.01
DMOCSA-2-3	0.74	0.01	0.90	0.01	0.82	0.00	0.90	0.02
DMOCSA-2-4	0.78	0.04	0.91	0.01	0.82	0.00	0.93	0.01
DMOCSA-2-5	0.72	0.03	0.90	0.01	0.82	0.00	0.89	0.00
DMOFPA-1	0.71	0.01	0.90	0.00	0.82	0.00	0.90	0.00
DMOFPA-2	0.75	0.01	0.91	0.00	0.82	0.00	0.89	0.01
DMOFPA-3	0.72	0.02	0.89	0.01	0.82	0.00	0.90	0.02
DMOFPA-4	0.80	0.01	0.93	0.00	0.82	0.00	0.94	0.01
DMOFPA-5	0.72	0.01	0.90	0.01	0.82	0.00	0.91	0.00
MOACS-1	0.80	0.14	0.97	0.02	0.82	0.00	0.91	0.01
MOACS-2	0.84	0.05	0.97	0.01	0.82	0.00	0.96	0.04
DMOBAT-1	0.73	0.02	0.90	0.01	0.82	0.00	0.89	0.01
DMOBAT-2	0.72	0.01	0.89	0.01	0.82	0.00	0.89	0.02
DMOBAT-3	0.72	0.01	0.89	0.01	0.82	0.00	0.89	0.00
DMOBAT-4	0.76	0.02	0.92	0.01	0.82	0.00	0.95	0.02
DMOBAT-5	0.73	0.02	0.90	0.01	0.82	0.00	0.90	0.02
DMOPSO-1	0.73	0.03	0.89	0.01	0.82	0.00	0.89	0.02
DMOPSO-2	0.73	0.02	0.90	0.01	0.82	0.00	0.90	0.01
DMOPSO-3	0.72	0.01	0.89	0.01	0.82	0.00	0.89	0.01
DMOPSO-4	0.75	0.06	0.92	0.02	0.82	0.00	0.95	0.06
DMOPSO-5	0.73	0.02	0.89	0.00	0.82	0.00	0.89	0.02
NSGA-II	0.71	0.01	0.89	0.02	0.82	0.00	0.90	0.02
SPEA2	0.74	0.04	0.89	0.01	0.82	0.00	0.90	0.02

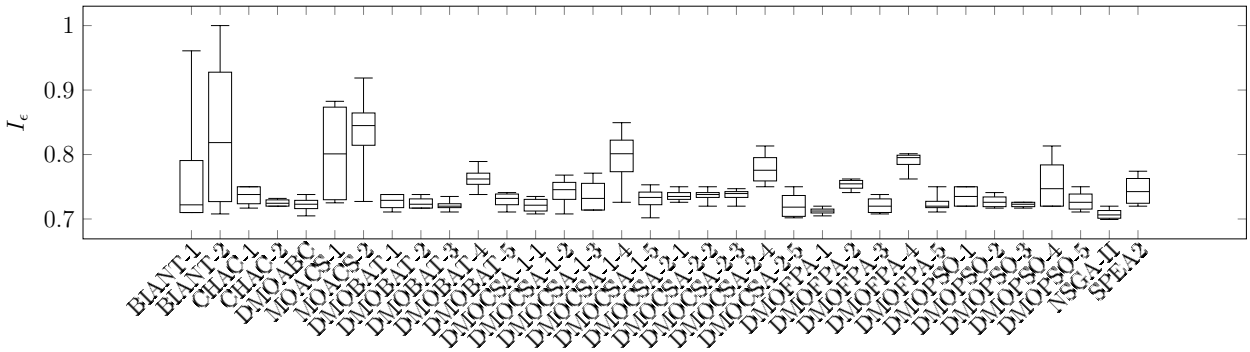

Figure C.50: Boxplot for I_ϵ: Mitchell-1

Table C.54: Median and interquartile range of I_Δ obtained by the optimisers for the Mitchell problems

	Mitchell-1 $\tilde{x} \pm IQR(x)$		Mitchell-2 $\tilde{x} \pm IQR(x)$		Mitchell-3 $\tilde{x} \pm IQR(x)$		Mitchell-4 $\tilde{x} \pm IQR(x)$	
BIANT-1	0.91	0.05	0.85	0.20	0.77	0.06	0.59	0.05
BIANT-2	0.89	0.01	0.80	0.10	0.79	0.11	0.89	0.14
CHAC-1	0.71	0.06	0.66	0.01	0.89	0.03	0.56	0.03
CHAC-2	0.75	0.03	0.70	0.03	0.91	0.04	0.59	0.16
DMOABC	0.79	0.07	0.69	0.04	0.90	0.02	0.42	0.17
DMOCSA-1-1	0.76	0.14	0.72	0.11	0.88	0.05	0.55	0.17
DMOCSA-1-2	0.79	0.03	0.79	0.03	0.90	0.05	0.63	0.17
DMOCSA-1-3	0.74	0.03	0.67	0.05	0.86	0.05	0.54	0.14
DMOCSA-1-4	0.64	0.06	0.68	0.07	0.82	0.04	0.41	0.22
DMOCSA-1-5	0.75	0.02	0.67	0.05	0.94	0.02	0.50	0.15
DMOCSA-2-1	0.78	0.04	0.78	0.02	0.92	0.03	0.49	0.03
DMOCSA-2-2	0.75	0.08	0.66	0.04	0.91	0.01	0.75	0.42
DMOCSA-2-3	0.81	0.02	0.67	0.04	0.92	0.03	0.53	0.08
DMOCSA-2-4	0.78	0.01	0.76	0.05	0.83	0.09	0.44	0.31
DMOCSA-2-5	0.80	0.05	0.73	0.12	0.90	0.08	0.51	0.18
DMOFPA-1	0.77	0.08	0.73	0.10	0.88	0.06	0.54	0.02
DMOFPA-2	0.74	0.05	0.68	0.04	0.88	0.06	0.56	0.20
DMOFPA-3	0.76	0.05	0.72	0.09	0.89	0.05	0.54	0.23
DMOFPA-4	0.71	0.09	0.84	0.06	0.82	0.05	0.76	0.45
DMOFPA-5	0.78	0.03	0.72	0.11	0.90	0.05	0.51	0.20
MOACS-1	0.68	0.16	0.86	0.12	0.82	0.03	0.56	0.04
MOACS-2	0.76	0.05	0.78	0.02	0.84	0.03	0.57	0.05
DMOBAT-1	0.78	0.04	0.73	0.12	0.92	0.06	0.52	0.06
DMOBAT-2	0.81	0.08	0.76	0.04	0.91	0.03	0.50	0.18
DMOBAT-3	0.81	0.02	0.69	0.03	0.92	0.02	0.53	0.02
DMOBAT-4	0.73	0.04	0.78	0.04	0.77	0.02	0.43	0.10
DMOBAT-5	0.79	0.04	0.72	0.13	0.89	0.07	0.51	0.12
DMOPSO-1	0.71	0.04	0.71	0.04	0.91	0.03	0.57	0.17
DMOPSO-2	0.82	0.03	0.73	0.09	0.89	0.11	0.46	0.22
DMOPSO-3	0.78	0.07	0.72	0.09	0.94	0.02	0.57	0.14
DMOPSO-4	0.75	0.07	0.80	0.08	0.81	0.02	0.92	0.12
DMOPSO-5	0.74	0.05	0.72	0.05	0.92	0.04	0.52	0.06
NSGA-II	0.72	0.06	0.71	0.02	0.90	0.03	0.53	0.14
SPEA2	0.77	0.04	0.69	0.02	0.92	0.04	0.54	0.05

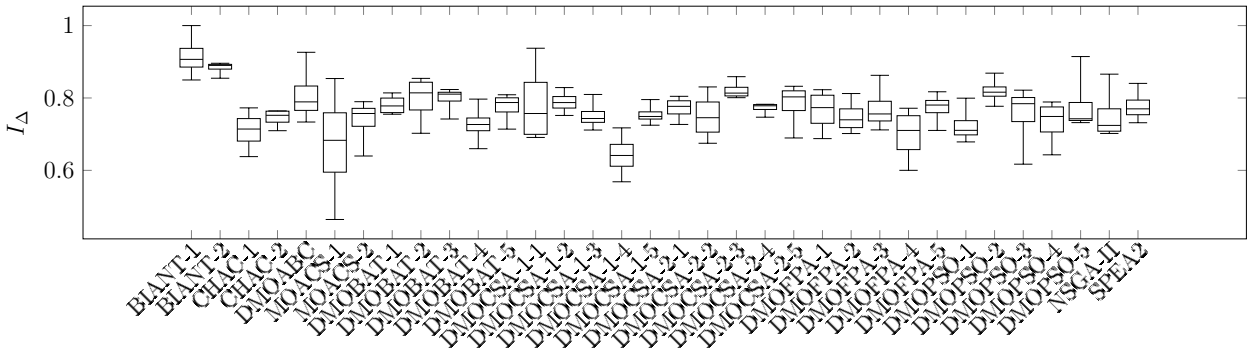

Figure C.51: Boxplot for I_Δ: Mitchell-1

Table C.55: Median and interquartile range of the computation time required by the optimisers for the Mitchell problems

	Mitchell-1 $\tilde{x} \pm IQR(x)$		Mitchell-2 $\tilde{x} \pm IQR(x)$		Mitchell-3 $\tilde{x} \pm IQR(x)$		Mitchell-4 $\tilde{x} \pm IQR(x)$	
BIANT-1	0.75	0.02	0.95	0.07	0.52	0.02	0.78	0.03
BIANT-2	0.80	0.04	0.93	0.10	0.53	0.02	0.78	0.03
CHAC-1	0.69	0.09	0.75	0.04	0.72	0.09	0.66	0.01
CHAC-2	0.80	0.16	0.74	0.07	0.62	0.14	0.65	0.00
DMOABC	0.87	0.20	0.86	0.07	0.94	0.14	0.75	0.00
DMOCSA-1-1	0.77	0.12	0.67	0.02	0.50	0.08	0.58	0.01
DMOCSA-1-2	0.60	0.02	0.67	0.06	0.67	0.10	0.57	0.01
DMOCSA-1-3	0.76	0.05	0.66	0.03	0.75	0.17	0.57	0.01
DMOCSA-1-4	0.55	0.01	0.62	0.03	0.44	0.09	0.57	0.02
DMOCSA-1-5	0.58	0.06	0.64	0.03	0.57	0.04	0.56	0.04
DMOCSA-2-1	0.70	0.11	0.72	0.05	0.66	0.10	0.63	0.01
DMOCSA-2-2	0.62	0.01	0.69	0.01	0.62	0.05	0.59	0.06
DMOCSA-2-3	0.76	0.08	0.72	0.04	0.85	0.15	0.64	0.05
DMOCSA-2-4	0.66	0.06	0.69	0.04	0.49	0.10	0.62	0.01
DMOCSA-2-5	0.65	0.03	0.73	0.01	0.75	0.18	0.64	0.01
DMOFPA-1	0.72	0.13	0.66	0.03	0.68	0.27	0.56	0.01
DMOFPA-2	0.70	0.09	0.68	0.04	0.51	0.11	0.60	0.03
DMOFPA-3	0.68	0.12	0.69	0.03	0.62	0.12	0.58	0.00
DMOFPA-4	0.31	0.01	0.35	0.01	0.45	0.34	0.31	0.06
DMOFPA-5	0.63	0.09	0.69	0.04	0.66	0.20	0.60	0.03
MOACS-1	0.77	0.02	0.84	0.05	0.51	0.03	0.88	0.03
MOACS-2	0.83	0.04	0.98	0.06	0.65	0.07	1.00	0.00
DMOBAT-1	0.59	0.10	0.66	0.07	0.47	0.07	0.58	0.02
DMOBAT-2	0.60	0.05	0.71	0.04	0.67	0.17	0.58	0.02
DMOBAT-3	0.79	0.12	0.71	0.03	0.62	0.12	0.59	0.01
DMOBAT-4	0.58	0.01	0.65	0.03	0.44	0.07	0.57	0.01
DMOBAT-5	0.67	0.17	0.67	0.03	0.55	0.11	0.59	0.01
DMOPSO-1	0.56	0.05	0.67	0.07	0.54	0.10	0.54	0.05
DMOPSO-2	0.65	0.13	0.67	0.06	0.67	0.10	0.56	0.02
DMOPSO-3	0.59	0.07	0.57	0.10	0.44	0.04	0.41	0.04
DMOPSO-4	0.52	0.07	0.66	0.16	0.54	0.28	0.52	0.02
DMOPSO-5	0.64	0.10	0.66	0.06	0.62	0.21	0.58	0.06
NSGA-II	0.62	0.03	0.72	0.03	0.63	0.15	0.65	0.01
SPEA2	0.50	0.01	0.56	0.03	0.53	0.11	0.51	0.00

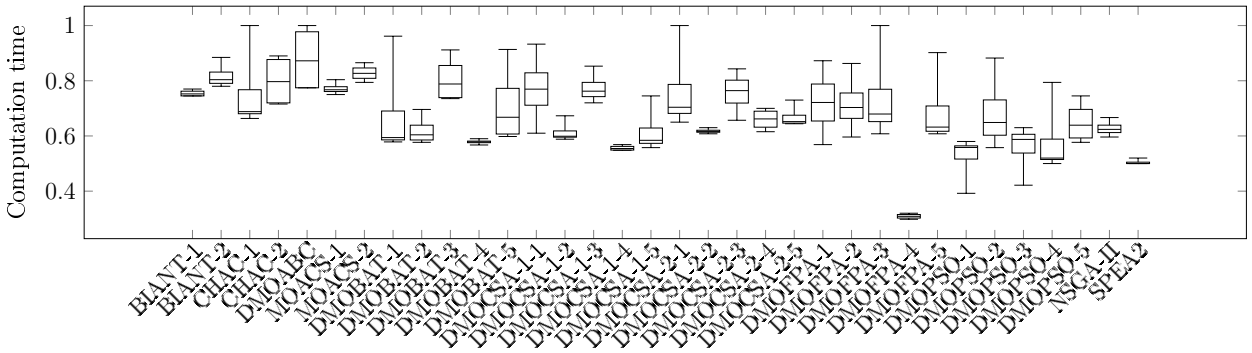

Figure C.52: Boxplot for the computation time: Mitchell-1

C.3.9 Problem Family: Mukherje

Table C.56: Median and interquartile range of I_{HV} obtained by the optimisers for the Mukherje problems

	Mukherje-1 $\tilde{x} \pm IQR(x)$		Mukherje-2 $\tilde{x} \pm IQR(x)$		Mukherje-3 $\tilde{x} \pm IQR(x)$	
BIANT-1	0.93	0.02	0.93	0.04	0.91	0.04
BIANT-2	0.93	0.03	0.90	0.04	0.93	0.03
CHAC-1	0.87	0.02	0.86	0.01	0.84	0.02
CHAC-2	0.87	0.01	0.87	0.02	0.84	0.01
DMOABC	0.86	0.00	0.85	0.01	0.84	0.01
DMOCSA-1-1	0.86	0.01	0.85	0.01	0.84	0.01
DMOCSA-1-2	0.86	0.02	0.85	0.01	0.84	0.01
DMOCSA-1-3	0.86	0.01	0.85	0.01	0.84	0.01
DMOCSA-1-4	0.86	0.00	0.86	0.02	0.84	0.01
DMOCSA-1-5	0.86	0.02	0.86	0.01	0.84	0.01
DMOCSA-2-1	0.85	0.01	0.86	0.01	0.84	0.00
DMOCSA-2-2	0.86	0.00	0.86	0.02	0.85	0.01
DMOCSA-2-3	0.86	0.01	0.85	0.01	0.84	0.01
DMOCSA-2-4	0.85	0.02	0.85	0.02	0.84	0.00
DMOCSA-2-5	0.86	0.01	0.85	0.01	0.84	0.02
DMOFPA-1	0.86	0.01	0.85	0.01	0.84	0.01
DMOFPA-2	0.85	0.01	0.86	0.02	0.84	0.01
DMOFPA-3	0.86	0.01	0.86	0.00	0.84	0.01
DMOFPA-4	0.86	0.01	0.85	0.01	0.84	0.02
DMOFPA-5	0.86	0.01	0.85	0.01	0.85	0.01
MOACS-1	0.88	0.02	0.88	0.02	0.90	0.01
MOACS-2	0.91	0.01	0.91	0.01	0.92	0.02
DMOBAT-1	0.85	0.01	0.85	0.01	0.84	0.01
DMOBAT-2	0.86	0.01	0.86	0.02	0.84	0.01
DMOBAT-3	0.86	0.01	0.86	0.01	0.84	0.02
DMOBAT-4	0.86	0.02	0.85	0.02	0.85	0.01
DMOBAT-5	0.85	0.01	0.85	0.02	0.85	0.01
DMOPSO-1	0.86	0.01	0.85	0.02	0.84	0.02
DMOPSO-2	0.85	0.01	0.86	0.02	0.84	0.00
DMOPSO-3	0.86	0.01	0.85	0.02	0.84	0.02
DMOPSO-4	0.86	0.01	0.86	0.00	0.84	0.01
DMOPSO-5	0.86	0.01	0.86	0.01	0.84	0.01
NSGA-II	0.86	0.01	0.86	0.02	0.85	0.01
SPEA2	0.86	0.01	0.86	0.02	0.85	0.01

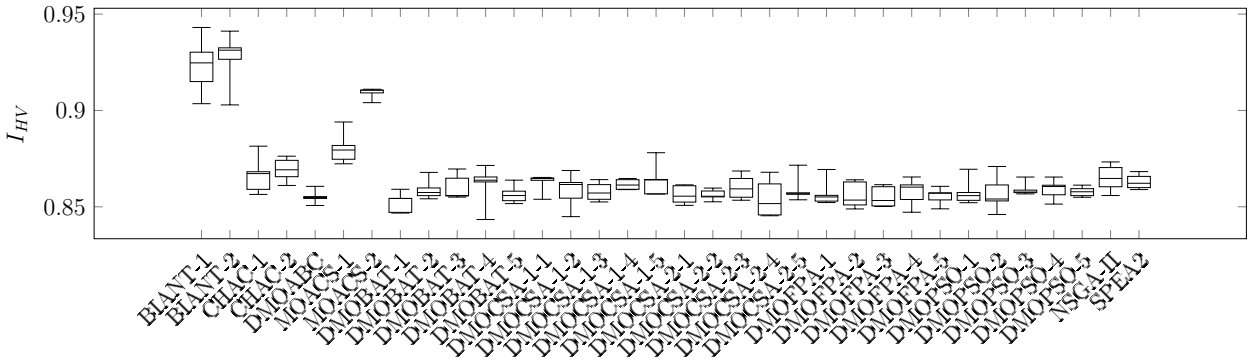

Figure C.53: Boxplot for I_{HV}: Mukherje-1

Table C.57: Median and interquartile range of I_{IGD} obtained by the optimisers for the Mukherje problems

	Mukherje-1 $\tilde{x} \pm IQR(x)$		Mukherje-2 $\tilde{x} \pm IQR(x)$		Mukherje-3 $\tilde{x} \pm IQR(x)$	
BIANT-1	0.48	0.08	0.56	0.01	0.47	0.08
BIANT-2	0.46	0.16	0.60	0.02	0.38	0.14
CHAC-1	0.88	0.02	0.83	0.03	0.83	0.11
CHAC-2	0.83	0.06	0.77	0.04	0.87	0.03
DMOABC	0.92	0.02	0.85	0.03	0.89	0.03
DMOCSA-1-1	0.87	0.03	0.84	0.02	0.86	0.05
DMOCSA-1-2	0.88	0.07	0.85	0.06	0.84	0.07
DMOCSA-1-3	0.89	0.06	0.83	0.03	0.88	0.04
DMOCSA-1-4	0.89	0.03	0.81	0.16	0.86	0.01
DMOCSA-1-5	0.85	0.04	0.80	0.03	0.89	0.04
DMOCSA-2-1	0.91	0.04	0.81	0.03	0.85	0.03
DMOCSA-2-2	0.93	0.02	0.80	0.04	0.82	0.06
DMOCSA-2-3	0.91	0.07	0.83	0.01	0.84	0.05
DMOCSA-2-4	0.92	0.08	0.80	0.16	0.83	0.02
DMOCSA-2-5	0.91	0.03	0.83	0.04	0.85	0.06
DMOFPA-1	0.90	0.03	0.84	0.03	0.83	0.06
DMOFPA-2	0.93	0.07	0.79	0.11	0.86	0.05
DMOFPA-3	0.91	0.05	0.85	0.00	0.86	0.04
DMOFPA-4	0.87	0.07	0.84	0.06	0.88	0.06
DMOFPA-5	0.89	0.03	0.81	0.02	0.83	0.06
MOACS-1	0.75	0.08	0.71	0.06	0.48	0.03
MOACS-2	0.63	0.00	0.58	0.03	0.44	0.03
DMOBAT-1	0.92	0.05	0.84	0.03	0.88	0.01
DMOBAT-2	0.89	0.03	0.83	0.13	0.87	0.03
DMOBAT-3	0.93	0.09	0.78	0.01	0.85	0.08
DMOBAT-4	0.85	0.02	0.84	0.01	0.90	0.04
DMOBAT-5	0.91	0.06	0.88	0.09	0.82	0.01
DMOPSO-1	0.91	0.02	0.88	0.06	0.90	0.01
DMOPSO-2	0.91	0.06	0.81	0.02	0.89	0.03
DMOPSO-3	0.89	0.02	0.88	0.05	0.86	0.10
DMOPSO-4	0.90	0.03	0.80	0.03	0.87	0.03
DMOPSO-5	0.93	0.03	0.85	0.08	0.86	0.05
NSGA-II	0.90	0.05	0.85	0.06	0.90	0.07
SPEA2	0.94	0.05	0.85	0.07	0.86	0.13

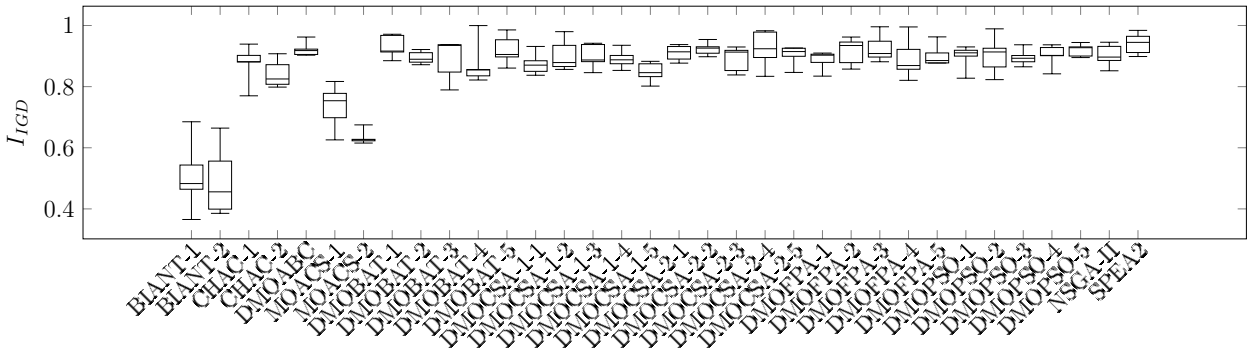

Figure C.54: Boxplot for I_{IGD}: Mukherje-1

Table C.58: Median and interquartile range of I_ϵ obtained by the optimisers for the Mukherje problems

	Mukherje-1 $\tilde{x} \pm IQR(x)$		Mukherje-2 $\tilde{x} \pm IQR(x)$		Mukherje-3 $\tilde{x} \pm IQR(x)$	
BIANT-1	0.78	0.12	0.66	0.11	0.79	0.08
BIANT-2	0.75	0.12	0.80	0.09	0.77	0.11
CHAC-1	0.34	0.00	0.35	0.00	0.43	0.01
CHAC-2	0.34	0.00	0.35	0.00	0.42	0.01
DMOABC	0.33	0.00	0.35	0.01	0.43	0.01
DMOCSA-1-1	0.33	0.01	0.36	0.00	0.43	0.01
DMOCSA-1-2	0.34	0.01	0.35	0.00	0.43	0.00
DMOCSA-1-3	0.34	0.00	0.36	0.01	0.43	0.01
DMOCSA-1-4	0.33	0.01	0.35	0.00	0.43	0.01
DMOCSA-1-5	0.33	0.00	0.35	0.01	0.43	0.00
DMOCSA-2-1	0.33	0.00	0.35	0.01	0.43	0.00
DMOCSA-2-2	0.33	0.01	0.35	0.00	0.43	0.00
DMOCSA-2-3	0.34	0.00	0.35	0.00	0.43	0.01
DMOCSA-2-4	0.34	0.01	0.35	0.01	0.42	0.01
DMOCSA-2-5	0.34	0.00	0.35	0.00	0.43	0.00
DMOFPA-1	0.33	0.00	0.35	0.01	0.43	0.00
DMOFPA-2	0.34	0.00	0.35	0.00	0.43	0.00
DMOFPA-3	0.34	0.00	0.35	0.00	0.43	0.01
DMOFPA-4	0.34	0.00	0.35	0.00	0.43	0.00
DMOFPA-5	0.33	0.00	0.35	0.00	0.42	0.01
MOACS-1	0.92	0.13	0.93	0.05	0.84	0.15
MOACS-2	0.46	0.04	0.51	0.04	0.56	0.04
DMOBAT-1	0.34	0.00	0.35	0.01	0.43	0.00
DMOBAT-2	0.33	0.01	0.35	0.00	0.43	0.01
DMOBAT-3	0.34	0.00	0.35	0.01	0.43	0.00
DMOBAT-4	0.33	0.01	0.35	0.00	0.42	0.00
DMOBAT-5	0.34	0.00	0.36	0.00	0.43	0.00
DMOPSO-1	0.33	0.01	0.35	0.01	0.43	0.01
DMOPSO-2	0.34	0.00	0.35	0.01	0.43	0.01
DMOPSO-3	0.34	0.01	0.35	0.01	0.43	0.01
DMOPSO-4	0.33	0.00	0.36	0.00	0.43	0.01
DMOPSO-5	0.33	0.01	0.35	0.00	0.43	0.01
NSGA-II	0.21	0.00	0.22	0.01	0.26	0.01
SPEA2	0.21	0.00	0.21	0.01	0.25	0.01

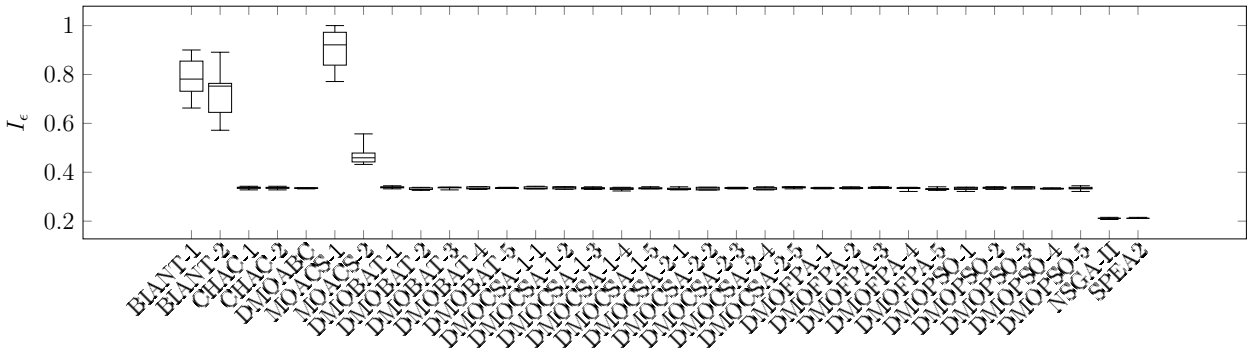

Figure C.55: Boxplot for I_ϵ: Mukherje-1

Table C.59: Median and interquartile range of I_Δ obtained by the optimisers for the Mukherje problems

	Mukherje-1 $\tilde{x} \pm IQR(x)$		Mukherje-2 $\tilde{x} \pm IQR(x)$		Mukherje-3 $\tilde{x} \pm IQR(x)$	
BIANT-1	0.44	0.05	0.48	0.08	0.49	0.08
BIANT-2	0.44	0.01	0.58	0.03	0.48	0.11
CHAC-1	0.74	0.05	0.73	0.06	0.78	0.02
CHAC-2	0.74	0.08	0.75	0.03	0.82	0.05
DMOABC	0.89	0.02	0.88	0.05	0.96	0.09
DMOCSA-1-1	0.83	0.03	0.82	0.03	0.88	0.07
DMOCSA-1-2	0.84	0.04	0.84	0.02	0.81	0.06
DMOCSA-1-3	0.82	0.03	0.87	0.07	0.88	0.05
DMOCSA-1-4	0.83	0.04	0.82	0.02	0.88	0.03
DMOCSA-1-5	0.84	0.04	0.77	0.00	0.85	0.02
DMOCSA-2-1	0.84	0.08	0.83	0.12	0.86	0.06
DMOCSA-2-2	0.87	0.11	0.89	0.09	0.83	0.06
DMOCSA-2-3	0.84	0.09	0.82	0.03	0.85	0.00
DMOCSA-2-4	0.80	0.07	0.79	0.12	0.83	0.01
DMOCSA-2-5	0.81	0.06	0.90	0.12	0.84	0.02
DMOFPA-1	0.85	0.07	0.80	0.06	0.82	0.05
DMOFPA-2	0.90	0.04	0.82	0.03	0.84	0.05
DMOFPA-3	0.86	0.03	0.83	0.08	0.85	0.03
DMOFPA-4	0.78	0.07	0.83	0.07	0.87	0.11
DMOFPA-5	0.83	0.02	0.87	0.07	0.84	0.01
MOACS-1	0.46	0.01	0.52	0.03	0.50	0.05
MOACS-2	0.35	0.03	0.38	0.05	0.36	0.01
DMOBAT-1	0.86	0.05	0.84	0.08	0.86	0.03
DMOBAT-2	0.82	0.02	0.81	0.07	0.87	0.05
DMOBAT-3	0.84	0.02	0.80	0.04	0.83	0.04
DMOBAT-4	0.84	0.07	0.84	0.08	0.90	0.02
DMOBAT-5	0.82	0.01	0.81	0.11	0.83	0.03
DMOPSO-1	0.84	0.03	0.81	0.07	0.88	0.08
DMOPSO-2	0.81	0.04	0.79	0.02	0.85	0.03
DMOPSO-3	0.80	0.01	0.83	0.03	0.86	0.05
DMOPSO-4	0.83	0.04	0.79	0.05	0.87	0.05
DMOPSO-5	0.79	0.02	0.79	0.05	0.89	0.06
NSGA-II	0.88	0.05	0.92	0.05	0.93	0.05
SPEA2	0.88	0.04	0.90	0.11	0.90	0.04

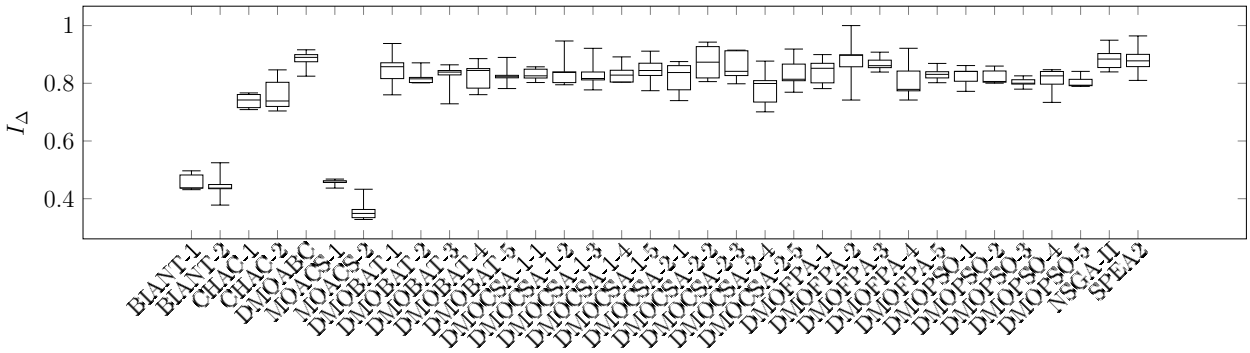

Figure C.56: Boxplot for I_Δ: Mukherje-1

Table C.60: Median and interquartile range of the computation time required by the optimisers for the Mukherje problems

	Mukherje-1 $\tilde{x} \pm IQR(x)$		Mukherje-2 $\tilde{x} \pm IQR(x)$		Mukherje-3 $\tilde{x} \pm IQR(x)$	
BIANT-1	0.87	0.27	0.62	0.16	0.84	0.34
BIANT-2	0.90	0.22	0.82	0.22	0.40	0.54
CHAC-1	0.47	0.04	0.61	0.06	0.29	0.40
CHAC-2	0.44	0.09	0.39	0.28	0.33	0.28
DMOABC	0.50	0.09	0.88	0.20	0.45	0.23
DMOCSA-1-1	0.41	0.23	0.48	0.23	0.39	0.33
DMOCSA-1-2	0.33	0.29	0.53	0.11	0.34	0.15
DMOCSA-1-3	0.32	0.13	0.42	0.04	0.21	0.12
DMOCSA-1-4	0.50	0.28	0.48	0.07	0.30	0.11
DMOCSA-1-5	0.39	0.21	0.59	0.23	0.21	0.03
DMOCSA-2-1	0.61	0.13	0.58	0.20	0.44	0.03
DMOCSA-2-2	0.53	0.15	0.46	0.04	0.54	0.15
DMOCSA-2-3	0.41	0.38	0.58	0.16	0.39	0.17
DMOCSA-2-4	0.54	0.21	0.53	0.28	0.45	0.30
DMOCSA-2-5	0.70	0.20	0.54	0.23	0.47	0.17
DMOFPA-1	0.34	0.16	0.30	0.31	0.40	0.22
DMOFPA-2	0.34	0.20	0.46	0.22	0.24	0.17
DMOFPA-3	0.46	0.12	0.43	0.30	0.36	0.11
DMOFPA-4	0.35	0.13	0.47	0.24	0.28	0.17
DMOFPA-5	0.38	0.06	0.26	0.29	0.42	0.01
MOACS-1	0.52	0.08	0.66	0.18	0.42	0.15
MOACS-2	0.39	0.24	0.53	0.06	0.50	0.11
DMOBAT-1	0.31	0.07	0.35	0.18	0.24	0.09
DMOBAT-2	0.34	0.15	0.42	0.23	0.27	0.11
DMOBAT-3	0.35	0.19	0.43	0.34	0.32	0.11
DMOBAT-4	0.38	0.31	0.50	0.22	0.33	0.09
DMOBAT-5	0.30	0.07	0.40	0.17	0.25	0.15
DMOPSO-1	0.52	0.17	0.29	0.07	0.28	0.15
DMOPSO-2	0.35	0.18	0.44	0.09	0.18	0.17
DMOPSO-3	0.55	0.18	0.31	0.63	0.33	0.11
DMOPSO-4	0.82	0.09	0.67	0.23	0.56	0.51
DMOPSO-5	0.47	0.28	0.36	0.04	0.32	0.04
NSGA-II	0.28	0.17	0.50	0.21	0.17	0.10
SPEA2	0.19	0.11	0.24	0.17	0.15	0.02

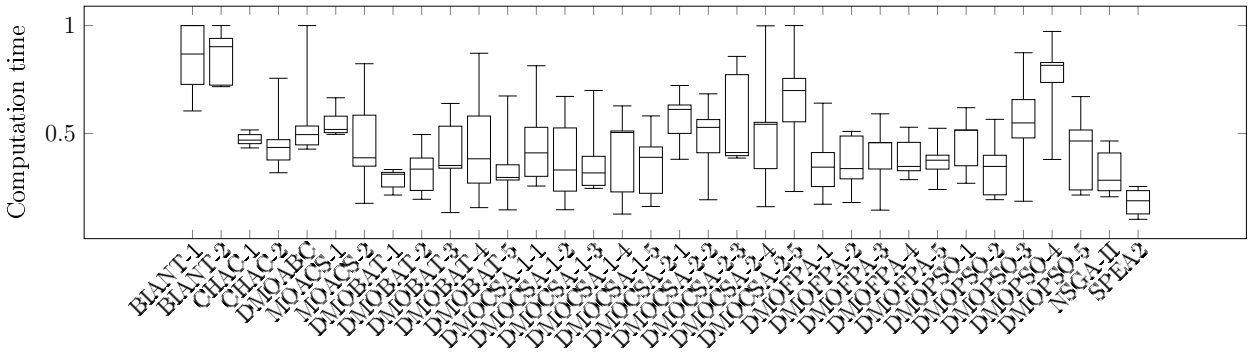

Figure C.57: Boxplot for the computation time: Mukherje-1

C.3.10 Problem Family: Roszieg

Table C.61: Median and interquartile range of I_{HV} obtained by the optimisers for the Roszieg problems

	Roszieg-1 $\tilde{x} \pm IQR(x)$		Roszieg-2 $\tilde{x} \pm IQR(x)$		Roszieg-3 $\tilde{x} \pm IQR(x)$		Roszieg-4 $\tilde{x} \pm IQR(x)$	
BIANT-1	0.97	0.03	0.36	0.00	0.92	0.05	0.68	0.00
BIANT-2	0.94	0.05	0.37	0.04	0.76	0.13	0.67	0.00
CHAC-1	0.99	0.01	0.48	0.00	0.99	0.01	0.68	0.00
CHAC-2	1.00	0.00	0.48	0.00	1.00	0.01	0.68	0.00
DMOABC	1.00	0.01	0.48	0.00	0.99	0.01	0.68	0.00
DMOCSA-1-1	1.00	0.01	0.48	0.00	0.99	0.01	0.68	0.00
DMOCSA-1-2	0.99	0.01	0.48	0.00	0.99	0.00	0.68	0.00
DMOCSA-1-3	1.00	0.01	0.47	0.00	0.98	0.01	0.68	0.00
DMOCSA-1-4	0.99	0.02	0.46	0.01	0.95	0.02	0.68	0.00
DMOCSA-1-5	1.00	0.01	0.48	0.00	0.98	0.02	0.68	0.00
DMOCSA-2-1	1.00	0.00	0.48	0.00	0.98	0.01	0.68	0.00
DMOCSA-2-2	1.00	0.01	0.48	0.00	0.98	0.01	0.68	0.00
DMOCSA-2-3	1.00	0.01	0.48	0.00	0.98	0.02	0.68	0.00
DMOCSA-2-4	0.98	0.01	0.46	0.01	0.96	0.00	0.68	0.00
DMOCSA-2-5	1.00	0.00	0.48	0.01	0.99	0.02	0.68	0.00
DMOFPA-1	1.00	0.00	0.47	0.00	0.99	0.00	0.68	0.00
DMOFPA-2	1.00	0.00	0.48	0.00	0.99	0.01	0.68	0.00
DMOFPA-3	1.00	0.01	0.48	0.00	0.98	0.01	0.68	0.00
DMOFPA-4	0.98	0.01	0.46	0.01	0.95	0.01	0.68	0.00
DMOFPA-5	1.00	0.01	0.48	0.01	0.99	0.01	0.68	0.00
MOACS-1	0.96	0.00	0.39	0.02	0.95	0.05	0.61	0.00
MOACS-2	0.96	0.04	0.38	0.03	0.88	0.13	0.63	0.00
DMOBAT-1	0.99	0.00	0.48	0.00	0.98	0.02	0.68	0.00
DMOBAT-2	1.00	0.01	0.48	0.00	0.99	0.00	0.68	0.00
DMOBAT-3	1.00	0.00	0.48	0.00	0.98	0.01	0.68	0.00
DMOBAT-4	0.99	0.00	0.46	0.00	0.95	0.01	0.68	0.00
DMOBAT-5	1.00	0.01	0.48	0.00	0.99	0.01	0.68	0.00
DMOPSO-1	1.00	0.00	0.48	0.00	0.99	0.01	0.68	0.00
DMOPSO-2	1.00	0.00	0.48	0.00	0.99	0.01	0.68	0.00
DMOPSO-3	1.00	0.00	0.48	0.00	0.99	0.01	0.68	0.00
DMOPSO-4	0.99	0.02	0.47	0.01	0.95	0.05	0.68	0.00
DMOPSO-5	1.00	0.01	0.48	0.00	0.98	0.01	0.68	0.00
NSGA-II	1.00	0.01	0.48	0.00	0.99	0.01	0.68	0.00
SPEA2	0.99	0.01	0.48	0.00	0.99	0.01	0.68	0.00

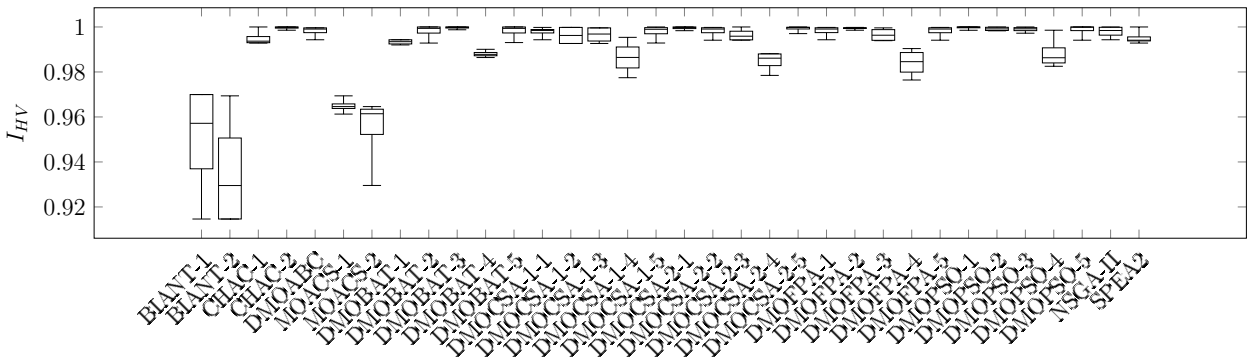

Figure C.58: Boxplot for I_{HV}: Roszieg-1

Table C.62: Median and interquartile range of I_{IGD} obtained by the optimisers for the Roszieg problems

	Roszieg-1 $\tilde{x} \pm IQR(x)$		Roszieg-2 $\tilde{x} \pm IQR(x)$		Roszieg-3 $\tilde{x} \pm IQR(x)$		Roszieg-4 $\tilde{x} \pm IQR(x)$	
BIANT-1	0.53	0.33	0.99	0.02	0.58	0.05	0.25	0.35
BIANT-2	0.83	0.42	0.96	0.06	0.93	0.17	0.42	0.00
CHAC-1	0.12	0.15	0.90	0.00	0.36	0.05	0.07	0.00
CHAC-2	0.04	0.01	0.90	0.00	0.28	0.01	0.07	0.00
DMOABC	0.04	0.04	0.90	0.00	0.34	0.05	0.07	0.00
DMOCSA-1-1	0.07	0.04	0.91	0.00	0.34	0.05	0.07	0.00
DMOCSA-1-2	0.11	0.14	0.91	0.00	0.29	0.03	0.07	0.00
DMOCSA-1-3	0.11	0.13	0.91	0.00	0.29	0.01	0.07	0.00
DMOCSA-1-4	0.09	0.04	0.91	0.00	0.47	0.07	0.07	0.00
DMOCSA-1-5	0.06	0.05	0.90	0.00	0.34	0.03	0.07	0.00
DMOCSA-2-1	0.04	0.01	0.90	0.00	0.31	0.02	0.07	0.00
DMOCSA-2-2	0.06	0.05	0.91	0.00	0.31	0.03	0.07	0.00
DMOCSA-2-3	0.12	0.12	0.90	0.00	0.29	0.03	0.07	0.00
DMOCSA-2-4	0.09	0.04	0.91	0.00	0.43	0.07	0.07	0.00
DMOCSA-2-5	0.04	0.01	0.91	0.00	0.35	0.04	0.07	0.00
DMOFPA-1	0.06	0.05	0.91	0.00	0.34	0.03	0.07	0.00
DMOFPA-2	0.04	0.01	0.90	0.00	0.29	0.03	0.07	0.00
DMOFPA-3	0.12	0.12	0.91	0.00	0.31	0.03	0.07	0.00
DMOFPA-4	0.17	0.03	0.91	0.01	0.47	0.05	0.07	0.00
DMOFPA-5	0.06	0.05	0.90	0.00	0.31	0.04	0.07	0.00
MOACS-1	0.44	0.02	0.95	0.07	0.56	0.09	0.44	0.15
MOACS-2	0.44	0.00	0.92	0.02	0.70	0.11	0.83	0.13
DMOBAT-1	0.13	0.14	0.90	0.00	0.30	0.04	0.07	0.00
DMOBAT-2	0.05	0.02	0.91	0.00	0.29	0.02	0.07	0.00
DMOBAT-3	0.04	0.01	0.91	0.00	0.32	0.05	0.07	0.00
DMOBAT-4	0.20	0.04	0.91	0.00	0.46	0.07	0.07	0.00
DMOBAT-5	0.05	0.06	0.91	0.00	0.29	0.02	0.07	0.00
DMOPSO-1	0.04	0.00	0.90	0.00	0.35	0.03	0.07	0.00
DMOPSO-2	0.04	0.00	0.90	0.00	0.35	0.05	0.07	0.00
DMOPSO-3	0.05	0.02	0.90	0.00	0.31	0.03	0.07	0.00
DMOPSO-4	0.13	0.10	0.91	0.01	0.47	0.08	0.07	0.00
DMOPSO-5	0.04	0.04	0.91	0.00	0.35	0.09	0.07	0.00
NSGA-II	0.06	0.06	0.90	0.00	0.32	0.07	0.07	0.00
SPEA2	0.12	0.13	0.91	0.00	0.33	0.01	0.07	0.00

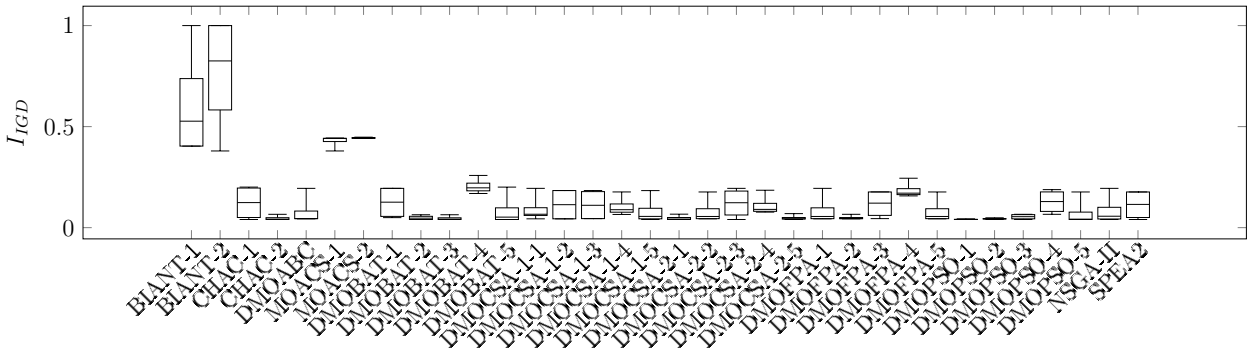

Figure C.59: Boxplot for I_{IGD}: Roszieg-1

Table C.63: Median and interquartile range of I_ϵ obtained by the optimisers for the Roszieg problems

	Roszieg-1 $\tilde{x} \pm IQR(x)$		Roszieg-2 $\tilde{x} \pm IQR(x)$		Roszieg-3 $\tilde{x} \pm IQR(x)$		Roszieg-4 $\tilde{x} \pm IQR(x)$	
BIANT-1	0.63	0.31	0.93	0.04	0.51	0.10	0.87	0.01
BIANT-2	0.88	0.31	0.93	0.01	0.73	0.42	0.87	0.00
CHAC-1	0.27	0.02	0.45	0.00	0.43	0.01	0.86	0.00
CHAC-2	0.18	0.00	0.45	0.00	0.43	0.02	0.86	0.00
DMOABC	0.18	0.02	0.44	0.02	0.43	0.01	0.86	0.00
DMOCSA-1-1	0.18	0.02	0.46	0.00	0.43	0.01	0.86	0.00
DMOCSA-1-2	0.22	0.08	0.46	0.00	0.43	0.01	0.86	0.00
DMOCSA-1-3	0.22	0.08	0.46	0.00	0.44	0.01	0.86	0.00
DMOCSA-1-4	0.27	0.04	0.47	0.01	0.47	0.01	0.86	0.00
DMOCSA-1-5	0.18	0.02	0.45	0.01	0.43	0.01	0.86	0.00
DMOCSA-2-1	0.18	0.00	0.46	0.00	0.45	0.02	0.86	0.00
DMOCSA-2-2	0.18	0.02	0.45	0.02	0.44	0.00	0.86	0.00
DMOCSA-2-3	0.22	0.08	0.45	0.02	0.44	0.01	0.86	0.00
DMOCSA-2-4	0.31	0.08	0.47	0.02	0.45	0.00	0.86	0.00
DMOCSA-2-5	0.18	0.00	0.46	0.01	0.43	0.01	0.86	0.00
DMOFPA-1	0.18	0.02	0.46	0.00	0.43	0.01	0.86	0.00
DMOFPA-2	0.18	0.00	0.45	0.00	0.43	0.00	0.86	0.00
DMOFPA-3	0.22	0.08	0.45	0.02	0.43	0.00	0.86	0.00
DMOFPA-4	0.31	0.10	0.46	0.01	0.46	0.00	0.86	0.00
DMOFPA-5	0.18	0.02	0.45	0.01	0.44	0.01	0.86	0.00
MOACS-1	0.51	0.00	0.88	0.06	0.57	0.18	0.90	0.04
MOACS-2	0.51	0.06	0.88	0.00	0.61	0.13	0.99	0.03
DMOBAT-1	0.27	0.00	0.45	0.00	0.43	0.01	0.86	0.00
DMOBAT-2	0.18	0.02	0.45	0.00	0.43	0.01	0.86	0.00
DMOBAT-3	0.18	0.00	0.45	0.00	0.43	0.01	0.86	0.00
DMOBAT-4	0.27	0.00	0.46	0.00	0.47	0.02	0.86	0.00
DMOBAT-5	0.18	0.02	0.45	0.00	0.44	0.01	0.86	0.00
DMOPSO-1	0.18	0.00	0.45	0.00	0.44	0.01	0.86	0.00
DMOPSO-2	0.18	0.00	0.46	0.00	0.43	0.00	0.86	0.00
DMOPSO-3	0.18	0.00	0.45	0.00	0.43	0.01	0.86	0.00
DMOPSO-4	0.27	0.05	0.47	0.02	0.46	0.03	0.86	0.00
DMOPSO-5	0.18	0.02	0.45	0.01	0.43	0.00	0.86	0.00
NSGA-II	0.18	0.02	0.45	0.00	0.43	0.00	0.86	0.00
SPEA2	0.27	0.02	0.45	0.02	0.43	0.01	0.86	0.00

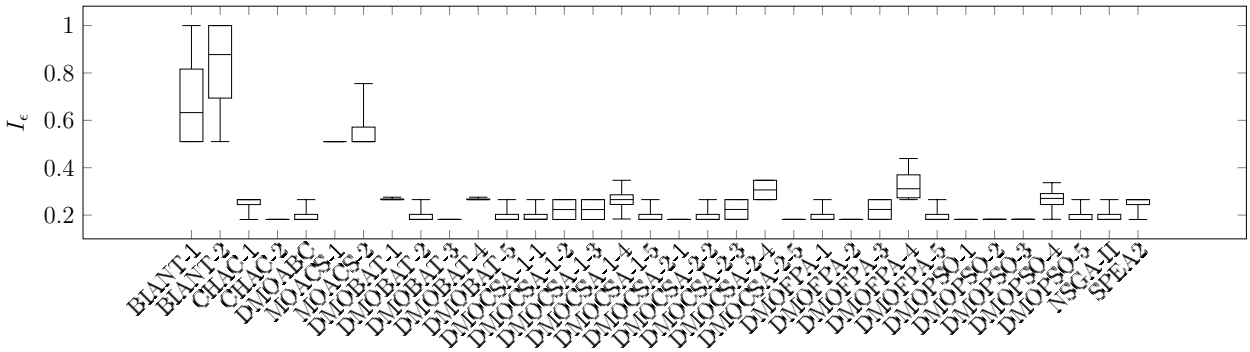

Figure C.60: Boxplot for I_ϵ: Roszieg-1

Table C.64: Median and interquartile range of I_Δ obtained by the optimisers for the Roszieg problems

	Roszieg-1 $\tilde{x} \pm IQR(x)$		Roszieg-2 $\tilde{x} \pm IQR(x)$		Roszieg-3 $\tilde{x} \pm IQR(x)$		Roszieg-4 $\tilde{x} \pm IQR(x)$	
BIANT-1	0.80	0.09	0.87	0.06	0.62	0.09	0.38	0.01
BIANT-2	0.86	0.08	0.80	0.04	0.72	0.15	0.38	0.00
CHAC-1	0.84	0.02	0.86	0.04	0.80	0.05	0.39	0.00
CHAC-2	0.84	0.02	0.85	0.03	0.69	0.13	0.39	0.00
DMOABC	0.77	0.10	0.85	0.08	0.81	0.08	0.39	0.00
DMOCSA-1-1	0.85	0.11	0.93	0.06	0.76	0.13	0.39	0.00
DMOCSA-1-2	0.87	0.02	0.91	0.06	0.72	0.04	0.39	0.00
DMOCSA-1-3	0.84	0.08	0.94	0.04	0.73	0.03	0.39	0.00
DMOCSA-1-4	0.69	0.15	0.86	0.05	0.59	0.13	0.39	0.00
DMOCSA-1-5	0.83	0.07	0.87	0.04	0.80	0.02	0.39	0.00
DMOCSA-2-1	0.83	0.05	0.92	0.03	0.75	0.07	0.39	0.00
DMOCSA-2-2	0.85	0.08	0.87	0.02	0.78	0.05	0.39	0.00
DMOCSA-2-3	0.90	0.16	0.87	0.05	0.77	0.05	0.39	0.00
DMOCSA-2-4	0.69	0.09	0.90	0.05	0.62	0.22	0.39	0.00
DMOCSA-2-5	0.86	0.05	0.87	0.07	0.77	0.13	0.39	0.00
DMOFPA-1	0.80	0.19	0.93	0.04	0.75	0.03	0.39	0.00
DMOFPA-2	0.81	0.02	0.93	0.04	0.71	0.03	0.39	0.00
DMOFPA-3	0.88	0.14	0.89	0.03	0.78	0.12	0.39	0.00
DMOFPA-4	0.79	0.18	0.85	0.10	0.64	0.09	0.39	0.00
DMOFPA-5	0.85	0.10	0.80	0.05	0.80	0.05	0.39	0.00
MOACS-1	0.70	0.04	0.84	0.08	0.70	0.06	0.49	0.11
MOACS-2	0.70	0.04	0.84	0.04	0.70	0.03	0.53	0.09
DMOBAT-1	0.84	0.04	0.93	0.02	0.75	0.07	0.39	0.00
DMOBAT-2	0.73	0.02	0.89	0.02	0.72	0.20	0.39	0.00
DMOBAT-3	0.84	0.03	0.89	0.07	0.75	0.15	0.39	0.00
DMOBAT-4	0.74	0.08	0.88	0.05	0.74	0.03	0.39	0.00
DMOBAT-5	0.74	0.02	0.95	0.01	0.68	0.15	0.39	0.00
DMOPSO-1	0.81	0.07	0.88	0.01	0.67	0.07	0.39	0.00
DMOPSO-2	0.88	0.02	0.87	0.05	0.76	0.04	0.39	0.00
DMOPSO-3	0.83	0.06	0.87	0.02	0.64	0.06	0.39	0.00
DMOPSO-4	0.75	0.03	0.88	0.02	0.75	0.07	0.39	0.00
DMOPSO-5	0.86	0.08	0.85	0.06	0.69	0.07	0.39	0.00
NSGA-II	0.86	0.10	0.83	0.04	0.81	0.03	0.39	0.00
SPEA2	0.92	0.16	0.85	0.07	0.76	0.11	0.39	0.00

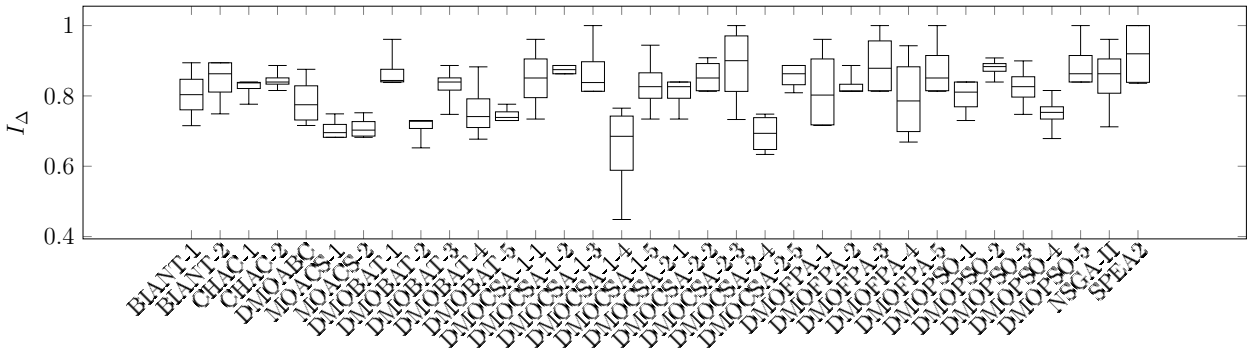

Figure C.61: Boxplot for I_Δ: Roszieg-1

Table C.65: Median and interquartile range of the computation time required by the optimisers for the Roszieg problems

	Roszieg-1 $\tilde{x} \pm IQR(x)$		Roszieg-2 $\tilde{x} \pm IQR(x)$		Roszieg-3 $\tilde{x} \pm IQR(x)$		Roszieg-4 $\tilde{x} \pm IQR(x)$	
BIANT-1	0.93	0.02	0.76	0.13	0.73	0.03	0.74	0.10
BIANT-2	0.96	0.06	0.78	0.18	0.77	0.03	0.95	0.07
CHAC-1	0.83	0.04	0.70	0.23	0.76	0.20	0.57	0.04
CHAC-2	0.83	0.02	0.72	0.10	0.68	0.11	0.55	0.04
DMOABC	0.94	0.02	0.77	0.16	0.82	0.15	0.65	0.04
DMOCSA-1-1	0.73	0.02	0.60	0.15	0.64	0.07	0.50	0.04
DMOCSA-1-2	0.72	0.02	0.63	0.21	0.64	0.09	0.50	0.04
DMOCSA-1-3	0.74	0.02	0.77	0.12	0.60	0.11	0.50	0.06
DMOCSA-1-4	0.72	0.03	0.63	0.06	0.57	0.06	0.49	0.05
DMOCSA-1-5	0.71	0.06	0.63	0.10	0.79	0.11	0.48	0.03
DMOCSA-2-1	0.79	0.03	0.68	0.20	0.66	0.09	0.56	0.09
DMOCSA-2-2	0.76	0.03	0.66	0.10	0.66	0.16	0.51	0.04
DMOCSA-2-3	0.80	0.05	0.82	0.13	0.75	0.10	0.54	0.04
DMOCSA-2-4	0.80	0.04	0.63	0.13	0.81	0.21	0.54	0.04
DMOCSA-2-5	0.81	0.02	0.69	0.09	0.75	0.07	0.55	0.05
DMOFPA-1	0.73	0.03	0.58	0.09	0.64	0.14	0.49	0.04
DMOFPA-2	0.75	0.02	0.67	0.12	0.78	0.30	0.51	0.04
DMOFPA-3	0.75	0.02	0.62	0.14	0.66	0.13	0.50	0.04
DMOFPA-4	0.44	0.04	0.32	0.12	0.33	0.02	0.27	0.02
DMOFPA-5	0.73	0.03	0.66	0.17	0.67	0.09	0.51	0.03
MOACS-1	0.90	0.03	0.79	0.23	0.82	0.09	0.85	0.15
MOACS-2	1.00	0.02	0.90	0.20	0.89	0.09	0.98	0.09
DMOBAT-1	0.73	0.05	0.67	0.19	0.73	0.18	0.49	0.04
DMOBAT-2	0.73	0.04	0.65	0.01	0.59	0.07	0.52	0.05
DMOBAT-3	0.76	0.02	0.65	0.14	0.63	0.14	0.51	0.04
DMOBAT-4	0.72	0.02	0.59	0.14	0.58	0.04	0.50	0.04
DMOBAT-5	0.75	0.04	0.74	0.05	0.67	0.10	0.51	0.04
DMOPSO-1	0.67	0.14	0.55	0.16	0.60	0.08	0.45	0.09
DMOPSO-2	0.72	0.04	0.62	0.06	0.56	0.09	0.48	0.03
DMOPSO-3	0.55	0.06	0.48	0.08	0.45	0.07	0.35	0.04
DMOPSO-4	0.73	0.13	0.59	0.17	0.55	0.04	0.47	0.06
DMOPSO-5	0.74	0.07	0.60	0.15	0.73	0.15	0.50	0.04
NSGA-II	0.84	0.03	0.72	0.10	0.74	0.07	0.64	0.04
SPEA2	0.64	0.03	0.52	0.13	0.54	0.08	0.45	0.03

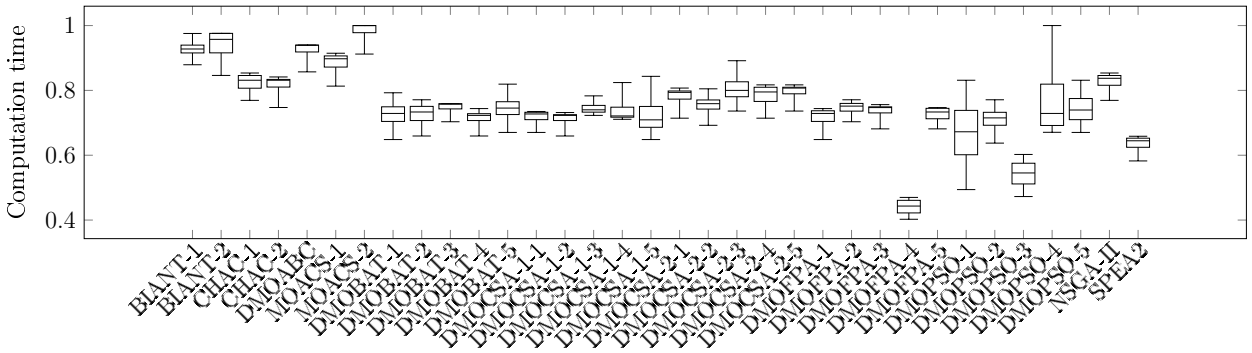

Figure C.62: Boxplot for the computation time: Roszieg-1

C.3.11 Problem Family: Sawyer

Table C.66: Median and interquartile range of I_{HV} obtained by the optimisers for the Sawyer problems

	Sawyer-1 $\tilde{x} \pm IQR(x)$		Sawyer-2 $\tilde{x} \pm IQR(x)$		Sawyer-3 $\tilde{x} \pm IQR(x)$		Sawyer-4 $\tilde{x} \pm IQR(x)$	
BIANT-1	0.92	0.00	0.96	0.00	0.86	0.00	0.85	0.00
BIANT-2	1.00	0.00	0.78	0.00	0.86	0.00	0.86	0.00
CHAC-1	1.00	0.00	1.00	0.00	1.00	0.00	0.99	0.00
CHAC-2	1.00	0.00	1.00	0.00	1.00	0.00	0.99	0.00
DMOABC	1.00	0.00	1.00	0.00	1.00	0.00	0.99	0.00
DMOCSA-1-1	1.00	0.00	1.00	0.00	1.00	0.00	0.99	0.00
DMOCSA-1-2	1.00	0.00	1.00	0.00	1.00	0.00	0.99	0.00
DMOCSA-1-3	1.00	0.00	1.00	0.00	1.00	0.00	0.99	0.00
DMOCSA-1-4	1.00	0.00	1.00	0.00	0.93	0.00	0.98	0.00
DMOCSA-1-5	1.00	0.00	1.00	0.00	1.00	0.00	0.99	0.00
DMOCSA-2-1	1.00	0.00	1.00	0.00	1.00	0.00	0.99	0.00
DMOCSA-2-2	1.00	0.00	1.00	0.00	1.00	0.00	0.99	0.00
DMOCSA-2-3	1.00	0.00	1.00	0.00	1.00	0.00	0.99	0.00
DMOCSA-2-4	1.00	0.00	1.00	0.00	1.00	0.00	0.98	0.00
DMOCSA-2-5	1.00	0.00	1.00	0.00	1.00	0.00	0.99	0.00
DMOFPA-1	1.00	0.00	1.00	0.00	1.00	0.00	0.99	0.00
DMOFPA-2	1.00	0.00	1.00	0.00	1.00	0.00	0.99	0.00
DMOFPA-3	1.00	0.00	1.00	0.00	1.00	0.00	0.99	0.00
DMOFPA-4	1.00	0.00	1.00	0.00	0.99	0.00	0.98	0.00
DMOFPA-5	1.00	0.00	1.00	0.00	1.00	0.00	1.00	0.00
MOACS-1	0.90	0.00	0.78	0.00	0.87	0.00	0.85	0.00
MOACS-2	0.90	0.00	0.78	0.00	0.86	0.00	0.85	0.00
DMOBAT-1	1.00	0.00	1.00	0.00	1.00	0.00	0.99	0.00
DMOBAT-2	1.00	0.00	1.00	0.00	1.00	0.00	0.99	0.00
DMOBAT-3	1.00	0.00	1.00	0.00	1.00	0.00	0.99	0.00
DMOBAT-4	1.00	0.00	1.00	0.00	0.99	0.00	0.98	0.00
DMOBAT-5	1.00	0.00	1.00	0.00	1.00	0.00	0.99	0.00
DMOPSO-1	1.00	0.00	1.00	0.00	1.00	0.00	0.99	0.00
DMOPSO-2	1.00	0.00	1.00	0.00	1.00	0.00	0.99	0.00
DMOPSO-3	1.00	0.00	1.00	0.00	1.00	0.00	0.99	0.00
DMOPSO-4	1.00	0.00	1.00	0.00	1.00	0.00	0.97	0.00
DMOPSO-5	1.00	0.00	1.00	0.00	1.00	0.00	1.00	0.00
NSGA-II	1.00	0.00	1.00	0.00	1.00	0.00	0.99	0.00
SPEA2	1.00	0.00	1.00	0.00	1.00	0.00	0.99	0.00

Table C.67: Median and interquartile range of I_{IGD} obtained by the optimisers for the Sawyer problems

	Sawyer-1 $\tilde{x} \pm IQR(x)$		Sawyer-2 $\tilde{x} \pm IQR(x)$		Sawyer-3 $\tilde{x} \pm IQR(x)$		Sawyer-4 $\tilde{x} \pm IQR(x)$	
BIANT-1	0.02	0.00	0.55	1.00	0.38	0.05	0.94	0.16
BIANT-2	0.73	0.72	1.00	0.48	0.38	0.07	0.93	0.13
CHAC-1	0.73	0.00	0.00	0.00	0.01	0.02	0.07	0.00
CHAC-2	0.73	0.00	0.00	0.00	0.09	0.02	0.08	0.00
DMOABC	0.73	0.00	0.00	0.00	0.09	0.02	0.07	0.00
DMOCSA-1-1	0.73	0.00	0.00	0.00	0.09	0.02	0.07	0.00
DMOCSA-1-2	0.73	0.00	0.00	0.00	0.05	0.09	0.08	0.00
DMOCSA-1-3	0.73	0.00	0.00	0.00	0.09	0.02	0.08	0.00
DMOCSA-1-4	0.73	0.00	0.00	0.00	0.26	0.04	0.11	0.19
DMOCSA-1-5	0.73	0.00	0.00	0.00	0.09	0.02	0.08	0.00
DMOCSA-2-1	0.73	0.00	0.00	0.00	0.01	0.02	0.07	0.00
DMOCSA-2-2	0.73	0.00	0.00	0.00	0.01	0.02	0.08	0.00
DMOCSA-2-3	0.73	0.00	0.00	0.00	0.01	0.02	0.07	0.00
DMOCSA-2-4	0.73	0.00	0.00	0.00	0.09	0.00	0.10	0.01
DMOCSA-2-5	0.73	0.00	0.00	0.00	0.01	0.00	0.08	0.00
DMOFPA-1	0.73	0.00	0.00	0.00	0.05	0.09	0.08	0.00
DMOFPA-2	0.73	0.00	0.00	0.00	0.05	0.09	0.08	0.00
DMOFPA-3	0.73	0.00	0.00	0.00	0.01	0.02	0.08	0.00
DMOFPA-4	0.73	0.00	0.00	0.00	0.09	0.06	0.12	0.01
DMOFPA-5	0.73	0.00	0.00	0.00	0.09	0.00	0.07	0.00
MOACS-1	0.63	0.00	1.00	0.00	0.39	0.06	0.96	0.14
MOACS-2	0.63	0.10	1.00	0.03	0.38	0.06	0.95	0.00
DMOBAT-1	0.73	0.00	0.00	0.00	0.01	0.00	0.08	0.00
DMOBAT-2	0.73	0.00	0.00	0.00	0.01	0.00	0.07	0.00
DMOBAT-3	0.73	0.00	0.00	0.00	0.01	0.00	0.07	0.00
DMOBAT-4	0.73	0.00	0.00	0.00	0.10	0.06	0.11	0.01
DMOBAT-5	0.73	0.00	0.00	0.00	0.01	0.00	0.07	0.00
DMOPSO-1	0.73	0.00	0.00	0.00	0.01	0.02	0.07	0.00
DMOPSO-2	0.73	0.00	0.00	0.00	0.01	0.02	0.07	0.00
DMOPSO-3	0.73	0.00	0.00	0.00	0.01	0.00	0.07	0.00
DMOPSO-4	0.73	0.00	0.00	0.00	0.10	0.04	0.08	0.00
DMOPSO-5	0.73	0.00	0.00	0.00	0.09	0.02	0.93	0.15
NSGA-II	0.73	0.00	0.00	0.00	0.05	0.08	0.50	0.23
SPEA2	0.73	0.00	0.00	0.00	0.09	0.00	0.07	0.00

Table C.68: Median and interquartile range of I_ϵ obtained by the optimisers for the Sawyer problems

	Sawyer-1 $\tilde{x} \pm IQR(x)$		Sawyer-2 $\tilde{x} \pm IQR(x)$		Sawyer-3 $\tilde{x} \pm IQR(x)$		Sawyer-4 $\tilde{x} \pm IQR(x)$	
BIANT-1	0.78	0.00	0.91	0.15	0.76	0.01	0.98	0.09
BIANT-2	0.78	0.00	1.00	0.09	0.76	0.01	0.95	0.08
CHAC-1	0.78	0.00	0.85	0.00	0.53	0.01	0.77	0.00
CHAC-2	0.78	0.00	0.85	0.00	0.53	0.01	0.77	0.00
DMOABC	0.78	0.00	0.85	0.00	0.53	0.00	0.77	0.00
DMOCSA-1-1	0.78	0.00	0.85	0.00	0.53	0.00	0.77	0.00
DMOCSA-1-2	0.78	0.00	0.85	0.00	0.53	0.00	0.77	0.00
DMOCSA-1-3	0.78	0.00	0.85	0.00	0.53	0.00	0.77	0.00
DMOCSA-1-4	0.78	0.00	0.85	0.00	0.64	0.01	0.78	0.01
DMOCSA-1-5	0.78	0.00	0.85	0.00	0.53	0.00	0.77	0.00
DMOCSA-2-1	0.78	0.00	0.85	0.00	0.53	0.00	0.77	0.00
DMOCSA-2-2	0.78	0.00	0.85	0.00	0.53	0.00	0.77	0.00
DMOCSA-2-3	0.78	0.00	0.85	0.00	0.53	0.00	0.76	0.00
DMOCSA-2-4	0.78	0.00	0.85	0.00	0.53	0.01	0.78	0.01
DMOCSA-2-5	0.78	0.00	0.85	0.00	0.53	0.00	0.77	0.00
DMOFPA-1	0.78	0.00	0.85	0.00	0.53	0.00	0.77	0.00
DMOFPA-2	0.78	0.00	0.85	0.00	0.53	0.00	0.77	0.00
DMOFPA-3	0.78	0.00	0.85	0.00	0.53	0.00	0.77	0.00
DMOFPA-4	0.78	0.00	0.85	0.00	0.54	0.12	0.79	0.01
DMOFPA-5	0.78	0.00	0.85	0.00	0.53	0.00	0.76	0.00
MOACS-1	1.00	0.00	1.00	0.00	0.76	0.01	0.99	0.09
MOACS-2	0.79	0.22	1.00	0.08	0.76	0.01	0.98	0.01
DMOBAT-1	0.78	0.00	0.85	0.00	0.53	0.00	0.77	0.00
DMOBAT-2	0.78	0.00	0.85	0.00	0.53	0.00	0.77	0.00
DMOBAT-3	0.78	0.00	0.85	0.00	0.53	0.01	0.77	0.00
DMOBAT-4	0.78	0.00	0.85	0.00	0.55	0.11	0.79	0.01
DMOBAT-5	0.78	0.00	0.85	0.00	0.53	0.00	0.77	0.00
DMOPSO-1	0.78	0.00	0.85	0.00	0.53	0.00	0.76	0.00
DMOPSO-2	0.78	0.00	0.85	0.00	0.53	0.00	0.77	0.00
DMOPSO-3	0.78	0.00	0.85	0.00	0.53	0.00	0.77	0.00
DMOPSO-4	0.78	0.00	0.85	0.00	0.54	0.11	0.77	0.00
DMOPSO-5	0.78	0.00	0.85	0.00	0.53	0.00	0.98	0.09
NSGA-II	0.78	0.00	0.85	0.00	0.53	0.01	0.80	0.02
SPEA2	0.78	0.00	0.85	0.00	0.53	0.00	0.77	0.00

Table C.69: Median and interquartile range of I_Δ obtained by the optimisers for the Sawyer problems

	Sawyer-1 $\tilde{x} \pm IQR(x)$		Sawyer-2 $\tilde{x} \pm IQR(x)$		Sawyer-3 $\tilde{x} \pm IQR(x)$		Sawyer-4 $\tilde{x} \pm IQR(x)$	
BIANT-1	0.06	0.04	0.72	0.28	0.77	0.04	0.84	0.04
BIANT-2	0.57	0.47	1.00	0.05	0.78	0.05	0.84	0.05
CHAC-1	0.57	0.00	0.72	0.00	0.94	0.03	0.97	0.00
CHAC-2	0.57	0.00	0.72	0.00	0.96	0.04	0.96	0.03
DMOABC	0.57	0.00	0.72	0.00	0.96	0.02	0.98	0.01
DMOCSA-1-1	0.57	0.00	0.72	0.00	0.96	0.01	0.98	0.00
DMOCSA-1-2	0.57	0.00	0.72	0.00	0.95	0.03	0.98	0.00
DMOCSA-1-3	0.57	0.00	0.72	0.00	0.96	0.01	0.97	0.02
DMOCSA-1-4	0.57	0.00	0.72	0.00	0.91	0.01	0.91	0.02
DMOCSA-1-5	0.57	0.00	0.72	0.00	0.96	0.01	0.98	0.00
DMOCSA-2-1	0.57	0.00	0.72	0.00	0.92	0.03	0.98	0.02
DMOCSA-2-2	0.57	0.00	0.72	0.00	0.92	0.03	0.98	0.01
DMOCSA-2-3	0.57	0.00	0.72	0.00	0.94	0.02	0.98	0.00
DMOCSA-2-4	0.57	0.00	0.72	0.00	0.93	0.02	0.91	0.01
DMOCSA-2-5	0.57	0.00	0.72	0.00	0.93	0.00	0.98	0.00
DMOFPA-1	0.57	0.00	0.72	0.00	0.94	0.05	0.97	0.02
DMOFPA-2	0.57	0.00	0.72	0.00	0.95	0.03	0.98	0.01
DMOFPA-3	0.57	0.00	0.72	0.00	0.91	0.01	0.97	0.02
DMOFPA-4	0.57	0.00	0.72	0.00	0.91	0.03	0.92	0.12
DMOFPA-5	0.57	0.00	0.72	0.00	0.96	0.00	0.99	0.00
MOACS-1	0.50	0.00	1.00	0.00	0.87	0.03	0.91	0.01
MOACS-2	0.50	0.06	1.00	0.29	0.80	0.04	0.88	0.03
DMOBAT-1	0.57	0.00	0.72	0.00	0.90	0.03	0.98	0.01
DMOBAT-2	0.57	0.00	0.72	0.00	0.92	0.02	0.98	0.00
DMOBAT-3	0.57	0.00	0.72	0.00	0.93	0.04	0.98	0.01
DMOBAT-4	0.57	0.00	0.72	0.00	0.85	0.05	0.88	0.02
DMOBAT-5	0.57	0.00	0.72	0.00	0.91	0.00	0.98	0.00
DMOPSO-1	0.57	0.00	0.72	0.00	0.91	0.02	0.98	0.01
DMOPSO-2	0.57	0.00	0.72	0.00	0.94	0.02	0.98	0.00
DMOPSO-3	0.57	0.00	0.72	0.00	0.92	0.02	0.98	0.00
DMOPSO-4	0.57	0.00	0.72	0.00	0.89	0.04	0.98	0.00
DMOPSO-5	0.57	0.00	0.72	0.00	0.95	0.04	0.91	0.04
NSGA-II	0.57	0.00	0.72	0.00	0.93	0.01	0.99	0.02
SPEA2	0.57	0.00	0.72	0.00	0.97	0.01	0.98	0.00

Table C.70: Median and interquartile range of the computation time required by the optimisers for the Sawyer problems

	Sawyer-1 $\tilde{x} \pm IQR(x)$		Sawyer-2 $\tilde{x} \pm IQR(x)$		Sawyer-3 $\tilde{x} \pm IQR(x)$		Sawyer-4 $\tilde{x} \pm IQR(x)$	
BIANT-1	0.92	0.03	0.93	0.21	0.92	0.06	0.97	0.02
BIANT-2	0.95	0.04	0.83	0.08	0.96	0.09	1.00	0.03
CHAC-1	0.75	0.02	0.62	0.05	0.72	0.05	0.78	0.07
CHAC-2	0.74	0.02	0.62	0.06	0.72	0.03	0.77	0.02
DMOABC	0.90	0.04	0.71	0.07	0.83	0.05	0.89	0.06
DMOCSA-1-1	0.65	0.02	0.53	0.06	0.66	0.10	0.67	0.05
DMOCSA-1-2	0.65	0.02	0.54	0.05	0.63	0.03	0.67	0.04
DMOCSA-1-3	0.65	0.02	0.54	0.06	0.63	0.01	0.72	0.06
DMOCSA-1-4	0.65	0.01	0.53	0.06	0.62	0.03	0.65	0.05
DMOCSA-1-5	0.64	0.01	0.50	0.05	0.60	0.04	0.65	0.04
DMOCSA-2-1	0.74	0.02	0.60	0.06	0.69	0.02	0.74	0.04
DMOCSA-2-2	0.70	0.02	0.58	0.06	0.66	0.05	0.72	0.05
DMOCSA-2-3	0.74	0.03	0.61	0.06	0.72	0.06	0.78	0.03
DMOCSA-2-4	0.72	0.03	0.60	0.06	0.74	0.11	0.72	0.01
DMOCSA-2-5	0.74	0.02	0.61	0.05	0.71	0.04	0.75	0.05
DMOFPA-1	0.65	0.03	0.54	0.06	0.61	0.03	0.69	0.05
DMOFPA-2	0.69	0.03	0.55	0.06	0.64	0.02	0.68	0.04
DMOFPA-3	0.66	0.02	0.54	0.05	0.64	0.04	0.70	0.04
DMOFPA-4	0.38	0.01	0.31	0.03	0.43	0.06	0.37	0.03
DMOFPA-5	0.67	0.03	0.54	0.06	0.65	0.09	0.69	0.05
MOACS-1	0.92	0.02	0.80	0.09	0.87	0.04	0.88	0.09
MOACS-2	1.00	0.00	0.93	0.07	0.97	0.07	0.87	0.09
DMOBAT-1	0.66	0.02	0.53	0.06	0.61	0.06	0.66	0.04
DMOBAT-2	0.66	0.01	0.54	0.06	0.63	0.09	0.67	0.05
DMOBAT-3	0.68	0.02	0.54	0.06	0.65	0.05	0.70	0.05
DMOBAT-4	0.67	0.01	0.54	0.05	0.65	0.11	0.66	0.07
DMOBAT-5	0.67	0.02	0.54	0.05	0.63	0.04	0.69	0.05
DMOPSO-1	0.63	0.13	0.43	0.06	0.59	0.11	0.66	0.03
DMOPSO-2	0.64	0.02	0.52	0.05	0.62	0.05	0.64	0.10
DMOPSO-3	0.52	0.03	0.43	0.08	0.53	0.01	0.64	0.08
DMOPSO-4	0.65	0.04	0.52	0.05	0.68	0.07	0.52	0.05
DMOPSO-5	0.66	0.01	0.53	0.05	0.63	0.04	0.97	0.06
NSGA-II	0.86	0.04	0.75	0.07	0.78	0.09	0.66	0.03
SPEA2	0.57	0.01	0.45	0.04	0.49	0.03	0.81	0.05

C.4 Friedman's nonparametric test

This section presents the detailed results of the Friedman's test.

C.4.1 Arc111's family problem

Table C.71: Average rankings returned by Friedman's nonparametric test for the Arc111 problems family according to all quality indicators

Algorithm	Ranking I_{HV}	I_{IGD}	I_{ϵ}	I_{Δ}	Time
BIANT-1	7.88	21.32	2.36	32.04	5.76
BIANT-2	5.04	22.60	2.56	31.80	8.28
CHAC-1	15.80	17.20	19.68	22.00	18.00
CHAC-2	15.08	17.88	19.96	24.76	18.62
DMOABC	21.76	14.36	20.32	10.72	7.32
DMOBAT-1	19.12	15.80	18.82	15.92	19.24
DMOBAT-2	20.00	15.60	16.58	12.80	18.52
DMOBAT-3	19.80	16.56	19.80	16.48	20.04
DMOBAT-4	21.80	13.60	18.72	14.12	22.16
DMOBAT-5	21.68	15.68	17.96	14.96	19.40
DMOCSA-1-1	20.48	14.00	16.92	12.72	11.08
DMOCSA-1-2	18.84	18.12	17.28	16.16	8.28
DMOCSA-2-1	19.40	16.24	19.52	16.76	9.80
DMOCSA-2-2	17.12	17.64	19.34	18.12	9.54
DMOCSA-2-3	18.76	16.80	19.86	18.24	11.78
DMOCSA-2-4	15.56	22.28	20.62	15.96	20.88
DMOCSA-2-5	17.64	19.88	19.86	18.84	17.40
DMOCSA-1-3	19.60	16.40	16.10	15.64	17.54
DMOCSA-1-4	22.60	15.28	18.60	14.28	22.44
DMOCSA-1-5	20.92	16.92	19.50	14.80	17.96
DMOFPA-1	20.12	15.48	20.40	13.32	27.66
DMOFPA-2	19.20	17.20	18.84	15.32	26.02
DMOFPA-3	18.44	18.96	17.24	18.60	21.56
DMOFPA-4	21.76	14.88	15.92	13.36	21.04
DMOFPA-5	19.96	15.64	16.34	13.96	20.66
DMOPSO-1	17.84	17.04	20.60	14.96	18.60
DMOPSO-2	20.84	16.56	14.94	16.48	19.66
DMOPSO-3	22.36	13.44	17.74	13.68	18.64
DMOPSO-4	21.92	13.60	18.58	14.80	25.16
DMOPSO-5	18.36	17.24	19.80	15.24	18.08
MOACS-1	10.16	25.56	1.08	32.12	5.66
MOACS-2	1.16	34.00	4.00	33.72	17.10
NSGA-II	10.48	17.00	33.64	8.44	19.28
SPEA2	13.52	14.24	31.52	13.88	31.84

* Rankings obtained by considering the average performance of each algorithm for the Arc111 problem instances

Table C.72: Unadjusted and adjusted p-values obtained for Arc111 through the application of Holm's post hoc procedure, using the MOACS-2 as control algorithm according to I_{HV}

Algorithm	Unadjusted p-value	Adjusted p-value
Others	<0.017	<0.034
BIANT-2	0.168	0.168

Table C.73: Unadjusted and adjusted p-values obtained for Arc111 through the application of Holm's post hoc procedure, using the MOACS-2 as control algorithm according to I_{IGD}

Algorithm	Unadjusted p-value	Adjusted p-value
All	<0.004	<0.004

Table C.74: Unadjusted and adjusted p-values obtained for Arc111 through the application of Holm's post hoc procedure, using the NSGA-II as control algorithm according to I_{ϵ}

Algorithm	Unadjusted p-value	Adjusted p-value
Others	<3.79E−06	<1.13E−05
SPEA2	0.452	0.452

Table C.75: Unadjusted and adjusted p-values obtained for Arc111 through the application of Holm's post hoc procedure, using the MOACS-2 as control algorithm according to I_{Δ}

Algorithm	Unadjusted p-value	Adjusted p-value
Others	<6.41E−04	<0.003
BIANT-2	4.98E−01	1.494
MOACS-1	5.89E−01	1.494
BIANT-1	0.593	1.494

Table C.76: Unadjusted and adjusted p-values obtained for Arc111 through the application of Holm's post hoc procedure, using the SPEA2 as control algorithm in accordance with the computation time

Algorithm	Unadjusted p-value	Adjusted p-value
Others	<8.46E−04	<0.003
DMOPSO-2	0.018	0.053
MOACS-2	0.039	0.078
MOACS-1	0.138	0.138

C.4.2 Buxey's family problem

Table C.77: Average rankings returned by Friedman's nonparametric test for the Buxey problems family according to all quality indicators

Algorithm	Ranking I_{HV}	I_{IGD}	I_ϵ	I_Δ	Time
BIANT-1	8.36	27.44	22.32	29.68	6.08
BIANT-2	4.84	29.88	23.60	31.36	5.58
CHAC-1	15.16	18.60	16.86	18.12	12.38
CHAC-2	13.48	19.40	16.26	15.12	14.22
DMOABC	14.92	20.84	16.26	13.64	6.40
DMOBAT-1	18.72	17.36	16.86	14.00	20.26
DMOBAT-2	16.48	18.28	16.26	17.68	21.18
DMOBAT-3	17.12	19.32	16.26	16.32	18.84
DMOBAT-4	29.48	6.56	16.26	17.08	27.48
DMOBAT-5	17.84	17.00	16.84	10.72	22.32
DMOCSA-1-1	20.00	16.80	16.26	15.96	19.74
DMOCSA-1-2	17.28	15.92	16.86	16.08	15.84
DMOCSA-2-1	18.52	16.52	16.86	14.60	13.58
DMOCSA-2-2	16.12	19.68	16.26	14.32	22.78
DMOCSA-2-3	18.92	16.60	16.86	15.20	13.56
DMOCSA-2-4	32.28	3.28	15.66	18.40	19.20
DMOCSA-2-5	17.92	19.56	16.26	16.40	19.18
DMOCSA-1-3	18.60	18.00	16.26	14.96	17.08
DMOCSA-1-4	32.64	2.28	16.26	13.64	26.02
DMOCSA-1-5	19.28	16.40	16.88	17.28	19.50
DMOFPA-1	17.40	19.28	16.26	19.72	5.26
DMOFPA-2	19.56	17.28	16.26	15.32	10.06
DMOFPA-3	16.84	18.68	16.26	16.44	21.76
DMOFPA-4	30.92	3.84	16.26	16.92	20.00
DMOFPA-5	19.72	17.44	16.26	15.28	19.78
DMOPSO-1	18.18	18.38	16.86	17.74	19.76
DMOPSO-2	16.96	19.28	16.86	15.32	19.08
DMOPSO-3	16.68	17.92	16.26	14.08	23.00
DMOPSO-4	26.72	8.36	16.26	17.64	19.88
DMOPSO-5	18.58	20.38	16.26	17.58	12.90
MOACS-1	3.52	31.28	29.44	32.80	14.52
MOACS-2	2.76	29.20	27.04	32.00	20.82
NSGA-II	9.28	16.84	16.26	10.52	15.32
SPEA2	9.92	17.12	16.26	13.08	31.64

* Rankings obtained by considering the average performance of each algorithm for the Buxey problem instances

Table C.78: Unadjusted and adjusted p-values obtained for Buxey through the application of Holm's post hoc procedure, using the MOACS-2 as control algorithm according to I_{HV}

Algorithm	Unadjusted p-value	Adjusted p-value
Others	<1.41E−04	<8.47E−04
SPEA2	1.10E−02	0.055
NSGA-II	2.06E−02	0.082
BIANT-1	4.68E−02	0.140
BIANT-2	4.60E−01	0.920
MOACS-1	0.787	0.920

Table C.79: Unadjusted and adjusted p-values obtained for Buxey through the application of Holm's post hoc procedure, using the MOACS-1 as control algorithm according to I_{IGD}

Algorithm	Unadjusted p-value	Adjusted p-value
Others	<2.10E−04	<8.40E−04
BIANT-1	1.73E−01	0.518
MOACS-2	4.60E−01	0.920
BIANT-2	0.619	0.920

Table C.80: Unadjusted and adjusted p-values obtained for Buxey through the application of Holm's post hoc procedure, using the MOACS-1 as control algorithm according to I_{ϵ}

Algorithm	Unadjusted p-value	Adjusted p-value
Others	<1.15E−02	<0.034
BIANT-2	3.81E−02	0.076
MOACS-2	3.94E−01	0.394

Table C.81: Unadjusted and adjusted p-values obtained for Buxey through the application of Holm's post hoc procedure, using the MOACS-1 as control algorithm according to I_{Δ}

Algorithm	Unadjusted p-value	Adjusted p-value
Others	<3.42E−06	<1.37E−05
BIANT-1	2.68E−01	0.804
BIANT-2	6.09E−01	1.218
MOACS-2	7.76E−01	1.218

Table C.82: Unadjusted and adjusted p-values obtained for Buxey through the application of Holm's post hoc procedure, using the SPEA2 as control algorithm in accordance with the computation time

Algorithm	Unadjusted p-value	Adjusted p-value
Others	<0.002	<0.007
DMOFPA-4	0.046	0.092
DMOCSA-1-4	0.140	0.140

C.4.3 Gunther family problem

Table C.83: Average rankings returned by Friedman's nonparametric test for the Gunther problems family according to all quality indicators

Algorithm	Ranking I_{HV}	I_{IGD}	I_ϵ	I_Δ	Time
BIANT-1	1.73	32.41	31.14	32.32	4.02
BIANT-2	3.64	29.18	30.36	31.86	2.64
CHAC-1	14.05	20.23	17.09	18.05	13.70
CHAC-2	18.64	19.32	14.89	17.14	14.55
DMOABC	16.91	19.05	15.57	13.09	6.50
DMOBAT-1	16.86	17.86	16.18	16.55	18.16
DMOBAT-2	15.68	22.59	15.55	16.41	20.00
DMOBAT-3	17.45	18.27	16.45	14.50	19.77
DMOBAT-4	32.00	3.45	14.89	17.14	24.57
DMOBAT-5	17.18	20.05	15.59	17.14	21.82
DMOCSA-1-1	16.68	19.95	14.89	13.41	14.20
DMOCSA-1-2	17.32	20.55	14.89	15.00	18.25
DMOCSA-2-1	17.09	20.91	14.89	15.86	11.18
DMOCSA-2-2	18.86	18.14	14.89	14.86	17.32
DMOCSA-2-3	16.27	20.68	14.89	15.91	11.52
DMOCSA-2-4	30.45	5.45	14.89	18.36	18.75
DMOCSA-2-5	15.27	17.59	16.23	15.14	18.80
DMOCSA-1-3	18.27	18.82	16.36	16.27	19.89
DMOCSA-1-4	32.23	2.82	14.89	12.77	26.73
DMOCSA-1-5	17.23	18.50	16.27	13.45	18.52
DMOFPA-1	17.41	17.82	16.20	16.55	9.64
DMOFPA-2	20.36	17.73	14.89	17.64	14.09
DMOFPA-3	19.09	19.18	15.77	15.73	21.45
DMOFPA-4	31.45	3.73	14.89	16.73	18.14
DMOFPA-5	17.32	18.32	16.25	16.59	21.61
DMOPSO-1	16.18	20.00	15.64	18.14	26.61
DMOPSO-2	19.09	17.86	16.91	15.86	18.20
DMOPSO-3	16.09	21.36	16.32	14.27	19.14
DMOPSO-4	27.68	8.77	14.89	16.82	26.45
DMOPSO-5	15.09	21.45	16.16	18.95	18.27
MOACS-1	15.00	10.82	32.73	32.59	11.93
MOACS-2	6.73	14.36	33.82	32.73	18.45
NSGA-II	8.77	19.68	14.89	7.68	18.98
SPEA2	10.91	18.09	14.89	9.50	31.14

* Rankings obtained by considering the average performance of each algorithm for the Gunther problem instances

Table C.84: Unadjusted and adjusted p-values obtained for Gunther through the application of Holm's post hoc procedure, using the BIANT-1 as control algorithm according to I_{HV}

Algorithm	Unadjusted p-value	Adjusted p-value
Others	<2.23E−03	<0.009
NSGA-II	1.90E−02	0.057
MOACS-2	9.59E−02	0.192
BIANT-2	5.25E−01	0.525

Table C.85: Unadjusted and adjusted p-values obtained for Gunther through the application of Holm's post hoc procedure, using the BIANT-1 as control algorithm according to I_{IGD}

Algorithm	Unadjusted p-value	Adjusted p-value
DMOBAT-2	<1.08E−03	<0.002
BIANT-2	2.82E−01	0.282

Table C.86: Unadjusted and adjusted p-values obtained for Gunther through the application of Holm's post hoc procedure, using the MOACS-2 as control algorithm according to I_{ϵ}

Algorithm	Unadjusted p-value	Adjusted p-value
Others	2.53E−08	<1.01E−07
BIANT-2	2.50E−01	0.750
BIANT-1	3.72E−01	0.750
MOACS-1	0.716	0.750

Table C.87: Unadjusted and adjusted p-values obtained for Gunther through the application of Holm's post hoc procedure, using the MOACS-2 as control algorithm according to I_{Δ}

Algorithm	Unadjusted p-value	Adjusted p-value
Others	<4.50E−06	<1.80E−05
BIANT-2	7.74E−01	2.321
BIANT-1	8.92E−01	2.321
MOACS-1	9.64E−01	2.321

Table C.88: Unadjusted and adjusted p-values obtained for Gunther through the application of Holm's post hoc procedure, using the SPEA2 as control algorithm in accordance with the computation time

Algorithm	Unadjusted p-value	Adjusted p-value
Others	<1.91E−03	<0.010
DMOCSA-1-4	2.87E−02	0.115
DMOPSO-2	0.119	0.357
DMOBAT-4	0.132	0.357
DMOFPA-4	0.142	0.357

C.4.4 Hahn family problem

Table C.89: Average rankings returned by Friedman's nonparametric test for the Hahn problems family according to all quality indicators

Algorithm	Ranking I_{HV}	I_{IGD}	I_ϵ	I_Δ	Time
BIANT-1	1.78	33.48	10.74	32.91	4.15
BIANT-2	1.61	33.43	13.13	32.39	3.48
CHAC-1	15.87	21.74	16.43	21.57	15.02
CHAC-2	17.22	18.70	15.78	19.52	16.67
DMOABC	18.26	18.09	17.11	13.04	8.22
DMOBAT-1	19.09	16.91	15.67	14.22	21.04
DMOBAT-2	18.96	16.30	14.89	18.35	17.76
DMOBAT-3	16.83	18.35	15.20	19.65	21.30
DMOBAT-4	27.78	7.78	12.89	12.13	21.78
DMOBAT-5	18.13	17.96	15.80	15.61	22.13
DMOCSA-1-1	17.74	16.83	17.20	15.26	12.70
DMOCSA-1-2	18.57	17.22	17.43	16.00	13.78
DMOCSA-2-1	19.04	15.65	16.26	16.87	10.15
DMOCSA-2-2	16.30	19.61	16.70	17.48	16.11
DMOCSA-2-3	17.30	18.87	17.33	15.35	13.11
DMOCSA-2-4	25.74	8.74	15.59	11.65	20.67
DMOCSA-2-5	19.70	16.87	17.07	15.61	20.93
DMOCSA-1-3	20.52	17.70	14.74	15.78	20.30
DMOCSA-1-4	28.57	5.13	15.35	16.52	25.80
DMOCSA-1-5	21.48	16.70	15.37	14.48	20.93
DMOFPA-1	20.91	16.09	17.26	18.00	12.43
DMOFPA-2	18.52	17.91	16.35	14.17	13.54
DMOFPA-3	19.22	15.30	17.50	15.00	20.22
DMOFPA-4	28.00	7.04	14.85	10.96	21.17
DMOFPA-5	20.26	16.70	15.33	14.17	16.57
DMOPSO-1	19.04	17.43	17.30	15.00	22.41
DMOPSO-2	17.17	19.09	17.24	16.35	19.63
DMOPSO-3	19.87	17.52	18.61	20.26	18.48
DMOPSO-4	26.04	9.17	12.46	13.22	24.85
DMOPSO-5	15.74	17.39	19.09	19.39	15.80
MOACS-1	3.70	25.52	27.35	32.39	11.04
MOACS-2	5.57	24.35	30.00	30.39	19.98
NSGA-II	9.13	20.17	31.89	10.22	19.59
SPEA2	11.35	15.26	29.11	11.09	33.22

* Rankings obtained by considering the average performance of each algorithm for the Hahn problem instances

Table C.90: Unadjusted and adjusted p-values obtained for Hahn through the application of Holm's post hoc procedure, using the BIANT-2 as control algorithm according to I_{HV}

Algorithm	Unadjusted p-value	Adjusted p-value
Others	<1.04E−02	<0.042
MOACS-2	1.78E−01	0.534
MOACS-1	4.77E−01	0.955
BIANT-1	0.953	0.955

Table C.91: Unadjusted and adjusted p-values obtained for Hahn through the application of Holm's post hoc procedure, using the BIANT-1 as control algorithm according to I_{IGD}

Algorithm	Unadjusted p-value	Adjusted p-value
Others	<6.01E−03	<0.012
BIANT-2	0.977	0.977

Table C.92: Unadjusted and adjusted p-values obtained for Hahn through the application of Holm's post hoc procedure, using the NSGA-II as control algorithm according to I_{ϵ}

Algorithm	Unadjusted p-value	Adjusted p-value
Others	<1.30E−05	<5.19E−05
MOACS-1	1.22E−01	0.365
SPEA2	3.43E−01	0.687
MOACS-2	0.520	0.687

Table C.93: Unadjusted and adjusted p-values obtained for Hahn through the application of Holm's post hoc procedure, using the BIANT-1 as control algorithm according to I_{Δ}

Algorithm	Unadjusted p-value	Adjusted p-value
Others	<1.11E−04	<4.46E−04
MOACS-2	3.90E−01	1.171
BIANT-2	8.59E−01	1.718
MOACS-1	0.859	1.718

Table C.94: Unadjusted and adjusted p-values obtained for Hahn through the application of Holm's post hoc procedure, using the SPEA2 as control algorithm in accordance with the computation time

Algorithm	Unadjusted p-value	Adjusted p-value
Others	<2.34E−04	<7.02E−04
DMOPSO-2	0.004	0.009
DMOFPA-4	0.012	0.012

C.4.5 Jackson family problem

Table C.95: Average rankings returned by Friedman's nonparametric test for the Jackson problems family according to all quality indicators

Algorithm	Ranking I_{HV}	I_{IGD}	I_{ϵ}	I_{Δ}	Time
BIANT-1	32.64	9.90	2.90	27.08	3.52
BIANT-2	32.56	10.42	3.06	23.08	3.56
CHAC-1	12.76	20.22	19.72	17.14	9.80
CHAC-2	12.54	21.44	21.54	18.76	13.20
DMOABC	14.14	18.32	19.82	15.72	5.72
DMOBAT-1	12.72	20.34	20.80	15.50	20.82
DMOBAT-2	10.34	23.08	21.82	18.44	23.00
DMOBAT-3	13.82	20.46	21.28	16.86	19.62
DMOBAT-4	23.04	12.68	14.56	17.98	24.92
DMOBAT-5	11.42	21.74	21.66	15.76	26.50
DMOCSA-1-1	12.90	20.60	20.86	14.90	13.58
DMOCSA-1-2	12.84	20.50	22.02	15.26	22.50
DMOCSA-2-1	12.98	19.48	20.90	12.92	9.24
DMOCSA-2-2	13.08	19.98	21.24	14.50	15.44
DMOCSA-2-3	15.46	21.16	20.94	17.96	10.36
DMOCSA-2-4	24.64	9.74	13.76	20.38	24.04
DMOCSA-2-5	13.78	19.18	20.06	16.76	16.14
DMOCSA-1-3	13.92	19.92	19.52	15.84	14.32
DMOCSA-1-4	28.50	7.98	12.52	20.66	33.80
DMOCSA-1-5	13.50	20.06	20.50	16.46	15.34
DMOFPA-1	14.08	20.32	19.72	16.60	4.56
DMOFPA-2	12.82	20.52	20.00	17.38	2.16
DMOFPA-3	14.00	19.28	19.62	14.58	25.04
DMOFPA-4	28.26	10.24	13.04	19.58	18.50
DMOFPA-5	15.06	18.86	18.94	15.10	11.96
DMOPSO-1	14.22	20.94	20.50	18.06	16.78
DMOPSO-2	14.12	18.76	19.74	15.56	16.44
DMOPSO-3	16.16	17.08	19.76	13.50	28.82
DMOPSO-4	20.70	14.98	17.64	13.96	27.30
DMOPSO-5	14.06	17.88	20.10	14.86	32.90
MOACS-1	32.20	11.88	4.38	25.16	28.18
MOACS-2	32.48	8.04	3.00	24.92	22.76
NSGA-II	15.70	19.58	19.36	17.32	3.16
SPEA2	13.56	19.44	19.72	16.46	31.02

* Rankings obtained by considering the average performance of each algorithm for the Jackson problem instances

Table C.96: Unadjusted and adjusted p-values obtained for Jackson through the application of Holm's post hoc procedure, using the DMOBAT-2 as control algorithm according to I_{HV}

Algorithm	Unadjusted p-value	Adjusted p-value
Others	<2.35E−04	<0.006
DMOPSO-3	3.88E−02	0.931
NSGA-II	5.70E−02	1.312
DMOCSA-2-3	6.91E−02	1.520
DMOFPA-5	9.38E−02	1.969
DMOPSO-1	1.68E−01	3.367
DMOABC	1.77E−01	3.369
DMOPSO-2	1.80E−01	3.369
DMOFPA-1	1.84E−01	3.369
DMOPSO-5	1.87E−01	3.369
DMOFPA-3	1.94E−01	3.369
DMOCSA-1-3	2.04E−01	3.369
DMOBAT-3	2.17E−01	3.369
DMOCSA-2-5	2.22E−01	3.369
SPEA2	2.53E−01	3.369
DMOCSA-1-5	2.62E−01	3.369
DMOCSA-2-2	3.31E−01	3.369
DMOCSA-2-1	3.49E−01	3.369
DMOCSA-1-1	3.63E−01	3.369
DMOCSA-1-2	3.75E−01	3.369
DMOFPA-2	3.79E−01	3.369
CHAC-1	3.90E−01	3.369
DMOBAT-1	3.98E−01	3.369
CHAC-2	4.35E−01	3.369
DMOBAT-5	0.701	3.369

Table C.97: Unadjusted and adjusted p-values obtained for Jackson through the application of Holm's post hoc procedure, using the DMOBAT-2 as control algorithm according to I_{IGD}

Algorithm	Unadjusted p-value	Adjusted p-value
Others	<4.03E−03	<0.101
DMOPSO-3	3.32E−02	0.796
DMOPSO-5	6.49E−02	1.492
DMOABC	9.10E−02	2.003
DMOPSO-2	1.25E−01	2.627
DMOFPA-5	1.34E−01	2.681
DMOCSA-2-5	1.66E−01	3.157
DMOFPA-3	1.77E−01	3.191
SPEA2	1.96E−01	3.336
DMOCSA-2-1	2.01E−01	3.336
NSGA-II	2.14E−01	3.336
DMOCSA-1-3	2.62E−01	3.667
DMOCSA-2-2	2.71E−01	3.667
DMOCSA-1-5	2.84E−01	3.667
CHAC-1	3.10E−01	3.667
DMOFPA-1	3.27E−01	3.667
DMOBAT-1	3.31E−01	3.667
DMOBAT-3	3.52E−01	3.667
DMOCSA-1-2	3.60E−01	3.667
DMOFPA-2	3.63E−01	3.667
DMOCSA-1-1	3.79E−01	3.667
DMOPSO-1	4.47E−01	3.667
DMOCSA-2-3	4.95E−01	3.667
CHAC-2	5.60E−01	3.667
DMOBAT-5	6.34E−01	3.667

Table C.98: Unadjusted and adjusted p-values obtained for Jackson through the application of Holm's post hoc procedure, using the DMOCSA-1-2 as control algorithm according to I_ϵ

Algorithm	Unadjusted p-value	Adjusted p-value
Others	<1.43E−03	<0.040
DMOCSA-2-4	3.36E−03	0.091
DMOBAT-4	8.08E−03	0.210
DMOPSO-4	1.20E−01	2.998
DMOFPA-5	2.74E−01	6.580
NSGA-II	3.45E−01	7.934
DMOCSA-1-3	3.75E−01	8.245
DMOFPA-3	3.94E−01	8.277
DMOFPA-1	4.14E−01	8.283
CHAC-1	4.14E−01	8.283
SPEA2	4.14E−01	8.283
DMOPSO-2	4.18E−01	8.283
DMOPSO-3	4.22E−01	8.283
DMOABC	4.35E−01	8.283
DMOFPA-2	4.73E−01	8.283
DMOCSA-2-5	4.87E−01	8.283
DMOPSO-5	4.95E−01	8.283
DMOPSO-1	5.89E−01	8.283
DMOCSA-1-5	5.89E−01	8.283
DMOBAT-1	6.65E−01	8.283
DMOCSA-1-1	6.80E−01	8.283
DMOCSA-2-1	6.91E−01	8.283
DMOCSA-2-3	7.01E−01	8.283
DMOCSA-2-2	7.82E−01	8.283
DMOBAT-3	7.93E−01	8.283
CHAC-2	8.65E−01	8.283
DMOBAT-5	8.98E−01	8.283
DMOBAT-2	0.943	8.283

Table C.99: Unadjusted and adjusted p-values obtained for Jackson through the application of Holm's post hoc procedure, using the BIANT-1 as control algorithm according to I_Δ

Algorithm	Unadjusted p-value	Adjusted p-value
Others	<7.75E−03	<0.047
DMOCSA-2-4	1.74E−02	0.087
DMOCSA-1-4	2.26E−02	0.091
BIANT-2	1.56E−01	0.467
MOACS-2	4.43E−01	0.886
MOACS-1	0.495	0.886

Table C.100: Unadjusted and adjusted p-values obtained for Jackson through the application of Holm's post hoc procedure, using the DMOFPA-4 as control algorithm in accordance with the computation time

Algorithm	Unadjusted p-value	Adjusted p-value
Others	<1.87E−03	<0.013
DMOCSA-1-5	9.55E−03	0.057
DMOPSO-2	2.10E−02	0.105
DMOPSO-4	4.60E−02	0.184
DMOPSO-1	7.70E−02	0.231
SPEA2	0.324	0.647
DMOPSO-3	0.749	0.749

C.4.6 Kilbrid family problem

Table C.101: Average rankings returned by Friedman's nonparametric test for the Kilbrid problems family according to all quality indicators

Algorithm	Ranking I_{HV}	I_{IGD}	I_{ϵ}	I_{Δ}	Time
BIANT-1	30.52	6.14	4.14	12.08	15.84
BIANT-2	31.40	3.90	3.94	7.88	14.30
CHAC-1	11.96	25.44	19.90	19.40	13.54
CHAC-2	12.80	21.80	21.04	19.96	14.06
DMOABC	13.48	23.76	23.18	20.24	5.06
DMOBAT-1	12.16	21.04	22.44	18.80	19.88
DMOBAT-2	17.88	19.60	17.66	17.12	20.56
DMOBAT-3	12.36	19.72	20.24	17.04	20.46
DMOBAT-4	25.64	11.24	8.74	22.80	21.40
DMOBAT-5	13.80	21.44	20.38	15.40	17.76
DMOCSA-1-1	16.12	21.00	21.04	20.00	10.26
DMOCSA-1-2	13.56	19.48	21.22	19.24	12.40
DMOCSA-2-1	14.40	22.08	16.96	20.00	10.02
DMOCSA-2-2	14.04	17.68	20.00	18.24	14.34
DMOCSA-2-3	15.00	19.36	23.12	17.40	10.34
DMOCSA-2-4	25.44	7.84	9.54	18.64	21.90
DMOCSA-2-5	14.16	20.72	19.34	18.20	17.76
DMOCSA-1-3	15.00	18.92	20.46	15.56	18.68
DMOCSA-1-4	27.76	7.72	8.50	21.20	29.20
DMOCSA-1-5	12.72	20.84	20.80	16.44	20.78
DMOFPA-1	13.76	18.08	20.26	18.28	18.24
DMOFPA-2	13.52	20.40	21.78	21.68	14.30
DMOFPA-3	14.16	19.76	18.42	18.68	18.40
DMOFPA-4	28.04	5.64	8.54	18.80	19.58
DMOFPA-5	14.32	19.60	20.62	17.68	16.36
DMOPSO-1	12.66	23.02	24.54	18.14	18.30
DMOPSO-2	13.92	22.12	22.42	19.28	16.12
DMOPSO-3	13.16	22.84	22.40	19.44	21.24
DMOPSO-4	19.60	16.36	16.84	19.16	23.56
DMOPSO-5	13.18	23.54	24.50	17.90	20.18
MOACS-1	32.24	3.32	2.80	9.68	9.96
MOACS-2	31.60	2.92	3.18	5.52	18.38
NSGA-II	12.48	22.80	21.64	17.48	19.74
SPEA2	12.16	24.88	24.42	17.64	32.10

* Rankings obtained by considering the average performance of each algorithm for the Kilbrid problem instances

Table C.102: Unadjusted and adjusted p-values obtained for Kilbrid through the application of Holm's post hoc procedure, using the CHAC-1 as control algorithm according to I_{HV}

Algorithm	Unadjusted p-value	Adjusted p-value
Others	<1.70E−06	<4.43E−05
DMOPSO-4	6.68E−03	0.167
DMOBAT-2	3.56E−02	0.854
DMOCSA-1-1	1.40E−01	3.213
DMOCSA-2-3	2.80E−01	6.170
DMOCSA-1-3	2.80E−01	6.170
DMOCSA-2-1	3.86E−01	7.727
DMOFPA-5	4.02E−01	7.727
DMOCSA-2-5	4.35E−01	7.826
DMOFPA-3	4.35E−01	7.826
DMOCSA-2-2	4.60E−01	7.826
DMOPSO-2	4.87E−01	7.826
DMOBAT-5	5.14E−01	7.826
DMOFPA-1	5.23E−01	7.826
DMOCSA-1-2	5.70E−01	7.826
DMOFPA-2	5.80E−01	7.826
DMOABC	5.89E−01	7.826
DMOPSO-5	6.65E−01	7.826
DMOPSO-3	6.70E−01	7.826
CHAC-2	7.66E−01	7.826
DMOCSA-1-5	7.87E−01	7.826
DMOPSO-1	8.04E−01	7.826
NSGA-II	8.54E−01	7.826
DMOBAT-3	8.87E−01	7.826
DMOBAT-1	9.43E−01	7.826
SPEA2	0.943	7.826

Table C.103: Unadjusted and adjusted p-values obtained for Kilbrid through the application of Holm's post hoc procedure, using the CHAC-1 as control algorithm according to I_{IGD}

Algorithm	Unadjusted p-value	Adjusted p-value
Others	<1.27E−03	<0.032
DMOCSA-2-2	5.87E−03	0.141
DMOFPA-1	8.97E−03	0.206
DMOCSA-1-3	2.06E−02	0.454
DMOCSA-2-3	3.09E−02	0.648
DMOCSA-1-2	3.43E−02	0.687
DMOFPA-5	3.81E−02	0.725
DMOBAT-2	3.81E−02	0.725
DMOBAT-3	4.23E−02	0.725
DMOFPA-3	4.37E−02	0.725
DMOFPA-2	7.36E−02	1.103
DMOCSA-2-5	9.38E−02	1.313
DMOCSA-1-5	1.02E−01	1.332
DMOCSA-1-1	1.15E−01	1.379
DMOBAT-1	1.18E−01	1.379
DMOBAT-5	1.56E−01	1.556
CHAC-2	1.96E−01	1.766
DMOCSA-2-1	2.33E−01	1.863
DMOPSO-2	2.39E−01	1.863
NSGA-II	3.49E−01	2.092
DMOPSO-3	3.56E−01	2.092
DMOPSO-1	3.90E−01	2.092
DMOPSO-5	5.00E−01	2.092
DMOABC	5.51E−01	2.092
SPEA2	0.842	2.092

Table C.104: Unadjusted and adjusted p-values obtained for Kilbrid through the application of Holm's post hoc procedure, using the DMOPSO-1 as control algorithm according to I_ϵ

Algorithm	Unadjusted p-value	Adjusted p-value
DMOCSA-2-4	<1.01E−07	<2.62E−06
DMOPSO-4	6.26E−03	0.157
DMOCSA-2-1	7.12E−03	0.171
DMOBAT-2	1.46E−02	0.335
DMOFPA-3	2.98E−02	0.655
DMOCSA-2-5	6.49E−02	1.362
CHAC-1	9.95E−02	1.990
DMOCSA-2-2	1.07E−01	2.033
DMOBAT-3	1.27E−01	2.283
DMOFPA-1	1.29E−01	2.283
DMOBAT-5	1.40E−01	2.283
DMOCSA-1-3	1.47E−01	2.283
DMOFPA-5	1.64E−01	2.296
DMOCSA-1-5	1.84E−01	2.395
CHAC-2	2.14E−01	2.568
DMOCSA-1-1	2.14E−01	2.568
DMOCSA-1-2	2.39E−01	2.568
NSGA-II	3.03E−01	2.729
DMOFPA-2	3.27E−01	2.729
DMOPSO-3	4.47E−01	3.132
DMOPSO-2	4.52E−01	3.132
DMOBAT-1	4.56E−01	3.132
DMOCSA-2-3	6.14E−01	3.132
DMOABC	6.29E−01	3.132
SPEA2	9.66E−01	3.132
DMOPSO-5	0.989	3.132

Table C.105: Unadjusted and adjusted p-values obtained for Kilbrid through the application of Holm's post hoc procedure, using the DMOBAT-4 as control algorithm in accordance with the Spread

Algorithm	Unadjusted p-value	Adjusted p-value
Others	<1.41E−04	<0.004
DMOBAT-5	0.009	0.250
DMOCSA-1-3	0.010	0.284
DMOCSA-1-5	0.024	0.646
DMOBAT-3	0.041	1.062
DMOBAT-2	0.044	1.093
DMOCSA-2-3	0.055	1.325
NSGA-II	0.059	1.355
SPEA2	0.067	1.473
DMOFPA-5	0.069	1.473
DMOPSO-5	0.082	1.638
DMOPSO-1	0.098	1.863
DMOCSA-2-5	0.102	1.863
DMOCSA-2-2	0.105	1.863
DMOFPA-1	0.109	1.863
DMOCSA-2-4	0.140	2.095
DMOFPA-3	0.144	2.095
DMOBAT-1	0.156	2.095
DMOFPA-4	0.156	2.095
DMOPSO-4	0.196	2.159
DMOCSA-1-2	0.206	2.159
DMOPSO-2	0.211	2.159
CHAC-1	0.227	2.159
DMOPSO-3	0.233	2.159
CHAC-2	0.313	2.159
DMOCSA-2-1	0.320	2.159
DMOCSA-1-1	0.320	2.159
DMOABC	0.363	2.159
DMOCSA-1-4	0.570	2.159
DMOFPA-2	0.691	2.159

Table C.106: Unadjusted and adjusted p-values obtained for Kilbrid through the application of Holm's post hoc procedure, using the SPEA2 as control algorithm in accordance with the computation time

Algorithm	Unadjusted p-value	Adjusted p-value
Others	<0.002	<0.005
DMOFPA-4	0.303	0.303

C.4.7 Lutz1 family problem

Table C.107: Average rankings returned by Friedman's nonparametric test for the Lutz1 problems family according to all quality indicators

Algorithm	Ranking I_{HV}	I_{IGD}	I_{ϵ}	I_{Δ}	Time
BIANT-1	31.70	3.40	3.28	25.00	4.68
BIANT-2	32.10	2.95	3.03	24.20	4.60
CHAC-1	10.43	25.43	25.00	19.20	8.68
CHAC-2	12.18	24.43	23.78	19.30	10.23
DMOABC	9.95	25.60	25.00	19.63	4.30
DMOBAT-1	11.67	23.98	22.30	18.83	24.63
DMOBAT-2	13.53	21.48	21.03	16.88	22.72
DMOBAT-3	11.60	23.60	23.23	19.25	21.82
DMOBAT-4	22.03	13.40	13.83	17.80	21.70
DMOBAT-5	13.53	22.45	20.98	16.95	27.28
DMOCSA-1-1	15.67	17.48	19.10	13.60	12.03
DMOCSA-1-2	16.20	16.60	18.75	12.05	13.50
DMOCSA-2-1	15.15	17.13	19.68	11.55	8.42
DMOCSA-2-2	17.75	17.08	17.20	14.45	10.83
DMOCSA-2-3	16.88	16.55	18.55	11.68	10.20
DMOCSA-2-4	22.22	15.53	13.78	18.03	25.72
DMOCSA-2-5	17.65	16.20	16.60	12.95	17.88
DMOCSA-1-3	17.28	17.48	17.20	14.95	17.03
DMOCSA-1-4	25.05	10.85	10.18	19.45	33.52
DMOCSA-1-5	16.78	16.00	17.98	11.63	18.18
DMOFPA-1	15.70	17.70	18.70	14.65	2.80
DMOFPA-2	17.88	16.93	17.05	13.23	1.20
DMOFPA-3	15.55	16.58	19.33	12.95	22.88
DMOFPA-4	24.80	12.68	10.73	18.33	20.88
DMOFPA-5	18.15	17.03	16.93	13.90	16.68
DMOPSO-1	9.65	25.30	24.78	20.18	20.53
DMOPSO-2	11.73	23.80	22.93	18.65	20.80
DMOPSO-3	12.90	23.45	23.00	20.43	30.60
DMOPSO-4	19.10	17.55	16.60	20.10	28.10
DMOPSO-5	12.65	23.40	22.30	17.68	29.90
MOACS-1	33.05	1.80	1.90	26.15	13.48
MOACS-2	33.15	1.85	1.80	25.05	28.15
NSGA-II	10.58	24.33	24.15	17.55	8.18
SPEA2	10.80	25.05	24.40	18.83	32.92

* Rankings obtained by considering the average performance of each algorithm for the Lutz1 problem instances

Table C.108: Unadjusted and adjusted p-values obtained for Lutz1 through the application of Holm's post hoc procedure, using the DMOPSO-1 as control algorithm according to I_{HV}

Algorithm	Unadjusted p-value	Adjusted p-value
Others	<8.50E−05	<0.002
DMOPSO-4	2.69E−03	0.067
DMOFPA-5	6.95E−03	0.167
DMOFPA-2	9.00E−03	0.207
DMOCSA-2-2	1.01E−02	0.222
DMOCSA-2-5	1.11E−02	0.233
DMOCSA-1-3	1.55E−02	0.309
DMOCSA-2-3	2.18E−02	0.414
DMOCSA-1-5	2.37E−02	0.426
DMOCSA-1-2	3.75E−02	0.638
DMOFPA-1	5.47E−02	0.875
DMOCSA-1-1	5.57E−02	0.875
DMOFPA-3	6.10E−02	0.875
DMOCSA-2-1	8.07E−02	1.049
DMOBAT-5	2.19E−01	2.622
DMOBAT-2	2.19E−01	2.622
DMOPSO-3	3.02E−01	3.020
DMOPSO-5	3.41E−01	3.067
CHAC-2	4.23E−01	3.381
DMOPSO-2	5.10E−01	3.570
DMOBAT-1	5.20E−01	3.570
DMOBAT-3	5.36E−01	3.570
SPEA2	7.15E−01	3.570
NSGA-II	7.69E−01	3.570
CHAC-1	8.06E−01	3.570
DMOABC	0.924	3.570

Table C.109: Unadjusted and adjusted p-values obtained for Lutz1 through the application of Holm's post hoc procedure, using the DMOBAT-3 as control algorithm according to I_{IGD}

Algorithm	Unadjusted p-value	Adjusted p-value
Others	<1.38E−03	0.000<03581143
DMOCSA-1-5	2.30E−03	0.057
DMOCSA-2-5	2.84E−03	0.068
DMOCSA-2-3	4.05E−03	0.093
DMOFPA-3	4.16E−03	0.093
DMOCSA-1-2	4.26E−03	0.093
DMOFPA-2	5.87E−03	0.117
DMOFPA-5	6.47E−03	0.123
DMOCSA-2-2	6.79E−03	0.123
DMOCSA-2-1	7.12E−03	0.123
DMOCSA-1-3	9.88E−03	0.158
DMOCSA-1-1	9.88E−03	0.158
DMOPSO-4	1.06E−02	0.158
DMOFPA-1	1.21E−02	0.158
DMOBAT-2	1.90E−01	2.283
DMOBAT-5	3.17E−01	3.489
DMOPSO-5	4.85E−01	4.848
DMOPSO-3	4.95E−01	4.848
DMOBAT-3	5.25E−01	4.848
DMOPSO-2	5.68E−01	4.848
DMOBAT-1	6.06E−01	4.848
NSGA-II	6.86E−01	4.848
CHAC-2	7.09E−01	4.848
SPEA2	8.61E−01	4.848
DMOPSO-1	9.24E−01	4.848
CHAC-1	0.956	4.848

Table C.110: Unadjusted and adjusted p-values obtained for Lutz1 through the application of Holm's post hoc procedure, using the DMOPSO-5 as control algorithm according to I_ϵ

Algorithm	Unadjusted p-value	Adjusted p-value
Others	<3.87E−04	<0.010
DMOPSO-4	7.64E−03	0.191
DMOCSA-2-5	7.64E−03	0.191
DMOFPA-5	1.03E−02	0.238
DMOFPA-2	1.16E−02	0.255
DMOCSA-2-2	1.33E−02	0.278
DMOCSA-1-3	1.33E−02	0.278
DMOCSA-1-5	2.57E−02	0.488
DMOCSA-2-3	4.05E−02	0.730
DMOFPA-1	4.54E−02	0.772
DMOCSA-1-2	4.72E−02	0.772
DMOCSA-1-1	6.10E−02	0.915
DMOFPA-3	7.15E−02	1.001
DMOCSA-2-1	9.08E−02	1.181
DMOBAT-5	2.01E−01	2.414
DMOBAT-2	2.07E−01	2.414
DMOBAT-1	3.91E−01	3.912
DMOPSO-5	3.91E−01	3.912
DMOPSO-2	5.10E−01	4.080
DMOPSO-3	5.25E−01	4.080
DMOBAT-3	5.73E−01	4.080
CHAC-2	6.97E−01	4.080
NSGA-II	7.87E−01	4.080
SPEA2	8.49E−01	4.080
DMOPSO-1	9.43E−01	4.080
CHAC-1	1	4.080

Table C.111: Unadjusted and adjusted p-values obtained for Lutz1 through the application of Holm's post hoc procedure, using the MOACS-1 as control algorithm according to I_{Δ}

Algorithm	Unadjusted p-value	Adjusted p-value
Others	<3.76E−04	<0.008
DMOBAT-2	3.23E−03	0.068
DMOBAT-5	3.48E−03	0.070
NSGA-II	6.31E−03	0.120
DMOPSO-5	7.12E−03	0.128
DMOBAT-4	8.01E−03	0.136
DMOCSA-2-4	9.88E−03	0.158
DMOFPA-4	1.30E−02	0.194
DMOPSO-2	1.72E−02	0.241
DMOBAT-1	2.00E−02	0.260
SPEA2	2.00E−02	0.260
CHAC-1	2.73E−02	0.300
DMOBAT-3	2.84E−02	0.300
CHAC-2	2.96E−02	0.300
DMOCSA-1-4	3.34E−02	0.300
DMOABC	3.83E−02	0.300
DMOPSO-4	5.47E−02	0.328
DMOPSO-1	5.78E−02	0.328
DMOPSO-3	6.91E−02	0.328
BIANT-2	5.36E−01	1.607
BIANT-1	7.15E−01	1.607
MOACS-2	0.727	1.607

Table C.112: Unadjusted and adjusted p-values obtained for Lutz1 through the application of Holm's post hoc procedure, using the DMOFPA-4 as control algorithm in accordance with the computation time

Algorithm	Unadjusted p-value	Adjusted p-value
Others	<4.71E−03	<0.038
DMOFPA-1	1.33E−02	0.093
DMOCSA-1-5	4.72E−02	0.283
DMOPSO-2	8.49E−02	0.425
DMOPSO-5	8.78E−02	0.425
DMOPSO-3	2.50E−01	0.749
DMOPSO-1	0.353	0.749
SPEA2	0.849	0.849

C.4.8 Mitchell family problem

Table C.113: Average rankings returned by Friedman's nonparametric test for the Mitchell problems family according to all quality indicators

Algorithm	Ranking I_{HV}	I_{IGD}	I_{ϵ}	I_{Δ}	Time
BIANT-1	21.63	3.50	15.38	12.50	9.94
BIANT-2	23.25	3.50	10.31	11.69	8.72
CHAC-1	14.88	27.88	18.13	21.19	9.56
CHAC-2	12.56	27.88	21.81	16.63	11.06
DMOABC	13.25	27.88	21.25	18.25	4.22
DMOBAT-1	15.06	24.88	20.81	16.00	19.47
DMOBAT-2	13.13	19.00	21.97	16.50	19.53
DMOBAT-3	12.28	20.75	22.25	16.31	17.38
DMOBAT-4	29.19	13.25	9.59	22.81	28.66
DMOBAT-5	14.25	18.75	19.06	17.56	23.50
DMOCSA-1-1	11.31	15.25	20.72	18.44	11.81
DMOCSA-1-2	16.78	14.50	16.16	12.09	16.44
DMOCSA-2-1	13.69	16.38	20.59	16.19	8.59
DMOCSA-2-2	15.00	14.25	18.47	17.00	18.00
DMOCSA-2-3	17.03	16.00	17.50	16.09	12.84
DMOCSA-2-4	27.63	20.00	10.69	19.81	19.44
DMOCSA-2-5	13.94	14.25	21.41	15.94	16.53
DMOCSA-1-3	13.88	11.63	20.47	20.75	16.94
DMOCSA-1-4	29.38	7.00	9.44	26.94	31.59
DMOCSA-1-5	15.63	13.75	19.44	18.25	15.75
DMOFPA-1	12.47	19.25	21.03	17.41	9.34
DMOFPA-2	17.34	17.00	16.63	19.47	5.09
DMOFPA-3	14.63	14.25	20.19	16.81	22.25
DMOFPA-4	30.25	19.25	7.53	17.69	17.56
DMOFPA-5	13.38	16.63	18.59	18.38	13.38
DMOPSO-1	13.63	27.88	21.25	17.63	26.25
DMOPSO-2	16.00	26.13	18.78	15.81	19.34
DMOPSO-3	12.72	26.25	22.44	15.50	26.47
DMOPSO-4	22.69	13.25	13.75	17.00	19.88
DMOPSO-5	11.72	27.88	23.06	16.78	29.56
MOACS-1	28.00	1.25	9.06	18.44	24.13
MOACS-2	30.69	1.75	7.47	17.75	18.31
NSGA-II	12.66	26.13	21.47	17.53	13.78
SPEA2	15.13	27.88	18.31	17.88	29.69

* Rankings obtained by considering the average performance of each algorithm for the Mitchell problem instances

Table C.114: Unadjusted and adjusted p-values obtained for Mitchell through the application of Holm's post hoc procedure, using the DMOCSA-1 as control algorithm according to I_{HV}

Algorithm	Unadjusted p-value	Adjusted p-value
Others	<1.23E−03	<0.032
BIANT-1	3.40E−03	0.085
DMOFPA-2	8.67E−02	2.081
DMOCSA-2-3	1.04E−01	2.399
DMOCSA-1-2	1.20E−01	2.648
DMOPSO-2	1.83E−01	3.844
DMOCSA-1-5	2.21E−01	4.412
SPEA2	2.79E−01	5.299
DMOBAT-1	2.87E−01	5.299
DMOCSA-2-2	2.95E−01	5.299
CHAC-1	3.12E−01	5.299
DMOFPA-3	3.47E−01	5.299
DMOBAT-5	4.04E−01	5.657
DMOCSA-2-5	4.56E−01	5.927
DMOCSA-1-3	4.67E−01	5.927
DMOCSA-2-1	5.00E−01	5.927
DMOPSO-1	5.11E−01	5.927
DMOFPA-5	5.58E−01	5.927
DMOABC	5.82E−01	5.927
DMOBAT-2	6.07E−01	5.927
DMOPSO-3	6.90E−01	5.927
NSGA-II	7.03E−01	5.927
CHAC-2	7.23E−01	5.927
DMOFPA-1	7.43E−01	5.927
DMOBAT-3	7.83E−01	5.927
DMOPSO-5	0.908	5.927

Table C.115: Unadjusted and adjusted p-values obtained for Mitchell through the application of Holm's post hoc procedure, using the DMOBAT-3 as control algorithm according to I_{IGD}

Algorithm	Unadjusted p-value	Adjusted p-value
Others	<6.20E−04	<0.015
DMOFPA-2	3.72E−02	0.893
CHAC-1	8.49E−02	1.953
SPEA2	1.05E−01	2.302
DMOCSA-1-3	1.06E−01	2.302
DMOCSA-2-3	1.08E−01	2.302
DMOPSO-1	1.85E−01	3.516
DMOABC	2.20E−01	3.961
DMOBAT-1	2.42E−01	4.109
DMOCSA-1-5	3.05E−01	4.876
DMOCSA-2-1	3.26E−01	4.885
DMOPSO-2	3.28E−01	4.885
CHAC-2	3.57E−01	4.885
DMOCSA-1-1	3.58E−01	4.885
DMOBAT-3	3.66E−01	4.885
DMOCSA-1-2	3.89E−01	4.885
DMOFPA-1	4.01E−01	4.885
DMOPSO-3	4.42E−01	4.885
DMOFPA-5	4.92E−01	4.885
DMOPSO-5	5.99E−01	4.885
DMOCSA-2-2	6.09E−01	4.885
DMOCSA-2-5	6.12E−01	4.885
DMOFPA-3	6.18E−01	4.885
NSGA-II	7.65E−01	4.885
DMOBAT-2	0.891	4.885

Table C.116: Unadjusted and adjusted p-values obtained for Mitchell through the application of Holm's post hoc procedure, using the DMOPSO-5 as control algorithm according to I_ϵ

Algorithm	Unadjusted p-value	Adjusted p-value
Others	<4.40E−04	<0.012
DMOPSO-4	8.17E−03	0.212
BIANT-1	2.90E−02	0.725
DMOCSA-1-2	4.98E−02	1.195
DMOFPA-2	6.75E−02	1.552
DMOCSA-2-3	1.14E−01	2.511
CHAC-1	1.61E−01	3.377
SPEA2	1.77E−01	3.546
DMOCSA-2-2	1.92E−01	3.648
DMOFPA-5	2.04E−01	3.678
DMOPSO-2	2.24E−01	3.808
DMOBAT-5	2.56E−01	4.095
DMOCSA-1-5	3.03E−01	4.548
DMOFPA-3	4.14E−01	5.798
DMOCSA-1-3	4.61E−01	5.997
DMOCSA-2-1	4.83E−01	5.997
DMOCSA-1-1	5.06E−01	5.997
DMOBAT-1	5.23E−01	5.997
DMOFPA-1	5.64E−01	5.997
DMOABC	6.07E−01	5.997
DMOPSO-1	6.07E−01	5.997
DMOCSA-2-5	6.38E−01	5.997
NSGA-II	6.51E−01	5.997
CHAC-2	7.23E−01	5.997
DMOBAT-2	7.56E−01	5.997
DMOBAT-3	8.17E−01	5.997
DMOPSO-3	0.859	5.997

Table C.117: Unadjusted and adjusted p-values obtained for Mitchell through the application of Holm's post hoc procedure, using the DMOCSA-1-4 as control algorithm according to I_{Δ}

Algorithm	Unadjusted p-value	Adjusted p-value
Others	<1.78E−03	<0.050
DMOBAT-1	1.89E−03	0.051
DMOCSA-2-3	2.07E−03	0.054
DMOCSA-2-1	2.26E−03	0.057
DMOBAT-3	2.55E−03	0.061
DMOBAT-2	3.03E−03	0.070
CHAC-2	3.40E−03	0.075
DMOPSO-5	3.92E−03	0.082
DMOFPA-3	4.03E−03	0.082
DMOCSA-2-2	4.76E−03	0.091
DMOPSO-4	4.76E−03	0.091
DMOFPA-1	6.79E−03	0.115
NSGA-II	7.55E−03	0.121
DMOBAT-5	7.75E−03	0.121
DMOPSO-1	8.17E−03	0.121
DMOFPA-4	8.61E−03	0.121
MOACS-2	9.07E−03	0.121
SPEA2	1.01E−02	0.121
DMOABC	1.36E−02	0.136
DMOCSA-1-5	1.36E−02	0.136
DMOFPA-5	1.50E−02	0.136
DMOCSA-1-1	1.58E−02	0.136
MOACS-1	1.58E−02	0.136
DMOFPA-2	3.39E−02	0.169
DMOCSA-2-4	4.30E−02	0.172
DMOCSA-1-3	7.88E−02	0.237
CHAC-1	1.02E−01	0.237
DMOBAT-4	0.241	0.241

Table C.118: Unadjusted and adjusted p-values obtained for Mitchell through the application of Holm's post hoc procedure, using the DMOFPA-4 as control algorithm in accordance with the computation time

Algorithm	Unadjusted p-value	Adjusted p-value
Others	<8.73E−04	<0.008
DMOBAT-1	7.96E−03	0.064
DMOCSA-1-5	2.15E−02	0.151
DMOPSO-4	3.39E−02	0.203
DMOBAT-4	1.29E−01	0.645
DMOPSO-1	1.45E−01	0.645
DMOCSA-1-4	4.04E−01	1.212
DMOPSO-3	0.564	1.212
SPEA2	0.588	1.212

C.4.9 Mukherje family problem

Table C.119: Average rankings returned by Friedman's nonparametric test for the Mukherje problems family according to all quality indicators

Algorithm	Ranking I_{HV}	I_{IGD}	I_ϵ	I_Δ	Time
BIANT-1	2.07	33.07	2.53	31.93	5.80
BIANT-2	1.73	32.53	2.27	31.93	5.20
CHAC-1	13.60	16.20	18.60	27.53	14.40
CHAC-2	11.87	20.40	18.30	24.80	17.70
DMOABC	21.67	12.07	20.10	7.13	6.70
DMOBAT-1	24.20	12.07	17.33	14.47	18.60
DMOBAT-2	20.13	15.67	22.93	16.07	17.80
DMOBAT-3	17.80	17.20	17.10	17.87	23.60
DMOBAT-4	18.73	15.07	20.23	11.07	19.90
DMOBAT-5	20.67	15.20	15.10	18.60	21.30
DMOCSA-1-1	18.20	18.60	15.43	14.33	12.80
DMOCSA-1-2	19.60	16.53	16.80	16.33	12.90
DMOCSA-2-1	21.73	16.47	21.77	15.73	10.90
DMOCSA-2-2	18.53	17.27	17.43	13.60	14.00
DMOCSA-2-3	18.00	17.93	19.60	14.53	11.30
DMOCSA-2-4	20.00	16.00	21.07	19.67	22.10
DMOCSA-2-5	19.80	17.73	16.73	15.60	20.50
DMOCSA-1-3	23.07	13.47	19.67	13.93	18.60
DMOCSA-1-4	19.00	17.27	21.27	12.67	21.20
DMOCSA-1-5	18.60	18.60	19.03	18.33	21.10
DMOFPA-1	21.20	16.80	16.20	16.07	9.90
DMOFPA-2	20.40	16.67	16.77	14.40	12.70
DMOFPA-3	22.47	12.00	15.67	13.53	25.70
DMOFPA-4	22.80	14.07	18.10	15.20	22.00
DMOFPA-5	20.47	17.33	24.13	13.87	20.70
DMOPSO-1	23.90	11.30	19.23	16.70	18.20
DMOPSO-2	21.67	16.33	15.23	17.40	23.40
DMOPSO-3	21.13	13.53	15.90	17.67	20.60
DMOPSO-4	20.33	15.40	18.93	17.47	22.70
DMOPSO-5	19.63	14.03	19.33	17.57	16.30
MOACS-1	4.20	31.33	1.20	32.20	7.90
MOACS-2	2.27	32.60	4.00	33.93	22.80
NSGA-II	13.07	12.73	33.40	5.60	23.80
SPEA2	12.47	11.53	33.60	7.27	31.90

* Rankings obtained by considering the average performance of each algorithm for the Mukherje problem instances

Table C.120: Unadjusted and adjusted p-values obtained for Mukherje through the application of Holm's post hoc procedure, using the BIANT-2 as control algorithm according to I_{HV}

Algorithm	Unadjusted p-value	Adjusted p-value
Others	<5.32E−03	<0.021
MOACS-1	4.98E−01	1.493
MOACS-2	8.83E−01	1.767
BIANT-1	0.927	1.767

Table C.121: Unadjusted and adjusted p-values obtained for Mukherje through the application of Holm's post hoc procedure, using the BIANT-1 as control algorithm according to I_{IGD}

Algorithm	Unadjusted p-value	Adjusted p-value
Others	<4.95E−04	<0.002
MOACS-1	6.34E−01	1.901
BIANT-2	8.83E−01	1.901
MOACS-2	0.898	1.901

Table C.122: Unadjusted and adjusted p-values obtained for Mukherje through the application of Holm's post hoc procedure, using the NSGA-II as control algorithm according to I_{ϵ}

Algorithm	Unadjusted p-value	Adjusted p-value
Others	<9.23E−03	<0.018
NSGA-II	0.956	0.956

Table C.123: Unadjusted and adjusted p-values obtained for Mukherje through the application of Holm's post hoc procedure, using the MOACS-2 as control algorithm according to I_{Δ}

Algorithm	Unadjusted p-value	Adjusted p-value
Others	<8.73E−05	<5.24E−04
CHAC-2	1.20E−02	0.060
CHAC-1	7.84E−02	0.314
BIANT-2	5.82E−01	1.747
BIANT-1	5.82E−01	1.747
MOACS-1	0.634	1.747

Table C.124: Unadjusted and adjusted p-values obtained for Mukherje through the application of Holm's post hoc procedure, using the SPEA2 as control algorithm in accordance with the computation time

Algorithm	Unadjusted p-value	Adjusted p-value
Others	<3.56E−03	<0.034
DMOBAT-2	6.85E−03	0.055
DMOFPA-1	7.43E−03	0.055
DMOPSO-2	1.20E−02	0.072
DMOPSO-5	1.30E−02	0.072
DMOBAT-5	1.99E−02	0.080
DMOCSA-1-3	2.30E−02	0.080
NSGA-II	0.026	0.080
DMOBAT-1	0.090	0.090

C.4.10 Roszieg family problem

Table C.125: Average rankings returned by Friedman's nonparametric test for the Roszieg problems family according to all quality indicators

Algorithm	Ranking I_{HV}	I_{IGD}	I_ϵ	I_Δ	Time
BIANT-1	31.04	4.53	4.88	22.13	6.60
BIANT-2	33.04	2.13	2.50	23.56	5.60
CHAC-1	13.07	20.13	21.56	16.41	9.70
CHAC-2	7.89	25.38	22.59	17.47	10.10
DMOABC	12.79	20.25	23.03	18.56	5.40
DMOBAT-1	17.57	19.91	19.72	13.31	22.80
DMOBAT-2	14.82	21.16	21.97	20.41	21.20
DMOBAT-3	11.68	22.41	24.25	15.41	18.50
DMOBAT-4	26.75	11.16	11.34	19.31	25.60
DMOBAT-5	12.93	22.28	21.09	16.63	20.90
DMOCSA-1-1	15.96	18.56	19.28	14.69	13.60
DMOCSA-1-2	14.61	18.91	18.81	13.81	15.60
DMOCSA-2-1	13.61	22.50	18.75	15.28	9.90
DMOCSA-2-2	14.54	18.72	19.88	15.22	13.60
DMOCSA-2-3	16.04	21.31	17.06	15.19	12.30
DMOCSA-2-4	26.04	13.25	10.44	21.88	23.70
DMOCSA-2-5	15.04	19.75	20.25	15.66	15.70
DMOCSA-1-3	17.39	21.63	18.53	13.97	19.40
DMOCSA-1-4	26.04	13.03	11.91	24.88	34.00
DMOCSA-1-5	14.96	20.28	21.44	15.16	19.00
DMOFPA-1	17.61	16.88	18.00	15.09	5.40
DMOFPA-2	11.79	23.66	25.28	17.63	2.20
DMOFPA-3	15.18	18.66	20.13	13.84	18.90
DMOFPA-4	26.39	11.53	10.72	20.63	20.50
DMOFPA-5	14.75	20.94	20.66	15.81	16.80
DMOPSO-1	10.39	23.91	22.72	20.16	23.50
DMOPSO-2	10.82	22.44	21.69	15.03	15.00
DMOPSO-3	11.07	21.47	21.69	19.13	27.70
DMOPSO-4	22.04	14.34	13.06	19.25	25.10
DMOPSO-5	11.18	18.41	24.06	17.72	31.70
MOACS-1	31.61	3.16	3.13	21.38	26.10
MOACS-2	32.75	2.22	2.81	18.88	19.60
NSGA-II	10.14	20.88	22.84	16.56	8.50
SPEA2	13.50	19.28	18.94	15.00	31.00

* Rankings obtained by considering the average performance of each algorithm for the Roszieg problem instances

Table C.126: Unadjusted and adjusted p-values obtained for Roszieg through the application of Holm's post hoc procedure, using the CHAC-2 as control algorithm according to I_{HV}

Algorithm	Unadjusted p-value	Adjusted p-value
Others	<1.72E−04	<0.004
DMOFPA-1	9.85E−03	0.236
DMOBAT-1	1.01E−02	0.236
DMOCSA-1-3	1.16E−02	0.255
DMOCSA-2-3	3.05E−02	0.641
DMOCSA-1-1	3.20E−02	0.641
DMOFPA-3	5.29E−02	1.005
DMOCSA-2-5	5.77E−02	1.039
DMOCSA-1-5	6.03E−02	1.039
DMOBAT-2	6.56E−02	1.050
DMOFPA-5	6.85E−02	1.050
DMOCSA-1-2	7.44E−02	1.050
DMOCSA-2-2	7.76E−02	1.050
DMOCSA-2-1	1.29E−01	1.548
SPEA2	1.36E−01	1.548
CHAC-1	1.69E−01	1.689
DMOBAT-5	1.81E−01	1.689
DMOABC	1.94E−01	1.689
DMOFPA-2	3.01E−01	2.107
DMOBAT-3	3.15E−01	2.107
DMOPSO-5	3.83E−01	2.107
DMOPSO-3	3.98E−01	2.107
DMOPSO-2	4.37E−01	2.107
DMOPSO-1	5.07E−01	2.107
NSGA-II	0.550	2.107

Table C.127: Unadjusted and adjusted p-values obtained for Roszieg through the application of Holm's post hoc procedure, using the CHAC-2 as control algorithm according to I_{IGD}

Algorithm	Unadjusted p-value	Adjusted p-value
Others	<1.73E−03	<0.043
DMOFPA-1	1.58E−02	0.378
DMOPSO-5	4.78E−02	1.099
DMOCSA-1-1	5.30E−02	1.166
DMOFPA-3	5.64E−02	1.183
DMOCSA-2-2	5.87E−02	1.183
DMOCSA-1-2	6.62E−02	1.257
SPEA2	8.35E−02	1.503
DMOCSA-2-5	1.10E−01	1.872
DMOBAT-1	1.20E−01	1.926
CHAC-1	1.36E−01	2.039
DMOABC	1.45E−01	2.039
DMOCSA-1-5	1.48E−01	2.039
NSGA-II	2.01E−01	2.414
DMOFPA-5	2.08E−01	2.414
DMOBAT-2	2.31E−01	2.414
DMOCSA-2-3	2.49E−01	2.414
DMOPSO-3	2.67E−01	2.414
DMOCSA-1-3	2.87E−01	2.414
DMOBAT-5	3.80E−01	2.414
DMOBAT-3	3.99E−01	2.414
DMOPSO-2	4.04E−01	2.414
DMOCSA-2-1	4.14E−01	2.414
DMOFPA-2	6.25E−01	2.414
DMOPSO-1	0.677	2.414

Table C.128: Unadjusted and adjusted p-values obtained for Roszieg through the application of Holm's post hoc procedure, using the DMOFPA-2 as control algorithm according to I_{ϵ}

Algorithm	Unadjusted p-value	Adjusted p-value
Others	<9.23E−03	<0.018
NSGA-II	0.956	0.956

Table C.129: Unadjusted and adjusted p-values obtained for Roszieg through the application of Holm's post hoc procedure, using the DMOCSA-1-4 as control algorithm according to I_{Δ}

Algorithm	Unadjusted p-value	Adjusted p-value
DMOBAT-1	1.02E−03	0.034
DMOCSA-1-2	1.68E−03	0.054
DMOFPA-3	1.73E−03	0.054
DMOCSA-1-3	1.95E−03	0.059
DMOCSA-1-1	3.81E−03	0.110
SPEA2	5.04E−03	0.141
DMOPSO-2	5.18E−03	0.141
DMOFPA-1	5.47E−03	0.142
DMOCSA-1-5	5.77E−03	0.144
DMOCSA-2-3	5.93E−03	0.144
DMOCSA-2-2	6.09E−03	0.144
DMOCSA-2-1	6.43E−03	0.144
DMOBAT-3	7.16E−03	0.150
DMOCSA-2-5	8.83E−03	0.177
DMOFPA-5	1.01E−02	0.191
CHAC-1	1.62E−02	0.291
NSGA-II	1.82E−02	0.310
DMOBAT-5	1.91E−02	0.310
CHAC-2	3.54E−02	0.531
DMOFPA-2	3.95E−02	0.553
DMOPSO-5	4.21E−02	0.553
DMOABC	7.30E−02	0.876
MOACS-2	8.83E−02	0.972
DMOPSO-3	1.02E−01	1.024
DMOPSO-4	1.10E−01	1.024
DMOBAT-4	1.14E−01	1.024
DMOPSO-1	1.80E−01	1.261
DMOBAT-2	2.04E−01	1.261
DMOFPA-4	2.27E−01	1.261
MOACS-1	3.20E−01	1.281
DMOCSA-2-4	3.94E−01	1.281
BIANT-1	4.35E−01	1.281
BIANT-2	0.709	1.281

Table C.130: Unadjusted and adjusted p-values obtained for Mukherje through the application of Holm's post hoc procedure, using the DMOFPA-4 as control algorithm in accordance with the computation time

Algorithm	Unadjusted p-value	Adjusted p-value
DMOFPA-1	<3.50E−03	<0.024
DMOPSO-2	1.17E−02	0.070
DMOCSA-1-4	1.66E−02	0.083
DMOPSO-4	2.42E−02	0.097
DMOPSO-1	7.16E−02	0.215
SPEA2	0.394	0.788
DMOPSO-3	0.506	0.788

C.4.11 Sawyer family problem

Table C.131: Average rankings returned by Friedman's nonparametric test for the Sawyer problems family according to all quality indicators

Algorithm	Ranking I_{HV}	I_{IGD}	I_{ϵ}	I_{Δ}	Time
BIANT-1	12.61	12.62	5.47	26.79	23.60
BIANT-2	16.25	8.91	5.71	22.32	22.10
CHAC-1	14.46	20.68	21.97	17.59	25.10
CHAC-2	12.43	17.44	20.03	15.79	29.00
DMOABC	22.07	18.94	21.74	14.18	3.00
DMOBAT-1	14.29	18.53	19.85	19.44	11.80
DMOBAT-2	30.14	21.35	19.82	17.41	13.90
DMOBAT-3	29.96	22.26	18.59	16.68	18.40
DMOBAT-4	13.00	14.06	14.38	22.29	34.00
DMOBAT-5	14.75	19.97	17.74	16.74	17.50
DMOCSA-1-1	15.43	19.15	20.41	13.24	9.40
DMOCSA-1-2	15.11	19.09	19.29	15.00	11.30
DMOCSA-2-1	14.25	20.85	21.09	15.88	10.40
DMOCSA-2-2	16.50	19.18	16.47	17.12	25.00
DMOCSA-2-3	13.36	20.15	19.44	15.85	18.30
DMOCSA-2-4	20.93	13.82	17.24	19.24	4.30
DMOCSA-2-5	15.25	20.50	17.41	16.85	1.90
DMOCSA-1-3	16.00	18.41	18.35	15.59	24.50
DMOCSA-1-4	22.07	13.24	15.26	20.71	22.30
DMOCSA-1-5	18.68	17.32	20.26	14.38	17.00
DMOFPA-1	17.96	17.85	2.18	16.47	21.00
DMOFPA-2	17.68	18.18	4.15	16.53	18.60
DMOFPA-3	17.14	18.56	19.24	17.82	2.10
DMOFPA-4	21.50	14.71	20.09	20.35	7.90
DMOFPA-5	15.07	18.29	21.41	12.62	8.90
DMOPSO-1	33.07	20.53	14.50	17.06	5.30
DMOPSO-2	31.39	21.91	20.18	14.26	22.30
DMOPSO-3	11.61	21.71	21.85	16.65	28.60
DMOPSO-4	12.93	16.18	22.65	18.38	31.10
DMOPSO-5	11.36	14.18	22.32	17.24	24.30
MOACS-1	12.18	11.26	18.74	22.24	17.50
MOACS-2	19.43	9.44	17.21	25.06	28.50
NSGA-II	12.93	16.44	18.41	15.26	8.50
SPEA2	13.21	19.29	21.56	11.97	27.60

* Rankings obtained by considering the average performance of each algorithm for the Sawyer problem instances

Table C.132: Unadjusted and adjusted p-values obtained for Sawyer through the application of Holm's post hoc procedure, using the DMOPSO-2 as control algorithm according to I_{HV}

Algorithm	Unadjusted p-value	Adjusted p-value
Others	<7.67E−07	<2.30E−05
DMOBAT-4	4.42E−03	0.128
DMOCSA-1-4	4.42E−03	0.128
DMOFPA-4	7.04E−03	0.190
DMOCSA-2-4	1.10E−02	0.286
DMOPSO-4	3.20E−02	0.800
DMOCSA-1-5	5.18E−02	1.242
DMOFPA-1	7.92E−02	1.821
DMOFPA-2	9.31E−02	2.047
DMOFPA-3	1.24E−01	2.609
DMOCSA-2-2	1.72E−01	3.436
DMOBAT-1	1.94E−01	3.679
DMOCSA-1-3	2.17E−01	3.913
DMOCSA-1-1	2.79E−01	4.749
DMOCSA-2-5	3.01E−01	4.816
DMOCSA-1-2	3.19E−01	4.816
DMOFPA-5	3.24E−01	4.816
CHAC-2	3.67E−01	4.816
DMOBAT-2	4.09E−01	4.909
DMOBAT-5	4.37E−01	4.909
DMOCSA-2-1	4.42E−01	4.909
DMOCSA-2-3	5.95E−01	5.356
SPEA2	6.22E−01	5.356
CHAC-1	6.62E−01	5.356
NSGA-II	6.76E−01	5.356
DMOPSO-1	6.76E−01	5.356
DMOABC	7.40E−01	5.356
DMOBAT-3	7.76E−01	5.356
DMOPSO-3	8.27E−01	5.356
DMOPSO-5	0.947	5.356

Table C.133: Unadjusted and adjusted p-values obtained for Sawyer through the application of Holm's post hoc procedure, using the DMOBAT-3 as control algorithm according to I_{IGD}

Algorithm	Unadjusted p-value	Adjusted p-value
Others	<1.28E−03	<0.040
BIANT-1	4.74E−03	0.142
DMOCSA-1-4	8.20E−03	0.238
DMOCSA-2-4	1.35E−02	0.377
DMOBAT-4	1.63E−02	0.440
DMOPSO-5	1.79E−02	0.465
DMOFPA-4	2.69E−02	0.672
DMOPSO-4	7.47E−02	1.792
NSGA-II	8.82E−02	2.029
DMOCSA-1-5	1.48E−01	3.256
CHAC-2	1.58E−01	3.316
DMOFPA-1	1.96E−01	3.930
DMOFPA-2	2.31E−01	4.395
DMOFPA-5	2.45E−01	4.411
DMOCSA-1-3	2.59E−01	4.411
DMOBAT-1	2.74E−01	4.411
DMOFPA-3	2.78E−01	4.411
DMOABC	3.31E−01	4.628
DMOCSA-1-2	3.52E−01	4.628
DMOCSA-1-1	3.61E−01	4.628
DMOCSA-2-2	3.66E−01	4.628
SPEA2	3.84E−01	4.628
DMOBAT-5	5.02E−01	4.628
DMOCSA-2-3	5.35E−01	4.628
DMOCSA-2-5	6.05E−01	4.628
DMOPSO-1	6.11E−01	4.628
CHAC-1	6.42E−01	4.628
DMOCSA-2-1	6.79E−01	4.628
DMOBAT-2	7.90E−01	4.628
DMOPSO-3	8.70E−01	4.628
DMOPSO-2	0.918	4.628

Table C.134: Unadjusted and adjusted p-values obtained for Sawyer through the application of Holm's post hoc procedure, using the DMOPSO-2 as control algorithm according to I_ϵ

Algorithm	Unadjusted p-value	Adjusted p-value
Others	<7.05E−07	<2.12E−05
DMOCSA-1-4	1.55E−02	0.451
DMOBAT-4	1.71E−02	0.478
DMOFPA-4	3.07E−02	0.828
DMOCSA-2-4	7.06E−02	1.835
DMOPSO-5	1.11E−01	2.779
DMOFPA-1	1.13E−01	2.779
DMOFPA-2	1.25E−01	2.883
DMOCSA-1-5	1.50E−01	3.309
DMOFPA-3	2.09E−01	4.382
NSGA-II	2.15E−01	4.382
DMOCSA-1-3	2.35E−01	4.460
DMOPSO-4	2.52E−01	4.538
DMOBAT-1	3.18E−01	5.404
DMOCSA-2-2	3.26E−01	5.404
DMOCSA-2-5	3.48E−01	5.404
DMOCSA-1-2	4.08E−01	5.718
DMOCSA-1-1	4.13E−01	5.718
CHAC-2	4.43E−01	5.718
DMOBAT-2	4.54E−01	5.718
DMOBAT-5	4.69E−01	5.718
DMOFPA-5	4.86E−01	5.718
DMOCSA-2-1	5.13E−01	5.718
DMOCSA-2-3	6.48E−01	5.718
DMOBAT-3	7.18E−01	5.718
SPEA2	7.50E−01	5.718
DMOABC	7.90E−01	5.718
DMOPSO-1	8.16E−01	5.718
CHAC-1	8.43E−01	5.718
DMOPSO-3	0.925	5.718

Table C.135: Unadjusted and adjusted p-values obtained for Sawyer through the application of Holm's post hoc procedure, using the BIANT-1 as control algorithm according to I_{Δ}

Algorithm	Unadjusted p-value	Adjusted p-value
Others	<1.40E−03	<0.031
DMOFPA-1	2.51E−03	0.053
DMOFPA-2	2.65E−03	0.053
DMOPSO-3	2.97E−03	0.056
DMOBAT-3	3.06E−03	0.056
DMOBAT-5	3.23E−03	0.056
DMOCSA-2-5	3.61E−03	0.058
DMOPSO-1	4.37E−03	0.066
DMOCSA-2-2	4.61E−03	0.066
DMOPSO-5	5.13E−03	0.067
DMOBAT-2	6.02E−03	0.072
CHAC-1	7.03E−03	0.077
DMOFPA-3	8.63E−03	0.086
DMOPSO-4	1.38E−02	0.124
DMOCSA-2-4	2.69E−02	0.215
DMOBAT-1	3.13E−02	0.219
DMOFPA-4	5.93E−02	0.356
DMOCSA-1-4	7.47E−02	0.373
MOACS-1	1.82E−01	0.728
DMOBAT-4	1.88E−01	0.728
BIANT-2	1.91E−01	0.728
MOACS-2	0.611	0.728

Table C.136: Unadjusted and adjusted p-values obtained for Mukherje through the application of Holm's post hoc procedure, using the DMOCSA-1-4 as control algorithm in accordance with the computation time

Algorithm	Unadjusted p-value	Adjusted p-value
Others	<5.56E−03	<0.044
DMOFPA-1	8.42E−03	0.059
DMOCSA-1-4	9.55E−03	0.059
SPEA2	6.41E−02	0.321
DMOPSO-1	1.09E−01	0.437
DMOPSO-2	0.113	0.437
DMOCSA-1-5	0.148	0.437
DMOPSO-3	0.399	0.437

C.4.12 Group analysis

Table C.137: Average rankings returned by Friedman's nonparametric test for both groups, Group 1 and Group 2

	Group 1					Group 2				
Algorithm	I_{HV}	I_{IGD}	I_{ϵ}	I_{Δ}	Time1	I_{HV}	I_{IGD}	I_{ϵ}	I_{Δ}	Time2
ABC	18.52	17.24	17.75	11.85	7.05	12.78	21.23	22.29	17.83	5.04
DMOBAT-1	19.29	16.29	16.99	15.05	21.87	13.77	21.00	21.03	17.09	22.01
DMOBAT-2	18.16	17.76	16.81	16.24	20.39	14.00	21.73	20.61	17.76	19.82
DMOBAT-3	17.85	17.99	17.00	16.90	19.80	12.46	21.92	21.94	17.00	15.24
DMOBAT-4	26.44	8.95	16.38	14.56	21.21	24.63	11.47	12.11	20.41	20.50
DMOBAT-5	19.05	17.26	16.39	15.06	19.74	13.25	22.01	20.64	16.38	17.61
BIANT-1	4.69	29.07	14.43	31.73	5.15	29.96	7.57	5.53	20.91	7.50
BIANT-2	3.55	29.19	15.07	31.85	5.11	30.66	6.34	4.52	18.50	6.75
CHAC-1	15.05	18.94	17.70	20.99	14.75	12.54	22.29	21.00	18.47	10.09
CHAC-2	15.46	19.03	17.00	19.95	16.28	12.24	22.00	21.77	18.22	11.57
DMOCSO-1-1	18.75	17.05	16.22	14.35	19.55	14.56	19.78	20.23	15.96	21.56
DMOCSO-1-2	18.25	17.70	16.67	15.90	19.16	14.64	19.14	19.77	14.90	21.82
DMOCSO-2-1	19.01	17.15	17.61	15.97	14.25	14.00	20.27	19.47	15.36	12.13
DMOCSO-2-2	17.28	18.56	16.94	15.85	13.78	14.98	19.03	19.47	16.08	15.89
DMOCSO-2-3	17.92	18.12	17.62	15.97	11.16	15.64	19.46	20.03	15.86	9.29
DMOCSO-2-4	25.09	10.91	17.35	16.60	16.09	24.53	10.92	12.40	19.58	13.94
DMOCSO-2-5	17.98	18.43	17.30	16.43	12.34	14.90	19.73	19.45	16.18	10.92
DMOCSO-1-3	19.80	17.12	16.39	15.41	20.46	15.42	19.16	19.19	16.00	20.06
DMOCSO-1-4	27.58	7.98	17.01	14.08	23.46	26.76	9.63	11.05	21.99	24.26
DMOCSO-1-5	19.64	17.30	17.33	15.51	21.37	15.02	19.18	19.73	15.41	24.00
DMOFPA-1	19.30	17.12	17.39	16.77	20.20	14.98	18.76	19.25	16.51	23.34
DMOFPA-2	19.56	17.40	16.66	15.42	19.25	14.96	19.41	19.76	17.78	17.07
DMOFPA-3	18.95	17.23	16.56	16.09	18.63	14.93	19.15	19.28	15.83	17.31
DMOFPA-4	27.25	8.39	15.86	14.59	24.64	26.82	9.67	10.97	19.20	32.54
DMOFPA-5	19.53	17.04	17.15	14.82	19.47	15.17	19.43	19.33	15.62	17.82
MOACS-1	7.47	24.69	19.36	32.44	13.36	31.80	6.09	3.78	20.24	7.85
MOACS-2	3.15	26.77	20.64	32.46	15.58	32.05	4.83	3.58	19.11	4.92
DMOPSO	17.41	18.39	18.05	17.70	19.60	12.64	20.27	21.91	16.95	20.97
DMOPSO-1	18.69	17.24	17.88	16.47	19.96	12.36	22.22	22.66	18.51	27.01
DMOPSO-2	18.98	17.94	16.29	16.19	23.82	13.18	21.52	21.39	16.64	25.54
DMOPSO-3	19.15	16.91	17.05	15.81	16.22	13.33	21.37	21.84	17.39	28.85
DMOPSO-4	24.83	10.76	16.08	15.88	10.35	20.46	15.47	16.32	17.84	20.50
NSGA-II	9.74	17.58	25.54	8.75	19.00	12.64	21.37	21.26	17.03	10.39
SPEA2	11.61	15.51	24.50	11.34	31.95	12.94	21.54	21.46	16.46	30.90

C.4.12.1 Unadjusted and adjusted p-values through the application of Holm's post hoc procedure for the problems of Group 1

Table C.138: Unadjusted and adjusted p-values obtained for problem instances of Group 1 through the application of Holm's post hoc procedure, using the MOACS-2 as control algorithm according to I_{HV}

Algorithm	Unadjusted p-value	Adjusted p-value
Others	<1.3E−03	<3.9E−03
BIANT-1	2.5E−01	5.1E−01
BIANT-2	7.7E−01	7.7E−01

Table C.139: Unadjusted and adjusted p-values obtained for problem instances of Group 1 through the application of Holm's post hoc procedure, using the BIANT-2 as control algorithm according to I_{IGD}

Algorithm	Unadjusted p-value	Adjusted p-value
Others	<8.0E−04	<2.4E−03
MOACS-2	7.2E−02	1.4E−01
BIANT-1	9.3E−01	9.3E−01

Table C.140: Unadjusted and adjusted p-values obtained for problem instances of Group 1 through the application of Holm's post hoc procedure, using the NSGA-II as control algorithm according to I_{ϵ}

Algorithm	Unadjusted p-value	Adjusted p-value
Others	<2.6E−04	<5.2E−04
SPEA2	4.4E−01	4.4E−01

Table C.141: Unadjusted and adjusted p-values obtained for problem instances of Group 1 through the application of Holm's post hoc procedure, using the MOACS-2 as control algorithm according to I_{Δ}

Algorithm	Unadjusted p-value	Adjusted p-value
Others	<1.3E−17	<5.2E−17
BIANT-1	5.8E−01	1.8E+00
BIANT-2	6.5E−01	1.8E+00
MOACS-1	9.8E−01	1.8E+00

Table C.142: Unadjusted and adjusted p-values obtained for problem instances of Group 1 through the application of Holm's post hoc procedure, using the SPEA2 as control algorithm in accordance with the computation time

Algorithm	Unadjusted p-value	Adjusted p-value
All	<5.3E−08	<5.3E−08

C.4.12.2 Unadjusted and adjusted p-values through the application of Holm's post hoc procedure for the problems of Group 2

Table C.143: Unadjusted and adjusted p-values obtained for problem instances of Group 2 through the application of Holm's post hoc procedure, using the CHAC-2 as control algorithm according to I_{HV}

Algorithm	Unadjusted p-value	Adjusted p-value
Others	<4.4E−10	<1.1E−08
DMOCSA-2-3	9.9E−03	2.4E−01
DMOCSA-1-3	1.6E−02	3.6E−01
DMOFPA-5	2.6E−02	5.8E−01
DMOCSA-1-5	3.5E−02	7.4E−01
DMOCSA-2-2	3.8E−02	7.5E−01
DMOFPA-1	3.8E−02	7.5E−01
DMOFPA-2	3.9E−02	7.5E−01
DMOFPA-3	4.2E−02	7.5E−01
DMOCSA-2-5	4.4E−02	7.5E−01
DMOCSA-1-2	6.9E−02	1.0E+00
DMOCSA-1	7.9E−02	1.1E+00
DMOCSA-2-1	1.8E−01	2.3E+00
DMOBAT-2	1.8E−01	2.3E+00
DMOBAT-1	2.4E−01	2.7E+00
DMOPSO-3	4.1E−01	4.1E+00
DMOBAT-5	4.4E−01	4.1E+00
DMOPSO-2	4.8E−01	4.1E+00
SPEA2	6.0E−01	4.2E+00
DMOABC	6.8E−01	4.2E+00
NSGA-II	7.6E−01	4.2E+00
DMOPSO-5	7.6E−01	4.2E+00
CHAC-1	8.2E−01	4.2E+00
DMOBAT-3	8.7E−01	4.2E+00
DMOPSO-1	9.2E−01	4.2E+00

Table C.144: Unadjusted and adjusted p-values obtained for problem instances of Group 2 through the application of Holm's post hoc procedure, using the CHAC-1 as control algorithm according to I_{IGD}

Algorithm	Unadjusted p-value	Adjusted p-value
Others	<1.3E−07	<3.2E−06

Table C.145: Unadjusted and adjusted p-values obtained for problem instances of Group 2 through the application of Holm's post hoc procedure, using the DMOPSO-1 as control algorithm according to I_ϵ

Algorithm	Unadjusted p-value	Adjusted p-value
Others	<8.90E−07	<2.23E−05
DMOFPA-1	6.2E−03	1.5E−01
DMOCSA-2-2	1.2E−02	2.7E−01
DMOCSA-1-2	1.5E−02	3.3E−01
DMOFPA-3	1.5E−02	3.3E−01
DMOCSA-1-3	1.6E−02	3.3E−01
DMOCSA-1-5	1.6E−02	3.3E−01
DMOFPA-2	2.6E−02	4.6E−01
DMOFPA-5	2.7E−02	4.6E−01
DMOCSA-2-3	2.9E−02	4.6E−01
DMOCSA-2-5	4.8E−02	7.1E−01
DMOCSA-1	5.2E−02	7.3E−01
DMOPSO-5	1.2E−01	1.5E+00
DMOCSA-2-1	1.2E−01	1.5E+00
DMOBAT-1	3.2E−01	3.5E+00
DMOABC	4.1E−01	4.1E+00
DMOPSO-3	4.8E−01	4.3E+00
NSGA-II	4.8E−01	4.3E+00
DMOPSO-2	5.5E−01	4.3E+00
SPEA2	5.6E−01	4.3E+00
DMOBAT-2	6.7E−01	4.3E+00
DMOBAT-3	7.8E−01	4.3E+00
CHAC-2	8.3E−01	4.3E+00
DMOBAT-5	8.3E−01	4.3E+00
DMOPSO-1	9.6E−01	4.3E+00

Table C.146: Unadjusted and adjusted p-values obtained for problem instances of Group 2 through the application of Holm's post hoc procedure, using the DMOCSA-1-4 as control algorithm according to I_Δ

Algorithm	Unadjusted p-value	Adjusted p-value
Others	<3.5E−03	<3.5E−02
CHAC-1	6.5E−03	5.8E−02
BIANT-2	6.9E−03	5.8E−02
DMOPSO-1	7.1E−03	5.8E−02
MOACS-2	2.6E−02	1.5E−01
DMOFPA-4	3.1E−02	1.5E−01
DMOCSA-2-4	6.2E−02	2.5E−01
MOACS-1	1.8E−01	5.3E−01
DMOBAT-4	2.2E−01	5.3E−01
BIANT-1	4.1E−01	5.3E−01

Table C.147: Unadjusted and adjusted p-values obtained for problem instances of Group 2 through the application of Holm's post hoc procedure, using the DMOFPA-4 as control algorithm in accordance with the computation time

Algorithm	Unadjusted p-value	Adjusted p-value
All	<5.3E−08	<5.3E−08

C.4.13 Best strategies Swarm Algorithms

This section presents the results of the Friedman's test for the choice of the best selection strategy.

C.4.13.1 Friedman's rankings

Table C.148: Average rankings returned by Friedman's nonparametric test for the DMOBAT

	All Problem				Group 1				Group 2			
	I_{HV}	I_{IGD}	I_{ϵ}	I_{Δ}	I_{HV}	I_{IGD}	I_{ϵ}	I_{Δ}	I_{HV}	I_{IGD}	I_{ϵ}	I_{Δ}
DMOBAT-1	2.78	3.18	3.15	2.89	2.84	3.15	3.01	2.88	2.73	3.21	3.27	2.89
DMOBAT-2	2.71	3.33	3.12	3.11	2.65	3.34	3.01	3.15	2.76	3.33	3.23	3.08
DMOBAT-3	2.53	3.37	3.25	3.03	2.62	3.35	3.02	3.27	2.44	3.39	3.46	2.81
DMOBAT-4	4.25	1.82	2.37	3.13	4.04	1.92	2.95	2.79	4.46	1.73	1.84	3.45
DMOBAT-5	2.73	3.29	3.11	2.84	2.85	3.25	3.01	2.91	2.61	3.34	3.20	2.77

Table C.149: Average rankings returned by Friedman's nonparametric test for the DMOCSO

	All problems				Group 1				Group 2			
	I_{HV}	I_{IGD}	I_{ϵ}	I_{Δ}	I_{HV}	I_{IGD}	I_{ϵ}	I_{Δ}	I_{HV}	I_{IGD}	I_{ϵ}	I_{Δ}
DMOCSO-1-1	4.83	5.98	5.73	5.22	4.97	5.85	5.19	5.09	4.68	6.11	6.24	5.33
DMOCSO-1-2	4.80	6.03	5.73	5.24	4.95	6.02	5.33	5.67	4.64	6.04	6.11	4.84
DMOCSO-1-3	5.15	5.94	5.60	5.31	5.34	5.78	5.23	5.38	4.97	6.09	5.93	5.25
DMOCSO-1-4	8.52	2.75	4.21	6.02	8.11	2.85	5.51	4.92	8.93	2.66	3.00	7.03
DMOCSO-1-5	5.05	5.96	5.86	5.29	5.43	5.84	5.62	5.45	4.68	6.08	6.08	5.16
DMOCSO-2-1	4.71	6.19	5.87	5.37	5.02	5.96	5.69	5.64	4.41	6.39	6.03	5.12
DMOCSO-2-2	4.61	6.22	5.74	5.46	4.41	6.43	5.48	5.62	4.80	6.04	5.99	5.31
DMOCSO-2-3	4.87	6.17	5.98	5.46	4.81	6.19	5.78	5.61	4.94	6.16	6.18	5.32
DMOCSO-2-4	7.68	3.51	4.48	6.07	7.15	3.91	5.60	5.82	8.20	3.15	3.44	6.30
DMOCSO-2-5	4.78	6.23	5.80	5.57	4.82	6.18	5.57	5.81	4.74	6.27	6.01	5.34

Table C.150: Average rankings returned by Friedman's nonparametric test for the DMOFPA

	All problems				Group 1				Group 2			
	I_{HV}	I_{IGD}	I_{ϵ}	I_{Δ}	I_{HV}	I_{IGD}	I_{ϵ}	I_{Δ}	I_{HV}	I_{IGD}	I_{ϵ}	I_{Δ}
DMOFPA-1	2.62	3.31	3.25	2.98	2.65	3.36	3.20	3.08	2.58	3.26	3.29	2.89
DMOFPA-2	2.67	3.36	3.17	3.06	2.77	3.35	2.98	3.00	2.57	3.37	3.34	3.12
DMOFPA-3	2.59	3.29	3.13	2.95	2.65	3.24	2.95	3.07	2.54	3.35	3.30	2.84
DMOFPA-4	4.44	1.71	2.28	3.16	4.17	1.80	2.82	2.94	4.70	1.63	1.79	3.37
DMOFPA-5	2.68	3.33	3.17	2.85	2.75	3.25	3.05	2.91	2.61	3.40	3.28	2.79

Table C.151: Average rankings returned by Friedman's nonparametric test for the DMOPSO

	All problems				Group 1				Group 2			
	I_{HV}	I_{IGD}	I_ϵ	I_Δ	I_{HV}	I_{IGD}	I_ϵ	I_Δ	I_{HV}	I_{IGD}	I_ϵ	I_Δ
DMOPSO-1	2.73	3.26	3.26	3.08	2.82	3.17	3.20	3.02	2.65	3.34	3.32	3.13
DMOPSO-2	2.85	3.26	2.96	2.88	2.89	3.30	2.86	2.99	2.82	3.23	3.05	2.78
DMOPSO-3	2.83	3.18	3.07	2.94	2.84	3.18	2.98	2.86	2.83	3.18	3.16	3.02
DMOPSO-4	3.84	2.14	2.55	3.00	3.80	2.05	2.80	2.83	3.89	2.21	2.32	3.16
DMOPSO-5	2.74	3.16	3.16	3.10	2.65	3.29	3.16	3.30	2.82	3.03	3.16	2.91

C.4.13.2 Unadjusted and adjusted p-values through the application of Holm's post hoc procedure to evaluate the selection of the best solution

C.4.13.2.1 DMOBAT

Table C.152: Unadjusted and adjusted p-values obtained for all problems through the application of Holm's post hoc procedure, using the DMOBAT-3 as control algorithm according to I_{HV}

Algorithm	Unadjusted p-value	Adjusted p-value
DMOBAT-4	2.85E−09	1.14E−08
DMOBAT-5	0.337	1.010
DMOBAT-2	0.400	1.010
DMOBAT-1	0.497	1.010

Table C.153: Unadjusted and adjusted p-values obtained for all problems through the application of Holm's post hoc procedure, using the DMOBAT-3 as control algorithm according to I_{IGD}

Algorithm	Unadjusted p-value	Adjusted p-value
DMOBAT-4	1.11E−25	4.43E−25
DMOBAT-1	2.09E−01	0.627
DMOBAT-5	6.05E−01	1.210
DMOBAT-2	0.813	1.210

Table C.154: Unadjusted and adjusted p-values obtained for all problems through the application of Holm's post hoc procedure, using the DMOBAT-3 as control algorithm according to I_ϵ

Algorithm	Unadjusted p-value	Adjusted p-value
DMOBAT-4	7.03E−17	2.81E−16
DMOBAT-5	3.09E−01	0.927
DMOBAT-1	5.13E−01	1.025
DMOBAT-2	5.53E−01	1.025

Table C.155: Unadjusted and adjusted p-values obtained for all problems through the application of Holm's post hoc procedure, using the DMOBAT-4 as control algorithm according to I_{Δ}

Algorithm	Unadjusted p-value	Adjusted p-value
DMOBAT-5	4.45E−02	0.178
DMOBAT-1	9.79E−02	0.294
DMOBAT-3	4.97E−01	0.993
DMOBAT-2	0.871	0.993

Table C.156: Unadjusted and adjusted p-values obtained for problem instances of Group 1 through the application of Holm's post hoc procedure, using the DMOBAT-3 as control algorithm according to I_{HV}

Algorithm	Unadjusted p-value	Adjusted p-value
DMOBAT-4	1.55E−17	6.21E−17
DMOBAT-1	0.163	0.488
DMOBAT-5	0.235	0.488
DMOBAT-2	0.770	0.770

Table C.157: Unadjusted and adjusted p-values obtained for problem instances of Group 1 through the application of Holm's post hoc procedure, using the DMOBAT-3 as control algorithm according to I_{ϵ}

Algorithm	Unadjusted p-value	Adjusted p-value
DMOBAT-4	2.16E−11	8.66E−11
DMOBAT-1	0.371	1.112
DMOBAT-5	0.639	1.278
DMOBAT-2	0.966	1.278

Table C.158: Unadjusted and adjusted p-values obtained for problem instances of Group 1 through the application of Holm's post hoc procedure, using the DMOBAT-3 as control algorithm according to I_{ϵ}

Algorithm	Unadjusted p-value	Adjusted p-value
DMOBAT-4	7.49E−01	2.996
DMOBAT-2	0.966	2.996
DMOBAT-5	0.966	2.996
DMOBAT-1	0.983	2.996

Table C.159: Unadjusted and adjusted p-values obtained for problem instances of Group 1 through the application of Holm's post hoc procedure, using the DMOBAT-3 as control algorithm according to I_{Δ}

Algorithm	Unadjusted p-value	Adjusted p-value
DMOBAT-4	2.38E−02	0.095
DMOBAT-1	0.067	0.200
DMOBAT-5	0.088	0.200
DMOBAT-2	0.551	0.551

Table C.160: Unadjusted and adjusted p-values obtained for all problems through the application of Holm's post hoc procedure, using the DMOBAT-3 as control algorithm according to I_{HV}

Algorithm	Unadjusted p-value	Adjusted p-value
DMOBAT-4	4.70E−22	1.88E−21
DMOBAT-2	0.126	0.379
DMOBAT-1	0.167	0.379
DMOBAT-5	0.402	0.402

Table C.161: Unadjusted and adjusted p-values obtained for all problems through the application of Holm's post hoc procedure, using the DMOBAT-3 as control algorithm according to I_{ϵ}

Algorithm	Unadjusted p-value	Adjusted p-value
DMOBAT-4	5.65E−16	2.26E−15
DMOBAT-1	0.378	1.134
DMOBAT-2	0.774	1.548
DMOBAT-5	0.790	1.548

Table C.162: Unadjusted and adjusted p-values obtained for all problems through the application of Holm's post hoc procedure, using the DMOBAT-3 as control algorithm according to I_{ϵ}

Algorithm	Unadjusted p-value	Adjusted p-value
DMOBAT-4	2.14E−15	8.58E−15
DMOBAT-5	0.197	0.590
DMOBAT-2	0.260	0.590
DMOBAT-1	0.356	0.590

Table C.163: Unadjusted and adjusted p-values obtained for all problems through the application of Holm's post hoc procedure, using the DMOBAT-4 as control algorithm according to I_{Δ}

Algorithm	Unadjusted p-value	Adjusted p-value
DMOBAT-5	8.98E−04	0.004
DMOBAT-3	0.002	0.006
DMOBAT-1	0.007	0.014
DMOBAT-2	0.068	0.068

C.4.13.2.2 DMOCSO

Table C.164: Unadjusted and adjusted p-values obtained for all problems through the application of Holm's post hoc procedure, using the DMOCSA-2-2 as control algorithm according to I_{HV}

Algorithm	Unadjusted p-value	Adjusted p-value
Others	<5.82E−27	<4.66E−26
DMOCSA-1-3	0.058	0.406
DMOCSA-1-5	0.122	0.734
DMOCSA-2-3	0.349	1.746
DMOCSA-1-1	0.444	1.778
DMOCSA-2-1	0.507	1.778
DMOCSA-2-5	0.548	1.778
DMOCSA-2-1	0.720	1.778

Table C.165: Unadjusted and adjusted p-values obtained for all problems through the application of Holm's post hoc procedure, using the DMOCSA-2-5 as control algorithm according to I_{ϵ}

Algorithm	Unadjusted p-value	Adjusted p-value
All	<0.007	<0.007

Table C.166: Unadjusted and adjusted p-values obtained for all problems through the application of Holm's post hoc procedure, using the DMOCSA-1-4 as control algorithm according to I_{ϵ}

Algorithm	Unadjusted p-value	Adjusted p-value
Others	<8.85E−07	<1.77E−06
DMOCSA-2-4	0.335	0.335

Table C.167: Unadjusted and adjusted p-values obtained for all problems through the application of Holm's post hoc procedure, using the DMOCSA-1-1 as control algorithm according to I_{Δ}

Algorithm	Unadjusted p-value	Adjusted p-value
Others	<4.63E−03	<0.037
DMOCSA-2-5	2.17E−01	1.519
DMOCSA-2-3	3.87E−01	2.325
DMOCSA-2-2	3.96E−01	2.325
DMOCSA-2-1	5.89E−01	2.356
DMOCSA-1-3	7.28E−01	2.356
DMOCSA-1-5	0.781	2.356
DMOCSA-2-1	0.938	2.356

Table C.168: Unadjusted and adjusted p-values obtained for problem instances of Group 1 through the application of Holm's post hoc procedure, using the DMOCSA-2-2 as control algorithm according to I_{HV}

Algorithm	Unadjusted p-value	Adjusted p-value
Others	<2.05E−11	<1.64E−10
DMOCSA-1-5	0.013	0.088
DMOCSA-1-3	0.023	0.139
DMOCSA-2-1	0.136	0.679
DMOCSA-1-1	0.167	0.679
DMOCSA-1-2	0.182	0.679
DMOCSA-2-5	0.316	0.679
DMOCSA-2-3	0.327	0.679

Table C.169: Unadjusted and adjusted p-values obtained for problem instances of Group 1 through the application of Holm's post hoc procedure, using the DMOCSA-2-2 as control algorithm according to I_{ϵ}

Algorithm	Unadjusted p-value	Adjusted p-value
Others	<6.90E−10	<5.52E−09
DMOCSA-1-3	0.114	0.797
DMOCSA-1-5	0.148	0.887
DMOCSA-1-1	0.154	0.887
DMOCSA-2-1	0.256	1.024
DMOCSA-1-2	0.316	1.024
DMOCSA-2-5	0.548	1.095
DMOCSA-2-3	0.563	1.095

Table C.170: Unadjusted and adjusted p-values obtained for problem instances of Group 1 through the application of Holm's post hoc procedure, using the DMOCSA-2-3 as control algorithm according to I_{ϵ}

Algorithm	Unadjusted p-value	Adjusted p-value
DMOCSA-1-1	1.48E−01	1.330
DMOCSA-1-3	1.82E−01	1.452
DMOCSA-1-2	0.270	1.892
DMOCSA-2-2	0.462	2.775
DMOCSA-1-4	0.511	2.775
DMOCSA-2-5	0.616	2.775
DMOCSA-2-4	0.672	2.775
DMOCSA-1-5	0.705	2.775
DMOCSA-2-1	0.832	2.775

Table C.171: Unadjusted and adjusted p-values obtained for problem instances of Group 1 through the application of Holm's post hoc procedure, using the DMOCSA-2-4 as control algorithm according to I_{Δ}

Algorithm	Unadjusted p-value	Adjusted p-value
DMOCSA-1-4	2.75E−02	0.247
DMOCSA-1-1	7.48E−02	0.599
DMOCSA-1-3	0.285	1.996
DMOCSA-1-5	0.361	2.167
DMOCSA-2-3	0.609	3.043
DMOCSA-2-2	0.624	3.043
DMOCSA-2-1	0.656	3.043
DMOCSA-1-2	0.722	3.043
DMOCSA-2-5	0.982	3.043

Table C.172: Unadjusted and adjusted p-values obtained for problem instances of Group 2 through the application of Holm's post hoc procedure, using the DMOCSA-2-1 as control algorithm according to I_{HV}

Algorithm	Unadjusted p-value	Adjusted p-value
Others	<3.40E−21	<2.72E−20
DMOCSA-1-3	0.165	1.154
DMOCSA-2-3	0.189	1.154
DMOCSA-2-2	0.336	1.679
DMOCSA-2-5	0.412	1.679
DMOCSA-1-5	0.498	1.679
DMOCSA-1-1	0.498	1.679
DMOCSA-1-2	0.562	1.679

Table C.173: Unadjusted and adjusted p-values obtained for problem instances of Group 2 through the application of Holm's post hoc procedure, using the DMOCSA-2-1 as control algorithm according to I_{ϵ}

Algorithm	Unadjusted p-value	Adjusted p-value
Others	<1.29E−16	<1.03E−15
DMOCSA-2-2	0.363	2.540
DMOCSA-1-2	0.369	2.540
DMOCSA-1-5	0.422	2.540
DMOCSA-1-3	0.441	2.540
DMOCSA-1-1	0.473	2.540
DMOCSA-2-3	0.549	2.540
DMOCSA-2-5	0.748	2.540

Table C.174: Unadjusted and adjusted p-values obtained for problem instances of Group 2 through the application of Holm's post hoc procedure, using the DMOCSA-1-1 as control algorithm according to I_ϵ

Algorithm	Unadjusted p-value	Adjusted p-value
Others	<9.33E−13	<7.46E−12
DMOCSA-1-3	0.435	3.042
DMOCSA-2-2	0.521	3.124
DMOCSA-2-5	0.556	3.124
DMOCSA-2-1	0.600	3.124
DMOCSA-1-5	0.684	3.124
DMOCSA-1-2	0.732	3.124
DMOCSA-2-3	0.872	3.124

Table C.175: Unadjusted and adjusted p-values obtained for problem instances of Group 2 through the application of Holm's post hoc procedure, using the DMOCSA-1-4 as control algorithm according to I_Δ

Algorithm	Unadjusted p-value	Adjusted p-value
Others	<1.60E−05	<5.42E−05
DMOCSA-2-4	0.061	0.061

C.4.13.2.3 DMOFPA

Table C.176: Unadjusted and adjusted p-values obtained for all problems through the application of Holm's post hoc procedure, using the DMOFPA-3 as control algorithm according to I_{HV}

Algorithm	Unadjusted p-value	Adjusted p-value
DMOFPA-4	3.77E−35	1.51E−34
DMOFPA-5	5.70E−01	1.711
DMOFPA-2	6.11E−01	1.711
DMOFPA-1	8.81E−01	1.711

Table C.177: Unadjusted and adjusted p-values obtained for all problems through the application of Holm's post hoc procedure, using the DMOFPA-2 as control algorithm according to I_ϵ

Algorithm	Unadjusted p-value	Adjusted p-value
DMOFPA-4	6.68E−29	2.67E−28
DMOFPA-3	6.58E−01	1.973
DMOFPA-1	7.23E−01	1.973
DMOFPA-5	8.13E−01	1.973

Table C.178: Unadjusted and adjusted p-values obtained for all problems through the application of Holm's post hoc procedure, using the DMOFPA-1 as control algorithm according to I_ϵ

Algorithm	Unadjusted p-value	Adjusted p-value
DMOFPA-4	1.04E−17	4.15E−17
DMOFPA-3	5.28E−01	1.584
DMOFPA-2	6.21E−01	1.584
DMOFPA-5	7.64E−01	1.584

Table C.179: Unadjusted and adjusted p-values obtained for all problems through the application of Holm's post hoc procedure, using the DMOFPA-4 as control algorithm according to I_Δ

Algorithm	Unadjusted p-value	Adjusted p-value
DMOFPA-5	3.34E−02	0.133
DMOFPA-3	1.52E−01	0.455
DMOFPA-1	2.20E−01	0.455
DMOFPA-2	4.97E−01	0.497

Table C.180: Unadjusted and adjusted p-values obtained for problem instances of Group 1 through the application of Holm's post hoc procedure, using the DMOFPA-3 as control algorithm according to I_{HV}

Algorithm	Unadjusted p-value	Adjusted p-value
DMOFPA-4	7.86E−13	3.14E−12
DMOFPA-2	5.51E−01	1.652
DMOFPA-5	6.09E−01	1.652
DMOFPA-1	9.66E−01	1.652

Table C.181: Unadjusted and adjusted p-values obtained for problem instances of Group 1 through the application of Holm's post hoc procedure, using the DMOFPA-2 as control algorithm according to I_ϵ

Algorithm	Unadjusted p-value	Adjusted p-value
DMOFPA-4	2.23E−13	8.93E−13
DMOFPA-3	5.51E−01	1.652
DMOFPA-5	5.79E−01	1.652
DMOFPA-2	9.66E−01	1.652

Table C.182: Unadjusted and adjusted p-values obtained for problem instances of Group 1 through the application of Holm's post hoc procedure, using the DMOFPA-1 as control algorithm according to I_ϵ

Algorithm	Unadjusted p-value	Adjusted p-value
DMOFPA-4	7.68E−02	0.307
DMOFPA-3	2.58E−01	0.775
DMOFPA-2	3.06E−01	0.775
DMOFPA-5	5.09E−01	0.775

Table C.183: Unadjusted and adjusted p-values obtained for problem instances of Group 1 through the application of Holm's post hoc procedure, using the DMOFPA-4 as control algorithm according to I_{Δ}

Algorithm	Unadjusted p-value	Adjusted p-value
DMOFPA-5	7.57E−02	0.303
DMOFPA-4	8.42E−02	0.303
DMOFPA-2	1.62E−01	0.323
DMOFPA-3	3.91E−01	0.391

Table C.184: Unadjusted and adjusted p-values obtained for problem instances of Group 2 through the application of Holm's post hoc procedure, using the DMOFPA-3 as control algorithm according to I_{HV}

Algorithm	Unadjusted p-value	Adjusted p-value
DMOFPA-4	6.77E−25	2.71E−24
DMOFPA-5	7.69E−01	2.308
DMOFPA-1	8.67E−01	2.308
DMOFPA-2	9.00E−01	2.308

Table C.185: Unadjusted and adjusted p-values obtained for problem instances of Group 2 through the application of Holm's post hoc procedure, using the DMOFPA-5 as control algorithm according to I_{ϵ}

Algorithm	Unadjusted p-value	Adjusted p-value
DMOFPA-4	6.15E−18	2.46E−17
DMOFPA-1	4.86E−01	1.458
DMOFPA-3	8.06E−01	1.611
DMOFPA-2	8.70E−01	1.611

Table C.186: Unadjusted and adjusted p-values obtained for problem instances of Group 2 through the application of Holm's post hoc procedure, using the DMOFPA-2 as control algorithm according to I_{ϵ}

Algorithm	Unadjusted p-value	Adjusted p-value
DMOFPA-4	3.34E−14	1.34E−13
DMOFPA-5	7.74E−01	2.322
DMOFPA-1	8.22E−01	2.322
DMOFPA-3	8.38E−01	2.322

Table C.187: Unadjusted and adjusted p-values obtained for problem instances of Group 2 through the application of Holm's post hoc procedure, using the DMOFPA-4 as control algorithm according to I_{Δ}

Algorithm	Unadjusted p-value	Adjusted p-value
DMOFPA-3	3.32E−03	0.013
DMOFPA-5	5.25E−03	0.016
DMOFPA-1	1.52E−02	0.030
DMOFPA-2	2.99E−01	0.299

C.4.13.2.4 DMOPSO

Table C.188: Unadjusted and adjusted p-values obtained for all problems through the application of Holm's post hoc procedure, using the DMOPSO-1 as control algorithm according to I_{HV}

Algorithm	Unadjusted p-value	Adjusted p-value
DMOPSO-4	1.00E−13	4.02E−13
DMOPSO-2	0.420	1.259
DMOPSO-3	0.501	1.259
DMOPSO-5	0.964	1.259

Table C.189: Unadjusted and adjusted p-values obtained for all problems through the application of Holm's post hoc procedure, using the DMOPSO-2 as control algorithm according to I_{ϵ}

Algorithm	Unadjusted p-value	Adjusted p-value
DMOPSO-4	7.48E−18	4.49E−17
DMOPSO-3	0.456	1.825
DMOPSO-1	0.596	1.825
DMOPSO-5	7.01E−01	1.825

Table C.190: Unadjusted and adjusted p-values obtained for all problems through the application of Holm's post hoc procedure, using the DMOPSO-1 as control algorithm according to I_{ϵ}

Algorithm	Unadjusted p-value	Adjusted p-value
DMOPSO-4	1.69E−06	6.75E−06
DMOPSO-2	0.043	0.129
DMOPSO-3	0.209	0.418
DMOPSO-5	0.516	0.516

Table C.191: Unadjusted and adjusted p-values obtained for all problems through the application of Holm's post hoc procedure, using the DMOPSO-5 as control algorithm according to I_{Δ}

Algorithm	Unadjusted p-value	Adjusted p-value
DMOPSO-2	1.48E−01	0.590
DMOPSO-3	0.301	0.903
DMOPSO-4	0.516	1.031
DMOPSO-1	0.906	1.031

Table C.192: Unadjusted and adjusted p-values obtained for problem instances of Group 1 through the application of Holm's post hoc procedure, using the DMOPSO-5 as control algorithm according to I_{HV}

Algorithm	Unadjusted p-value	Adjusted p-value
DMOPSO-4	6.65E−15	2.66E−14
DMOPSO-3	1.13E−01	0.339
DMOPSO-2	2.34E−01	0.467
DMOPSO-1	2.50E−01	0.467

Table C.193: Unadjusted and adjusted p-values obtained for problem instances of Group 1 through the application of Holm's post hoc procedure, using the DMOPSO-2 as control algorithm according to I_{ϵ}

Algorithm	Unadjusted p-value	Adjusted p-value
DMOPSO-4	5.17E−09	2.07E−08
DMOPSO-1	5.51E−01	1.652
DMOPSO-3	5.79E−01	1.652
DMOPSO-5	9.66E−01	1.652

Table C.194: Unadjusted and adjusted p-values obtained for problem instances of Group 1 through the application of Holm's post hoc procedure, using the DMOPSO-1 as control algorithm according to I_{ϵ}

Algorithm	Unadjusted p-value	Adjusted p-value
DMOPSO-4	6.67E−02	0.267
DMOPSO-2	1.15E−01	0.344
DMOPSO-3	3.16E−01	0.633
DMOPSO-5	8.65E−01	0.865

Table C.195: Unadjusted and adjusted p-values obtained for problem instances of Group 1 through the application of Holm's post hoc procedure, using the DMOPSO-5 as control algorithm according to I_{Δ}

Algorithm	Unadjusted p-value	Adjusted p-value
DMOPSO-4	2.66E−02	0.106
DMOPSO-3	4.07E−02	0.122
DMOPSO-2	1.47E−01	0.294
DMOPSO-1	1.86E−01	0.294

Table C.196: Unadjusted and adjusted p-values obtained for problem instances of Group 2 through the application of Holm's post hoc procedure, using the DMOPSO-1 as control algorithm according to I_{HV}

Algorithm	Unadjusted p-value	Adjusted p-value
DMOPSO-4	3.51E−09	1.40E−08
DMOPSO-3	3.91E−01	1.172
DMOPSO-5	4.14E−01	1.172
DMOPSO-2	4.26E−01	1.172

Table C.197: Unadjusted and adjusted p-values obtained for problem instances of Group 2 through the application of Holm's post hoc procedure, using the DMOPSO-1 as control algorithm according to I_ϵ

Algorithm	Unadjusted p-value	Adjusted p-value
DMOPSO-4	3.51E−08	1.40E−07
DMOPSO-5	1.24E−01	0.373
DMOPSO-3	4.36E−01	0.872
DMOPSO-2	5.66E−01	0.872

Table C.198: Unadjusted and adjusted p-values obtained for problem instances of Group 2 through the application of Holm's post hoc procedure, using the DMOPSO-1 as control algorithm according to I_ϵ

Algorithm	Unadjusted p-value	Adjusted p-value
DMOPSO-4	1.07E−06	4.28E−06
DMOPSO-2	1.97E−01	0.590
DMOPSO-3	4.36E−01	0.872
DMOPSO-5	4.61E−01	0.872

Table C.199: Unadjusted and adjusted p-values obtained for problem instances of Group 2 through the application of Holm's post hoc procedure, using the DMOPSO-4 as control algorithm according to I_Δ

Algorithm	Unadjusted p-value	Adjusted p-value
DMOPSO-2	6.51E−02	0.260
DMOPSO-5	2.19E−01	0.656
DMOPSO-3	4.86E−01	0.972
DMOPSO-1	9.02E−01	0.972

Appendix D

Detailed Analysis and Results of Chapter 5: Influence of the Dominance Rules

---

Abstract

The present chapter presents the various analyses of Chapter 5, and (i) the values of the various quality indicators obtained by each dominance rule for each problem instance and (ii) the detailed values of the Friedman's test.

D.1 Detailed values of the metrics

This section presents the procedure used for the definition of the parameters of the various optimization algorithms and dominance rules.

D.1.1 Problem Family: Arc111

Table D.1: Median and interquartile range of I_{HV} obtained by the optimisers for the Arc111 problems

	Arc111-1 $\tilde{x} \pm IQR(x)$		Arc111-2 $\tilde{x} \pm IQR(x)$		Arc111-3 $\tilde{x} \pm IQR(x)$		Arc111-4 $\tilde{x} \pm IQR(x)$		Arc111-5 $\tilde{x} \pm IQR(x)$	
BIANT-1	0.88	0.00	0.88	0.02	0.86	0.04	0.90	0.02	0.87	0.03
BIANT-2	0.89	0.01	0.88	0.02	0.87	0.01	0.86	0.02	0.89	0.02
CHAC-1	0.88	0.00	0.85	0.01	0.85	0.01	0.85	0.01	0.86	0.01
CHAC-1-L	0.88	0.01	0.85	0.01	0.85	0.01	0.85	0.01	0.86	0.01
CHAC-2	0.88	0.01	0.85	0.01	0.85	0.00	0.85	0.01	0.86	0.01
CHAC-2-L	0.88	0.00	0.86	0.01	0.85	0.01	0.85	0.01	0.86	0.01
MOACS-1	0.84	0.01	0.87	0.00	0.87	0.01	0.88	0.01	0.87	0.01
MOACS-1-S-CDAS	0.81	0.03	0.84	0.01	0.86	0.04	0.86	0.02	0.86	0.01
MOACS-1-L	0.85	0.01	0.87	0.01	0.87	0.00	0.88	0.01	0.87	0.01
MOACS-2	0.90	0.01	0.92	0.00	0.92	0.01	0.92	0.00	0.91	0.01
MOACS-2-S-CDAS	0.82	0.04	0.91	0.01	0.92	0.01	0.92	0.01	0.91	0.01
MOACS-2-L	0.91	0.01	0.92	0.00	0.92	0.00	0.92	0.01	0.91	0.00
DMOPSO-5	0.87	0.01	0.85	0.01	0.85	0.01	0.85	0.01	0.85	0.01
DMOPSO-1	0.87	0.01	0.85	0.00	0.85	0.01	0.85	0.01	0.85	0.01
DMOPSO-2	0.87	0.00	0.85	0.01	0.85	0.01	0.84	0.01	0.85	0.01
DMOPSO-3	0.87	0.01	0.85	0.00	0.85	0.01	0.84	0.01	0.85	0.01
DMOPSO-4	0.87	0.01	0.85	0.01	0.84	0.00	0.84	0.01	0.85	0.00
DMOPSO-1-L	0.87	0.01	0.85	0.01	0.85	0.01	0.85	0.01	0.85	0.01
NSGA-II	0.88	0.00	0.86	0.01	0.86	0.01	0.86	0.02	0.86	0.01
NSGA-II-L	0.88	0.01	0.86	0.01	0.86	0.02	0.86	0.02	0.86	0.01
SPEA2	0.88	0.01	0.85	0.01	0.85	0.01	0.86	0.01	0.86	0.01
SPEA2-L	0.88	0.01	0.86	0.01	0.86	0.01	0.85	0.02	0.86	0.01

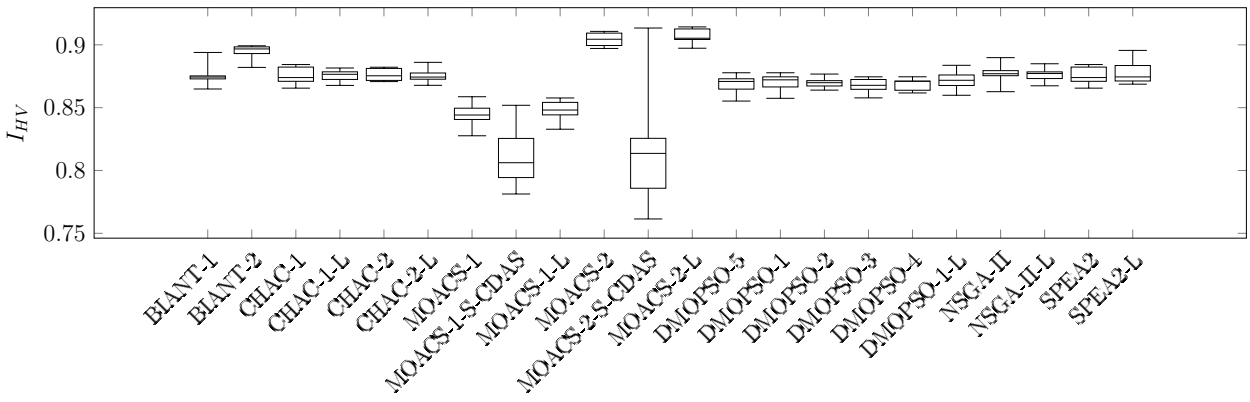

Figure D.1: Boxplot for I_{HV}: Arc111-1

Table D.2: Median and interquartile range of I_{IGD} obtained by the optimisers for the Arc111 problems

	Arc111-1 $\tilde{x} \pm IQR(x)$		Arc111-2 $\tilde{x} \pm IQR(x)$		Arc111-3 $\tilde{x} \pm IQR(x)$		Arc111-4 $\tilde{x} \pm IQR(x)$		Arc111-5 $\tilde{x} \pm IQR(x)$	
BIANT-1	0.40	0.04	0.77	0.03	0.87	0.23	0.59	0.10	0.61	0.12
BIANT-2	0.39	0.02	0.70	0.14	0.80	0.11	0.75	0.07	0.60	0.08
CHAC-1	0.39	0.01	0.89	0.05	0.71	0.03	0.83	0.05	0.58	0.03
CHAC-1-L	0.40	0.02	0.88	0.04	0.70	0.02	0.84	0.07	0.59	0.05
CHAC-2	0.40	0.01	0.89	0.06	0.71	0.01	0.84	0.05	0.57	0.03
CHAC-2-L	0.40	0.02	0.87	0.03	0.71	0.01	0.84	0.10	0.58	0.03
MOACS-1	0.47	0.07	0.67	0.03	0.50	0.04	0.54	0.03	0.43	0.02
MOACS-1-S-CDAS	0.68	0.19	0.83	0.22	0.64	0.19	0.71	0.11	0.50	0.06
MOACS-1-L	0.46	0.03	0.69	0.07	0.52	0.05	0.53	0.03	0.42	0.05
MOACS-2	0.25	0.02	0.47	0.04	0.34	0.04	0.39	0.02	0.32	0.02
MOACS-2-S-CDAS	0.70	0.27	0.49	0.05	0.39	0.06	0.40	0.03	0.33	0.04
MOACS-2-L	0.26	0.03	0.48	0.02	0.37	0.04	0.39	0.03	0.33	0.02
DMOPSO-5	0.42	0.02	0.86	0.06	0.69	0.02	0.83	0.04	0.59	0.05
DMOPSO-1	0.41	0.04	0.90	0.05	0.71	0.04	0.84	0.05	0.59	0.03
DMOPSO-2	0.41	0.01	0.89	0.06	0.70	0.02	0.85	0.07	0.59	0.03
DMOPSO-3	0.42	0.03	0.91	0.01	0.71	0.01	0.85	0.02	0.59	0.02
DMOPSO-4	0.42	0.02	0.87	0.02	0.72	0.01	0.85	0.02	0.61	0.02
DMOPSO-1-L	0.41	0.02	0.89	0.05	0.71	0.02	0.83	0.06	0.60	0.01
NSGA-II	0.42	0.02	0.91	0.06	0.70	0.02	0.83	0.10	0.59	0.04
NSGA-II-L	0.41	0.02	0.89	0.08	0.70	0.06	0.84	0.12	0.61	0.03
SPEA2	0.42	0.01	0.90	0.08	0.72	0.03	0.85	0.02	0.59	0.03
SPEA2-L	0.42	0.04	0.87	0.06	0.70	0.02	0.84	0.08	0.59	0.01

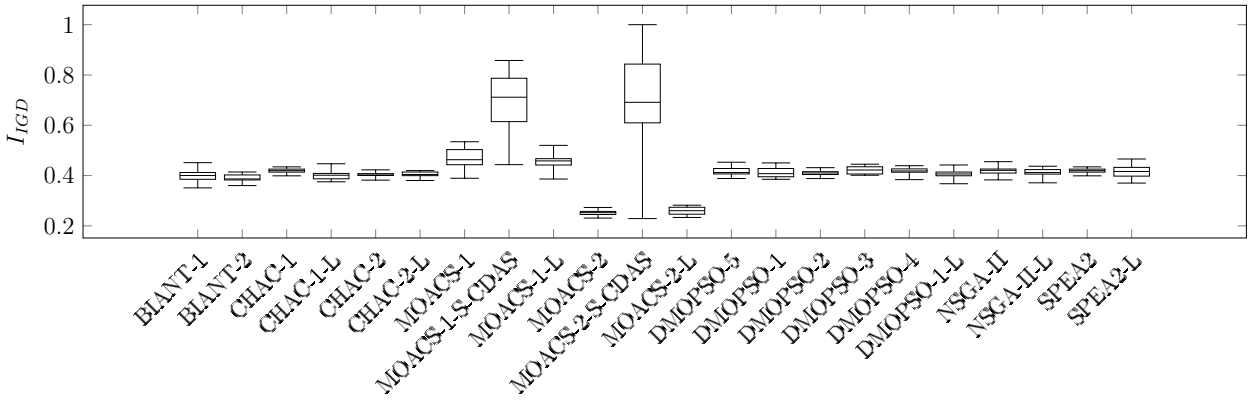

Figure D.2: Boxplot for I_{IGD}: Arc111-1

Table D.3: Median and interquartile range of I_ϵ obtained by the optimisers for the Arc111 problems

	Arc111-1 $\tilde{x} \pm IQR(x)$		Arc111-2 $\tilde{x} \pm IQR(x)$		Arc111-3 $\tilde{x} \pm IQR(x)$		Arc111-4 $\tilde{x} \pm IQR(x)$		Arc111-5 $\tilde{x} \pm IQR(x)$	
BIANT-1	0.54	0.03	0.62	0.10	0.52	0.02	0.59	0.01	0.53	0.10
BIANT-2	0.52	0.02	0.56	0.04	0.52	0.01	0.59	0.03	0.51	0.03
CHAC-1	0.18	0.00	0.25	0.00	0.24	0.00	0.28	0.00	0.24	0.00
CHAC-1-L	0.18	0.00	0.25	0.00	0.24	0.00	0.28	0.00	0.24	0.00
CHAC-2	0.18	0.00	0.25	0.00	0.24	0.00	0.28	0.00	0.24	0.00
CHAC-2-L	0.18	0.00	0.25	0.00	0.24	0.00	0.28	0.01	0.24	0.00
MOACS-1	0.67	0.05	0.72	0.05	0.63	0.04	0.70	0.04	0.60	0.04
MOACS-1-S-CDAS	0.80	0.11	0.89	0.10	0.73	0.20	0.86	0.11	0.65	0.08
MOACS-1-L	0.65	0.04	0.72	0.04	0.63	0.02	0.71	0.07	0.62	0.06
MOACS-2	0.36	0.04	0.38	0.02	0.32	0.03	0.39	0.05	0.36	0.05
MOACS-2-S-CDAS	0.79	0.10	0.40	0.03	0.33	0.02	0.38	0.04	0.33	0.03
MOACS-2-L	0.34	0.06	0.37	0.04	0.33	0.02	0.40	0.05	0.36	0.02
DMOPSO-5	0.18	0.00	0.25	0.01	0.24	0.00	0.28	0.00	0.24	0.00
DMOPSO-1	0.18	0.00	0.25	0.00	0.24	0.00	0.28	0.00	0.24	0.00
DMOPSO-2	0.18	0.00	0.25	0.00	0.24	0.01	0.28	0.00	0.24	0.00
DMOPSO-3	0.18	0.00	0.25	0.01	0.24	0.00	0.28	0.01	0.24	0.00
DMOPSO-4	0.18	0.00	0.25	0.00	0.24	0.00	0.28	0.01	0.24	0.00
DMOPSO-1-L	0.18	0.00	0.25	0.00	0.24	0.00	0.28	0.00	0.24	0.00
NSGA-II	0.10	0.00	0.14	0.00	0.15	0.00	0.17	0.00	0.20	0.00
NSGA-II-L	0.10	0.00	0.14	0.00	0.15	0.00	0.18	0.01	0.20	0.00
SPEA2	0.11	0.00	0.17	0.01	0.17	0.00	0.18	0.00	0.21	0.00
SPEA2-L	0.10	0.00	0.15	0.00	0.15	0.00	0.18	0.01	0.21	0.00

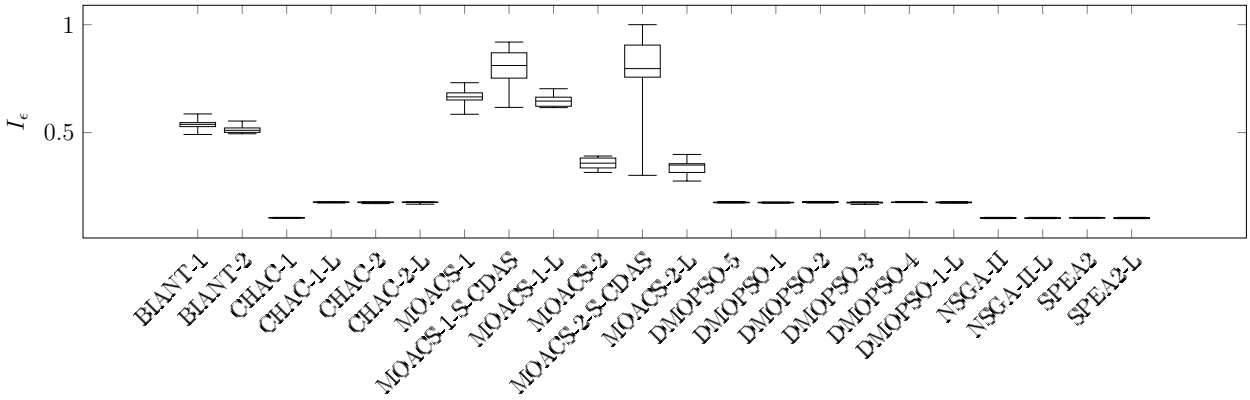

Figure D.3: Boxplot for I_ϵ: Arc111-1

Table D.4: Median and interquartile range of I_Δ obtained by the optimisers for the Arc111 problems

	Arc111-1		Arc111-2		Arc111-3		Arc111-4		Arc111-5	
	$\tilde{x}$	$IQR(x)$	$\tilde{x}$	$IQR(x)$	$\tilde{x}$	$IQR(x)$	$\tilde{x}$	$IQR(x)$	$\tilde{x}$	$IQR(x)$
BIANT-1	0.55	0.02	0.65	0.03	0.66	0.09	0.54	0.01	0.69	0.06
BIANT-2	0.56	0.01	0.61	0.12	0.67	0.08	0.61	0.07	0.67	0.03
CHAC-1	0.73	0.03	0.86	0.05	0.87	0.05	0.82	0.05	0.80	0.05
CHAC-1-L	0.76	0.07	0.82	0.08	0.84	0.10	0.80	0.06	0.82	0.06
CHAC-2	0.75	0.06	0.83	0.04	0.86	0.01	0.81	0.05	0.82	0.08
CHAC-2-L	0.75	0.10	0.84	0.06	0.85	0.10	0.81	0.08	0.81	0.05
MOACS-1	0.59	0.04	0.62	0.07	0.62	0.08	0.60	0.07	0.65	0.03
MOACS-1-S-CDAS	0.67	0.05	0.72	0.08	0.70	0.08	0.67	0.06	0.70	0.07
MOACS-1-L	0.61	0.05	0.66	0.07	0.63	0.07	0.62	0.03	0.64	0.04
MOACS-2	0.43	0.03	0.55	0.06	0.41	0.07	0.46	0.07	0.55	0.09
MOACS-2-S-CDAS	0.67	0.03	0.60	0.07	0.56	0.08	0.53	0.04	0.59	0.09
MOACS-2-L	0.42	0.08	0.51	0.12	0.48	0.12	0.49	0.05	0.54	0.03
DMOPSO-5	0.84	0.05	0.87	0.06	0.87	0.05	0.84	0.04	0.88	0.08
DMOPSO-1	0.84	0.07	0.87	0.04	0.89	0.06	0.84	0.04	0.90	0.07
DMOPSO-2	0.83	0.07	0.88	0.08	0.87	0.08	0.87	0.09	0.87	0.03
DMOPSO-3	0.82	0.05	0.89	0.06	0.87	0.04	0.84	0.08	0.87	0.05
DMOPSO-4	0.84	0.05	0.87	0.07	0.87	0.07	0.86	0.04	0.88	0.02
DMOPSO-1-L	0.83	0.06	0.87	0.09	0.88	0.07	0.86	0.08	0.88	0.03
NSGA-II	0.85	0.07	0.93	0.06	0.92	0.06	0.91	0.04	0.89	0.06
NSGA-II-L	0.85	0.08	0.88	0.06	0.89	0.06	0.89	0.09	0.90	0.06
SPEA2	0.86	0.03	0.91	0.10	0.89	0.06	0.87	0.07	0.86	0.03
SPEA2-L	0.86	0.08	0.89	0.03	0.90	0.05	0.87	0.05	0.88	0.08

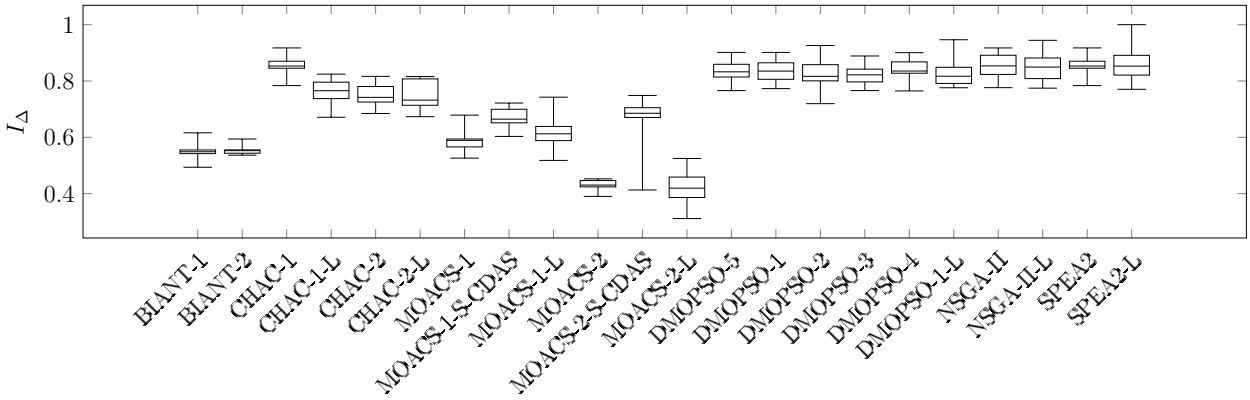

Figure D.4: Boxplot for I_Δ: Arc111-1

Table D.5: Median and interquartile range of the computation time required by the optimisers for the Arc111 problems

	Arc111-1 $\tilde{x} \pm IQR(x)$		Arc111-2 $\tilde{x} \pm IQR(x)$		Arc111-3 $\tilde{x} \pm IQR(x)$		Arc111-4 $\tilde{x} \pm IQR(x)$		Arc111-5 $\tilde{x} \pm IQR(x)$	
BIANT-1	0.55	0.22	0.36	0.08	0.81	0.05	0.58	0.07	0.78	0.08
BIANT-2	0.82	0.16	0.33	0.17	0.63	0.04	0.27	0.02	0.80	0.04
CHAC-1	0.33	0.07	0.19	0.06	0.44	0.24	0.23	0.19	1.94	0.06
CHAC-1-L	0.34	0.13	0.22	0.09	0.60	0.23	0.32	0.11	1.79	0.06
CHAC-2	0.38	0.09	0.18	0.06	0.44	0.26	0.23	0.12	0.99	0.06
CHAC-2-L	0.44	0.17	0.20	0.13	0.58	0.16	0.25	0.09	0.77	0.06
MOACS-1	0.23	0.11	0.15	0.03	0.25	0.04	0.14	0.02	0.53	0.02
MOACS-1-S-CDAS	0.25	0.10	0.12	0.04	0.40	0.12	0.20	0.07	1.13	0.04
MOACS-1-L	0.26	0.17	0.11	0.03	0.33	0.22	0.15	0.04	0.81	0.05
MOACS-2	0.26	0.10	0.12	0.04	0.32	0.11	0.17	0.07	0.64	0.04
MOACS-2-S-CDAS	0.24	0.15	0.13	0.07	0.30	0.07	0.15	0.05	0.87	0.04
MOACS-2-L	0.22	0.09	0.12	0.01	0.27	0.09	0.18	0.08	0.68	0.03
DMOPSO-5	0.31	0.13	0.19	0.07	0.41	0.16	0.27	0.05	1.38	0.03
DMOPSO-1	0.39	0.13	0.21	0.08	0.46	0.14	0.27	0.07	1.09	0.05
DMOPSO-2	0.27	0.11	0.13	0.03	0.40	0.21	0.17	0.04	0.80	0.04
DMOPSO-3	0.41	0.15	0.28	0.11	0.47	0.15	0.25	0.06	1.03	0.06
DMOPSO-4	0.61	0.19	0.38	0.14	0.75	0.25	0.38	0.27	1.00	0.02
DMOPSO-1-L	0.35	0.23	0.17	0.07	0.39	0.16	0.25	0.07	1.00	0.04
NSGA-II	0.28	0.14	0.15	0.04	0.41	0.30	0.26	0.15	1.00	0.02
NSGA-II-L	0.23	0.04	0.13	0.01	0.41	0.13	0.20	0.12	0.87	0.04
SPEA2	0.13	0.02	0.08	0.02	0.21	0.15	0.12	0.05	0.48	0.03
SPEA2-L	0.14	0.02	0.08	0.02	0.22	0.07	0.11	0.04	0.54	0.02

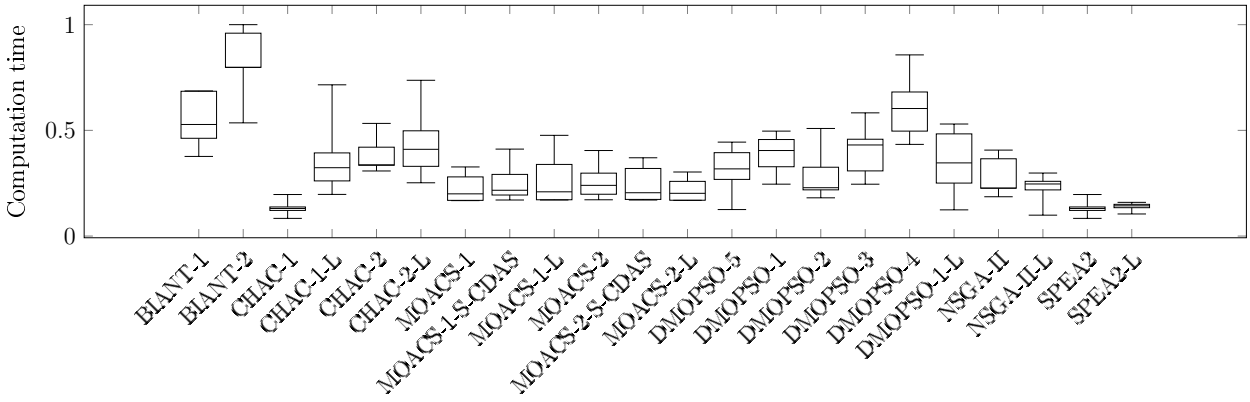

Figure D.5: Boxplot for the computation time: Arc111-1

Table D.6: C-metric for the Arc111-1 problem instance

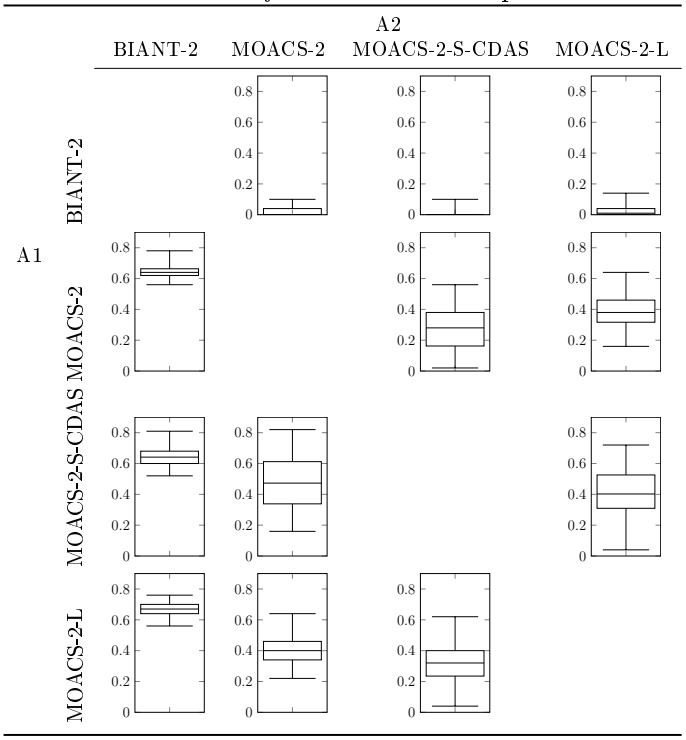

Table D.7: C-metric for the Arc111-2 problem instance

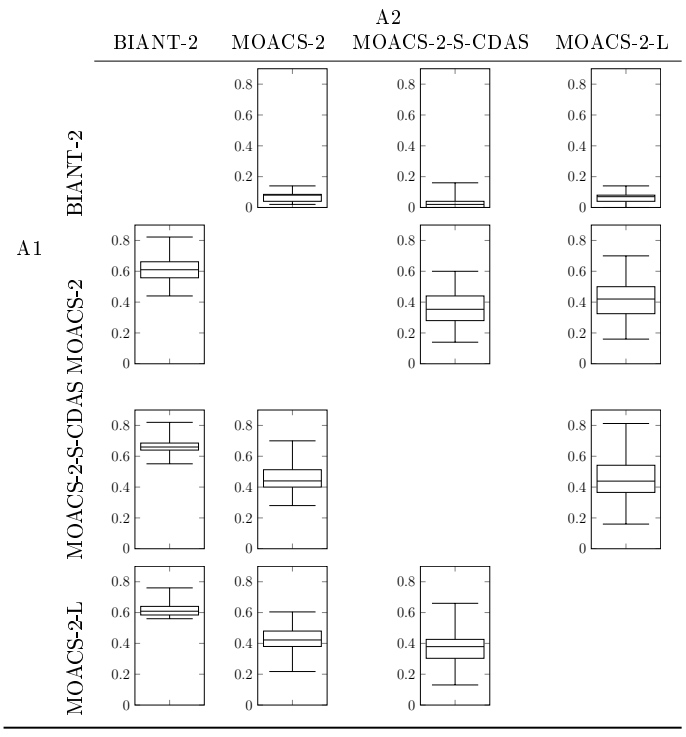

Table D.8: C-metric for the Arc111-3 problem instance

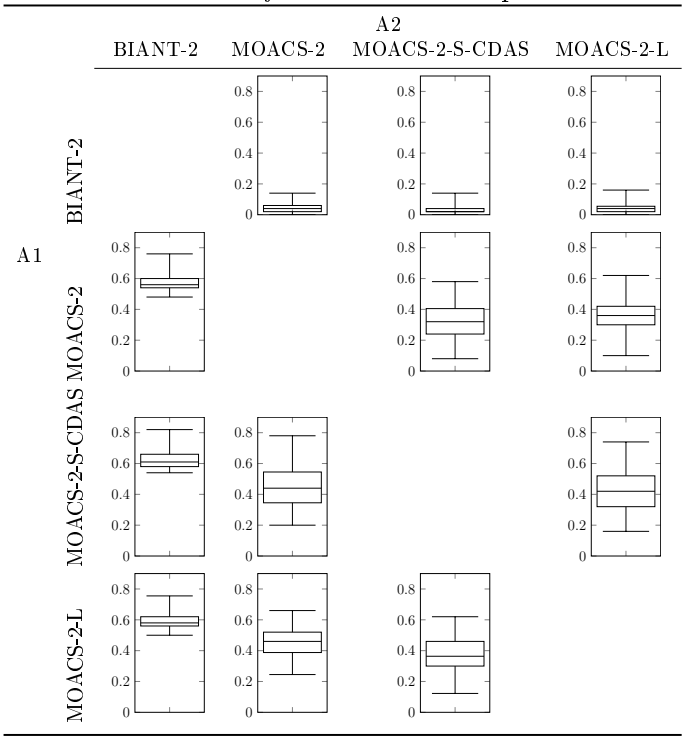

Table D.9: C-metric for the Arc111-1 problem instance

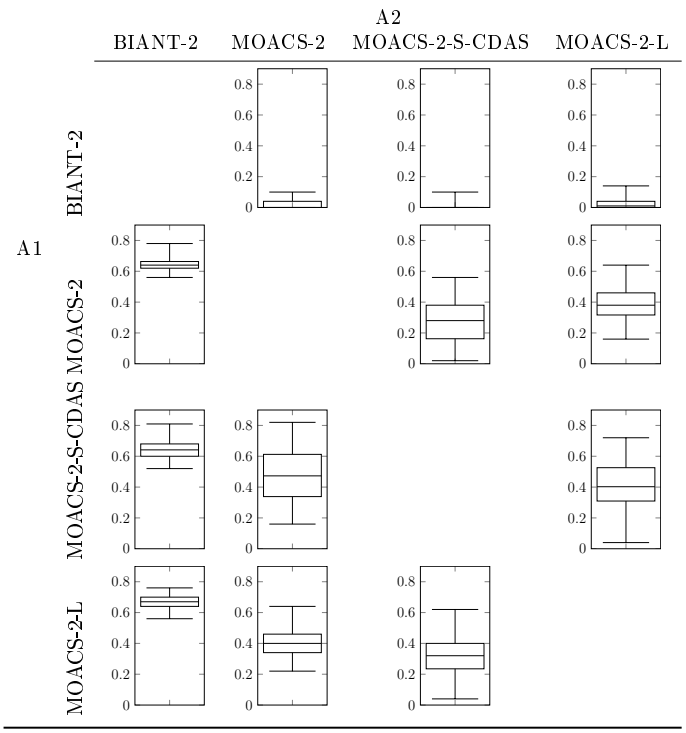

Table D.10: C-metric for the Arc111-5 problem instance

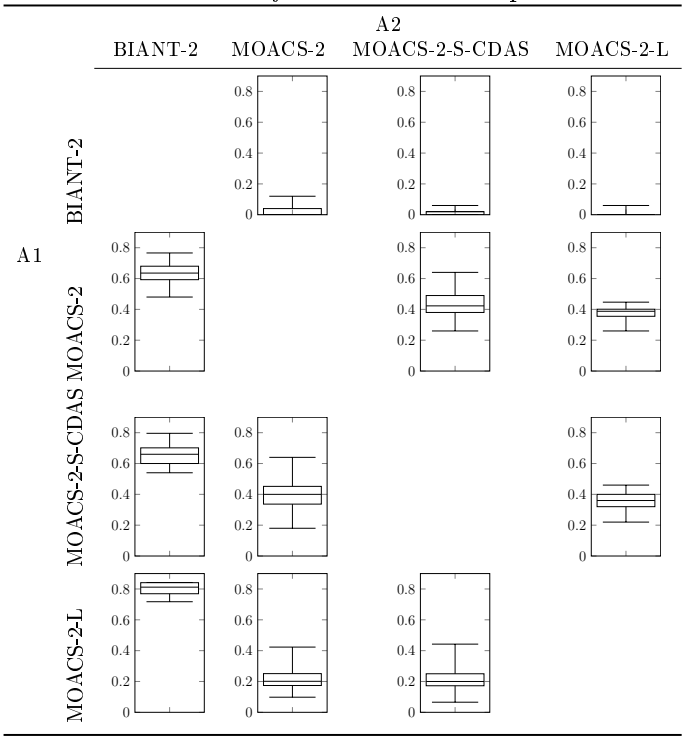

D.1.2 Problem Family: Buxey

Table D.11: Median and interquartile range of I_{HV} obtained by the optimisers for the Buxey problems

	Buxey-1 $\tilde{x} \pm IQR(x)$		Buxey-2 $\tilde{x} \pm IQR(x)$		Buxey-3 $\tilde{x} \pm IQR(x)$		Buxey-4 $\tilde{x} \pm IQR(x)$		Buxey-5 $\tilde{x} \pm IQR(x)$	
BIANT-1	0.94	0.02	0.93	0.02	0.93	0.02	0.92	0.01	0.92	0.01
BIANT-2	0.95	0.01	0.94	0.03	0.93	0.02	0.93	0.03	0.93	0.02
CHAC-1	0.93	0.01	0.92	0.01	0.92	0.00	0.90	0.00	0.90	0.02
CHAC-1-L	0.93	0.01	0.92	0.01	0.92	0.01	0.90	0.01	0.91	0.01
CHAC-2	0.93	0.01	0.92	0.01	0.91	0.01	0.90	0.01	0.91	0.01
CHAC-2-L	0.93	0.01	0.92	0.01	0.92	0.01	0.91	0.01	0.91	0.01
MOACS-1	0.94	0.01	0.95	0.01	0.94	0.01	0.93	0.01	0.95	0.01
MOACS-1-S-CDAS	0.93	0.01	0.95	0.01	0.95	0.01	0.93	0.01	0.95	0.01
MOACS-1-L	0.94	0.01	0.95	0.00	0.94	0.01	0.93	0.01	0.95	0.01
MOACS-2	0.94	0.01	0.95	0.01	0.95	0.01	0.94	0.01	0.95	0.01
MOACS-2-S-CDAS	0.94	0.01	0.95	0.01	0.95	0.01	0.93	0.01	0.96	0.01
MOACS-2-L	0.94	0.01	0.95	0.00	0.95	0.01	0.94	0.01	0.95	0.01
DMOPSO-5	0.93	0.01	0.92	0.01	0.91	0.01	0.90	0.00	0.91	0.00
DMOPSO-1	0.93	0.01	0.92	0.00	0.91	0.01	0.90	0.01	0.91	0.01
DMOPSO-2	0.93	0.01	0.92	0.00	0.91	0.00	0.90	0.01	0.90	0.01
DMOPSO-3	0.93	0.01	0.92	0.01	0.91	0.01	0.90	0.00	0.91	0.00
DMOPSO-4	0.91	0.03	0.91	0.01	0.89	0.03	0.88	0.02	0.89	0.02
DMOPSO-1-L	0.93	0.01	0.92	0.01	0.91	0.01	0.90	0.01	0.90	0.01
NSGA-II	0.94	0.01	0.93	0.01	0.92	0.01	0.91	0.02	0.91	0.01
NSGA-II-L	0.94	0.01	0.93	0.01	0.92	0.01	0.91	0.01	0.92	0.00
SPEA2	0.93	0.01	0.93	0.01	0.92	0.00	0.91	0.01	0.91	0.01
SPEA2-L	0.93	0.01	0.93	0.01	0.92	0.00	0.91	0.02	0.91	0.01

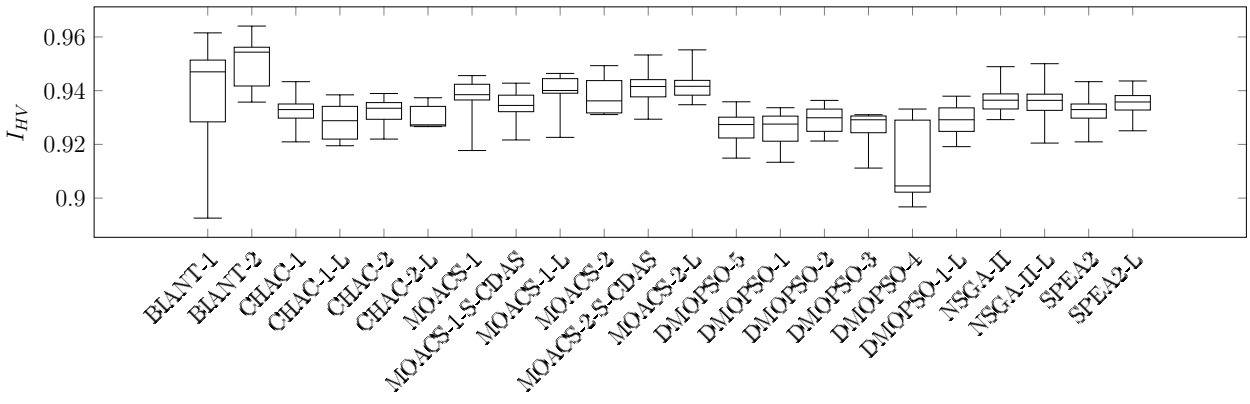

Figure D.6: Boxplot for I_{HV}: Buxey-1

Table D.12: Median and interquartile range of I_{IGD} obtained by the optimisers for the Buxey problems

	Buxey-1 $\tilde{x} \pm IQR(x)$		Buxey-2 $\tilde{x} \pm IQR(x)$		Buxey-3 $\tilde{x} \pm IQR(x)$		Buxey-4 $\tilde{x} \pm IQR(x)$		Buxey-5 $\tilde{x} \pm IQR(x)$	
BIANT-1	0.63	0.21	0.55	0.08	0.46	0.10	0.44	0.04	0.52	0.05
BIANT-2	0.55	0.14	0.51	0.07	0.48	0.06	0.40	0.08	0.47	0.09
CHAC-1	0.71	0.11	0.66	0.07	0.63	0.08	0.66	0.05	0.68	0.13
CHAC-1-L	0.70	0.09	0.69	0.08	0.62	0.05	0.64	0.06	0.65	0.13
CHAC-2	0.68	0.07	0.71	0.10	0.66	0.08	0.64	0.02	0.66	0.10
CHAC-2-L	0.70	0.10	0.68	0.09	0.59	0.08	0.60	0.02	0.64	0.04
MOACS-1	0.69	0.06	0.52	0.06	0.43	0.04	0.39	0.02	0.31	0.05
MOACS-1-S-CDAS	0.71	0.06	0.53	0.07	0.42	0.04	0.37	0.02	0.34	0.05
MOACS-1-L	0.68	0.06	0.51	0.03	0.44	0.04	0.40	0.02	0.32	0.04
MOACS-2	0.74	0.15	0.59	0.09	0.41	0.03	0.39	0.03	0.36	0.05
MOACS-2-S-CDAS	0.72	0.09	0.59	0.08	0.40	0.09	0.42	0.07	0.34	0.06
MOACS-2-L	0.69	0.05	0.56	0.05	0.42	0.06	0.39	0.04	0.38	0.04
DMOPSO-5	0.69	0.05	0.69	0.07	0.62	0.08	0.63	0.03	0.63	0.06
DMOPSO-1	0.72	0.08	0.67	0.08	0.60	0.05	0.62	0.07	0.65	0.10
DMOPSO-2	0.68	0.09	0.69	0.03	0.66	0.06	0.65	0.10	0.66	0.09
DMOPSO-3	0.71	0.11	0.70	0.12	0.62	0.09	0.65	0.07	0.70	0.11
DMOPSO-4	0.85	0.18	0.83	0.13	0.80	0.23	0.79	0.16	0.80	0.16
DMOPSO-1-L	0.67	0.07	0.73	0.14	0.68	0.13	0.66	0.06	0.65	0.12
NSGA-II	0.71	0.03	0.70	0.04	0.62	0.05	0.59	0.09	0.70	0.15
NSGA-II-L	0.72	0.15	0.70	0.07	0.64	0.05	0.66	0.10	0.60	0.03
SPEA2	0.72	0.07	0.69	0.10	0.68	0.12	0.63	0.05	0.69	0.11
SPEA2-L	0.68	0.07	0.68	0.14	0.64	0.07	0.64	0.10	0.65	0.11

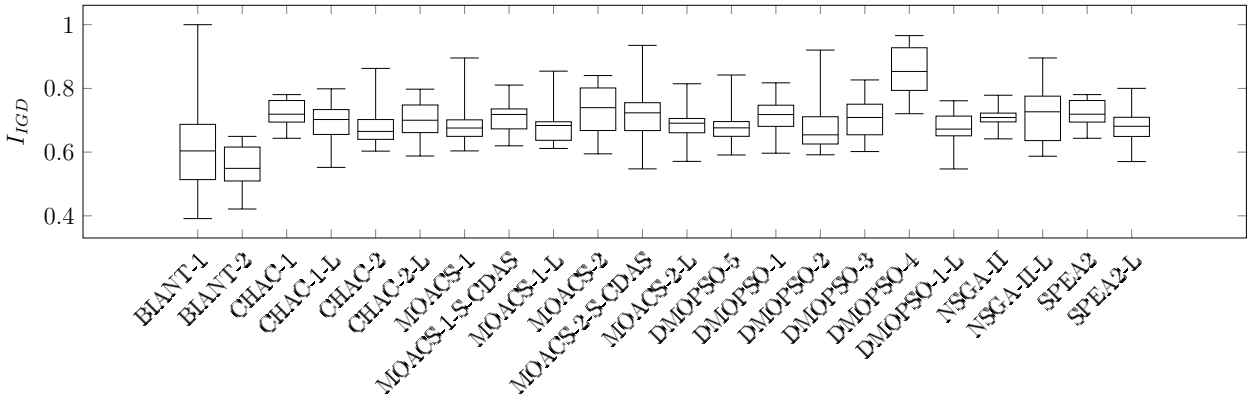

Figure D.7: Boxplot for I_{IGD}: Buxey-1

Table D.13: Median and interquartile range of I_ϵ obtained by the optimisers for the Buxey problems

	Buxey-1		Buxey-2		Buxey-3		Buxey-4		Buxey-5	
	$\tilde{x}$	$IQR(x)$	$\tilde{x}$	$IQR(x)$	$\tilde{x}$	$IQR(x)$	$\tilde{x}$	$IQR(x)$	$\tilde{x}$	$IQR(x)$
BIANT-1	0.42	0.29	0.39	0.20	0.50	0.23	0.53	0.34	0.68	0.01
BIANT-2	0.31	0.16	0.47	0.23	0.73	0.44	0.25	0.04	0.61	0.31
CHAC-1	1.00	0.00	1.00	0.00	0.64	0.00	0.26	0.00	0.77	0.00
CHAC-1-L	1.00	0.00	1.00	0.00	0.64	0.00	0.26	0.00	0.77	0.00
CHAC-2	1.00	0.00	1.00	0.00	0.65	0.00	0.26	0.00	0.77	0.00
CHAC-2-L	1.00	0.00	0.99	0.00	0.65	0.00	0.26	0.00	0.77	0.00
MOACS-1	0.23	0.05	0.16	0.06	0.33	0.07	0.31	0.21	0.22	0.07
MOACS-1-S-CDAS	0.27	0.06	0.18	0.09	0.31	0.04	0.35	0.11	0.22	0.05
MOACS-1-L	0.23	0.09	0.16	0.05	0.32	0.05	0.37	0.14	0.26	0.09
MOACS-2	0.22	0.05	0.15	0.12	0.36	0.16	0.45	0.15	0.31	0.04
MOACS-2-S-CDAS	0.17	0.09	0.16	0.11	0.38	0.15	0.45	0.10	0.21	0.11
MOACS-2-L	0.23	0.05	0.19	0.12	0.42	0.13	0.34	0.17	0.51	0.51
DMOPSO-5	1.00	0.00	1.00	0.00	0.64	0.00	0.26	0.00	0.77	0.00
DMOPSO-1	0.99	0.00	1.00	0.00	0.65	0.00	0.26	0.00	0.77	0.00
DMOPSO-2	1.00	0.00	1.00	0.00	0.65	0.00	0.26	0.00	0.77	0.00
DMOPSO-3	0.99	0.00	1.00	0.00	0.64	0.00	0.26	0.00	0.77	0.00
DMOPSO-4	1.00	0.00	1.00	0.00	0.65	0.00	0.26	0.00	0.77	0.00
DMOPSO-1-L	1.00	0.00	1.00	0.00	0.65	0.00	0.26	0.00	0.77	0.00
NSGA-II	1.00	0.00	1.00	0.00	0.65	0.00	0.26	0.00	0.77	0.00
NSGA-II-L	1.00	0.00	1.00	0.00	0.65	0.00	0.26	0.00	0.77	0.00
SPEA2	1.00	0.00	0.95	0.00	0.65	0.00	0.26	0.00	0.77	0.00
SPEA2-L	0.99	0.00	1.00	0.00	0.65	0.00	0.26	0.00	0.77	0.00

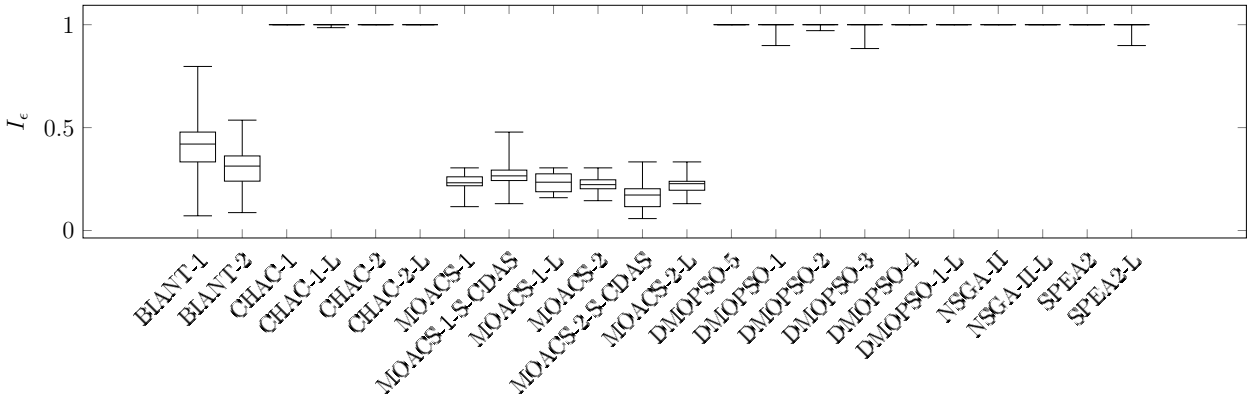

Figure D.8: Boxplot for I_ϵ: Buxey-1

Table D.14: Median and interquartile range of I_Δ obtained by the optimisers for the Buxey problems

	Buxey-1 $\tilde{x} \pm IQR(x)$		Buxey-2 $\tilde{x} \pm IQR(x)$		Buxey-3 $\tilde{x} \pm IQR(x)$		Buxey-4 $\tilde{x} \pm IQR(x)$		Buxey-5 $\tilde{x} \pm IQR(x)$	
BIANT-1	0.73	0.06	0.62	0.09	0.71	0.10	0.69	0.03	0.63	0.10
BIANT-2	0.61	0.05	0.68	0.10	0.69	0.09	0.64	0.02	0.67	0.09
CHAC-1	0.83	0.04	0.84	0.05	0.88	0.05	0.86	0.01	0.83	0.11
CHAC-1-L	0.87	0.07	0.84	0.04	0.88	0.06	0.83	0.06	0.80	0.04
CHAC-2	0.85	0.05	0.84	0.05	0.91	0.05	0.84	0.02	0.81	0.10
CHAC-2-L	0.90	0.07	0.85	0.04	0.84	0.05	0.86	0.04	0.79	0.05
MOACS-1	0.63	0.03	0.58	0.11	0.63	0.09	0.64	0.04	0.55	0.09
MOACS-1-S-CDAS	0.59	0.12	0.60	0.10	0.66	0.07	0.63	0.07	0.52	0.07
MOACS-1-L	0.60	0.04	0.61	0.08	0.64	0.06	0.68	0.09	0.58	0.04
MOACS-2	0.58	0.11	0.58	0.11	0.70	0.22	0.72	0.09	0.55	0.06
MOACS-2-S-CDAS	0.62	0.05	0.61	0.11	0.69	0.14	0.67	0.13	0.54	0.08
MOACS-2-L	0.62	0.10	0.57	0.13	0.69	0.08	0.68	0.08	0.60	0.16
DMOPSO-5	0.85	0.05	0.85	0.06	0.88	0.10	0.84	0.08	0.82	0.03
DMOPSO-1	0.86	0.05	0.84	0.06	0.87	0.06	0.86	0.04	0.85	0.04
DMOPSO-2	0.86	0.09	0.87	0.05	0.88	0.04	0.85	0.05	0.82	0.05
DMOPSO-3	0.83	0.08	0.86	0.06	0.88	0.07	0.84	0.07	0.84	0.07
DMOPSO-4	0.82	0.01	0.86	0.04	0.86	0.02	0.85	0.07	0.84	0.03
DMOPSO-1-L	0.81	0.03	0.85	0.06	0.88	0.07	0.85	0.04	0.85	0.06
NSGA-II	0.89	0.07	0.88	0.03	0.89	0.05	0.90	0.07	0.90	0.15
NSGA-II-L	0.90	0.08	0.89	0.07	0.88	0.04	0.86	0.05	0.87	0.08
SPEA2	0.88	0.10	0.87	0.08	0.89	0.07	0.87	0.03	0.86	0.04
SPEA2-L	0.90	0.06	0.86	0.06	0.86	0.12	0.87	0.05	0.85	0.07

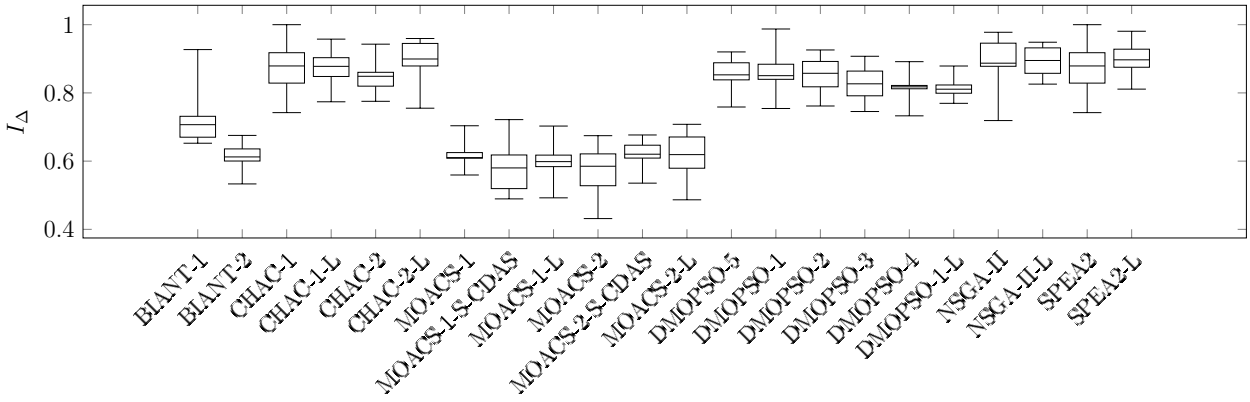

Figure D.9: Boxplot for I_Δ: Buxey-1

Table D.15: Median and interquartile range of the computation time required by the optimisers for the Buxey problems

	Buxey-1		Buxey-2		Buxey-3		Buxey-4		Buxey-5	
	$\tilde{x}$	$IQR(x)$	$\tilde{x}$	$IQR(x)$	$\tilde{x}$	$IQR(x)$	$\tilde{x}$	$IQR(x)$	$\tilde{x}$	$IQR(x)$
BIANT-1	0.52	0.34	0.43	0.19	0.46	0.09	0.54	0.27	0.40	0.30
BIANT-2	0.58	0.22	0.33	0.14	0.46	0.07	0.47	0.20	0.42	0.20
CHAC-1	0.28	0.10	0.18	0.05	0.37	0.10	0.28	0.10	0.29	0.11
CHAC-1-L	0.29	0.15	0.23	0.10	0.32	0.11	0.33	0.08	0.37	0.18
CHAC-2	0.32	0.09	0.20	0.05	0.33	0.02	0.29	0.04	0.26	0.12
CHAC-2-L	0.33	0.23	0.22	0.07	0.33	0.12	0.32	0.04	0.28	0.10
MOACS-1	0.38	0.19	0.26	0.10	0.49	0.09	0.45	0.17	0.57	0.19
MOACS-1-S-CDAS	0.44	0.18	0.29	0.14	0.58	0.22	0.68	0.25	0.58	0.36
MOACS-1-L	0.34	0.06	0.29	0.08	0.42	0.09	0.39	0.13	0.52	0.22
MOACS-2	0.34	0.08	0.21	0.05	0.38	0.25	0.32	0.08	0.41	0.09
MOACS-2-S-CDAS	0.36	0.11	0.30	0.11	0.45	0.21	0.43	0.23	0.45	0.17
MOACS-2-L	0.33	0.11	0.26	0.06	0.33	0.11	0.40	0.10	0.47	0.14
DMOPSO-5	0.20	0.05	0.16	0.04	0.25	0.05	0.26	0.04	0.26	0.09
DMOPSO-1	0.21	0.08	0.17	0.08	0.26	0.08	0.30	0.12	0.27	0.10
DMOPSO-2	0.23	0.06	0.17	0.04	0.24	0.09	0.24	0.09	0.23	0.05
DMOPSO-3	0.24	0.06	0.18	0.08	0.30	0.11	0.28	0.07	0.35	0.06
DMOPSO-4	0.29	0.07	0.23	0.12	0.28	0.06	0.31	0.15	0.26	0.06
DMOPSO-1-L	0.22	0.14	0.15	0.05	0.27	0.19	0.23	0.07	0.24	0.10
NSGA-II	0.25	0.12	0.18	0.06	0.30	0.08	0.30	0.06	0.27	0.12
NSGA-II-L	0.21	0.08	0.15	0.04	0.18	0.07	0.18	0.05	0.25	0.05
SPEA2	0.14	0.04	0.10	0.03	0.14	0.03	0.16	0.01	0.14	0.03
SPEA2-L	0.13	0.03	0.10	0.02	0.15	0.05	0.15	0.02	0.15	0.04

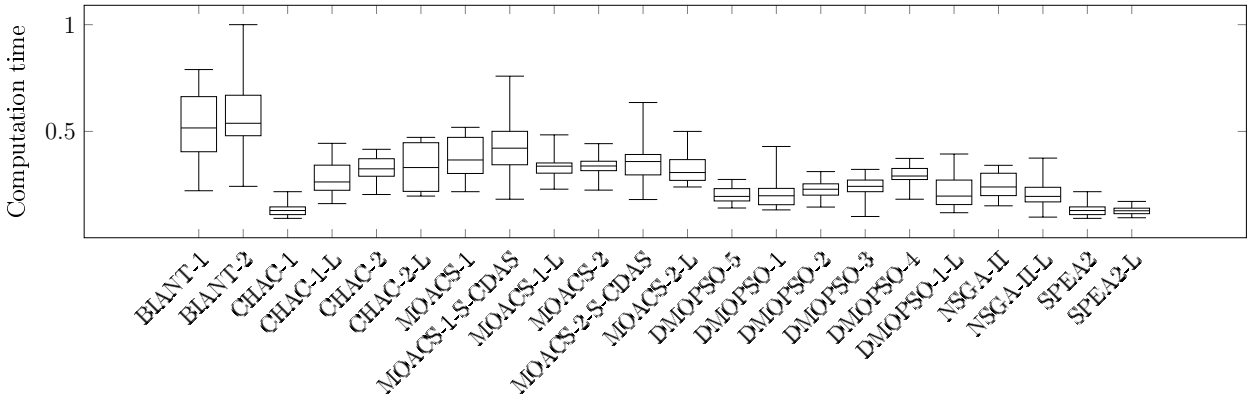

Figure D.10: Boxplot for the computation time: Buxey-1

Table D.16: C-metric for the Buxey-2 problem instance

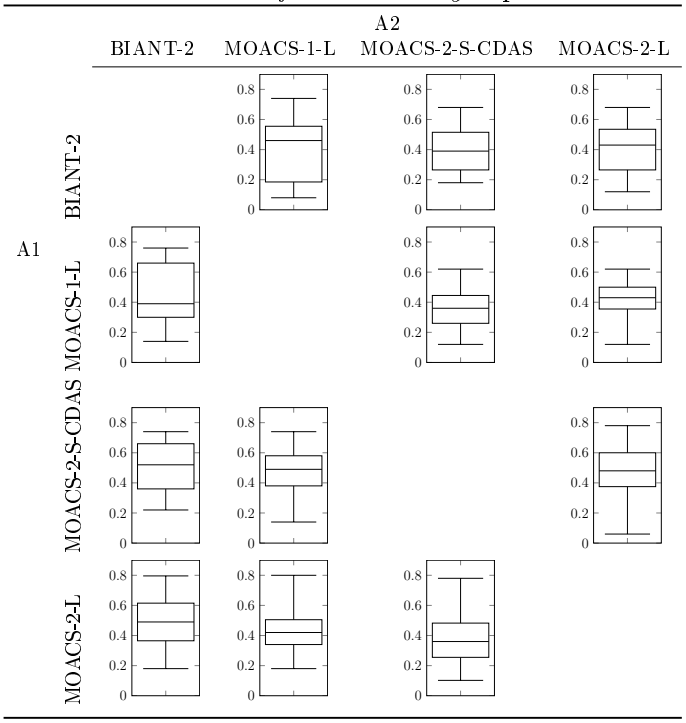

Table D.17: C-metric for the Buxey-1 problem instance

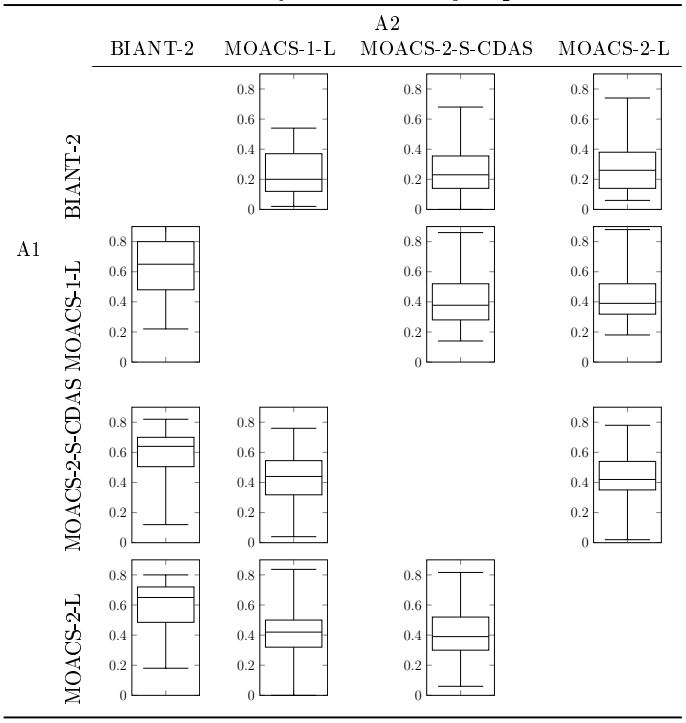

Table D.18: C-metric for the Buxey-3 problem instance

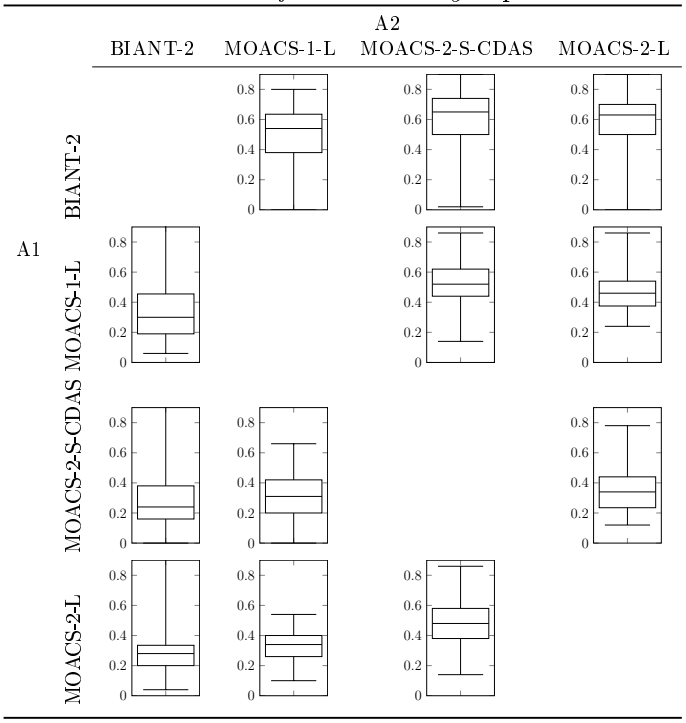

Table D.19: C-metric for the Buxey-4 problem instance

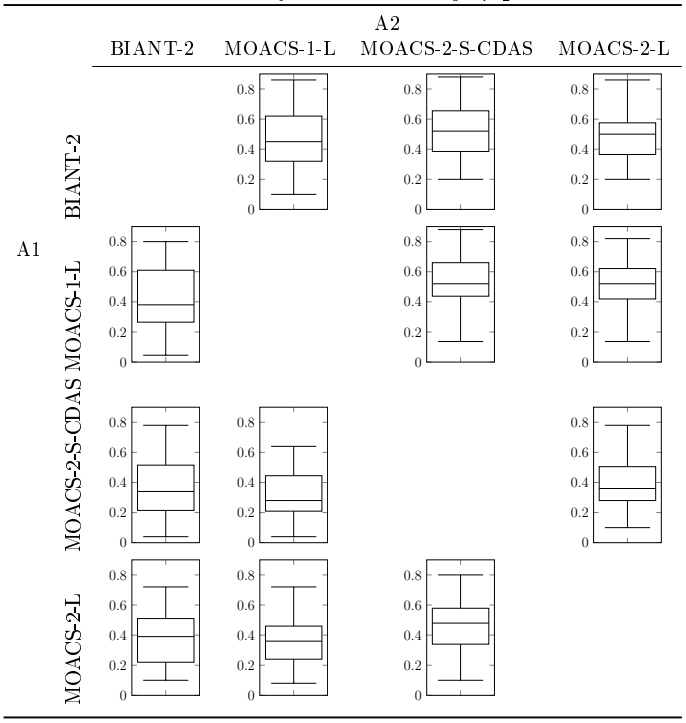

Table D.20: C-metric for the Buxey-5 problem instance

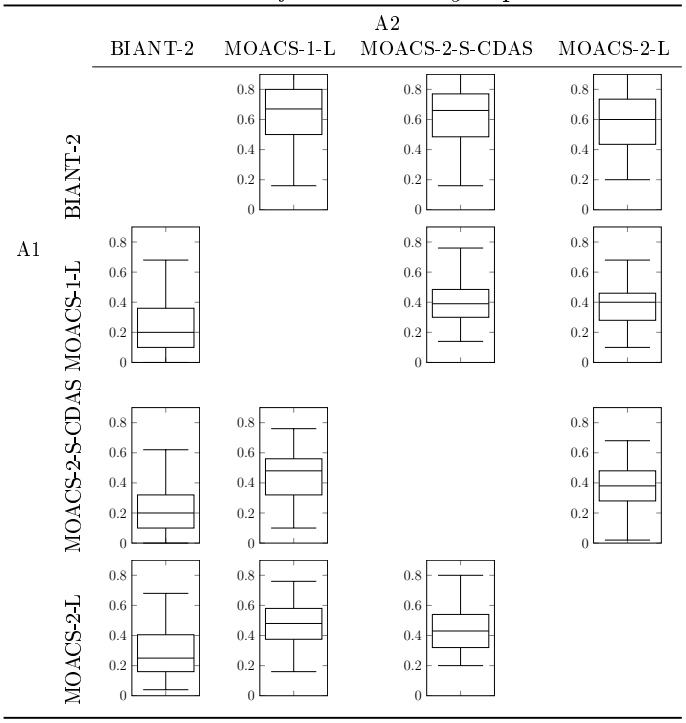

D.1.3 Problem Family: Gunther

Table D.21: Median and interquartile range of I_{HV} obtained by the optimisers for the Gunther problems

	Gunther-1 $\tilde{x} \pm IQR(x)$		Gunther-2 $\tilde{x} \pm IQR(x)$		Gunther-3 $\tilde{x} \pm IQR(x)$		Gunther-4 $\tilde{x} \pm IQR(x)$		Gunther-5 $\tilde{x} \pm IQR(x)$	
BIANT-1	0.96	0.01	0.96	0.01	0.96	0.02	0.94	0.02	0.94	0.00
BIANT-2	0.95	0.01	0.94	0.04	0.95	0.02	0.96	0.00	0.96	0.00
CHAC-1	0.93	0.01	0.92	0.01	0.92	0.01	0.92	0.01	0.91	0.01
CHAC-1-L	0.92	0.01	0.92	0.01	0.92	0.01	0.92	0.00	0.91	0.01
CHAC-2	0.92	0.01	0.92	0.01	0.92	0.01	0.92	0.01	0.90	0.01
CHAC-2-L	0.92	0.01	0.92	0.01	0.91	0.01	0.92	0.00	0.91	0.01
MOACS-1	0.92	0.00	0.92	0.01	0.92	0.00	0.92	0.01	0.93	0.00
MOACS-1-S-CDAS	0.92	0.00	0.92	0.01	0.91	0.01	0.93	0.00	0.93	0.01
MOACS-1-L	0.92	0.00	0.92	0.01	0.91	0.00	0.93	0.01	0.93	0.01
MOACS-2	0.93	0.01	0.93	0.01	0.92	0.01	0.94	0.01	0.94	0.01
MOACS-2-S-CDAS	0.93	0.01	0.93	0.00	0.92	0.01	0.94	0.01	0.94	0.01
MOACS-2-L	0.93	0.00	0.93	0.01	0.92	0.01	0.93	0.01	0.94	0.01
DMOPSO-5	0.92	0.01	0.92	0.00	0.92	0.00	0.92	0.00	0.91	0.01
DMOPSO-1	0.93	0.00	0.92	0.01	0.92	0.00	0.92	0.00	0.91	0.01
DMOPSO-2	0.92	0.01	0.92	0.01	0.92	0.01	0.92	0.00	0.91	0.01
DMOPSO-3	0.93	0.01	0.92	0.01	0.92	0.01	0.92	0.01	0.91	0.01
DMOPSO-4	0.91	0.00	0.91	0.02	0.90	0.02	0.90	0.02	0.89	0.01
DMOPSO-1-L	0.93	0.01	0.92	0.01	0.92	0.01	0.92	0.01	0.91	0.01
NSGA-II	0.93	0.01	0.92	0.01	0.92	0.00	0.93	0.01	0.91	0.01
NSGA-II-L	0.93	0.01	0.93	0.01	0.92	0.00	0.93	0.01	0.91	0.01
SPEA2	0.93	0.01	0.93	0.01	0.92	0.01	0.93	0.01	0.92	0.01
SPEA2-L	0.93	0.01	0.92	0.01	0.92	0.01	0.92	0.01	0.91	0.01

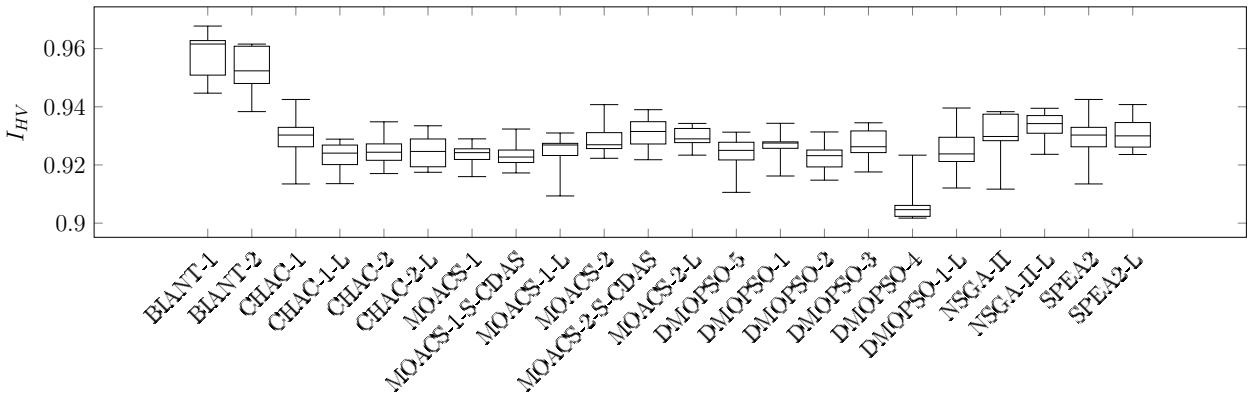

Figure D.11: Boxplot for I_{HV}: Gunther-1

Table D.22: Median and interquartile range of I_{IGD} obtained by the optimisers for the Gunther problems

	Gunther-1 $\tilde{x} \pm IQR(x)$		Gunther-2 $\tilde{x} \pm IQR(x)$		Gunther-3 $\tilde{x} \pm IQR(x)$		Gunther-4 $\tilde{x} \pm IQR(x)$		Gunther-5 $\tilde{x} \pm IQR(x)$	
BIANT-1	0.61	0.10	0.38	0.10	0.47	0.11	0.45	0.12	0.51	0.03
BIANT-2	0.51	0.01	0.66	0.29	0.53	0.19	0.42	0.05	0.39	0.08
CHAC-1	0.78	0.07	0.74	0.13	0.79	0.11	0.71	0.05	0.74	0.07
CHAC-1-L	0.78	0.04	0.72	0.07	0.74	0.07	0.70	0.04	0.72	0.10
CHAC-2	0.79	0.06	0.73	0.07	0.71	0.04	0.70	0.06	0.80	0.08
CHAC-2-L	0.75	0.07	0.70	0.04	0.75	0.03	0.70	0.05	0.74	0.02
MOACS-1	0.79	0.03	0.81	0.07	0.75	0.02	0.76	0.05	0.68	0.05
MOACS-1-S-CDAS	0.79	0.04	0.81	0.09	0.82	0.09	0.75	0.03	0.66	0.06
MOACS-1-L	0.76	0.06	0.79	0.09	0.82	0.05	0.76	0.09	0.68	0.07
MOACS-2	0.80	0.08	0.82	0.07	0.82	0.09	0.76	0.16	0.68	0.05
MOACS-2-S-CDAS	0.77	0.09	0.83	0.05	0.80	0.07	0.74	0.08	0.68	0.07
MOACS-2-L	0.80	0.05	0.81	0.06	0.81	0.06	0.77	0.13	0.67	0.06
DMOPSO-5	0.77	0.06	0.70	0.04	0.75	0.11	0.71	0.05	0.73	0.13
DMOPSO-1	0.76	0.03	0.71	0.10	0.75	0.08	0.70	0.03	0.78	0.11
DMOPSO-2	0.78	0.02	0.75	0.08	0.74	0.12	0.72	0.03	0.75	0.07
DMOPSO-3	0.78	0.06	0.72	0.04	0.73	0.03	0.74	0.06	0.74	0.11
DMOPSO-4	0.93	0.03	0.83	0.15	0.87	0.12	0.88	0.13	0.89	0.06
DMOPSO-1-L	0.80	0.04	0.71	0.07	0.75	0.06	0.74	0.05	0.75	0.04
NSGA-II	0.79	0.05	0.73	0.04	0.74	0.06	0.71	0.04	0.77	0.07
NSGA-II-L	0.79	0.05	0.71	0.07	0.74	0.08	0.71	0.07	0.80	0.09
SPEA2	0.83	0.06	0.75	0.08	0.78	0.08	0.71	0.03	0.74	0.08
SPEA2-L	0.80	0.07	0.74	0.03	0.73	0.04	0.76	0.07	0.79	0.05

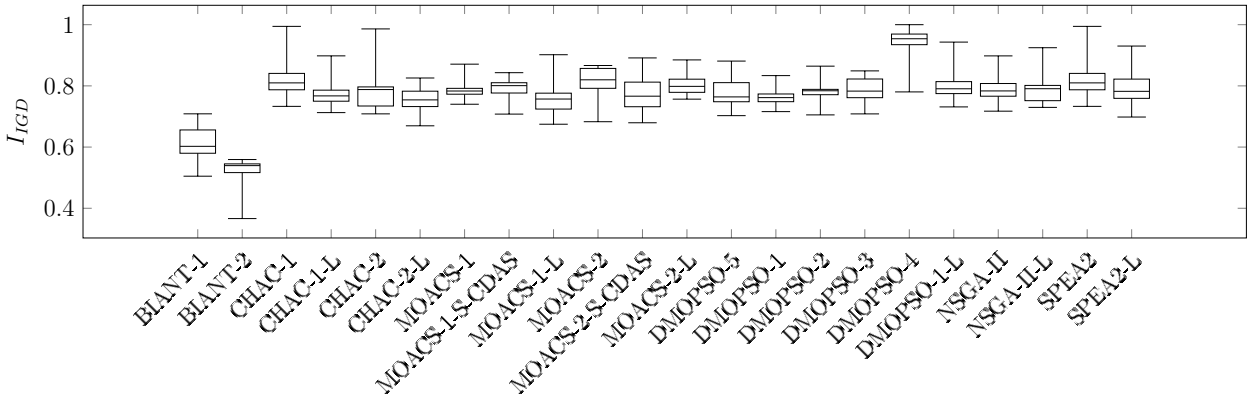

Figure D.12: Boxplot for I_{IGD}: Gunther-1

Table D.23: Median and interquartile range of I_ϵ obtained by the optimisers for the Gunther problems

	Gunther-1 $\tilde{x} \pm IQR(x)$		Gunther-2 $\tilde{x} \pm IQR(x)$		Gunther-3 $\tilde{x} \pm IQR(x)$		Gunther-4 $\tilde{x} \pm IQR(x)$		Gunther-5 $\tilde{x} \pm IQR(x)$	
BIANT-1	0.48	0.16	0.53	0.23	0.53	0.24	0.30	0.06	0.89	0.05
BIANT-2	0.63	0.12	0.47	0.19	0.48	0.11	0.34	0.08	0.59	0.04
CHAC-1	0.90	0.00	1.00	0.00	0.99	0.00	1.00	0.00	0.97	0.00
CHAC-1-L	0.96	0.00	1.00	0.00	1.00	0.00	0.99	0.00	1.00	0.00
CHAC-2	0.96	0.00	1.00	0.00	1.00	0.00	1.00	0.00	1.00	0.00
CHAC-2-L	0.96	0.00	1.00	0.00	1.00	0.00	1.00	0.00	1.00	0.00
MOACS-1	0.21	0.01	0.20	0.03	0.20	0.03	0.20	0.02	0.72	0.05
MOACS-1-S-CDAS	0.22	0.02	0.18	0.04	0.20	0.04	0.17	0.04	0.69	0.08
MOACS-1-L	0.22	0.01	0.19	0.08	0.20	0.05	0.21	0.06	0.72	0.03
MOACS-2	0.18	0.04	0.20	0.07	0.17	0.06	0.13	0.06	0.44	0.05
MOACS-2-S-CDAS	0.19	0.05	0.18	0.05	0.16	0.04	0.17	0.06	0.47	0.07
MOACS-2-L	0.19	0.05	0.17	0.04	0.19	0.05	0.16	0.06	0.45	0.03
DMOPSO-5	0.96	0.00	0.99	0.00	1.00	0.00	1.00	0.00	0.97	0.00
DMOPSO-1	0.96	0.00	1.00	0.00	1.00	0.00	1.00	0.00	0.93	0.00
DMOPSO-2	0.96	0.00	0.99	0.00	1.00	0.00	1.00	0.00	1.00	0.00
DMOPSO-3	0.95	0.00	1.00	0.00	1.00	0.00	0.94	0.00	0.97	0.00
DMOPSO-4	0.96	0.00	1.00	0.00	1.00	0.00	1.00	0.00	1.00	0.00
DMOPSO-1-L	0.96	0.00	1.00	0.00	0.97	0.00	1.00	0.00	0.99	0.00
NSGA-II	0.96	0.00	0.99	0.00	1.00	0.00	1.00	0.00	1.00	0.00
NSGA-II-L	0.95	0.00	1.00	0.00	0.98	0.00	1.00	0.00	0.88	0.00
SPEA2	0.96	0.00	1.00	0.00	0.99	0.00	1.00	0.00	0.95	0.00
SPEA2-L	0.96	0.00	1.00	0.00	1.00	0.00	1.00	0.00	1.00	0.00

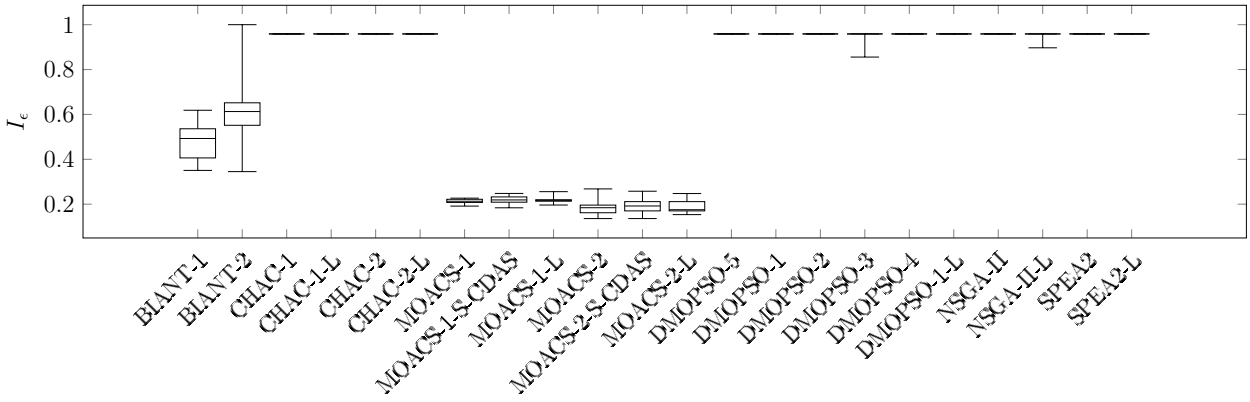

Figure D.13: Boxplot for I_ϵ: Gunther-1

Table D.24: Median and interquartile range of I_Δ obtained by the optimisers for the Gunther problems

	Gunther-1 $\tilde{x} \pm IQR(x)$		Gunther-2 $\tilde{x} \pm IQR(x)$		Gunther-3 $\tilde{x} \pm IQR(x)$		Gunther-4 $\tilde{x} \pm IQR(x)$		Gunther-5 $\tilde{x} \pm IQR(x)$	
BIANT-1	0.65	0.05	0.51	0.11	0.54	0.05	0.58	0.11	0.66	0.08
BIANT-2	0.64	0.15	0.61	0.12	0.62	0.09	0.58	0.06	0.61	0.07
CHAC-1	0.82	0.07	0.84	0.06	0.85	0.09	0.81	0.05	0.83	0.05
CHAC-1-L	0.79	0.06	0.80	0.07	0.81	0.04	0.78	0.07	0.84	0.06
CHAC-2	0.84	0.13	0.80	0.08	0.83	0.05	0.80	0.10	0.86	0.04
CHAC-2-L	0.84	0.10	0.83	0.09	0.84	0.06	0.81	0.03	0.85	0.04
MOACS-1	0.58	0.03	0.54	0.14	0.60	0.05	0.57	0.06	0.64	0.06
MOACS-1-S-CDAS	0.59	0.14	0.55	0.08	0.53	0.04	0.58	0.13	0.64	0.07
MOACS-1-L	0.55	0.15	0.54	0.08	0.55	0.10	0.58	0.09	0.63	0.05
MOACS-2	0.57	0.13	0.57	0.11	0.56	0.07	0.57	0.08	0.60	0.06
MOACS-2-S-CDAS	0.57	0.16	0.55	0.09	0.59	0.08	0.63	0.19	0.66	0.13
MOACS-2-L	0.55	0.08	0.57	0.17	0.56	0.09	0.63	0.10	0.62	0.14
DMOPSO-5	0.84	0.08	0.79	0.04	0.82	0.07	0.82	0.06	0.82	0.08
DMOPSO-1	0.87	0.05	0.81	0.05	0.82	0.03	0.83	0.08	0.85	0.05
DMOPSO-2	0.86	0.08	0.84	0.14	0.83	0.07	0.81	0.05	0.85	0.04
DMOPSO-3	0.87	0.08	0.84	0.05	0.84	0.07	0.81	0.09	0.83	0.10
DMOPSO-4	0.86	0.07	0.81	0.04	0.85	0.06	0.84	0.10	0.84	0.04
DMOPSO-1-L	0.84	0.04	0.83	0.06	0.81	0.05	0.84	0.09	0.81	0.04
NSGA-II	0.91	0.05	0.90	0.05	0.91	0.02	0.90	0.05	0.89	0.06
NSGA-II-L	0.89	0.07	0.85	0.04	0.88	0.10	0.86	0.10	0.91	0.03
SPEA2	0.91	0.08	0.87	0.05	0.87	0.04	0.84	0.10	0.87	0.06
SPEA2-L	0.89	0.07	0.88	0.03	0.84	0.08	0.86	0.03	0.86	0.06

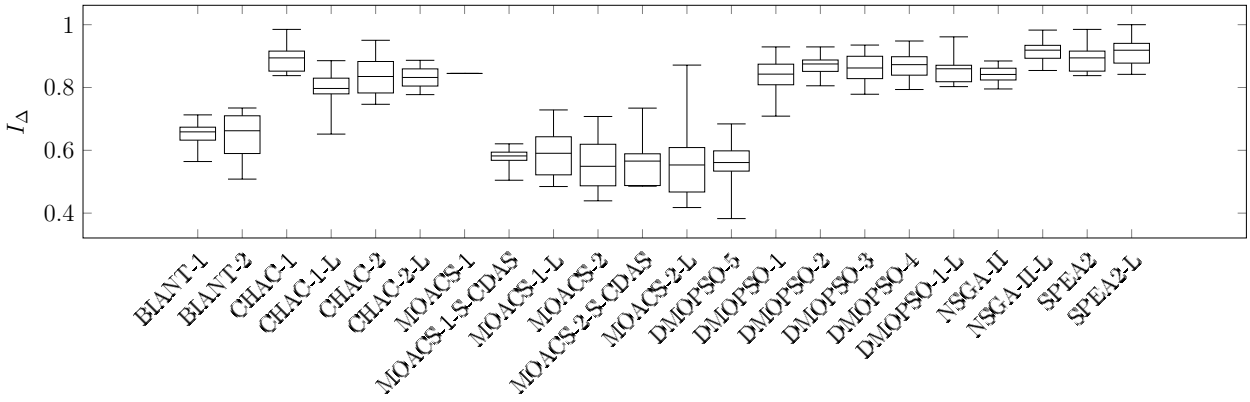

Figure D.14: Boxplot for I_Δ: Gunther-1

Table D.25: Median and interquartile range of the computation time required by the optimisers for the Gunther problems

	Gunther-1 $\tilde{x} \pm IQR(x)$		Gunther-2 $\tilde{x} \pm IQR(x)$		Gunther-3 $\tilde{x} \pm IQR(x)$		Gunther-4 $\tilde{x} \pm IQR(x)$		Gunther-5 $\tilde{x} \pm IQR(x)$	
BIANT-1	0.48	0.11	0.51	0.18	0.52	0.22	0.56	0.22	0.59	0.22
BIANT-2	0.49	0.37	0.57	0.15	0.63	0.27	0.70	0.38	0.81	0.29
CHAC-1	0.20	0.07	0.26	0.12	0.25	0.14	0.32	0.09	0.34	0.12
CHAC-1-L	0.21	0.12	0.28	0.13	0.31	0.16	0.40	0.12	0.37	0.10
CHAC-2	0.20	0.12	0.27	0.11	0.29	0.09	0.35	0.10	0.32	0.09
CHAC-2-L	0.19	0.09	0.30	0.06	0.23	0.03	0.34	0.11	0.33	0.16
MOACS-1	0.30	0.17	0.31	0.11	0.35	0.09	0.42	0.15	0.29	0.10
MOACS-1-S-CDAS	0.32	0.21	0.39	0.18	0.37	0.18	0.60	0.32	0.50	0.27
MOACS-1-L	0.31	0.17	0.42	0.30	0.32	0.09	0.41	0.15	0.35	0.07
MOACS-2	0.23	0.10	0.25	0.11	0.29	0.14	0.53	0.27	0.32	0.18
MOACS-2-S-CDAS	0.25	0.15	0.36	0.15	0.42	0.18	0.52	0.28	0.30	0.05
MOACS-2-L	0.21	0.05	0.31	0.18	0.36	0.13	0.39	0.11	0.32	0.13
DMOPSO-5	0.16	0.06	0.24	0.04	0.23	0.07	0.29	0.05	0.26	0.08
DMOPSO-1	0.17	0.07	0.23	0.09	0.20	0.12	0.32	0.08	0.24	0.10
DMOPSO-2	0.15	0.03	0.19	0.07	0.19	0.07	0.24	0.06	0.23	0.12
DMOPSO-3	0.20	0.03	0.22	0.07	0.23	0.06	0.25	0.08	0.35	0.10
DMOPSO-4	0.17	0.05	0.46	0.18	0.29	0.07	0.31	0.09	0.33	0.10
DMOPSO-1-L	0.13	0.03	0.23	0.05	0.23	0.05	0.23	0.10	0.25	0.04
NSGA-II	0.16	0.02	0.23	0.09	0.25	0.03	0.30	0.07	0.21	0.08
NSGA-II-L	0.13	0.05	0.22	0.10	0.20	0.08	0.26	0.09	0.18	0.08
SPEA2	0.09	0.04	0.14	0.05	0.12	0.02	0.16	0.06	0.17	0.04
SPEA2-L	0.09	0.03	0.11	0.02	0.12	0.03	0.14	0.05	0.13	0.03

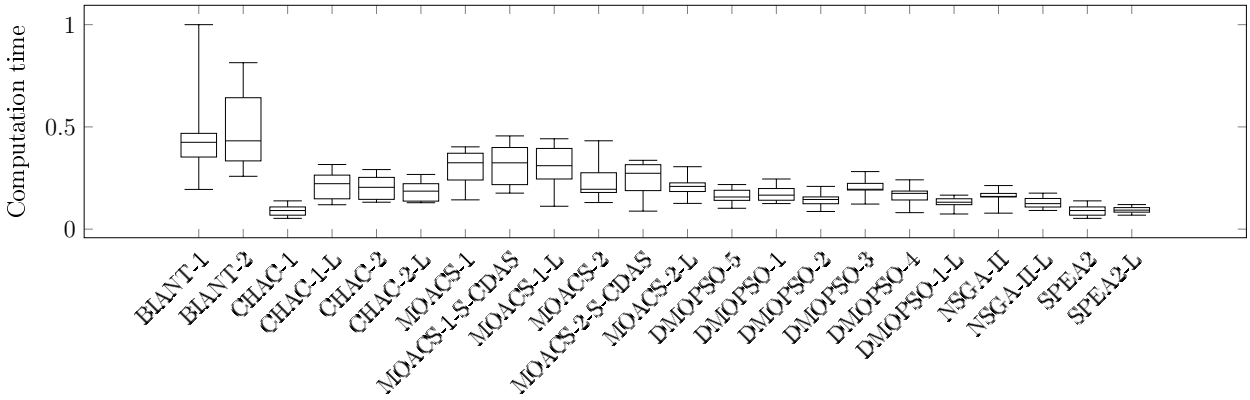

Figure D.15: Boxplot for the computation time: Gunther-1

Table D.26: C-metric for the Gunther-1 problem instance

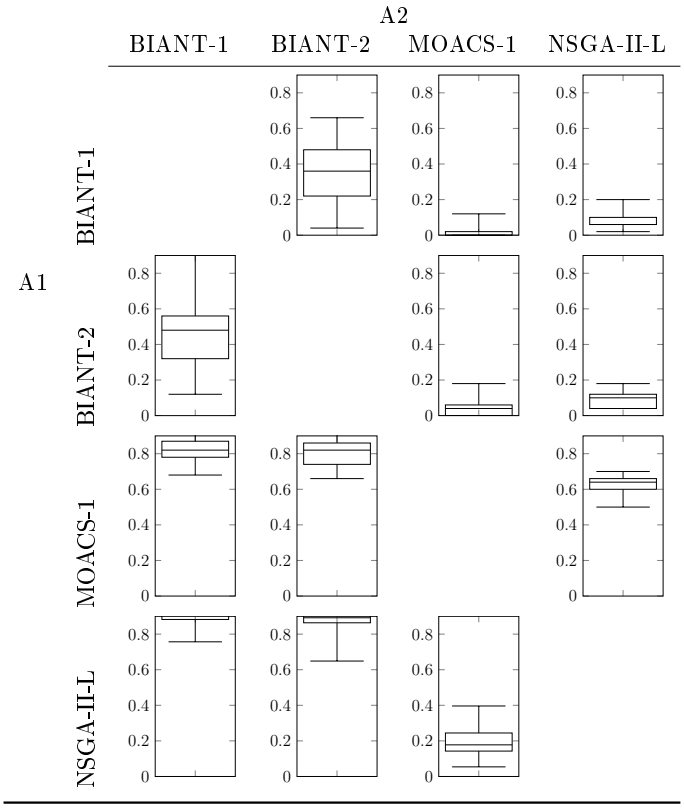

Table D.27: C-metric for the Gunther-2 problem instance

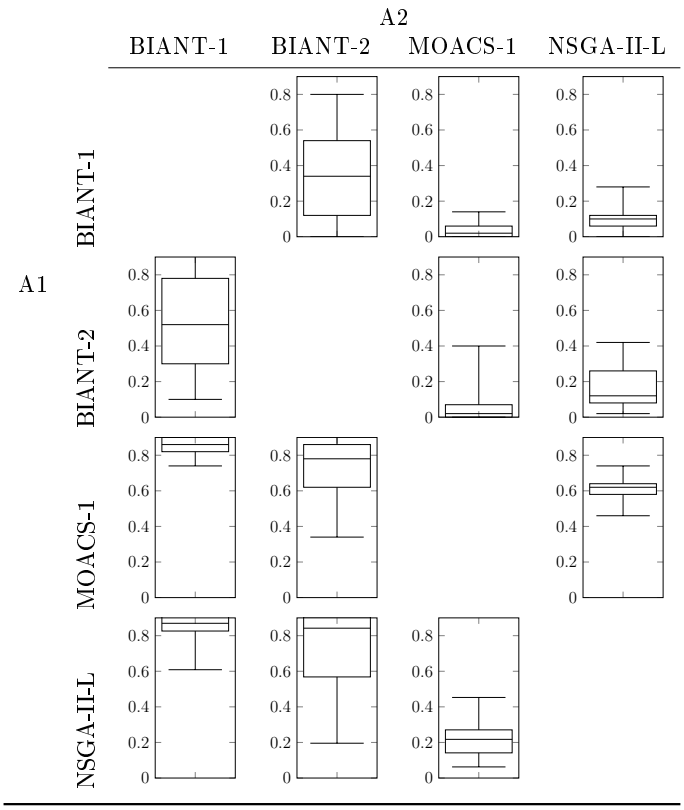

Table D.28: C-metric for the Gunther-3 problem instance

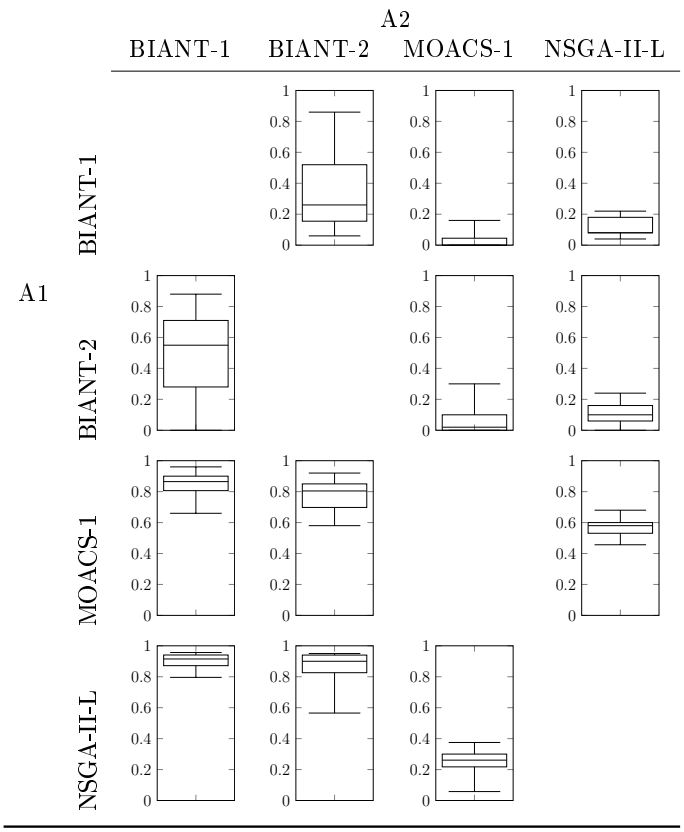

Table D.29: C-metric for the Gunther-4 problem instance

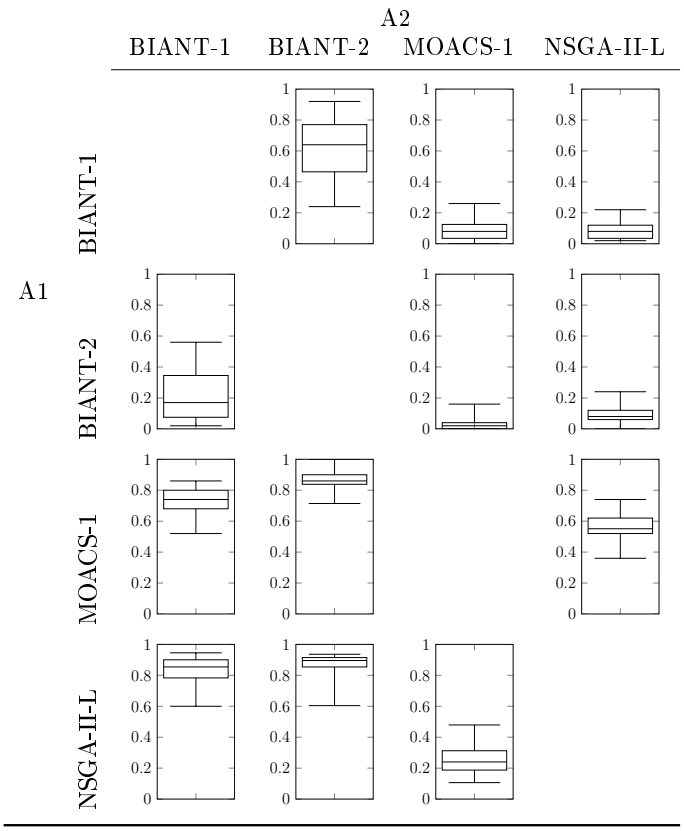

Table D.30: C-metric for the Gunther-5 problem instance

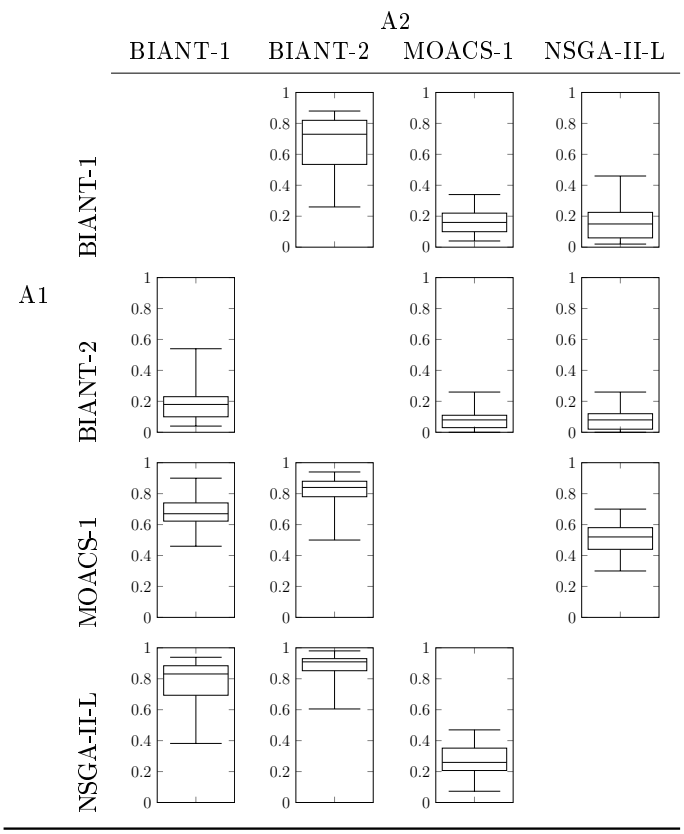

D.1.4 Problem Family: Hahn

Table D.31: Median and interquartile range of I_{HV} obtained by the optimisers for the Hahn problems

	Hahn-1 $\tilde{x} \pm IQR(x)$		Hahn-2 $\tilde{x} \pm IQR(x)$		Hahn-3 $\tilde{x} \pm IQR(x)$		Hahn-4 $\tilde{x} \pm IQR(x)$		Hahn-5 $\tilde{x} \pm IQR(x)$	
BIANT-1	0.94	0.02	0.95	0.01	0.95	0.01	0.94	0.02	0.94	0.01
BIANT-2	0.94	0.03	0.95	0.01	0.95	0.02	0.94	0.01	0.94	0.01
CHAC-1	0.90	0.01	0.89	0.01	0.88	0.01	0.88	0.00	0.86	0.01
CHAC-1-L	0.89	0.00	0.89	0.01	0.88	0.01	0.88	0.01	0.86	0.01
CHAC-2	0.89	0.01	0.89	0.01	0.88	0.00	0.88	0.01	0.86	0.01
CHAC-2-L	0.89	0.01	0.89	0.00	0.89	0.01	0.87	0.01	0.86	0.00
MOACS-1	0.91	0.00	0.92	0.01	0.91	0.01	0.91	0.01	0.92	0.01
MOACS-1-S-CDAS	0.91	0.01	0.92	0.01	0.91	0.00	0.91	0.01	0.92	0.01
MOACS-1-L	0.92	0.00	0.92	0.01	0.91	0.01	0.91	0.00	0.93	0.01
MOACS-2	0.92	0.01	0.93	0.01	0.93	0.01	0.88	0.05	0.93	0.01
MOACS-2-S-CDAS	0.92	0.01	0.93	0.01	0.92	0.00	0.92	0.01	0.94	0.01
MOACS-2-L	0.92	0.01	0.93	0.01	0.92	0.01	0.92	0.01	0.94	0.01
DMOPSO-5	0.89	0.01	0.89	0.01	0.88	0.01	0.88	0.01	0.86	0.02
DMOPSO-1	0.89	0.01	0.89	0.01	0.88	0.01	0.87	0.01	0.86	0.01
DMOPSO-2	0.89	0.01	0.89	0.01	0.88	0.01	0.88	0.01	0.86	0.01
DMOPSO-3	0.89	0.01	0.89	0.00	0.88	0.01	0.88	0.01	0.86	0.01
DMOPSO-4	0.88	0.02	0.88	0.01	0.87	0.01	0.87	0.00	0.85	0.01
DMOPSO-1-L	0.89	0.01	0.89	0.01	0.88	0.01	0.88	0.01	0.86	0.02
NSGA-II	0.90	0.01	0.90	0.01	0.89	0.01	0.89	0.01	0.87	0.01
NSGA-II-L	0.90	0.01	0.89	0.00	0.89	0.01	0.88	0.01	0.87	0.02
SPEA2	0.89	0.01	0.90	0.01	0.89	0.01	0.88	0.00	0.87	0.00
SPEA2-L	0.90	0.00	0.90	0.01	0.89	0.01	0.88	0.01	0.87	0.01

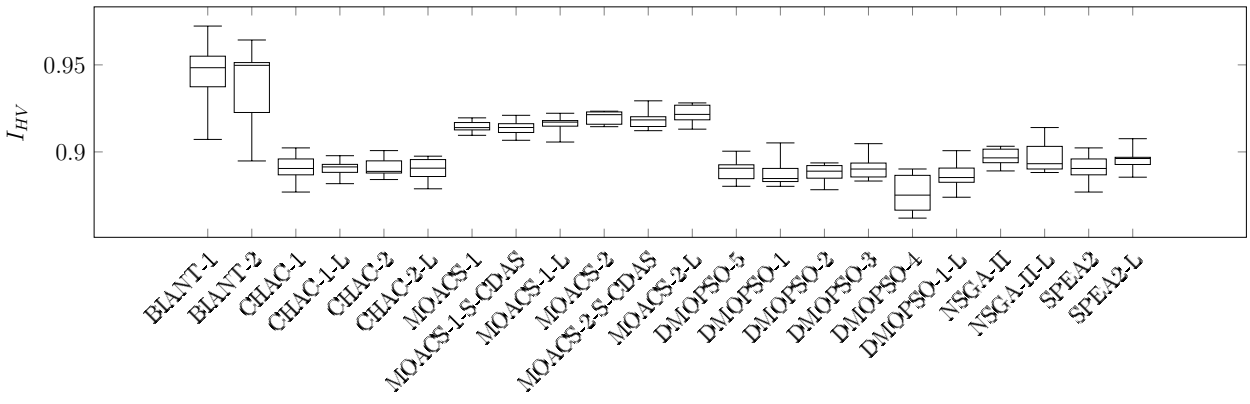

Figure D.16: Boxplot for I_{HV}: Hahn-1

Table D.32: Median and interquartile range of I_{IGD} obtained by the optimisers for the Hahn problems

	Hahn-1 $\tilde{x} \pm IQR(x)$		Hahn-2 $\tilde{x} \pm IQR(x)$		Hahn-3 $\tilde{x} \pm IQR(x)$		Hahn-4 $\tilde{x} \pm IQR(x)$		Hahn-5 $\tilde{x} \pm IQR(x)$	
BIANT-1	0.47	0.21	0.36	0.12	0.37	0.04	0.23	0.04	0.27	0.04
BIANT-2	0.40	0.19	0.35	0.08	0.35	0.05	0.22	0.05	0.27	0.04
CHAC-1	0.79	0.06	0.87	0.04	0.80	0.09	0.35	0.02	0.81	0.17
CHAC-1-L	0.78	0.10	0.87	0.06	0.78	0.06	0.36	0.02	0.78	0.09
CHAC-2	0.78	0.04	0.85	0.06	0.81	0.02	0.36	0.02	0.84	0.13
CHAC-2-L	0.81	0.10	0.87	0.04	0.77	0.07	0.37	0.01	0.82	0.08
MOACS-1	0.69	0.06	0.68	0.05	0.61	0.03	0.30	0.02	0.45	0.02
MOACS-1-S-CDAS	0.69	0.02	0.69	0.04	0.63	0.03	0.30	0.02	0.41	0.05
MOACS-1-L	0.69	0.05	0.68	0.04	0.61	0.04	0.30	0.02	0.39	0.05
MOACS-2	0.69	0.08	0.69	0.05	0.57	0.03	0.43	0.13	0.42	0.02
MOACS-2-S-CDAS	0.72	0.06	0.66	0.05	0.59	0.05	0.30	0.03	0.38	0.03
MOACS-2-L	0.70	0.05	0.64	0.03	0.60	0.07	0.29	0.01	0.36	0.06
DMOPSO-5	0.80	0.07	0.88	0.05	0.80	0.07	0.36	0.02	0.82	0.15
DMOPSO-1	0.80	0.09	0.89	0.07	0.82	0.12	0.36	0.03	0.82	0.12
DMOPSO-2	0.81	0.09	0.86	0.06	0.86	0.09	0.35	0.02	0.80	0.07
DMOPSO-3	0.80	0.07	0.88	0.06	0.82	0.03	0.35	0.02	0.79	0.09
DMOPSO-4	0.91	0.03	0.90	0.06	0.87	0.07	0.38	0.01	0.92	0.13
DMOPSO-1-L	0.83	0.07	0.88	0.12	0.79	0.08	0.35	0.03	0.80	0.16
NSGA-II	0.81	0.08	0.86	0.08	0.80	0.09	0.35	0.02	0.82	0.07
NSGA-II-L	0.81	0.03	0.90	0.03	0.79	0.08	0.36	0.04	0.83	0.04
SPEA2	0.84	0.12	0.86	0.05	0.83	0.09	0.36	0.02	0.83	0.00
SPEA2-L	0.80	0.08	0.87	0.08	0.81	0.04	0.36	0.02	0.84	0.03

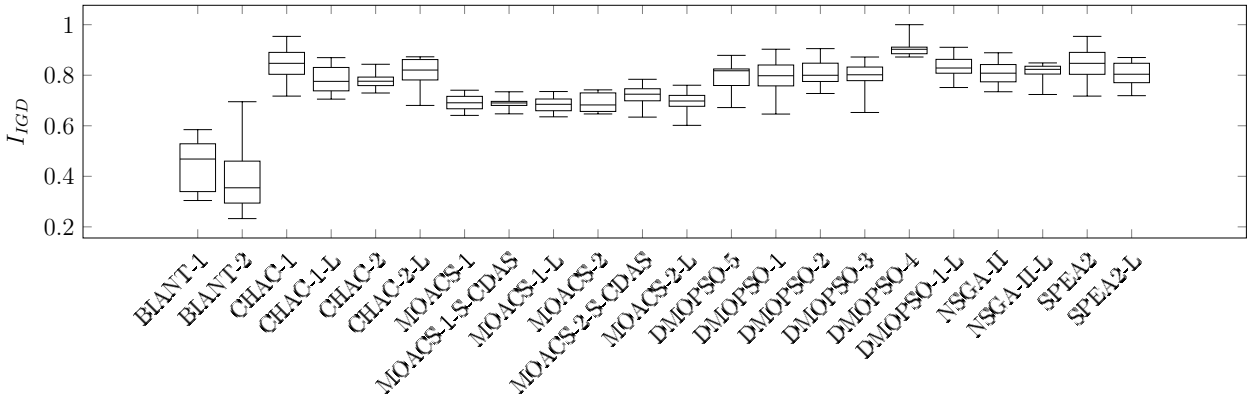

Figure D.17: Boxplot for I_{IGD}: Hahn-1

Table D.33: Median and interquartile range of I_ϵ obtained by the optimisers for the Hahn problems

	Hahn-1		Hahn-2		Hahn-3		Hahn-4		Hahn-5	
	$\tilde{x}$	$IQR(x)$	$\tilde{x}$	$IQR(x)$	$\tilde{x}$	$IQR(x)$	$\tilde{x}$	$IQR(x)$	$\tilde{x}$	$IQR(x)$
BIANT-1	0.52	0.09	0.87	0.12	0.85	0.14	0.22	0.02	0.62	0.04
BIANT-2	0.52	0.25	0.84	0.04	0.76	0.17	0.20	0.04	0.67	0.27
CHAC-1	0.51	0.00	0.79	0.01	0.67	0.02	0.17	0.01	0.53	0.00
CHAC-1-L	0.57	0.13	0.78	0.01	0.67	0.01	0.17	0.01	0.52	0.01
CHAC-2	0.57	0.13	0.79	0.01	0.68	0.01	0.17	0.01	0.53	0.01
CHAC-2-L	0.57	0.13	0.78	0.01	0.67	0.02	0.16	0.00	0.53	0.01
MOACS-1	0.25	0.01	0.73	0.04	0.66	0.10	0.16	0.01	0.50	0.03
MOACS-1-S-CDAS	0.29	0.10	0.74	0.03	0.65	0.06	0.18	0.02	0.52	0.04
MOACS-1-L	0.26	0.03	0.75	0.04	0.65	0.08	0.16	0.01	0.53	0.02
MOACS-2	0.30	0.07	0.64	0.15	0.51	0.08	0.29	0.16	0.39	0.11
MOACS-2-S-CDAS	0.29	0.11	0.54	0.09	0.52	0.07	0.14	0.03	0.41	0.10
MOACS-2-L	0.26	0.08	0.54	0.03	0.56	0.16	0.14	0.03	0.41	0.08
DMOPSO-5	0.54	0.13	0.79	0.01	0.67	0.01	0.16	0.01	0.52	0.01
DMOPSO-1	0.56	0.13	0.78	0.02	0.67	0.01	0.17	0.01	0.52	0.01
DMOPSO-2	0.60	0.00	0.79	0.02	0.67	0.00	0.16	0.01	0.52	0.01
DMOPSO-3	0.53	0.10	0.79	0.02	0.67	0.02	0.16	0.00	0.52	0.01
DMOPSO-4	0.60	0.00	0.79	0.02	0.69	0.00	0.17	0.00	0.54	0.01
DMOPSO-1-L	0.58	0.10	0.78	0.01	0.67	0.01	0.16	0.01	0.52	0.00
NSGA-II	0.55	0.13	0.57	0.00	0.58	0.12	0.15	0.00	0.35	0.00
NSGA-II-L	0.56	0.13	0.60	0.13	0.55	0.00	0.15	0.03	0.35	0.01
SPEA2	0.62	0.00	0.64	0.13	0.59	0.12	0.16	0.03	0.35	0.00
SPEA2-L	0.53	0.10	0.61	0.13	0.60	0.12	0.15	0.02	0.37	0.01

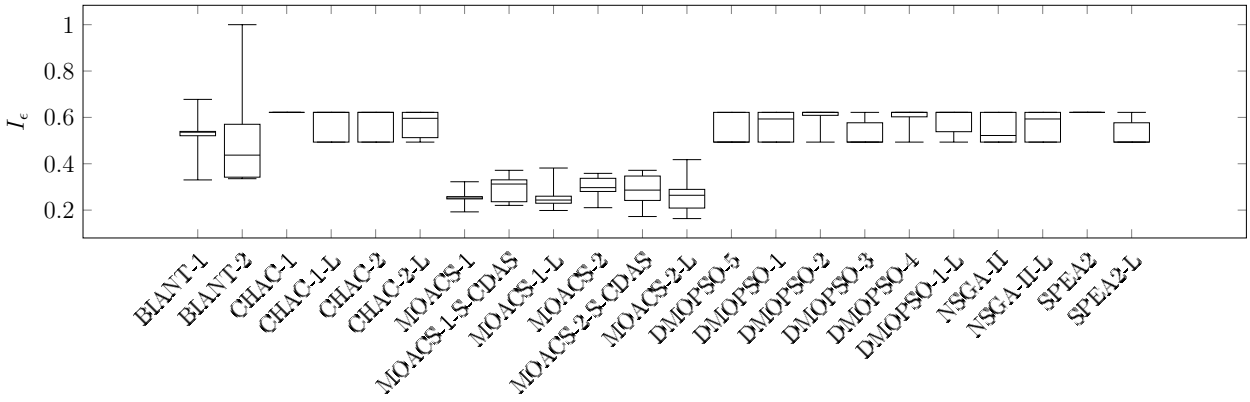

Figure D.18: Boxplot for I_ϵ: Hahn-1

Table D.34: Median and interquartile range of I_Δ obtained by the optimisers for the Hahn problems

	Hahn-1		Hahn-2		Hahn-3		Hahn-4		Hahn-5	
	$\tilde{x}$	$IQR(x)$	$\tilde{x}$	$IQR(x)$	$\tilde{x}$	$IQR(x)$	$\tilde{x}$	$IQR(x)$	$\tilde{x}$	$IQR(x)$
BIANT-1	0.42	0.10	0.39	0.03	0.44	0.02	0.43	0.11	0.36	0.12
BIANT-2	0.39	0.14	0.45	0.05	0.46	0.06	0.42	0.05	0.34	0.09
CHAC-1	0.81	0.03	0.84	0.03	0.83	0.08	0.82	0.08	0.88	0.06
CHAC-1-L	0.77	0.06	0.84	0.03	0.80	0.05	0.81	0.10	0.87	0.05
CHAC-2	0.77	0.08	0.83	0.04	0.84	0.05	0.84	0.03	0.88	0.03
CHAC-2-L	0.80	0.03	0.83	0.03	0.83	0.02	0.80	0.00	0.91	0.00
MOACS-1	0.39	0.05	0.41	0.09	0.44	0.05	0.45	0.07	0.37	0.05
MOACS-1-S-CDAS	0.39	0.02	0.41	0.06	0.45	0.10	0.45	0.05	0.34	0.06
MOACS-1-L	0.36	0.04	0.45	0.04	0.45	0.05	0.43	0.01	0.37	0.04
MOACS-2	0.37	0.05	0.41	0.10	0.45	0.07	0.54	0.11	0.35	0.05
MOACS-2-S-CDAS	0.38	0.09	0.41	0.05	0.41	0.07	0.42	0.06	0.35	0.12
MOACS-2-L	0.38	0.02	0.41	0.06	0.42	0.05	0.43	0.08	0.33	0.05
DMOPSO-5	0.82	0.07	0.85	0.08	0.85	0.03	0.84	0.09	0.90	0.02
DMOPSO-1	0.81	0.10	0.88	0.07	0.87	0.09	0.85	0.04	0.91	0.04
DMOPSO-2	0.81	0.02	0.87	0.04	0.87	0.05	0.84	0.06	0.90	0.04
DMOPSO-3	0.81	0.06	0.87	0.04	0.86	0.13	0.82	0.11	0.90	0.06
DMOPSO-4	0.83	0.04	0.87	0.02	0.86	0.07	0.91	0.00	0.92	0.03
DMOPSO-1-L	0.83	0.04	0.86	0.06	0.87	0.07	0.84	0.03	0.89	0.01
NSGA-II	0.85	0.05	0.91	0.11	0.91	0.03	0.89	0.06	0.94	0.06
NSGA-II-L	0.85	0.04	0.91	0.11	0.89	0.07	0.93	0.07	0.91	0.05
SPEA2	0.85	0.08	0.89	0.08	0.95	0.05	0.86	0.04	0.91	0.05
SPEA2-L	0.84	0.10	0.89	0.03	0.90	0.06	0.90	0.03	0.92	0.03

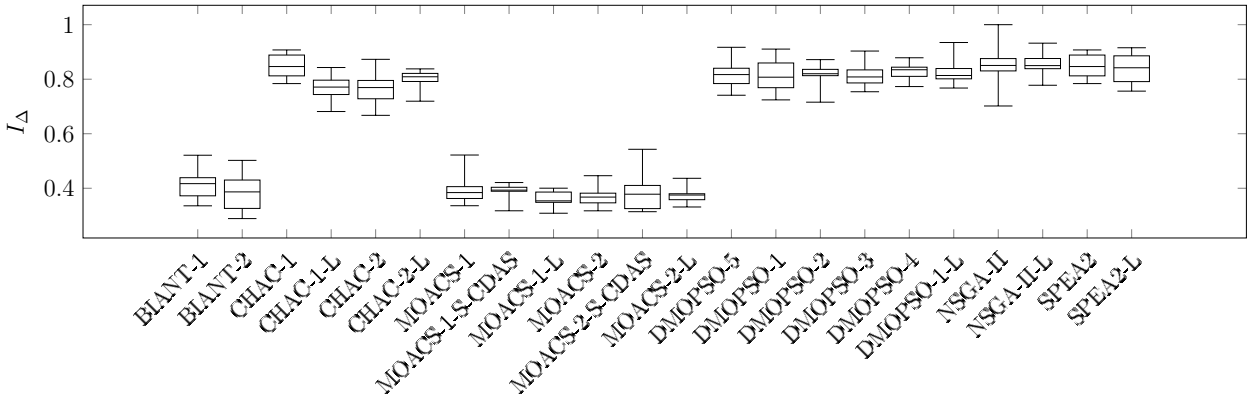

Figure D.19: Boxplot for I_Δ: Hahn-1

Table D.35: Median and interquartile range of the computation time required by the optimisers for the Hahn problems

	Hahn-1		Hahn-2		Hahn-3		Hahn-4		Hahn-5	
	$\tilde{x} \pm IQR(x)$		$\tilde{x} \pm IQR(x)$		$\tilde{x} \pm IQR(x)$		$\tilde{x} \pm IQR(x)$		$\tilde{x} \pm IQR(x)$	
BIANT-1	0.74	0.14	0.17	0.10	0.51	0.33	0.45	0.18	0.40	0.17
BIANT-2	0.54	0.09	0.23	0.07	0.58	0.12	0.59	0.42	0.52	0.53
CHAC-1	0.35	0.11	0.10	0.03	0.25	0.06	0.15	0.01	0.19	0.04
CHAC-1-L	0.35	0.09	0.11	0.02	0.30	0.14	0.16	0.05	0.20	0.09
CHAC-2	0.32	0.15	0.10	0.04	0.23	0.12	0.17	0.03	0.19	0.08
CHAC-2-L	0.31	0.07	0.12	0.01	0.29	0.10	0.19	0.08	0.23	0.05
MOACS-1	0.39	0.18	0.13	0.06	0.22	0.09	0.23	0.04	0.27	0.08
MOACS-1-S-CDAS	0.48	0.16	0.15	0.04	0.37	0.23	0.21	0.15	0.26	0.08
MOACS-1-L	0.41	0.12	0.13	0.06	0.28	0.17	0.19	0.09	0.26	0.09
MOACS-2	0.29	0.26	0.09	0.04	0.36	0.23	0.21	0.19	0.26	0.11
MOACS-2-S-CDAS	0.33	0.09	0.11	0.03	0.30	0.12	0.22	0.08	0.27	0.10
MOACS-2-L	0.43	0.31	0.12	0.07	0.28	0.17	0.17	0.07	0.26	0.19
DMOPSO-5	0.36	0.10	0.08	0.04	0.22	0.05	0.15	0.04	0.18	0.10
DMOPSO-1	0.40	0.15	0.20	0.03	0.24	0.05	0.13	0.03	0.17	0.11
DMOPSO-2	0.26	0.15	0.08	0.02	0.14	0.04	0.13	0.04	0.16	0.05
DMOPSO-3	0.39	0.08	0.18	0.05	0.23	0.11	0.18	0.05	0.24	0.05
DMOPSO-4	0.38	0.36	0.15	0.00	0.32	0.21	0.25	0.12	0.32	0.04
DMOPSO-1-L	0.28	0.13	0.08	0.02	0.21	0.06	0.15	0.05	0.15	0.07
NSGA-II	0.30	0.12	0.09	0.03	0.16	0.08	0.17	0.04	0.17	0.07
NSGA-II-L	0.25	0.08	0.08	0.03	0.21	0.06	0.12	0.03	0.12	0.04
SPEA2	0.13	0.06	0.04	0.01	0.10	0.02	0.07	0.02	0.08	0.03
SPEA2-L	0.15	0.06	0.05	0.01	0.10	0.01	0.08	0.02	0.11	0.01

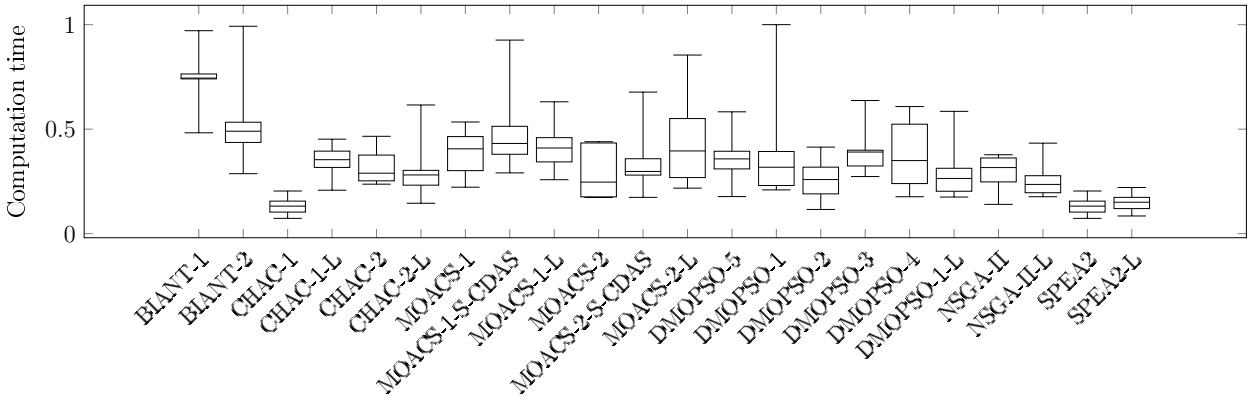

Figure D.20: Boxplot for the computation time: Hahn-1

Table D.36: C-metric for the Hahn-1 problem instance

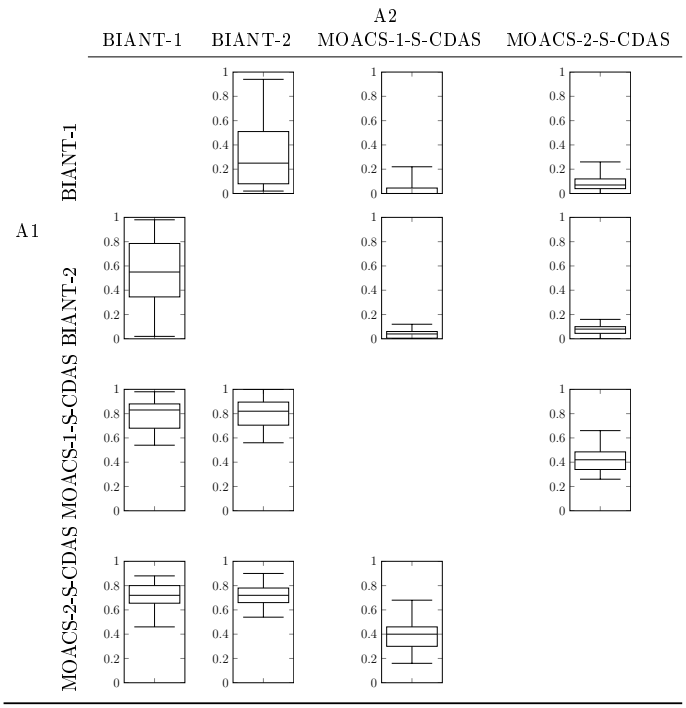

Table D.37: C-metric for the Hahn-2 problem instance

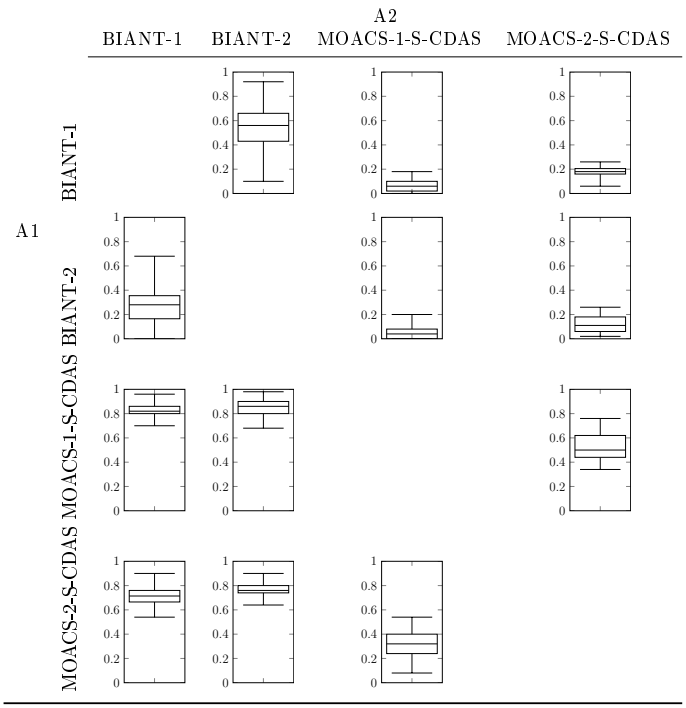

Table D.38: C-metric for the Hahn-3 problem instance

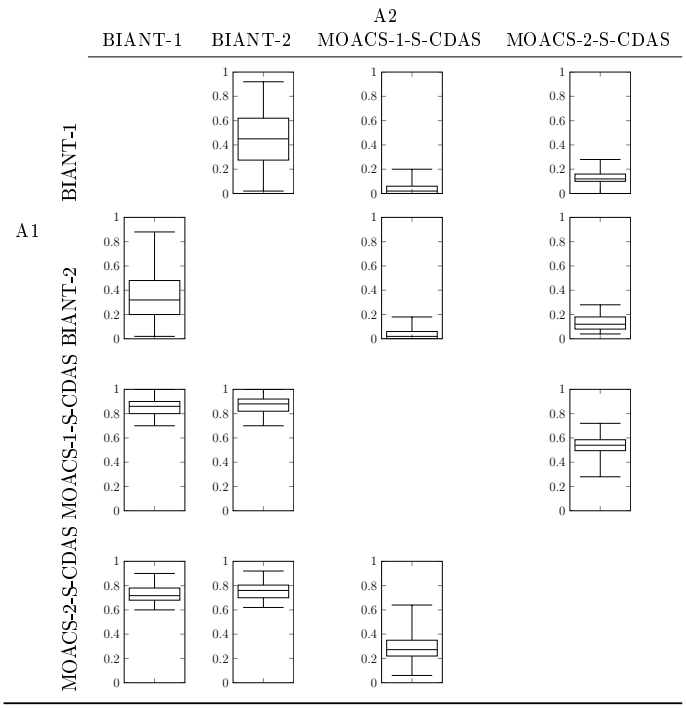

Table D.39: C-metric for the Hahn-4 problem instance

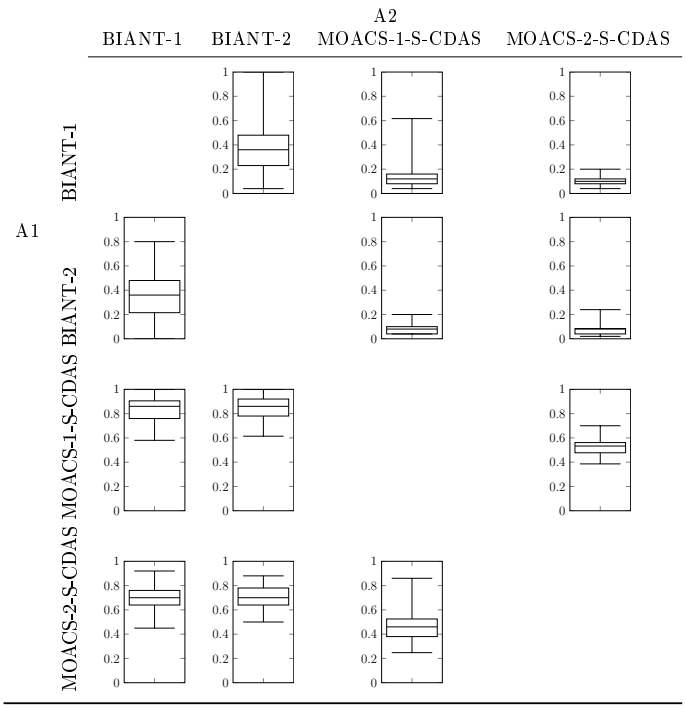

Table D.40: C-metric for the Hahn-5 problem instance

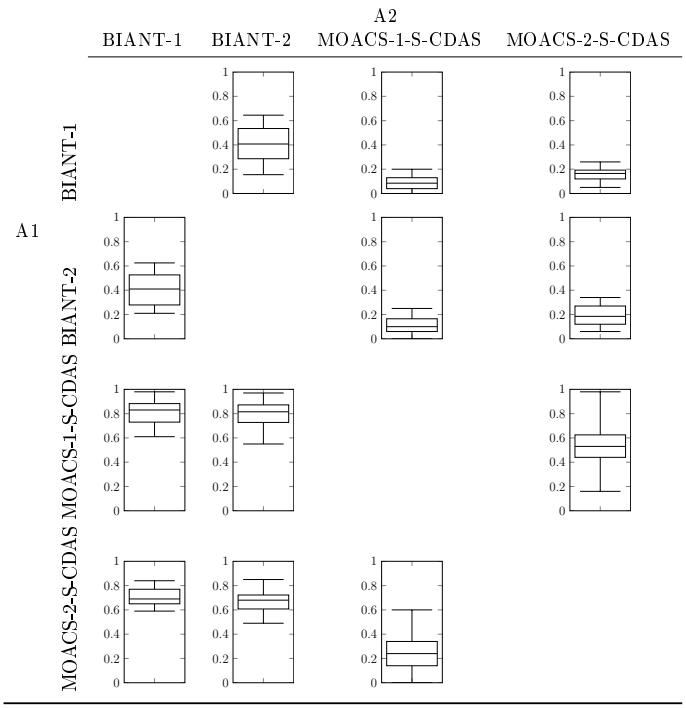

D.1.5 Problem Family: Jackson

Table D.41: Median and interquartile range of I_{HV} obtained by the optimisers for the Jackson problems

	Jackson-1 $\tilde{x} \pm IQR(x)$		Jackson-2 $\tilde{x} \pm IQR(x)$		Jackson-3 $\tilde{x} \pm IQR(x)$		Jackson-4 $\tilde{x} \pm IQR(x)$		Jackson-5 $\tilde{x} \pm IQR(x)$	
BIANT-1	0.51	0.00	0.52	0.03	0.60	0.02	0.93	0.02	0.49	0.00
BIANT-2	0.50	0.00	0.53	0.03	0.62	0.01	0.89	0.03	0.49	0.00
CHAC-1	0.58	0.00	0.58	0.00	0.63	0.00	0.98	0.02	0.50	0.00
CHAC-1-L	0.58	0.00	0.58	0.00	0.63	0.00	0.98	0.00	0.50	0.00
CHAC-2	0.58	0.00	0.58	0.00	0.63	0.00	0.98	0.02	0.50	0.00
CHAC-2-L	0.58	0.00	0.58	0.00	0.63	0.00	0.98	0.02	0.50	0.00
MOACS-1	0.53	0.00	0.53	0.01	0.62	0.00	0.92	0.01	0.50	0.00
MOACS-1-S-CDAS	0.53	0.00	0.53	0.01	0.62	0.00	0.92	0.01	0.50	0.00
MOACS-1-L	0.52	0.02	0.53	0.00	0.62	0.00	0.92	0.02	0.50	0.00
MOACS-2	0.52	0.01	0.53	0.00	0.62	0.00	0.90	0.02	0.50	0.00
MOACS-2-S-CDAS	0.53	0.00	0.53	0.00	0.61	0.01	0.89	0.00	0.50	0.00
MOACS-2-L	0.53	0.01	0.53	0.00	0.62	0.00	0.88	0.02	0.50	0.00
DMOPSO-5	0.58	0.00	0.58	0.00	0.63	0.00	0.98	0.00	0.50	0.00
DMOPSO-1	0.58	0.00	0.58	0.00	0.63	0.00	0.98	0.02	0.50	0.00
DMOPSO-2	0.58	0.00	0.58	0.00	0.63	0.00	0.98	0.00	0.50	0.00
DMOPSO-3	0.58	0.00	0.58	0.00	0.63	0.00	0.98	0.00	0.50	0.00
DMOPSO-4	0.58	0.00	0.58	0.00	0.63	0.00	0.98	0.00	0.50	0.00
DMOPSO-1-L	0.58	0.00	0.58	0.00	0.63	0.00	0.98	0.02	0.50	0.00
NSGA-II	0.58	0.00	0.58	0.00	0.63	0.00	0.98	0.00	0.50	0.00
NSGA-II-L	0.58	0.00	0.58	0.00	0.63	0.00	0.98	0.00	0.50	0.00
SPEA2	0.58	0.00	0.58	0.00	0.63	0.00	0.99	0.02	0.50	0.00
SPEA2-L	0.58	0.00	0.58	0.00	0.63	0.00	0.97	0.00	0.50	0.00

Table D.42: Median and interquartile range of I_{IGD} obtained by the optimisers for the Jackson problems

	Jackson-1 $\tilde{x} \pm IQR(x)$		Jackson-2 $\tilde{x} \pm IQR(x)$		Jackson-3 $\tilde{x} \pm IQR(x)$		Jackson-4 $\tilde{x} \pm IQR(x)$		Jackson-5 $\tilde{x} \pm IQR(x)$	
BIANT-1	0.99	0.00	0.81	0.19	0.81	0.14	0.47	0.08	0.85	0.00
BIANT-2	0.99	0.00	0.78	0.22	0.73	0.01	0.63	0.20	0.81	0.00
CHAC-1	0.99	0.00	0.60	0.00	0.71	0.00	0.11	0.14	1.00	0.00
CHAC-1-L	0.99	0.00	0.60	0.00	0.71	0.00	0.14	0.00	1.00	0.00
CHAC-2	0.99	0.00	0.60	0.00	0.71	0.00	0.12	0.14	1.00	0.00
CHAC-2-L	0.99	0.00	0.60	0.00	0.71	0.00	0.12	0.15	1.00	0.00
MOACS-1	0.99	0.00	0.72	0.07	0.73	0.01	0.32	0.04	0.81	0.00
MOACS-1-S-CDAS	0.99	0.00	0.71	0.01	0.73	0.01	0.30	0.03	0.85	0.00
MOACS-1-L	0.99	0.00	0.68	0.01	0.74	0.01	0.31	0.04	0.81	0.00
MOACS-2	0.99	0.00	0.66	0.01	0.73	0.00	0.39	0.13	0.81	0.00
MOACS-2-S-CDAS	0.99	0.00	0.66	0.01	0.74	0.01	0.43	0.00	0.83	0.00
MOACS-2-L	0.99	0.00	0.69	0.01	0.73	0.00	0.48	0.09	0.83	0.00
DMOPSO-5	0.99	0.00	0.60	0.00	0.71	0.00	0.14	0.01	1.00	0.00
DMOPSO-1	0.99	0.00	0.60	0.00	0.71	0.00	0.13	0.14	1.00	0.00
DMOPSO-2	0.99	0.00	0.60	0.00	0.71	0.00	0.15	0.01	1.00	0.00
DMOPSO-3	0.99	0.00	0.60	0.00	0.71	0.00	0.16	0.01	1.00	0.00
DMOPSO-4	0.99	0.00	0.60	0.00	0.72	0.00	0.15	0.00	0.92	0.19
DMOPSO-1-L	0.99	0.00	0.60	0.00	0.72	0.00	0.12	0.14	1.00	0.00
NSGA-II	0.99	0.00	0.60	0.00	0.71	0.00	0.16	0.00	1.00	0.00
NSGA-II-L	0.99	0.00	0.60	0.00	0.71	0.00	0.16	0.00	1.00	0.00
SPEA2	0.99	0.00	0.60	0.00	0.71	0.00	0.10	0.14	1.00	0.00
SPEA2-L	0.99	0.00	0.60	0.00	0.71	0.00	0.18	0.01	1.00	0.00

Table D.44: Median and interquartile range of I_{Δ} obtained by the optimisers for the Jackson problems

	Jackson-1 $\tilde{x} \pm IQR(x)$		Jackson-2 $\tilde{x} \pm IQR(x)$		Jackson-3 $\tilde{x} \pm IQR(x)$		Jackson-4 $\tilde{x} \pm IQR(x)$		Jackson-5 $\tilde{x} \pm IQR(x)$	
BIANT-1	0.92	0.00	0.92	0.05	0.78	0.04	0.78	0.07	0.80	0.04
BIANT-2	0.93	0.03	0.89	0.03	0.82	0.01	0.85	0.10	0.81	0.05
CHAC-1	1.00	0.00	1.00	0.00	0.85	0.01	0.85	0.07	0.85	0.00
CHAC-1-L	1.00	0.00	1.00	0.00	0.86	0.01	0.86	0.10	0.85	0.00
CHAC-2	1.00	0.00	1.00	0.00	0.86	0.01	0.85	0.06	0.85	0.00
CHAC-2-L	1.00	0.00	1.00	0.00	0.86	0.01	0.85	0.04	0.85	0.00
MOACS-1	0.93	0.02	0.90	0.03	0.71	0.03	0.79	0.19	0.86	0.03
MOACS-1-S-CDAS	0.93	0.01	0.90	0.04	0.70	0.09	0.78	0.25	0.85	0.04
MOACS-1-L	0.93	0.05	0.89	0.04	0.70	0.08	0.83	0.22	0.87	0.02
MOACS-2	0.89	0.02	0.86	0.05	0.74	0.07	0.77	0.17	0.85	0.05
MOACS-2-S-CDAS	0.90	0.03	0.87	0.03	0.76	0.04	0.87	0.07	0.85	0.01
MOACS-2-L	0.90	0.02	0.86	0.03	0.73	0.09	0.86	0.10	0.86	0.03
DMOPSO-5	1.00	0.00	1.00	0.00	0.86	0.01	0.86	0.07	0.85	0.00
DMOPSO-1	1.00	0.00	1.00	0.00	0.85	0.01	0.87	0.10	0.85	0.00
DMOPSO-2	1.00	0.00	1.00	0.00	0.86	0.02	0.88	0.05	0.85	0.00
DMOPSO-3	1.00	0.00	1.00	0.00	0.86	0.01	0.88	0.03	0.85	0.00
DMOPSO-4	1.00	0.00	1.00	0.01	0.85	0.05	0.91	0.05	0.86	0.02
DMOPSO-1-L	1.00	0.00	1.00	0.00	0.86	0.01	0.85	0.06	0.85	0.00
NSGA-II	1.00	0.00	1.00	0.00	0.85	0.01	0.89	0.03	0.85	0.00
NSGA-II-L	1.00	0.00	1.00	0.00	0.86	0.01	0.87	0.09	0.85	0.00
SPEA2	1.00	0.00	1.00	0.00	0.86	0.01	0.86	0.06	0.85	0.00
SPEA2-L	1.00	0.00	1.00	0.00	0.86	0.01	0.88	0.05	0.85	0.00

Table D.45: Median and interquartile range of the computation time required by the optimisers for the Jackson problems

	Jackson-1 $\tilde{x} \pm IQR(x)$		Jackson-2 $\tilde{x} \pm IQR(x)$		Jackson-3 $\tilde{x} \pm IQR(x)$		Jackson-4 $\tilde{x} \pm IQR(x)$		Jackson-5 $\tilde{x} \pm IQR(x)$	
BIANT-1	0.45	0.04	0.03	0.00	0.04	0.00	0.34	0.01	0.11	0.00
BIANT-2	0.43	0.05	0.03	0.00	0.04	0.00	0.36	0.02	0.11	0.01
CHAC-1	0.34	0.01	0.02	0.00	0.03	0.00	0.27	0.00	0.09	0.00
CHAC-1-L	0.28	0.10	0.02	0.01	0.03	0.01	0.21	0.09	0.07	0.03
CHAC-2	0.33	0.00	0.02	0.00	0.03	0.00	0.26	0.00	0.09	0.00
CHAC-2-L	0.29	0.11	0.02	0.01	0.03	0.01	0.23	0.11	0.07	0.03
MOACS-1	0.45	0.01	0.03	0.00	0.04	0.00	0.31	0.01	0.10	0.00
MOACS-1-S-CDAS	0.67	0.25	0.13	0.02	0.23	0.04	0.42	0.06	0.40	0.09
MOACS-1-L	0.46	0.01	0.03	0.00	0.04	0.00	0.32	0.01	0.10	0.00
MOACS-2	0.50	0.05	0.04	0.00	0.04	0.00	0.37	0.00	0.10	0.00
MOACS-2-S-CDAS	0.83	0.07	0.05	0.01	0.36	0.03	0.44	0.18	0.50	0.05
MOACS-2-L	0.51	0.03	0.04	0.00	0.04	0.00	0.36	0.02	0.10	0.00
DMOPSO-5	0.31	0.01	0.02	0.00	0.03	0.00	0.25	0.01	0.08	0.00
DMOPSO-1	0.25	0.10	0.02	0.01	0.03	0.01	0.20	0.10	0.06	0.03
DMOPSO-2	0.31	0.00	0.02	0.00	0.03	0.00	0.25	0.00	0.08	0.00
DMOPSO-3	0.25	0.02	0.02	0.00	0.12	0.00	0.19	0.01	0.06	0.00
DMOPSO-4	0.29	0.04	0.02	0.00	0.03	0.00	0.22	0.02	0.07	0.00
DMOPSO-1-L	0.31	0.00	0.02	0.00	0.03	0.00	0.25	0.00	0.08	0.00
NSGA-II	0.45	0.01	0.03	0.00	0.04	0.00	0.34	0.00	0.10	0.00
NSGA-II-L	0.34	0.09	0.02	0.00	0.02	0.00	0.21	0.00	0.05	0.00
SPEA2	0.28	0.00	0.02	0.00	0.03	0.00	0.23	0.00	0.08	0.00
SPEA2-L	0.31	0.05	0.02	0.00	0.03	0.00	0.23	0.01	0.08	0.00

Table D.43: Median and interquartile range of I_ϵ obtained by the optimisers for the Jackson problems

	Jackson-1 $\tilde{x} \pm IQR(x)$		Jackson-2 $\tilde{x} \pm IQR(x)$		Jackson-3 $\tilde{x} \pm IQR(x)$		Jackson-4 $\tilde{x} \pm IQR(x)$		Jackson-5 $\tilde{x} \pm IQR(x)$	
BIANT-1	0.93	0.03	0.77	0.24	0.39	0.00	0.56	0.37	0.38	0.00
BIANT-2	0.95	0.04	0.49	0.68	0.41	0.04	0.54	0.37	0.38	0.00
CHAC-1	0.17	0.00	0.19	0.00	0.35	0.00	0.15	0.04	0.37	0.00
CHAC-1-L	0.17	0.00	0.19	0.00	0.35	0.00	0.16	0.00	0.37	0.00
CHAC-2	0.17	0.00	0.19	0.00	0.35	0.00	0.15	0.04	0.37	0.00
CHAC-2-L	0.17	0.00	0.19	0.00	0.35	0.00	0.15	0.04	0.37	0.00
MOACS-1	0.30	0.00	0.39	0.20	0.41	0.05	0.17	0.00	0.37	0.00
MOACS-1-S-CDAS	0.27	0.00	0.33	0.00	0.38	0.04	0.17	0.00	0.37	0.00
MOACS-1-L	0.43	0.58	0.27	0.00	0.39	0.02	0.17	0.00	0.37	0.00
MOACS-2	0.20	0.02	0.19	0.00	0.59	0.21	0.21	0.02	0.37	0.00
MOACS-2-S-CDAS	0.20	0.02	0.19	0.00	0.63	0.29	0.19	0.01	0.37	0.00
MOACS-2-L	0.20	0.02	0.27	0.01	0.50	0.09	0.21	0.00	0.37	0.00
DMOPSO-5	0.17	0.00	0.19	0.00	0.35	0.00	0.16	0.00	0.37	0.00
DMOPSO-1	0.17	0.00	0.19	0.00	0.35	0.00	0.16	0.04	0.37	0.00
DMOPSO-2	0.17	0.00	0.19	0.00	0.35	0.00	0.16	0.00	0.37	0.00
DMOPSO-3	0.17	0.00	0.19	0.00	0.35	0.00	0.17	0.00	0.37	0.00
DMOPSO-4	0.17	0.00	0.19	0.00	0.36	0.03	0.16	0.00	0.37	0.00
DMOPSO-1-L	0.17	0.00	0.19	0.00	0.35	0.00	0.15	0.04	0.37	0.00
NSGA-II	0.17	0.00	0.19	0.00	0.35	0.00	0.16	0.00	0.37	0.00
NSGA-II-L	0.17	0.00	0.19	0.00	0.35	0.00	0.16	0.00	0.37	0.00
SPEA2	0.17	0.00	0.19	0.00	0.35	0.00	0.16	0.03	0.37	0.00
SPEA2-L	0.17	0.00	0.19	0.00	0.35	0.00	0.17	0.00	0.37	0.00

D.1.6 Problem Family: Lutz1

Table D.46: Median and interquartile range of I_{HV} obtained by the optimisers for the Lutz1 problems

	Lutz1-1		Lutz1-2		Lutz1-3		Lutz1-4		Lutz1-5	
	$\tilde{x}$	$IQR(x)$	$\tilde{x}$	$IQR(x)$	$\tilde{x}$	$IQR(x)$	$\tilde{x}$	$IQR(x)$	$\tilde{x}$	$IQR(x)$
BIANT-1	0.89	0.00	0.94	0.03	0.91	0.03	0.90	0.02	0.88	0.02
BIANT-2	0.89	0.00	0.91	0.05	0.88	0.02	0.87	0.05	0.88	0.03
CHAC-1	0.91	0.00	1.00	0.00	1.00	0.00	1.00	0.00	1.00	0.00
CHAC-1-L	0.91	0.00	1.00	0.00	1.00	0.00	1.00	0.00	1.00	0.00
CHAC-2	0.91	0.00	1.00	0.00	1.00	0.00	1.00	0.00	1.00	0.00
CHAC-2-L	0.91	0.00	1.00	0.00	1.00	0.00	1.00	0.00	1.00	0.00
MOACS-1	0.89	0.00	0.88	0.08	0.81	0.10	0.78	0.13	0.75	0.09
MOACS-1-S-CDAS	0.88	0.00	0.90	0.10	0.79	0.11	0.76	0.06	0.78	0.08
MOACS-1-L	0.89	0.00	0.88	0.09	0.81	0.10	0.75	0.08	0.75	0.08
MOACS-2	0.89	0.00	0.86	0.02	0.73	0.03	0.78	0.03	0.79	0.07
MOACS-2-S-CDAS	0.89	0.00	0.82	0.06	0.75	0.07	0.77	0.03	0.80	0.04
MOACS-2-L	0.89	0.00	0.84	0.02	0.71	0.02	0.72	0.05	0.78	0.07
DMOPSO-5	0.91	0.00	1.00	0.00	1.00	0.00	1.00	0.00	1.00	0.00
DMOPSO-1	0.91	0.00	1.00	0.00	1.00	0.00	1.00	0.00	1.00	0.00
DMOPSO-2	0.91	0.00	1.00	0.00	1.00	0.00	1.00	0.00	1.00	0.00
DMOPSO-3	0.91	0.00	1.00	0.00	1.00	0.00	1.00	0.00	1.00	0.00
DMOPSO-4	0.91	0.00	1.00	0.00	1.00	0.00	1.00	0.00	1.00	0.00
DMOPSO-1-L	0.91	0.00	1.00	0.00	1.00	0.00	1.00	0.00	1.00	0.00
NSGA-II	0.91	0.00	1.00	0.00	1.00	0.00	1.00	0.00	1.00	0.00
NSGA-II-L	0.91	0.00	1.00	0.00	1.00	0.00	1.00	0.00	1.00	0.00
SPEA2	0.91	0.00	1.00	0.00	1.00	0.00	1.00	0.00	1.00	0.00
SPEA2-L	0.91	0.00	1.00	0.00	1.00	0.00	1.00	0.00	1.00	0.00

Table D.47: Median and interquartile range of I_{IGD} obtained by the optimisers for the Lutz1 problems

	Lutz1-1 $\tilde{x} \pm IQR(x)$		Lutz1-2 $\tilde{x} \pm IQR(x)$		Lutz1-3 $\tilde{x} \pm IQR(x)$		Lutz1-4 $\tilde{x} \pm IQR(x)$		Lutz1-5 $\tilde{x} \pm IQR(x)$	
BIANT-1	1.00	0.00	0.47	0.14	0.33	0.12	0.39	0.07	0.45	0.05
BIANT-2	1.00	0.00	0.36	0.11	0.53	0.14	0.47	0.07	0.51	0.06
CHAC-1	0.92	0.00	0.00	0.00	0.00	0.00	0.01	0.00	0.00	0.00
CHAC-1-L	0.92	0.00	0.00	0.00	0.00	0.00	0.01	0.00	0.00	0.00
CHAC-2	0.92	0.00	0.00	0.00	0.00	0.00	0.01	0.00	0.00	0.00
CHAC-2-L	0.92	0.00	0.00	0.00	0.00	0.00	0.01	0.00	0.00	0.00
MOACS-1	1.00	0.00	0.50	0.17	0.63	0.30	0.76	0.31	0.73	0.18
MOACS-1-S-CDAS	0.93	0.00	0.49	0.11	0.68	0.27	0.76	0.21	0.65	0.16
MOACS-1-L	1.00	0.00	0.51	0.16	0.61	0.25	0.78	0.27	0.74	0.12
MOACS-2	1.00	0.00	0.55	0.06	0.77	0.07	0.71	0.08	0.65	0.23
MOACS-2-S-CDAS	1.00	0.00	0.64	0.12	0.73	0.22	0.70	0.08	0.61	0.08
MOACS-2-L	1.00	0.00	0.59	0.09	0.84	0.09	0.85	0.15	0.69	0.17
DMOPSO-5	0.92	0.00	0.00	0.00	0.00	0.00	0.01	0.00	0.00	0.00
DMOPSO-1	0.92	0.00	0.00	0.00	0.00	0.00	0.01	0.00	0.00	0.00
DMOPSO-2	0.92	0.00	0.00	0.00	0.00	0.00	0.01	0.00	0.00	0.00
DMOPSO-3	0.92	0.00	0.00	0.00	0.00	0.00	0.01	0.01	0.00	0.00
DMOPSO-4	0.92	0.00	0.05	0.12	0.03	0.01	0.03	0.01	0.01	0.01
DMOPSO-1-L	0.92	0.00	0.00	0.00	0.00	0.00	0.01	0.00	0.00	0.00
NSGA-II	0.92	0.00	0.00	0.00	0.00	0.00	0.01	0.00	0.00	0.00
NSGA-II-L	0.92	0.00	0.00	0.00	0.00	0.00	0.01	0.00	0.00	0.00
SPEA2	0.92	0.00	0.00	0.00	0.00	0.00	0.01	0.00	0.00	0.00
SPEA2-L	0.92	0.00	0.00	0.00	0.00	0.00	0.01	0.00	0.00	0.00

Table D.49: Median and interquartile range of I_{Δ} obtained by the optimisers for the Lutz1 problems

	Lutz1-1 $\tilde{x} \pm IQR(x)$		Lutz1-2 $\tilde{x} \pm IQR(x)$		Lutz1-3 $\tilde{x} \pm IQR(x)$		Lutz1-4 $\tilde{x} \pm IQR(x)$		Lutz1-5 $\tilde{x} \pm IQR(x)$	
BIANT-1	1.00	0.00	0.87	0.08	0.80	0.11	0.78	0.21	0.77	0.06
BIANT-2	1.00	0.00	0.87	0.08	0.91	0.08	0.84	0.10	0.82	0.03
CHAC-1	0.98	0.00	0.93	0.00	0.93	0.00	0.97	0.01	0.98	0.00
CHAC-1-L	0.98	0.00	0.93	0.00	0.93	0.00	0.97	0.01	0.98	0.00
CHAC-2	0.98	0.00	0.93	0.00	0.93	0.00	0.97	0.02	0.98	0.00
CHAC-2-L	0.98	0.00	0.93	0.00	0.94	0.00	0.97	0.01	0.98	0.00
MOACS-1	1.00	0.00	0.90	0.03	0.75	0.22	0.75	0.18	0.78	0.09
MOACS-1-S-CDAS	0.92	0.00	0.89	0.08	0.78	0.09	0.82	0.11	0.69	0.14
MOACS-1-L	1.00	0.00	0.88	0.11	0.80	0.05	0.72	0.17	0.78	0.03
MOACS-2	1.00	0.00	0.88	0.02	0.82	0.13	0.74	0.14	0.77	0.12
MOACS-2-S-CDAS	1.00	0.00	0.80	0.18	0.79	0.10	0.80	0.03	0.74	0.14
MOACS-2-L	1.00	0.00	0.80	0.16	0.81	0.10	0.78	0.16	0.71	0.22
DMOPSO-5	0.98	0.00	0.93	0.00	0.93	0.00	0.98	0.00	0.98	0.00
DMOPSO-1	0.98	0.00	0.93	0.00	0.92	0.00	0.97	0.01	0.98	0.00
DMOPSO-2	0.98	0.00	0.93	0.00	0.93	0.00	0.97	0.01	0.98	0.00
DMOPSO-3	0.98	0.00	0.93	0.00	0.92	0.00	0.97	0.01	0.98	0.00
DMOPSO-4	0.98	0.00	0.96	0.07	0.91	0.03	0.95	0.04	0.97	0.03
DMOPSO-1-L	0.98	0.00	0.93	0.00	0.93	0.00	0.97	0.01	0.98	0.00
NSGA-II	0.98	0.00	0.93	0.00	0.93	0.00	0.97	0.02	0.98	0.00
NSGA-II-L	0.98	0.00	0.93	0.00	0.93	0.00	0.98	0.01	0.98	0.00
SPEA2	0.98	0.00	0.93	0.00	0.93	0.00	0.97	0.00	0.98	0.00
SPEA2-L	0.98	0.00	0.93	0.00	0.93	0.00	0.98	0.02	0.98	0.00

Table D.50: Median and interquartile range of the computation time required by the optimisers for the Lutz1 problems

	Lutz1-1 $\tilde{x} \pm IQR(x)$		Lutz1-2 $\tilde{x} \pm IQR(x)$		Lutz1-3 $\tilde{x} \pm IQR(x)$		Lutz1-4 $\tilde{x} \pm IQR(x)$		Lutz1-5 $\tilde{x} \pm IQR(x)$	
BIANT-1	0.09	0.00	0.07	0.00	0.06	0.00	0.08	0.01	0.06	0.01
BIANT-2	0.09	0.00	0.08	0.00	0.06	0.00	0.07	0.01	0.06	0.00
CHAC-1	0.08	0.00	0.06	0.00	0.05	0.00	0.05	0.00	0.05	0.00
CHAC-1-L	0.07	0.01	0.06	0.01	0.05	0.00	0.05	0.01	0.05	0.01
CHAC-2	0.08	0.00	0.06	0.00	0.05	0.00	0.05	0.00	0.05	0.00
CHAC-2-L	0.08	0.00	0.07	0.00	0.05	0.00	0.06	0.01	0.05	0.01
MOACS-1	0.12	0.00	0.08	0.00	0.06	0.00	0.08	0.01	0.06	0.00
MOACS-1-S-CDAS	0.73	0.26	0.78	0.18	0.67	0.15	0.69	0.23	0.62	0.11
MOACS-1-L	0.12	0.00	0.09	0.00	0.06	0.00	0.07	0.00	0.06	0.00
MOACS-2	0.13	0.00	0.10	0.00	0.07	0.00	0.08	0.01	0.08	0.01
MOACS-2-S-CDAS	0.72	0.02	0.61	0.07	0.46	0.09	0.61	0.07	0.54	0.09
MOACS-2-L	0.13	0.00	0.10	0.01	0.08	0.00	0.08	0.00	0.07	0.00
DMOPSO-5	0.06	0.00	0.05	0.00	0.04	0.00	0.04	0.00	0.04	0.00
DMOPSO-1	0.05	0.02	0.05	0.01	0.03	0.01	0.04	0.01	0.04	0.01
DMOPSO-2	0.06	0.00	0.05	0.00	0.04	0.00	0.05	0.00	0.04	0.00
DMOPSO-3	0.06	0.01	0.05	0.01	0.04	0.00	0.04	0.00	0.04	0.01
DMOPSO-4	0.07	0.00	0.06	0.01	0.05	0.00	0.06	0.01	0.05	0.01
DMOPSO-1-L	0.06	0.00	0.05	0.00	0.04	0.00	0.05	0.00	0.04	0.00
NSGA-II	0.10	0.00	0.07	0.00	0.05	0.00	0.06	0.00	0.05	0.00
NSGA-II-L	0.07	0.00	0.05	0.00	0.03	0.00	0.04	0.00	0.04	0.01
SPEA2	0.05	0.00	0.04	0.00	0.03	0.00	0.03	0.00	0.03	0.00
SPEA2-L	0.05	0.00	0.04	0.00	0.03	0.00	0.03	0.00	0.03	0.00

Table D.48: Median and interquartile range of I_ϵ obtained by the optimisers for the Lutz1 problems

	Lutz1-1 $\tilde{x} \pm IQR(x)$		Lutz1-2 $\tilde{x} \pm IQR(x)$		Lutz1-3 $\tilde{x} \pm IQR(x)$		Lutz1-4 $\tilde{x} \pm IQR(x)$		Lutz1-5 $\tilde{x} \pm IQR(x)$	
BIANT-1	1.00	0.00	0.87	0.02	0.86	0.02	0.74	0.01	0.58	0.19
BIANT-2	1.00	0.00	0.89	0.05	0.90	0.03	0.70	0.02	0.52	0.05
CHAC-1	0.89	0.00	0.78	0.00	0.75	0.00	0.62	0.00	0.42	0.00
CHAC-1-L	0.89	0.00	0.78	0.00	0.75	0.00	0.63	0.00	0.42	0.00
CHAC-2	0.89	0.00	0.78	0.00	0.75	0.00	0.62	0.00	0.42	0.00
CHAC-2-L	0.89	0.00	0.78	0.00	0.75	0.00	0.62	0.00	0.42	0.00
MOACS-1	1.00	0.00	0.88	0.02	0.92	0.11	0.86	0.21	0.82	0.20
MOACS-1-S-CDAS	0.93	0.00	0.88	0.02	0.93	0.10	0.86	0.13	0.75	0.09
MOACS-1-L	1.00	0.00	0.88	0.03	0.91	0.09	0.91	0.13	0.79	0.15
MOACS-2	1.00	0.00	0.90	0.00	0.96	0.03	0.84	0.02	0.72	0.21
MOACS-2-S-CDAS	1.00	0.00	0.91	0.01	0.95	0.05	0.86	0.03	0.67	0.11
MOACS-2-L	1.00	0.00	0.89	0.01	0.98	0.00	0.92	0.14	0.77	0.08
DMOPSO-5	0.89	0.00	0.78	0.00	0.75	0.00	0.62	0.00	0.42	0.00
DMOPSO-1	0.89	0.00	0.78	0.00	0.75	0.00	0.62	0.00	0.42	0.00
DMOPSO-2	0.89	0.00	0.78	0.00	0.75	0.00	0.62	0.00	0.42	0.00
DMOPSO-3	0.89	0.00	0.78	0.00	0.75	0.00	0.63	0.00	0.42	0.00
DMOPSO-4	0.89	0.00	0.78	0.00	0.75	0.00	0.63	0.01	0.42	0.01
DMOPSO-1-L	0.89	0.00	0.78	0.00	0.75	0.00	0.62	0.00	0.42	0.00
NSGA-II	0.89	0.00	0.78	0.00	0.75	0.00	0.62	0.00	0.42	0.00
NSGA-II-L	0.89	0.00	0.78	0.00	0.75	0.00	0.62	0.00	0.42	0.00
SPEA2	0.89	0.00	0.78	0.00	0.75	0.00	0.63	0.00	0.42	0.00
SPEA2-L	0.89	0.00	0.78	0.00	0.75	0.00	0.62	0.00	0.42	0.00

D.1.7 Problem Family: Kilbrid

Table D.51: Median and interquartile range of I_{HV} obtained by the optimisers for the Kilbrid problems

	Kilbrid-1 $\tilde{x} \pm IQR(x)$		Kilbrid-2 $\tilde{x} \pm IQR(x)$		Kilbrid-3 $\tilde{x} \pm IQR(x)$		Kilbrid-4 $\tilde{x} \pm IQR(x)$		Kilbrid-5 $\tilde{x} \pm IQR(x)$	
BIANT-1	0.48	0.11	0.90	0.06	0.87	0.06	0.83	0.03	0.89	0.06
BIANT-2	0.50	0.11	0.94	0.01	0.83	0.06	0.88	0.04	0.85	0.10
CHAC-1	0.74	0.01	0.97	0.02	0.94	0.01	0.95	0.02	0.95	0.01
CHAC-1-L	0.73	0.01	0.97	0.01	0.95	0.02	0.95	0.01	0.95	0.01
CHAC-2	0.74	0.01	0.97	0.01	0.95	0.01	0.95	0.02	0.94	0.01
CHAC-2-L	0.73	0.00	0.97	0.01	0.95	0.01	0.96	0.01	0.95	0.01
MOACS-1	0.61	0.04	0.92	0.01	0.87	0.04	0.85	0.03	0.85	0.05
MOACS-1-S-CDAS	0.60	0.04	0.92	0.02	0.87	0.06	0.85	0.06	0.84	0.03
MOACS-1-L	0.59	0.01	0.92	0.03	0.86	0.06	0.87	0.06	0.86	0.04
MOACS-2	0.54	0.11	0.94	0.01	0.84	0.05	0.84	0.02	0.85	0.03
MOACS-2-S-CDAS	0.55	0.18	0.93	0.04	0.84	0.02	0.86	0.04	0.84	0.04
MOACS-2-L	0.55	0.11	0.94	0.02	0.84	0.03	0.86	0.01	0.86	0.02
DMOPSO-5	0.73	0.01	0.97	0.01	0.95	0.01	0.95	0.02	0.95	0.01
DMOPSO-1	0.74	0.01	0.97	0.00	0.95	0.01	0.95	0.01	0.95	0.01
DMOPSO-2	0.73	0.01	0.97	0.02	0.94	0.01	0.95	0.01	0.94	0.01
DMOPSO-3	0.74	0.00	0.97	0.01	0.95	0.01	0.95	0.02	0.95	0.01
DMOPSO-4	0.72	0.01	0.96	0.02	0.92	0.02	0.95	0.02	0.93	0.03
DMOPSO-1-L	0.73	0.01	0.96	0.01	0.94	0.02	0.95	0.02	0.95	0.01
NSGA-II	0.74	0.01	0.97	0.00	0.94	0.02	0.95	0.01	0.94	0.01
NSGA-II-L	0.74	0.00	0.97	0.01	0.93	0.02	0.93	0.01	0.95	0.01
SPEA2	0.73	0.01	0.97	0.01	0.95	0.02	0.95	0.01	0.94	0.01
SPEA2-L	0.74	0.01	0.97	0.02	0.94	0.02	0.95	0.01	0.95	0.01

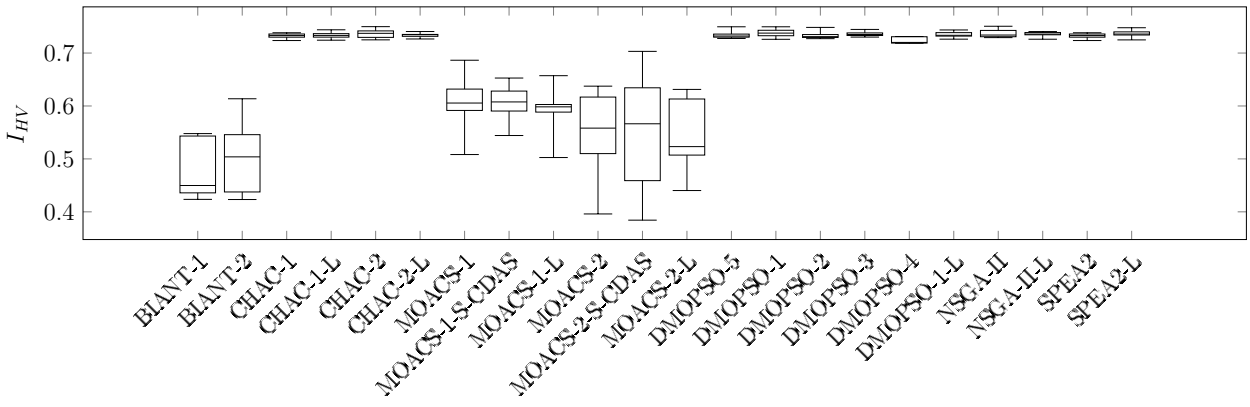

Figure D.21: Boxplot for I_{HV}: Kilbrid-1

Table D.52: Median and interquartile range of I_{IGD} obtained by the optimisers for the Kilbrid problems

	Kilbrid-1 $\tilde{x} \pm IQR(x)$		Kilbrid-2 $\tilde{x} \pm IQR(x)$		Kilbrid-3 $\tilde{x} \pm IQR(x)$		Kilbrid-4 $\tilde{x} \pm IQR(x)$		Kilbrid-5 $\tilde{x} \pm IQR(x)$	
BIANT-1	0.75	0.14	0.68	0.22	0.65	0.09	0.69	0.11	0.23	0.16
BIANT-2	0.59	0.23	0.55	0.03	0.72	0.03	0.54	0.13	0.31	0.19
CHAC-1	0.18	0.00	0.28	0.02	0.43	0.04	0.30	0.07	0.16	0.02
CHAC-1-L	0.18	0.00	0.28	0.05	0.43	0.04	0.29	0.02	0.16	0.01
CHAC-2	0.18	0.00	0.36	0.11	0.44	0.06	0.29	0.02	0.17	0.01
CHAC-2-L	0.18	0.00	0.28	0.01	0.43	0.03	0.29	0.02	0.16	0.01
MOACS-1	0.37	0.07	0.60	0.03	0.60	0.03	0.62	0.10	0.46	0.18
MOACS-1-S-CDAS	0.37	0.08	0.59	0.04	0.63	0.09	0.63	0.13	0.45	0.17
MOACS-1-L	0.40	0.04	0.60	0.03	0.65	0.03	0.63	0.12	0.49	0.16
MOACS-2	0.54	0.27	0.58	0.03	0.64	0.05	0.61	0.08	0.45	0.07
MOACS-2-S-CDAS	0.54	0.44	0.62	0.07	0.61	0.07	0.62	0.09	0.54	0.20
MOACS-2-L	0.53	0.26	0.55	0.03	0.62	0.12	0.59	0.10	0.45	0.17
DMOPSO-5	0.18	0.00	0.29	0.04	0.45	0.02	0.31	0.06	0.16	0.01
DMOPSO-1	0.17	0.00	0.27	0.04	0.47	0.02	0.31	0.03	0.17	0.01
DMOPSO-2	0.18	0.00	0.34	0.22	0.47	0.04	0.31	0.05	0.18	0.02
DMOPSO-3	0.18	0.00	0.25	0.08	0.47	0.01	0.30	0.01	0.16	0.02
DMOPSO-4	0.18	0.00	0.33	0.08	0.53	0.09	0.32	0.06	0.21	0.03
DMOPSO-1-L	0.18	0.00	0.41	0.24	0.46	0.03	0.29	0.03	0.17	0.01
NSGA-II	0.17	0.00	0.28	0.06	0.46	0.04	0.31	0.02	0.17	0.01
NSGA-II-L	0.18	0.00	0.29	0.02	0.48	0.06	0.38	0.05	0.16	0.01
SPEA2	0.18	0.00	0.32	0.06	0.44	0.04	0.30	0.04	0.17	0.01
SPEA2-L	0.18	0.00	0.31	0.02	0.46	0.04	0.30	0.02	0.17	0.02

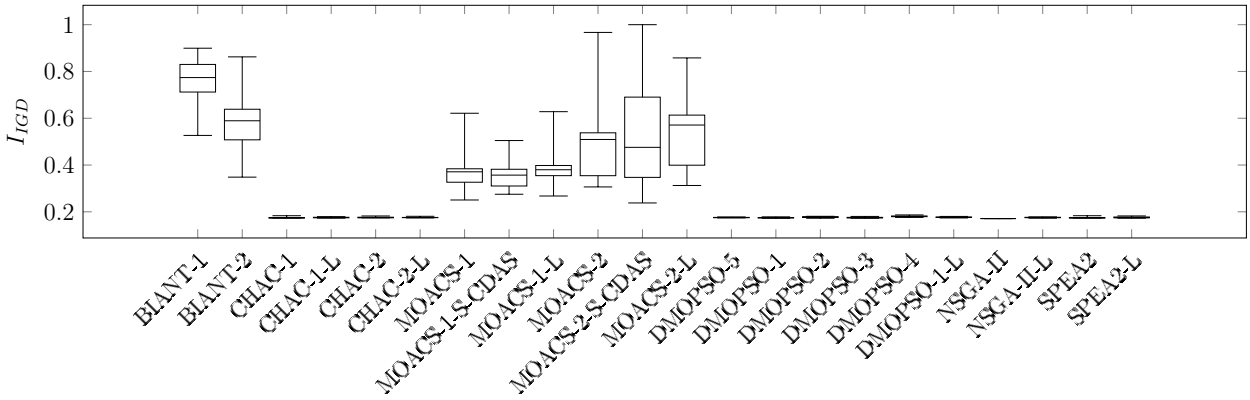

Figure D.22: Boxplot for I_{IGD}: Kilbrid-1

Table D.53: Median and interquartile range of I_ϵ obtained by the optimisers for the Kilbrid problems

	Kilbrid-1 $\tilde{x} \pm IQR(x)$		Kilbrid-2 $\tilde{x} \pm IQR(x)$		Kilbrid-3 $\tilde{x} \pm IQR(x)$		Kilbrid-4 $\tilde{x} \pm IQR(x)$		Kilbrid-5 $\tilde{x} \pm IQR(x)$	
BIANT-1	0.95	0.06	0.93	0.03	0.84	0.07	0.90	0.02	0.76	0.08
BIANT-2	0.94	0.06	0.91	0.01	0.89	0.07	0.84	0.05	0.80	0.10
CHAC-1	0.87	0.00	0.90	0.02	0.75	0.00	0.75	0.01	0.69	0.01
CHAC-1-L	0.87	0.00	0.90	0.01	0.75	0.00	0.74	0.02	0.69	0.01
CHAC-2	0.87	0.00	0.90	0.01	0.75	0.00	0.75	0.01	0.69	0.01
CHAC-2-L	0.87	0.00	0.90	0.02	0.75	0.00	0.75	0.00	0.68	0.01
MOACS-1	0.89	0.02	0.93	0.01	0.85	0.03	0.89	0.04	0.81	0.05
MOACS-1-S-CDAS	0.89	0.02	0.92	0.01	0.86	0.09	0.89	0.07	0.83	0.03
MOACS-1-L	0.90	0.01	0.92	0.02	0.85	0.07	0.87	0.08	0.81	0.04
MOACS-2	0.92	0.05	0.92	0.01	0.89	0.06	0.92	0.03	0.83	0.03
MOACS-2-S-CDAS	0.92	0.08	0.93	0.03	0.90	0.03	0.89	0.05	0.84	0.04
MOACS-2-L	0.92	0.05	0.92	0.01	0.89	0.03	0.89	0.01	0.82	0.03
DMOPSO-5	0.87	0.00	0.90	0.01	0.75	0.00	0.75	0.00	0.69	0.01
DMOPSO-1	0.87	0.00	0.90	0.01	0.75	0.00	0.75	0.01	0.69	0.01
DMOPSO-2	0.87	0.00	0.90	0.01	0.75	0.00	0.75	0.01	0.69	0.01
DMOPSO-3	0.87	0.00	0.90	0.01	0.75	0.00	0.75	0.01	0.69	0.01
DMOPSO-4	0.87	0.00	0.91	0.01	0.76	0.02	0.75	0.00	0.70	0.01
DMOPSO-1-L	0.87	0.00	0.91	0.00	0.75	0.00	0.75	0.01	0.69	0.00
NSGA-II	0.87	0.00	0.90	0.01	0.75	0.00	0.75	0.00	0.69	0.01
NSGA-II-L	0.87	0.00	0.90	0.01	0.75	0.01	0.76	0.00	0.69	0.02
SPEA2	0.87	0.00	0.90	0.01	0.75	0.00	0.74	0.01	0.69	0.01
SPEA2-L	0.87	0.00	0.90	0.01	0.75	0.00	0.75	0.00	0.69	0.01

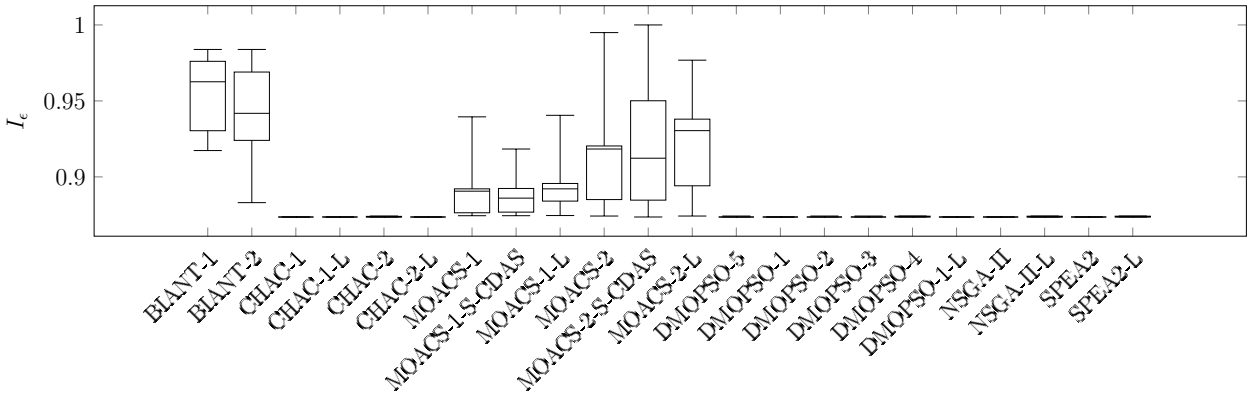

Figure D.23: Boxplot for I_ϵ: Kilbrid-1

Table D.54: Median and interquartile range of I_Δ obtained by the optimisers for the Kilbrid problems

	Kilbrid-1 $\tilde{x} \pm IQR(x)$		Kilbrid-2 $\tilde{x} \pm IQR(x)$		Kilbrid-3 $\tilde{x} \pm IQR(x)$		Kilbrid-4 $\tilde{x} \pm IQR(x)$		Kilbrid-5 $\tilde{x} \pm IQR(x)$	
BIANT-1	0.85	0.07	0.78	0.12	0.82	0.15	0.82	0.03	0.90	0.02
BIANT-2	0.86	0.10	0.90	0.09	0.88	0.03	0.86	0.09	0.98	0.02
CHAC-1	0.86	0.04	0.65	0.06	0.76	0.10	0.78	0.07	0.76	0.06
CHAC-1-L	0.87	0.05	0.63	0.11	0.78	0.06	0.80	0.05	0.74	0.06
CHAC-2	0.87	0.05	0.68	0.12	0.77	0.07	0.78	0.04	0.76	0.10
CHAC-2-L	0.87	0.03	0.62	0.06	0.79	0.05	0.74	0.03	0.76	0.08
MOACS-1	0.90	0.05	0.84	0.07	0.81	0.12	0.80	0.03	0.84	0.08
MOACS-1-S-CDAS	0.85	0.08	0.84	0.10	0.79	0.12	0.83	0.07	0.83	0.06
MOACS-1-L	0.82	0.05	0.75	0.13	0.82	0.05	0.82	0.06	0.82	0.13
MOACS-2	0.90	0.09	0.85	0.07	0.90	0.05	0.85	0.05	0.89	0.05
MOACS-2-S-CDAS	0.91	0.06	0.87	0.16	0.82	0.06	0.88	0.03	0.87	0.04
MOACS-2-L	0.88	0.05	0.91	0.06	0.87	0.08	0.86	0.06	0.91	0.08
DMOPSO-5	0.87	0.02	0.63	0.13	0.79	0.04	0.79	0.11	0.78	0.08
DMOPSO-1	0.87	0.03	0.66	0.10	0.77	0.10	0.77	0.12	0.79	0.04
DMOPSO-2	0.88	0.02	0.64	0.05	0.77	0.06	0.80	0.07	0.80	0.04
DMOPSO-3	0.87	0.01	0.64	0.09	0.77	0.06	0.78	0.02	0.75	0.11
DMOPSO-4	0.89	0.03	0.65	0.17	0.75	0.08	0.75	0.09	0.74	0.04
DMOPSO-1-L	0.88	0.04	0.66	0.10	0.80	0.09	0.81	0.06	0.78	0.07
NSGA-II	0.80	0.00	0.71	0.11	0.78	0.05	0.79	0.16	0.79	0.12
NSGA-II-L	0.87	0.01	0.68	0.08	0.77	0.08	0.73	0.07	0.74	0.06
SPEA2	0.87	0.03	0.67	0.06	0.80	0.05	0.74	0.06	0.80	0.06
SPEA2-L	0.87	0.03	0.65	0.07	0.77	0.07	0.79	0.07	0.73	0.10

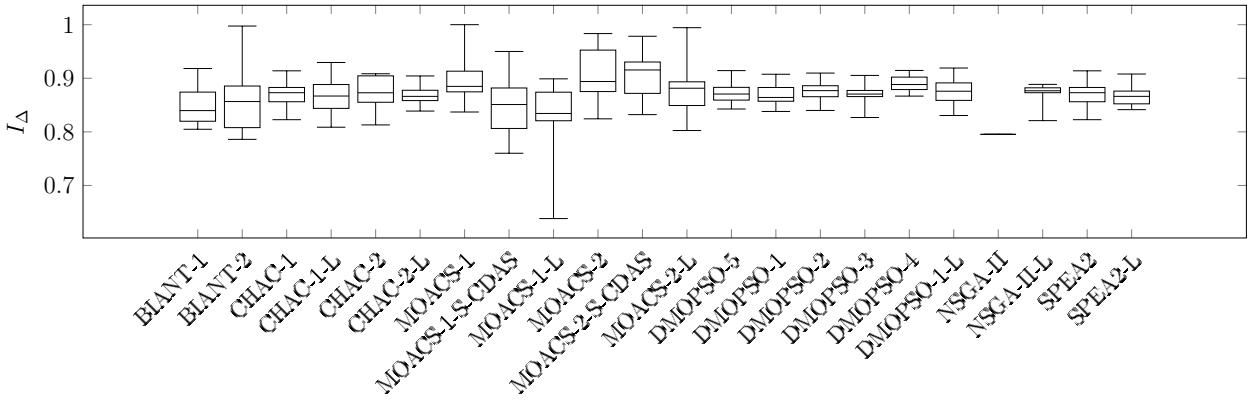

Figure D.24: Boxplot for I_Δ: Kilbrid-1

Table D.55: Median and interquartile range of the computation time required by the optimisers for the Kilbrid problems

	Kilbrid-1 $\tilde{x} \pm IQR(x)$		Kilbrid-2 $\tilde{x} \pm IQR(x)$		Kilbrid-3 $\tilde{x} \pm IQR(x)$		Kilbrid-4 $\tilde{x} \pm IQR(x)$		Kilbrid-5 $\tilde{x} \pm IQR(x)$	
BIANT-1	0.03	0.00	0.04	0.00	0.01	0.00	0.02	0.00	0.02	0.00
BIANT-2	0.03	0.00	0.04	0.00	0.02	0.00	0.02	0.00	0.02	0.00
CHAC-1	0.03	0.01	0.04	0.00	0.02	0.00	0.03	0.00	0.03	0.00
CHAC-1-L	0.03	0.00	0.04	0.01	0.02	0.00	0.03	0.01	0.03	0.01
CHAC-2	0.03	0.01	0.04	0.00	0.02	0.01	0.03	0.01	0.03	0.01
CHAC-2-L	0.03	0.01	0.03	0.01	0.02	0.01	0.03	0.01	0.03	0.00
MOACS-1	0.03	0.00	0.04	0.00	0.02	0.00	0.02	0.00	0.02	0.00
MOACS-1-S-CDAS	0.49	0.15	0.79	0.08	0.51	0.28	0.62	0.17	0.53	0.13
MOACS-1-L	0.03	0.00	0.04	0.00	0.02	0.00	0.03	0.00	0.02	0.01
MOACS-2	0.03	0.00	0.04	0.00	0.02	0.00	0.03	0.00	0.02	0.00
MOACS-2-S-CDAS	0.32	0.10	0.59	0.11	0.25	0.09	0.31	0.01	0.35	0.14
MOACS-2-L	0.03	0.00	0.04	0.00	0.02	0.00	0.03	0.01	0.02	0.00
DMOPSO	0.03	0.00	0.03	0.00	0.02	0.00	0.03	0.00	0.03	0.01
DMOPSO-1	0.02	0.00	0.03	0.01	0.01	0.00	0.02	0.00	0.02	0.01
DMOPSO-2	0.02	0.00	0.03	0.00	0.02	0.00	0.02	0.00	0.02	0.00
DMOPSO-3	0.03	0.00	0.03	0.00	0.02	0.01	0.03	0.01	0.03	0.02
DMOPSO-4	0.03	0.01	0.04	0.01	0.02	0.00	0.04	0.00	0.04	0.03
DMOPSO-L	0.02	0.00	0.03	0.00	0.02	0.01	0.03	0.01	0.02	0.01
NSGA-II	0.03	0.00	0.03	0.00	0.02	0.00	0.03	0.00	0.02	0.01
NSGA-II-L	0.02	0.01	0.02	0.00	0.01	0.00	0.02	0.01	0.02	0.01
SPEA2	0.02	0.00	0.02	0.00	0.01	0.00	0.02	0.01	0.02	0.00
SPEA2-L	0.02	0.00	0.03	0.00	0.01	0.00	0.02	0.00	0.01	0.00

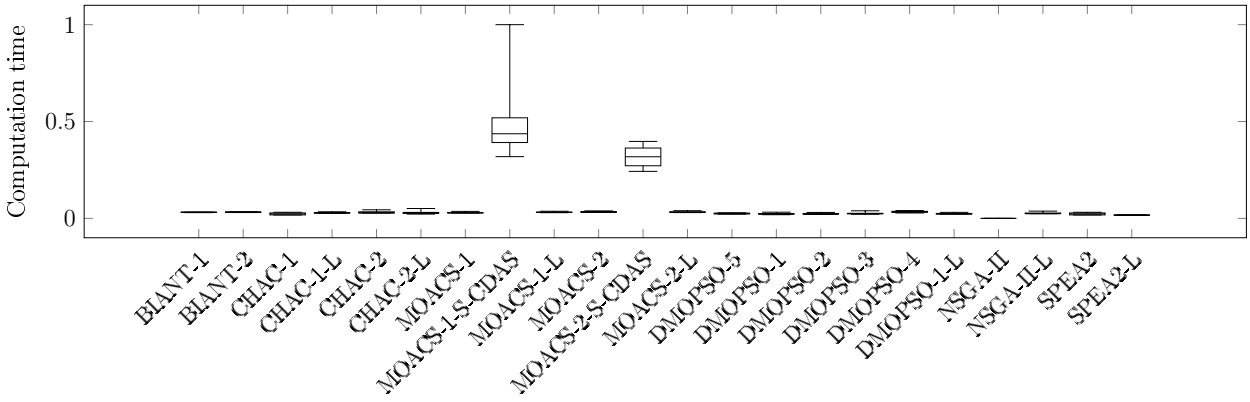

Figure D.25: Boxplot for the computation time: Kilbrid-1

D.1.8 Problem Family: Mitchell

Table D.56: Median and interquartile range of I_{HV} obtained by the optimisers for the Mitchell problems

	Mitchell-1 $\tilde{x} \pm IQR(x)$		Mitchell-2 $\tilde{x} \pm IQR(x)$		Mitchell-3 $\tilde{x} \pm IQR(x)$		Mitchell-4 $\tilde{x} \pm IQR(x)$	
BIANT-1	0.88	0.15	0.91	0.04	0.54	0.02	0.88	0.01
BIANT-2	0.84	0.22	0.91	0.01	0.53	0.01	0.88	0.00
CHAC-1	0.95	0.03	0.99	0.01	0.59	0.01	0.86	0.01
CHAC-1-L	0.96	0.03	0.99	0.02	0.59	0.01	0.87	0.01
CHAC-2	0.95	0.02	0.99	0.02	0.59	0.01	0.86	0.01
CHAC-2-L	0.97	0.01	0.99	0.02	0.59	0.00	0.87	0.00
MOACS-1	0.86	0.17	0.86	0.04	0.56	0.01	0.84	0.02
MOACS-1-S-CDAS	0.84	0.24	0.86	0.05	0.55	0.01	0.84	0.01
MOACS-1-L	0.87	0.18	0.86	0.05	0.55	0.02	0.84	0.00
MOACS-2	0.80	0.07	0.87	0.02	0.55	0.01	0.81	0.04
MOACS-2-S-CDAS	0.79	0.05	0.87	0.02	0.55	0.01	0.78	0.03
MOACS-2-L	0.80	0.07	0.86	0.05	0.55	0.02	0.79	0.08
DMOPSO-5	0.95	0.02	0.99	0.02	0.58	0.01	0.86	0.02
DMOPSO-1	0.95	0.03	0.99	0.01	0.58	0.00	0.87	0.02
DMOPSO-2	0.95	0.03	0.99	0.01	0.58	0.00	0.86	0.00
DMOPSO-3	0.96	0.01	0.99	0.01	0.59	0.01	0.87	0.01
DMOPSO-4	0.90	0.09	0.97	0.01	0.57	0.02	0.82	0.05
DMOPSO-1-L	0.95	0.03	0.99	0.02	0.59	0.01	0.86	0.01
NSGA-II	0.96	0.02	0.98	0.01	0.59	0.00	0.86	0.01
NSGA-II-L	0.95	0.04	0.99	0.01	0.58	0.01	0.87	0.01
SPEA2	0.95	0.04	0.99	0.01	0.59	0.01	0.86	0.01
SPEA2-L	0.95	0.02	0.99	0.02	0.59	0.01	0.86	0.02

,

Table D.57: Median and interquartile range of I_{IGD} obtained by the optimisers for the Mitchell problems

	Mitchell-1 $\tilde{x} \pm IQR(x)$		Mitchell-2 $\tilde{x} \pm IQR(x)$		Mitchell-3 $\tilde{x} \pm IQR(x)$		Mitchell-4 $\tilde{x} \pm IQR(x)$	
BIANT-1	0.41	0.22	0.52	0.38	0.92	0.04	0.47	0.25
BIANT-2	0.44	0.34	0.51	0.20	0.94	0.02	0.34	0.08
CHAC-1	0.10	0.03	0.19	0.12	0.86	0.02	0.34	0.14
CHAC-1-L	0.10	0.04	0.21	0.00	0.87	0.02	0.32	0.08
CHAC-2	0.10	0.03	0.19	0.11	0.86	0.00	0.38	0.12
CHAC-2-L	0.09	0.02	0.20	0.01	0.86	0.01	0.34	0.15
MOACS-1	0.30	0.09	0.76	0.23	0.93	0.00	0.60	0.25
MOACS-1-S-CDAS	0.43	0.61	0.67	0.08	0.93	0.01	0.55	0.46
MOACS-1-L	0.29	0.21	0.74	0.16	0.93	0.08	0.50	0.11
MOACS-2	0.37	0.10	0.71	0.19	0.92	0.03	0.84	0.06
MOACS-2-S-CDAS	0.30	0.07	0.68	0.25	0.94	0.02	0.76	0.06
MOACS-2-L	0.36	0.09	0.68	0.16	0.93	0.02	0.67	0.36
DMOPSO-5	0.10	0.02	0.17	0.15	0.88	0.03	0.36	0.09
DMOPSO-1	0.11	0.02	0.22	0.00	0.86	0.01	0.30	0.09
DMOPSO-2	0.11	0.02	0.14	0.17	0.88	0.03	0.34	0.10
DMOPSO-3	0.09	0.02	0.14	0.19	0.87	0.01	0.34	0.09
DMOPSO-4	0.15	0.09	0.28	0.01	0.92	0.10	0.58	0.25
DMOPSO-1-L	0.10	0.03	0.22	0.01	0.86	0.01	0.36	0.03
NSGA-II	0.10	0.02	0.23	0.01	0.87	0.02	0.36	0.05
NSGA-II-L	0.10	0.03	0.15	0.20	0.87	0.01	0.40	0.13
SPEA2	0.11	0.06	0.21	0.00	0.87	0.04	0.36	0.03
SPEA2-L	0.10	0.03	0.19	0.10	0.86	0.01	0.32	0.23

Table D.59: Median and interquartile range of I_{Δ} obtained by the optimisers for the Mitchell problems

	Mitchell-1 $\tilde{x} \pm IQR(x)$		Mitchell-2 $\tilde{x} \pm IQR(x)$		Mitchell-3 $\tilde{x} \pm IQR(x)$		Mitchell-4 $\tilde{x} \pm IQR(x)$	
BIANT-1	0.92	0.05	0.83	0.20	0.83	0.06	0.60	0.05
BIANT-2	0.88	0.01	0.77	0.10	0.84	0.10	0.84	0.14
CHAC-1	0.74	0.07	0.70	0.10	0.92	0.06	0.62	0.09
CHAC-1-L	0.77	0.14	0.69	0.03	0.91	0.01	0.66	0.10
CHAC-2	0.80	0.07	0.70	0.06	0.90	0.05	0.61	0.08
CHAC-2-L	0.79	0.09	0.68	0.02	0.90	0.02	0.68	0.02
MOACS-1	0.66	0.23	0.84	0.12	0.82	0.08	0.63	0.07
MOACS-1-S-CDAS	0.72	0.12	0.81	0.13	0.80	0.14	0.63	0.08
MOACS-1-L	0.67	0.11	0.80	0.08	0.79	0.12	0.60	0.06
MOACS-2	0.71	0.12	0.78	0.03	0.83	0.06	0.60	0.06
MOACS-2-S-CDAS	0.75	0.10	0.78	0.02	0.81	0.04	0.64	0.07
MOACS-2-L	0.75	0.09	0.80	0.07	0.83	0.07	0.65	0.12
DMOPSO-5	0.78	0.05	0.72	0.09	0.92	0.06	0.60	0.12
DMOPSO-1	0.74	0.07	0.68	0.05	0.92	0.08	0.56	0.16
DMOPSO-2	0.79	0.05	0.73	0.09	0.91	0.08	0.65	0.34
DMOPSO-3	0.77	0.07	0.72	0.09	0.92	0.04	0.56	0.06
DMOPSO-4	0.73	0.06	0.77	0.10	0.83	0.01	0.78	0.37
DMOPSO-1-L	0.78	0.03	0.69	0.02	0.93	0.02	0.62	0.21
NSGA-II	0.77	0.09	0.69	0.03	0.92	0.02	0.68	0.43
NSGA-II-L	0.81	0.05	0.71	0.05	0.92	0.05	0.58	0.06
SPEA2	0.77	0.06	0.69	0.04	0.91	0.06	0.63	0.11
SPEA2-L	0.75	0.05	0.71	0.07	0.91	0.07	0.55	0.10

Table D.60: Median and interquartile range of the computation time required by the optimisers for the Mitchell problems

	Mitchell-1 $\tilde{x} \pm IQR(x)$		Mitchell-2 $\tilde{x} \pm IQR(x)$		Mitchell-3 $\tilde{x} \pm IQR(x)$		Mitchell-4 $\tilde{x} \pm IQR(x)$	
BIANT-1	0.05	0.00	0.05	0.00	0.06	0.00	0.07	0.00
BIANT-2	0.05	0.00	0.05	0.01	0.06	0.00	0.07	0.00
CHAC-1	0.05	0.01	0.04	0.00	0.09	0.02	0.06	0.00
CHAC-1-L	0.04	0.01	0.03	0.01	0.07	0.02	0.05	0.01
CHAC-2	0.05	0.01	0.04	0.00	0.08	0.02	0.06	0.00
CHAC-2-L	0.05	0.02	0.04	0.01	0.08	0.03	0.06	0.02
MOACS-1	0.05	0.00	0.04	0.00	0.07	0.00	0.08	0.00
MOACS-1-S-CDAS	0.63	0.21	0.73	0.21	0.66	0.19	0.66	0.12
MOACS-1-L	0.05	0.00	0.05	0.00	0.07	0.01	0.08	0.01
MOACS-2	0.05	0.00	0.05	0.00	0.08	0.01	0.10	0.00
MOACS-2-S-CDAS	0.64	0.24	0.41	0.03	0.61	0.19	0.72	0.04
MOACS-2-L	0.05	0.00	0.05	0.00	0.07	0.01	0.09	0.00
DMOPSO-5	0.04	0.01	0.03	0.00	0.07	0.01	0.06	0.00
DMOPSO-1	0.03	0.01	0.03	0.01	0.06	0.02	0.04	0.02
DMOPSO-2	0.04	0.01	0.03	0.00	0.07	0.02	0.05	0.00
DMOPSO-3	0.03	0.01	0.03	0.01	0.07	0.03	0.04	0.00
DMOPSO-4	0.03	0.00	0.03	0.01	0.08	0.05	0.05	0.00
DMOPSO-1-L	0.04	0.00	0.03	0.00	0.08	0.01	0.05	0.00
NSGA-II	0.04	0.00	0.04	0.00	0.08	0.02	0.06	0.00
NSGA-II-L	0.02	0.00	0.02	0.00	0.06	0.05	0.04	0.00
SPEA2	0.03	0.00	0.03	0.00	0.06	0.02	0.05	0.00
SPEA2-L	0.03	0.00	0.03	0.00	0.06	0.01	0.05	0.00

Table D.58: Median and interquartile range of I_ϵ obtained by the optimisers for the Mitchell problems

	Mitchell-1 $\tilde{x} \pm IQR(x)$		Mitchell-2 $\tilde{x} \pm IQR(x)$		Mitchell-3 $\tilde{x} \pm IQR(x)$		Mitchell-4 $\tilde{x} \pm IQR(x)$	
BIANT-1	0.77	0.08	0.93	0.03	0.87	0.07	0.84	0.01
BIANT-2	0.82	0.2	0.93	0.01	0.84	0.01	0.85	0.02
CHAC-1	0.72	0.03	0.88	0.01	0.82	0.00	0.85	0.02
CHAC-1-L	0.72	0.02	0.88	0.02	0.82	0.00	0.84	0.02
CHAC-2	0.72	0.02	0.88	0.02	0.82	0.00	0.85	0.02
CHAC-2-L	0.71	0.00	0.88	0.01	0.82	0.00	0.84	0.01
MOACS-1	0.81	0.15	0.96	0.03	0.82	0	0.87	0.02
MOACS-1-S-CDAS	0.82	0.2	0.96	0.03	0.82	0	0.88	0.01
MOACS-1-L	0.8	0.16	0.96	0.03	0.83	0	0.88	0.00
MOACS-2	0.86	0.06	0.95	0.02	0.82	0.00	0.9	0.05
MOACS-2-S-CDAS	0.85	0.04	0.95	0.02	0.82	0.00	0.93	0.03
MOACS-2-L	0.85	0.06	0.95	0.03	0.82	0.00	0.92	0.07
DMOPSO-5	0.72	0.01	0.88	0.02	0.82	0.00	0.85	0.02
DMOPSO-1	0.72	0.03	0.88	0.01	0.82	0.00	0.85	0.02
DMOPSO-2	0.72	0.03	0.89	0.01	0.82	0.00	0.85	0.01
DMOPSO-3	0.71	0.01	0.88	0.01	0.82	0.00	0.85	0.01
DMOPSO-4	0.77	0.09	0.9	0.01	0.82	0.00	0.89	0.04
DMOPSO-1-L	0.73	0.03	0.88	0.01	0.82	0.00	0.85	0.02
NSGA-II	0.71	0.02	0.89	0.00	0.82	0.00	0.85	0.01
NSGA-II-L	0.73	0.04	0.88	0.01	0.82	0.00	0.85	0.01
SPEA2	0.73	0.03	0.88	0.01	0.82	0.00	0.85	0.01
SPEA2-L	0.72	0.02	0.88	0.02	0.82	0.00	0.85	0.02

D.1.9 Problem Family: Mukherje

Table D.61: Median and interquartile range of I_{HV} obtained by the optimisers for the Mukherje problems

	Mukherje-1 $\tilde{x} \pm IQR(x)$		Mukherje-2 $\tilde{x} \pm IQR(x)$		Mukherje-3 $\tilde{x} \pm IQR(x)$	
BIANT-1	0.93	0.02	0.92	0.01	0.91	0.01
BIANT-2	0.93	0.01	0.91	0.02	0.92	0.03
CHAC-1	0.87	0.01	0.86	0.00	0.85	0.01
CHAC-1-L	0.87	0.01	0.86	0.01	0.85	0.01
CHAC-2	0.87	0.01	0.87	0.00	0.85	0.00
CHAC-2-L	0.87	0.01	0.86	0.01	0.85	0.01
MOACS-1	0.88	0.01	0.89	0.01	0.89	0.02
MOACS-1-S-CDAS	0.82	0.04	0.82	0.01	0.85	0.01
MOACS-1-L	0.88	0.01	0.89	0.01	0.90	0.00
MOACS-2	0.91	0.00	0.91	0.01	0.92	0.01
MOACS-2-S-CDAS	0.91	0.01	0.91	0.00	0.91	0.00
MOACS-2-L	0.91	0.00	0.91	0.01	0.92	0.01
DMOPSO-5	0.86	0.00	0.86	0.01	0.84	0.01
DMOPSO-1	0.86	0.01	0.85	0.01	0.84	0.01
DMOPSO-2	0.86	0.01	0.86	0.00	0.84	0.01
DMOPSO-3	0.86	0.00	0.86	0.01	0.85	0.01
DMOPSO-4	0.86	0.00	0.86	0.00	0.84	0.00
DMOPSO-1-L	0.86	0.00	0.86	0.00	0.85	0.01
NSGA-II	0.87	0.01	0.87	0.00	0.85	0.01
NSGA-II-L	0.87	0.01	0.87	0.01	0.85	0.01
SPEA2	0.87	0.01	0.86	0.01	0.85	0.01
SPEA2-L	0.86	0.01	0.86	0.01	0.85	0.00

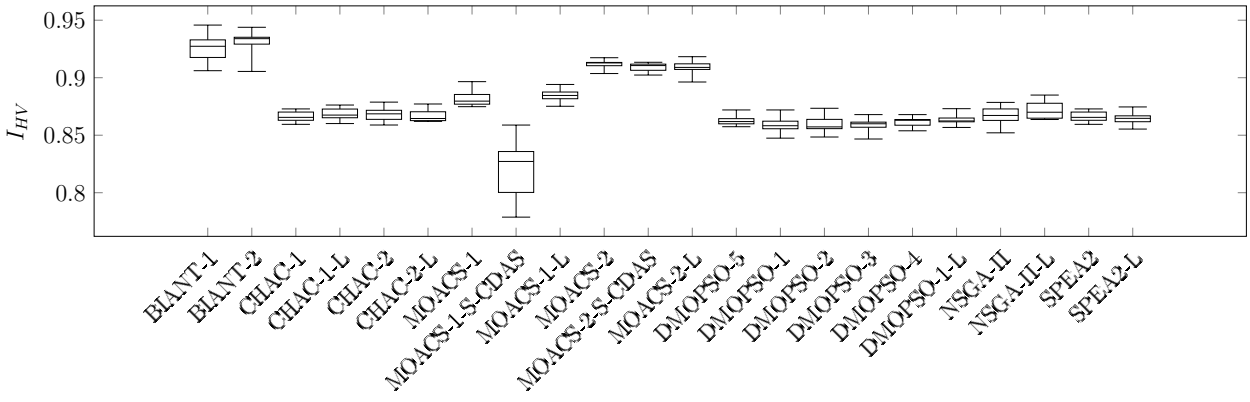

Figure D.26: Boxplot for I_{HV}: Mukherje-1

Table D.62: Median and interquartile range of I_{IGD} obtained by the optimisers for the Mukherje problems

	Mukherje-1 $\tilde{x} \pm IQR(x)$		Mukherje-2 $\tilde{x} \pm IQR(x)$		Mukherje-3 $\tilde{x} \pm IQR(x)$	
BIANT-1	0.24	0.05	0.31	0.01	0.34	0.12
BIANT-2	0.23	0.06	0.36	0.05	0.29	0.15
CHAC-1	0.48	0.04	0.56	0.03	0.63	0.07
CHAC-1-L	0.48	0.03	0.55	0.04	0.63	0.03
CHAC-2	0.48	0.04	0.53	0.05	0.64	0.05
CHAC-2-L	0.49	0.04	0.56	0.05	0.62	0.06
MOACS-1	0.34	0.03	0.37	0.07	0.33	0.03
MOACS-1-S-CDAS	0.72	0.32	0.78	0.13	0.67	0.12
MOACS-1-L	0.33	0.01	0.36	0.01	0.31	0.03
MOACS-2	0.30	0.01	0.33	0.02	0.30	0.02
MOACS-2-S-CDAS	0.30	0.02	0.33	0.03	0.30	0.03
MOACS-2-L	0.30	0.03	0.32	0.02	0.31	0.01
DMOPSO-5	0.51	0.02	0.55	0.05	0.64	0.04
DMOPSO-1	0.51	0.02	0.57	0.04	0.66	0.01
DMOPSO-2	0.51	0.04	0.56	0.04	0.64	0.05
DMOPSO-3	0.50	0.02	0.57	0.05	0.62	0.05
DMOPSO-4	0.50	0.02	0.55	0.02	0.64	0.02
DMOPSO-1-L	0.50	0.01	0.56	0.01	0.63	0.02
NSGA-II	0.50	0.04	0.57	0.03	0.64	0.04
NSGA-II-L	0.49	0.03	0.56	0.05	0.63	0.06
SPEA2	0.53	0.06	0.58	0.04	0.64	0.05
SPEA2-L	0.53	0.04	0.58	0.03	0.64	0.03

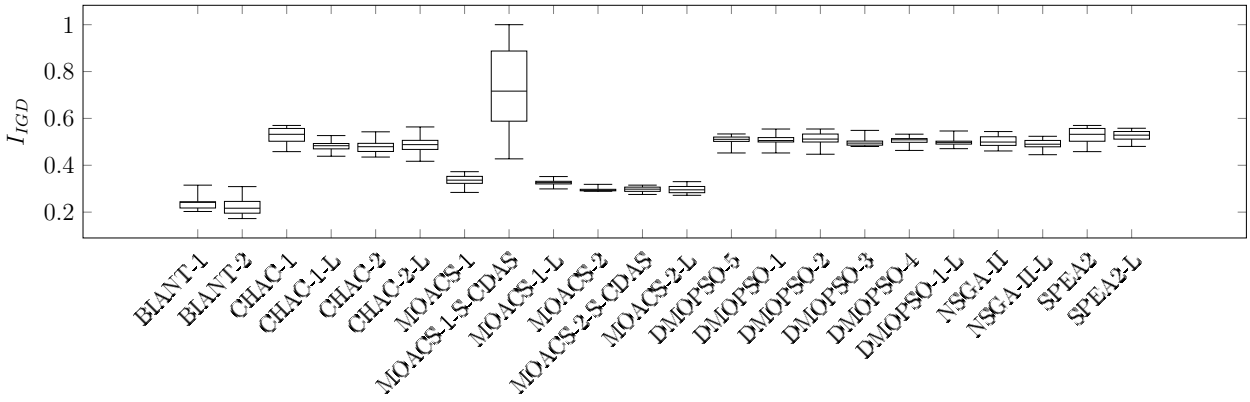

Figure D.27: Boxplot for I_{IGD}: Mukherje-1

Table D.63: Median and interquartile range of I_ϵ obtained by the optimisers for the Mukherje problems

	Mukherje-1 $\tilde{x} \pm IQR(x)$		Mukherje-2 $\tilde{x} \pm IQR(x)$		Mukherje-3 $\tilde{x} \pm IQR(x)$	
BIANT-1	0.44	0.07	0.40	0.06	0.44	0.06
BIANT-2	0.40	0.07	0.46	0.05	0.44	0.06
CHAC-1	0.19	0.00	0.20	0.01	0.24	0.00
CHAC-1-L	0.19	0.00	0.20	0.00	0.24	0.00
CHAC-2	0.19	0.00	0.20	0.00	0.24	0.00
CHAC-2-L	0.19	0.00	0.20	0.00	0.24	0.00
MOACS-1	0.50	0.06	0.49	0.10	0.50	0.07
MOACS-1-S-CDAS	0.83	0.22	0.86	0.06	0.81	0.10
MOACS-1-L	0.48	0.03	0.46	0.05	0.46	0.06
MOACS-2	0.27	0.04	0.28	0.04	0.31	0.03
MOACS-2-S-CDAS	0.29	0.03	0.28	0.01	0.31	0.07
MOACS-2-L	0.29	0.01	0.29	0.03	0.30	0.03
DMOPSO-5	0.19	0.00	0.20	0.00	0.24	0.00
DMOPSO-1	0.18	0.00	0.20	0.00	0.24	0.00
DMOPSO-2	0.19	0.00	0.20	0.00	0.24	0.00
DMOPSO-3	0.19	0.00	0.21	0.00	0.24	0.00
DMOPSO-4	0.19	0.00	0.21	0.00	0.24	0.00
DMOPSO-1-L	0.18	0.00	0.20	0.00	0.24	0.00
NSGA-II	0.11	0.00	0.12	0.01	0.14	0.00
NSGA-II-L	0.11	0.00	0.12	0.01	0.14	0.00
SPEA2	0.11	0.00	0.12	0.01	0.15	0.00
SPEA2-L	0.12	0.00	0.13	0.00	0.15	0.00

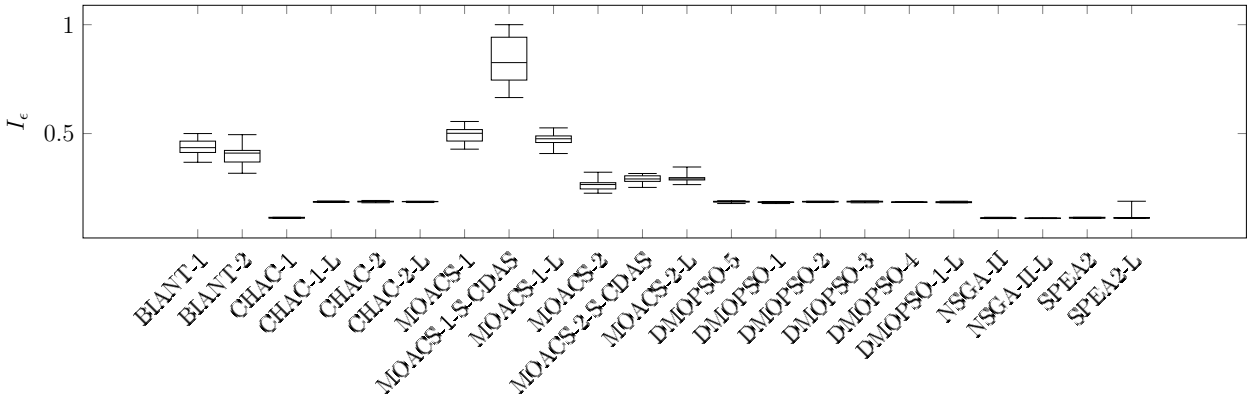

Figure D.28: Boxplot for I_ϵ: Mukherje-1

Table D.64: Median and interquartile range of I_Δ obtained by the optimisers for the Mukherje problems

	Mukherje-1 $\tilde{x} \pm IQR(x)$		Mukherje-2 $\tilde{x} \pm IQR(x)$		Mukherje-3 $\tilde{x} \pm IQR(x)$	
BIANT-1	0.46	0.05	0.46	0.08	0.51	0.08
BIANT-2	0.45	0.01	0.53	0.03	0.50	0.11
CHAC-1	0.77	0.05	0.76	0.03	0.78	0.05
CHAC-1-L	0.79	0.10	0.80	0.05	0.79	0.02
CHAC-2	0.79	0.09	0.79	0.06	0.81	0.06
CHAC-2-L	0.79	0.09	0.77	0.07	0.78	0.04
MOACS-1	0.49	0.02	0.49	0.03	0.47	0.06
MOACS-1-S-CDAS	0.75	0.05	0.69	0.06	0.60	0.09
MOACS-1-L	0.49	0.07	0.49	0.06	0.45	0.08
MOACS-2	0.35	0.03	0.33	0.07	0.35	0.02
MOACS-2-S-CDAS	0.42	0.07	0.40	0.06	0.42	0.09
MOACS-2-L	0.39	0.05	0.37	0.06	0.38	0.07
DMOPSO-5	0.86	0.05	0.85	0.05	0.85	0.05
DMOPSO-1	0.87	0.05	0.83	0.03	0.84	0.07
DMOPSO-2	0.88	0.05	0.84	0.06	0.84	0.04
DMOPSO-3	0.86	0.04	0.87	0.03	0.82	0.06
DMOPSO-4	0.84	0.04	0.83	0.04	0.85	0.05
DMOPSO-1-L	0.87	0.03	0.81	0.04	0.84	0.06
NSGA-II	0.91	0.04	0.91	0.04	0.91	0.06
NSGA-II-L	0.90	0.08	0.89	0.08	0.90	0.05
SPEA2	0.91	0.06	0.92	0.04	0.88	0.04
SPEA2-L	0.92	0.04	0.91	0.06	0.89	0.06

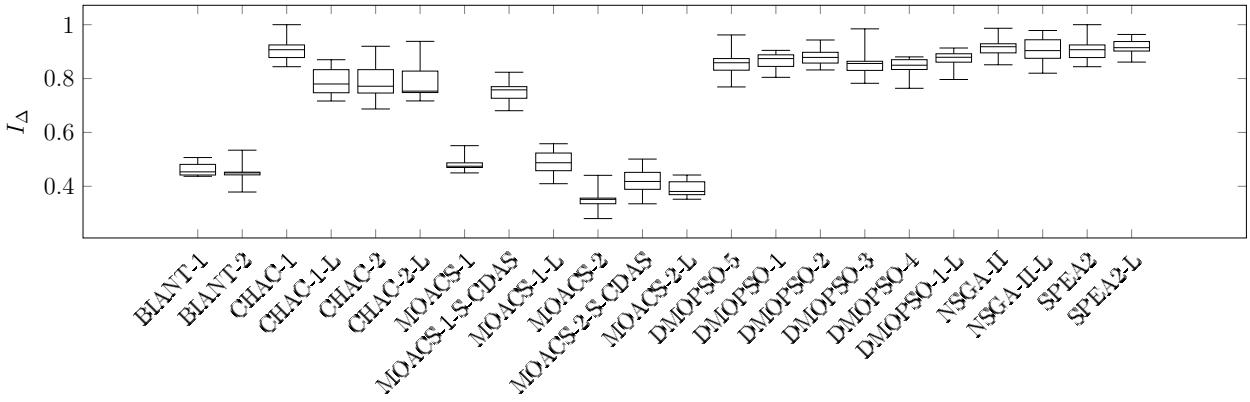

Figure D.29: Boxplot for I_Δ: Mukherje-1

Table D.65: Median and interquartile range of the computation time required by the optimisers for the Mukherje problems

	Mukherje-1 $\tilde{x} \pm IQR(x)$		Mukherje-2 $\tilde{x} \pm IQR(x)$		Mukherje-3 $\tilde{x} \pm IQR(x)$	
BIANT-1	0.35	0.04	1.75	0.07	0.68	0.20
BIANT-2	0.34	0.01	2.21	0.12	0.51	0.35
CHAC-1	0.40	0.02	2.94	0.08	0.37	0.21
CHAC-1-L	0.50	0.02	4.23	0.16	0.32	0.16
CHAC-2	0.33	0.01	2.65	0.14	0.33	0.09
CHAC-2-L	0.19	0.01	2.05	0.19	0.39	0.14
MOACS-1	0.33	0.02	3.06	0.13	0.39	0.23
MOACS-1-S-CDAS	0.44	0.01	4.59	0.29	0.58	0.25
MOACS-1-L	0.48	0.02	3.50	0.20	0.54	0.23
MOACS-2	0.28	0.02	2.41	0.06	0.44	0.27
MOACS-2-S-CDAS	0.36	0.01	2.30	0.09	0.37	0.19
MOACS-2-L	1.30	0.02	3.27	0.08	0.31	0.20
DMOPSO-5	0.41	0.01	2.65	0.08	0.28	0.07
DMOPSO-1	0.27	0.01	2.21	0.20	0.26	0.07
DMOPSO-2	0.27	0.01	2.24	0.08	0.27	0.04
DMOPSO-3	0.34	0.02	2.38	0.09	0.35	0.07
DMOPSO-4	0.28	0.02	1.88	0.02	0.47	0.27
DMOPSO-1-L	0.27	0.00	2.18	0.04	0.27	0.11
NSGA-II	0.21	0.01	2.06	0.15	0.23	0.09
NSGA-II-L	0.25	0.01	1.90	0.11	0.20	0.09
SPEA2	0.16	0.01	1.10	0.06	0.12	0.05
SPEA2-L	0.15	0.00	1.29	0.02	0.14	0.05

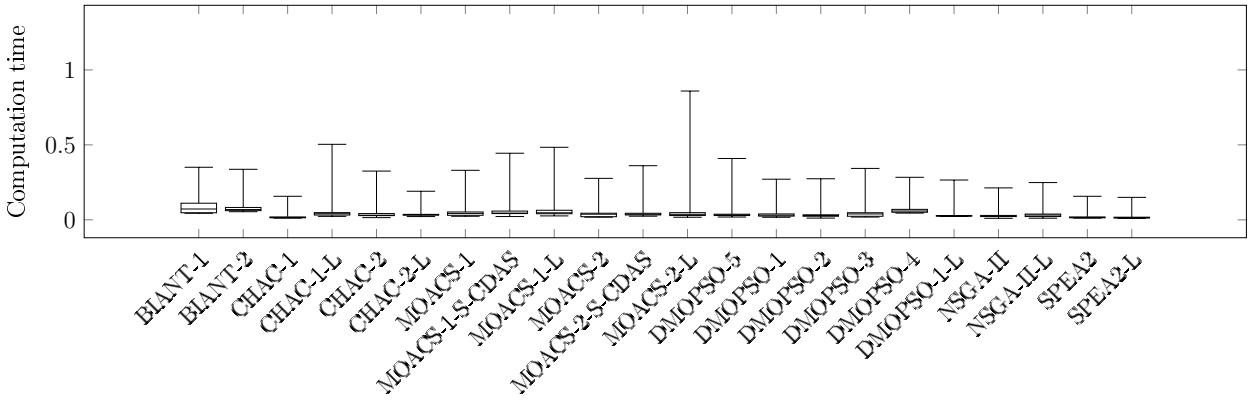

Figure D.30: Boxplot for the computation time: Mukherje-1

Table D.66: C-metric for the Mukherje-1 problem instance

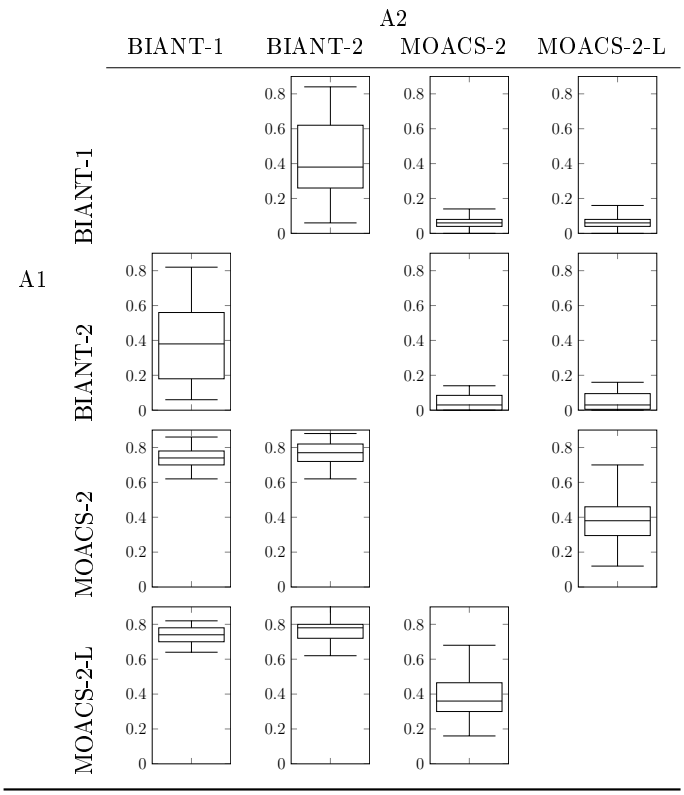

Table D.67: C-metric for the Mukherje-2 problem instance

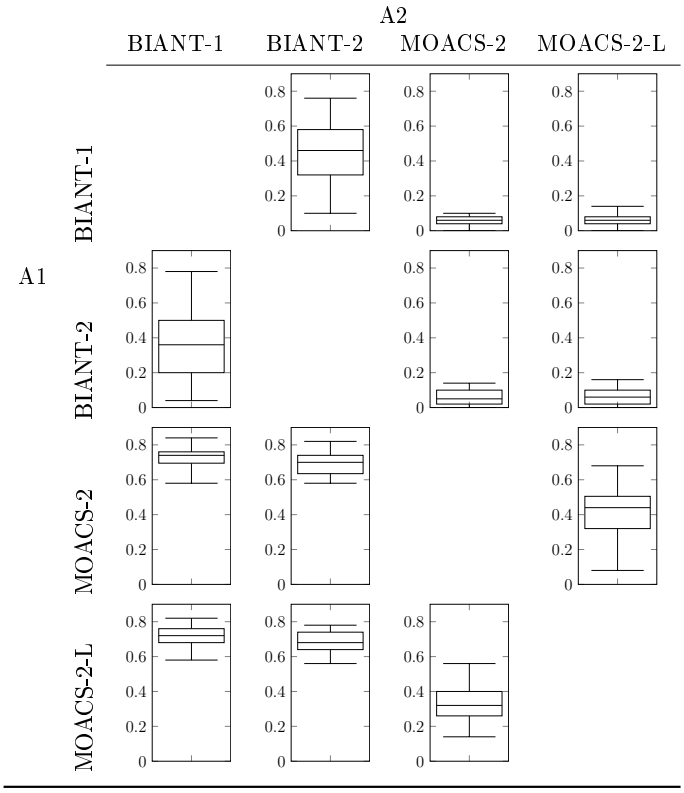

Table D.68: C-metric for the Mukherje-3 problem instance

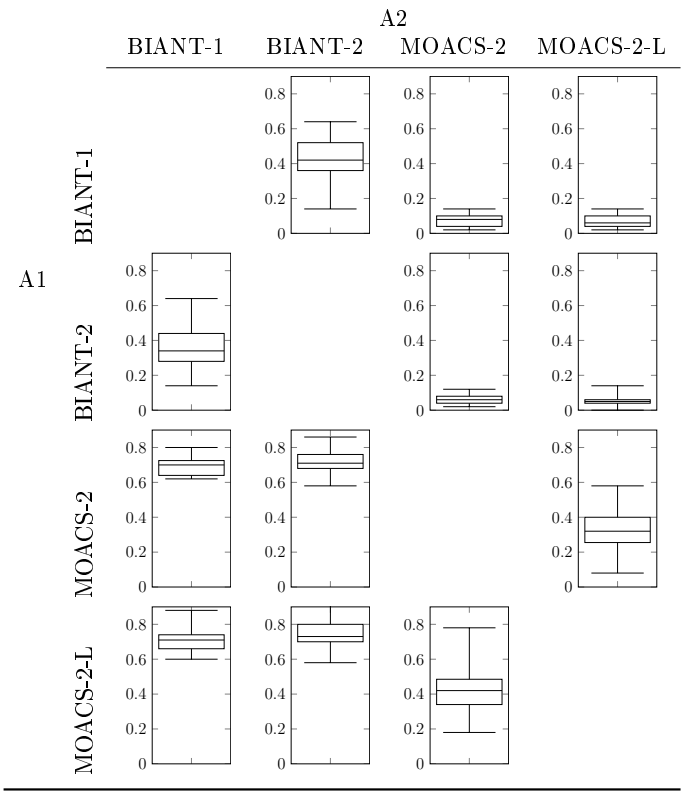

D.1.10 Problem Family: Roszieg

Table D.69: Median and interquartile range of I_{HV} obtained by the optimisers for the Roszieg problems

	Roszieg-1 $\tilde{x} \pm IQR(x)$		Roszieg-2 $\tilde{x} \pm IQR(x)$		Roszieg-3 $\tilde{x} \pm IQR(x)$		Roszieg-4 $\tilde{x} \pm IQR(x)$	
BIANT-1	0.95	0.03	0.37	0.01	0.94	0.02	0.78	0.00
BIANT-2	0.94	0.04	0.37	0.02	0.85	0.09	0.78	0.00
CHAC-1	1.00	0.00	0.48	0.00	0.99	0.01	0.79	0.00
CHAC-1-L	1.00	0.01	0.48	0.00	0.99	0.01	0.79	0.00
CHAC-2	1.00	0.00	0.48	0.00	0.99	0.01	0.79	0.00
CHAC-2-L	1.00	0.00	0.48	0.00	0.99	0.01	0.79	0.00
MOACS-1	0.97	0.00	0.39	0.01	0.93	0.06	0.72	0.08
MOACS-1-S-CDAS	0.96	0.00	0.38	0.02	0.92	0.07	0.73	0.02
MOACS-1-L	0.96	0.00	0.38	0.00	0.90	0.07	0.75	0.02
MOACS-2	0.96	0.01	0.38	0.01	0.91	0.05	0.69	0.12
MOACS-2-S-CDAS	0.96	0.01	0.36	0.02	0.90	0.05	0.70	0.14
MOACS-2-L	0.95	0.02	0.37	0.01	0.91	0.11	0.72	0.11
DMOPSO-5	1.00	0.01	0.48	0.00	0.99	0.01	0.79	0.00
DMOPSO-1	1.00	0.00	0.48	0.00	0.99	0.00	0.79	0.00
DMOPSO-2	1.00	0.00	0.48	0.00	0.99	0.00	0.79	0.00
DMOPSO-3	1.00	0.01	0.48	0.00	0.99	0.00	0.79	0.00
DMOPSO-4	0.99	0.01	0.47	0.00	0.97	0.01	0.79	0.00
DMOPSO-1-L	1.00	0.00	0.48	0.00	0.99	0.01	0.79	0.00
NSGA-II	1.00	0.00	0.48	0.00	0.99	0.00	0.79	0.00
NSGA-II-L	1.00	0.01	0.48	0.00	0.99	0.00	0.79	0.00
SPEA2	1.00	0.00	0.48	0.00	0.99	0.00	0.79	0.00
SPEA2-L	1.00	0.01	0.48	0.00	0.99	0.00	0.79	0.00

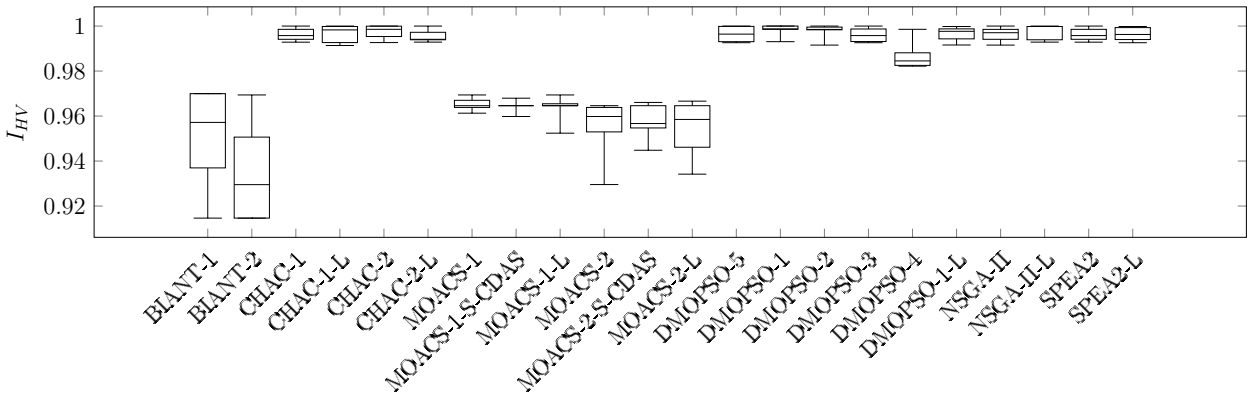

Figure D.31: Boxplot for I_{HV}: Roszieg-1

Table D.70: Median and interquartile range of I_{IGD} obtained by the optimisers for the Roszieg problems

	Roszieg-1 $\tilde{x} \pm IQR(x)$		Roszieg-2 $\tilde{x} \pm IQR(x)$		Roszieg-3 $\tilde{x} \pm IQR(x)$		Roszieg-4 $\tilde{x} \pm IQR(x)$	
BIANT-1	0.61	0.25	0.97	0.02	0.57	0.05	0.22	0.39
BIANT-2	0.79	0.31	0.96	0.06	0.87	0.17	0.41	0.00
CHAC-1	0.11	0.15	0.90	0.00	0.34	0.06	0.02	0.00
CHAC-1-L	0.08	0.03	0.90	0.00	0.33	0.05	0.02	0.00
CHAC-2	0.08	0.03	0.90	0.00	0.31	0.08	0.02	0.00
CHAC-2-L	0.13	0.10	0.90	0.00	0.32	0.08	0.02	0.00
MOACS-1	0.42	0.03	0.96	0.04	0.62	0.18	0.55	0.25
MOACS-1-S-CDAS	0.44	0.00	0.96	0.04	0.66	0.22	0.54	0.05
MOACS-1-L	0.43	0.01	0.96	0.06	0.68	0.20	0.47	0.02
MOACS-2	0.44	0.00	0.95	0.07	0.70	0.14	0.68	0.41
MOACS-2-S-CDAS	0.44	0.01	0.98	0.00	0.72	0.16	0.62	0.43
MOACS-2-L	0.44	0.02	0.97	0.05	0.71	0.28	0.58	0.34
DMOPSO-5	0.11	0.14	0.90	0.00	0.33	0.11	0.02	0.00
DMOPSO-1	0.08	0.03	0.90	0.00	0.32	0.04	0.02	0.00
DMOPSO-2	0.06	0.02	0.90	0.00	0.33	0.05	0.02	0.00
DMOPSO-3	0.09	0.09	0.90	0.00	0.32	0.04	0.02	0.00
DMOPSO-4	0.14	0.08	0.90	0.01	0.46	0.04	0.02	0.00
DMOPSO-1-L	0.08	0.03	0.90	0.00	0.32	0.04	0.02	0.00
NSGA-II	0.08	0.03	0.90	0.00	0.33	0.05	0.02	0.00
NSGA-II-L	0.11	0.14	0.90	0.01	0.33	0.07	0.02	0.00
SPEA2	0.10	0.13	0.90	0.00	0.32	0.03	0.02	0.00
SPEA2-L	0.09	0.09	0.90	0.00	0.30	0.03	0.02	0.00

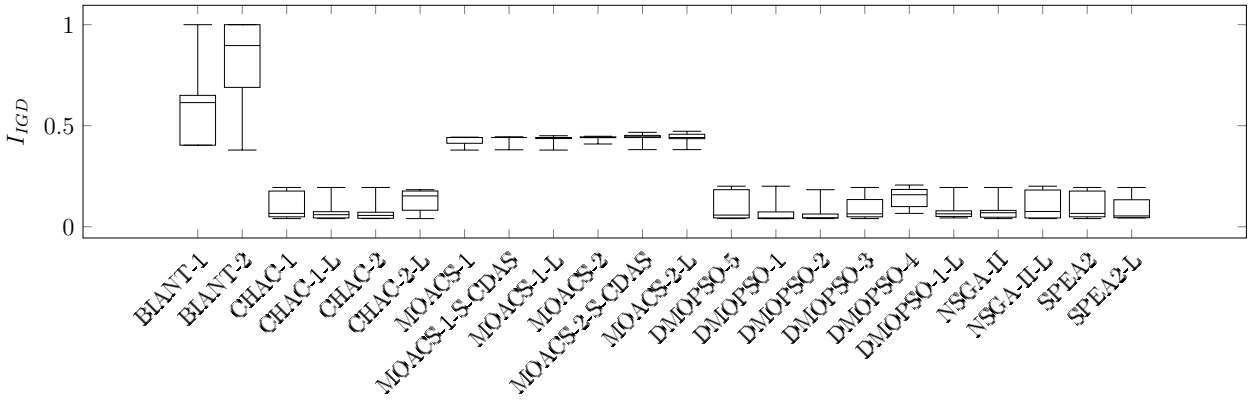

Figure D.32: Boxplot for I_{IGD}: Roszieg-1

Table D.71: Median and interquartile range of I_ϵ obtained by the optimisers for the Roszieg problems

	Roszieg-1 $\tilde{x} \pm IQR(x)$		Roszieg-2 $\tilde{x} \pm IQR(x)$		Roszieg-3 $\tilde{x} \pm IQR(x)$		Roszieg-4 $\tilde{x} \pm IQR(x)$	
BIANT-1	0.69	0.31	0.84	0.07	0.52	0.10	0.87	0.01
BIANT-2	0.82	0.31	0.93	0.00	0.72	0.41	0.87	0.00
CHAC-1	0.22	0.08	0.45	0.01	0.43	0.01	0.86	0.00
CHAC-1-L	0.21	0.08	0.45	0.00	0.43	0.01	0.86	0.00
CHAC-2	0.21	0.06	0.44	0.01	0.43	0.02	0.86	0.00
CHAC-2-L	0.23	0.08	0.45	0.01	0.42	0.00	0.86	0.00
MOACS-1	0.51	0.00	0.85	0.01	0.62	0.25	0.92	0.06
MOACS-1-S-CDAS	0.51	0.00	0.88	0.00	0.64	0.34	0.91	0.02
MOACS-1-L	0.52	0.00	0.85	0.00	0.72	0.34	0.89	0.01
MOACS-2	0.56	0.04	0.89	0.02	0.66	0.18	0.95	0.10
MOACS-2-S-CDAS	0.52	0.00	0.89	0.01	0.70	0.20	0.93	0.11
MOACS-2-L	0.53	0.05	0.89	0.03	0.71	0.33	0.92	0.09
DMOPSO-5	0.22	0.08	0.45	0.00	0.43	0.01	0.86	0.00
DMOPSO-1	0.20	0.00	0.45	0.00	0.43	0.01	0.86	0.00
DMOPSO-2	0.20	0.00	0.45	0.02	0.42	0.00	0.86	0.00
DMOPSO-3	0.22	0.08	0.45	0.00	0.42	0.00	0.86	0.00
DMOPSO-4	0.28	0.07	0.48	0.02	0.46	0.03	0.86	0.00
DMOPSO-1-L	0.22	0.08	0.44	0.02	0.42	0.01	0.86	0.00
NSGA-II	0.22	0.08	0.45	0.00	0.43	0.01	0.86	0.00
NSGA-II-L	0.22	0.08	0.44	0.01	0.43	0.01	0.86	0.00
SPEA2	0.22	0.08	0.45	0.00	0.42	0.01	0.86	0.00
SPEA2-L	0.22	0.08	0.45	0.00	0.43	0.01	0.86	0.00

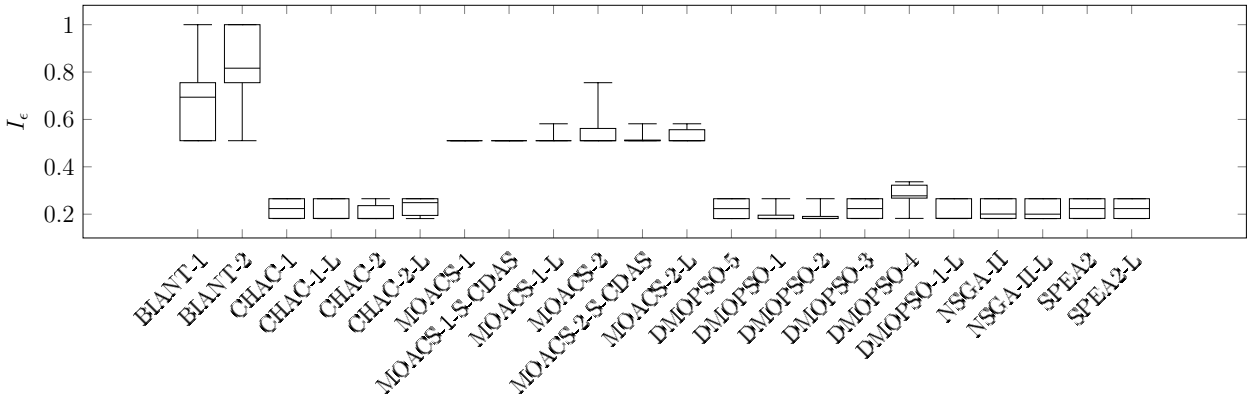

Figure D.33: Boxplot for I_ϵ: Roszieg-1

Table D.72: Median and interquartile range of I_Δ obtained by the optimisers for the Roszieg problems

	Roszieg-1 $\tilde{x} \pm IQR(x)$		Roszieg-2 $\tilde{x} \pm IQR(x)$		Roszieg-3 $\tilde{x} \pm IQR(x)$		Roszieg-4 $\tilde{x} \pm IQR(x)$	
BIANT-1	0.80	0.09	0.89	0.03	0.66	0.09	0.36	0.01
BIANT-2	0.84	0.08	0.80	0.02	0.70	0.15	0.35	0.00
CHAC-1	0.85	0.11	0.89	0.07	0.75	0.09	0.36	0.00
CHAC-1-L	0.83	0.09	0.90	0.04	0.78	0.09	0.36	0.00
CHAC-2	0.88	0.10	0.86	0.05	0.71	0.13	0.36	0.00
CHAC-2-L	0.91	0.04	0.91	0.08	0.77	0.03	0.36	0.00
MOACS-1	0.71	0.05	0.84	0.06	0.69	0.07	0.53	0.13
MOACS-1-S-CDAS	0.69	0.00	0.86	0.06	0.65	0.08	0.51	0.26
MOACS-1-L	0.70	0.03	0.83	0.05	0.68	0.11	0.41	0.04
MOACS-2	0.71	0.05	0.86	0.08	0.74	0.06	0.53	0.16
MOACS-2-S-CDAS	0.71	0.02	0.91	0.07	0.71	0.11	0.51	0.22
MOACS-2-L	0.70	0.03	0.89	0.07	0.72	0.17	0.54	0.39
DMOPSO-5	0.86	0.05	0.90	0.06	0.69	0.10	0.36	0.00
DMOPSO-1	0.82	0.06	0.90	0.02	0.71	0.10	0.36	0.00
DMOPSO-2	0.85	0.06	0.89	0.05	0.73	0.14	0.36	0.00
DMOPSO-3	0.86	0.11	0.85	0.07	0.71	0.15	0.36	0.00
DMOPSO-4	0.76	0.03	0.91	0.02	0.70	0.08	0.36	0.00
DMOPSO-1-L	0.84	0.11	0.89	0.05	0.71	0.15	0.36	0.00
NSGA-II	0.85	0.06	0.86	0.05	0.80	0.02	0.36	0.00
NSGA-II-L	0.86	0.10	0.89	0.03	0.75	0.14	0.36	0.00
SPEA2	0.90	0.12	0.89	0.08	0.78	0.10	0.36	0.00
SPEA2-L	0.90	0.12	0.92	0.04	0.69	0.14	0.39	0.00

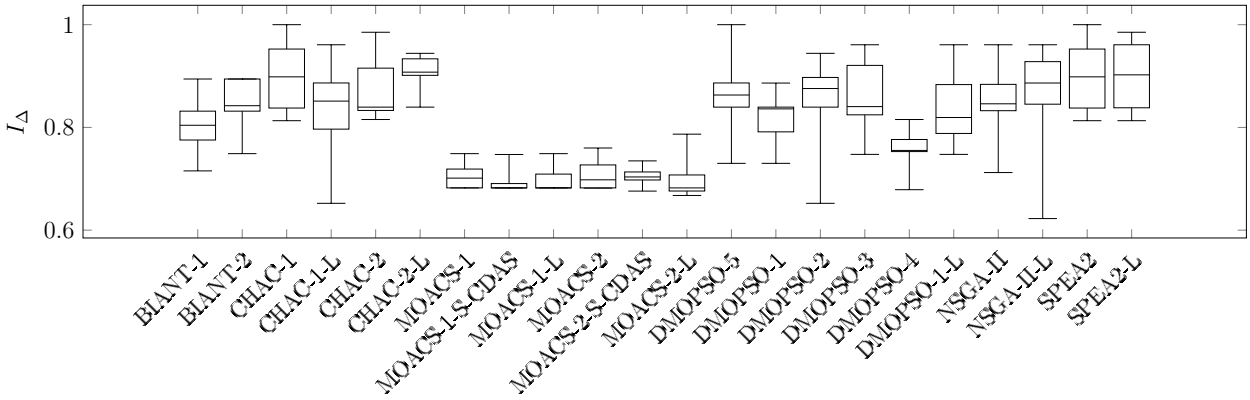

Figure D.34: Boxplot for I_Δ: Roszieg-1

Table D.73: Median and interquartile range of the computation time required by the optimisers for the Roszieg problems

	Roszieg-1 $\tilde{x} \pm IQR(x)$		Roszieg-2 $\tilde{x} \pm IQR(x)$		Roszieg-3 $\tilde{x} \pm IQR(x)$		Roszieg-4 $\tilde{x} \pm IQR(x)$	
BIANT-1	0.15	0.01	0.37	0.01	0.07	0.01	0.05	0.00
BIANT-2	0.15	0.01	0.37	0.02	0.07	0.00	0.06	0.01
CHAC-1	0.13	0.00	0.48	0.00	0.07	0.02	0.04	0.00
CHAC-1-L	0.12	0.03	0.48	0.00	0.06	0.02	0.03	0.01
CHAC-2	0.13	0.00	0.48	0.00	0.07	0.01	0.04	0.00
CHAC-2-L	0.13	0.03	0.48	0.00	0.07	0.01	0.03	0.01
MOACS-1	0.15	0.00	0.39	0.01	0.07	0.01	0.05	0.01
MOACS-1-S-CDAS	0.71	0.11	0.38	0.02	0.72	0.20	0.60	0.10
MOACS-1-L	0.15	0.00	0.38	0.00	0.07	0.00	0.05	0.01
MOACS-2	0.16	0.00	0.38	0.01	0.08	0.01	0.07	0.01
MOACS-2-S-CDAS	0.54	0.17	0.36	0.02	0.57	0.18	0.52	0.15
MOACS-2-L	0.16	0.00	0.37	0.01	0.08	0.00	0.08	0.02
DMOPSO-5	0.12	0.00	0.48	0.00	0.06	0.01	0.03	0.00
DMOPSO-1	0.10	0.04	0.48	0.00	0.05	0.02	0.02	0.01
DMOPSO-2	0.11	0.00	0.48	0.00	0.06	0.02	0.03	0.00
DMOPSO-3	0.10	0.01	0.48	0.00	0.06	0.03	0.03	0.00
DMOPSO-4	0.12	0.02	0.47	0.00	0.05	0.00	0.03	0.00
DMOPSO-1-L	0.11	0.00	0.48	0.00	0.06	0.01	0.03	0.00
NSGA-II	0.14	0.00	0.48	0.00	0.07	0.01	0.04	0.00
NSGA-II-L	0.09	0.00	0.48	0.00	0.04	0.02	0.03	0.00
SPEA2	0.10	0.00	0.48	0.00	0.05	0.00	0.03	0.00
SPEA2-L	0.10	0.00	0.48	0.00	0.05	0.01	0.03	0.00

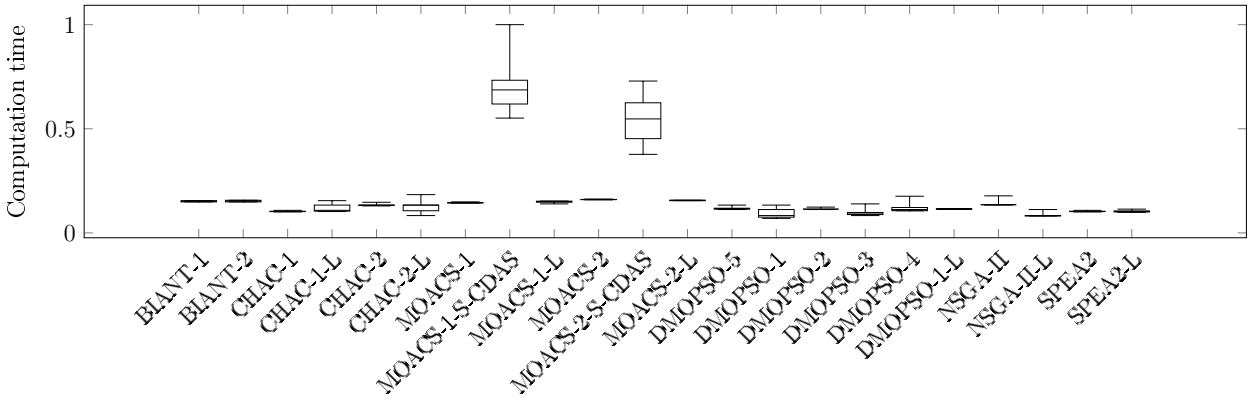

Figure D.35: Boxplot for the computation time: Roszieg-1

D.1.11 Problem Family: Sawyer

Table D.74: Median and interquartile range of I_{HV} obtained by the optimisers for the Sawyer problems

	Sawyer-1		Sawyer-2		Sawyer-3		Sawyer-4	
	$\tilde{x}$	$IQR(x)$	$\tilde{x}$	$IQR(x)$	$\tilde{x}$	$IQR(x)$	$\tilde{x}$	$IQR(x)$
BIANT-1	0.93	0.00	0.90	0.22	0.87	0.01	0.87	0.03
BIANT-2	0.96	0.08	0.85	0.16	0.88	0.03	0.88	0.03
CHAC-1	1.00	0.00	1.00	0.00	1.00	0.00	0.99	0.00
CHAC-1-L	1.00	0.00	1.00	0.00	1.00	0.00	0.99	0.00
CHAC-2	1.00	0.00	1.00	0.00	1.00	0.00	0.99	0.00
CHAC-2-L	1.00	0.00	1.00	0.00	1.00	0.00	0.99	0.00
MOACS-1	0.50	0.28	0.78	0.00	0.87	0.02	0.87	0.03
MOACS-1-S-CDAS	0.78	0.53	0.83	0.10	0.87	0.01	0.85	0.00
MOACS-1-L	0.91	0.08	0.81	0.00	0.86	0.01	0.86	0.00
MOACS-2	0.74	0.67	0.82	0.04	0.88	0.02	0.86	0.00
MOACS-2-S-CDAS	0.78	0.53	0.81	0.01	0.92	0.08	0.85	0.01
MOACS-2-L	0.86	0.08	0.80	0.00	0.88	0.01	0.87	0.05
DMOPSO-5	1.00	0.00	1.00	0.00	1.00	0.00	0.87	0.08
DMOPSO-1	1.00	0.00	1.00	0.00	1.00	0.00	0.99	0.00
DMOPSO-2	1.00	0.00	1.00	0.00	1.00	0.00	0.99	0.00
DMOPSO-3	1.00	0.00	1.00	0.00	1.00	0.00	0.99	0.00
DMOPSO-4	1.00	0.00	1.00	0.00	0.98	0.01	0.99	0.00
DMOPSO-1-L	1.00	0.00	1.00	0.00	1.00	0.00	0.98	0.03
NSGA-II	1.00	0.00	1.00	0.00	1.00	0.00	0.99	0.00
NSGA-II-L	1.00	0.00	1.00	0.00	1.00	0.00	0.99	0.00
SPEA2	1.00	0.00	1.00	0.00	1.00	0.00	0.99	0.00
SPEA2-L	1.00	0.00	1.00	0.00	1.00	0.00	0.99	0.00

Table D.75: Median and interquartile range of I_{IGD} obtained by the optimisers for the Sawyer problems

	Sawyer-1 $\tilde{x} \pm IQR(x)$		Sawyer-2 $\tilde{x} \pm IQR(x)$		Sawyer-3 $\tilde{x} \pm IQR(x)$		Sawyer-4 $\tilde{x} \pm IQR(x)$	
BIANT-1	0.16	0.00	0.43	0.55	0.30	0.09	0.88	0.08
BIANT-2	0.55	0.18	0.72	0.48	0.34	0.07	0.85	0.13
CHAC-1	0.73	0.00	0.00	0.00	0.05	0.09	0.07	0.00
CHAC-1-L	0.73	0.00	0.00	0.00	0.04	0.09	0.07	0.00
CHAC-2	0.73	0.00	0.00	0.00	0.06	0.08	0.08	0.00
CHAC-2-L	0.73	0.00	0.00	0.00	0.06	0.09	0.07	0.00
MOACS-1	0.45	0.31	1.00	0.00	0.38	0.06	0.88	0.07
MOACS-1-S-CDAS	0.56	0.10	0.89	0.01	0.38	0.06	0.95	0.00
MOACS-1-L	0.51	0.56	0.86	0.00	0.38	0.06	0.92	0.00
MOACS-2	0.60	0.10	0.92	0.01	0.36	0.03	0.92	0.00
MOACS-2-S-CDAS	0.56	0.10	0.90	0.02	0.25	0.20	0.92	0.02
MOACS-2-L	0.64	0.08	0.97	0.00	0.35	0.06	0.86	0.15
DMOPSO-5	0.73	0.00	0.00	0.00	0.05	0.09	0.87	0.25
DMOPSO-1	0.73	0.00	0.00	0.00	0.05	0.09	0.07	0.00
DMOPSO-2	0.73	0.00	0.00	0.00	0.05	0.09	0.07	0.00
DMOPSO-3	0.73	0.00	0.00	0.00	0.05	0.09	0.08	0.00
DMOPSO-4	0.73	0.00	0.00	0.00	0.11	0.00	0.07	0.00
DMOPSO-1-L	0.73	0.00	0.00	0.00	0.06	0.09	0.33	0.41
NSGA-II	0.73	0.00	0.00	0.00	0.05	0.09	0.07	0.00
NSGA-II-L	0.73	0.00	0.00	0.00	0.06	0.09	0.07	0.00
SPEA2	0.73	0.00	0.00	0.00	0.08	0.00	0.08	0.00
SPEA2-L	0.73	0.00	0.00	0.00	0.07	0.06	0.07	0.00

Table D.77: Median and interquartile range of I_{Δ} obtained by the optimisers for the Sawyer problems

	Sawyer-1 $\tilde{x} \pm IQR(x)$		Sawyer-2 $\tilde{x} \pm IQR(x)$		Sawyer-3 $\tilde{x} \pm IQR(x)$		Sawyer-4 $\tilde{x} \pm IQR(x)$	
BIANT-1	0.19	0.16	0.65	0.23	0.76	0.08	0.85	0.03
BIANT-2	0.37	0.47	0.79	0.04	0.80	0.05	0.87	0.06
CHAC-1	0.57	0.00	0.61	0.00	0.94	0.03	0.97	0.02
CHAC-1-L	0.57	0.00	0.61	0.00	0.93	0.03	0.98	0.02
CHAC-2	0.57	0.00	0.61	0.00	0.94	0.04	0.97	0.03
CHAC-2-L	0.57	0.00	0.61	0.00	0.95	0.04	0.97	0.01
MOACS-1	0.38	0.20	0.84	0.00	0.84	0.07	0.90	0.02
MOACS-1-S-CDAS	0.45	0.06	0.80	0.00	0.85	0.04	0.88	0.03
MOACS-1-L	0.41	0.37	0.76	0.00	0.87	0.03	0.90	0.03
MOACS-2	0.48	0.06	0.77	0.06	0.80	0.02	0.90	0.03
MOACS-2-S-CDAS	0.45	0.06	0.75	0.12	0.82	0.11	0.89	0.02
MOACS-2-L	0.51	0.05	0.80	0.00	0.84	0.04	0.89	0.04
DMOPSO-5	0.57	0.00	0.61	0.00	0.95	0.04	0.90	0.02
DMOPSO-1	0.57	0.00	0.61	0.00	0.93	0.04	0.98	0.01
DMOPSO-2	0.57	0.00	0.61	0.00	0.94	0.03	0.98	0.01
DMOPSO-3	0.57	0.00	0.61	0.00	0.95	0.04	0.98	0.01
DMOPSO-4	0.57	0.00	0.61	0.00	0.88	0.05	0.98	0.00
DMOPSO-1-L	0.57	0.00	0.61	0.00	0.96	0.06	0.97	0.03
NSGA-II	0.57	0.00	0.61	0.00	0.94	0.02	0.97	0.01
NSGA-II-L	0.57	0.00	0.61	0.00	0.94	0.03	0.98	0.02
SPEA2	0.57	0.00	0.61	0.00	0.96	0.02	0.98	0.01
SPEA2-L	0.57	0.00	0.61	0.00	0.95	0.02	0.98	0.02

Table D.78: Median and interquartile range of the computation time required by the optimisers for the Sawyer problems

	Sawyer-1 $\tilde{x} \pm IQR(x)$		Sawyer-2 $\tilde{x} \pm IQR(x)$		Sawyer-3 $\tilde{x} \pm IQR(x)$		Sawyer-4 $\tilde{x} \pm IQR(x)$	
BIANT-1	0.07	0.00	0.03	0.00	0.09	0.00	0.06	0.01
BIANT-2	0.07	0.00	0.03	0.00	0.09	0.00	0.07	0.01
CHAC-1	0.06	0.00	0.02	0.00	0.07	0.00	0.05	0.00
CHAC-1-L	0.05	0.01	0.02	0.00	0.06	0.01	0.05	0.01
CHAC-2	0.06	0.00	0.02	0.00	0.07	0.00	0.05	0.00
CHAC-2-L	0.05	0.00	0.02	0.00	0.07	0.01	0.05	0.00
MOACS-1	0.07	0.00	0.03	0.00	0.09	0.00	0.06	0.00
MOACS-1-S-CDAS	0.63	0.50	0.19	0.04	0.76	0.08	0.06	0.00
MOACS-1-L	0.07	0.00	0.03	0.00	0.09	0.00	0.81	0.10
MOACS-2	0.07	0.00	0.03	0.00	0.09	0.01	0.06	0.00
MOACS-2-S-CDAS	0.88	0.06	0.16	0.01	0.73	0.09	0.06	0.00
MOACS-2-L	0.07	0.00	0.03	0.00	0.09	0.00	0.86	0.18
DMOPSO-5	0.05	0.00	0.02	0.00	0.07	0.01	0.06	0.00
DMOPSO-1	0.04	0.02	0.01	0.01	0.05	0.02	0.04	0.00
DMOPSO-2	0.05	0.00	0.02	0.00	0.06	0.00	0.04	0.01
DMOPSO-3	0.04	0.00	0.01	0.00	0.05	0.01	0.04	0.00
DMOPSO-4	0.05	0.00	0.02	0.00	0.07	0.01	0.04	0.00
DMOPSO-1-L	0.05	0.00	0.02	0.00	0.06	0.00	0.04	0.00
NSGA-II	0.07	0.00	0.02	0.00	0.08	0.00	0.04	0.00
NSGA-II-L	0.04	0.00	0.02	0.00	0.05	0.00	0.05	0.00
SPEA2	0.04	0.00	0.01	0.00	0.05	0.00	0.04	0.00
SPEA2-L	0.04	0.00	0.01	0.00	0.05	0.00	0.03	0.00

Table D.76: Median and interquartile range of I_ϵ obtained by the optimisers for the Sawyer problems

	Sawyer-1 $\tilde{x} \pm IQR(x)$		Sawyer-2 $\tilde{x} \pm IQR(x)$		Sawyer-3 $\tilde{x} \pm IQR(x)$		Sawyer-4 $\tilde{x} \pm IQR(x)$	
BIANT-1	0.79	0.00	0.92	0.15	0.76	0.00	0.93	0.06
BIANT-2	0.79	0.00	0.96	0.09	0.70	0.10	0.97	0.01
CHAC-1	0.78	0.00	0.85	0.00	0.53	0.00	0.77	0.00
CHAC-1-L	0.78	0.00	0.85	0.00	0.53	0.00	0.77	0.00
CHAC-2	0.78	0.00	0.85	0.00	0.53	0.00	0.77	0.00
CHAC-2-L	0.78	0.00	0.85	0.00	0.53	0.00	0.77	0.01
MOACS-1	0.94	0.10	1.00	0.00	0.74	0.03	0.94	0.06
MOACS-1-S-CDAS	0.85	0.16	0.97	0.05	0.75	0.02	0.98	0.01
MOACS-1-L	0.81	0.00	0.98	0.00	0.75	0.01	0.96	0.00
MOACS-2	0.87	0.22	0.97	0.02	0.76	0.01	0.96	0.01
MOACS-2-S-CDAS	0.85	0.16	0.98	0.01	0.67	0.21	0.96	0.01
MOACS-2-L	0.83	0.01	0.99	0.00	0.71	0.03	0.93	0.10
DMOPSO-5	0.78	0.00	0.85	0.00	0.53	0.00	0.93	0.14
DMOPSO-1	0.78	0.00	0.85	0.00	0.53	0.01	0.77	0.01
DMOPSO-2	0.78	0.00	0.85	0.00	0.53	0.00	0.77	0.00
DMOPSO-3	0.78	0.00	0.85	0.00	0.53	0.00	0.77	0.00
DMOPSO-4	0.78	0.00	0.85	0.00	0.56	0.01	0.77	0.00
DMOPSO-1-L	0.78	0.00	0.85	0.00	0.53	0.00	0.79	0.01
NSGA-II	0.78	0.00	0.85	0.00	0.53	0.00	0.77	0.01
NSGA-II-L	0.78	0.00	0.85	0.00	0.53	0.01	0.77	0.01
SPEA2	0.78	0.00	0.85	0.00	0.53	0.00	0.77	0.00
SPEA2-L	0.78	0.00	0.85	0.00	0.53	0.01	0.77	0.01

D.1.12 Summarize of the I_C values obtained by the various dominance rules

Table D.79: $I_C(A_1, A_2)$ values obtained between the CHAC-1 and CHAC-1-L for all problems

		A_2			A2	
Problem	Algorithm	1	2	Problem	1	2
Arc111-1	1		0.42	Kilbrid-1		0.09
	2	0.37			0.14	
Arc111-2	1		0.34	Kilbrid-2		0.18
	2	0.41			0.35	
Arc111-3	1		0.41	Kilbrid-3		0.32
	2	0.40			0.36	
Arc111-4	1		0.42	Kilbrid-4		0.28
	2	0.38			0.29	
Arc111-5	1		0.40	Kilbrid-5		0.29
	2	0.38			0.32	
Buxey-1	1		0.36	Lutz1-1		0.00
	2	0.44			0.00	
Buxey-2	1		0.43	Lutz1-2		0.00
	2	0.42			0.00	
Buxey-3	1		0.30	Lutz1-3		0.00
	2	0.46			0.00	
Buxey-4	1		0.38	Lutz1-4		0.03
	2	0.40			0.06	
Buxey-5	1		0.40	Lutz1-5		0.00
	2	0.33			0.00	
Gunther-1	1		0.36	Mitchell-1		0.20
	2	0.42			0.19	
Gunther-2	1		0.40	Mitchell-2		0.05
	2	0.38			0.00	
Gunther-3 A_1	1		0.49	Mitchell-3		0.30
	2	0.33			0.38	
Gunther-4	1		0.44	Mitchell-4		0.27
	2	0.35			0.17	
Gunther-5	1		0.38	Mukherje-1		0.34
	2	0.41			0.38	
Hahn-1	1		0.35	Mukherje-2		0.36
	2	0.42			0.38	
Hahn-2	1		0.40	Mukherje-3		0.38
	2	0.35			0.37	
Hahn-3	1		0.40	Roszieg-1		0.00
	2	0.36			0.00	
Hahn-4	1		0.33	Roszieg-2		0.23
	2	0.40			0.23	
Hahn-5	1		0.40	Roszieg-3		0.39
	2	0.42			0.36	
Jackson-1	1		0.00	Roszieg-4		0.00
	2	0.00			0.00	
Jackson-2	1		0.00	Sawyer-1		0.00
	2	0.00			0.00	
Jackson-3	1		0.00	Sawyer-2		0.00
	2	0.08			0.00	
Jackson-4	1		0.00	Sawyer-3		0.00
	2	0.00			0.00	
Jackson-5	1		0.00	Sawyer-4		0.00
	2	0.00			0.00	

* In order to ease the readiness of the table, the CHAC-1 and CHAC-1-L are associated to respectively the number 1 and 2

Table D.80: $I_C(A_1, A_2)$ values obtained between the CHAC-2 and CHAC-2-L for all problems

		A_2			A2	
Problem	Algorithm	1	2	Problem	1	2
Arc111-1	1		0.34	Kilbrid-1		0.14
	2	0.40			0.10	
Arc111-2	1		0.38	Kilbrid-2		0.28
	2	0.40			0.38	
Arc111-3	1		0.46	Kilbrid-3		0.40
	2	0.36			0.29	
Arc111-4	1		0.38	Kilbrid-4		0.30
	2	0.44			0.34	
Arc111-5	1		0.38	Kilbrid-5		0.36
	2	0.38			0.29	
Buxey-1	1		0.40	Lutz1-1		0.00
	2	0.41			0.00	
Buxey-2	1		0.42	Lutz1-2		0.00
	2	0.36			0.00	
Buxey-3	1		0.47	Lutz1-3		0.00
	2	0.35			0.00	
Buxey-4	1		0.43	Lutz1-4		0.06
	2	0.42			0.03	
Buxey-5	1		0.32	Lutz1-5		0.00
	2	0.40			0.00	
Gunther-1	1		0.43	Mitchell-1		0.22
	2	0.39			0.10	
Gunther-2	1		0.40	Mitchell-2		0.05
	2	0.40			0.00	
Gunther-3 A_1	1		0.28	Mitchell-3		0.37
	2	0.48			0.29	
Gunther-4	1		0.39	Mitchell-4		0.29
	2	0.41			0.22	
Gunther-5	1		0.42	Mukherje-1		0.37
	2	0.42			0.40	
Hahn-1	1		0.40	Mukherje-2		0.38
	2	0.43			0.34	
Hahn-2	1		0.41	Mukherje-3		0.42
	2	0.31			0.33	
Hahn-3	1		0.36	Roszieg-1		0.00
	2	0.39			0.00	
Hahn-4	1		0.38	Roszieg-2		0.20
	2	0.38			0.31	
Hahn-5	1		0.41	Roszieg-3		0.32
	2	0.44			0.38	
Jackson-1	1		0.00	Roszieg-4		0.00
	2	0.00			0.00	
Jackson-2	1		0.00	Sawyer-1		0.00
	2	0.00			0.00	
Jackson-3	1		0.04	Sawyer-2		0.00
	2	0.04			0.00	
Jackson-4	1		0.00	Sawyer-3		0.00
	2	0.00			0.00	
Jackson-5	1		0.00	Sawyer-4		0.04
	2	0.00			0	

* In order to ease the readiness of the table, the CHAC-2 and CHAC-2-L are associated to respectively the number 1 and 2

Table D.81: $I_C(A_1, A_2)$ values obtained between the MOACS-1 and MOACS-1-L for all problems

		A_2			A2	
Problem	Algorithm	1	2	Problem	1	2
Arc111-1	1		0.42	Kilbrid-1		0.29
	2	0.47			0.40	
Arc111-2	1		0.39	Kilbrid-2		0.47
	2	0.48			0.33	
Arc111-3	1		0.44	Kilbrid-3		0.32
	2	0.42			0.60	
Arc111-4	1		0.47	Kilbrid-4		0.49
	2	0.40			0.34	
Arc111-5	1		0.48	Kilbrid-5		0.45
	2	0.39			0.38	
Buxey-1	1		0.43	Lutz1-1		0.00
	2	0.35			0.00	
Buxey-2	1		0.46	Lutz1-2		0.27
	2	0.34			0.18	
Buxey-3	1		0.39	Lutz1-3		0.33
	2	0.42			0.35	
Buxey-4	1		0.40	Lutz1-4		0.32
	2	0.44			0.23	
Buxey-5	1		0.36	Lutz1-5		0.36
	2	0.44			0.42	
Gunther-1	1		0.47	Mitchell-1		0.56
	2	0.32			0.33	
Gunther-2	1		0.48	Mitchell-2		0.20
	2	0.30			0.14	
Gunther-3 A_1	1		0.28	Mitchell-3		0.14
	2	0.56			0.21	
Gunther-4	1		0.40	Mitchell-4		0.17
	2	0.40			0.00	
Gunther-5	1		0.48	Mukherje-1		0.38
	2	0.35			0.42	
Hahn-1	1		0.40	Mukherje-2		0.34
	2	0.35			0.42	
Hahn-2	1		0.38	Mukherje-3		0.41
	2	0.38			0.35	
Hahn-3	1		0.42	Roszieg-1		0.00
	2	0.34			0.00	
Hahn-4	1		0.33	Roszieg-2		0.25
	2	0.40			0.29	
Hahn-5	1		0.56	Roszieg-3		0.22
	2	0.22			0.38	
Jackson-1	1		0.00	Roszieg-4		0.50
	2	0.05			0.00	
Jackson-2	1		0.05	Sawyer-1		0.50
	2	0.05			0.00	
Jackson-3	1		0.25	Sawyer-2		0.00
	2	0.27			0.00	
Jackson-4	1		0.00	Sawyer-3		0.00
	2	0.00			0.07	
Jackson-5	1		0.00	Sawyer-4		0
	2	0.00			0.13	

* In order to ease the readiness of the table, the MOACS-1 and MOACS-1-L are associated to respectively the number 1 and 2

Table D.82: $I_C(A_1, A_2)$ values obtained between the MOACS-2 and MOACS-2-L for all problems

		A_2			A2	
Problem	Algorithm	1	2	Problem	1	2
Arc111-1	1		0.38	Kilbrid-1		0.19
	2	0.40			0.07	
Arc111-2	1		0.42	Kilbrid-2		0.14
	2	0.42			0.41	
Arc111-3	1		0.36	Kilbrid-3		0.21
	2	0.46			0.49	
Arc111-4	1		0.40	Kilbrid-4		0.35
	2	0.38			0.31	
Arc111-5	1		0.42	Kilbrid-5		0.35
	2	0.40			0.31	
Buxey-1	1		0.52	Lutz1-1		0.00
	2	0.34			0.00	
Buxey-2	1		0.47	Lutz1-2		0.09
	2	0.34			0.40	
Buxey-3	1		0.38	Lutz1-3		0.31
	2	0.39			0.38	
Buxey-4	1		0.38	Lutz1-4		0.22
	2	0.50			0.43	
Buxey-5	1		0.48	Lutz1-5		0.25
	2	0.36			0.33	
Gunther-1	1		0.44	Mitchell-1		0.33
	2	0.40			0.27	
Gunther-2	1		0.44	Mitchell-2		0.17
	2	0.38			0.16	
Gunther-3 A_1	1		0.40	Mitchell-3		0.21
	2	0.43			0.26	
Gunther-4	1		0.42	Mitchell-4		0.14
	2	0.48			0.14	
Gunther-5	1		0.42	Mukherje-1		0.38
	2	0.42			0.36	
Hahn-1	1		0.38	Mukherje-2		0.44
	2	0.38			0.32	
Hahn-2	1		0.44	Mukherje-3		0.32
	2	0.32			0.42	
Hahn-3	1		0.28	Roszieg-1		0.00
	2	0.46			0.12	
Hahn-4	1		0.42	Roszieg-2		0.14
	2	0.33			0.44	
Hahn-5	1		0.63	Roszieg-3		0.29
	2	0.16			0.25	
Jackson-1	1		0.00	Roszieg-4		0.33
	2	0.06			0.00	
Jackson-2	1		0.00	Sawyer-1		0.00
	2	0.06			0.00	
Jackson-3	1		0.06	Sawyer-2		0.00
	2	0.23			0.00	
Jackson-4	1		0.00	Sawyer-3		0.00
	2	0.08			0.16	
Jackson-5	1		0.00	Sawyer-4		0.12
	2	0.00			0.05	

* In order to ease the readiness of the table, the MOACS-2 and MOACS-2-L are associated to respectively the number 1 and 2

Table D.83: $I_C(A_1, A_2)$ values obtained between the MOACS-1 and MOACS-1-S-CDAS for all problems

		A_2			A2	
Problem	Algorithm	1	2	Problem	1	2
Arc111-1	1		0.33	Kilbrid-1		0.21
	2	0.52			0.50	
Arc111-2	1		0.39	Kilbrid-2		0.33
	2	0.50			0.29	
Arc111-3	1		0.48	Kilbrid-3		0.44
	2	0.40			0.44	
Arc111-4	1		0.40	Kilbrid-4		0.37
	2	0.42			0.47	
Arc111-5	1		0.42	Kilbrid-5		0.47
	2	0.45			0.42	
Buxey-1	1		0.34	Lutz1-1		0.00
	2	0.44			0.00	
Buxey-2	1		0.43	Lutz1-2		0.30
	2	0.40			0.17	
Buxey-3	1		0.47	Lutz1-3		0.25
	2	0.34			0.41	
Buxey-4	1		0.52	Lutz1-4		0.24
	2	0.34			0.40	
Buxey-5	1		0.28	Lutz1-5		0.45
	2	0.50			0.25	
Gunther-1	1		0.39	Mitchell-1		0.50
	2	0.43			0.43	
Gunther-2	1		0.44	Mitchell-2		0.33
	2	0.38			0.14	
Gunther-3 A_1	1		0.28	Mitchell-3		0.14
	2	0.56			0.22	
Gunther-4	1		0.46	Mitchell-4		0.17
	2	0.34			0.00	
Gunther-5	1		0.53	Mukherje-1		0.22
	2	0.31			0.54	
Hahn-1	1		0.38	Mukherje-2		0.26
	2	0.36			0.45	
Hahn-2	1		0.38	Mukherje-3		0.28
	2	0.38			0.44	
Hahn-3	1		0.39	Roszieg-1		0.00
	2	0.34			0.00	
Hahn-4	1		0.28	Roszieg-2		0.29
	2	0.48			0.29	
Hahn-5	1		0.46	Roszieg-3		0.22
	2	0.24			0.14	
Jackson-1	1		0.05	Roszieg-4		0.33
	2	0.00			0.00	
Jackson-2	1		0.00	Sawyer-1		0.50
	2	0.06			0.00	
Jackson-3	1		0.28	Sawyer-2		0.00
	2	0.28			0.00	
Jackson-4	1		0.00	Sawyer-3		0.00
	2	0.00			0.06	
Jackson-5	1		0.00	Sawyer-4		0.00
	2	0.00			0.05	

* In order to ease the readiness of the table, the MOACS-1 and MOACS-1-S-CDAS are associated to respectively the number 1 and 2

Table D.84: $I_C(A_1, A_2)$ values obtained between the MOACS-2 and MOACS-2-S-CDAS for all problems

		A_2			A2	
Problem	Algorithm	1	2	Problem	1	2
Arc111-1	1		0.28	Kilbrid-1		0.12
	2	0.47			0.07	
Arc111-2	1		0.35	Kilbrid-2		0.14
	2	0.44			0.14	
Arc111-3	1		0.32	Kilbrid-3		0.20
	2	0.44			0.45	
Arc111-4	1		0.38	Kilbrid-4		0.30
	2	0.40			0.41	
Arc111-5	1		0.44	Kilbrid-5		0.32
	2	0.36			0.33	
Buxey-1	1		0.48	Lutz1-1		0.00
	2	0.36			0.00	
Buxey-2	1		0.40	Lutz1-2		0.08
	2	0.38			0.27	
Buxey-3	1		0.47	Lutz1-3		0.43
	2	0.32			0.29	
Buxey-4	1		0.42	Lutz1-4		0.33
	2	0.41			0.31	
Buxey-5	1		0.46	Lutz1-5		0.27
	2	0.34			0.53	
Gunther-1	1		0.50	Mitchell-1		0.33
	2	0.34			0.30	
Gunther-2	1		0.44	Mitchell-2		0.20
	2	0.43			0.14	
Gunther-3 A_1	1		0.44	Mitchell-3		0.17
	2	0.36			0.28	
Gunther-4	1		0.48	Mitchell-4		0.00
	2	0.42			0.17	
Gunther-5	1		0.42	Mukherje-1		0.40
	2	0.44			0.36	
Hahn-1	1		0.33	Mukherje-2		0.38
	2	0.41			0.38	
Hahn-2	1		0.48	Mukherje-3		0.31
	2	0.30			0.42	
Hahn-3	1		0.32	Roszieg-1		0.13
	2	0.45			0.13	
Hahn-4	1		0.42	Roszieg-2		0.14
	2	0.31			0.38	
Hahn-5	1		0.56	Roszieg-3		0.29
	2	0.20			0.29	
Jackson-1	1		0.06	Roszieg-4		0.00
	2	0.00			0.00	
Jackson-2	1		0.00	Sawyer-1		0.00
	2	0.00			0.00	
Jackson-3	1		0.08	Sawyer-2		0.00
	2	0.18			0.00	
Jackson-4	1		0.00	Sawyer-3		0.00
	2	0.08			0.07	
Jackson-5	1		0.00	Sawyer-4		0.15
	2	0.00			0.00	

* In order to ease the readiness of the table, the MOACS-2 and MOACS-2-S-CDAS are associated to respectively the number 1 and 2

D.2 General Friedman's nonparametric test applied for the various dominance rules and all problems

D.2.1 Group analysis

D.2.1.1 Group 1

Table D.85: Unadjusted and adjusted p-values obtained for problem instances of Group 1 through the application of Holm's post hoc procedure, using the MOACS-2-L as control algorithm according to I_{HV}

Algorithm	Unadjusted p-value	Adjusted p-value
Others	<0.000	<1.42E−05
BIANT-1	0.136	0.543
MOACS-2-S-CDAS	0.308	0.925
MOACS-2	0.600	1.199
BIANT-2	0.629	1.199

Table D.86: Unadjusted and adjusted p-values obtained for problem instances of Group 1 through the application of Holm's post hoc procedure, using the BIANT-2 as control algorithm according to I_{IGD}

Algorithm	Unadjusted p-value	Adjusted p-value
Others	<0.007	<0.029
MOACS-2	0.035	0.105
MOACS-2-L	0.111	0.221
BIANT-1	0.703	0.703

Table D.87: Unadjusted and adjusted p-values obtained for problem instances of Group 1 through the application of Holm's post hoc procedure, using the NSGA-II-L as control algorithm according to I_ϵ

Algorithm	Unadjusted p-value	Adjusted p-value
Others	<0.004	<0.026
SPEA2	0.249	1.494
SPEA2-L	0.463	2.316
MOACS-2	0.600	2.401
MOACS-2-S-CDAS	0.660	2.401
NSGA-II	0.698	2.401
MOACS-2-L	0.846	2.401

Table D.88: Unadjusted and adjusted p-values obtained for problem instances of Group 1 through the application of Holm's post hoc procedure, using the MOACS-2-L as control algorithm according to I_{Δ}

Algorithm	Unadjusted p-value	Adjusted p-value
Others	<0.000	<4.30E−25
MOACS-1-S-CDAS	0.035	0.246
BIANT-1	0.045	0.271
BIANT-2	0.051	0.271
MOACS-1-L	0.200	0.798
MOACS-1	0.234	0.798
MOACS-2-S-CDAS	0.504	1.009
MOACS-2	0.876	1.009

Table D.89: Unadjusted and adjusted p-values obtained for problem instances of Group 1 through the application of Holm's post hoc procedure, using the SPEA2-L as control algorithm in accordance with the computation time

Algorithm	Unadjusted p-value	Adjusted p-value
<NSGA-II-L	0.000	<1.20E−05
SPEA2	0.836	0.836

D.2.1.2 Group 2

Table D.90: Unadjusted and adjusted p-values obtained for problem instances of Group 2 through the application of Holm's post hoc procedure, using the CHAC-2-L as control algorithm according to I_{HV}

Algorithm	Unadjusted p-value	Adjusted p-value
Others	<0.017	<0.221
DMOPSO	0.285	3.414
NSGA-II-L	0.379	4.166
DMOPSO-2	0.497	4.974
SPEA2	0.527	4.974
DMOPSO-L	0.539	4.974
SPEA2-L	0.545	4.974
CHAC-1	0.547	4.974
DMOPSO-3	0.615	4.974
NSGA-II	0.633	4.974
DMOPSO-1	0.647	4.974
CHAC-1-L	0.695	4.974
CHAC-2	0.771	4.974

Table D.91: Unadjusted and adjusted p-values obtained for problem instances of Group 2 through the application of Holm's post hoc procedure, using the CHAC-2-L as control algorithm according to I_{IGD}

Algorithm	Unadjusted p-value	Adjusted p-value
Others	<0.000	<8.31E−23
DMOPSO-4	0.036	0.462
DMOPSO	0.194	2.333
DMOPSO-L	0.395	4.344
NSGA-II-L	0.441	4.412
SPEA2	0.581	5.226
SPEA2-L	0.604	5.226
CHAC-1	0.632	5.226
DMOPSO-2	0.729	5.226
CHAC-2	0.764	5.226
NSGA-II	0.773	5.226
DMOPSO-1	0.784	5.226
CHAC-1-L	0.804	5.226
DMOPSO-3	0.866	5.226

Table D.92: Unadjusted and adjusted p-values obtained for problem instances of Group 2 through the application of Holm's post hoc procedure, using the CHAC-2-L as control algorithm according to I_{ϵ}

Algorithm	Unadjusted p-value	Adjusted p-value
Others	<0.000	<2.88E−25
DMOPSO-4	0.092	1.197
DMOPSO	0.531	6.378
CHAC-1	0.577	6.378
NSGA-II-L	0.587	6.378
SPEA2-L	0.620	6.378
SPEA2	0.642	6.378
DMOPSO-2	0.652	6.378
DMOPSO-L	0.671	6.378
CHAC-1-L	0.704	6.378
DMOPSO-3	0.789	6.378
NSGA-II	0.791	6.378
DMOPSO-1	0.805	6.378
CHAC-2	0.854	6.378

Table D.93: Unadjusted and adjusted p-values obtained for problem instances of Group 2 through the application of Holm's post hoc procedure, using the MOACS-1-S-CDAS as control algorithm according to I_{Δ}

Algorithm	Unadjusted p-value	Adjusted p-value
Others	<0.001	<0.008
MOACS-2-S-CDAS	0.030	0.212
BIANT-2	0.035	0.212
MOACS-2-L	0.041	0.212
MOACS-2	0.064	0.256
MOACS-1	0.175	0.524
MOACS-1-L	0.553	1.105
BIANT-1	0.838	1.105

Table D.94: Unadjusted and adjusted p-values obtained for problem instances of Group 2 through the application of Holm's post hoc procedure, using the SPEA2 as control algorithm in accordance with the computation time

Algorithm	Unadjusted p-value	Adjusted p-value
Others	<0.000	<0.002
DMOPSO-3	0.237	0.710
NSGA-II-L	0.422	0.845
SPEA2-L	0.637	0.845

Appendix E

Detailed Analysis and Results of Chapter 5: Influence of the Local Search

---

Abstract

The present chapter presents the various analyses of Chapter 6, and (i) the values of the various quality indicators obtained by the local search for each problem instance and (ii) the detailed values of the Friedman's test.

E.1 Detailed values of the metrics

This section presents the procedure used for the definition of the parameters of the various optimization algorithms.

E.1.1 Problem Family: Arc111

Table E.1: Median and interquartile range of I_{HV} obtained by the optimisers for the Arc111 problems

	Arc111-1 $\tilde{x} \pm IQR(x)$		Arc111-2 $\tilde{x} \pm IQR(x)$		Arc111-3 $\tilde{x} \pm IQR(x)$		Arc111-4 $\tilde{x} \pm IQR(x)$		Arc111-5 $\tilde{x} \pm IQR(x)$	
BIANT-1	0.87	0.00	0.88	0.02	0.88	0.04	0.90	0.02	0.85	0.03
BIANT-2	0.89	0.01	0.89	0.02	0.86	0.01	0.86	0.02	0.90	0.02
CHAC-1	0.87	0.00	0.85	0.01	0.85	0.01	0.85	0.01	0.86	0.01
CHAC-1-L	0.87	0.01	0.85	0.01	0.85	0.01	0.85	0.01	0.86	0.01
CHAC-2	0.87	0.01	0.85	0.01	0.85	0.00	0.85	0.01	0.86	0.01
CHAC-2-L	0.87	0.00	0.85	0.01	0.85	0.01	0.85	0.01	0.86	0.01
MOACS-1	0.84	0.01	0.87	0.00	0.87	0.01	0.88	0.01	0.87	0.01
MOACS-1-S-CDAS	0.80	0.03	0.84	0.01	0.87	0.04	0.86	0.02	0.87	0.01
MOACS-1-L	0.85	0.01	0.87	0.01	0.87	0.00	0.88	0.01	0.87	0.01
MOACS-2	0.90	0.01	0.92	0.00	0.92	0.01	0.92	0.00	0.91	0.01
MOACS-2-S-CDAS	0.81	0.04	0.91	0.01	0.92	0.01	0.92	0.01	0.91	0.01
MOACS-2-L	0.90	0.01	0.91	0.00	0.92	0.00	0.92	0.01	0.91	0.00
MOACS-2-L-LS	0.90	0.01	0.91	0.01	0.92	0.01	0.92	0.01	0.91	0.00
NSGA-II	0.87	0.00	0.85	0.01	0.86	0.01	0.85	0.02	0.86	0.01
NSGA-L	0.87	0.01	0.86	0.01	0.86	0.02	0.86	0.02	0.86	0.01
NSGA-II-L-LS	0.87	0.01	0.85	0.01	0.85	0.01	0.85	0.01	0.85	0.01
SPEA2	0.87	0.01	0.85	0.01	0.85	0.01	0.86	0.01	0.86	0.01
SPEA2-LS	0.87	0.00	0.85	0.01	0.86	0.01	0.86	0.00	0.86	0.01
SPEA2-L	0.87	0.01	0.86	0.01	0.86	0.01	0.85	0.02	0.86	0.01

Table E.2: Median and interquartile range of I_{IGD} obtained by the optimisers for the Arc111 problems

	Arc111-1 $\tilde{x} \pm IQR(x)$		Arc111-2 $\tilde{x} \pm IQR(x)$		Arc111-3 $\tilde{x} \pm IQR(x)$		Arc111-4 $\tilde{x} \pm IQR(x)$		Arc111-5 $\tilde{x} \pm IQR(x)$	
BIANT-1	0.54	0.02	0.65	0.10	0.52	0.02	0.58	0.01	0.57	0.10
BIANT-2	0.51	0.02	0.54	0.04	0.55	0.01	0.59	0.03	0.52	0.03
CHAC-1	0.18	0.01	0.25	0.00	0.24	0.00	0.28	0.00	0.24	0.00
CHAC-1-L	0.18	0.00	0.25	0.00	0.24	0.00	0.28	0.00	0.24	0.00
CHAC-2	0.18	0.00	0.25	0.00	0.24	0.00	0.28	0.00	0.24	0.00
CHAC-2-L	0.18	0.00	0.25	0.00	0.24	0.00	0.28	0.01	0.24	0.00
MOACS-1	0.67	0.04	0.74	0.05	0.63	0.04	0.70	0.04	0.60	0.04
MOACS-1-S-CDAS	0.82	0.13	0.91	0.10	0.68	0.20	0.87	0.11	0.64	0.08
MOACS-1-L	0.64	0.04	0.72	0.04	0.62	0.02	0.72	0.07	0.63	0.06
MOACS-2	0.36	0.05	0.39	0.02	0.32	0.03	0.39	0.05	0.35	0.05
MOACS-2-S-CDAS	0.81	0.18	0.40	0.03	0.34	0.02	0.39	0.04	0.34	0.03
MOACS-2-L	0.35	0.05	0.38	0.04	0.32	0.02	0.40	0.05	0.36	0.02
MOACS-2-L-LS	0.34	0.04	0.38	0.07	0.32	0.03	0.38	0.03	0.32	0.03
NSGA-II	0.10	0.00	0.14	0.00	0.15	0.00	0.17	0.00	0.20	0.00
NSGA-L	0.10	0.00	0.14	0.00	0.15	0.00	0.18	0.01	0.20	0.00
NSGA-II-L-LS	0.10	0.00	0.15	0.00	0.15	0.00	0.17	0.00	0.20	0.00
SPEA2	0.10	0.00	0.15	0.01	0.15	0.00	0.17	0.00	0.20	0.00
SPEA2-LS	0.10	0.00	0.14	0.00	0.15	0.00	0.17	0.00	0.20	0.00
SPEA2-L	0.10	0.00	0.14	0.00	0.15	0.00	0.17	0.01	0.20	0.00

Table E.3: Median and interquartile range of I_ϵ obtained by the optimisers for the Arc111 problems

	Arc111-1 $\tilde{x} \pm IQR(x)$		Arc111-2 $\tilde{x} \pm IQR(x)$		Arc111-3 $\tilde{x} \pm IQR(x)$		Arc111-4 $\tilde{x} \pm IQR(x)$		Arc111-5 $\tilde{x} \pm IQR(x)$	
BIANT-1	0.54	0.02	0.65	0.10	0.52	0.02	0.58	0.01	0.57	0.10
BIANT-2	0.51	0.02	0.54	0.04	0.55	0.01	0.59	0.03	0.52	0.03
CHAC-1	0.18	0.01	0.25	0.00	0.24	0.00	0.28	0.00	0.24	0.00
CHAC-1-L	0.18	0.00	0.25	0.00	0.24	0.00	0.28	0.00	0.24	0.00
CHAC-2	0.18	0.00	0.25	0.00	0.24	0.00	0.28	0.00	0.24	0.00
CHAC-2-L	0.18	0.00	0.25	0.00	0.24	0.00	0.28	0.01	0.24	0.00
MOACS-1	0.67	0.04	0.74	0.05	0.63	0.04	0.70	0.04	0.60	0.04
MOACS-1-S-CDAS	0.82	0.13	0.91	0.10	0.68	0.20	0.87	0.11	0.64	0.08
MOACS-1-L	0.64	0.04	0.72	0.04	0.62	0.02	0.72	0.07	0.63	0.06
MOACS-2	0.36	0.05	0.39	0.02	0.32	0.03	0.39	0.05	0.35	0.05
MOACS-2-S-CDAS	0.81	0.18	0.40	0.03	0.34	0.02	0.39	0.04	0.34	0.03
MOACS-2-L	0.35	0.05	0.38	0.04	0.32	0.02	0.40	0.05	0.36	0.02
MOACS-2-L-LS	0.34	0.04	0.38	0.07	0.32	0.03	0.38	0.03	0.32	0.03
NSGA-II	0.10	0.00	0.14	0.00	0.15	0.00	0.17	0.00	0.20	0.00
NSGA-II-L	0.10	0.00	0.14	0.00	0.15	0.00	0.18	0.01	0.20	0.00
NSGA-II-L-LS	0.10	0.00	0.15	0.00	0.15	0.00	0.17	0.00	0.20	0.00
SPEA2	0.10	0.00	0.15	0.01	0.15	0.00	0.17	0.00	0.20	0.00
SPEA2-LS	0.10	0.00	0.14	0.00	0.15	0.00	0.17	0.00	0.20	0.00
SPEA2-L	0.10	0.00	0.14	0.00	0.15	0.00	0.17	0.01	0.20	0.00

Table E.4: Median and interquartile range of I_Δ obtained by the optimisers for the Arc111 problems

	Buxey-1 $\tilde{x} \pm IQR(x)$		Buxey-2 $\tilde{x} \pm IQR(x)$		Buxey-3 $\tilde{x} \pm IQR(x)$		Buxey-4 $\tilde{x} \pm IQR(x)$		Buxey-5 $\tilde{x} \pm IQR(x)$	
BIANT-1	0.55	0.02	0.60	0.01	0.65	0.09	0.54	0.01	0.70	0.06
BIANT-2	0.55	0.01	0.55	0.11	0.68	0.08	0.63	0.07	0.67	0.03
CHAC-1	0.75	0.03	0.81	0.05	0.87	0.05	0.81	0.05	0.82	0.05
CHAC-1-L	0.77	0.03	0.77	0.07	0.83	0.10	0.79	0.06	0.81	0.06
CHAC-2	0.73	0.06	0.77	0.04	0.85	0.01	0.80	0.05	0.82	0.08
CHAC-2-L	0.77	0.09	0.79	0.06	0.84	0.10	0.82	0.08	0.83	0.05
MOACS-1	0.59	0.04	0.58	0.06	0.61	0.08	0.58	0.07	0.65	0.03
MOACS-1-S-CDAS	0.66	0.05	0.69	0.08	0.71	0.08	0.69	0.06	0.72	0.07
MOACS-1-L	0.60	0.05	0.63	0.07	0.62	0.07	0.63	0.03	0.64	0.04
MOACS-2	0.43	0.03	0.51	0.05	0.40	0.07	0.45	0.07	0.53	0.09
MOACS-2-S-CDAS	0.69	0.03	0.58	0.06	0.57	0.08	0.52	0.04	0.59	0.09
MOACS-2-L	0.42	0.08	0.50	0.11	0.49	0.12	0.47	0.05	0.54	0.03
MOACS-2-L-LS	0.43	0.06	0.44	0.07	0.50	0.07	0.47	0.09	0.53	0.10
NSGA-II	0.85	0.07	0.87	0.06	0.93	0.06	0.91	0.04	0.86	0.06
NSGA-II-L	0.85	0.08	0.83	0.06	0.88	0.06	0.89	0.09	0.90	0.06
NSGA-II-L-LS	0.85	0.03	0.89	0.08	0.90	0.02	0.90	0.07	0.90	0.05
SPEA2	0.85	0.03	0.87	0.09	0.89	0.06	0.88	0.07	0.86	0.03
SPEA2-LS	0.83	0.04	0.85	0.05	0.89	0.06	0.90	0.05	0.89	0.07
SPEA2-L	0.84	0.08	0.85	0.03	0.90	0.05	0.88	0.05	0.87	0.08

Table E.5: Median and interquartile range of the computation time required by the optimisers for the Arc111 problems

	Arc111-1 $\tilde{x} \pm IQR(x)$		Arc111-2 $\tilde{x} \pm IQR(x)$		Arc111-3 $\tilde{x} \pm IQR(x)$		Arc111-4 $\tilde{x} \pm IQR(x)$		Arc111-5 $\tilde{x} \pm IQR(x)$	
BIANT-1	0.38	0.16	0.80	0.16	0.62	0.03	0.51	0.07	0.14	0.08
BIANT-2	0.69	0.15	0.59	0.34	0.39	0.03	0.27	0.02	0.15	0.04
CHAC-1	0.25	0.05	0.39	0.13	0.35	0.18	0.22	0.19	0.11	0.06
CHAC-1-L	0.23	0.02	0.42	0.18	0.44	0.17	0.29	0.10	0.15	0.06
CHAC-2	0.24	0.06	0.32	0.11	0.35	0.18	0.23	0.12	0.10	0.06
CHAC-2-L	0.30	0.13	0.35	0.26	0.44	0.11	0.22	0.09	0.09	0.06
MOACS-1	0.14	0.08	0.27	0.05	0.17	0.03	0.13	0.02	0.07	0.02
MOACS-1-S-CDAS	0.16	0.07	0.21	0.09	0.28	0.09	0.21	0.07	0.10	0.04
MOACS-1-L	0.15	0.12	0.18	0.06	0.18	0.16	0.12	0.04	0.07	0.05
MOACS-2	0.17	0.07	0.21	0.09	0.23	0.08	0.15	0.07	0.08	0.04
MOACS-2-S-CDAS	0.15	0.11	0.25	0.13	0.23	0.05	0.12	0.05	0.08	0.04
MOACS-2-L	0.15	0.06	0.21	0.03	0.19	0.06	0.18	0.08	0.06	0.03
MOACS-2-L-LS	0.16	0.12	0.27	0.07	0.28	0.11	0.22	0.17	0.10	0.08
NSGA-II	0.16	0.10	0.31	0.09	0.27	0.21	0.25	0.15	0.09	0.02
NSGA-II-L	0.18	0.03	0.25	0.02	0.29	0.10	0.19	0.12	0.08	0.04
NSGA-II-L-LS	0.12	0.03	0.18	0.12	0.19	0.05	0.13	0.05	0.06	0.02
SPEA2	0.09	0.01	0.17	0.04	0.15	0.11	0.10	0.05	0.05	0.03
SPEA2-LS	0.12	0.04	0.13	0.10	0.17	0.08	0.14	0.03	0.05	0.04
SPEA2-L	0.10	0.01	0.14	0.04	0.15	0.05	0.11	0.04	0.05	0.02

E.1.2 Problem Family: Buxey

Table E.6: Median and interquartile range of I_{HV} obtained by the optimisers for the Buxey problems

	Buxey-1		Buxey-2		Buxey-3		Buxey-4		Buxey-5	
	$\tilde{x}$	$IQR(x)$	$\tilde{x}$	$IQR(x)$	$\tilde{x}$	$IQR(x)$	$\tilde{x}$	$IQR(x)$	$\tilde{x}$	$IQR(x)$
BIANT-1	0.95	0.02	0.94	0.02	0.93	0.02	0.93	0.01	0.92	0.01
BIANT-2	0.95	0.01	0.94	0.03	0.92	0.02	0.93	0.03	0.94	0.02
CHAC-1	0.92	0.01	0.92	0.01	0.92	0.00	0.90	0.00	0.91	0.02
CHAC-1-L	0.93	0.01	0.92	0.01	0.91	0.01	0.90	0.01	0.91	0.01
CHAC-2	0.93	0.01	0.92	0.01	0.91	0.01	0.90	0.01	0.91	0.01
CHAC-2-L	0.93	0.01	0.92	0.01	0.92	0.01	0.91	0.01	0.91	0.01
MOACS-1	0.94	0.01	0.95	0.01	0.95	0.01	0.93	0.01	0.95	0.01
MOACS-1-S-CDAS	0.93	0.01	0.95	0.01	0.95	0.01	0.93	0.01	0.95	0.01
MOACS-1-L	0.94	0.01	0.95	0.00	0.94	0.01	0.93	0.01	0.95	0.01
MOACS-2	0.94	0.01	0.95	0.01	0.95	0.01	0.94	0.01	0.95	0.01
MOACS-2-S-CDAS	0.94	0.01	0.95	0.01	0.95	0.01	0.93	0.01	0.96	0.01
MOACS-2-L	0.94	0.01	0.95	0.00	0.95	0.01	0.94	0.01	0.95	0.01
MOACS-2-L-LS	0.94	0.01	0.95	0.01	0.96	0.01	0.94	0.01	0.95	0.01
NSGA-II	0.94	0.01	0.93	0.01	0.92	0.01	0.91	0.02	0.92	0.01
NSGA-L	0.93	0.01	0.93	0.01	0.92	0.01	0.91	0.01	0.92	0.00
NSGA-II-L-LS	0.94	0.01	0.92	0.01	0.91	0.01	0.90	0.01	0.91	0.01
SPEA2	0.94	0.00	0.93	0.01	0.92	0.00	0.91	0.01	0.91	0.01
SPEA2-LS	0.94	0.01	0.93	0.01	0.91	0.02	0.91	0.01	0.91	0.01
SPEA2-L	0.93	0.01	0.93	0.01	0.92	0.00	0.91	0.02	0.91	0.01

Table E.7: Median and interquartile range of I_{IGD} obtained by the optimisers for the Buxey problems

	Buxey-1		Buxey-2		Buxey-3		Buxey-4		Buxey-5	
	$\tilde{x}$	$IQR(x)$	$\tilde{x}$	$IQR(x)$	$\tilde{x}$	$IQR(x)$	$\tilde{x}$	$IQR(x)$	$\tilde{x}$	$IQR(x)$
BIANT-1	0.42	0.41	0.39	0.20	0.62	0.22	0.59	0.34	0.65	0.01
BIANT-2	0.28	0.14	0.49	0.23	0.84	0.44	0.23	0.04	0.50	0.31
CHAC-1	0.87	0.00	1.00	0.00	0.65	0.00	0.26	0.00	0.77	0.00
CHAC-1-L	0.87	0.00	1.00	0.00	0.65	0.00	0.26	0.00	0.77	0.00
CHAC-2	0.87	0.00	1.00	0.00	0.65	0.00	0.26	0.00	0.77	0.00
CHAC-2-L	0.87	0.00	1.00	0.00	0.65	0.00	0.26	0.00	0.77	0.00
MOACS-1	0.21	0.04	0.16	0.06	0.32	0.07	0.34	0.21	0.23	0.07
MOACS-1-L	0.21	0.08	0.16	0.05	0.30	0.05	0.39	0.14	0.21	0.09
MOACS-2	0.20	0.05	0.14	0.12	0.32	0.16	0.45	0.15	0.22	0.04
MOACS-2-S-CDAS	0.15	0.08	0.18	0.11	0.36	0.15	0.41	0.10	0.25	0.11
MOACS-2-L	0.20	0.04	0.20	0.12	0.34	0.13	0.31	0.17	0.55	0.51
MOACS-2-L-LS	0.24	0.10	0.17	0.05	0.29	0.22	0.37	0.19	0.31	0.09
NSGA-II	0.87	0.00	1.00	0.00	0.65	0.00	0.26	0.00	0.77	0.00
NSGA-L	0.87	0.00	1.00	0.00	0.65	0.00	0.26	0.00	0.77	0.00
NSGA-II-L-LS	0.87	0.00	1.00	0.00	0.65	0.00	0.26	0.00	0.77	0.00
SPEA2	0.87	0.00	1.00	0.00	0.65	0.00	0.26	0.00	0.77	0.00
SPEA2-LS	0.87	0.00	1.00	0.00	0.65	0.00	0.26	0.00	0.77	0.00
SPEA2-L	0.87	0.00	1.00	0.00	0.65	0.00	0.26	0.00	0.77	0.00

Table E.8: Median and interquartile range of I_ϵ obtained by the optimisers for the Buxey problems

	Buxey-1 $\tilde{x} \pm IQR(x)$		Buxey-2 $\tilde{x} \pm IQR(x)$		Buxey-3 $\tilde{x} \pm IQR(x)$		Buxey-4 $\tilde{x} \pm IQR(x)$		Buxey-5 $\tilde{x} \pm IQR(x)$	
BIANT-1	0.42	0.41	0.39	0.20	0.62	0.22	0.59	0.34	0.65	0.01
BIANT-2	0.28	0.14	0.49	0.23	0.84	0.44	0.23	0.04	0.50	0.31
CHAC-1	0.87	0.00	1.00	0.00	0.65	0.00	0.26	0.00	0.77	0.00
CHAC-1-L	0.87	0.00	1.00	0.00	0.65	0.00	0.26	0.00	0.77	0.00
CHAC-2	0.87	0.00	1.00	0.00	0.65	0.00	0.26	0.00	0.77	0.00
CHAC-2-L	0.87	0.00	1.00	0.00	0.65	0.00	0.26	0.00	0.77	0.00
MOACS-1	0.21	0.04	0.16	0.06	0.32	0.07	0.34	0.21	0.23	0.07
MOACS-1-L	0.21	0.08	0.16	0.05	0.30	0.05	0.39	0.14	0.21	0.09
MOACS-2	0.20	0.05	0.14	0.12	0.32	0.16	0.45	0.15	0.22	0.04
MOACS-2-S-CDAS	0.15	0.08	0.18	0.11	0.36	0.15	0.41	0.10	0.25	0.11
MOACS-2-L	0.20	0.04	0.20	0.12	0.34	0.13	0.31	0.17	0.55	0.51
MOACS-2-L-CHC	0.24	0.10	0.17	0.05	0.29	0.22	0.37	0.19	0.31	0.09
NSGA-II	0.87	0.00	1.00	0.00	0.65	0.00	0.26	0.00	0.77	0.00
NSGA-L	0.87	0.00	1.00	0.00	0.65	0.00	0.26	0.00	0.77	0.00
NSGA-L-CHC	0.87	0.00	1.00	0.00	0.65	0.00	0.26	0.00	0.77	0.00
SPEA2	0.87	0.00	1.00	0.00	0.65	0.00	0.26	0.00	0.77	0.00
SPEA2-CHC	0.87	0.00	1.00	0.00	0.65	0.00	0.26	0.00	0.77	0.00
SPEA2-L	0.87	0.00	1.00	0.00	0.65	0.00	0.26	0.00	0.77	0.00

Table E.9: Median and interquartile range of I_Δ obtained by the optimisers for the Buxey problems

	Buxey-1 $\tilde{x} \pm IQR(x)$		Buxey-2 $\tilde{x} \pm IQR(x)$		Buxey-3 $\tilde{x} \pm IQR(x)$		Buxey-4 $\tilde{x} \pm IQR(x)$		Buxey-5 $\tilde{x} \pm IQR(x)$	
BIANT-1	0.68	0.06	0.66	0.10	0.66	0.10	0.66	0.03	0.66	0.10
BIANT-2	0.61	0.05	0.70	0.10	0.67	0.08	0.61	0.02	0.65	0.09
CHAC-1	0.83	0.04	0.84	0.05	0.84	0.05	0.84	0.01	0.83	0.11
CHAC-1-L	0.88	0.07	0.86	0.04	0.83	0.05	0.81	0.06	0.81	0.04
CHAC-2	0.85	0.05	0.86	0.05	0.85	0.04	0.83	0.02	0.82	0.10
CHAC-2-L	0.92	0.07	0.84	0.04	0.78	0.05	0.85	0.03	0.78	0.05
MOACS-1	0.61	0.03	0.57	0.11	0.59	0.08	0.62	0.04	0.53	0.09
MOACS-1-S-CDAS	0.57	0.12	0.57	0.10	0.64	0.07	0.63	0.07	0.52	0.07
MOACS-1-L	0.60	0.04	0.63	0.08	0.61	0.06	0.66	0.09	0.57	0.04
MOACS-2	0.59	0.11	0.53	0.11	0.66	0.21	0.72	0.09	0.53	0.06
MOACS-2-S-CDAS	0.62	0.05	0.60	0.11	0.67	0.13	0.67	0.13	0.53	0.08
MOACS-2-L	0.62	0.10	0.56	0.13	0.65	0.08	0.66	0.08	0.62	0.16
MOACS-2-L-LS	0.62	0.13	0.58	0.05	0.60	0.04	0.65	0.11	0.55	0.05
NSGA-II	0.88	0.07	0.89	0.00	0.83	0.05	0.90	0.07	0.92	0.15
NSGA-II-L	0.91	0.08	0.91	0.03	0.84	0.04	0.85	0.05	0.88	0.08
NSGA-II-L-LS	0.91	0.06	0.88	0.07	0.89	0.07	0.86	0.09	0.85	0.05
SPEA2	0.88	0.10	0.90	0.09	0.82	0.07	0.86	0.03	0.86	0.04
SPEA2-LS	0.90	0.07	0.90	0.08	0.87	0.05	0.81	0.07	0.86	0.04
SPEA2-L	0.89	0.06	0.84	0.08	0.83	0.11	0.83	0.05	0.84	0.07

Table E.10: Median and interquartile range of the computation time required by the optimisers for the Buxey problems

	Buxey-1 $\tilde{x} \pm IQR(x)$		Buxey-2 $\tilde{x} \pm IQR(x)$		Buxey-3 $\tilde{x} \pm IQR(x)$		Buxey-4 $\tilde{x} \pm IQR(x)$		Buxey-5 $\tilde{x} \pm IQR(x)$	
BIANT-1	0.40	0.11	0.42	0.18	0.45	0.22	0.56	0.22	0.58	0.22
BIANT-2	0.37	0.37	0.44	0.15	0.53	0.27	0.80	0.38	0.78	0.29
CHAC-1	0.19	0.07	0.26	0.12	0.25	0.14	0.33	0.09	0.34	0.12
CHAC-1-L	0.23	0.13	0.28	0.11	0.29	0.15	0.37	0.11	0.36	0.10
CHAC-2	0.20	0.12	0.27	0.11	0.27	0.09	0.34	0.10	0.33	0.09
CHAC-2-L	0.18	0.09	0.29	0.06	0.21	0.03	0.33	0.11	0.32	0.16
MOACS-1	0.35	0.17	0.33	0.11	0.36	0.09	0.35	0.15	0.27	0.10
MOACS-1-S-CDAS	0.34	0.21	0.41	0.18	0.35	0.18	0.61	0.32	0.51	0.27
MOACS-1-L	0.34	0.17	0.43	0.30	0.31	0.09	0.34	0.15	0.37	0.07
MOACS-2	0.19	0.10	0.24	0.11	0.30	0.14	0.55	0.27	0.30	0.18
MOACS-2-S-CDAS	0.28	0.15	0.31	0.15	0.37	0.18	0.47	0.28	0.27	0.05
MOACS-2-L	0.21	0.05	0.27	0.18	0.34	0.13	0.32	0.11	0.31	0.13
MOACS-2-L-LS	0.18	0.12	0.27	0.18	0.27	0.13	0.35	0.16	0.39	0.18
NSGA-II	0.16	0.02	0.22	0.09	0.26	0.03	0.30	0.07	0.21	0.08
NSGA-II-L	0.12	0.05	0.23	0.10	0.20	0.08	0.25	0.09	0.18	0.08
NSGA-II-L-LS	0.08	0.03	0.12	0.05	0.13	0.08	0.14	0.07	0.13	0.05
SPEA2	0.09	0.04	0.12	0.05	0.12	0.02	0.15	0.06	0.17	0.04
SPEA2-LS	0.07	0.03	0.15	0.06	0.11	0.04	0.13	0.04	0.13	0.04
SPEA2-L	0.09	0.03	0.11	0.02	0.12	0.03	0.12	0.05	0.13	0.03

E.1.3 Problem Family: Gunther

Table E.11: Median and interquartile range of I_{HV} obtained by the optimisers for the Gunther problems

	Gunther-1 $\tilde{x} \pm IQR(x)$		Gunther-2 $\tilde{x} \pm IQR(x)$		Gunther-3 $\tilde{x} \pm IQR(x)$		Gunther-4 $\tilde{x} \pm IQR(x)$		Gunther-5 $\tilde{x} \pm IQR(x)$	
BIANT-1	0.96	0.01	0.96	0.01	0.96	0.02	0.94	0.02	0.94	0.00
BIANT-2	0.95	0.01	0.94	0.04	0.94	0.02	0.96	0.00	0.96	0.00
CHAC-1	0.92	0.01	0.92	0.01	0.92	0.01	0.92	0.01	0.91	0.01
CHAC-1-L	0.92	0.01	0.92	0.01	0.92	0.01	0.92	0.00	0.91	0.01
CHAC-2	0.92	0.01	0.92	0.01	0.92	0.01	0.92	0.01	0.90	0.01
CHAC-2-L	0.92	0.01	0.92	0.01	0.91	0.01	0.92	0.00	0.91	0.01
MOACS-1	0.92	0.00	0.91	0.01	0.92	0.00	0.92	0.01	0.93	0.00
MOACS-1-S-CDAS	0.92	0.00	0.92	0.01	0.91	0.01	0.92	0.00	0.93	0.01
MOACS-1-L	0.93	0.00	0.92	0.01	0.91	0.00	0.92	0.01	0.93	0.01
MOACS-2	0.93	0.01	0.93	0.01	0.92	0.01	0.93	0.01	0.94	0.01
MOACS-2-S-CDAS	0.93	0.01	0.93	0.00	0.92	0.01	0.93	0.01	0.94	0.01
MOACS-2-L	0.93	0.00	0.92	0.01	0.92	0.01	0.93	0.01	0.94	0.01
MOACS-2-L-LS	0.93	0.00	0.93	0.01	0.93	0.01	0.94	0.01	0.95	0.00
NSGA-II	0.93	0.01	0.93	0.01	0.92	0.00	0.93	0.01	0.91	0.01
NSGA-L	0.93	0.01	0.92	0.00	0.92	0.01	0.93	0.01	0.91	0.01
NSGA-II-L-LS	0.93	0.01	0.93	0.01	0.92	0.00	0.92	0.01	0.90	0.01
SPEA2	0.93	0.01	0.93	0.01	0.92	0.00	0.93	0.01	0.92	0.01
SPEA2-LS	0.93	0.01	0.92	0.01	0.92	0.01	0.92	0.01	0.91	0.01
SPEA2-L	0.93	0.01	0.92	0.01	0.92	0.01	0.92	0.01	0.91	0.01

Table E.12: Median and interquartile range of I_{IGD} obtained by the optimisers for the Gunther problems

	Gunther-1 $\tilde{x} \pm IQR(x)$		Gunther-2 $\tilde{x} \pm IQR(x)$		Gunther-3 $\tilde{x} \pm IQR(x)$		Gunther-4 $\tilde{x} \pm IQR(x)$		Gunther-5 $\tilde{x} \pm IQR(x)$	
BIANT-1	0.51	0.16	0.49	0.23	0.53	0.24	0.28	0.06	0.93	0.02
BIANT-2	0.60	0.12	0.44	0.19	0.47	0.11	0.24	0.08	0.60	0.06
CHAC-1	0.96	0.00	1.00	0.00	1.00	0.00	1.00	0.00	1.00	0.00
CHAC-1-L	0.96	0.00	1.00	0.00	1.00	0.00	1.00	0.00	1.00	0.00
CHAC-2	0.96	0.00	1.00	0.00	1.00	0.00	1.00	0.00	1.00	0.00
CHAC-2-L	0.96	0.00	1.00	0.00	1.00	0.00	1.00	0.00	1.00	0.00
MOACS-1	0.21	0.01	0.20	0.03	0.20	0.03	0.19	0.02	0.71	0.05
MOACS-1-S-CDAS	0.22	0.02	0.17	0.04	0.20	0.04	0.17	0.04	0.70	0.08
MOACS-1-L	0.22	0.01	0.19	0.08	0.20	0.05	0.21	0.06	0.71	0.03
MOACS-2	0.18	0.04	0.20	0.07	0.17	0.06	0.12	0.06	0.42	0.05
MOACS-2-S-CDAS	0.19	0.05	0.20	0.05	0.16	0.04	0.17	0.06	0.46	0.07
MOACS-2-L	0.18	0.05	0.17	0.04	0.20	0.05	0.16	0.06	0.46	0.03
MOACS-2-L-LS	0.34	0.08	0.33	0.03	0.24	0.08	0.18	0.06	0.46	0.07
NSGA-II	0.96	0.00	1.00	0.00	1.00	0.00	1.00	0.00	1.00	0.00
NSGA-L	0.96	0.00	1.00	0.00	1.00	0.00	1.00	0.00	1.00	0.00
NSGA-II-L-LS	0.96	0.00	1.00	0.00	1.00	0.00	1.00	0.00	1.00	0.00
SPEA2	0.96	0.00	1.00	0.00	1.00	0.00	1.00	0.00	1.00	0.00
SPEA2-LS	0.96	0.00	1.00	0.00	1.00	0.00	1.00	0.00	1.00	0.00
SPEA2-L	0.96	0.00	1.00	0.00	1.00	0.00	1.00	0.00	1.00	0.00

Table E.13: Median and interquartile range of I_ϵ obtained by the optimisers for the Gunther problems

	Gunther-1 $\tilde{x} \pm IQR(x)$		Gunther-2 $\tilde{x} \pm IQR(x)$		Gunther-3 $\tilde{x} \pm IQR(x)$		Gunther-4 $\tilde{x} \pm IQR(x)$		Gunther-5 $\tilde{x} \pm IQR(x)$	
BIANT-1	0.51	0.16	0.49	0.23	0.53	0.24	0.28	0.06	0.93	0.02
BIANT-2	0.60	0.12	0.44	0.19	0.47	0.11	0.24	0.08	0.60	0.06
CHAC-1	0.96	0.00	1.00	0.00	1.00	0.00	1.00	0.00	1.00	0.00
CHAC-1-L	0.96	0.00	1.00	0.00	1.00	0.00	1.00	0.00	1.00	0.00
CHAC-2	0.96	0.00	1.00	0.00	1.00	0.00	1.00	0.00	1.00	0.00
CHAC-2-L	0.96	0.00	1.00	0.00	1.00	0.00	1.00	0.00	1.00	0.00
MOACS-1	0.21	0.01	0.20	0.03	0.20	0.03	0.19	0.02	0.71	0.05
MOACS-1-S-CDAS	0.22	0.02	0.17	0.04	0.20	0.04	0.17	0.04	0.70	0.08
MOACS-1-L	0.22	0.01	0.19	0.08	0.20	0.05	0.21	0.06	0.71	0.03
MOACS-2	0.18	0.04	0.20	0.07	0.17	0.06	0.12	0.06	0.42	0.05
MOACS-2-S-CDAS	0.19	0.05	0.20	0.05	0.16	0.04	0.17	0.06	0.46	0.07
MOACS-2-L	0.18	0.05	0.17	0.04	0.20	0.05	0.16	0.06	0.46	0.03
MOACS-2-L-CHC	0.34	0.08	0.33	0.03	0.24	0.08	0.18	0.06	0.46	0.07
NSGA-II	0.96	0.00	1.00	0.00	1.00	0.00	1.00	0.00	1.00	0.00
NSGA-L	0.96	0.00	1.00	0.00	1.00	0.00	1.00	0.00	1.00	0.00
NSGA-L-CHC	0.96	0.00	1.00	0.00	1.00	0.00	1.00	0.00	1.00	0.00
SPEA2	0.96	0.00	1.00	0.00	1.00	0.00	1.00	0.00	1.00	0.00
SPEA2-CHC	0.96	0.00	1.00	0.00	1.00	0.00	1.00	0.00	1.00	0.00
SPEA2-L	0.96	0.00	1.00	0.00	1.00	0.00	1.00	0.00	1.00	0.00

Table E.14: Median and interquartile range of I_Δ obtained by the optimisers for the Gunther problems

	Gunther-1 $\tilde{x} \pm IQR(x)$		Gunther-2 $\tilde{x} \pm IQR(x)$		Gunther-3 $\tilde{x} \pm IQR(x)$		Gunther-4 $\tilde{x} \pm IQR(x)$		Gunther-5 $\tilde{x} \pm IQR(x)$	
BIANT-1	0.65	0.05	0.51	0.11	0.52	0.05	0.56	0.11	0.65	0.08
BIANT-2	0.67	0.14	0.65	0.12	0.64	0.09	0.62	0.06	0.60	0.07
CHAC-1	0.80	0.07	0.84	0.06	0.85	0.09	0.80	0.05	0.81	0.05
CHAC-1-L	0.78	0.06	0.80	0.07	0.81	0.04	0.79	0.07	0.84	0.06
CHAC-2	0.81	0.12	0.80	0.08	0.84	0.05	0.80	0.10	0.86	0.04
CHAC-2-L	0.79	0.10	0.80	0.09	0.82	0.06	0.85	0.03	0.87	0.04
MOACS-1	0.57	0.03	0.55	0.14	0.61	0.05	0.56	0.06	0.65	0.06
MOACS-1-S-CDAS	0.57	0.14	0.54	0.08	0.53	0.04	0.58	0.13	0.64	0.07
MOACS-1-L	0.52	0.14	0.52	0.08	0.55	0.10	0.56	0.09	0.63	0.05
MOACS-2	0.53	0.13	0.55	0.11	0.56	0.07	0.59	0.08	0.59	0.06
MOACS-2-S-CDAS	0.51	0.16	0.57	0.09	0.61	0.08	0.62	0.19	0.64	0.13
MOACS-2-L	0.55	0.08	0.57	0.17	0.57	0.09	0.62	0.10	0.61	0.14
MOACS-2-L-LS	0.61	0.16	0.61	0.08	0.55	0.10	0.55	0.11	0.58	0.10
NSGA-II	0.90	0.05	0.79	0.04	0.91	0.02	0.90	0.05	0.88	0.06
NSGA-L	0.88	0.07	0.80	0.05	0.89	0.05	0.85	0.10	0.91	0.03
NSGA-II-L-LS	0.89	0.04	0.82	0.14	0.86	0.06	0.87	0.10	0.88	0.07
SPEA2	0.90	0.08	0.83	0.05	0.86	0.04	0.84	0.10	0.88	0.06
SPEA2-LS	0.88	0.07	0.81	0.04	0.87	0.08	0.86	0.04	0.87	0.05
SPEA2-L	0.85	0.07	0.84	0.06	0.84	0.08	0.86	0.03	0.86	0.06

Table E.15: Median and interquartile range of the computation time required by the optimisers for the Gunther problems

	Gunther-1 $\tilde{x} \pm IQR(x)$		Gunther-2 $\tilde{x} \pm IQR(x)$		Gunther-3 $\tilde{x} \pm IQR(x)$		Gunther-4 $\tilde{x} \pm IQR(x)$		Gunther-5 $\tilde{x} \pm IQR(x)$	
BIANT-1	0.48	0.11	0.51	0.18	0.52	0.22	0.56	0.22	0.59	0.22
BIANT-2	0.49	0.37	0.57	0.15	0.63	0.27	0.70	0.38	0.81	0.29
CHAC-1	0.20	0.07	0.26	0.12	0.25	0.14	0.32	0.09	0.34	0.12
CHAC-1-L	0.21	0.12	0.28	0.13	0.31	0.16	0.40	0.12	0.37	0.10
CHAC-2	0.20	0.12	0.27	0.11	0.29	0.09	0.35	0.10	0.32	0.09
CHAC-2-L	0.19	0.09	0.30	0.06	0.23	0.03	0.34	0.11	0.33	0.16
MOACS-1	0.30	0.17	0.31	0.11	0.35	0.09	0.42	0.15	0.29	0.10
MOACS-1-S-CDAS	0.32	0.21	0.39	0.18	0.37	0.18	0.60	0.32	0.50	0.27
MOACS-1-L	0.31	0.17	0.42	0.30	0.32	0.09	0.41	0.15	0.35	0.07
MOACS-2	0.23	0.10	0.25	0.11	0.29	0.14	0.53	0.27	0.32	0.18
MOACS-2-S-CDAS	0.25	0.15	0.36	0.15	0.42	0.18	0.52	0.28	0.30	0.05
MOACS-2-L	0.21	0.05	0.31	0.18	0.36	0.13	0.39	0.11	0.32	0.13
DMOPSO-5	0.16	0.06	0.24	0.04	0.23	0.07	0.29	0.05	0.26	0.08
DMOPSO-1	0.17	0.07	0.23	0.09	0.20	0.12	0.32	0.08	0.24	0.10
DMOPSO-2	0.15	0.03	0.19	0.07	0.19	0.07	0.24	0.06	0.23	0.12
DMOPSO-3	0.20	0.03	0.22	0.07	0.23	0.06	0.25	0.08	0.35	0.10
DMOPSO-4	0.17	0.05	0.46	0.18	0.29	0.07	0.31	0.09	0.33	0.10
DMOPSO-1-L	0.13	0.03	0.23	0.05	0.23	0.05	0.23	0.10	0.25	0.04
NSGA-II	0.16	0.02	0.23	0.09	0.25	0.03	0.30	0.07	0.21	0.08
NSGA-II-L	0.13	0.05	0.22	0.10	0.20	0.08	0.26	0.09	0.18	0.08
SPEA2	0.09	0.04	0.14	0.05	0.12	0.02	0.16	0.06	0.17	0.04
SPEA2-L	0.09	0.03	0.11	0.02	0.12	0.03	0.14	0.05	0.13	0.03

E.1.4 Problem Family: Hahn

Table E.16: Median and interquartile range of I_{HV} obtained by the optimisers for the Hahn problems

	Hahn-1		Hahn-2		Hahn-3		Hahn-4		Hahn-5	
	$\tilde{x}$	$IQR(x)$	$\tilde{x}$	$IQR(x)$	$\tilde{x}$	$IQR(x)$	$\tilde{x}$	$IQR(x)$	$\tilde{x}$	$IQR(x)$
BIANT-1	0.95	0.02	0.95	0.01	0.94	0.01	0.94	0.01	0.94	0.01
BIANT-2	0.95	0.03	0.95	0.01	0.95	0.01	0.94	0.01	0.93	0.02
CHAC-1	0.90	0.01	0.89	0.01	0.88	0.01	0.87	0.00	0.86	0.01
CHAC-1-L	0.89	0.00	0.89	0.01	0.89	0.01	0.88	0.01	0.86	0.01
CHAC-2	0.89	0.01	0.89	0.01	0.88	0.00	0.88	0.01	0.85	0.01
CHAC-2-L	0.89	0.01	0.89	0.00	0.88	0.01	0.87	0.01	0.86	0.00
MOACS-1	0.91	0.00	0.92	0.01	0.91	0.01	0.91	0.00	0.92	0.01
MOACS-1-S-CDAS	0.92	0.01	0.92	0.01	0.91	0.00	0.90	0.01	0.92	0.01
MOACS-1-L	0.92	0.00	0.92	0.01	0.91	0.01	0.91	0.00	0.93	0.01
MOACS-2	0.92	0.01	0.93	0.01	0.93	0.01	0.92	0.14	0.93	0.01
MOACS-2-S-CDAS	0.92	0.01	0.94	0.01	0.92	0.00	0.92	0.01	0.94	0.01
MOACS-2-L	0.92	0.01	0.93	0.01	0.92	0.01	0.92	0.00	0.94	0.00
MOACS-2-L-LS	0.92	0.00	0.93	0.00	0.93	0.01	0.92	0.01	0.94	0.01
NSGA-II	0.90	0.01	0.90	0.01	0.89	0.01	0.88	0.00	0.86	0.01
NSGA-L	0.89	0.01	0.90	0.00	0.89	0.01	0.88	0.01	0.86	0.01
NSGA-II-L-LS	0.89	0.01	0.89	0.01	0.89	0.01	0.87	0.00	0.86	0.01
SPEA2	0.89	0.01	0.90	0.01	0.89	0.01	0.88	0.00	0.87	0.01
SPEA2-LS	0.89	0.01	0.89	0.01	0.89	0.01	0.88	0.00	0.86	0.01
SPEA2-L	0.90	0.00	0.90	0.01	0.89	0.01	0.89	0.00	0.86	0.01

Table E.17: Median and interquartile range of I_{IGD} obtained by the optimisers for the Hahn problems

	Hahn-1		Hahn-2		Hahn-3		Hahn-4		Hahn-5	
	$\tilde{x}$	$IQR(x)$	$\tilde{x}$	$IQR(x)$	$\tilde{x}$	$IQR(x)$	$\tilde{x}$	$IQR(x)$	$\tilde{x}$	$IQR(x)$
BIANT-1	0.54	0.09	0.83	0.09	0.85	0.14	0.22	0.02	0.55	0.15
BIANT-2	0.35	0.25	0.85	0.11	0.68	0.14	0.20	0.03	0.65	0.24
CHAC-1	0.49	0.00	0.80	0.01	0.66	0.02	0.17	0.01	0.53	0.00
CHAC-1-L	0.62	0.13	0.78	0.01	0.67	0.01	0.17	0.01	0.53	0.01
CHAC-2	0.62	0.13	0.78	0.01	0.67	0.01	0.17	0.01	0.53	0.01
CHAC-2-L	0.62	0.13	0.78	0.01	0.67	0.02	0.16	0.00	0.53	0.00
MOACS-1	0.25	0.01	0.74	0.04	0.65	0.10	0.16	0.01	0.50	0.03
MOACS-1-S-CDAS	0.31	0.10	0.73	0.03	0.62	0.06	0.17	0.03	0.51	0.03
MOACS-1-L	0.24	0.03	0.73	0.04	0.62	0.08	0.16	0.01	0.54	0.01
MOACS-2	0.30	0.07	0.70	0.15	0.47	0.07	0.13	0.04	0.40	0.11
MOACS-2-S-CDAS	0.28	0.11	0.50	0.09	0.50	0.07	0.13	0.04	0.38	0.07
MOACS-2-L	0.26	0.08	0.53	0.03	0.51	0.16	0.13	0.06	0.40	0.10
MOACS-2-L-LS	0.40	0.12	0.70	0.06	0.57	0.11	0.18	0.03	0.47	0.17
NSGA-II	0.49	0.13	0.56	0.00	0.53	0.12	0.14	0.00	0.35	0.01
NSGA-L	0.62	0.13	0.56	0.13	0.53	0.00	0.14	0.03	0.36	0.01
NSGA-II-L-LS	0.62	0.06	0.56	0.13	0.53	0.00	0.14	0.03	0.36	0.01
SPEA2	0.62	0.00	0.68	0.13	0.53	0.12	0.14	0.02	0.35	0.00
SPEA2-LS	0.62	0.13	0.56	0.00	0.59	0.12	0.14	0.03	0.35	0.01
SPEA2-L	0.49	0.10	0.56	0.13	0.59	0.12	0.16	0.01	0.35	0.00

Table E.18: Median and interquartile range of I_ϵ obtained by the optimisers for the Hahn problems

	Hahn-1		Hahn-2		Hahn-3		Hahn-4		Hahn-5	
	$\tilde{x}$	$IQR(x)$	$\tilde{x}$	$IQR(x)$	$\tilde{x}$	$IQR(x)$	$\tilde{x}$	$IQR(x)$	$\tilde{x}$	$IQR(x)$
BIANT-1	0.54	0.09	0.83	0.09	0.85	0.14	0.22	0.02	0.55	0.15
BIANT-2	0.35	0.25	0.85	0.11	0.68	0.14	0.20	0.03	0.65	0.24
CHAC-1	0.49	0.00	0.80	0.01	0.66	0.02	0.17	0.01	0.53	0.00
CHAC-1-L	0.62	0.13	0.78	0.01	0.67	0.01	0.17	0.01	0.53	0.01
CHAC-2	0.62	0.13	0.78	0.01	0.67	0.01	0.17	0.01	0.53	0.01
CHAC-2-L	0.62	0.13	0.78	0.01	0.67	0.02	0.16	0.00	0.53	0.00
MOACS-1	0.25	0.01	0.74	0.04	0.65	0.10	0.16	0.01	0.50	0.03
MOACS-1-S-CDAS	0.31	0.10	0.73	0.03	0.62	0.06	0.17	0.03	0.51	0.03
MOACS-1-L	0.24	0.03	0.73	0.04	0.62	0.08	0.16	0.01	0.54	0.01
MOACS-2	0.30	0.07	0.70	0.15	0.47	0.07	0.13	0.04	0.40	0.11
MOACS-2-S-CDAS	0.28	0.11	0.50	0.09	0.50	0.07	0.13	0.04	0.38	0.07
MOACS-2-L	0.26	0.08	0.53	0.03	0.51	0.16	0.13	0.06	0.40	0.10
MOACS-2-L-CHC	0.40	0.12	0.70	0.06	0.57	0.11	0.18	0.03	0.47	0.17
NSGA-II	0.49	0.13	0.56	0.00	0.53	0.12	0.14	0.00	0.35	0.01
NSGA-L	0.62	0.13	0.56	0.13	0.53	0.00	0.14	0.03	0.36	0.01
NSGA-L-CHC	0.62	0.06	0.56	0.13	0.53	0.00	0.14	0.03	0.36	0.01
SPEA2	0.62	0.00	0.68	0.13	0.53	0.12	0.14	0.02	0.35	0.00
SPEA2-CHC	0.62	0.13	0.56	0.00	0.59	0.12	0.14	0.03	0.35	0.01
SPEA2-L	0.49	0.10	0.56	0.13	0.59	0.12	0.16	0.01	0.35	0.00

Table E.19: Median and interquartile range of I_Δ obtained by the optimisers for the Hahn problems

	Hahn-1		Hahn-2		Hahn-3		Hahn-4		Hahn-5	
	$\tilde{x}$	$IQR(x)$	$\tilde{x}$	$IQR(x)$	$\tilde{x}$	$IQR(x)$	$\tilde{x}$	$IQR(x)$	$\tilde{x}$	$IQR(x)$
BIANT-1	0.41	0.10	0.39	0.03	0.45	0.02	0.44	0.09	0.36	0.07
BIANT-2	0.39	0.14	0.42	0.05	0.47	0.05	0.42	0.07	0.35	0.08
CHAC-1	0.81	0.03	0.85	0.03	0.82	0.08	0.81	0.09	0.89	0.06
CHAC-1-L	0.77	0.06	0.85	0.03	0.79	0.09	0.80	0.09	0.87	0.07
CHAC-2	0.77	0.08	0.85	0.04	0.83	0.05	0.84	0.05	0.88	0.04
CHAC-2-L	0.82	0.03	0.82	0.03	0.83	0.02	0.78	0.05	0.89	0.01
MOACS-1	0.37	0.05	0.43	0.09	0.46	0.05	0.44	0.07	0.39	0.05
MOACS-1-S-CDAS	0.40	0.02	0.43	0.06	0.45	0.10	0.44	0.06	0.34	0.06
MOACS-1-L	0.35	0.04	0.45	0.04	0.44	0.05	0.42	0.01	0.38	0.04
MOACS-2	0.37	0.05	0.36	0.10	0.44	0.07	0.42	0.04	0.33	0.03
MOACS-2-S-CDAS	0.36	0.09	0.41	0.05	0.41	0.07	0.42	0.07	0.35	0.11
MOACS-2-L	0.37	0.02	0.40	0.06	0.41	0.05	0.43	0.07	0.32	0.05
MOACS-2-L-LS	0.36	0.05	0.41	0.07	0.47	0.13	0.46	0.04	0.34	0.03
NSGA-II	0.85	0.05	0.92	0.11	0.90	0.03	0.89	0.07	0.95	0.04
NSGA-II-L	0.85	0.04	0.91	0.11	0.90	0.07	0.94	0.07	0.92	0.07
NSGA-II-L-LS	0.86	0.04	0.88	0.04	0.92	0.03	0.92	0.05	0.92	0.04
SPEA2	0.84	0.08	0.89	0.08	0.92	0.03	0.90	0.06	0.88	0.01
SPEA2-LS	0.84	0.05	0.90	0.02	0.89	0.07	0.83	0.04	0.91	0.05
SPEA2-L	0.85	0.10	0.90	0.03	0.91	0.06	0.64	0.03	0.91	0.04

Table E.20: Median and interquartile range of the computation time required by the optimisers for the Hahn problems

	Hahn-1 $\tilde{x} \pm IQR(x)$		Hahn-2 $\tilde{x} \pm IQR(x)$		Hahn-3 $\tilde{x} \pm IQR(x)$		Hahn-4 $\tilde{x} \pm IQR(x)$		Hahn-5 $\tilde{x} \pm IQR(x)$	
BIANT-1	0.76	0.14	0.49	0.30	0.49	0.33	0.40	0.19	0.37	0.17
BIANT-2	0.46	0.09	0.69	0.22	0.60	0.12	0.65	0.25	0.48	0.31
CHAC-1	0.33	0.12	0.30	0.09	0.24	0.06	0.14	0.03	0.20	0.05
CHAC-1-L	0.36	0.08	0.34	0.08	0.33	0.17	0.15	0.07	0.22	0.09
CHAC-2	0.29	0.15	0.28	0.12	0.22	0.12	0.18	0.04	0.19	0.08
CHAC-2-L	0.28	0.07	0.37	0.03	0.29	0.10	0.24	0.12	0.25	0.07
MOACS-1	0.43	0.18	0.32	0.19	0.20	0.09	0.23	0.04	0.29	0.09
MOACS-1-S-CDAS	0.43	0.16	0.43	0.13	0.39	0.23	0.20	0.19	0.26	0.14
MOACS-1-L	0.39	0.12	0.34	0.19	0.25	0.17	0.18	0.08	0.31	0.11
MOACS-2	0.20	0.26	0.28	0.10	0.36	0.23	0.24	0.11	0.26	0.18
MOACS-2-S-CDAS	0.30	0.09	0.29	0.07	0.30	0.12	0.22	0.10	0.30	0.11
MOACS-2-L	0.38	0.31	0.37	0.22	0.26	0.17	0.16	0.04	0.29	0.19
MOACS-2-L-LS	0.39	0.12	0.32	0.18	0.23	0.14	0.17	0.09	0.32	0.16
NSGA-II	0.34	0.13	0.26	0.08	0.13	0.08	0.18	0.06	0.19	0.07
NSGA-II-L	0.22	0.08	0.23	0.08	0.21	0.06	0.12	0.04	0.14	0.05
NSGA-II-L-LS	0.22	0.10	0.14	0.08	0.13	0.08	0.09	0.04	0.11	0.06
SPEA2	0.13	0.06	0.12	0.02	0.11	0.02	0.08	0.02	0.08	0.03
SPEA2-LS	0.14	0.06	0.12	0.04	0.12	0.07	0.07	0.04	0.07	0.04
SPEA2-L	0.15	0.06	0.15	0.03	0.10	0.01	0.07	0.02	0.13	0.04

E.1.5 Problem Family: Jackson

Table E.21: Median and interquartile range of I_{HV} obtained by the optimisers for the Jackson problems

	Jackson-1 $\tilde{x} \pm IQR(x)$		Jackson-2 $\tilde{x} \pm IQR(x)$		Jackson-3 $\tilde{x} \pm IQR(x)$		Jackson-4 $\tilde{x} \pm IQR(x)$		Jackson-5 $\tilde{x} \pm IQR(x)$	
BIANT-1	0.51	0.00	0.59	0.04	0.57	0.03	0.92	0.02	0.49	0.00
BIANT-2	0.51	0.00	0.61	0.03	0.58	0.01	0.89	0.03	0.49	0.00
CHAC-1	0.59	0.00	0.68	0.00	0.59	0.00	0.98	0.02	0.49	0.00
CHAC-1-L	0.59	0.00	0.68	0.00	0.59	0.00	0.97	0.00	0.49	0.00
CHAC-2	0.59	0.00	0.68	0.00	0.59	0.00	0.97	0.02	0.49	0.00
CHAC-2-L	0.59	0.00	0.68	0.00	0.59	0.00	0.98	0.02	0.49	0.00
MOACS-1	0.54	0.00	0.62	0.01	0.57	0.00	0.92	0.01	0.49	0.00
MOACS-1-S-CDAS	0.54	0.00	0.62	0.01	0.57	0.00	0.92	0.01	0.49	0.00
MOACS-1-L	0.54	0.02	0.62	0.00	0.57	0.00	0.92	0.02	0.49	0.00
MOACS-2	0.53	0.01	0.62	0.00	0.57	0.00	0.91	0.02	0.49	0.00
MOACS-2-S-CDAS	0.53	0.00	0.62	0.00	0.57	0.00	0.89	0.00	0.49	0.00
MOACS-2-L	0.53	0.01	0.62	0.01	0.57	0.00	0.89	0.02	0.49	0.00
MOACS-2-L-LS	0.58	0.00	0.67	0.00	0.58	0.00	0.92	0.02	0.49	0.00
NSGA-II	0.59	0.00	0.68	0.00	0.59	0.00	0.97	0.00	0.49	0.00
NSGA-L	0.59	0.00	0.68	0.00	0.59	0.00	0.97	0.00	0.49	0.00
NSGA-II-L-LS	0.59	0.00	0.68	0.00	0.59	0.00	0.97	0.00	0.49	0.00
SPEA2	0.59	0.00	0.68	0.00	0.59	0.00	0.99	0.02	0.49	0.00
SPEA2-LS	0.59	0.00	0.68	0.00	0.59	0.00	0.98	0.02	0.49	0.00
SPEA2-L	0.59	0.00	0.68	0.00	0.59	0.00	0.97	0.00	0.49	0.00

Table E.22: Median and interquartile range of I_{IGD} obtained by the optimisers for the Jackson problems

	Jackson-1 $\tilde{x} \pm IQR(x)$		Jackson-2 $\tilde{x} \pm IQR(x)$		Jackson-3 $\tilde{x} \pm IQR(x)$		Jackson-4 $\tilde{x} \pm IQR(x)$		Jackson-5 $\tilde{x} \pm IQR(x)$	
BIANT-1	0.93	0.05	0.90	0.76	0.38	0.00	0.38	0.37	0.90	0.00
BIANT-2	0.97	0.04	0.20	0.68	0.38	0.04	0.38	0.37	0.90	0.00
CHAC-1	0.17	0.00	0.19	0.00	0.35	0.00	0.17	0.04	0.90	0.00
CHAC-1-L	0.17	0.00	0.19	0.00	0.35	0.00	0.17	0.00	0.90	0.00
CHAC-2	0.17	0.00	0.19	0.00	0.35	0.00	0.17	0.04	0.90	0.00
CHAC-2-L	0.17	0.00	0.19	0.00	0.35	0.00	0.17	0.04	0.90	0.00
MOACS-1	0.20	0.00	0.19	0.20	0.39	0.05	0.17	0.00	0.90	0.00
MOACS-1-S-CDAS	0.20	0.00	0.19	0.00	0.38	0.04	0.17	0.00	0.90	0.00
MOACS-1-L	0.20	0.58	0.19	0.00	0.39	0.02	0.17	0.00	0.90	0.00
MOACS-2	0.20	0.02	0.19	0.00	0.54	0.21	0.18	0.02	0.90	0.00
MOACS-2-S-CDAS	0.20	0.02	0.19	0.00	0.54	0.29	0.19	0.01	0.90	0.00
MOACS-2-L	0.20	0.02	0.19	0.01	0.50	0.09	0.19	0.00	0.90	0.00
MOACS-2-L-LS	0.17	0.00	0.19	0.00	0.35	0.00	0.17	0.00	0.90	0.00
NSGA-II	0.17	0.00	0.19	0.00	0.35	0.00	0.17	0.00	0.90	0.00
NSGA-L	0.17	0.00	0.19	0.00	0.35	0.00	0.17	0.00	0.90	0.00
NSGA-II-L-LS	0.17	0.00	0.19	0.00	0.35	0.00	0.17	0.00	0.90	0.00
SPEA2	0.17	0.00	0.19	0.00	0.35	0.00	0.15	0.04	0.90	0.00
SPEA2-LS	0.17	0.00	0.19	0.00	0.35	0.00	0.17	0.04	0.90	0.00
SPEA2-L	0.17	0.00	0.19	0.00	0.35	0.00	0.17	0.00	0.90	0.00

Table E.23: Median and interquartile range of I_ϵ obtained by the optimisers for the Jackson problems

	Jackson-1 $\tilde{x} \pm IQR(x)$		Jackson-2 $\tilde{x} \pm IQR(x)$		Jackson-3 $\tilde{x} \pm IQR(x)$		Jackson-4 $\tilde{x} \pm IQR(x)$		Jackson-5 $\tilde{x} \pm IQR(x)$	
BIANT-1	0.93	0.05	0.90	0.76	0.38	0.00	0.38	0.37	0.90	0.00
BIANT-2	0.97	0.04	0.20	0.68	0.38	0.04	0.38	0.37	0.90	0.00
CHAC-1	0.17	0.00	0.19	0.00	0.35	0.00	0.17	0.04	0.90	0.00
CHAC-1-L	0.17	0.00	0.19	0.00	0.35	0.00	0.17	0.00	0.90	0.00
CHAC-2	0.17	0.00	0.19	0.00	0.35	0.00	0.17	0.04	0.90	0.00
CHAC-2-L	0.17	0.00	0.19	0.00	0.35	0.00	0.17	0.04	0.90	0.00
MOACS-1	0.20	0.00	0.19	0.20	0.39	0.05	0.17	0.00	0.90	0.00
MOACS-1-S-CDAS	0.20	0.00	0.19	0.00	0.38	0.04	0.17	0.00	0.90	0.00
MOACS-1-L	0.20	0.58	0.19	0.00	0.39	0.02	0.17	0.00	0.90	0.00
MOACS-2	0.20	0.02	0.19	0.00	0.54	0.21	0.18	0.02	0.90	0.00
MOACS-2-S-CDAS	0.20	0.02	0.19	0.00	0.54	0.29	0.19	0.01	0.90	0.00
MOACS-2-L	0.20	0.02	0.19	0.01	0.50	0.09	0.19	0.00	0.90	0.00
MOACS-2-L-CHC	0.17	0.00	0.19	0.00	0.35	0.00	0.17	0.00	0.90	0.00
NSGA-II	0.17	0.00	0.19	0.00	0.35	0.00	0.17	0.00	0.90	0.00
NSGA-L	0.17	0.00	0.19	0.00	0.35	0.00	0.17	0.00	0.90	0.00
NSGA-L-CHC	0.17	0.00	0.19	0.00	0.35	0.00	0.17	0.00	0.90	0.00
SPEA2	0.17	0.00	0.19	0.00	0.35	0.00	0.15	0.04	0.90	0.00
SPEA2-CHC	0.17	0.00	0.19	0.00	0.35	0.00	0.17	0.04	0.90	0.00
SPEA2-L	0.17	0.00	0.19	0.00	0.35	0.00	0.17	0.00	0.90	0.00

Table E.24: Median and interquartile range of I_Δ obtained by the optimisers for the Jackson problems

	Jackson-1 $\tilde{x} \pm IQR(x)$		Jackson-2 $\tilde{x} \pm IQR(x)$		Jackson-3 $\tilde{x} \pm IQR(x)$		Jackson-4 $\tilde{x} \pm IQR(x)$		Jackson-5 $\tilde{x} \pm IQR(x)$	
BIANT-1	0.92	0.00	0.85	0.05	0.90	0.05	0.76	0.07	0.79	0.05
BIANT-2	0.94	0.03	0.84	0.03	0.95	0.01	0.82	0.10	0.83	0.05
CHAC-1	1.00	0.00	0.94	0.00	0.97	0.01	0.82	0.07	0.87	0.00
CHAC-1-L	1.00	0.00	0.94	0.00	0.99	0.02	0.84	0.09	0.87	0.00
CHAC-2	1.00	0.00	0.94	0.00	0.98	0.01	0.82	0.06	0.87	0.00
CHAC-2-L	1.00	0.00	0.94	0.00	0.98	0.01	0.84	0.04	0.87	0.00
MOACS-1	0.93	0.02	0.85	0.02	0.81	0.03	0.82	0.18	0.89	0.03
MOACS-1-S-CDAS	0.93	0.01	0.85	0.04	0.79	0.10	0.83	0.25	0.86	0.04
MOACS-1-L	0.94	0.05	0.84	0.03	0.79	0.09	0.86	0.22	0.89	0.02
MOACS-2	0.89	0.02	0.81	0.05	0.84	0.08	0.76	0.17	0.88	0.05
MOACS-2-S-CDAS	0.90	0.03	0.82	0.03	0.88	0.05	0.87	0.07	0.87	0.01
MOACS-2-L	0.90	0.02	0.81	0.03	0.84	0.10	0.90	0.10	0.88	0.03
MOACS-2-L-LS	0.97	0.02	0.89	0.04	0.89	0.02	1.00	0.02	0.86	0.01
NSGA-II	1.00	0.00	0.94	0.00	0.97	0.01	0.89	0.03	0.87	0.00
NSGA-II-L	1.00	0.00	0.94	0.00	0.98	0.01	0.87	0.08	0.87	0.00
NSGA-II-L-LS	1.00	0.00	0.94	0.00	0.98	0.01	0.84	0.04	0.87	0.00
SPEA2	1.00	0.00	0.94	0.00	0.99	0.01	0.85	0.07	0.87	0.00
SPEA2-LS	1.00	0.00	0.94	0.00	0.98	0.02	0.85	0.03	0.87	0.00
SPEA2-L	1.00	0.00	0.94	0.00	0.98	0.02	0.87	0.05	0.87	0.00

Table E.25: Median and interquartile range of the computation time required by the optimisers for the Jackson problems

	Jackson-1		Jackson-2		Jackson-3		Jackson-4		Jackson-5	
	$\tilde{x}$	$IQR(x)$	$\tilde{x}$	$IQR(x)$	$\tilde{x}$	$IQR(x)$	$\tilde{x}$	$IQR(x)$	$\tilde{x}$	$IQR(x)$
BIANT-1	0.44	0.04	0.03	0.00	0.06	0.00	0.34	0.01	0.11	0.01
BIANT-2	0.42	0.07	0.03	0.00	0.06	0.00	0.35	0.02	0.09	0.00
CHAC-1	0.34	0.01	0.02	0.00	0.05	0.00	0.27	0.00	0.06	0.03
CHAC-1-L	0.24	0.11	0.02	0.01	0.04	0.02	0.18	0.09	0.09	0.00
CHAC-2	0.33	0.00	0.02	0.00	0.05	0.00	0.26	0.00	0.09	0.04
CHAC-2-L	0.33	0.13	0.02	0.01	0.05	0.02	0.26	0.11	0.05	0.02
MOACS-1	0.44	0.01	0.03	0.00	0.06	0.00	0.31	0.01	0.31	0.07
MOACS-1-S-CDAS	0.60	0.26	0.04	0.02	0.29	0.07	0.38	0.06	0.10	0.00
MOACS-1-L	0.46	0.02	0.03	0.00	0.06	0.00	0.32	0.01	0.10	0.00
MOACS-2	0.49	0.05	0.04	0.00	0.06	0.00	0.37	0.00	0.49	0.06
MOACS-2-S-CDAS	0.88	0.08	0.05	0.01	0.59	0.04	0.39	0.18	0.10	0.00
MOACS-2-L	0.51	0.04	0.04	0.00	0.06	0.01	0.36	0.02	0.05	0.00
MOACS-2-L-LS	0.25	0.03	0.02	0.00	0.03	0.00	0.17	0.00	0.10	0.00
NSGA-II	0.45	0.01	0.03	0.00	0.06	0.00	0.35	0.00	0.05	0.00
NSGA-L	0.30	0.10	0.02	0.00	0.04	0.00	0.21	0.00	0.04	0.01
NSGA-II-L-LS	0.17	0.06	0.01	0.00	0.03	0.00	0.13	0.02	0.08	0.00
SPEA2	0.28	0.00	0.02	0.00	0.05	0.00	0.23	0.00	0.04	0.01
SPEA2-LS	0.14	0.04	0.01	0.00	0.02	0.01	0.12	0.03	0.08	0.00
SPEA2-L	0.28	0.05	0.02	0.00	0.05	0.00	0.23	0.01	0.08	0.01

E.1.6 Problem Family: Kilbrid

Table E.26: Median and interquartile range of I_{HV} obtained by the optimisers for the Kilbrid problems

	Kilbrid-1 $\tilde{x} \pm IQR(x)$		Kilbrid-2 $\tilde{x} \pm IQR(x)$		Kilbrid-3 $\tilde{x} \pm IQR(x)$		Kilbrid-4 $\tilde{x} \pm IQR(x)$		Kilbrid-5 $\tilde{x} \pm IQR(x)$	
BIANT-1	0.45	0.11	0.93	0.06	0.85	0.06	0.82	0.03	0.90	0.06
BIANT-2	0.50	0.11	0.94	0.01	0.81	0.06	0.90	0.04	0.80	0.10
CHAC-1	0.74	0.01	0.97	0.02	0.95	0.01	0.94	0.02	0.93	0.01
CHAC-1-L	0.73	0.01	0.98	0.01	0.95	0.02	0.96	0.01	0.93	0.01
CHAC-2	0.74	0.01	0.97	0.01	0.95	0.01	0.95	0.02	0.93	0.01
CHAC-2-L	0.73	0.00	0.97	0.01	0.95	0.01	0.96	0.01	0.94	0.01
MOACS-1	0.61	0.04	0.92	0.01	0.86	0.04	0.83	0.03	0.83	0.04
MOACS-1-S-CDAS	0.60	0.01	0.93	0.02	0.88	0.06	0.84	0.06	0.83	0.03
MOACS-1-L	0.61	0.04	0.92	0.03	0.86	0.06	0.85	0.06	0.84	0.04
MOACS-2	0.57	0.18	0.95	0.01	0.83	0.05	0.84	0.02	0.83	0.03
MOACS-2-S-CDAS	0.70	0.02	0.93	0.04	0.83	0.02	0.85	0.04	0.83	0.04
MOACS-2-L	0.52	0.11	0.95	0.02	0.83	0.03	0.85	0.01	0.84	0.02
MOACS-2-L-LS	0.56	0.11	0.95	0.02	0.91	0.06	0.92	0.03	0.91	0.08
NSGA-II	0.73	0.01	0.97	0.00	0.93	0.02	0.95	0.01	0.94	0.01
NSGA-L	0.74	0.00	0.97	0.01	0.93	0.02	0.95	0.01	0.93	0.01
NSGA-II-L-LS	0.73	0.01	0.96	0.01	0.93	0.02	0.94	0.01	0.92	0.01
SPEA2	0.73	0.01	0.97	0.01	0.95	0.02	0.95	0.01	0.93	0.01
SPEA2-LS	0.74	0.01	0.97	0.01	0.95	0.01	0.95	0.01	0.93	0.01
SPEA2-L	0.73	0.01	0.98	0.02	0.94	0.02	0.95	0.01	0.93	0.01

Table E.27: Median and interquartile range of I_{IGD} obtained by the optimisers for the Kilbrid problems

	Kilbrid-1 $\tilde{x} \pm IQR(x)$		Kilbrid-2 $\tilde{x} \pm IQR(x)$		Kilbrid-3 $\tilde{x} \pm IQR(x)$		Kilbrid-4 $\tilde{x} \pm IQR(x)$		Kilbrid-5 $\tilde{x} \pm IQR(x)$	
BIANT-1	0.97	0.06	0.91	0.03	0.86	0.07	0.90	0.02	0.73	0.08
BIANT-2	0.94	0.06	0.91	0.01	0.90	0.07	0.81	0.05	0.82	0.10
CHAC-1	0.87	0.00	0.90	0.02	0.75	0.00	0.75	0.01	0.69	0.01
CHAC-1-L	0.87	0.00	0.90	0.01	0.75	0.00	0.75	0.02	0.69	0.01
CHAC-2	0.87	0.00	0.91	0.01	0.75	0.00	0.75	0.01	0.69	0.01
CHAC-2-L	0.87	0.00	0.90	0.02	0.75	0.00	0.75	0.00	0.68	0.01
MOACS-1	0.89	0.02	0.92	0.01	0.86	0.03	0.91	0.04	0.83	0.05
MOACS-1-S-CDAS	0.88	0.02	0.92	0.01	0.83	0.09	0.91	0.07	0.83	0.03
MOACS-1-L	0.89	0.01	0.93	0.02	0.86	0.07	0.89	0.08	0.81	0.04
MOACS-2	0.91	0.05	0.91	0.01	0.90	0.06	0.91	0.03	0.84	0.03
MOACS-2-S-CDAS	0.91	0.08	0.93	0.03	0.90	0.03	0.90	0.05	0.83	0.04
MOACS-2-L	0.93	0.05	0.91	0.01	0.90	0.03	0.90	0.01	0.83	0.03
MOACS-2-L-LS	0.87	0.00	0.91	0.01	0.81	0.07	0.81	0.03	0.76	0.09
NSGA-II	0.87	0.00	0.90	0.01	0.75	0.00	0.75	0.00	0.69	0.01
NSGA-L	0.87	0.00	0.90	0.01	0.75	0.01	0.75	0.00	0.69	0.02
NSGA-II-L-LS	0.87	0.00	0.91	0.01	0.75	0.00	0.75	0.00	0.70	0.01
SPEA2	0.87	0.00	0.90	0.01	0.75	0.00	0.75	0.01	0.69	0.01
SPEA2-LS	0.87	0.00	0.90	0.02	0.75	0.00	0.74	0.02	0.69	0.01
SPEA2-L	0.87	0.00	0.90	0.01	0.75	0.00	0.75	0.00	0.69	0.01

Table E.28: Median and interquartile range of I_ϵ obtained by the optimisers for the Kilbrid problems

	Kilbrid-1 $\tilde{x} \pm IQR(x)$		Kilbrid-2 $\tilde{x} \pm IQR(x)$		Kilbrid-3 $\tilde{x} \pm IQR(x)$		Kilbrid-4 $\tilde{x} \pm IQR(x)$		Kilbrid-5 $\tilde{x} \pm IQR(x)$	
BIANT-1	0.97	0.06	0.91	0.03	0.86	0.07	0.90	0.02	0.73	0.08
BIANT-2	0.94	0.06	0.91	0.01	0.90	0.07	0.81	0.05	0.82	0.10
CHAC-1	0.87	0.00	0.90	0.02	0.75	0.00	0.75	0.01	0.69	0.01
CHAC-1-L	0.87	0.00	0.90	0.01	0.75	0.00	0.75	0.02	0.69	0.01
CHAC-2	0.87	0.00	0.91	0.01	0.75	0.00	0.75	0.01	0.69	0.01
CHAC-2-L	0.87	0.00	0.90	0.02	0.75	0.00	0.75	0.00	0.68	0.01
MOACS-1	0.89	0.02	0.92	0.01	0.86	0.03	0.91	0.04	0.83	0.05
MOACS-1-S-CDAS	0.88	0.02	0.92	0.01	0.83	0.09	0.91	0.07	0.83	0.03
MOACS-1-L	0.89	0.01	0.93	0.02	0.86	0.07	0.89	0.08	0.81	0.04
MOACS-2	0.91	0.05	0.91	0.01	0.90	0.06	0.91	0.03	0.84	0.03
MOACS-2-S-CDAS	0.91	0.08	0.93	0.03	0.90	0.03	0.90	0.05	0.83	0.04
MOACS-2-L	0.93	0.05	0.91	0.01	0.90	0.03	0.90	0.01	0.83	0.03
MOACS-2-L-CHC	0.87	0.00	0.91	0.01	0.81	0.07	0.81	0.03	0.76	0.09
NSGA-II	0.87	0.00	0.90	0.01	0.75	0.00	0.75	0.00	0.69	0.01
NSGA-L	0.87	0.00	0.90	0.01	0.75	0.01	0.75	0.00	0.69	0.02
NSGA-L-CHC	0.87	0.00	0.91	0.01	0.75	0.00	0.75	0.00	0.70	0.01
SPEA2	0.87	0.00	0.90	0.01	0.75	0.00	0.75	0.01	0.69	0.01
SPEA2-CHC	0.87	0.00	0.90	0.02	0.75	0.00	0.74	0.02	0.69	0.01
SPEA2-L	0.87	0.00	0.90	0.01	0.75	0.00	0.75	0.00	0.69	0.01

Table E.29: Median and interquartile range of I_Δ obtained by the optimisers for the Kilbrid problems

	Kilbrid-1 $\tilde{x} \pm IQR(x)$		Kilbrid-2 $\tilde{x} \pm IQR(x)$		Kilbrid-3 $\tilde{x} \pm IQR(x)$		Kilbrid-4 $\tilde{x} \pm IQR(x)$		Kilbrid-5 $\tilde{x} \pm IQR(x)$	
BIANT-1	0.83	0.07	0.84	0.12	0.79	0.14	0.81	0.03	0.86	0.02
BIANT-2	0.85	0.10	0.96	0.09	0.78	0.03	0.83	0.09	0.94	0.02
CHAC-1	0.85	0.04	0.65	0.06	0.71	0.09	0.74	0.07	0.73	0.06
CHAC-1-L	0.86	0.03	0.63	0.11	0.71	0.05	0.75	0.05	0.71	0.06
CHAC-2	0.87	0.05	0.66	0.12	0.71	0.06	0.78	0.04	0.72	0.09
CHAC-2-L	0.86	0.03	0.63	0.06	0.73	0.04	0.72	0.03	0.74	0.08
MOACS-1	0.88	0.05	0.87	0.07	0.71	0.11	0.77	0.03	0.81	0.08
MOACS-1-S-CDAS	0.85	0.08	0.84	0.10	0.72	0.11	0.78	0.07	0.81	0.06
MOACS-1-L	0.84	0.05	0.72	0.13	0.76	0.05	0.79	0.06	0.76	0.12
MOACS-2	0.89	0.09	0.86	0.07	0.83	0.05	0.82	0.04	0.86	0.05
MOACS-2-S-CDAS	0.92	0.06	0.91	0.16	0.75	0.06	0.84	0.03	0.84	0.04
MOACS-2-L	0.87	0.05	0.93	0.06	0.79	0.07	0.82	0.06	0.88	0.08
MOACS-2-L-LS	0.91	0.01	0.91	0.08	0.82	0.08	0.87	0.03	0.91	0.07
NSGA-II	0.88	0.01	0.69	0.11	0.70	0.05	0.74	0.15	0.74	0.12
NSGA-L	0.87	0.03	0.69	0.08	0.71	0.07	0.70	0.07	0.70	0.06
NSGA-II-L-LS	0.87	0.02	0.65	0.10	0.71	0.08	0.77	0.10	0.72	0.07
SPEA2	0.86	0.03	0.64	0.10	0.73	0.05	0.74	0.06	0.77	0.08
SPEA2-LS	0.85	0.03	0.62	0.08	0.72	0.07	0.75	0.08	0.72	0.10
SPEA2-L	0.86	0.04	0.66	0.07	0.72	0.06	0.78	0.07	0.68	0.10

Table E.30: Median and interquartile range of the computation time required by the optimisers for the Kilbrid problems

	Kilbrid-1 $\tilde{x} \pm IQR(x)$		Kilbrid-2 $\tilde{x} \pm IQR(x)$		Kilbrid-3 $\tilde{x} \pm IQR(x)$		Kilbrid-4 $\tilde{x} \pm IQR(x)$		Kilbrid-5 $\tilde{x} \pm IQR(x)$	
BIANT-1	0.03	0.00	0.04	0.00	0.01	0.00	0.02	0.00	0.02	0.00
BIANT-2	0.03	0.01	0.04	0.00	0.02	0.00	0.02	0.00	0.02	0.00
CHAC-1	0.03	0.00	0.04	0.00	0.02	0.00	0.03	0.00	0.03	0.00
CHAC-1-L	0.03	0.01	0.04	0.00	0.02	0.00	0.02	0.01	0.03	0.00
CHAC-2	0.03	0.01	0.04	0.00	0.02	0.01	0.03	0.01	0.03	0.01
CHAC-2-L	0.03	0.02	0.04	0.01	0.02	0.01	0.03	0.01	0.02	0.00
MOACS-1	0.03	0.00	0.04	0.00	0.01	0.00	0.02	0.00	0.02	0.00
MOACS-1-S-CDAS	0.03	0.00	0.79	0.08	0.42	0.28	0.59	0.17	0.48	0.13
MOACS-1-L	0.32	0.10	0.04	0.00	0.02	0.00	0.02	0.00	0.02	0.01
MOACS-2	0.03	0.00	0.04	0.00	0.01	0.00	0.02	0.00	0.02	0.00
MOACS-2-S-CDAS	0.02	0.00	0.56	0.11	0.22	0.09	0.31	0.01	0.26	0.14
MOACS-2-L	0.02	0.00	0.04	0.00	0.01	0.00	0.02	0.01	0.02	0.00
MOACS-2-L-LS	0.02	0.01	0.03	0.00	0.02	0.01	0.03	0.00	0.03	0.02
NSGA-II	0.02	0.01	0.03	0.00	0.02	0.00	0.03	0.00	0.02	0.01
NSGA-II-L	0.02	0.00	0.02	0.00	0.01	0.00	0.02	0.01	0.02	0.01
NSGA-II-L-LS	0.01	0.00	0.02	0.00	0.01	0.00	0.02	0.01	0.01	0.01
SPEA2	0.02	0.00	0.02	0.00	0.01	0.00	0.02	0.01	0.02	0.00
SPEA2-LS	0.01	0.00	0.02	0.01	0.01	0.00	0.01	0.01	0.01	0.01
SPEA2-L	0.02	0.00	0.02	0.00	0.01	0.00	0.02	0.00	0.01	0.00

E.1.7 Problem Family: Lutz1

Table E.31: Median and interquartile range of I_{HV} obtained by the optimisers for the Lutz1 problems

	Lutz1-1		Lutz1-2		Lutz1-3		Lutz1-4		Lutz1-5	
	$\tilde{x}$	$IQR(x)$	$\tilde{x}$	$IQR(x)$	$\tilde{x}$	$IQR(x)$	$\tilde{x}$	$IQR(x)$	$\tilde{x}$	$IQR(x)$
BIANT-1	0.89	0.00	0.96	0.01	0.90	0.02	0.93	0.02	0.86	0.02
BIANT-2	0.89	0.00	0.87	0.08	0.88	0.05	0.86	0.02	0.87	0.03
CHAC-1	0.91	0.00	1.00	0.00	1.00	0.00	1.00	0.00	1.00	0.00
CHAC-1-L	0.91	0.00	1.00	0.00	1.00	0.00	1.00	0.00	1.00	0.00
CHAC-2	0.91	0.00	1.00	0.00	1.00	0.00	1.00	0.00	1.00	0.00
CHAC-2-L	0.91	0.00	1.00	0.00	1.00	0.00	1.00	0.00	1.00	0.00
MOACS-1	0.89	0.00	0.87	0.10	0.76	0.13	0.78	0.10	0.76	0.09
MOACS-1-S-CDAS	0.89	0.00	0.86	0.10	0.77	0.06	0.74	0.10	0.77	0.08
MOACS-1-L	0.89	0.00	0.87	0.11	0.73	0.08	0.82	0.10	0.74	0.08
MOACS-2	0.89	0.00	0.87	0.02	0.79	0.03	0.73	0.05	0.81	0.07
MOACS-2-S-CDAS	0.89	0.00	0.84	0.05	0.77	0.03	0.75	0.08	0.80	0.04
MOACS-2-L	0.89	0.00	0.84	0.02	0.71	0.05	0.72	0.02	0.79	0.07
MOACS-2-L-LS	0.91	0.00	0.98	0.02	0.93	0.01	0.95	0.04	0.95	0.02
NSGA-II	0.91	0.00	1.00	0.00	1.00	0.00	1.00	0.00	1.00	0.00
NSGA-L	0.91	0.00	1.00	0.00	1.00	0.00	1.00	0.00	1.00	0.00
NSGA-II-L-LS	0.91	0.00	1.00	0.00	1.00	0.00	1.00	0.00	1.00	0.00
SPEA2	0.91	0.00	1.00	0.00	1.00	0.00	1.00	0.00	1.00	0.00
SPEA2-LS	0.91	0.00	1.00	0.00	1.00	0.00	1.00	0.00	1.00	0.00
SPEA2-L	0.91	0.00	1.00	0.00	1.00	0.00	1.00	0.00	1.00	0.00

Table E.32: Median and interquartile range of I_{IGD} obtained by the optimisers for the Lutz1 problems

	Lutz1-1		Lutz1-2		Lutz1-3		Lutz1-4		Lutz1-5	
	$\tilde{x}$	$IQR(x)$	$\tilde{x}$	$IQR(x)$	$\tilde{x}$	$IQR(x)$	$\tilde{x}$	$IQR(x)$	$\tilde{x}$	$IQR(x)$
BIANT-1	1.00	0.00	0.87	0.02	0.86	0.02	0.72	0.00	0.58	0.19
BIANT-2	1.00	0.00	0.87	0.05	0.89	0.06	0.71	0.04	0.47	0.05
CHAC-1	0.89	0.00	0.78	0.00	0.75	0.00	0.62	0.00	0.42	0.00
CHAC-1-L	0.89	0.00	0.78	0.00	0.75	0.00	0.62	0.00	0.42	0.00
CHAC-2	0.89	0.00	0.78	0.00	0.75	0.00	0.62	0.00	0.42	0.00
CHAC-2-L	0.89	0.00	0.78	0.00	0.75	0.00	0.62	0.00	0.42	0.00
MOACS-1	1.00	0.00	0.89	0.02	0.90	0.11	0.83	0.21	0.78	0.20
MOACS-1-S-CDAS	1.00	0.00	0.89	0.02	0.95	0.10	0.83	0.13	0.74	0.09
MOACS-1-L	1.00	0.00	0.89	0.03	0.88	0.09	0.97	0.13	0.78	0.15
MOACS-2	1.00	0.00	0.89	0.00	0.98	0.03	0.83	0.02	0.70	0.21
MOACS-2-S-CDAS	1.00	0.00	0.90	0.01	0.98	0.05	0.84	0.03	0.68	0.11
MOACS-2-L	1.00	0.00	0.89	0.01	0.98	0.00	0.97	0.14	0.75	0.08
MOACS-2-L-LS	0.89	0.00	0.81	0.07	0.85	0.03	0.69	0.04	0.46	0.00
NSGA-II	0.89	0.00	0.78	0.00	0.75	0.00	0.62	0.00	0.42	0.00
NSGA-II-L	0.89	0.00	0.78	0.00	0.75	0.00	0.62	0.00	0.42	0.00
NSGA-II-L-LS	0.89	0.00	0.78	0.00	0.75	0.00	0.62	0.00	0.42	0.00
SPEA2	0.89	0.00	0.78	0.00	0.75	0.00	0.62	0.00	0.42	0.00
SPEA2-LS	0.89	0.00	0.78	0.00	0.75	0.00	0.62	0.00	0.42	0.00
SPEA2-L	0.89	0.00	0.78	0.00	0.75	0.00	0.62	0.00	0.42	0.00

Table E.33: Median and interquartile range of I_ϵ obtained by the optimisers for the Lutz1 problems

	Lutz1-1 $\tilde{x} \pm IQR(x)$		Lutz1-2 $\tilde{x} \pm IQR(x)$		Lutz1-3 $\tilde{x} \pm IQR(x)$		Lutz1-4 $\tilde{x} \pm IQR(x)$		Lutz1-5 $\tilde{x} \pm IQR(x)$	
BIANT-1	1.00	0.00	0.87	0.02	0.86	0.02	0.72	0.00	0.58	0.19
BIANT-2	1.00	0.00	0.87	0.05	0.89	0.06	0.71	0.04	0.47	0.05
CHAC-1	0.89	0.00	0.78	0.00	0.75	0.00	0.62	0.00	0.42	0.00
CHAC-1-L	0.89	0.00	0.78	0.00	0.75	0.00	0.62	0.00	0.42	0.00
CHAC-2	0.89	0.00	0.78	0.00	0.75	0.00	0.62	0.00	0.42	0.00
CHAC-2-L	0.89	0.00	0.78	0.00	0.75	0.00	0.62	0.00	0.42	0.00
MOACS-1	1.00	0.00	0.89	0.02	0.90	0.11	0.83	0.21	0.78	0.20
MOACS-1-S-CDAS	1.00	0.00	0.89	0.02	0.95	0.10	0.83	0.13	0.74	0.09
MOACS-1-L	1.00	0.00	0.89	0.03	0.88	0.09	0.97	0.13	0.78	0.15
MOACS-2	1.00	0.00	0.89	0.00	0.98	0.03	0.83	0.02	0.70	0.21
MOACS-2-S-CDAS	1.00	0.00	0.90	0.01	0.98	0.05	0.84	0.03	0.68	0.11
MOACS-2-L	1.00	0.00	0.89	0.01	0.98	0.00	0.97	0.14	0.75	0.08
MOACS-2-L-CHC	0.89	0.00	0.81	0.07	0.85	0.03	0.69	0.04	0.46	0.00
NSGA-II	0.89	0.00	0.78	0.00	0.75	0.00	0.62	0.00	0.42	0.00
NSGA-L	0.89	0.00	0.78	0.00	0.75	0.00	0.62	0.00	0.42	0.00
NSGA-L-CHC	0.89	0.00	0.78	0.00	0.75	0.00	0.62	0.00	0.42	0.00
SPEA2	0.89	0.00	0.78	0.00	0.75	0.00	0.62	0.00	0.42	0.00
SPEA2-CHC	0.89	0.00	0.78	0.00	0.75	0.00	0.62	0.00	0.42	0.00
SPEA2-L	0.89	0.00	0.78	0.00	0.75	0.00	0.62	0.00	0.42	0.00

Table E.34: Median and interquartile range of I_Δ obtained by the optimisers for the Lutz1 problems

	Lutz1-1 $\tilde{x} \pm IQR(x)$		Lutz1-2 $\tilde{x} \pm IQR(x)$		Lutz1-3 $\tilde{x} \pm IQR(x)$		Lutz1-4 $\tilde{x} \pm IQR(x)$		Lutz1-5 $\tilde{x} \pm IQR(x)$	
BIANT-1	1.00	0.00	0.81	0.08	0.78	0.11	0.79	0.21	0.79	0.06
BIANT-2	1.00	0.00	0.81	0.07	0.92	0.08	0.85	0.10	0.86	0.03
CHAC-1	0.98	0.00	0.86	0.00	0.93	0.00	0.97	0.01	0.99	0.00
CHAC-1-L	0.98	0.00	0.86	0.00	0.93	0.00	0.97	0.01	0.99	0.00
CHAC-2	0.98	0.00	0.86	0.00	0.93	0.00	0.97	0.02	0.99	0.00
CHAC-2-L	0.98	0.00	0.86	0.00	0.93	0.00	0.97	0.01	0.99	0.00
MOACS-1	1.00	0.00	0.85	0.03	0.73	0.22	0.73	0.18	0.83	0.09
MOACS-1-S-CDAS	1.00	0.00	0.84	0.08	0.80	0.09	0.83	0.11	0.71	0.14
MOACS-1-L	1.00	0.00	0.82	0.10	0.82	0.05	0.74	0.17	0.79	0.03
MOACS-2	1.00	0.00	0.83	0.02	0.82	0.13	0.75	0.14	0.75	0.13
MOACS-2-S-CDAS	1.00	0.00	0.76	0.16	0.77	0.10	0.84	0.03	0.78	0.14
MOACS-2-L	1.00	0.00	0.75	0.15	0.80	0.10	0.75	0.16	0.71	0.22
MOACS-2-L-LS	0.99	0.01	0.89	0.09	0.70	0.07	0.83	0.07	0.92	0.06
NSGA-II	0.98	0.00	0.86	0.00	0.93	0.00	0.97	0.02	0.99	0.00
NSGA-L	0.98	0.00	0.86	0.00	0.93	0.00	0.98	0.01	0.99	0.00
NSGA-II-L-LS	0.98	0.00	0.86	0.00	0.93	0.03	0.97	0.02	0.99	0.00
SPEA2	0.98	0.00	0.86	0.00	0.93	0.00	0.97	0.00	0.99	0.00
SPEA2-LS	0.98	0.00	0.86	0.00	0.93	0.00	0.97	0.03	0.99	0.00
SPEA2-L	0.98	0.00	0.86	0.00	0.93	0.00	0.98	0.02	0.99	0.00

Table E.35: Median and interquartile range of the computation time required by the optimisers for the Lutz1 problems

	Lutz1-1 $\tilde{x} \pm IQR(x)$		Lutz1-2 $\tilde{x} \pm IQR(x)$		Lutz1-3 $\tilde{x} \pm IQR(x)$		Lutz1-4 $\tilde{x} \pm IQR(x)$		Lutz1-5 $\tilde{x} \pm IQR(x)$	
BIANT-1	0.09	0.00	0.07	0.00	0.06	0.00	0.08	0.01	0.06	0.01
BIANT-2	0.09	0.00	0.08	0.00	0.06	0.00	0.07	0.01	0.05	0.00
CHAC-1	0.08	0.00	0.07	0.00	0.05	0.00	0.05	0.00	0.05	0.00
CHAC-1-L	0.07	0.01	0.06	0.01	0.04	0.01	0.05	0.01	0.05	0.01
CHAC-2	0.08	0.00	0.06	0.00	0.05	0.00	0.05	0.00	0.05	0.00
CHAC-2-L	0.08	0.00	0.06	0.00	0.05	0.00	0.05	0.01	0.05	0.01
MOACS-1	0.12	0.00	0.08	0.00	0.06	0.00	0.07	0.01	0.06	0.00
MOACS-1-S-CDAS	0.75	0.26	0.78	0.18	0.64	0.15	0.73	0.23	0.58	0.11
MOACS-1-L	0.12	0.00	0.09	0.00	0.06	0.00	0.07	0.00	0.06	0.00
MOACS-2	0.13	0.00	0.10	0.00	0.07	0.00	0.08	0.01	0.07	0.01
MOACS-2-S-CDAS	0.72	0.02	0.60	0.07	0.42	0.09	0.55	0.07	0.52	0.09
MOACS-2-L	0.13	0.00	0.10	0.01	0.07	0.00	0.08	0.00	0.07	0.00
MOACS-2-L-LS	0.07	0.00	0.05	0.00	0.04	0.00	0.04	0.00	0.05	0.02
NSGA-II	0.10	0.00	0.07	0.00	0.05	0.00	0.05	0.00	0.05	0.00
NSGA-II-L	0.07	0.00	0.05	0.00	0.03	0.00	0.04	0.00	0.04	0.01
NSGA-II-L-LS	0.04	0.00	0.03	0.00	0.02	0.00	0.03	0.01	0.02	0.01
SPEA2	0.05	0.00	0.04	0.00	0.03	0.00	0.03	0.00	0.03	0.00
SPEA2-LS	0.03	0.01	0.02	0.01	0.02	0.01	0.02	0.01	0.02	0.01
SPEA2-L	0.05	0.00	0.04	0.00	0.03	0.00	0.03	0.00	0.03	0.00

E.1.8 Problem Family: Mitchell

Table E.36: Median and interquartile range of I_{HV} obtained by the optimisers for the Mitchell problems

	Mitchell-1 $\tilde{x} \pm IQR(x)$		Mitchell-2 $\tilde{x} \pm IQR(x)$		Mitchell-3 $\tilde{x} \pm IQR(x)$		Mitchell-4 $\tilde{x} \pm IQR(x)$	
BIANT-1	0.95	0.09	0.89	0.05	0.60	0.02	0.98	0.01
BIANT-2	0.85	0.22	0.90	0.01	0.59	0.01	0.98	0.00
CHAC-1	0.95	0.03	0.99	0.01	0.65	0.01	0.97	0.01
CHAC-1-L	0.95	0.03	1.00	0.01	0.65	0.01	0.98	0.01
CHAC-2	0.95	0.02	0.99	0.02	0.64	0.01	0.97	0.02
CHAC-2-L	0.96	0.01	0.99	0.02	0.65	0.00	0.98	0.01
MOACS-1	0.83	0.17	0.86	0.04	0.61	0.01	0.95	0.02
MOACS-1-S-CDAS	0.85	0.24	0.84	0.05	0.60	0.01	0.94	0.01
MOACS-1-L	0.90	0.18	0.87	0.05	0.60	0.02	0.93	0.00
MOACS-2	0.79	0.07	0.87	0.02	0.60	0.01	0.91	0.05
MOACS-2-S-CDAS	0.79	0.05	0.87	0.02	0.60	0.02	0.89	0.03
MOACS-2-L	0.80	0.07	0.86	0.05	0.60	0.02	0.90	0.09
MOACS-2-L-LS	0.97	0.02	0.92	0.02	0.61	0.01	0.96	0.02
NSGA-II	0.96	0.02	0.98	0.01	0.64	0.00	0.97	0.01
NSGA-L	0.95	0.04	1.00	0.01	0.64	0.01	0.97	0.01
NSGA-II-L-LS	0.93	0.05	0.99	0.01	0.63	0.02	0.96	0.02
SPEA2	0.94	0.03	0.99	0.01	0.64	0.01	0.97	0.02
SPEA2-LS	0.93	0.03	0.99	0.02	0.64	0.00	0.97	0.02
SPEA2-L	0.95	0.02	1.00	0.02	0.65	0.01	0.96	0.02

Table E.37: Median and interquartile range of I_{IGD} obtained by the optimisers for the Mitchell problems

	Mitchell-1 $\tilde{x} \pm IQR(x)$		Mitchell-2 $\tilde{x} \pm IQR(x)$		Mitchell-3 $\tilde{x} \pm IQR(x)$		Mitchell-4 $\tilde{x} \pm IQR(x)$	
BIANT-1	0.71	0.08	0.94	0.03	0.84	0.07	0.84	0.01
BIANT-2	0.81	0.2	0.93	0.01	0.85	0.01	0.85	0.02
CHAC-1	0.72	0.03	0.88	0.01	0.82	0.00	0.85	0.02
CHAC-1-L	0.72	0.02	0.87	0.02	0.82	0.00	0.84	0.02
CHAC-2	0.72	0.02	0.88	0.02	0.82	0.00	0.85	0.02
CHAC-2-L	0.71	0.00	0.88	0.01	0.82	0.00	0.84	0.01
MOACS-1	0.82	0.15	0.96	0.03	0.82	0.00	0.86	0.02
MOACS-1-S-CDAS	0.79	0.2	0.97	0.03	0.82	0.00	0.88	0.01
MOACS-1-L	0.76	0.16	0.95	0.03	0.82	0.00	0.88	0.00
MOACS-2	0.85	0.06	0.95	0.02	0.82	0.00	0.9	0.05
MOACS-2-S-CDAS	0.85	0.04	0.96	0.02	0.82	0.00	0.92	0.03
MOACS-2-L	0.84	0.06	0.95	0.03	0.82	0.00	0.91	0.07
MOACS-2-L-CHC	0.71	0.01	0.93	0.00	0.82	0.00	0.85	0.02
NSGA-II	0.71	0.02	0.89	0.00	0.82	0.00	0.85	0.01
NSGA-L	0.72	0.04	0.88	0.01	0.82	0.00	0.85	0.01
NSGA-L-CHC	0.74	0.05	0.89	0.01	0.82	0.00	0.85	0.01
SPEA2	0.72	0.03	0.88	0.01	0.82	0.00	0.85	0.01
SPEA2-CHC	0.74	0.03	0.88	0.01	0.82	0.00	0.85	0.02
SPEA2-L	0.72	0.02	0.88	0.02	0.82	0.00	0.85	0.02

Table E.38: Median and interquartile range of I_ϵ obtained by the optimisers for the Mitchell problems

	Mitchell-1 $\tilde{x} \pm IQR(x)$		Mitchell-2 $\tilde{x} \pm IQR(x)$		Mitchell-3 $\tilde{x} \pm IQR(x)$		Mitchell-4 $\tilde{x} \pm IQR(x)$	
BIANT-1	0.71	0.08	0.94	0.03	0.84	0.07	0.84	0.01
BIANT-2	0.81	0.20	0.93	0.01	0.85	0.01	0.85	0.02
CHAC-1	0.72	0.03	0.88	0.01	0.82	0.00	0.85	0.02
CHAC-1-L	0.72	0.02	0.87	0.02	0.82	0.00	0.84	0.02
CHAC-2	0.72	0.02	0.88	0.02	0.82	0.00	0.85	0.02
CHAC-2-L	0.71	0.00	0.88	0.01	0.82	0.00	0.84	0.01
MOACS-1	0.82	0.15	0.96	0.03	0.82	0.00	0.86	0.02
MOACS-1-CADS	0.79	0.20	0.97	0.03	0.82	0.00	0.88	0.01
MOACS-1-L	0.76	0.16	0.95	0.03	0.82	0.00	0.88	0.00
MOACS-2	0.85	0.06	0.95	0.02	0.82	0.00	0.90	0.05
MOACS-2-CDAS	0.85	0.04	0.96	0.02	0.82	0.00	0.92	0.03
MOACS-2-L	0.84	0.06	0.95	0.03	0.82	0.00	0.91	0.07
MOACS-2-L-CHC	0.71	0.01	0.93	0.00	0.82	0.00	0.85	0.02
NSGA2	0.71	0.02	0.89	0.00	0.82	0.00	0.85	0.01
NSGA-L	0.72	0.04	0.88	0.01	0.82	0.00	0.85	0.01
NSGA-L-CHC	0.74	0.05	0.89	0.01	0.82	0.00	0.85	0.01
SPEA2	0.72	0.03	0.88	0.01	0.82	0.00	0.85	0.01
SPEA2-CHC	0.74	0.03	0.88	0.01	0.82	0.00	0.85	0.02
SPEA2-L	0.72	0.02	0.88	0.02	0.82	0.00	0.85	0.02

Table E.39: Median and interquartile range of I_Δ obtained by the optimisers for the Mitchell problems

	Mitchell-1 $\tilde{x} \pm IQR(x)$		Mitchell-2 $\tilde{x} \pm IQR(x)$		Mitchell-3 $\tilde{x} \pm IQR(x)$		Mitchell-4 $\tilde{x} \pm IQR(x)$	
BIANT-1	0.91	0.05	0.84	0.20	0.79	0.061	0.59	0.05
BIANT-2	0.89	0.01	0.79	0.10	0.81	0.11	0.89	0.14
CHAC-1	0.74	0.07	0.67	0.10	0.92	0.06	0.56	0.09
CHAC-1-L	0.76	0.14	0.68	0.03	0.92	0.01	0.57	0.10
CHAC-2	0.79	0.07	0.68	0.06	0.92	0.05	0.56	0.08
CHAC-2-L	0.82	0.09	0.67	0.02	0.90	0.02	0.62	0.02
MOACS-1	0.73	0.23	0.82	0.12	0.84	0.08	0.57	0.07
MOACS-1-S-CDAS	0.73	0.12	0.78	0.13	0.82	0.14	0.64	0.08
MOACS-1-L	0.71	0.11	0.78	0.08	0.81	0.12	0.60	0.06
MOACS-2	0.75	0.12	0.78	0.03	0.85	0.06	0.61	0.06
MOACS-2-S-CDAS	0.77	0.10	0.80	0.02	0.82	0.04	0.61	0.07
MOACS-2-L	0.75	0.09	0.80	0.07	0.85	0.07	0.64	0.12
MOACS-2-L-LS	0.81	0.05	0.80	0.05	0.93	0.04	0.60	0.07
NSGA-II	0.74	0.09	0.68	0.03	0.93	0.02	0.54	0.43
NSGA-II-L	0.81	0.05	0.70	0.05	0.91	0.05	0.58	0.06
NSGA-II-L-LS	0.77	0.09	0.72	0.06	0.91	0.04	0.49	0.12
SPEA2	0.76	0.06	0.68	0.04	0.91	0.06	0.56	0.11
SPEA2-LS	0.78	0.10	0.69	0.04	0.89	0.06	0.61	0.09
SPEA2-L	0.75	0.05	0.68	0.07	0.92	0.07	0.54	0.10

Table E.40: Median and interquartile range of the computation time required by the optimisers for the Mitchell problems

	Mitchell-1 $\tilde{x} \pm IQR(x)$		Mitchell-2 $\tilde{x} \pm IQR(x)$		Mitchell-3 $\tilde{x} \pm IQR(x)$		Mitchell-4 $\tilde{x} \pm IQR(x)$	
BIANT-1	0.05	0.00	0.05	0.00	0.06	0.01	0.07	0.00
BIANT-2	0.05	0.00	0.05	0.01	0.06	0.00	0.07	0.00
CHAC-1	0.04	0.01	0.04	0.00	0.09	0.02	0.06	0.00
CHAC-1-L	0.04	0.01	0.03	0.01	0.07	0.02	0.05	0.01
CHAC-2	0.04	0.01	0.04	0.00	0.08	0.02	0.06	0.00
CHAC-2-L	0.04	0.02	0.04	0.01	0.08	0.03	0.06	0.01
MOACS-1	0.05	0.00	0.04	0.00	0.06	0.00	0.08	0.00
MOACS-1-S-CDAS	0.58	0.21	0.70	0.21	0.58	0.19	0.63	0.12
MOACS-1-L	0.05	0.00	0.05	0.00	0.07	0.01	0.08	0.01
MOACS-2	0.05	0.00	0.05	0.00	0.07	0.01	0.09	0.00
MOACS-2-S-CDAS	0.55	0.24	0.37	0.03	0.65	0.19	0.70	0.04
MOACS-2-L	0.05	0.00	0.05	0.00	0.07	0.01	0.09	0.00
MOACS-2-L-LS	0.03	0.00	0.03	0.00	0.04	0.02	0.05	0.00
NSGA-II	0.04	0.00	0.04	0.00	0.08	0.02	0.06	0.00
NSGA-II-L	0.02	0.00	0.02	0.00	0.04	0.05	0.04	0.00
NSGA-II-L-LS	0.02	0.01	0.02	0.00	0.04	0.02	0.04	0.01
SPEA2	0.03	0.00	0.03	0.00	0.05	0.02	0.05	0.00
SPEA2-LS	0.02	0.01	0.02	0.01	0.05	0.01	0.03	0.01
SPEA2-L	0.03	0.00	0.03	0.00	0.06	0.01	0.05	0.00

E.1.9 Problem Family: Mukherje

Table E.41: Median and interquartile range of I_{HV} obtained by the optimisers for the Mukherje problems

	Mukherje-1 $\tilde{x} \pm IQR(x)$		Mukherje-2 $\tilde{x} \pm IQR(x)$		Mukherje-3 $\tilde{x} \pm IQR(x)$	
BIANT-1	0.93	0.02	0.93	0.01	0.92	0.01
BIANT-2	0.93	0.01	0.92	0.02	0.92	0.03
CHAC-1	0.87	0.01	0.86	0.00	0.85	0.01
CHAC-1-L	0.87	0.01	0.86	0.01	0.85	0.01
CHAC-2	0.87	0.01	0.86	0.00	0.85	0.00
CHAC-2-L	0.86	0.01	0.86	0.01	0.85	0.01
MOACS-1	0.88	0.01	0.89	0.01	0.89	0.02
MOACS-1-S-CDAS	0.83	0.04	0.83	0.01	0.84	0.01
MOACS-1-L	0.88	0.01	0.89	0.01	0.90	0.00
MOACS-2	0.91	0.00	0.91	0.01	0.92	0.01
MOACS-2-S-CDAS	0.91	0.01	0.91	0.00	0.92	0.00
MOACS-2-L	0.91	0.00	0.91	0.01	0.92	0.01
MOACS-2-L-LS	0.91	0.01	0.91	0.01	0.91	0.00
NSGA-II	0.87	0.01	0.86	0.00	0.85	0.01
NSGA-L	0.87	0.01	0.86	0.01	0.86	0.01
NSGA-II-L-LS	0.86	0.01	0.86	0.01	0.85	0.01
SPEA2	0.87	0.01	0.86	0.01	0.85	0.01
SPEA2-LS	0.87	0.01	0.86	0.01	0.85	0.01
SPEA2-L	0.86	0.01	0.86	0.01	0.85	0.00

Table E.42: Median and interquartile range of I_{IGD} obtained by the optimisers for the Mukherje problems

	Mukherje-1 $\tilde{x} \pm IQR(x)$		Mukherje-2 $\tilde{x} \pm IQR(x)$		Mukherje-3 $\tilde{x} \pm IQR(x)$	
BIANT-1	0.43	0.07	0.38	0.06	0.45	0.06
BIANT-2	0.42	0.07	0.47	0.05	0.44	0.06
CHAC-1	0.19	0.00	0.20	0.01	0.24	0.00
CHAC-1-L	0.19	0.00	0.20	0.00	0.24	0.00
CHAC-2	0.19	0.00	0.20	0.00	0.24	0.00
CHAC-2-L	0.19	0.00	0.20	0.00	0.24	0.00
MOACS-1	0.51	0.06	0.49	0.10	0.49	0.07
MOACS-1-S-CDAS	0.82	0.22	0.85	0.06	0.89	0.10
MOACS-1-L	0.48	0.03	0.47	0.05	0.46	0.06
MOACS-2	0.26	0.04	0.29	0.04	0.31	0.03
MOACS-2-S-CDAS	0.29	0.03	0.28	0.01	0.33	0.07
MOACS-2-L	0.29	0.01	0.29	0.03	0.30	0.03
MOACS-2-L-LS	0.30	0.04	0.31	0.03	0.33	0.02
NSGA-II	0.11	0.00	0.12	0.01	0.14	0.00
NSGA-L	0.11	0.00	0.12	0.01	0.14	0.00
NSGA-II-L-LS	0.11	0.00	0.13	0.00	0.14	0.00
SPEA2	0.11	0.00	0.13	0.01	0.14	0.00
SPEA2-LS	0.11	0.00	0.12	0.01	0.14	0.10
SPEA2-L	0.11	0.00	0.12	0.00	0.14	0.00

Table E.43: Median and interquartile range of I_ϵ obtained by the optimisers for the Mukherje problems

	Mukherje-1 $\tilde{x} \pm IQR(x)$		Mukherje-2 $\tilde{x} \pm IQR(x)$		Mukherje-3 $\tilde{x} \pm IQR(x)$	
BIANT-1	0.43	0.07	0.38	0.06	0.45	0.06
BIANT-2	0.42	0.07	0.47	0.05	0.44	0.06
CHAC-1	0.19	0.00	0.20	0.01	0.24	0.00
CHAC-1-L	0.19	0.00	0.20	0.00	0.24	0.00
CHAC-2	0.19	0.00	0.20	0.00	0.24	0.00
CHAC-2-L	0.19	0.00	0.20	0.00	0.24	0.00
MOACS-1	0.51	0.06	0.49	0.10	0.49	0.07
MOACS-1-S-CDAS	0.82	0.22	0.85	0.06	0.89	0.10
MOACS-1-L	0.48	0.03	0.47	0.05	0.46	0.06
MOACS-2	0.26	0.04	0.29	0.04	0.31	0.03
MOACS-2-S-CDAS	0.29	0.03	0.28	0.01	0.33	0.07
MOACS-2-L	0.29	0.01	0.29	0.03	0.30	0.03
MOACS-2-L-CHC	0.30	0.04	0.31	0.03	0.33	0.02
NSGA-II	0.11	0.00	0.12	0.01	0.14	0.00
NSGA-L	0.11	0.00	0.12	0.01	0.14	0.00
NSGA-L-CHC	0.11	0.00	0.13	0.00	0.14	0.00
SPEA2	0.11	0.00	0.13	0.01	0.14	0.00
SPEA2-CHC	0.11	0.00	0.12	0.01	0.14	0.10
SPEA2-L	0.11	0.00	0.12	0.00	0.14	0.00

Table E.44: Median and interquartile range of I_Δ obtained by the optimisers for the Mukherje problems

	Mukherje-1 $\tilde{x} \pm IQR(x)$		Mukherje-2 $\tilde{x} \pm IQR(x)$		Mukherje-3 $\tilde{x} \pm IQR(x)$	
BIANT-1	0.44	0.05	0.43	0.08	0.48	0.08
BIANT-2	0.45	0.01	0.54	0.03	0.47	0.11
CHAC-1	0.76	0.05	0.76	0.03	0.77	0.05
CHAC-1-L	0.76	0.09	0.80	0.05	0.79	0.02
CHAC-2	0.76	0.09	0.78	0.06	0.80	0.06
CHAC-2-L	0.75	0.09	0.77	0.07	0.77	0.04
MOACS-1	0.47	0.02	0.48	0.03	0.45	0.06
MOACS-1-S-CDAS	0.76	0.05	0.71	0.06	0.63	0.09
MOACS-1-L	0.48	0.07	0.49	0.06	0.45	0.08
MOACS-2	0.35	0.03	0.32	0.07	0.35	0.02
MOACS-2-S-CDAS	0.41	0.07	0.40	0.06	0.43	0.09
MOACS-2-L	0.37	0.05	0.38	0.06	0.39	0.07
MOACS-2-L-LS	0.38	0.06	0.43	0.04	0.36	0.06
NSGA-II	0.91	0.04	0.91	0.04	0.91	0.06
NSGA-II-L	0.90	0.08	0.90	0.08	0.89	0.05
NSGA-II-L-LS	0.92	0.05	0.91	0.07	0.89	0.03
SPEA2	0.90	0.05	0.92	0.04	0.89	0.04
SPEA2-LS	0.92	0.03	0.92	0.02	0.88	0.06
SPEA2-L	0.91	0.04	0.90	0.06	0.88	0.06

Table E.45: Median and interquartile range of the computation time required by the optimisers for the Mukherje problems

	Mukherje-1 $\tilde{x} \pm IQR(x)$		Mukherje-2 $\tilde{x} \pm IQR(x)$		Mukherje-3 $\tilde{x} \pm IQR(x)$	
BIANT-1	0.06	0.04	0.32	0.07	0.64	0.20
BIANT-2	0.06	0.01	0.42	0.12	0.41	0.35
CHAC-1	0.04	0.02	0.29	0.08	0.35	0.21
CHAC-1-L	0.04	0.02	0.30	0.18	0.30	0.16
CHAC-2	0.03	0.01	0.25	0.14	0.33	0.09
CHAC-2-L	0.03	0.01	0.35	0.19	0.43	0.14
MOACS-1	0.04	0.02	0.35	0.13	0.37	0.23
MOACS-1-S-CDAS	0.04	0.01	0.36	0.29	0.54	0.25
MOACS-1-L	0.04	0.02	0.28	0.20	0.58	0.23
MOACS-2	0.04	0.02	0.27	0.06	0.39	0.27
MOACS-2-S-CDAS	0.04	0.01	0.23	0.09	0.35	0.19
MOACS-2-L	0.04	0.02	0.33	0.08	0.35	0.20
MOACS-2-L-LS	0.04	0.02	0.22	0.17	0.32	0.24
NSGA-II	0.02	0.01	0.22	0.15	0.22	0.09
NSGA-II-L	0.03	0.01	0.20	0.11	0.16	0.09
NSGA-II-L-LS	0.02	0.01	0.15	0.08	0.18	0.06
SPEA2	0.02	0.01	0.10	0.06	0.13	0.05
SPEA2-LS	0.02	0.00	0.10	0.08	0.18	0.05
SPEA2-L	0.01	0.00	0.12	0.02	0.12	0.05

E.1.10 Problem Family: Roszieg

Table E.46: Median and interquartile range of I_{HV} obtained by the optimisers for the Roszieg problems

	Roszieg-1 $\tilde{x} \pm IQR(x)$		Roszieg-2 $\tilde{x} \pm IQR(x)$		Roszieg-3 $\tilde{x} \pm IQR(x)$		Roszieg-4 $\tilde{x} \pm IQR(x)$	
BIANT-1	0.96	0.03	0.75	0.01	0.94	0.02	1.00	0.01
BIANT-2	0.94	0.03	0.77	0.04	0.85	0.08	0.99	0.00
CHAC-1	1.00	0.00	0.99	0.01	0.98	0.01	1.00	0.00
CHAC-1-L	1.00	0.01	0.99	0.00	0.98	0.01	1.00	0.00
CHAC-2	1.00	0.00	0.99	0.00	0.98	0.01	1.00	0.00
CHAC-2-L	1.00	0.00	0.99	0.00	0.98	0.01	1.00	0.00
MOACS-1	0.97	0.00	0.80	0.03	0.94	0.06	0.95	0.10
MOACS-1-S-CDAS	0.97	0.00	0.79	0.04	0.92	0.07	0.96	0.03
MOACS-1-L	0.97	0.00	0.79	0.01	0.89	0.07	0.97	0.02
MOACS-2	0.96	0.01	0.78	0.01	0.91	0.05	0.80	0.16
MOACS-2-S-CDAS	0.96	0.01	0.75	0.04	0.91	0.05	0.96	0.17
MOACS-2-L	0.96	0.02	0.75	0.02	0.93	0.11	0.96	0.14
MOACS-2-L-LS	0.97	0.00	0.97	0.01	0.99	0.00	1.00	0.00
NSGA-II	1.00	0.00	0.99	0.01	0.98	0.00	1.00	0.00
NSGA-L	1.00	0.00	0.99	0.00	0.98	0.00	1.00	0.00
NSGA-II-L-LS	1.00	0.00	0.99	0.00	0.98	0.00	1.00	0.00
SPEA2	1.00	0.00	0.99	0.00	0.98	0.00	1.00	0.00
SPEA2-LS	1.00	0.00	0.99	0.00	0.98	0.00	1.00	0.00
SPEA2-L	1.00	0.00	0.99	0.00	0.98	0.00	1.00	0.00

Table E.47: Median and interquartile range of I_{IGD} obtained by the optimisers for the Roszieg problems

	Roszieg-1 $\tilde{x} \pm IQR(x)$		Roszieg-2 $\tilde{x} \pm IQR(x)$		Roszieg-3 $\tilde{x} \pm IQR(x)$		Roszieg-4 $\tilde{x} \pm IQR(x)$	
BIANT-1	0.63	0.31	0.93	0.04	0.50	0.10	0.87	0.01
BIANT-2	0.88	0.31	0.93	0.01	0.72	0.41	0.87	0.00
CHAC-1	0.22	0.08	0.45	0.01	0.43	0.01	0.86	0.00
CHAC-1-L	0.18	0.08	0.45	0.00	0.42	0.01	0.86	0.00
CHAC-2	0.18	0.06	0.45	0.01	0.43	0.02	0.86	0.00
CHAC-2-L	0.27	0.08	0.45	0.02	0.42	0.00	0.86	0.00
MOACS-1	0.51	0.00	0.88	0.01	0.52	0.25	0.90	0.06
MOACS-1-S-CDAS	0.51	0.00	0.88	0.00	0.58	0.34	0.89	0.02
MOACS-1-L	0.51	0.00	0.88	0.00	0.74	0.34	0.88	0.01
MOACS-2	0.51	0.04	0.88	0.02	0.59	0.18	0.99	0.10
MOACS-2-S-CDAS	0.51	0.00	0.88	0.01	0.61	0.20	0.89	0.11
MOACS-2-L	0.51	0.05	0.88	0.03	0.61	0.33	0.89	0.09
MOACS-2-L-LS	0.51	0.00	0.48	0.03	0.42	0.01	0.86	0.00
NSGA-II	0.18	0.08	0.45	0.00	0.42	0.01	0.86	0.00
NSGA-L	0.18	0.08	0.45	0.01	0.43	0.01	0.86	0.00
NSGA-II-L-LS	0.18	0.08	0.45	0.01	0.43	0.00	0.86	0.00
SPEA2	0.22	0.08	0.45	0.00	0.42	0.01	0.86	0.00
SPEA2-LS	0.18	0.08	0.45	0.00	0.42	0.00	0.86	0.00
SPEA2-L	0.22	0.08	0.45	0.00	0.43	0.01	0.86	0.00

Table E.48: Median and interquartile range of I_ϵ obtained by the optimisers for the Roszieg problems

	Roszieg-1 $\tilde{x} \pm IQR(x)$		Roszieg-2 $\tilde{x} \pm IQR(x)$		Roszieg-3 $\tilde{x} \pm IQR(x)$		Roszieg-4 $\tilde{x} \pm IQR(x)$	
BIANT-1	0.63	0.31	0.93	0.04	0.50	0.10	0.87	0.01
BIANT-2	0.88	0.31	0.93	0.01	0.72	0.41	0.87	0.00
CHAC-1	0.22	0.08	0.45	0.01	0.43	0.01	0.86	0.00
CHAC-1-L	0.18	0.08	0.45	0.00	0.42	0.01	0.86	0.00
CHAC-2	0.18	0.06	0.45	0.01	0.43	0.02	0.86	0.00
CHAC-2-L	0.27	0.08	0.45	0.02	0.42	0.00	0.86	0.00
MOACS-1	0.51	0.00	0.88	0.01	0.52	0.25	0.90	0.06
MOACS-1-S-CDAS	0.51	0.00	0.88	0.00	0.58	0.34	0.89	0.02
MOACS-1-L	0.51	0.00	0.88	0.00	0.74	0.34	0.88	0.01
MOACS-2	0.51	0.04	0.88	0.02	0.59	0.18	0.99	0.10
MOACS-2-S-CDAS	0.51	0.00	0.88	0.01	0.61	0.20	0.89	0.11
MOACS-2-L	0.51	0.05	0.88	0.03	0.61	0.33	0.89	0.09
MOACS-2-L-CHC	0.51	0.00	0.48	0.03	0.42	0.01	0.86	0.00
NSGA-II	0.18	0.08	0.45	0.00	0.42	0.01	0.86	0.00
NSGA-L	0.18	0.08	0.45	0.01	0.43	0.01	0.86	0.00
NSGA-L-CHC	0.18	0.08	0.45	0.01	0.43	0.00	0.86	0.00
SPEA2	0.22	0.08	0.45	0.00	0.42	0.01	0.86	0.00
SPEA2-CHC	0.18	0.08	0.45	0.00	0.42	0.00	0.86	0.00
SPEA2-L	0.22	0.08	0.45	0.00	0.43	0.01	0.86	0.00

Table E.49: Median and interquartile range of I_Δ obtained by the optimisers for the Roszieg problems

	Roszieg-1 $\tilde{x} \pm IQR(x)$		Roszieg-2 $\tilde{x} \pm IQR(x)$		Roszieg-3 $\tilde{x} \pm IQR(x)$		Roszieg-4 $\tilde{x} \pm IQR(x)$	
BIANT-1	0.79	0.09	0.88	0.06	0.62	0.09	0.36	0.01
BIANT-2	0.85	0.08	0.81	0.04	0.72	0.15	0.35	0.00
CHAC-1	0.83	0.11	0.88	0.07	0.77	0.09	0.36	0.00
CHAC-1-L	0.85	0.09	0.90	0.04	0.77	0.09	0.36	0.00
CHAC-2	0.83	0.10	0.87	0.05	0.71	0.13	0.36	0.00
CHAC-2-L	0.90	0.04	0.90	0.08	0.77	0.03	0.36	0.00
MOACS-1	0.69	0.05	0.84	0.06	0.68	0.07	0.49	0.13
MOACS-1-S-CDAS	0.67	0.00	0.88	0.06	0.66	0.08	0.40	0.26
MOACS-1-L	0.67	0.03	0.83	0.05	0.68	0.11	0.36	0.04
MOACS-2	0.68	0.05	0.85	0.08	0.76	0.06	0.49	0.16
MOACS-2-S-CDAS	0.69	0.02	0.94	0.07	0.70	0.11	0.49	0.22
MOACS-2-L	0.67	0.03	0.90	0.07	0.71	0.17	0.46	0.39
MOACS-2-L-LS	0.87	0.05	0.88	0.06	0.75	0.07	0.36	0.00
NSGA-II	0.83	0.06	0.86	0.05	0.81	0.02	0.36	0.00
NSGA-L	0.87	0.10	0.88	0.03	0.74	0.14	0.36	0.00
NSGA-II-L-LS	0.83	0.15	0.92	0.06	0.79	0.13	0.36	0.00
SPEA2	0.88	0.12	0.88	0.08	0.76	0.10	0.36	0.00
SPEA2-LS	0.83	0.05	0.89	0.02	0.72	0.10	0.36	0.00
SPEA2-L	0.90	0.12	0.92	0.04	0.71	0.14	0.36	0.00

Table E.50: Median and interquartile range of the computation time required by the optimisers for the Roszieg problems

	Roszieg-1 $\tilde{x} \pm IQR(x)$		Roszieg-2 $\tilde{x} \pm IQR(x)$		Roszieg-3 $\tilde{x} \pm IQR(x)$		Roszieg-4 $\tilde{x} \pm IQR(x)$	
BIANT-2	0.15	0.01	0.13	0.00	0.07	0.00	0.06	0.01
CHAC-1	0.14	0.00	0.12	0.01	0.06	0.02	0.04	0.00
CHAC-1-L	0.11	0.03	0.09	0.03	0.05	0.02	0.03	0.01
CHAC-2	0.13	0.00	0.11	0.01	0.06	0.01	0.04	0.00
CHAC-2-L	0.13	0.03	0.11	0.02	0.07	0.01	0.04	0.01
MOACS-1	0.15	0.00	0.13	0.01	0.07	0.01	0.05	0.01
MOACS-1-S-CDAS	0.69	0.11	0.64	0.12	0.70	0.20	0.55	0.10
MOACS-1-L	0.15	0.00	0.13	0.01	0.07	0.00	0.05	0.01
MOACS-2	0.16	0.00	0.15	0.01	0.07	0.01	0.06	0.01
MOACS-2-S-CDAS	0.55	0.17	0.70	0.10	0.57	0.18	0.49	0.15
MOACS-2-L	0.16	0.00	0.15	0.01	0.08	0.00	0.07	0.02
MOACS-2-L-LS	0.09	0.00	0.08	0.00	0.04	0.01	0.03	0.00
NSGA-II	0.14	0.00	0.11	0.02	0.07	0.01	0.04	0.00
NSGA-II-L	0.08	0.00	0.07	0.02	0.04	0.02	0.03	0.00
NSGA-II-L-LS	0.07	0.01	0.06	0.02	0.04	0.02	0.02	0.00
SPEA2	0.10	0.00	0.09	0.01	0.05	0.00	0.03	0.00
SPEA2-LS	0.06	0.02	0.06	0.02	0.03	0.01	0.02	0.00
SPEA2-L	0.10	0.00	0.09	0.01	0.05	0.01	0.03	0.00

E.1.11 Problem Family: Sawyer

Table E.51: Median and interquartile range of I_{HV} obtained by the optimisers for the Sawyer problems

	Sawyer-1 $\tilde{x} \pm IQR(x)$		Sawyer-2 $\tilde{x} \pm IQR(x)$		Sawyer-3 $\tilde{x} \pm IQR(x)$		Sawyer-4 $\tilde{x} \pm IQR(x)$	
BIANT-1	0.92	0.00	0.93	0.22	0.86	0.01	0.86	0.03
BIANT-2	1.00	0.08	0.78	0.16	0.86	0.03	0.86	0.03
CHAC-1	1.00	0.00	1.00	0.00	1.00	0.00	1.00	0.00
CHAC-1-L	1.00	0.00	1.00	0.00	1.00	0.00	1.00	0.00
CHAC-2	1.00	0.00	1.00	0.00	1.00	0.00	1.00	0.00
CHAC-2-L	1.00	0.00	1.00	0.00	1.00	0.00	1.00	0.00
MOACS-1	0.33	0.28	0.78	0.00	0.87	0.02	0.85	0.03
MOACS-1-S-CDAS	0.95	0.53	0.78	0.10	0.87	0.01	0.85	0.00
MOACS-1-L	1.00	0.08	0.78	0.00	0.86	0.01	0.85	0.00
MOACS-2	0.95	0.67	0.78	0.04	0.88	0.02	0.85	0.00
MOACS-2-S-CDAS	0.95	0.53	0.78	0.01	0.89	0.08	0.84	0.01
MOACS-2-L	1.00	0.08	0.78	0.00	0.86	0.01	0.85	0.05
MOACS-2-L-LS	1.00	0.00	1.00	0.00	0.99	0.05	0.85	0.08
NSGA-II	1.00	0.00	1.00	0.00	1.00	0.00	0.97	0.02
NSGA-L	1.00	0.00	1.00	0.00	1.00	0.00	1.00	0.00
NSGA-II-L-LS	1.00	0.00	1.00	0.00	1.00	0.00	1.00	0.00
SPEA2	1.00	0.00	1.00	0.00	1.00	0.00	1.00	0.00
SPEA2-LS	1.00	0.00	1.00	0.00	1.00	0.00	1.00	0.00
SPEA2-L	1.00	0.00	1.00	0.00	1.00	0.00	1.00	0.00

Table E.52: Median and interquartile range of I_{IGD} obtained by the optimisers for the Sawyer problems

	Sawyer-1 $\tilde{x} \pm IQR(x)$		Sawyer-2 $\tilde{x} \pm IQR(x)$		Sawyer-3 $\tilde{x} \pm IQR(x)$		Sawyer-4 $\tilde{x} \pm IQR(x)$	
BIANT-1	0.78	0.00	0.91	0.15	0.98	0.01	0.97	0.06
BIANT-2	0.78	0.00	1.00	0.09	0.99	0.08	0.96	0.05
CHAC-1	0.78	0.00	0.85	0.00	0.69	0.00	0.77	0.00
CHAC-1-L	0.78	0.00	0.85	0.00	0.69	0.00	0.77	0.00
CHAC-2	0.78	0.00	0.85	0.00	0.69	0.00	0.77	0.00
CHAC-2-L	0.78	0.00	0.85	0.00	0.69	0.00	0.76	0.01
MOACS-1	1.00	0.10	1.00	0.00	0.98	0.04	0.98	0.06
MOACS-1-S-CDAS	0.79	0.16	1.00	0.05	0.98	0.02	0.98	0.01
MOACS-1-L	0.78	0.00	1.00	0.00	0.98	0.01	0.98	0.00
MOACS-2	0.79	0.22	1.00	0.02	0.98	0.01	0.98	0.01
MOACS-2-S-CDAS	0.79	0.16	1.00	0.01	0.98	0.27	0.99	0.01
MOACS-2-L	0.78	0.01	1.00	0.00	0.98	0.04	0.99	0.10
MOACS-2-L-LS	0.78	0.00	0.85	0.00	0.71	0.11	0.99	0.14
NSGA-II	0.78	0.00	0.85	0.00	0.69	0.00	0.80	0.01
NSGA-L	0.78	0.00	0.85	0.00	0.69	0.01	0.77	0.01
NSGA-II-L-LS	0.78	0.00	0.85	0.00	0.69	0.01	0.77	0.00
SPEA2	0.78	0.00	0.85	0.00	0.69	0.00	0.76	0.01
SPEA2-LS	0.78	0.00	0.85	0.00	0.69	0.00	0.77	0.01
SPEA2-L	0.78	0.00	0.85	0.00	0.69	0.01	0.76	0.00

Table E.53: Median and interquartile range of I_ϵ obtained by the optimisers for the Sawyer problems

	Sawyer-1 $\tilde{x} \pm IQR(x)$		Sawyer-2 $\tilde{x} \pm IQR(x)$		Sawyer-3 $\tilde{x} \pm IQR(x)$		Sawyer-4 $\tilde{x} \pm IQR(x)$	
BIANT-1	0.78	0.00	0.91	0.15	0.98	0.01	0.97	0.06
BIANT-2	0.78	0.00	1.00	0.09	0.99	0.08	0.96	0.05
CHAC-1	0.78	0.00	0.85	0.00	0.69	0.00	0.77	0.00
CHAC-1-L	0.78	0.00	0.85	0.00	0.69	0.00	0.77	0.00
CHAC-2	0.78	0.00	0.85	0.00	0.69	0.00	0.77	0.00
CHAC-2-L	0.78	0.00	0.85	0.00	0.69	0.00	0.76	0.01
MOACS-1	1.00	0.10	1.00	0.00	0.98	0.04	0.98	0.06
MOACS-1-S-CDAS	0.79	0.16	1.00	0.05	0.98	0.02	0.98	0.01
MOACS-1-L	0.78	0.00	1.00	0.00	0.98	0.01	0.98	0.00
MOACS-2	0.79	0.22	1.00	0.02	0.98	0.01	0.98	0.01
MOACS-2-S-CDAS	0.79	0.16	1.00	0.01	0.98	0.27	0.99	0.01
MOACS-2-L	0.78	0.01	1.00	0.00	0.98	0.04	0.99	0.10
MOACS-2-L-CHC	0.78	0.00	0.85	0.00	0.71	0.11	0.99	0.14
NSGA-II	0.78	0.00	0.85	0.00	0.69	0.00	0.80	0.01
NSGA-L	0.78	0.00	0.85	0.00	0.69	0.01	0.77	0.01
NSGA-L-CHC	0.78	0.00	0.85	0.00	0.69	0.01	0.77	0.00
SPEA2	0.78	0.00	0.85	0.00	0.69	0.00	0.76	0.01
SPEA2-CHC	0.78	0.00	0.85	0.00	0.69	0.00	0.77	0.01
SPEA2-L	0.78	0.00	0.85	0.00	0.69	0.01	0.76	0.00

Table E.54: Median and interquartile range of I_Δ obtained by the optimisers for the Sawyer problems

	Sawyer-1 $\tilde{x} \pm IQR(x)$		Sawyer-2 $\tilde{x} \pm IQR(x)$		Sawyer-3 $\tilde{x} \pm IQR(x)$		Sawyer-4 $\tilde{x} \pm IQR(x)$	
BIANT-1	0.10	0.07	0.61	0.23	0.77	0.04	0.86	0.03
BIANT-2	1.00	0.83	0.84	0.04	0.78	0.05	0.87	0.06
CHAC-1	1.00	0.00	0.61	0.00	0.95	0.03	0.98	0.02
CHAC-1-L	1.00	0.00	0.61	0.00	0.93	0.03	0.99	0.02
CHAC-2	1.00	0.00	0.61	0.00	0.95	0.04	0.99	0.03
CHAC-2-L	1.00	0.00	0.61	0.00	0.94	0.04	0.98	0.01
MOACS-1	0.89	0.36	0.84	0.00	0.86	0.07	0.91	0.02
MOACS-1-S-CDAS	0.94	0.11	0.84	0.00	0.85	0.04	0.89	0.03
MOACS-1-L	1.00	0.65	0.84	0.00	0.87	0.03	0.91	0.03
MOACS-2	0.94	0.11	0.84	0.06	0.81	0.02	0.91	0.03
MOACS-2-S-CDAS	0.94	0.11	0.84	0.12	0.86	0.11	0.90	0.02
MOACS-2-L	1.00	0.08	0.84	0.00	0.85	0.04	0.90	0.04
MOACS-2-L-LS	1.00	0.00	0.61	0.00	0.94	0.08	0.91	0.02
NSGA-II	1.00	0.00	0.61	0.00	0.94	0.02	0.97	0.02
NSGA-II-L	1.00	0.00	0.61	0.00	0.95	0.03	0.98	0.02
NSGA-II-L-LS	1.00	0.00	0.61	0.00	0.95	0.03	0.99	0.01
SPEA2	1.00	0.00	0.61	0.00	0.96	0.02	0.98	0.02
SPEA2-LS	1.00	0.00	0.61	0.00	0.95	0.02	0.99	0.02
SPEA2-L	1.00	0.00	0.61	0.00	0.96	0.02	1.00	0.01

Table E.55: Median and interquartile range of the computation time required by the optimisers for the Sawyer problems

	Sawyer-1 $\tilde{x} \pm IQR(x)$		Sawyer-2 $\tilde{x} \pm IQR(x)$		Sawyer-3 $\tilde{x} \pm IQR(x)$		Sawyer-4 $\tilde{x} \pm IQR(x)$	
BIANT-1	0.07	0.00	0.13	0.02	0.09	0.00	0.06	0.01
BIANT-2	0.07	0.00	0.11	0.01	0.09	0.00	0.07	0.01
CHAC-1	0.06	0.00	0.08	0.00	0.07	0.00	0.05	0.00
CHAC-1-L	0.05	0.01	0.07	0.01	0.06	0.01	0.04	0.01
CHAC-2	0.06	0.00	0.08	0.00	0.07	0.00	0.05	0.00
CHAC-2-L	0.06	0.00	0.08	0.00	0.07	0.01	0.05	0.00
MOACS-1	0.07	0.00	0.11	0.00	0.09	0.00	0.06	0.00
MOACS-1-S-CDAS	0.60	0.50	0.82	0.18	0.76	0.08	0.06	0.00
MOACS-1-L	0.07	0.00	0.11	0.01	0.09	0.00	0.84	0.10
MOACS-2	0.08	0.00	0.13	0.01	0.09	0.01	0.06	0.00
MOACS-2-S-CDAS	0.87	0.06	0.66	0.03	0.72	0.09	0.06	0.00
MOACS-2-L	0.07	0.00	0.12	0.01	0.09	0.00	0.90	0.18
MOACS-2-L-LS	0.04	0.00	0.07	0.00	0.05	0.00	0.06	0.00
NSGA-II	0.06	0.00	0.10	0.00	0.08	0.00	0.04	0.00
NSGA-II-L	0.04	0.00	0.07	0.00	0.05	0.00	0.05	0.00
NSGA-II-L-LS	0.03	0.00	0.05	0.00	0.04	0.00	0.04	0.00
SPEA2	0.04	0.00	0.06	0.00	0.05	0.00	0.03	0.00
SPEA2-LS	0.02	0.01	0.04	0.01	0.03	0.01	0.03	0.00
SPEA2-L	0.04	0.00	0.06	0.00	0.05	0.00	0.02	0.01

E.2 Friedman's nonparametric test

This section presents the detailed results of the Friedman's test.

E.2.1 Group analysis

E.2.1.1 Group 1

Table E.56: Unadjusted and adjusted p-values obtained for all problems through the application of Holm's post hoc procedure, using the MOACS-2-L-LS as control algorithm according to I_{HV}

Algorithm	Unadjusted p-value	Adjusted p-value
Others	<1.21E−08	<7.27E−08
BIANT-1	0.031	0.156
MOACS-2-S-CDAS	0.067	0.266
MOACS-2	0.168	0.504
BIANT-2	0.274	0.548
MOACS-2-L	0.405	0.548

Table E.57: Unadjusted and adjusted p-values obtained for problem instances of Group 1 through the application of Holm's post hoc procedure, using the MOACS-2-L-LS as control algorithm according to I_{IGD}

Algorithm	Unadjusted p-value	Adjusted p-value
Others	<0.003	<0.009
BIANT-1	0.030	0.060
BIANT-2	0.079	0.079

Table E.58: Unadjusted and adjusted p-values obtained for problem instances of Group 1 through the application of Holm's post hoc procedure, using the MOACS-2-L as control algorithm according to I_ϵ

Algorithm	Unadjusted p-value	Adjusted p-value
Others	<7.06E−04	<0.007
MOACS-2-L-LS	0.006	0.055
NSGA-II-L-LS	0.093	0.745
SPEA2-LS	0.129	0.903
SPEA2-L	0.133	0.903
SPEA2	0.177	0.903
NSGA-II	0.361	1.442
NSGA-L	0.593	1.778
MOACS-2-S-CDAS	0.687	1.778
MOACS-2	0.692	1.778

Table E.59: Unadjusted and adjusted p-values obtained for problem instances of Group 1 through the application of Holm's post hoc procedure, using the MOACS-2 as control algorithm according to I_Δ

Algorithm	Unadjusted p-value	Adjusted p-value
Others	<5.59E−26	<5.03E−25
MOACS-1-S-CDAS	0.015	0.122
BIANT-1	0.016	0.122
BIANT-2	0.020	0.122
MOACS-1-L	0.112	0.559
MOACS-1	0.150	0.600
MOACS-2-S-CDAS	0.472	1.415
MOACS-2-L-LS	0.745	1.490
MOACS-2-L	0.963	1.490

Table E.60: Unadjusted and adjusted p-values obtained for problem instances of Group 1 through the application of Holm's post hoc procedure, using the SPEA2-LS as control algorithm in accordance with the computation time

Algorithm	Unadjusted p-value	Adjusted p-value
Others	<1.32E−06	<5.28E−06
NSGA-II-L-LS	2.00E−01	0.599
SPEA2	0.749	1.497
SPEA2-L	0.868	1.497

E.2.1.2 Group 2

Table E.61: Unadjusted and adjusted p-values obtained for problem instances of Group 2 through the application of Holm's post hoc procedure, using the CHAC-2-L as control algorithm according to I_{HV}

Algorithm	Unadjusted p-value	Adjusted p-value
Others	<3.68E−03	<0.037
NSGA-II	1.49E−01	1.345
SPEA2-L	2.86E−01	2.228
NSGA-II-L	0.314	2.228
CHAC-1	0.344	2.228
SPEA2	0.355	2.228
SPEA2-LS	0.451	2.228
CHAC-2	0.552	2.228
CHAC-1-L	0.578	2.228

Table E.62: Unadjusted and adjusted p-values obtained for problem instances of Group 2 through the application of Holm's post hoc procedure, using the CHAC-2-L as control algorithm according to I_{IGD}

Algorithm	Unadjusted p-value	Adjusted p-value
Others	<1.03E−11	<1.03E−10
NSGA-II-L-LS	5.05E−02	0.454
NSGA-II	3.74E−01	2.992
NSGA-L	4.06E−01	2.992
SPEA2-LS	0.484	2.992
SPEA2-L	0.495	2.992
CHAC-1-L	0.582	2.992
CHAC-1	0.582	2.992
SPEA2	0.598	2.992
CHAC-2	0.642	2.992

Table E.63: Unadjusted and adjusted p-values obtained for problem instances of Group 2 through the application of Holm's post hoc procedure, using the CHAC-2-L as control algorithm according to I_{ϵ}

Algorithm	Unadjusted p-value	Adjusted p-value
Others	<6.79E−09	<7.47E−08
NSGA-II-L-LS	0.024	0.243
CHAC-1	0.224	2.015
SPEA2-L	0.306	2.445
NSGA-II	0.396	2.445
NSGA-L	0.453	2.445
SPEA2	0.466	2.445
CHAC-2	0.493	2.445
CHAC-1-L	0.714	2.445
SPEA2-LS	0.900	2.445

Table E.64: Unadjusted and adjusted p-values obtained for problem instances of Group 2 through the application of Holm's post hoc procedure, using the MOACS-1-S-CDAS as control algorithm according to I_{Δ}

Algorithm	Unadjusted p-value	Adjusted p-value
Others	<1.83E−04	<3.66E−04
NSGA-II-L-LS	0.529	0.529

Table E.65: Unadjusted and adjusted p-values obtained for problem instances of Group 2 through the application of Holm's post hoc procedure, using the SPEA2-LS as control algorithm in accordance with the computation time

Algorithm	Unadjusted p-value	Adjusted p-value
Others	<1.83E−04	<3.66E−04
NSGA-II-L-LS	5.29E−01	0.529

E.3 C-Metric details for the problems of the Group 1

E.3.1 Problem Family: Arc111

Table E.66: $\tilde{C}_{A_1,A_2}$ for the Arc111-1 problem

		A2			
		BIANT-1	BIANT-2	MOACS-2	MOACS-2-L-LS
A1	BIANT-1		0.82	0.04	0.06
	BIANT-2	0.08		0	0.02
	MOACS-2	0.62	0.64		0.46
	MOACS-2-L-LS	0.6	0.65	0.32	

Table E.67: Interquartile of C_{A_1,A_2} for the Arc111-1 problem

		A2			
		BIANT-1	BIANT-2	MOACS-2	MOACS-2-L-LS
A1	BIANT-1		0.34	0.02	0.04
	BIANT-2	0.22		0.04	0.06
	MOACS-2	0.07	0.04		0.13
	MOACS-2-L-LS	0.07	0.09	0.11	

Table E.68: $\tilde{C}_{A_1,A_2}$ for the Arc111-2 problem

		A2			
		BIANT-1	BIANT-2	MOACS-2	MOACS-2-L-LS
A1	BIANT-1		0.18	0.04	0.04
	BIANT-2	0.58		0.08	0.07
	MOACS-2	0.61	0.61		0.40
	MOACS-2-L-LS	0.64	0.66	0.38	

Table E.69: Interquartile of C_{A_1,A_2} for the Arc111-2 problem

		A2			
		BIANT-1	BIANT-2	MOACS-2	MOACS-2-L-LS
A1	BIANT-1		0.48	0.06	0.06
	BIANT-2	0.44	0.4	0.05	0.06
	MOACS-2	0.1	0.1	0.14	0.14
	MOACS-2-L-LS	0.1	0.1	0.12	0.14

Table E.70: $\tilde{C}_{A_1,A_2}$ for the Arc111-3 problem

		A2			
		BIANT-1	BIANT-2	MOACS-2	MOACS-2-L-LS
A1	BIANT-1		0.32	0.08	0.07
	BIANT-2	0.48		0.04	0.04
	MOACS-2	0.56	0.56		0.45
	MOACS-2-L-LS	0.58	0.6	0.34	

Table E.71: Interquartile of C_{A_1,A_2} for the Arc111-3 problem

		A2			
		BIANT-1	BIANT-2	MOACS-2	MOACS-2-L-LS
A1	BIANT-1		0.4	0.06	0.06
	BIANT-2	0.52		0.04	0.04
	MOACS-2	0.09	0.06		0.15
	MOACS-2-L-LS	0.08	0.08	0.11	

Table E.72: $\tilde{C}_{A_1,A_2}$ for the Arc111-4 problem

		A2			
		BIANT-1	BIANT-2	MOACS-2	MOACS-2-L-LS
A1	BIANT-1		0.32	0.04	0.08
	BIANT-2	0.4		0.06	0.08
	MOACS-2	0.61	0.56		0.49
	MOACS-2-L-LS	0.66	0.58	0.3	

Table E.73: Interquartile of C_{A_1,A_2} for the Arc111-4 problem

		A2			
		BIANT-1	BIANT-2	MOACS-2	MOACS-2-L-LS
A1	BIANT-1		0.24	0.04	0.06
	BIANT-2	0.36		0.04	0.06
	MOACS-2	0.07	0.05		0.13
	MOACS-2-L-LS	0.1	0.09	0.16	

E.3.2 Problem Family: Buxey

Table E.74: $\tilde{C}_{A_1,A_2}$ for the Buxey-1 problem

		A2			
		BIANT-1	BIANT-2	MOACS-2	MOACS-2-L-LS
A1	BIANT-1		0.56	0.28	0.32
	BIANT-2	0.24		0.22	0.26
	MOACS-2	0.62	0.66		0.58
	MOACS-2-L-LS	0.56	0.64	0.3	

Table E.75: Interquartile of C_{A_1,A_2} for the Buxey-1 problem

		A2			
		BIANT-1	BIANT-2	MOACS-2	MOACS-2-L-LS
A1	BIANT-1		0.32	0.3	0.33
	BIANT-2	0.28		0.19	0.25
	MOACS-2	0.33	0.22		0.18
	MOACS-2-L-LS	0.38	0.29	0.23	

Table E.76: $\tilde{C}_{A_1,A_2}$ for the Buxey-2 problem

		A2			
		BIANT-1	BIANT-2	MOACS-2	MOACS-2-L-LS
A1	BIANT-1		0.18	0.04	0.04
	BIANT-2	0.58	0.34	0.08	0.07
	MOACS-2	0.61	0.61	0.4	0.40
	MOACS-2-L-LS	0.64	0.66	0.38	0.40

Table E.77: Interquartile of C_{A_1,A_2} for the Buxey-2 problem

		A2			
		BIANT-1	BIANT-2	MOACS-2	MOACS-2-L-LS
A1	BIANT-1		0.4	0.42	0.52
	BIANT-2	0.42		0.36	0.53
	MOACS-2	0.42	0.51		0.59
	MOACS-2-L-LS	0.31	0.39	0.23	

Table E.78: $\tilde{C}_{A_1,A_2}$ for the Buxey-3 problem

		A2			
		BIANT-1	BIANT-2	MOACS-2	MOACS-2-L-LS
A1	BIANT-1		0.44	0.54	0.64
	BIANT-2	0.46		0.59	0.72
	MOACS-2	0.36	0.28		0.54
	MOACS-2-L-LS	0.3	0.18	0.3	

Table E.79: Interquartile of C_{A_1,A_2} for the Buxey-3 problem

		A2			
		BIANT-1	BIANT-2	MOACS-2	MOACS-2-L-LS
A1	BIANT-1		0.54	0.35	0.36
	BIANT-2	0.38		0.22	0.27
	MOACS-2	0.29	0.19		0.18
	MOACS-2-L-LS	0.29	0.2	0.21	

Table E.80: $\tilde{C}_{A_1,A_2}$ for the Buxey-4 problem

		A2			
		BIANT-1	BIANT-2	MOACS-2	MOACS-2-L-LS
A1	BIANT-1		0.28	0.46	0.49
	BIANT-2	0.56		0.54	0.55
	MOACS-2	0.44	0.32		0.42
	MOACS-2-L-LS	0.4	0.3	0.44	

Table E.81: Interquartile of C_{A_1,A_2} for the Buxey-4 problem

		A2			
		BIANT-1	BIANT-2	MOACS-2	MOACS-2-L-LS
A1	BIANT-1		0.2	0.15	0.16
	BIANT-2	0.28		0.21	0.31
	MOACS-2	0.21	0.22		0.15
	MOACS-2-L-LS	0.15	0.27	0.15	

E.3.3 Problem Family: Gunther

Table E.82: $\tilde{C}_{A_1,A_2}$ for the Gunther-1 problem

		A2			
		BIANT-1	BIANT-2	MOACS-2	MOACS-2-L-LS
A1	BIANT-1		0.36	0.02	0.04
	BIANT-2	0.48		0.06	0.06
	MOACS-2	0.79	0.75		0.60
	MOACS-2-L-LS	0.83	0.78	0.28	

Table E.83: Interquartile of C_{A_1,A_2} for the Gunther-1 problem

		A2			
		BIANT-1	BIANT-2	MOACS-2	MOACS-2-L-LS
A1	BIANT-1		0.26	0.06	0.04
	BIANT-2	0.24		0.1	0.06
	MOACS-2	0.12	0.15		0.16
	MOACS-2-L-LS	0.09	0.1	0.16	

Table E.84: $\tilde{C}_{A_1,A_2}$ for the Gunther-2 problem

		A2			
		BIANT-1	BIANT-2	MOACS-2	MOACS-2-L-LS
A1	BIANT-1		0.34	0.04	0.06
	BIANT-2	0.52		0.08	0.10
	MOACS-2	0.82	0.74		0.53
	MOACS-2-L-LS	0.82	0.74	0.29	

Table E.85: Interquartile of C_{A_1,A_2} for the Gunther-2 problem

		A2			
		BIANT-1	BIANT-2	MOACS-2	MOACS-2-L-LS
A1	BIANT-1		0.42	0.03	0.10
	BIANT-2	0.48		0.13	0.23
	MOACS-2	0.08	0.24		0.15
	MOACS-2-L-LS	0.13	0.34	0.17	

Table E.86: $\tilde{C}_{A_1,A_2}$ for the Gunther-3 problem

		A2			
		BIANT-1	BIANT-2	MOACS-2	MOACS-2-L-LS
A1	BIANT-1		0.26	0.02	0.02
	BIANT-2	0.55		0.06	0.07
	MOACS-2	0.82	0.74		0.56
	MOACS-2-L-LS	0.85	0.8	0.29	

Table E.87: Interquartile of C_{A_1,A_2} for the Gunther-3 problem

		A2			
		BIANT-1	BIANT-2	MOACS-2	MOACS-2-L-LS
A1	BIANT-1		0.37	0.05	0.09
	BIANT-2	0.43		0.13	0.14
	MOACS-2	0.1	0.14		0.19
	MOACS-2-L-LS	0.14	0.16	0.2	

Table E.88: $\tilde{C}_{A_1,A_2}$ for the Gunther-4 problem

		A2			
		BIANT-1	BIANT-2	MOACS-2	MOACS-2-L-LS
A1	BIANT-1		0.64	0.17	0.17
	BIANT-2	0.17		0.07	0.04
	MOACS-2	0.67	0.78		0.51
	MOACS-2-L-LS	0.66	0.78	0.34	

Table E.89: Interquartile of C_{A_1,A_2} for the Gunther-4 problem

		A2			
		BIANT-1	BIANT-2	MOACS-2	MOACS-2-L-LS
A1	BIANT-1		0.31	0.13	0.16
	BIANT-2	0.27		0.11	0.08
	MOACS-2	0.12	0.14		0.27
	MOACS-2-L-LS	0.13	0.16	0.22	

Table E.90: $\tilde{C}_{A_1,A_2}$ for the Gunther-5 problem

		A2			
		BIANT-1	BIANT-2	MOACS-2	MOACS-2-L-LS
A1	BIANT-1		0.73	0.22	0.36
	BIANT-2	0.18		0.14	0.16
	MOACS-2	0.64	0.77		0.66
	MOACS-2-L-LS	0.49	0.74	0.22	

Table E.91: Interquartile of C_{A_1,A_2} for the Gunther-5 problem

		A2			
		BIANT-1	BIANT-2	MOACS-2	MOACS-2-L-LS
A1	BIANT-1		0.29	0.12	0.21
	BIANT-2	0.13		0.1	0.14
	MOACS-2	0.14	0.09		0.20
	MOACS-2-L-LS	0.18	0.17	0.13	

E.3.4 Problem Family: Hahn

Table E.92: $\tilde{C}_{A_1,A_2}$ for the Hahn-1 problem

		A2			
		BIANT-1	BIANT-2	MOACS-2	MOACS-2-L-LS
A1	BIANT-1		0.25	0.07	0.04
	BIANT-2	0.55		0.06	0.06
	MOACS-2	0.73	0.72		0.44
	MOACS-2-L-LS	0.81	0.8	0.32	

Table E.93: Interquartile of C_{A_1,A_2} for the Hahn-1 problem

		A2			
		BIANT-1	BIANT-2	MOACS-2	MOACS-2-L-LS
A1	BIANT-1		0.43	0.1	0.13
	BIANT-2	0.44		0.06	0.08
	MOACS-2	0.15	0.15		0.14
	MOACS-2-L-LS	0.19	0.18	0.14	

Table E.94: $\tilde{C}_{A_1,A_2}$ for the Hahn-2 problem

		A2			
		BIANT-1	BIANT-2	MOACS-2	MOACS-2-L-LS
A1	BIANT-1		0.56	0.15	0.14
	BIANT-2	0.28		0.1	0.07
	MOACS-2	0.74	0.78		0.54
	MOACS-2-L-LS	0.74	0.83	0.3	

Table E.95: Interquartile of C_{A_1,A_2} for the Hahn-2 problem

		A2			
		BIANT-1	BIANT-2	MOACS-2	MOACS-2-L-LS
A1	BIANT-1		0.23	0.06	0.05
	BIANT-2	0.19		0.09	0.15
	MOACS-2	0.11	0.1		0.14
	MOACS-2-L-LS	0.11	0.15	0.1	

Table E.96: $\tilde{C}_{A_1,A_2}$ for the Hahn-3 problem

		A2			
		BIANT-1	BIANT-2	MOACS-2	MOACS-2-L-LS
A1	BIANT-1		0.45	0.12	0.09
	BIANT-2	0.32		0.1	0.10
	MOACS-2	0.72	0.76		0.43
	MOACS-2-L-LS	0.76	0.79	0.36	

Table E.97: Interquartile of C_{A_1,A_2} for the Hahn-3 problem

		A2			
		BIANT-1	BIANT-2	MOACS-2	MOACS-2-L-LS
A1	BIANT-1		0.35	0.1	0.07
	BIANT-2	0.28		0.1	0.10
	MOACS-2	0.08	0.1		0.16
	MOACS-2-L-LS	0.11	0.13	0.14	

Table E.98: $\tilde{C}_{A_1,A_2}$ for the Hahn-4 problem

		A2			
		BIANT-1	BIANT-2	MOACS-2	MOACS-2-L-LS
A1	BIANT-1		0.32	0.08	0.10
	BIANT-2	0.4		0.08	0.10
	MOACS-2	0.74	0.7		0.50
	MOACS-2-L-LS	0.78	0.76	0.24	

Table E.99: Interquartile of C_{A_1,A_2} for the Hahn-4 problem

		A2			
		BIANT-1	BIANT-2	MOACS-2	MOACS-2-L-LS
A1	BIANT-1		0.35	0.13	0.09
	BIANT-2	0.33		0.14	0.10
	MOACS-2	0.12	0.14		0.16
	MOACS-2-L-LS	0.16	0.19	0.2	

E.3.5 Problem Family: Mukherje

Table E.100: $\tilde{C}_{A_1,A_2}$ for the Mukherje-1 problem

		A2			
		BIANT-1	BIANT-2	MOACS-2	MOACS-2-L-LS
A1	BIANT-1		0.38	0.06	0.06
	BIANT-2	0.38		0.03	0.02
	MOACS-2	0.74	0.77		0.44
	MOACS-2-L-LS	0.8	0.82	0.34	

Table E.101: Interquartile of C_{A_1,A_2} for the Mukherje-1 problem

		A2			
		BIANT-1	BIANT-2	MOACS-2	MOACS-2-L-LS
A1	BIANT-1		0.36	0.04	0.06
	BIANT-2	0.38		0.09	0.08
	MOACS-2	0.08	0.1		0.14
	MOACS-2-L-LS	0.1	0.12	0.12	

Table E.102: $\tilde{C}_{A_1,A_2}$ for the Mukherje-2 problem

		A2			
		BIANT-1	BIANT-2	MOACS-2	MOACS-2-L-LS
A1	BIANT-1		0.46	0.06	0.06
	BIANT-2	0.36		0.05	0.08
	MOACS-2	0.74	0.7		0.49
	MOACS-2-L-LS	0.78	0.72	0.29	

Table E.103: Interquartile of C_{A_1,A_2} for the Mukherje-2 problem

		A2			
		BIANT-1	BIANT-2	MOACS-2	MOACS-2-L-LS
A1	BIANT-1		0.26	0.04	0.04
	BIANT-2	0.3		0.08	0.08
	MOACS-2	0.07	0.11		0.14
	MOACS-2-L-LS	0.12	0.1	0.16	

Table E.104: $\tilde{C}_{A_1,A_2}$ for the Mukherje-3 problem

		A2			
		BIANT-1	BIANT-2	MOACS-2	MOACS-2-L-LS
A1	BIANT-1		0.42	0.08	0.06
	BIANT-2	0.34		0.06	0.04
	MOACS-2	0.7	0.71		0.42
	MOACS-2-L-LS	0.72	0.76	0.32	

Table E.105: Interquartile of C_{A_1,A_2} for the Mukherje-3 problem

		A2			
		BIANT-1	BIANT-2	MOACS-2	MOACS-2-L-LS
A1	BIANT-1		0.16	0.06	0.06
	BIANT-2	0.16		0.04	0.02
	MOACS-2	0.09	0.08		0.14
	MOACS-2-L-LS	0.08	0.1	0.14	

Appendix F

Detailed Information, Analysis and Results of Chapter 6

Abstract

The present chapter presents the various analyses of Chapter 7, and (i) the generic description of the events modifying the system under study in the simulation model, (ii) the values of the various quality indicators obtained by each optimisers for each problem instance and (ii) the detailed values of the Friedman's test.

F.1 Generic Description of the Events Modifying the System

This section presents generic flowcharts of the simulation module.

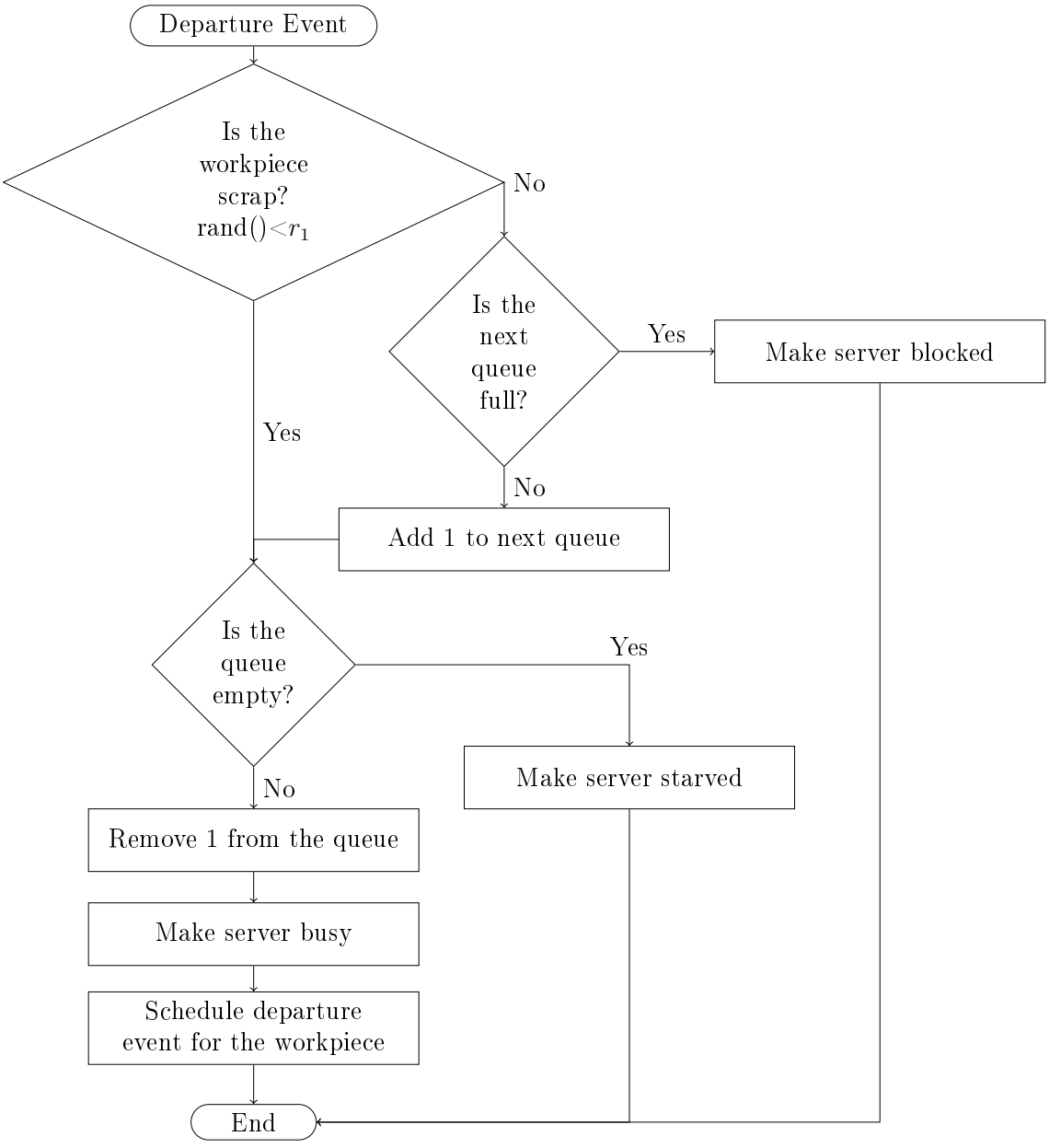

Figure F.1: Description of the departure event of the first subsystem

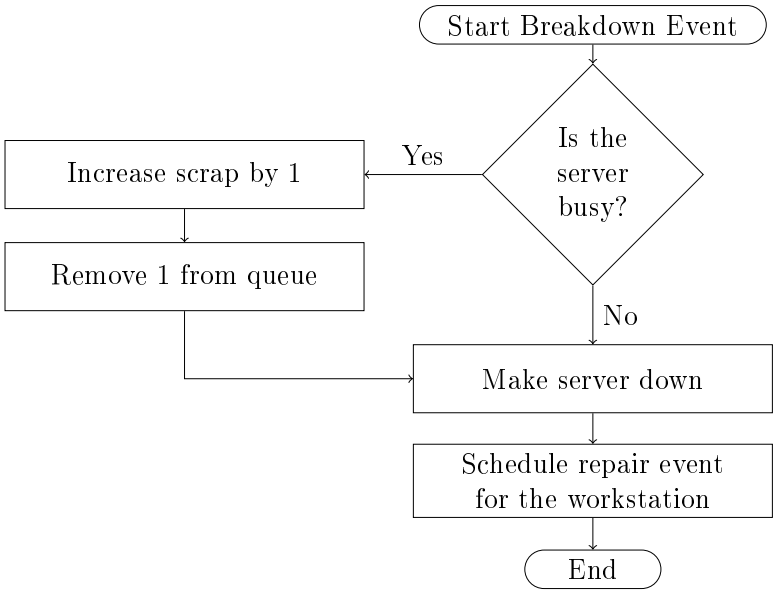

Figure F.2: Description of the breakdown event of the first subsystem

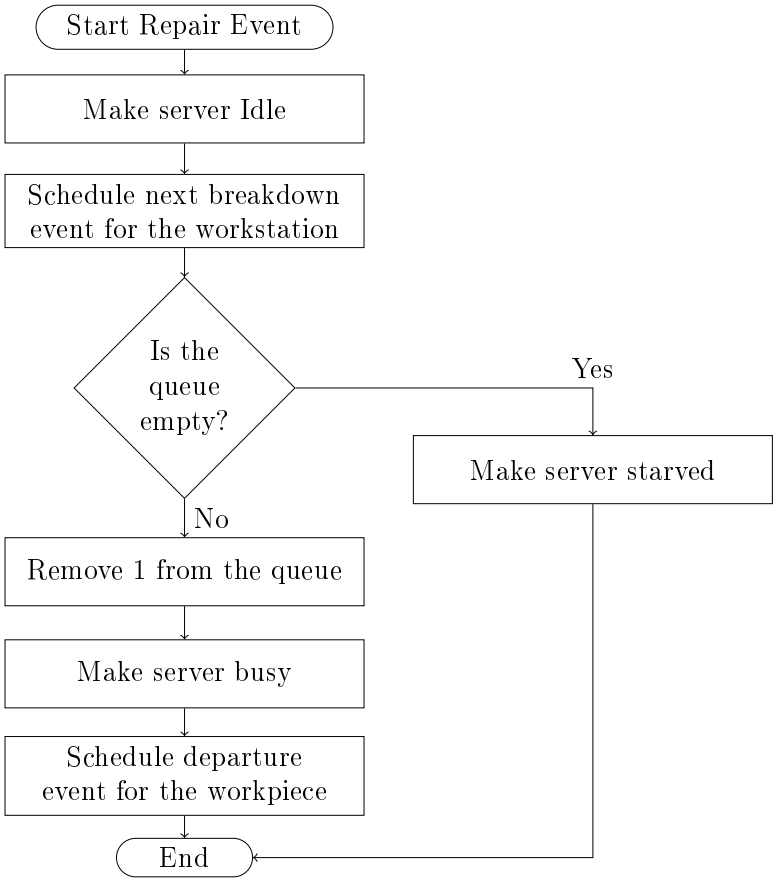

Figure F.3: Description of the repair event of the first subsystem

F.2 Comparison of transition probability for the MOAS

The section presents the results of the analysis of the choice of the transition rule for the multi-objective simulated annealing local search.

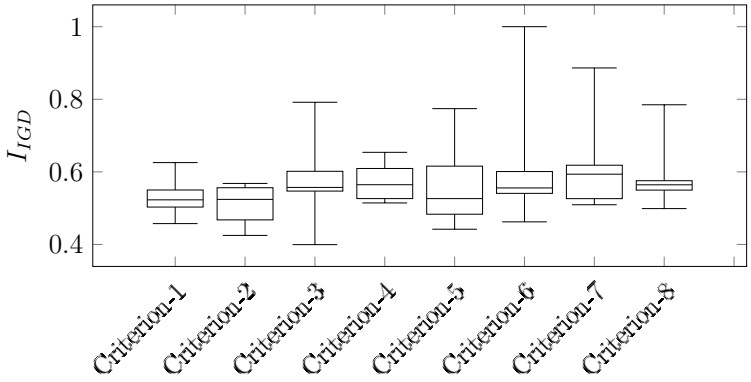

Figure F.4: Boxplot for I_{HV} obtained by various acceptance criteria for Arc111-1

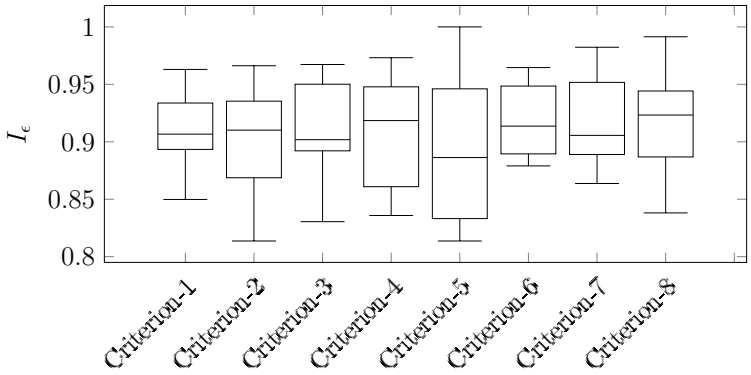

Figure F.5: Boxplot for I_{IGD} obtained by various acceptance criteria for Arc111-1

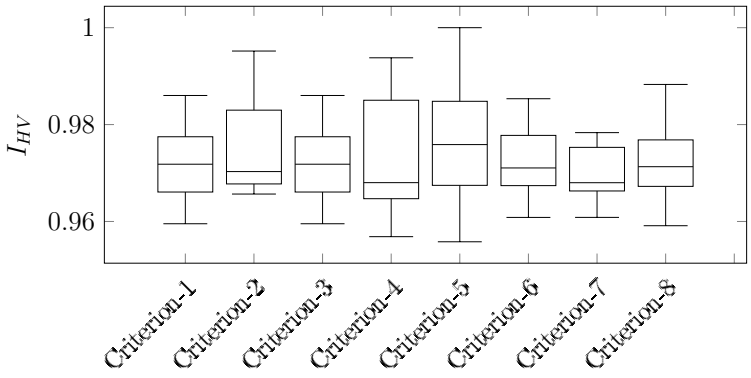

Figure F.6: Boxplot for I_{ϵ} obtained by various acceptance criteria for Arc111-1

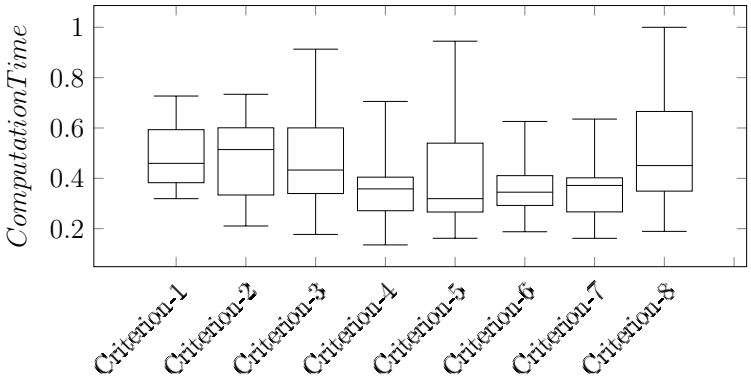

Figure F.7: Boxplot for I_Δ obtained by various acceptance criteria for Arc111-1

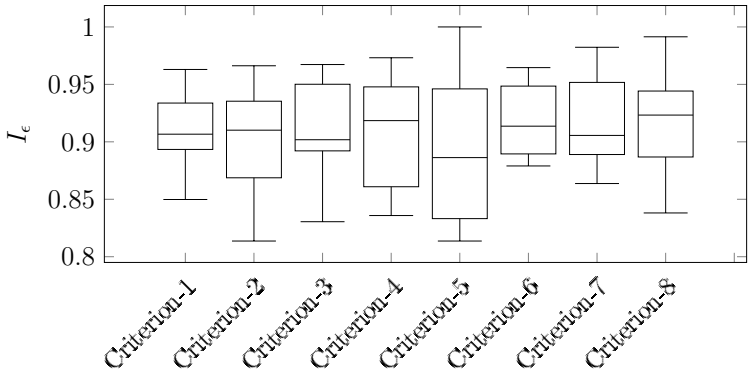

Figure F.8: Boxplot for the computation time obtained by various acceptance criteria for Arc111-1

Table F.1: Average rankings of the transition criteria returned by Friedman's nonparametric test for I_{HV} when considering the Arc111-1 problem instance

Algorithm	Ranking
C1	4.600
C2	4.000
C3	4.800
C4	4.800
C5	3.400
C6	4.300
C7	5.900
C8	4.200

Table F.2: Unadjusted and adjusted $p-$values obtained for the Arc111-1 through the application of Holm's post hoc procedure, using the C5 as control algorithm according to I_{HV}

Algorithm	Unadjusted $p-$value	Adjusted $p-$value
C7	0.029	0.203
C3	0.160	0.960
C8	0.273	1.363
C4	0.277	1.363
C1	0.290	1.363
C6	0.459	1.363
C2	0.557	1.363

Table F.3: Average rankings of the transition criteria returned by Friedman's nonparametric test for I_{IGD} when considering the Arc111-1 problem instance

Algorithm	Ranking
C1	5.700
C2	6.000
C3	4.200
C4	3.800
C5	5.000
C6	4.600
C7	3.000
C8	3.700

Table F.4: Unadjusted and adjusted $p-$values obtained for the Arc111-1 through the application of Holm's post hoc procedure, using the C2 as control algorithm according to I_{IGD}

Algorithm	Unadjusted $p-$value	Adjusted $p-$value
C7	0.001	0.006
C8	0.008	0.049
C4	0.020	0.102
C3	0.024	0.102
C6	0.070	0.211
C5	0.229	0.458
C1	0.501	0.501

Table F.5: Average rankings of the transition criteria returned by Friedman's nonparametric test for I_ϵ when considering the Arc111-1 problem instance

Algorithm	Ranking
C1	4.400
C2	4.900
C3	4.450
C4	4.800
C5	5.250
C6	4.050
C7	3.350
C8	4.800

Table F.6: Unadjusted and adjusted $p-$values obtained for the Arc111-1 through the application of Holm's post hoc procedure, using the C5 as control algorithm according to I_ϵ

Algorithm	Unadjusted $p-$value	Adjusted $p-$value
C7	0.033	0.229
C6	0.240	1.443
C1	0.246	1.443
C3	0.268	1.443
C4	0.301	1.443
C8	0.422	1.443
C2	0.479	1.443

Table F.7: Average rankings of the transition criteria returned by Friedman's nonparametric test for I_Δ when considering the Arc111-1 problem instance

Algorithm	Ranking
C1	4.300
C2	4.600
C3	4.400
C4	5.300
C5	5.600
C6	3.400
C7	4.000
C8	4.400

Table F.8: Unadjusted and adjusted $p-$values obtained for the Arc111-1 through the application of Holm's post hoc procedure, using the C5 as control algorithm according to I_Δ

Algorithm	Unadjusted $p-$value	Adjusted $p-$value
C6	0.061	0.424
C7	0.108	0.648
C8	0.197	0.986
C1	0.201	0.986
C3	0.361	1.082
C2	0.424	1.082
C4	0.870	1.082

Table F.9: Average rankings of the transition criteria returned by Friedman's nonparametric test for the computation time when considering the Arc111-1 problem instance

Algorithm	Ranking
C1	3.700
C2	3.600
C3	3.800
C4	5.300
C5	4.700
C6	5.2500
C7	5.5500
C8	4.100

Table F.10: Unadjusted and adjusted $p-$values obtained for the Arc111-1 through the application of Holm's post hoc procedure, using the C5 as control algorithm according to I_{Δ}

Algorithm	Unadjusted $p-$value	Adjusted $p-$value
C2	0.022	0.156
C1	0.031	0.185
C3	0.048	0.240
C8	0.074	0.297
C5	0.167	0.502
C6	0.476	0.953
C4	0.718	0.953

F.3 Detailed values of the metrics

This section presents the procedure used for the definition of the parameters of the various optimization algorithms.

F.3.1 Problem Family: Arc111

Table F.11: Median and interquartile range of I_{HV} obtained by the optimisers for the Arc111 problems

	Arc111-1 $\tilde{x} \pm IQR(x)$		Arc111-2 $\tilde{x} \pm IQR(x)$		Arc111-3 $\tilde{x} \pm IQR(x)$		Arc111-4 $\tilde{x} \pm IQR(x)$		Arc111-5 $\tilde{x} \pm IQR(x)$	
NSGA-II	0.95	0.01	0.95	0.01	0.93	0.01	0.95	0.00	0.94	0.01
NSGA-II-ACO-1	0.95	0.01	0.94	0.01	0.93	0.01	0.95	0.01	0.94	0.01
NSGA-II-ACO-2	0.95	0.01	0.94	0.01	0.94	0.02	0.95	0.01	0.94	0.00
NSGA-II-LS	0.94	0.01	0.94	0.01	0.93	0.02	0.95	0.01	0.94	0.00
SPEA2	0.95	0.01	0.95	0.01	0.94	0.01	0.95	0.01	0.95	0.01
SPEA2-LS	0.95	0.01	0.95	0.01	0.94	0.00	0.96	0.01	0.96	0.01

Table F.12: Median and interquartile range of I_{IGD} obtained by the optimisers for the Arc111 problems

	Arc111-1 $\tilde{x} \pm IQR(x)$		Arc111-2 $\tilde{x} \pm IQR(x)$		Arc111-3 $\tilde{x} \pm IQR(x)$		Arc111-4 $\tilde{x} \pm IQR(x)$		Arc111-5 $\tilde{x} \pm IQR(x)$	
NSGA-II	0.74	0.15	0.78	0.13	0.78	0.21	0.86	0.06	0.72	0.12
NSGA-II-ACO-1	0.77	0.04	0.85	0.08	0.86	0.13	0.91	0.07	0.74	0.19
NSGA-II-ACO-2	0.73	0.07	0.86	0.13	0.78	0.13	0.88	0.06	0.72	0.14
NSGA-II-LS	0.76	0.04	0.92	0.10	0.90	0.13	0.88	0.10	0.72	0.05
SPEA2	0.66	0.06	0.67	0.07	0.71	0.11	0.74	0.07	0.61	0.08
SPEA2-LS	0.72	0.07	0.77	0.15	0.71	0.07	0.74	0.05	0.68	0.06

Table F.13: Median and interquartile range of I_ϵ obtained by the optimisers for the Arc111 problems

	Arc111-1 $\tilde{x} \pm IQR(x)$		Arc111-2 $\tilde{x} \pm IQR(x)$		Arc111-3 $\tilde{x} \pm IQR(x)$		Arc111-4 $\tilde{x} \pm IQR(x)$		Arc111-5 $\tilde{x} \pm IQR(x)$	
NSGA-II	0.97	0.02	0.94	0.02	0.93	0.03	0.93	0.01	0.92	0.02
NSGA-II-ACO-1	0.96	0.01	0.94	0.04	0.95	0.04	0.94	0.03	0.96	0.09
NSGA-II-ACO-2	0.97	0.01	0.96	0.04	0.91	0.05	0.95	0.03	0.92	0.04
NSGA-II-LS	0.98	0.04	0.96	0.05	0.93	0.06	0.94	0.03	0.92	0.02
SPEA2	0.95	0.03	0.94	0.01	0.91	0.05	0.92	0.04	0.91	0.04
SPEA2-LS	0.95	0.03	0.94	0.04	0.91	0.07	0.91	0.02	0.87	0.06

Table F.14: Median and interquartile range of I_Δ obtained by the optimisers for the Arc111 problems

	Arc111-1 $\tilde{x} \pm IQR(x)$		Arc111-2 $\tilde{x} \pm IQR(x)$		Arc111-3 $\tilde{x} \pm IQR(x)$		Arc111-4 $\tilde{x} \pm IQR(x)$		Arc111-5 $\tilde{x} \pm IQR(x)$	
NSGA-II	0.83	0.13	0.84	0.07	0.81	0.10	0.79	0.13	0.89	0.07
NSGA-II-ACO-1	0.80	0.09	0.86	0.08	0.79	0.05	0.82	0.08	0.95	0.03
NSGA-II-ACO-2	0.77	0.11	0.81	0.04	0.83	0.02	0.85	0.12	0.90	0.02
NSGA-II-LS	0.81	0.07	0.82	0.06	0.77	0.07	0.86	0.08	0.90	0.11
SPEA2	0.80	0.08	0.78	0.07	0.78	0.12	0.76	0.05	0.87	0.06
SPEA2-LS	0.78	0.06	0.84	0.10	0.77	0.07	0.76	0.09	0.89	0.05

Table F.15: Median and interquartile range of the computation time required by the optimisers for the Arc111 problems

	Arc111-1 $\tilde{x} \pm IQR(x)$		Arc111-2 $\tilde{x} \pm IQR(x)$		Arc111-3 $\tilde{x} \pm IQR(x)$		Arc111-4 $\tilde{x} \pm IQR(x)$		Arc111-5 $\tilde{x} \pm IQR(x)$	
NSGA-II	0.02	0.00	0.02	0.00	0.02	0.00	0.03	0.00	0.04	0.00
NSGA-II-ACO-1	0.49	0.20	0.30	0.19	0.35	0.16	0.56	0.17	0.76	0.15
NSGA-II-ACO-2	0.44	0.24	0.62	0.23	0.77	0.34	0.67	0.34	0.93	0.15
NSGA-II-LS	0.12	0.01	0.14	0.00	0.14	0.00	0.18	0.00	0.22	0.00
SPEA2	0.12	0.09	0.13	0.11	0.11	0.11	0.15	0.14	0.23	0.17
SPEA2-LS	0.03	0.00	0.04	0.00	0.03	0.00	0.05	0.00	0.06	0.01

F.3.2 Problem Family: Buxey

Table F.16: Median and interquartile range of I_{HV} obtained by the optimisers for the Buxey problems

	Buxey-1 $\tilde{x} \pm IQR(x)$		Buxey-2 $\tilde{x} \pm IQR(x)$		Buxey-3 $\tilde{x} \pm IQR(x)$		Buxey-4 $\tilde{x} \pm IQR(x)$		Buxey-5 $\tilde{x} \pm IQR(x)$	
NSGA-II	0.95	0.01	0.94	0.01	0.93	0.00	0.95	0.01	0.94	0.01
NSGA-II-ACO-1	0.94	0.01	0.96	0.01	0.94	0.01	0.94	0.02	0.94	0.00
NSGA-II-ACO-2	0.94	0.00	0.95	0.01	0.94	0.01	0.94	0.01	0.95	0.01
NSGA-II-LS	0.94	0.01	0.95	0.01	0.94	0.00	0.94	0.00	0.95	0.01
SPEA2	0.95	0.01	0.96	0.01	0.95	0.02	0.95	0.01	0.95	0.00
SPEA2-LS	0.96	0.01	0.96	0.02	0.95	0.00	0.95	0.01	0.96	0.01

Table F.17: Median and interquartile range of I_{IGD} obtained by the optimisers for the Buxey problems

	Buxey-1 $\tilde{x} \pm IQR(x)$		Buxey-2 $\tilde{x} \pm IQR(x)$		Buxey-3 $\tilde{x} \pm IQR(x)$		Buxey-4 $\tilde{x} \pm IQR(x)$		Buxey-5 $\tilde{x} \pm IQR(x)$	
NSGA-II	0.82	0.03	0.73	0.10	0.74	0.11	0.79	0.09	0.61	0.05
NSGA-II-ACO-1	0.89	0.16	0.65	0.05	0.75	0.15	0.75	0.17	0.54	0.05
NSGA-II-ACO-2	0.83	0.05	0.66	0.06	0.72	0.06	0.82	0.06	0.60	0.12
NSGA-II-LS	0.86	0.12	0.62	0.06	0.72	0.05	0.81	0.06	0.61	0.17
SPEA2	0.73	0.05	0.57	0.08	0.62	0.07	0.61	0.11	0.52	0.20
SPEA2-LS	0.71	0.04	0.64	0.12	0.77	0.18	0.69	0.08	0.50	0.07

Table F.18: Median and interquartile range of I_ϵ obtained by the optimisers for the Buxey problems

	Buxey-1 $\tilde{x} \pm IQR(x)$		Buxey-2 $\tilde{x} \pm IQR(x)$		Buxey-3 $\tilde{x} \pm IQR(x)$		Buxey-4 $\tilde{x} \pm IQR(x)$		Buxey-5 $\tilde{x} \pm IQR(x)$	
NSGA-II	0.61	0.22	0.89	0.27	0.86	0.08	0.70	0.10	0.77	0.07
NSGA-II-ACO-1	0.86	0.19	0.59	0.33	0.72	0.21	0.73	0.14	0.72	0.15
NSGA-II-ACO-2	0.69	0.11	0.51	0.19	0.80	0.15	0.73	0.03	0.69	0.19
NSGA-II-LS	0.74	0.15	0.58	0.26	0.68	0.09	0.73	0.09	0.66	0.23
SPEA2	0.69	0.14	0.64	0.13	0.63	0.13	0.73	0.15	0.63	0.19
SPEA2-LS	0.63	0.20	0.71	0.32	0.73	0.14	0.71	0.16	0.64	0.14

Table F.19: Median and interquartile range of I_Δ obtained by the optimisers for the Buxey problems

	Buxey-1 $\tilde{x} \pm IQR(x)$		Buxey-2 $\tilde{x} \pm IQR(x)$		Buxey-3 $\tilde{x} \pm IQR(x)$		Buxey-4 $\tilde{x} \pm IQR(x)$		Buxey-5 $\tilde{x} \pm IQR(x)$	
NSGA-II	0.78	0.06	0.87	0.10	0.84	0.05	0.79	0.04	0.77	0.07
NSGA-II-ACO-1	0.87	0.03	0.81	0.03	0.74	0.07	0.82	0.12	0.81	0.15
NSGA-II-ACO-2	0.80	0.04	0.89	0.11	0.82	0.06	0.83	0.08	0.83	0.07
NSGA-II-LS	0.86	0.12	0.80	0.02	0.85	0.06	0.81	0.03	0.79	0.05
SPEA2	0.85	0.09	0.86	0.13	0.83	0.06	0.82	0.05	0.84	0.07
SPEA2-LS	0.79	0.10	0.81	0.11	0.80	0.12	0.80	0.12	0.78	0.02

Table F.20: Median and interquartile range of the computation time required by the optimisers for the Buxey problems

	Buxey-1 $\tilde{x} \pm IQR(x)$		Buxey-2 $\tilde{x} \pm IQR(x)$		Buxey-3 $\tilde{x} \pm IQR(x)$		Buxey-4 $\tilde{x} \pm IQR(x)$		Buxey-5 $\tilde{x} \pm IQR(x)$	
NSGA-II	0.01	0.00	0.02	0.00	0.02	0.00	0.02	0.00	0.03	0.00
NSGA-II-ACO-1	0.46	0.26	0.43	0.09	0.39	0.04	0.51	0.17	0.45	0.04
NSGA-II-ACO-2	0.38	0.15	0.54	0.35	0.66	0.40	0.64	0.23	0.70	0.15
NSGA-II-LS	0.09	0.00	0.12	0.00	0.09	0.04	0.12	0.00	0.15	0.00
SPEA2	0.08	0.06	0.12	0.09	0.11	0.08	0.08	0.08	0.15	0.11
SPEA2-LS	0.03	0.00	0.04	0.00	0.04	0.00	0.04	0.00	0.05	0.00

F.3.3 Problem Family: Gunther

Table F.21: Median and interquartile range of I_{HV} obtained by the optimisers for the Gunther problems

	Gunther-1 $\tilde{x} \pm IQR(x)$		Gunther-2 $\tilde{x} \pm IQR(x)$		Gunther-3 $\tilde{x} \pm IQR(x)$		Gunther-4 $\tilde{x} \pm IQR(x)$		Gunther-5 $\tilde{x} \pm IQR(x)$	
NSGA-II	0.94	0.02	0.94	0.00	0.94	0.01	0.96	0.01	0.95	0.01
NSGA-II-ACO-1	0.94	0.01	0.95	0.01	0.95	0.01	0.96	0.00	0.95	0.00
NSGA-II-ACO-2	0.94	0.01	0.95	0.01	0.94	0.00	0.95	0.01	0.95	0.01
NSGA-II-LS	0.95	0.00	0.95	0.00	0.94	0.00	0.95	0.00	0.95	0.01
SPEA2	0.95	0.01	0.96	0.01	0.95	0.01	0.96	0.00	0.96	0.00
SPEA2-LS	0.95	0.02	0.95	0.01	0.95	0.00	0.96	0.00	0.96	0.00

Table F.22: Median and interquartile range of I_{IGD} obtained by the optimisers for the Gunther problems

	Gunther-1 $\tilde{x} \pm IQR(x)$		Gunther-2 $\tilde{x} \pm IQR(x)$		Gunther-3 $\tilde{x} \pm IQR(x)$		Gunther-4 $\tilde{x} \pm IQR(x)$		Gunther-5 $\tilde{x} \pm IQR(x)$	
NSGA-II	0.79	0.15	0.75	0.06	0.66	0.10	0.65	0.12	0.87	0.05
NSGA-II-ACO-1	0.77	0.06	0.78	0.06	0.68	0.09	0.70	0.23	0.98	0.19
NSGA-II-ACO-2	0.82	0.02	0.79	0.15	0.69	0.04	0.62	0.11	0.88	0.04
NSGA-II-LS	0.75	0.03	0.70	0.06	0.73	0.13	0.63	0.07	0.85	0.05
SPEA2	0.67	0.03	0.65	0.11	0.62	0.05	0.52	0.03	0.77	0.07
SPEA2-LS	0.69	0.07	0.65	0.04	0.62	0.07	0.57	0.10	0.77	0.07

Table F.23: Median and interquartile range of I_ϵ obtained by the optimisers for the Gunther problems

	Gunther-1 $\tilde{x} \pm IQR(x)$		Gunther-2 $\tilde{x} \pm IQR(x)$		Gunther-3 $\tilde{x} \pm IQR(x)$		Gunther-4 $\tilde{x} \pm IQR(x)$		Gunther-5 $\tilde{x} \pm IQR(x)$	
NSGA-II	0.86	0.24	0.83	0.11	0.84	0.18	0.70	0.18	0.86	0.09
NSGA-II-ACO-1	0.83	0.32	0.74	0.06	0.67	0.31	0.71	0.11	0.84	0.01
NSGA-II-ACO-2	0.82	0.16	0.81	0.17	0.94	0.03	0.77	0.15	0.93	0.06
NSGA-II-LS	0.70	0.14	0.76	0.04	0.87	0.15	0.71	0.13	0.81	0.07
SPEA2	0.72	0.15	0.77	0.29	0.70	0.10	0.63	0.09	0.83	0.03
SPEA2-LS	0.73	0.29	0.76	0.06	0.82	0.16	0.69	0.10	0.89	0.09

Table F.24: Median and interquartile range of I_Δ obtained by the optimisers for the Gunther problems

	Gunther-1 $\tilde{x} \pm IQR(x)$		Gunther-2 $\tilde{x} \pm IQR(x)$		Gunther-3 $\tilde{x} \pm IQR(x)$		Gunther-4 $\tilde{x} \pm IQR(x)$		Gunther-5 $\tilde{x} \pm IQR(x)$	
NSGA-II	0.75	0.12	0.79	0.10	0.81	0.10	0.85	0.07	0.79	0.12
NSGA-II-ACO-1	0.80	0.08	0.80	0.12	0.88	0.03	0.81	0.09	0.74	0.18
NSGA-II-ACO-2	0.78	0.04	0.88	0.02	0.90	0.11	0.78	0.08	0.79	0.02
NSGA-II-LS	0.79	0.03	0.79	0.16	0.83	0.04	0.79	0.03	0.75	0.08
SPEA2	0.81	0.09	0.85	0.05	0.83	0.14	0.81	0.08	0.72	0.12
SPEA2-LS	0.82	0.04	0.86	0.10	0.84	0.04	0.81	0.08	0.75	0.07

Table F.25: Median and interquartile range of the computation time required by the optimisers for the Gunther problems

	Gunther-1 $\tilde{x} \pm IQR(x)$		Gunther-2 $\tilde{x} \pm IQR(x)$		Gunther-3 $\tilde{x} \pm IQR(x)$		Gunther-4 $\tilde{x} \pm IQR(x)$		Gunther-5 $\tilde{x} \pm IQR(x)$	
NSGA-II	0.04	0.01	0.03	0.00	0.03	0.00	0.03	0.00	0.04	0.00
NSGA-II-ACO-1	0.48	0.31	0.62	0.26	0.53	0.02	0.53	0.18	0.58	0.37
NSGA-II-ACO-2	0.69	0.29	0.54	0.10	0.61	0.24	0.75	0.18	0.79	0.21
NSGA-II-LS	0.22	0.00	0.15	0.00	0.18	0.00	0.16	0.00	0.21	0.00
SPEA2	0.21	0.12	0.12	0.08	0.14	0.08	0.14	0.08	0.15	0.11
SPEA2-LS	0.06	0.00	0.04	0.00	0.05	0.00	0.04	0.00	0.06	0.00

F.3.4 Problem Family: Hahn

Table F.26: Median and interquartile range of I_{HV} obtained by the optimisers for the Hahn problems

	Hahn-1		Hahn-2		Hahn-3		Hahn-4		Hahn-5	
	$\tilde{x}$	$IQR(x)$	$\tilde{x}$	$IQR(x)$	$\tilde{x}$	$IQR(x)$	$\tilde{x}$	$IQR(x)$	$\tilde{x}$	$IQR(x)$
NSGA-II	0.94	0.02	0.94	0.00	0.94	0.01	0.96	0.01	0.95	0.01
NSGA-II-ACO-1	0.94	0.01	0.95	0.01	0.95	0.01	0.96	0.00	0.95	0.00
NSGA-II-ACO-2	0.94	0.01	0.95	0.01	0.94	0.00	0.95	0.01	0.95	0.01
NSGA-II-LS	0.95	0.00	0.95	0.00	0.94	0.00	0.95	0.00	0.95	0.01
SPEA2	0.95	0.01	0.96	0.01	0.95	0.01	0.96	0.00	0.96	0.00
SPEA2-LS	0.95	0.02	0.95	0.01	0.95	0.00	0.96	0.00	0.96	0.00

Table F.27: Median and interquartile range of I_{IGD} obtained by the optimisers for the Hahn problems

	Hahn-1		Hahn-2		Hahn-3		Hahn-4		Hahn-5	
	$\tilde{x}$	$IQR(x)$	$\tilde{x}$	$IQR(x)$	$\tilde{x}$	$IQR(x)$	$\tilde{x}$	$IQR(x)$	$\tilde{x}$	$IQR(x)$
NSGA-II	0.96	0.09	0.89	0.03	0.89	0.11	0.87	0.05	0.88	0.05
NSGA-II-ACO-1	0.93	0.06	0.89	0.04	0.85	0.05	0.89	0.08	0.84	0.08
NSGA-II-ACO-2	0.96	0.12	0.93	0.07	0.88	0.05	0.84	0.06	0.93	0.10
NSGA-II-LS	0.91	0.03	0.90	0.06	0.90	0.06	0.81	0.05	0.83	0.20
SPEA2	0.79	0.09	0.75	0.12	0.79	0.06	0.72	0.08	0.74	0.02
SPEA2-LS	0.80	0.15	0.80	0.10	0.83	0.12	0.77	0.07	0.78	0.04

Table F.28: Median and interquartile range of I_{ϵ} obtained by the optimisers for the Hahn problems

	Hahn-1		Hahn-2		Hahn-3		Hahn-4		Hahn-5	
	$\tilde{x}$	$IQR(x)$	$\tilde{x}$	$IQR(x)$	$\tilde{x}$	$IQR(x)$	$\tilde{x}$	$IQR(x)$	$\tilde{x}$	$IQR(x)$
NSGA-II	0.84	0.09	0.92	0.07	0.91	0.07	0.87	0.02	0.90	0.05
NSGA-II-ACO-1	0.92	0.06	0.93	0.02	0.90	0.01	0.87	0.03	0.90	0.03
NSGA-II-ACO-2	0.90	0.07	0.83	0.08	0.93	0.06	0.97	0.08	0.94	0.15
NSGA-II-LS	0.88	0.04	0.92	0.13	0.96	0.04	0.91	0.07	0.84	0.05
SPEA2	0.83	0.05	0.87	0.06	0.92	0.10	0.88	0.04	0.85	0.05
SPEA2-LS	0.78	0.22	0.86	0.04	0.83	0.08	0.90	0.06	0.85	0.02

Table F.29: Median and interquartile range of I_{Δ} obtained by the optimisers for the Hahn problems

	Hahn-1		Hahn-2		Hahn-3		Hahn-4		Hahn-5	
	$\tilde{x}$	$IQR(x)$	$\tilde{x}$	$IQR(x)$	$\tilde{x}$	$IQR(x)$	$\tilde{x}$	$IQR(x)$	$\tilde{x}$	$IQR(x)$
NSGA-II	0.82	0.15	0.73	0.04	0.84	0.04	0.80	0.05	0.80	0.17
NSGA-II-ACO-1	0.80	0.09	0.81	0.15	0.87	0.13	0.80	0.04	0.81	0.05
NSGA-II-ACO-2	0.79	0.23	0.76	0.07	0.85	0.04	0.80	0.03	0.86	0.08
NSGA-II-LS	0.78	0.06	0.80	0.12	0.95	0.13	0.80	0.10	0.79	0.16
SPEA2	0.85	0.08	0.74	0.08	0.86	0.10	0.79	0.08	0.79	0.14
SPEA2-LS	0.85	0.07	0.80	0.04	0.91	0.10	0.78	0.11	0.80	0.03

Table F.30: Median and interquartile range of the computation time required by the optimisers for the Hahn problems

	Hahn-1 $\tilde{x} \pm IQR(x)$		Hahn-2 $\tilde{x} \pm IQR(x)$		Hahn-3 $\tilde{x} \pm IQR(x)$		Hahn-4 $\tilde{x} \pm IQR(x)$		Hahn-5 $\tilde{x} \pm IQR(x)$	
NSGA-II	0.03	0.00	0.03	0.00	0.03	0.00	0.02	0.00	0.03	0.00
NSGA-II-ACO-1	0.30	0.37	0.44	0.01	0.72	0.22	0.52	0.10	0.75	0.26
NSGA-II-ACO-2	0.84	0.50	0.60	0.18	0.43	0.34	0.59	0.12	0.63	0.34
NSGA-II-LS	0.19	0.00	0.20	0.00	0.20	0.00	0.14	0.01	0.21	0.00
SPEA2	0.18	0.10	0.18	0.11	0.19	0.11	0.13	0.08	0.17	0.12
SPEA2-LS	0.05	0.00	0.05	0.00	0.05	0.00	0.04	0.00	0.05	0.00

F.3.5 Problem Family: Jackson

Table F.31: Median and interquartile range of I_{HV} obtained by the optimisers for the Jackson problems

	Jackson-1 $\tilde{x} \pm IQR(x)$		Jackson-2 $\tilde{x} \pm IQR(x)$		Jackson-3 $\tilde{x} \pm IQR(x)$		Jackson-4 $\tilde{x} \pm IQR(x)$		Jackson-5 $\tilde{x} \pm IQR(x)$	
NSGA-II	1.00	0.00	1.00	0.00	1.00	0.00	0.98	0.01	0.99	0.00
NSGA-II-ACO-1	1.00	0.00	1.00	0.00	0.99	0.00	1.00	0.00	0.99	0.00
NSGA-II-ACO-2	1.00	0.00	1.00	0.00	0.99	0.00	1.00	0.00	1.00	0.01
NSGA-II-LS	1.00	0.00	1.00	0.00	0.99	0.00	1.00	0.00	0.99	0.00
SPEA2	1.00	0.00	1.00	0.00	1.00	0.00	1.00	0.01	1.00	0.00
SPEA2-LS	1.00	0.00	1.00	0.00	1.00	0.00	1.00	0.02	1.00	0.00

Table F.32: Median and interquartile range of I_{IGD} obtained by the optimisers for the Jackson problems

	Jackson-1 $\tilde{x} \pm IQR(x)$		Jackson-2 $\tilde{x} \pm IQR(x)$		Jackson-3 $\tilde{x} \pm IQR(x)$		Jackson-4 $\tilde{x} \pm IQR(x)$		Jackson-5 $\tilde{x} \pm IQR(x)$	
NSGA-II	0.75	0.06	0.97	0.54	0.47	0.25	0.64	0.37	0.32	0.21
NSGA-II-ACO-1	0.72	0.08	0.98	0.19	0.51	0.15	0.16	0.02	0.46	0.02
NSGA-II-ACO-2	0.72	0.04	0.26	0.71	0.53	0.23	0.15	0.03	0.41	0.04
NSGA-II-LS	0.71	0.09	0.97	0.55	0.53	0.42	0.62	0.01	0.46	0.01
SPEA2	0.68	0.03	0.98	0.02	0.40	0.16	0.62	0.42	0.23	0.38
SPEA2-LS	0.66	0.05	0.98	0.03	0.38	0.21	0.62	0.01	0.40	0.00

Table F.33: Median and interquartile range of I_ϵ obtained by the optimisers for the Jackson problems

	Jackson-1 $\tilde{x} \pm IQR(x)$		Jackson-2 $\tilde{x} \pm IQR(x)$		Jackson-3 $\tilde{x} \pm IQR(x)$		Jackson-4 $\tilde{x} \pm IQR(x)$		Jackson-5 $\tilde{x} \pm IQR(x)$	
NSGA-II	1.00	0.00	1.00	0.00	0.74	0.03	0.94	0.05	0.90	0.00
NSGA-II-ACO-1	1.00	0.00	1.00	0.00	0.77	0.08	0.85	0.10	0.90	0.00
NSGA-II-ACO-2	1.00	0.00	1.00	0.00	0.78	0.14	0.91	0.08	0.89	0.01
NSGA-II-LS	1.00	0.00	1.00	0.00	0.90	0.22	0.91	0.06	0.90	0.00
SPEA2	1.00	0.00	1.00	0.00	0.73	0.04	0.91	0.06	0.89	0.00
SPEA2-LS	1.00	0.00	1.00	0.00	0.73	0.03	0.91	0.04	0.89	0.00

Table F.34: Median and interquartile range of I_Δ obtained by the optimisers for the Jackson problems

	Jackson-1 $\tilde{x} \pm IQR(x)$		Jackson-2 $\tilde{x} \pm IQR(x)$		Jackson-3 $\tilde{x} \pm IQR(x)$		Jackson-4 $\tilde{x} \pm IQR(x)$		Jackson-5 $\tilde{x} \pm IQR(x)$	
NSGA-II	0.99	0.00	0.97	0.06	0.57	0.03	0.80	0.06	0.91	0.08
NSGA-II-ACO-1	0.99	0.00	0.96	0.02	0.62	0.19	0.78	0.03	0.91	0.08
NSGA-II-ACO-2	0.99	0.01	0.93	0.07	0.70	0.22	0.78	0.05	0.85	0.04
NSGA-II-LS	0.99	0.00	0.98	0.05	0.69	0.24	0.86	0.12	0.89	0.05
SPEA2	0.99	0.00	0.97	0.01	0.64	0.07	0.83	0.05	0.90	0.05
SPEA2-LS	0.99	0.01	0.97	0.02	0.70	0.24	0.88	0.01	0.85	0.06

Table F.35: Median and interquartile range of the computation time required by the optimisers for the Jackson problems

	Jackson-1 $\tilde{x} \pm IQR(x)$		Jackson-2 $\tilde{x} \pm IQR(x)$		Jackson-3 $\tilde{x} \pm IQR(x)$		Jackson-4 $\tilde{x} \pm IQR(x)$		Jackson-5 $\tilde{x} \pm IQR(x)$	
NSGA-II	0.99	0.00	0.97	0.06	0.57	0.03	0.80	0.06	0.91	0.08
NSGA-II-ACO-1	0.99	0.00	0.96	0.02	0.62	0.19	0.78	0.03	0.91	0.08
NSGA-II-ACO-2	0.99	0.01	0.93	0.07	0.70	0.22	0.78	0.05	0.85	0.04
NSGA-II-LS	0.99	0.00	0.98	0.05	0.69	0.24	0.86	0.12	0.89	0.05
SPEA2	0.99	0.00	0.97	0.01	0.64	0.07	0.83	0.05	0.90	0.05
SPEA2-LS	0.99	0.01	0.97	0.02	0.70	0.24	0.88	0.01	0.85	0.06

F.3.6 Problem Family: Lutz1

Table F.36: Median and interquartile range of I_{HV} obtained by the optimisers for the Lutz1 problems

	Lutz1-1 $\tilde{x} \pm IQR(x)$		Lutz1-2 $\tilde{x} \pm IQR(x)$		Lutz1-3 $\tilde{x} \pm IQR(x)$		Lutz1-4 $\tilde{x} \pm IQR(x)$		Lutz1-5 $\tilde{x} \pm IQR(x)$	
NSGA-II	0.99	0.00	0.99	0.00	0.99	0.00	0.99	0.00	0.98	0.01
NSGA-II-ACO-1	0.99	0.01	0.99	0.00	0.99	0.00	0.99	0.00	0.99	0.00
NSGA-II-ACO-2	0.99	0.00	1.00	0.00	0.99	0.00	0.99	0.00	0.99	0.00
NSGA-II-LS	0.99	0.00	0.99	0.00	0.99	0.00	0.99	0.00	0.98	0.01
SPEA2	0.99	0.00	1.00	0.00	0.99	0.00	0.99	0.00	0.99	0.00
SPEA2-LS	0.99	0.00	1.00	0.00	0.99	0.00	0.99	0.00	0.99	0.00

Table F.37: Median and interquartile range of I_{IGD} obtained by the optimisers for the Lutz1 problems

	Lutz1-1 $\tilde{x} \pm IQR(x)$		Lutz1-2 $\tilde{x} \pm IQR(x)$		Lutz1-3 $\tilde{x} \pm IQR(x)$		Lutz1-4 $\tilde{x} \pm IQR(x)$		Lutz1-5 $\tilde{x} \pm IQR(x)$	
NSGA-II	0.99	0.59	0.80	0.07	0.78	0.51	0.49	0.08	0.65	0.25
NSGA-II-ACO-1	0.57	0.82	0.91	0.08	0.36	0.25	0.43	0.07	0.34	0.24
NSGA-II-ACO-2	0.99	0.83	0.87	0.02	0.69	0.29	0.43	0.13	0.34	0.17
NSGA-II-LS	0.99	0.00	0.81	0.23	0.35	0.61	0.52	0.09	0.72	0.20
SPEA2	0.99	0.00	0.79	0.27	0.83	0.39	0.34	0.10	0.63	0.33
SPEA2-LS	0.99	0.82	0.73	0.12	0.25	0.08	0.33	0.11	0.22	0.17

Table F.38: Median and interquartile range of I_ϵ obtained by the optimisers for the Lutz1 problems

	Lutz1-1 $\tilde{x} \pm IQR(x)$		Lutz1-2 $\tilde{x} \pm IQR(x)$		Lutz1-3 $\tilde{x} \pm IQR(x)$		Lutz1-4 $\tilde{x} \pm IQR(x)$		Lutz1-5 $\tilde{x} \pm IQR(x)$	
NSGA-II	1.00	0.00	1.00	0.00	0.99	0.00	0.99	0.01	0.96	0.03
NSGA-II-ACO-1	1.00	0.00	1.00	0.00	0.99	0.00	0.99	0.00	0.92	0.02
NSGA-II-ACO-2	1.00	0.00	1.00	0.00	0.99	0.00	0.99	0.00	0.92	0.01
NSGA-II-LS	1.00	0.00	1.00	0.00	0.99	0.00	1.00	0.01	0.94	0.04
SPEA2	1.00	0.00	1.00	0.00	0.99	0.00	0.99	0.00	0.91	0.00
SPEA2-LS	1.00	0.00	1.00	0.00	0.99	0.00	0.99	0.00	0.91	0.01

Table F.39: Median and interquartile range of I_Δ obtained by the optimisers for the Lutz1 problems

	Lutz1-1 $\tilde{x} \pm IQR(x)$		Lutz1-2 $\tilde{x} \pm IQR(x)$		Lutz1-3 $\tilde{x} \pm IQR(x)$		Lutz1-4 $\tilde{x} \pm IQR(x)$		Lutz1-5 $\tilde{x} \pm IQR(x)$	
NSGA-II	0.70	0.07	0.93	0.07	0.88	0.07	0.88	0.04	0.88	0.08
NSGA-II-ACO-1	0.75	0.18	0.85	0.06	0.92	0.07	0.87	0.02	0.84	0.06
NSGA-II-ACO-2	0.82	0.02	0.84	0.04	0.90	0.06	0.92	0.05	0.83	0.13
NSGA-II-LS	0.70	0.01	0.87	0.08	0.79	0.16	0.87	0.01	0.79	0.15
SPEA2	0.79	0.20	0.94	0.06	0.90	0.06	0.92	0.03	0.81	0.03
SPEA2-LS	0.71	0.18	0.94	0.06	0.81	0.14	0.90	0.06	0.77	0.04

Table F.40: Median and interquartile range of the computation time required by the optimisers for the Lutz1 problems

	Lutz1-1		Lutz1-2		Lutz1-3		Lutz1-4		Lutz1-5	
	$\tilde{x}$	$IQR(x)$	$\tilde{x}$	$IQR(x)$	$\tilde{x}$	$IQR(x)$	$\tilde{x}$	$IQR(x)$	$\tilde{x}$	$IQR(x)$
NSGA-II	0.01	0.01	0.03	0.00	0.03	0.00	0.02	0.00	0.02	0.01
NSGA-II-ACO-1	0.54	0.10	0.69	0.09	0.60	0.08	0.46	0.38	0.47	0.31
NSGA-II-ACO-2	0.60	0.15	0.81	0.19	0.54	0.39	0.35	0.32	0.71	0.56
NSGA-II-LS	0.09	0.01	0.15	0.03	0.15	0.00	0.13	0.02	0.10	0.03
SPEA2	0.06	0.04	0.09	0.08	0.13	0.08	0.12	0.08	0.11	0.09
SPEA2-LS	0.02	0.01	0.04	0.00	0.04	0.00	0.04	0.00	0.05	0.00

F.3.7 Problem Family: Kilbrid

Table F.41: Median and interquartile range of I_{HV} obtained by the optimisers for the Kilbrid problems

	Kilbrid-1 $\tilde{x} \pm IQR(x)$		Kilbrid-2 $\tilde{x} \pm IQR(x)$		Kilbrid-3 $\tilde{x} \pm IQR(x)$		Kilbrid-4 $\tilde{x} \pm IQR(x)$		Kilbrid-5 $\tilde{x} \pm IQR(x)$	
NSGA-II	0.95	0.01	0.95	0.01	0.93	0.00	0.94	0.01	0.95	0.01
NSGA-II-ACO-1	0.96	0.01	0.95	0.01	0.93	0.01	0.94	0.00	0.96	0.00
NSGA-II-ACO-2	0.96	0.01	0.95	0.01	0.93	0.01	0.94	0.00	0.96	0.00
NSGA-II-LS	0.96	0.01	0.94	0.01	0.93	0.00	0.95	0.01	0.95	0.02
SPEA2	0.96	0.01	0.96	0.01	0.94	0.00	0.95	0.01	0.97	0.00
SPEA2-LS	0.97	0.01	0.96	0.01	0.95	0.02	0.95	0.01	0.97	0.01

Table F.42: Median and interquartile range of I_{IGD} obtained by the optimisers for the Kilbrid problems

	Kilbrid-1 $\tilde{x} \pm IQR(x)$		Kilbrid-2 $\tilde{x} \pm IQR(x)$		Kilbrid-3 $\tilde{x} \pm IQR(x)$		Kilbrid-4 $\tilde{x} \pm IQR(x)$		Kilbrid-5 $\tilde{x} \pm IQR(x)$	
NSGA-II	0.86	0.16	0.63	0.06	0.81	0.03	0.74	0.08	0.69	0.09
NSGA-II-ACO-1	0.87	0.06	0.65	0.05	0.78	0.12	0.83	0.05	0.71	0.17
NSGA-II-ACO-2	0.78	0.10	0.67	0.07	0.82	0.06	0.74	0.14	0.64	0.12
NSGA-II-LS	0.82	0.08	0.74	0.12	0.89	0.21	0.62	0.08	0.80	0.12
SPEA2	0.71	0.08	0.57	0.11	0.72	0.06	0.60	0.22	0.55	0.03
SPEA2-LS	0.71	0.06	0.54	0.10	0.69	0.09	0.65	0.13	0.56	0.05

Table F.43: Median and interquartile range of I_ϵ obtained by the optimisers for the Kilbrid problems

	Kilbrid-1 $\tilde{x} \pm IQR(x)$		Kilbrid-2 $\tilde{x} \pm IQR(x)$		Kilbrid-3 $\tilde{x} \pm IQR(x)$		Kilbrid-4 $\tilde{x} \pm IQR(x)$		Kilbrid-5 $\tilde{x} \pm IQR(x)$	
NSGA-II	0.99	0.00	0.99	0.00	0.98	0.01	0.98	0.02	0.98	0.01
NSGA-II-ACO-1	1.00	0.00	0.98	0.01	0.99	0.02	0.99	0.00	0.97	0.01
NSGA-II-ACO-2	1.00	0.00	0.98	0.00	0.98	0.02	0.99	0.01	0.97	0.01
NSGA-II-LS	0.99	0.00	0.99	0.00	0.97	0.01	0.97	0.01	0.99	0.02
SPEA2	0.99	0.00	0.98	0.00	0.96	0.01	0.97	0.01	0.97	0.00
SPEA2-LS	0.99	0.00	0.98	0.00	0.97	0.02	0.96	0.01	0.97	0.01

Table F.44: Median and interquartile range of I_Δ obtained by the optimisers for the Kilbrid problems

	Kilbrid-1 $\tilde{x} \pm IQR(x)$		Kilbrid-2 $\tilde{x} \pm IQR(x)$		Kilbrid-3 $\tilde{x} \pm IQR(x)$		Kilbrid-4 $\tilde{x} \pm IQR(x)$		Kilbrid-5 $\tilde{x} \pm IQR(x)$	
NSGA-II	0.83	0.08	0.84	0.14	0.84	0.05	0.80	0.11	0.88	0.04
NSGA-II-ACO-1	0.82	0.04	0.73	0.08	0.77	0.13	0.79	0.08	0.83	0.05
NSGA-II-ACO-2	0.82	0.09	0.75	0.06	0.84	0.16	0.73	0.07	0.84	0.05
NSGA-II-LS	0.81	0.06	0.83	0.10	0.77	0.07	0.74	0.07	0.82	0.17
SPEA2-LS	0.77	0.12	0.77	0.07	0.79	0.05	0.74	0.08	0.90	0.05
SPEA2	0.77	0.08	0.83	0.13	0.75	0.13	0.70	0.09	0.82	0.12

Table F.45: Median and interquartile range of the computation time required by the optimisers for the Kilbrid problems

	Kilbrid-1				Kilbrid-2				Kilbrid-3	
	HV									
Algo	$HV_\vee$	$\bar{HV}$	HV_σ	$HV_\wedge$	$HV_\vee$	$\bar{HV}$	HV_σ	$HV_\wedge$		
NSGA-II	0.02	0.00	0.01	0.01	0.01	0.00	0.03	0.00	0.01	0.01
NSGA-II-ACO-1	0.46	0.17	0.41	0.21	0.28	0.13	0.81	0.10	0.21	0.09
NSGA-II-ACO-2	0.63	0.12	0.62	0.19	0.50	0.23	0.69	0.17	0.43	0.25
NSGA-II-LS	0.14	0.02	0.06	0.03	0.06	0.03	0.16	0.02	0.07	0.03
SPEA2	0.10	0.10	0.05	0.07	0.06	0.06	0.08	0.10	0.07	0.06
SPEA2-LS	0.04	0.00	0.02	0.01	0.01	0.01	0.04	0.02	0.02	0.01

F.3.8 Problem Family: Mitchell

Table F.46: Median and interquartile range of I_{HV} obtained by the optimisers for the Mitchell problems

	Roszieg-1 $\tilde{x} \pm IQR(x)$		Roszieg-2 $\tilde{x} \pm IQR(x)$		Roszieg-3 $\tilde{x} \pm IQR(x)$		Roszieg-4 $\tilde{x} \pm IQR(x)$	
NSGA-II	0.93	0.01	0.96	0.01	0.96	0.00	0.92	0.01
NSGA-II-ACO-1	0.94	0.02	0.95	0.01	0.96	0.00	0.92	0.00
NSGA-II-ACO-2	0.93	0.01	0.94	0.02	0.96	0.00	0.93	0.01
NSGA-II-LS	0.93	0.01	0.93	0.03	0.96	0.00	0.94	0.01
SPEA2	0.95	0.00	0.97	0.01	0.97	0.01	0.95	0.02
SPEA2-LS	0.95	0.01	0.96	0.02	0.97	0.01	0.94	0.02

Table F.47: Median and interquartile range of I_{IGD} obtained by the optimisers for the Mitchell problems

	Mitchell-1 $\tilde{x} \pm IQR(x)$		Mitchell-2 $\tilde{x} \pm IQR(x)$		Mitchell-3 $\tilde{x} \pm IQR(x)$		Mitchell-4 $\tilde{x} \pm IQR(x)$	
NSGA-II	0.78	0.11	0.66	0.13	0.81	0.10	0.64	0.06
NSGA-II-ACO-1	0.69	0.10	0.78	0.13	0.85	0.11	0.76	0.11
NSGA-II-ACO-2	0.74	0.03	0.62	0.14	0.83	0.14	0.84	0.31
NSGA-II-LS	0.77	0.02	0.86	0.13	0.81	0.25	0.61	0.18
SPEA2	0.52	0.02	0.70	0.36	0.68	0.06	0.59	0.20
SPEA2-LS	0.55	0.19	0.65	0.24	0.64	0.09	0.64	0.16

Table F.48: Median and interquartile range of I_ϵ obtained by the optimisers for the Mitchell problems

	Roszieg-1 $\tilde{x} \pm IQR(x)$		Roszieg-2 $\tilde{x} \pm IQR(x)$		Roszieg-3 $\tilde{x} \pm IQR(x)$		Roszieg-4 $\tilde{x} \pm IQR(x)$	
NSGA-II	0.97	0.03	0.99	0.01	0.99	0.01	0.99	0.00
NSGA-II-ACO-1	0.94	0.04	0.99	0.01	0.97	0.04	0.98	0.01
NSGA-II-ACO-2	0.95	0.02	0.99	0.01	0.99	0.04	1.00	0.01
NSGA-II-LS	0.95	0.01	0.99	0.01	0.99	0.01	0.98	0.01
SPEA2	0.94	0.02	0.98	0.01	0.96	0.03	0.98	0.01
SPEA2-LS	0.94	0.03	0.99	0.01	0.93	0.06	0.97	0.01

Table F.49: Median and interquartile range of I_Δ obtained by the optimisers for the Mitchell problems

	Mitchell-1 $\tilde{x} \pm IQR(x)$		Mitchell-2 $\tilde{x} \pm IQR(x)$		Mitchell-3 $\tilde{x} \pm IQR(x)$		Mitchell-4 $\tilde{x} \pm IQR(x)$	
NSGA-II	0.73	0.08	0.79	0.13	0.72	0.10	0.74	0.29
NSGA-II-ACO-1	0.74	0.09	0.81	0.07	0.75	0.02	0.82	0.12
NSGA-II-ACO-2	0.69	0.01	0.86	0.12	0.78	0.07	0.74	0.11
NSGA-II-LS	0.70	0.10	0.91	0.14	0.80	0.06	0.86	0.17
SPEA2	0.75	0.11	0.80	0.01	0.78	0.10	0.78	0.21
SPEA2-LS	0.79	0.15	0.80	0.08	0.77	0.06	0.86	0.15

Table F.50: Median and interquartile range of the computation time required by the optimisers for the Mitchell problems

	Mitchell-1 $\tilde{x} \pm IQR(x)$		Mitchell-2 $\tilde{x} \pm IQR(x)$		Mitchell-3 $\tilde{x} \pm IQR(x)$		Mitchell-4 $\tilde{x} \pm IQR(x)$	
NSGA-II	0.01	0.00	0.01	0.00	0.03	0.00	0.02	0.00
NSGA-II-ACO-1	0.37	0.07	0.25	0.07	0.46	0.14	0.68	0.28
NSGA-II-ACO-2	0.48	0.22	0.34	0.20	0.56	0.36	0.72	0.10
NSGA-II-LS	0.06	0.01	0.06	0.02	0.13	0.01	0.09	0.02
SPEA2	0.10	0.06	0.05	0.02	0.13	0.07	0.10	0.05
SPEA2-LS	0.03	0.01	0.02	0.01	0.05	0.00	0.04	0.00

F.3.9 Problem Family: Mukherje

Table F.51: Median and interquartile range of I_{HV} obtained by the optimisers for the Mukherje problems

	Mukherje-1 $\tilde{x} \pm IQR(x)$		Mukherje-2 $\tilde{x} \pm IQR(x)$		Mukherje-3 $\tilde{x} \pm IQR(x)$	
NSGA-II	0.94	0.01	0.95	0.01	0.94	0.01
NSGA-II-ACO-1	0.94	0.00	0.95	0.00	0.94	0.00
NSGA-II-ACO-2	0.95	0.01	0.95	0.01	0.94	0.01
NSGA-II-LS	0.95	0.01	0.95	0.00	0.94	0.00
SPEA2	0.96	0.01	0.96	0.01	0.95	0.01
SPEA2-LS	0.95	0.01	0.96	0.01	0.95	0.01

Table F.52: Median and interquartile range of I_{IGD} obtained by the optimisers for the Mukherje problems

	Mukherje-1 $\tilde{x} \pm IQR(x)$		Mukherje-2 $\tilde{x} \pm IQR(x)$		Mukherje-3 $\tilde{x} \pm IQR(x)$	
NSGA-II	0.73	0.11	0.80	0.12	0.90	0.09
NSGA-II-ACO-1	0.74	0.06	0.91	0.08	0.85	0.08
NSGA-II-ACO-2	0.76	0.04	0.82	0.02	0.87	0.10
NSGA-II-LS	0.73	0.02	0.84	0.06	0.89	0.05
SPEA2	0.62	0.16	0.82	0.09	0.79	0.10
SPEA2-LS	0.71	0.10	0.77	0.14	0.74	0.06

Table F.53: Median and interquartile range of I_{ϵ} obtained by the optimisers for the Mukherje problems

	Mukherje-1 $\tilde{x} \pm IQR(x)$		Mukherje-2 $\tilde{x} \pm IQR(x)$		Mukherje-3 $\tilde{x} \pm IQR(x)$	
NSGA-II	0.91	0.10	0.92	0.01	0.92	0.09
NSGA-II-ACO-1	0.93	0.09	0.90	0.02	0.93	0.08
NSGA-II-ACO-2	0.89	0.02	0.93	0.05	0.89	0.01
NSGA-II-LS	0.91	0.03	0.94	0.04	0.95	0.04
SPEA2	0.85	0.03	0.91	0.02	0.89	0.08
SPEA2-LS	0.90	0.05	0.88	0.07	0.86	0.07

Table F.54: Median and interquartile range of I_{Δ} obtained by the optimisers for the Mukherje problems

	Mukherje-1 $\tilde{x} \pm IQR(x)$		Mukherje-2 $\tilde{x} \pm IQR(x)$		Mukherje-3 $\tilde{x} \pm IQR(x)$	
NSGA-II	0.81	0.04	0.83	0.07	0.84	0.08
NSGA-II-ACO-1	0.89	0.04	0.88	0.07	0.83	0.05
NSGA-II-ACO-2	0.88	0.09	0.84	0.10	0.85	0.09
NSGA-II-LS	0.83	0.07	0.81	0.09	0.81	0.01
SPEA2	0.81	0.05	0.86	0.08	0.82	0.04
SPEA2-LS	0.83	0.06	0.89	0.07	0.87	0.08

Table F.55: Median and interquartile range of the computation time required by the optimisers for the Mukherje problems

	Mukherje-1 $\tilde{x} \pm IQR(x)$		Mukherje-2 $\tilde{x} \pm IQR(x)$		Mukherje-3 $\tilde{x} \pm IQR(x)$	
NSGA-II	0.03	0.00	0.03	0.00	0.02	0.00
NSGA-II-ACO-1	0.42	0.18	0.40	0.41	0.56	0.20
NSGA-II-ACO-2	0.73	0.18	0.67	0.43	0.72	0.43
NSGA-II-LS	0.17	0.00	0.19	0.00	0.16	0.00
SPEA2	0.04	0.00	0.05	0.00	0.04	0.00
SPEA2-LS	0.16	0.06	0.18	0.11	0.13	0.09

F.3.10 Problem Family: Roszieg

Table F.56: Median and interquartile range of I_{HV} obtained by the optimisers for the Roszieg problems

	Roszieg-1 $\tilde{x} \pm IQR(x)$		Roszieg-2 $\tilde{x} \pm IQR(x)$		Roszieg-3 $\tilde{x} \pm IQR(x)$		Roszieg-4 $\tilde{x} \pm IQR(x)$	
NSGA-II	0.99	0.00	0.98	0.00	0.95	0.01	0.99	0.00
NSGA-II-ACO-1	0.99	0.00	0.98	0.00	0.96	0.02	0.99	0.00
NSGA-II-ACO-2	0.99	0.00	0.98	0.01	0.95	0.00	0.99	0.00
NSGA-II-LS	0.98	0.00	0.97	0.00	0.95	0.01	0.99	0.00
SPEA2	0.99	0.00	0.98	0.00	0.96	0.00	1.00	0.00
SPEA2-LS	0.99	0.00	0.98	0.00	0.97	0.00	1.00	0.00

Table F.57: Median and interquartile range of I_{IGD} obtained by the optimisers for the Roszieg problems

	Roszieg-1 $\tilde{x} \pm IQR(x)$		Roszieg-2 $\tilde{x} \pm IQR(x)$		Roszieg-3 $\tilde{x} \pm IQR(x)$		Roszieg-4 $\tilde{x} \pm IQR(x)$	
NSGA-II	0.72	0.18	0.43	0.25	0.73	0.21	0.21	0.04
NSGA-II-ACO-1	0.82	0.10	0.53	0.31	0.80	0.17	0.59	0.80
NSGA-II-ACO-2	0.72	0.09	0.39	0.19	0.66	0.02	0.25	0.07
NSGA-II-LS	0.91	0.20	0.58	0.17	0.58	0.05	0.29	0.72
SPEA2	0.64	0.04	0.56	0.20	0.55	0.06	0.58	0.80
SPEA2-LS	0.63	0.05	0.52	0.02	0.48	0.12	0.97	0.77

Table F.58: Median and interquartile range of I_ϵ obtained by the optimisers for the Roszieg problems

	Roszieg-1 $\tilde{x} \pm IQR(x)$		Roszieg-2 $\tilde{x} \pm IQR(x)$		Roszieg-3 $\tilde{x} \pm IQR(x)$		Roszieg-4 $\tilde{x} \pm IQR(x)$	
NSGA-II	0.69	0.23	0.92	0.02	0.98	0.03	1.00	0.00
NSGA-II-ACO-1	0.68	0.10	0.93	0.06	0.97	0.03	1.00	0.00
NSGA-II-ACO-2	0.69	0.02	0.93	0.02	0.96	0.01	1.00	0.00
NSGA-II-LS	1.00	0.30	0.94	0.02	0.96	0.02	1.00	0.00
SPEA2	0.67	0.00	0.94	0.03	0.96	0.01	1.00	0.00
SPEA2-LS	0.67	0.01	0.94	0.01	0.94	0.01	0.99	0.01

Table F.59: Median and interquartile range of I_Δ obtained by the optimisers for the Roszieg problems

	Roszieg-1 $\tilde{x} \pm IQR(x)$		Roszieg-2 $\tilde{x} \pm IQR(x)$		Roszieg-3 $\tilde{x} \pm IQR(x)$		Roszieg-4 $\tilde{x} \pm IQR(x)$	
NSGA-II	0.92	0.04	0.85	0.08	0.80	0.07	0.60	0.01
NSGA-II-ACO-1	0.88	0.05	0.81	0.06	0.75	0.08	0.74	0.08
NSGA-II-ACO-2	0.92	0.11	0.85	0.05	0.77	0.09	0.99	0.26
NSGA-II-LS	0.93	0.02	0.87	0.07	0.92	0.19	0.74	0.16
SPEA2	0.87	0.03	0.85	0.05	0.76	0.11	0.66	0.14
SPEA2-LS	0.85	0.06	0.87	0.11	0.81	0.12	0.73	0.04

Table F.60: Median and interquartile range of the computation time required by the optimisers for the Roszieg problems

	Roszieg-1 $\tilde{x} \pm IQR(x)$		Roszieg-2 $\tilde{x} \pm IQR(x)$		Roszieg-3 $\tilde{x} \pm IQR(x)$		Roszieg-4 $\tilde{x} \pm IQR(x)$	
NSGA-II	0.03	0.00	0.02	0.00	0.02	0.00	0.01	0.00
NSGA-II-ACO-1	0.65	0.23	0.52	0.14	0.74	0.11	0.59	0.14
NSGA-II-ACO-2	0.70	0.29	0.75	0.27	0.40	0.46	0.29	0.16
NSGA-II-LS	0.12	0.01	0.12	0.01	0.10	0.03	0.05	0.01
SPEA2	0.13	0.07	0.08	0.07	0.08	0.05	0.05	0.03
SPEA2-LS	0.05	0.00	0.04	0.00	0.04	0.01	0.02	0.01

F.3.11 Problem Family: Sawyer

Table F.61: Median and interquartile range of I_{HV} obtained by the optimisers for the Sawyer problems

	Sawyer-1 $\tilde{x} \pm IQR(x)$		Sawyer-2 $\tilde{x} \pm IQR(x)$		Sawyer-3 $\tilde{x} \pm IQR(x)$		Sawyer-4 $\tilde{x} \pm IQR(x)$	
NSGA-II	0.97	0.01	0.98	0.01	0.98	0.01	0.98	0.01
NSGA-II-ACO-1	0.97	0.00	0.98	0.00	0.98	0.00	0.98	0.01
NSGA-II-ACO-2	0.97	0.01	0.99	0.00	0.98	0.00	0.98	0.01
NSGA-II-LS	0.97	0.01	0.98	0.00	0.98	0.00	0.97	0.01
SPEA2	0.97	0.00	0.99	0.00	0.98	0.00	0.98	0.00
SPEA2-LS	0.98	0.01	0.99	0.01	0.99	0.00	0.98	0.01

Table F.62: Median and interquartile range of I_{IGD} obtained by the optimisers for the Sawyer problems

	Sawyer-1 $\tilde{x} \pm IQR(x)$		Sawyer-2 $\tilde{x} \pm IQR(x)$		Sawyer-3 $\tilde{x} \pm IQR(x)$		Sawyer-4 $\tilde{x} \pm IQR(x)$	
NSGA-II	0.14	0.01	0.86	0.22	0.98	0.01	0.77	0.14
NSGA-II-ACO-1	0.15	0.01	0.76	0.15	0.73	0.50	0.80	0.09
NSGA-II-ACO-2	0.14	0.01	0.79	0.09	0.97	0.49	0.73	0.06
NSGA-II-LS	0.15	0.02	0.74	0.07	0.49	0.02	0.77	0.24
SPEA2	0.14	0.00	0.61	0.14	0.98	0.37	0.64	0.10
SPEA2-LS	0.13	0.01	0.70	0.10	0.97	0.49	0.66	0.07

Table F.63: Median and interquartile range of I_ϵ obtained by the optimisers for the Sawyer problems

	Sawyer-1 $\tilde{x} \pm IQR(x)$		Sawyer-2 $\tilde{x} \pm IQR(x)$		Sawyer-3 $\tilde{x} \pm IQR(x)$		Sawyer-4 $\tilde{x} \pm IQR(x)$	
NSGA-II	1.00	0.00	1.00	0.00	1.00	0.00	1.00	0.00
NSGA-II-ACO-1	1.00	0.00	1.00	0.00	1.00	0.00	1.00	0.00
NSGA-II-ACO-2	1.00	0.00	1.00	0.00	1.00	0.00	1.00	0.01
NSGA-II-LS	1.00	0.00	1.00	0.00	1.00	0.00	1.00	0.00
SPEA2	1.00	0.00	1.00	0.00	1.00	0.00	0.99	0.00
SPEA2-LS	1.00	0.00	1.00	0.00	1.00	0.00	0.99	0.00

Table F.64: Median and interquartile range of I_Δ obtained by the optimisers for the Sawyer problems

	Sawyer-1 $\tilde{x} \pm IQR(x)$		Sawyer-2 $\tilde{x} \pm IQR(x)$		Sawyer-3 $\tilde{x} \pm IQR(x)$		Sawyer-4 $\tilde{x} \pm IQR(x)$	
NSGA-II	0.95	0.10	0.76	0.19	0.85	0.06	0.74	0.04
NSGA-II-ACO-1	0.99	0.01	0.79	0.17	0.86	0.01	0.77	0.09
NSGA-II-ACO-2	0.91	0.13	0.75	0.12	0.91	0.07	0.79	0.18
NSGA-II-LS	0.98	0.08	0.73	0.09	0.85	0.07	0.83	0.10
SPEA2	0.99	0.05	0.72	0.13	0.83	0.02	0.84	0.10
SPEA2-LS	0.92	0.08	0.66	0.11	0.92	0.01	0.92	0.13

Table F.65: Median and interquartile range of the computation time required by the optimisers for the Sawyer problems

	Sawyer-1 $\tilde{x} \pm IQR(x)$		Sawyer-2 $\tilde{x} \pm IQR(x)$		Sawyer-3 $\tilde{x} \pm IQR(x)$		Sawyer-4 $\tilde{x} \pm IQR(x)$	
NSGA-II	0.02	0.01	0.01	0.01	0.03	0.00	0.02	0.00
NSGA-II-ACO-1	0.67	0.24	0.54	0.17	0.88	0.36	0.50	0.09
NSGA-II-ACO-2	0.53	0.19	0.47	0.24	0.73	0.25	0.77	0.21
NSGA-II-LS	0.08	0.02	0.11	0.00	0.18	0.00	0.12	0.05
SPEA2	0.08	0.04	0.07	0.06	0.16	0.11	0.11	0.07
SPEA2-LS	0.04	0.00	0.03	0.01	0.06	0.00	0.04	0.00

Bibliography

[1] B. Akay. Synchronous and asynchronous Pareto-based multi-objective Artificial Bee Colony algorithms. *Journal of Global Optimization*, 57(2):415–445, 2013.

[2] S. Akpinar and A. Baykasoğlu. Modeling and solving mixed-model assembly line balancing problem with setups. Part I: A mixed integer linear programming model. *Journal of Manufacturing Systems*, 33(1):177–187, 2014.

[3] S. Akpinar and A. Baykasoğlu. Modeling and solving mixed-model assembly line balancing problem with setups. Part II: A multiple colony hybrid bees algorithm. *Journal of Manufacturing Systems*, 33(4):445–461, oct 2014.

[4] S. Akpinar and G. Mirac Bayhan. A hybrid genetic algorithm for mixed model assembly line balancing problem with parallel workstations and zoning constraints. *Engineering Applications of Artificial Intelligence*, 24(3):449–457, 2011.

[5] S. Akpinar, G. Mirac Bayhan, and A. Baykasoglu. Hybridizing ant colony optimization via genetic algorithm for mixed-model assembly line balancing problem with sequence dependent setup times between tasks. *Applied Soft Computing*, 13(1):574–589, jan 2013.

[6] F. Altiparmak, B. Dengiz, and A. A. Bulgak. Buffer allocation and performance modeling in asynchronous assembly system operations: An artificial neural network metamodeling approach. *Applied Soft Computing Journal*, 7(3):946–956, 2007.

[7] J. Alvarez-Benitez and R. Everson. A MOPSO algorithm based exclusively on pareto dominance concepts. In *Evolutionary Multi-Criterion Optimization*, volume 3410, pages 459–473. Springer Berlin Heidelberg, 2005.

[8] M. Amen. An exact method for cost-oriented assembly line balancing. *International Journal of Production Economics*, 64(1-3):187–195, 2000.

[9] M. Amiri and A. Mohtashami. Buffer allocation in unreliable production lines based on design of experiments, simulation, and genetic algorithm. *International Journal of Advanced Manufacturing Technology*, 62(1-4):371–383, 2012.

[10] C. Andrés, C. Miralles, and R. Pastor. Balancing and scheduling tasks in assembly lines with sequence-dependent setup times. *European Journal of Operational Research*, 187(3):1212–1223, 2008.

[11] D. Angus and C. Woodward. Multiple objective ant colony optimisation, mar 2009.

[12] J. Antony. Design of Experiments and its Role Within Six Sigma. In *Design of Experiments for Engineers and Scientists*, pages 201–208. Elsevier, 2014.

[13] K. Ağpak and H. Gökçen. Assembly line balancing: Two resource constrained cases. *International Journal of Production Economics*, 96(1):129–140, apr 2005.

[14] K. Ağpak and H. Gökçen. A chance-constrained approach to stochastic line balancing problem. *European Journal of Operational Research*, 180(3):1098–1115, aug 2007.

[15] A. L. Arcus. a Computer Method of Sequencing Operations for Assembly Lines. *International Journal of Production Research*, 4(4):259–277, jan 1965.

[16] J. S. Arora. Jan A. Snyman, Practical Mathematical Optimization: An introduction to basic optimization theory and classical and new gradient-based algorithms. *Structural and Multidisciplinary Optimization*, 31(3):249–249, mar 2006.

[17] Y. Asiedu and P. Gu. Product life cycle cost analysis: state of the art review. *International Journal of Production Research*, 36(4):883–908, apr 1998.

[18] A. Aziz. Modeling and Performance Evaluation of a Series-parallel Flow Line System with Finite Buffers. *Information Systems and Operational Research*, 48(2):103–120, 2010.

[19] T. Back. Selective pressure in evolutionary algorithms: a characterization of selection mechanisms. In *Proceedings of the First IEEE Conference on Evolutionary Computation. IEEE World Congress on Computational Intelligence*, volume 5, pages 57–62. IEEE, 1994.

[20] U. Bahalke, A. Yolmeh, and K. Shahanaghi. Meta-heuristics to solve single-machine scheduling problem with sequence-dependent setup time and deteriorating jobs. *International Journal of Advanced Manufacturing Technology*, 50(5-8):749–759, 2010.

[21] K. R. Baker and D. Trietsch. *Principles of Sequencing and Scheduling*. John Wiley & Sons, Inc., Hoboken, NJ, USA, mar 2009.

[22] J. Balakrishnan, C. H. Cheng, K. C. Ho, and K. K. Yang. The application of single-pass heuristics for U-lines. *Journal of Manufacturing Systems*, 28(1):28–40, 2009.

[23] J. C. Bansal, P. K. Singh, M. Saraswat, A. Verma, S. S. Jadon, and A. Abraham. Inertia Weight strategies in Particle Swarm Optimization. In *2011 Third World Congress on Nature and Biologically Inspired Computing*, pages 633–640. IEEE, oct 2011.

[24] B. Barán and M. Schaerer. A Multiobjective Ant Colony System for Vehicle Routing Problem with Time Windows. *Proceedings of the 21st IASTED International Conference on Applied Informatics*, pages 97–102, 2003.

[25] J. F. Bard. Assembly line balancing with parallel workstations and dead time. *International Journal of Production Research*, 27(6):1005–1018, 1989.

[26] J. J. Bartholdi. Balancing two-sided assembly lines: a case study. *International Journal of Production Research*, 31(10):2447–2461, oct 1993.

[27] J. A. Barton, D. M. Love, and G. D. Taylor. Design determines 70% of cost? A review of implications for design evaluation. *Journal of Engineering Design*, 12(1):47–58, 2001.

[28] T. Bartz-Beielstein. *Experimental Research in Evolutionary Computation: The New Experimentalism*. Springer, 2006.

[29] O. Battaïa and A. Dolgui. Reduction approaches for a generalized line balancing problem. *Computers & Operations Research*, 39(10):2337–2345, 2012.

[30] O. Battaïa and A. Dolgui. A taxonomy of line balancing problems and their solution approaches. *International Journal of Production Economics*, 142(2):259–277, apr 2013.

[31] D. Battini, X. Delorme, A. Dolgui, A. Persona, and F. Sgarbossa. Ergonomics in assembly line balancing based on energy expenditure: a multi-objective model. *International Journal of Production Research*, 7543(October):1–22, 2015.

[32] D. Battini, A. Persona, and A. Regattieri. Buffer size design linked to reliability performance: A simulative study. *Computers & Industrial Engineering*, 56(4):1633–1641, 2009.

[33] J. Bautista, R. Alfaro-Pozo, and C. Batalla-García. GRASP approach to a min-max problem of ergonomic risk in restricted assembly lines. In *Lecture Notes in Computer Science (including subseries Lecture Notes in Artificial Intelligence and Lecture Notes in Bioinformatics)*, volume 9422, pages 278–288. Springer Verlag, 2015.

[34] J. Bautista, C. Batalla, and R. Alfaro. Incorporating Ergonomics Factors into the TSALBP. In *IFIP Advances in Information and Communication Technology*, volume 397, pages 413–420. Springer, 2013.

[35] J. Bautista, C. Batalla, R. Alfaro, and A. Cano. Extended models for TSALBP with ergonomic risk constraints. *IFAC Proceedings Volumes*, 46(9):839–844, 2013.

[36] J. Bautista and J. Pereira. Ant algorithms for a time and space constrained assembly line balancing problem. *European Journal of Operational Research*, 177(3):2016–2032, mar 2007.

[37] J. Bautista and J. Pereira. Procedures for the Time and Space constrained Assembly Line Balancing Problem. *European Journal of Operational Research*, 212(3):473–481, aug 2011.

[38] I. Baybars. Survey of exact algorithms for the simple assembly line balancing problem. *Management Science*, 32(8):909–932, 1986.

[39] A. Baykasoğlu and T. Dereli. Simple and U-type Assembly Line Balancing by Using an Ant Colony Based Algorithm. *Mathematical and Computational Applications*, 14(3):1–12, apr 2009.

[40] A. Baykasoğlu, T. Dereli, and I. Sabuncu. An ant colony algorithm for solving budget constrained and unconstrained dynamic facility layout problems. *Omega*, 34(4):385–396, aug 2006.

[41] C. Becker and A. Scholl. A survey on problems and methods in generalized assembly line balancing. *European Journal of Operational Research*, 168(3):694–715, feb 2006.

[42] J. Bekker. Multi-objective buffer space allocation with the cross-entropy method. *International Journal of Simulation Modelling*, 12(1):50–61, 2013.

[43] D. Ben-Arieh and L. Qian. Activity-based cost management for design and development stage. *International Journal of Production Economics*, 83(2):169–183, 2003.

[44] A. Bernard, J. Daaboul, F. Laroche, and C. Da Cunha. Mass Customisation as a Competitive Factor for Sustainability. In *Enabling Manufacturing Competitiveness and Economic Sustainability*, pages 18–25. Springer Berlin Heidelberg, Berlin, Heidelberg, 2012.

[45] N. Beume. S-Metric calculation by considering dominated hypervolume as Klee's measure problem. *Evolutionary computation*, 17(4):477–492, dec 2009.

[46] L. Bianchi, M. Dorigo, L. M. Gambardella, and W. J. Gutjahr. A survey on metaheuristics for stochastic combinatorial optimization. *Natural Computing*, 8(2):239–287, 2009.

[47] C. Blum and C. Miralles. On solving the assembly line worker assignment and balancing problem via beam search. In *Computers & Operations Research*, volume 38, pages 328–339. Elsevier, 2011.

[48] L. Borba and M. Ritt. A heuristic and a branch-and-bound algorithm for the Assembly Line Worker Assignment and Balancing Problem. *Computers & Operations Research*, 45:87–96, may 2014.

[49] I. Boussaïd, J. Lepagnot, and P. Siarry. A survey on optimization metaheuristics. *Information Sciences*, 237(February):82–117, 2013.

[50] N. Boysen, M. Fliedner, and A. Scholl. A classification of assembly line balancing problems. *European Journal of Operational Research*, 183(2):674–693, dec 2007.

[51] N. Boysen, M. Fliedner, and A. Scholl. Assembly line balancing: Which model to use when? *International Journal of Production Economics*, 111(2):509–528, 2008.

[52] N. Boysen, M. Fliedner, and A. Scholl. Assembly line balancing: Joint precedence graphs under high product variety. *IIE Transactions*, 41(3):183–193, jan 2009.

[53] W. J. Braun. *Beitrag zur Festlegung der Arbeitsteilung in manuellen Montagesystemen*. PhD thesis, Universität Karlsruhe, 1995.

[54] K. Bringmann and T. Friedrich. Approximation quality of the hypervolume indicator. *Artificial Intelligence*, 195:265–290, 2013.

[55] J. Bukchin, E. M. Dar-El, and J. Rubinovitz. Mixed model assembly line design in a make-to-order environment. *Computers & Industrial Engineering*, 41(4):405–421, 2002.

[56] J. Bukchin and J. Rubinovitz. A weighted approach for assembly line design with station paralleling and equipment selection. *IIE Transactions*, 35(1):73–85, jan 2003.

[57] J. Bukchin and M. Tzur. Design of flexible assembly line to minimize equipment cost. *IIE Transactions*, 32(7):585–598, 2000.

[58] Y. Bukchin and I. Rabinowitch. A branch-and-bound based solution approach for the mixed-model assembly line-balancing problem for minimizing stations and task duplication costs. *European Journal of Operational Research*, 174(1):492–508, 2006.

[59] H.-J. Bullinger and D. Ammer. *Systematische Montageplanung: Handbuch für die Praxis*. Hanser, München, 1986.

[60] K. B.zandin. *MOST Work Measurement system*. Industrial Engineering: A Series of Reference Books and Textboo. Taylor & Francis, 2003.

[61] B. Cakir, F. Altiparmak, and B. Dengiz. Multi-objective optimization of a stochastic assembly line balancing: A hybrid simulated annealing algorithm. *Computers & Industrial Engineering*, 60(3):376–384, apr 2011.

[62] L. Capacho. *ASALBP : the Alternative Subgraphs Assembly Line Balancing Problem . Formalization and Resolution Procedures Liliana Capacho Betancourt*. PhD thesis, Technical University of Catalonia, 2007.

[63] L. Capacho and R. Pastor. The ASALB Problem with Processing Alternatives Involving Different Tasks: Definition, Formalization and Resolution. *Computational Science and Its Applications-ICCSA*, 3982:554–563, 2006.

[64] L. Capacho and R. Pastor. ASALBP: the alternative subgraphs assembly line balancing problem. *International Journal of Production Research*, 46(November 2013):3503–3516, jul 2008.

[65] L. Capacho, R. Pastor, A. Dolgui, and O. Guschinskaya. An evaluation of constructive heuristic methods for solving the alternative subgraphs assembly line balancing problem. In *Journal of Heuristics*, volume 15, pages 109–132, 2009.

[66] L. Capacho, R. Pastor, O. Guschinskaya, and A. Dolgui. Heuristic Methods to Solve the Alternative Subgraphs Assembly Line Balancing Problem. In *2006 IEEE International Conference on Automation Science and Engineering*, pages 501–506. IEEE, 2006.

[67] M. Caramia and P. Dell'Olmo. *Multi-objective Management in Freight Logistics*. Springer London, London, 2008.

[68] K. Chandrasekaran, K. b. Ramani, R. Sriram, I. Horváth, A. Bernard, R. Harik, and W. Gao. The evolution, challenges, and future of knowledge representation in product design systems. *CAD Computer Aided Design*, 45(2):204–228, 2013.

[69] K. Chandrasekaran and S. P. Simon. Multi-objective scheduling problem: Hybrid approach using fuzzy assisted cuckoo search algorithm. *Swarm and Evolutionary Computation*, 5:1–16, aug 2012.

[70] A. Charnes, W. W. Cooper, and R. O. Ferguson. Optimal estimation of executive compensation by linear programming. *Management Science*, 1(2):138–151, 1955.

[71] A. V. Chechkin, R. Metzler, J. Klafter, and V. Y. Gonchar. Introduction to the Theory of Lévy Flights. In *Anomalous Transport*, volume 1, pages 129–162. Wiley-VCH Verlag GmbH & Co. KGaA, Weinheim, Germany, 1980.

[72] H. Chehade, L. Amodeo, and F. Yalaoui. Ant Colony Optimization For Multiobjective Buffers Sizing Problems. In *Ant Colony Optimization - Methods and Applications*, number Mi. InTech, feb 2011.

[73] H. Chehade, F. Yalaoui, L. Amodeo, and F. Dugardin. Buffers sizing in assembly lines using a Lorenz multiobjective ant colony optimization algorithm. In *International Conference on Machine and Web Intelligence*, pages 283–287, 2010.

[74] G. Chen. Real-time analysis and control of serial production lines for energy efficient manufacturing. *ProQuest Dissertations and Theses*, page 150, 2014.

[75] J. C. Chen, C.-C. Chen, L.-H. Su, H.-B. Wu, and C.-J. Sun. Assembly line balancing in garment industry. *Expert Systems with Applications*, 39(11):10073–10081, sep 2012.

[76] W.-C. Chiang, T. L. Urban, and X. Xu. A bi-objective metaheuristic approach to unpaced synchronous production line-balancing problems. *International Journal of Production Research*, 50(1):293–306, 2012.

[77] M. Chica, J. Bautista, Ó. Cordón, and S. Damas. A multiobjective model and evolutionary algorithms for robust time and space assembly line balancing under uncertain demand. *Omega*, 58:55–68, 2016.

[78] M. Chica, Ó. Cordón, and S. Damas. An advanced multiobjective genetic algorithm design for the time and space assembly line balancing problem. *Computers & Industrial Engineering*, 61(1):103–117, aug 2011.

[79] M. Chica, Ó. Cordón, and S. Damas. Tackling the 1/3 variant of the time and space assembly line balancing problem by means of a multiobjective genetic algorithm. *2011 IEEE Congress of Evolutionary Computation*, pages 1367–1374, 2011.

[80] M. Chica, Ó. Cordón, S. Damas, and J. Bautista. A multiobjective GRASP for the 1/3 variant of the time and space assembly line balancing problem. In *Lecture Notes in Computer Science (including subseries Lecture Notes in Artificial Intelligence and Lecture Notes in Bioinformatics)*, volume 6098 LNAI, pages 656–665, 2010.

[81] M. Chica, Ó. Cordón, S. Damas, and J. Bautista. Multiobjective constructive heuristics for the 1/3 variant of the time and space assembly line balancing problem: ACO and random greedy search. *Information Sciences*, 180(18):3465–3487, 2010.

[82] M. Chica, Ó. Cordón, S. Damas, and J. Bautista. A new diversity induction mechanism for a multi-objective ant colony algorithm to solve a real-world time and space assembly line balancing problem. *Memetic Computing*, 3(1):15–24, 2011.

[83] M. Chica, Ó. Cordón, S. Damas, and J. Bautista. Including different kinds of preferences in a multi-objective ant algorithm for time and space assembly line balancing on different Nissan scenarios. *Expert Systems with Applications*, 38(1):709–720, jan 2011.

[84] B. K. Choi and D. Kang. *Modeling and Simulation of Discrete-Event Systems*. Wiley, 2013.

[85] M. Christmansson, A.-C. Falck, J. Amprazis, M. Forsman, L. Rasmusson, and R. Kadefors. Modified method time measurements for ergonomic planning of production systems in the manufacturing industry. *International Journal of Production Research*, 38(17):4051–4059, nov 2000.

[86] P. Chutima and P. Chimklai. Multi-objective two-sided mixed-model assembly line balancing using particle swarm optimisation with negative knowledge. *Computers & Industrial Engineering*, 62(1):39–55, feb 2012.

[87] C. A. Coello Coello, L. Jain, and X. Wu. Recent Trends in Evolutionary Multiobjective Optimization. In *Evolutionary Multiobjective Optimization*, pages 7–32. Springer, 2005.

[88] C. A. Coello Coello, G. B. Lamont, and D. A. V. Veldhuizen. *Evolutionary Algorithms for Solving Multi-Objective Problems*. Genetic and Evolutionary Computation Series. Springer US, Boston, MA, 2007.

[89] C. A. Coello Coello, G. T. Pulido, and E. M. Montes. Current and Future Research Trends in Evolutionary Multiobjective Optimization. In *Information Processing with Evolutionary Algorithms*, pages 213–231. Springer-Verlag, London, 2005.

[90] C. A. Coello Coello and M. Reyes-Sierra. A Study of the Parallelization of a Coevolutionary Multi-objective Evolutionary Algorithm. In *Proceedings of the Third Mexican International Conference on Artificial Intelligence (MICAI'2004)*, pages 688–697, 2004.

[91] C. A. Coello Coello and M. Reyes-Sierra. Multi-Objective Particle Swarm Optimizers: A Survey of the State-of-the-Art. *International Journal of Computational Intelligence Research*, 2(3):287–308, 2006.

[92] M. Colledani, M. Ekvall, T. Lundholm, P. Moriggi, A. Polato, and T. Tolio. Analytical methods to support continuous improvements at Scania. *International Journal of Production Research*, 48(7):1913–1945, apr 2010.

[93] A. Corominas, L. Ferrer, and R. Pastor. Assembly line balancing: general resource-constrained case. *International Journal of Production Research*, 49(12):3527–3542, 2011.

[94] A. Costa, A. Alfieri, A. Matta, and S. Fichera. A parallel tabu search for solving the primal buffer allocation problem in serial production systems. *Computers & Operations Research*, 64:97–112, dec 2015.

[95] M. K. Coughlin and M. J. Scott. An Activity-Based Costing Method to Support Market-Driven Top-Down Product Family Design. In *Volume 3A: 39th Design Automation Conference*, volume 3 A, page V03AT03A026. ASME, aug 2013.

[96] F. R. B. Cruz, T. Van Woensel, and J. M. Smith. Buffer and throughput trade-offs in M/G/1/K queueing networks: A bi-criteria approach. *International Journal of Production Economics*, 125(2):224–234, 2010.

[97] Z. Cui and X. Gu. An improved discrete artificial bee colony algorithm to minimize the makespan on hybrid flow shop problems. *Neurocomputing*, 148:248–259, 2015.

[98] J. Daaboul, C. Da Cunha, A. Bernard, and F. Laroche. Design for mass customization: Product variety vs. process variety. *CIRP Annals - Manufacturing Technology*, 60(1):169–174, 2011.

[99] S. Daoud, H. Chehade, F. Yalaoui, and L. Amodeo. Solving a robotic assembly line balancing problem using efficient hybrid methods. *Journal of Heuristics*, 20(3):235–259, 2014.

[100] S. Daoud, F. Yalaoui, L. Amodeo, H. Chehade, and P. Duperray. An adaptive harmony search algorithm to solve a robotic assembly line balancing problem. *10th International Industrial Simulation Conference 2012, ISC 2012*, pages 193–199, 2012.

[101] L. Davis. Handbook of Genetic Algorithms. *Computer*, pages 1–6, 1991.

[102] H. de Garis. Introduction to Evolutionary Computing. *Evolutionary Computation*, 12(2):269–271, jun 2004.

[103] K. Deb. *Multi-Objective Optimization Using Evolutionary Algorithms*. John Wiley & sons, LTD, 2001.

[104] K. Deb. Multi-objective Optimisation Using Evolutionary Algorithms: An Introduction. In L. Wang, A. H. C. Ng, and K. Deb, editors, *Multi-objective Evolutionary Optimisation for Product Design and Manufacturing*, pages 3–34. Springer London, London, 2011.

[105] K. Deb, A. Pratap, S. Agarwal, and T. Meyarivan. A fast and elitist multiobjective genetic algorithm: NSGA-II. *IEEE Transactions on Evolutionary Computation*, 6(2):182–197, apr 2002.

[106] L. Demir, S. Tunali, and D. T. Eliiyi. An adaptive tabu search approach for buffer allocation problem in unreliable non-homogenous production lines. *Computers & Operations Research*, 39(7):1477–1486, 2012.

[107] L. Demir, S. Tunali, and D. T. Eliiyi. The state of the art on buffer allocation problem: A comprehensive survey, 2014.

[108] L. Demir, S. Tunali, D. T. Eliiyi, and A. Løkketangen. Two approaches for solving the buffer allocation problem in unreliable production lines. *Computers & Operations Research*, 40(10):2556–2563, oct 2013.

[109] L. Demir, S. Tunali, and A. Løkketangen. A tabu search approach for buffer allocation in production lines with unreliable machines. *Engineering Optimization*, 43(2):213–231, feb 2011.

[110] J. Derrac, S. García, D. Molina, and F. Herrera. A practical tutorial on the use of nonparametric statistical tests as a methodology for comparing evolutionary and swarm intelligence algorithms. *Swarm and Evolutionary Computation*, 1(1):3–18, 2011.

[111] M. Despeisse, M. R. Oates, and P. D. Ball. Sustainable manufacturing tactics and cross-functional factory modelling. *Journal of Cleaner Production*, 42:31–41, 2013.

[112] Deutsches Institut für Normung. DIN 8580: Fertigungsverfahren – Begriffe, Einteilung. Technical report, Beuth, Berlin, 2003.

[113] Deutsches Institut für Normung. *Grundsätze der Ergonomie für die Gestaltung von Arbeitssystemen (DIN EN ISO 6385:2004)*. Beuth, 2004.

[114] G. Di Gironimo, C. Di Martino, A. Lanzotti, A. Marzano, and G. Russo. Improving MTM-UAS to predetermine automotive maintenance times. *International Journal on Interactive Design and Manufacturing*, 6(4):265–273, 2012.

[115] A. Dolgui, A. Eremeev, A. Kolokolov, and V. Sigaev. A Genetic Algorithm for the Allocation of Buffer Storage Capacities in a Production Line with Unreliable Machines. *Journal of Mathematical Modelling and Algorithms*, 1(2):89–104, 2002.

[116] A. Dolgui, A. Eremeev, M. Y. Kovalyov, and V. Sigaev. Complexity of Buffer Capacity Allocation Problems for Production Lines with Unreliable Machines. *Journal of Mathematical Modelling and Algorithms*, 12(2):155–165, 2013.

[117] A. Dolgui, A. V. Eremeev, and V. Sigaev. HBBA: Hybrid algorithm for buffer allocation in tandem production lines. *Journal of Intelligent Manufacturing*, 18(3):411–420, 2007.

[118] A. Dolgui, N. Guschinsky, and G. Levin. Enhanced mixed integer programming model for a transfer line design problem. *Computers & Industrial Engineering*, 62(2):570–578, mar 2012.

[119] G. Dong and W. W. Guo. A Cooperative Ant Colony System and Genetic Algorithm for TSPs. In *Lecture Notes in Computer Science (including subseries Lecture Notes in Artificial Intelligence and Lecture Notes in Bioinformatics)*, volume 6145 LNCS, pages 597–604. Springer Berlin Heidelberg, 2010.

[120] M. Dorigo and L. M. Gambardella. Ant colony system: A cooperative learning approach to the traveling salesman problem. *IEEE Transactions on Evolutionary Computation*, 1(1):53–66, 1997.

[121] M. Dorigo, V. Maniezzo, and A. Colorni. The ant systems: optimization by a colony of cooperative agents. *IEEE Transactions on Man, Machine and Cybernetics-Part B*, 26(1):1–13, 1996.

[122] F. Dugardin, F. Yalaoui, and L. Amodeo. New multi-objective method to solve reentrant hybrid flow shop scheduling problem. *European Journal of Operational Research*, 203(1):22–31, may 2010.

[123] J.-D. Duh and D. G. Brown. Knowledge-informed Pareto simulated annealing for multiobjective spatial allocation. *Computers Environment and Urban Systems*, 31(3):253–281, 2007.

[124] R. C. Eberhart and J. Kennedy. A new optimizer using particle swarm theory. In *Proceedings of the sixth international symposium on micro machine and human science*, volume 1, pages 39–43, 1995.

[125] M. Ehrgott, X. Gandibleux, and A. Przybylski. Exact Methods for Multi-Objective Combinatorial Optimisation. In *Multiple Criteria Decision Analysis*, pages 817–850. Springer, 2016.

[126] G. Eichfelder. *Adaptive Scalarization Methods in Multiobjective Optimization*. Vector Optimization. Springer Berlin Heidelberg, Berlin, Heidelberg, 2008.

[127] G. Eichfelder. Scalarizations for adaptively solving multi-objective optimization problems. *Computational Optimization and Applications*, 44(2):249–273, 2009.

[128] Y. R. Elhaddad. Combined Simulated Annealing and Genetic Algorithm to Solve Optimization Problems. *International Journal of Computer, Electrical, Automation, Control and Information Engineering*, 6(8):1047–1049, 2012.

[129] P. Eliseo, R. Aguirre, P. F. Pérez, M. D. Guadalupe, and C. Ortiz. Multi-Objective Optimization Using Bat Algorithm to Solve Multiprocessor Scheduling and Workload Allocation Problem. *Computer Science*, 2(2):41–51, 2015.

[130] E. Erel and S. C. Sarin. A survey of the assembly line balancing procedures. *Production Planning & Control*, 9(5):414–434, jan 1998.

[131] S. Eskilander. *Design for automatic assembly*. PhD thesis, Royal Institute of Technology, 2001.

[132] R. Esmaeilbeigi, B. Naderi, and P. Charkhgard. The type E simple assembly line balancing problem: A mixed integer linear programming formulation. *Computers & Operations Research*, 64:168–177, 2015.

[133] G. R. Esmaeilian, S. Sulaiman, N. Ismail, M. Hamedi, and M. M. H. M. Ahmad. A tabu search approach for mixed-model parallel assembly line balancing problem (type II). *International Journal of Industrial and Systems Engineering*, 8(4):407, 2011.

[134] P. Fattahi, A. Roshani, and A. Roshani. A mathematical model and ant colony algorithm for multi-manned assembly line balancing problem. *The International Journal of Advanced Manufacturing Technology*, 53(1-4):363–378, mar 2011.

[135] C. Feldmann. *Eine Methode für die integrierte rechnergestützte Montageplanung*, volume 104 of *Forschungsberichte iwb*. Springer Berlin Heidelberg, Berlin, Heidelberg, 1997.

[136] F. Field, R. E. Kirchain, and R. Roth. Process cost modeling: Strategic engineering and economic evaluation of materials technologies. *Journal of Metals*, 59(10):21–32, oct 2007.

[137] B. Finel, A. Dolgui, and F. Vernadat. A random search and backtracking procedure for transfer line balancing. *International Journal of Computer Integrated Manufacturing*, 21(4):376–387, 2008.

[138] S. K. Fixson. Product architecture assessment: A tool to link product, process, and supply chain design decisions. *Journal of Operations Management*, 23(3-4):345–369, 2005.

[139] M. Fleischer. The Measure of Pareto Optima. Applications to Multi-objective Metaheuristics. *Lecture Notes in Computer Science*, 2632:519–533, 2003.

[140] C. M. Fonseca and P. J. Fleming. An Overview of Evolutionary Algorithms in Multiobjective Optimization. *Evolutionary Computation*, 3(1):1–16, mar 1995.

[141] C. M. Fonseca and P. J. Fleming. On the performance assessment and comparison of stochastic multiobjective optimizers. *Lecture Notes in Computer Science*, 1141(Emo):584—-593, 1996.

[142] C. M. Fonseca, V. Grunert da Fonseca, and L. Paquete. Exploring the Performance of Stochastic Multiobjective Optimisers with the Second-Order Attainment Function. In *Evolutionary Multi-Criterion Optimization*, pages 250–264, Guanajuato, M{é}xico, 2005.

[143] M. J. French. *Conceptual Design for Engineers*. Springer London, London, 1999.

[144] M. Friedman. The Use of Ranks to Avoid the Assumption of Normality Implicit in the Analysis of Variance. *Journal of the American Statistical Association*, 32(200):675–701, dec 1937.

[145] M. Friedman. A comparison of alternative tests of significance for the problem of m rankings. *The Annals of Mathematical Statistics*, 11(1):86–92, 1940.

[146] E. R. H. Fuchs, F. R. Field, R. Roth, and R. E. Kirchain. Strategic materials selection in the automobile body: Economic opportunities for polymer composite design. *Composites Science and Technology*, 68(9):1989–2002, 2008.

[147] G. M. Gaddis and M. L. Gaddis. Introduction to biostatistics: Part 4, statistical inference techniques in hypothesis testing. *Annals of Emergency Medicine*, 19(7):820–825, 1990.

[148] R. Gamberini, A. Grassi, and B. Rimini. A new multi-objective heuristic algorithm for solving the stochastic assembly line re-balancing problem. *International Journal of Production Economics*, 102(2):226–243, apr 2006.

[149] C. García-Martínez, Ó. Cordón, and F. Herrera. A taxonomy and an empirical analysis of multiple objective ant colony optimization algorithms for the bi-criteria TSP. *European Journal of Operational Research*, 180(1):116–148, jul 2007.

[150] A. Garcia-Najera and J. A. Bullinaria. An improved multi-objective evolutionary algorithm for the vehicle routing problem with time windows. *Computers & Operations Research*, 38(1):287–300, jan 2011.

[151] S. B. Gershwin. An efficient decomposition method for the approximate evaluation of tandem queues with finite storage space and blocking. *Operational Research*, 35(2):291–305, 1987.

[152] S. B. Gershwin. *Manufacturing Systems Engineering*. Prentice Hall, 1994.

[153] A. Gherboudj, A. Layeb, and S. Chikhi. Solving 0-1 knapsack problems by a discrete binary version of cuckoo search algorithm. *International Journal of Bio-Inspired Computation*, 4(4):229, 2012.

[154] S. Ghosh and R. J. Gagnon. A comprehensive literature review and analysis of the design, balancing and scheduling of assembly systems. *International Journal of Production Research*, 27(4):637–670, 1989.

[155] F. Glover. Tabu Search—Part I. *ORSA Journal on Computing*, 1(3):190–206, aug 1989.

[156] F. Glover. Tabu Search—Part II. *ORSA Journal on Computing*, 4(1):4–32, 1990.

[157] D.-w. Gong, Y. Zhang, and J.-h. Zhang. Multi-objective Particle Swarm Optimization Based on. In *Advances in Intelligent Computing*, pages 571–580. Springer, 2005.

[158] M. K. Govil and M. C. Fu. Queueing theory in manufacturing: A survey. *Journal of Manufacturing Systems*, 18(3):214–240, 1999.

[159] S. Graves and D. Whitney. A mathematical programming procedure for equipment selection and system evaluation in programmable assembly. In *1979 18th IEEE Conference on Decision and Control including the Symposium on Adaptive Processes*, volume 2, pages 531–536. IEEE, dec 1979.

[160] S. C. Graves and B. W. Lamar. Integer programming procedure for assembly system design problems. *Operations Research*, 31(3):522–545, 1983.

[161] S. C. Graves and C. H. Redfield. Equipment selection and task assignment for multiproduct assembly system design. *International Journal of Flexible Manufacturing Systems*, 1(1):31–50, 1988.

[162] R. Grob and H. Haffner. *Planungsleitlinien Arbeitsstrukturierung: Systematik zur Gestaltung von Arbeitssystemen*. Siemens-Aktienges, Berlin, 1982.

[163] P. Guo, W. Cheng, and Y. Wang. Parallel machine scheduling with step-deteriorating jobs and setup times by a hybrid discrete cuckoo search algorithm. *Engineering Optimization*, 47(11):1564–1585, nov 2015.

[164] Z. X. Guo, W. K. Wong, S. Y. S. Leung, J. T. Fan, and S. F. Chan. A genetic-algorithm-based optimization model for solving the flexible assembly line balancing problem with work sharing and workstation revisiting. *IEEE Transactions on Systems, Man and Cybernetics Part C: Applications and Reviews*, 38(2):218–228, 2008.

[165] O. Guschinskaya and A. Dolgui. Comparison of exact and heuristic methods for a transfer line balancing problem. *International Journal of Production Economics*, 120(2):276–286, 2009.

[166] O. Guschinskaya, E. Gurevsky, A. Dolgui, and A. V. Eremeev. Metaheuristic approaches for the design of machining lines. *The International Journal of Advanced Manufacturing Technology*, 55(1-4):11–22, jul 2011.

[167] Y. Y. Haimes, L. S. Lasdon, and D. A. Wismer. On a Bicriterion Formulation of the Problems of Integrated System Identification and System Optimization. *IEEE Journals & Magazines*, 47(July):296–297, 1971.

[168] N. Hamta, S. Fatemi Ghomi, M. Hakimi-Asiabar, and P. Hooshangi Tabrizi. Multi-objective assembly line balancing problem with bounded processing times, learning effect, and sequence-dependent setup times. In *2011 IEEE International Conference on Industrial Engineering and Engineering Management*, pages 768–772. IEEE, dec 2011.

[169] N. Hamta, S. Fatemi Ghomi, F. Jolai, and M. Akbarpour Shirazi. A hybrid PSO algorithm for a multi-objective assembly line balancing problem with flexible operation times, sequence-dependent setup times and learning effect. *International Journal of Production Economics*, 141(1):99–111, 2013.

[170] N. Hamta, S. Fatemi Ghomi, F. Jolai, and U. Bahalke. Bi-criteria assembly line balancing by considering flexible operation times. *Applied Mathematical Modelling*, 35(12):5592–5608, dec 2011.

[171] O. Hasançebi and S. Carbas. Bat inspired algorithm for discrete size optimization of steel frames. *Advances in Engineering Software*, 67:173–185, jan 2014.

[172] E. A. Hassan, A. I. Hafez, A. E. Hassanien, and A. A. Fahmy. A Discrete Bat Algorithm for the Community Detection Problem. In E. Onieva, I. Santos, E. Osaba, H. Quintián, and E. Corchado, editors, *Lecture Notes in Artificial Intelligence (Subseries of Lecture Notes in Computer Science)*, volume 9121 of *Lecture Notes in Computer Science*, pages 188–199. Springer International Publishing, Cham, 2015.

[173] Ö. Hazır, X. Delorme, and A. Dolgui. A Survey on Cost and Profit Oriented Assembly Line Balancing. *IFAC Proceedings Volumes*, 47(3):6159–6167, aug 2014.

[174] Ö. Hazır, X. Delorme, and A. Dolgui. A review of cost and profit oriented line design and balancing problems and solution approaches. *Annual Reviews in Control*, 40(October 2015):14–24, 2015.

[175] Ö. Hazır and A. Dolgui. Assembly line balancing under uncertainty: Robust optimization models and exact solution method. *Computers & Industrial Engineering*, 65(2):261–267, 2013.

[176] M. Held, R. M. Karp, and R. Shareshian. Assembly-Line Balancing-Dynamic Programming with Precedence Constraints. *Operations Research*, 11(3):442–459, jun 1963.

[177] J. M. Henrioud, L. Relange, and C. Perrard. Assembly sequences, assembly constraints, precedence graphs. In *Proceedings of the IEEE International Symposium on Assembly and Task Planning*, volume 2003-January, pages 90–95. IEEE, 2003.

[178] G. Hernandez, C. C. Seepersad, and F. Mistree. *Engineering Design*. Springer London, London, 2007.

[179] F. Herrera, M. Lozano, and A. M. Sánchez. A taxonomy for the crossover operator for real-coded genetic algorithms: An experimental study. *International Journal of Intelligent Systems*, 18(3):309–338, 2003.

[180] T. R. Hoffmann. Eureka. A hybrid system for assembly line balancing. *Management Science*, 38(1):39–47, 1992.

[181] P. Holtewert, J. Oesterle, A. Bruns, and H. Wirtz. Detaillierungsgrad von Simulationsmodellen. *Productivity Management*, 19(5):31ff, 2014.

[182] S. J. Hu, J. Ko, L. Weyand, H. A. Elmaraghy, T. K. Lien, Y. Koren, H. Bley, G. Chryssolouris, N. Nasr, and M. Shpitalni. Assembly system design and operations for product variety. *CIRP Annals - Manufacturing Technology*, 60(2):715–733, 2011.

[183] W. Huang and T. W. S. Chow. Network topological optimization for packet routing using multi-objective simulated annealing method. *Physica A: Statistical Mechanics and its Applications*, 389(4):871–880, 2010.

[184] J. Huidong and W. Man-Leung. Adaptive diversity maintenance and convergence guarantee in multiobjective evolutionary algorithms. In *The 2003 Congress on Evolutionary Computation, 2003. CEC '03.*, volume 4, pages 2498–2505. IEEE, 2003.

[185] K. F. Hyde. Recognising deductive processes in qualitative research. *Qualitative Market Research: An International Journal*, 3(2):82–90, jun 2000.

[186] S. Iredi, D. Merkle, and M. Middendorf. *Evolutionary Multi-Criterion Optimization*, volume 1993 of *Lecture Notes in Computer Science*. Springer Berlin Heidelberg, Berlin, Heidelberg, 2001.

[187] H. Ishibuchi, N. Akedo, and Y. Nojima. Behavior of Multiobjective Evolutionary Algorithms on Many-Objective Knapsack Problems. *IEEE Transactions on Evolutionary Computation*, 19(2):264–283, 2015.

[188] J. R. Jackson. A Computing Procedure for a Line Balancing Problem, 1956.

[189] T. Jansen. Evolutionary Algorithms and Other Randomized Search Heuristics. In *Analyzing Evolutionary Algorithms*, Natural Computing Series, pages 7–29. Springer Berlin Heidelberg, Berlin, Heidelberg, 2013.

[190] F. Jarrahi and W. Abdul-Kader. Performance evaluation of a multi-product production line: An approximation method. *Applied Mathematical Modelling*, 39(13):3619–3636, jul 2015.

[191] S. Jiang, Y. S. Ong, J. Zhang, and L. Feng. Consistencies and contradictions of performance metrics in multiobjective optimization. *IEEE Transactions on Cybernetics*, 44(12):2391–2404, 2014.

[192] J. Jiao, L. Zhang, and S. Pokharel. Process platform planning for variety coordination from design to production in mass customization manufacturing. *IEEE Transactions on Engineering Management*, 54(1):112–129, 2007.

[193] J. Jiao, L. Zhang, and K. Prasanna. Process variety modeling for process configuration in mass customization: An approach based on object-oriented Petri nets with changeable structures. *International Journal of Flexible Manufacturing Systems*, 16(4 SPEC. ISS.):335–361, 2004.

[194] C. F. Johnson. Deductive versus inductive reasoning: A closer look at economics. *Social Science Journal*, 33(3):287–299, 1996.

[195] M. D. Johnson and R. E. Kirchain. Quantifying the effects of product family decisions on material selection: A process-based costing approach. *International Journal of Production Economics*, 120(2):653–668, 2009.

[196] R. V. Johnson. Optimally Balancing Large Assembly Lines with "Fable". *Management Science*, 34(2):240–253, feb 1988.

[197] L. Jourdan, M. Basseur, and E. G. Talbi. Hybridizing exact methods and metaheuristics: A taxonomy. *European Journal of Operational Research*, 199(3):620–629, 2009.

[198] J. Kallrath and A. Schreieck. Discrete optimisation and real world problems. In *High-performance computing and networking*, pages 351–359. Springer, 1995.

[199] J.-G. Kang and D. Brissaud. A Product Lifecycle Costing System with Imprecise End-of-Life Data. In *Advances in Life Cycle Engineering for Sustainable Manufacturing Businesses*, pages 467–472. Springer London, London, 2007.

[200] Y. Kara, C. Özgüven, N. Y. Seçme, and C.-T. Chang. Multi-objective approaches to balance mixed-model assembly lines for model mixes having precedence conflicts and duplicable common tasks. *The International Journal of Advanced Manufacturing Technology*, 52(5-8):725–737, feb 2011.

[201] Y. Kara, C. Özgüven, N. Yalçın, and Y. Atasagun. Balancing straight and U-shaped assembly lines with resource dependent task times. *International Journal of Production Research*, 49(21):6387–6405, 2011.

[202] D. Karaboga and B. Basturk. A powerful and efficient algorithm for numerical function optimization: Artificial bee colony (ABC) algorithm. *Journal of Global Optimization*, 39(3):459–471, 2007.

[203] G. Karafotias, M. Hoogendoorn, and A. E. Eiben. Parameter Control in Evolutionary Algorithms: Trends and Challenges. *IEEE Transactions on Evolutionary Computation*, 19(2):167–187, 2015.

[204] Y. Kaya, M. Uyar, and R. Tekin. A Novel Crossover Operator for Genetic Algorithms: Ring Crossover. *Computing Research Repository*, page 5, may 2011.

[205] A. Kazemi and A. Sedighi. A Cost-oriented Model for Multi-manned Assembly Line Balancing Problem. *Journal of Optimization in Industrial Engineering*, 13:13–25, 2013.

[206] S. M. Kazemi, R. Ghodsi, M. Rabbani, and R. Tavakkoli-Moghaddam. A novel two-stage genetic algorithm for a mixed-model U-line balancing problem with duplicated tasks. *International Journal of Advanced Manufacturing Technology*, 55(9-12):1111–1122, 2011.

[207] C. Ke and J. M. Henrioud. Systematic generation of assembly precedence graphs. In *Proceedings of the 1994 IEEE International Conference on Robotics and Automation*, pages 1476–1482. IEEE Comput. Soc. Press, 1994.

[208] T. Kellegöz and B. Toklu. An efficient branch and bound algorithm for assembly line balancing problems with parallel multi-manned workstations. *Computers & Operations Research*, 39(12):3344–3360, 2012.

[209] R. Keller, T. Alink, C. Pfeifer, C. M. Eckert, P. J. Clarkson, and A. Albers. Product models in design: a combined use of two models to assess change risks. In *16th International Conference on Engineering Design, ICED 2007*, volume DS 42, pages 673–674, 2007.

[210] M. Khouja, D. E. Booth, M. Suh, and J. K. Mahaney. Statistical procedures for task assignment and robot selection in assembly cells. *International Journal of Computer Integrated Manufacturing*, 13(2):95–106, jan 2000.

[211] O. Kilincci. A Petri net-based heuristic for simple assembly line balancing problem of type 2. *International Journal of Advanced Manufacturing Technology*, 46(1-4):329–338, 2010.

[212] O. Kilincci. Firing sequences backward algorithm for simple assembly line balancing problem of type 1. *Computers & Industrial Engineering*, 60(4):830–839, may 2011.

[213] D. Kim, J. Park, and I. Moon. Integrated Mixed-Model Assembly Line Balancing with Unskilled Temporary Workers. In S. Umeda, M. Nakano, H. Mizuyama, H. Hibino, D. Kiritsis, and G. von Cieminski, editors, *IFIP Advances in Information and Communication Technology*, volume 460 of *IFIP Advances in Information and Communication Technology*, pages 324–331. Springer International Publishing, Cham, 2015.

[214] H. Kim and S. Park. Strong cutting plane algorithm for the robotic assembly line balancing problem. *International Journal of Production Research*, 33(8):2311–2323, 1995.

[215] Y. K. Kim, Y. Kim, and Y. J. Kim. Two-sided assembly line balancing: A genetic algorithm approach. *Production Planning & Control*, 11(1):44–53, jan 2000.

[216] S. Kirkpatrick, C. D. Gelatt, M. P. Vecchi, C. Gelatt Jr, and M. P. Vecchi. Optimization by simulated annealing. *Science*, 220(4598):671–80, may 1983.

[217] H. Klindworth, C. Otto, and A. Scholl. On a learning precedence graph concept for the automotive industry. *European Journal of Operational Research*, 217(2):259–269, mar 2012.

[218] S. Klos and P. Trebuna. Using Computer Simulation Method to Improve Throughput of Production Systems by Buffers and Workers Allocation. *Management and Production Engineering Review*, 6(4):60–69, 2015.

[219] J. Knowles. A summary-attainment-surface plotting method for visualizing the performance of stochastic multiobjective optimizers. In *5th International Conference on Intelligent Systems Design and Applications (ISDA'05)*, volume 2005, pages 552–557. IEEE, 2005.

[220] Y. Koren. *The Global Manufacturing Revolution: Product-Process-Business Integration and Reconfigurable Systems*. Wiley, 2010.

[221] S. Y. Kose and O. Kilincci. Hybrid Simulated Annealing/Genetic Algorithm Approach To Buffer Allocation Problem In Unreliable Production Lines. In *Uncertainty Modeling in Knowledge Engineering and Decision Making*, volume 46, pages 981–986. World Scientific Publishing Company, oct 2012.

[222] M. M. Kostreva, W. Ogryczak, and A. Wierzbicki. Equitable aggregations and multiple criteria analysis. *European Journal of Operational Research*, 158(2):362–377, 2004.

[223] G. Kovács and K. M. Spens. Abductive reasoning in logistics research. *International Journal of Physical Distribution & Logistics Management*, 35(2):132–144, feb 2005.

[224] O. Kramer. Evolutionary self-adaptation: A survey of operators and strategy parameters. *Evolutionary Intelligence*, 3(2):51–65, 2010.

[225] J. Krause, J. Cordeiro, R. S. Parpinelli, and H. S. A. Lopes. A Survey of Swarm Algorithms Applied to Discrete Optimization Problems. *Swarm Intelligence and Bio-Inspired Computation*, pages 169–191, 2013.

[226] I. Kucukkoc and D. Z. Zhang. Mathematical model and agent based solution approach for the simultaneous balancing and sequencing of mixed-model parallel two-sided assembly lines. *International Journal of Production Economics*, 158(February 2015):314–333, 2014.

[227] I. Kucukkoc and D. Z. Zhang. Mixed-model Parallel Two-sided Assembly Line Balancing Problem: A Flexible Agent-based Ant Colony Optimization Approach. *Computers & Industrial Engineering*, 2016.

[228] A. Kumar. From mass customization to mass personalization: A strategic transformation. *International Journal of Flexible Manufacturing Systems*, 19(4):533–547, 2007.

[229] S. D. Lapierre and A. B. Ruiz. Balancing assembly lines: an industrial case study. *Journal of the Operational Research Society*, 55(6):589–597, 2004.

[230] M. Laumanns, L. Thiele, K. Deb, and E. Zitzler. Combining convergence and diversity in evolutionary multiobjective optimization. *Evolutionary computation*, 10(3):263–282, 2002.

[231] M. Laumanns, E. Zitzler, and L. Thiele. A unified model for multi-objective evolutionary algorithms with elitism. In *Proceedings of the 2000 Congress on Evolutionary Computation*, volume 1, pages 46–53. IEEE, 2000.

[232] A. Layer, E. Brinke, and F. Houten. Recent and future trends in cost estimation. *International Journal of Computer Integrated Manufacturing*, 15(6):499–510, 2002.

[233] K. Le and D. Landa-Silva. Obtaining better non-dominated sets using volume dominance. *2007 IEEE Congress on Evolutionary Computation*, D:3119–3126, 2007.

[234] K. Le, D. Landa-Silva, and H. Li. An Improved Version of Volume Dominance for Multi-Objective Optimisation. *Evolutionary Multi-Criterion Optimization*, 5467:231–245, 2009.

[235] D. Lei. Multi-objective production scheduling: A survey. *International Journal of Advanced Manufacturing Technology*, 43(9-10):925–938, 2009.

[236] D. Lei and X. Guo. Variable neighborhood search for the second type of two-sided assembly line balancing problem. *Computers & Operations Research*, 72:183–188, 2016.

[237] J. Lemesre, C. Dhaenens, and E. G. Talbi. Parallel partitioning method (PPM): A new exact method to solve bi-objective problems. *Computers & Operations Research*, 34(8):2450–2462, aug 2007.

[238] R. Levantesi, A. Matta, and T. Tolio. Performance evaluation of continuous production lines with machines having different processing times and multiple failure modes. *Performance Evaluation*, 51(2-4):247–268, 2003.

[239] G. Levitin, J. Rubinovitz, and B. Shnits. A genetic algorithm for robotic assembly line balancing. *European Journal of Operational Research*, 168(3):811–825, 2006.

[240] M. Lewis and N. Slack. *Operations Management: Critical Perspectives on Business and Management*. Number Bd. 2 in Critical perspectives on business and management. Routledge, 2003.

[241] J. Li, D. E. Blumenfeld, and J. M. Alden. Comparisons of two-machine line models in throughput analysis. *International Journal of Production Research*, 44(7):1375–1398, 2006.

[242] J. Li, D. E. Blumenfeld, N. Huang, and J. M. Alden. Throughput analysis of production systems: recent advances and future topics. *International Journal of Production Research*, 47(14):3823–3851, 2009.

[243] J. Li and S. M. Meerkov. *Production Systems Engineering*. Springer US, Boston, MA, 2009.

[244] L. Li, Y. Qian, Y. M. Yang, and K. Du. A fast algorithm for buffer allocation problem. *International Journal of Production Research*, 7543(December), 2015.

[245] X. Li, H. Chehade, F. Yalaoui, and L. Amodeo. Lorenz dominance based metaheuristic to solve a hybrid flowshop scheduling problem with sequence dependent setup times. In *2011 International Conference on Communications, Computing and Control Applications (CCCA)*, pages 1–6. IEEE, mar 2011.

[246] K. Lian, C. Zhang, L. Gao, and X. Shao. A modified colonial competitive algorithm for the mixed-model U-line balancing and sequencing problem. *International Journal of Production Research*, 50(18):5117–5131, 2012.

[247] L. Lin and M. Gen. Multiobjective Genetic Algorithm for Bicriteria Network Design Problems. In *Intelligent and Evolutionary Systems*, Decision Engineering, pages 141–161. Springer Berlin Heidelberg, Berlin, Heidelberg, 2008.

[248] B. Liu and P. Meng. Hybrid Algorithm Combining Ant Colony Algorithm with Genetic Algorithm for Continuous Domain. *2008 The 9th International Conference for Young Computer Scientists*, pages 1819–1824, 2008.

[249] S. B. Liu, K. M. Ng, and H. L. Ong. Branch-and-bound algorithms for simple assembly line balancing problem. *International Journal of Advanced Manufacturing Technology*, 36(1-2):169–177, 2008.

[250] Y.-F. Liu and S.-Y. Liu. A hybrid discrete artificial bee colony algorithm for permutation flowshop scheduling problem. *Applied Soft Computing*, 13(3):1459–1463, 2013.

[251] M. López-Ibáñez and T. Stützle. An experimental analysis of design choices of multi-objective ant colony optimization algorithms. *Swarm Intelligence*, 6(3):207–232, 2012.

[252] M. López-Ibáñez, T. Stützle, and L. Paquete. Graphical tools for the analysis of bi-objective optimization algorithms. *Proceedings of the 12th Annual conference on Genetic and evolutionary computation - GECCO '10*, page 1959, 2010.

[253] Q. Luo, Y. Zhou, J. Xie, M. Ma, and L. Li. Discrete Bat Algorithm for Optimal Problem of Permutation Flow Shop Scheduling. *The Scientific World Journal*, 2014:1–15, 2014.

[254] J. L. C. Macaskill. Production-Line Balances for Mixed-Model Lines. *Management Science*, 19(4-part-1):423–434, dec 1972.

[255] S. Mahdavi, M. E. Shiri, and S. Rahnamayan. Metaheuristics in large-scale global continues optimization: A survey. *Information Sciences*, 295(October):407–428, 2015.

[256] N. Manavizadeh, N. S. Hosseini, M. Rabbani, and F. Jolai. A Simulated Annealing algorithm for a mixed model assembly U-line balancing type-I problem considering human efficiency and Just-In-Time approach. *Computers & Industrial Engineering*, 64(2):669–685, 2013.

[257] N. Manavizadeh, M. Rabbani, D. Moshtaghi, and F. Jolai. Mixed-model assembly line balancing in the make-to-order and stochastic environment using multi-objective evolutionary algorithms. *Expert Systems with Applications*, 39(15):12026–12031, 2012.

[258] L. Marti, J. García, A. Berlanga, and J. M. Molina. An approach to stopping criteria for multi-objective optimization evolutionary algorithms: The MGBM criterion. In *2009 IEEE Congress on Evolutionary Computation*, pages 1263–1270. IEEE, may 2009.

[259] Y. Massim, F. Yalaoui, L. Amodeo, E. Chatelet, and A. Zeblah. Efficient combined immune-decomposition algorithm for optimal buffer allocation in production lines for throughput and profit maximization. *Computers & Operations Research*, 37(4):611–620, 2010.

[260] H. B. Maynard, G. J. Stegemerten, and J. L. Schwab. *Methods-Time Measurement*. Gauthier-Villard, 1948.

[261] T. McNamara, S. Shaaban, and S. Hudson. Simulation of unbalanced buffer allocation in unreliable unpaced production lines. *International Journal of Production Research*, 51(6):1922–1936, 2012.

[262] J. Mehnen and N. Henkenjohann. Systematic analyses of multi-objective evolutionary algorithms applied to real-world problems using statistical design of experiments. *Manufacturing Engineering*, pages 171–178, 2004.

[263] J. Melorose, R. Perroy, and S. Careas. Data Classification: Algorithms and Applications. In Intergovernmental Panel on Climate Change, editor, *Climate Change 2013 - The Physical Science Basis*, volume 1, pages 1–30. Cambridge University Press, Cambridge, 2015.

[264] Z. Meng and Q. Chen. Hybrid genetic-ant colony algorithm based job scheduling method research of arc welding robot. In *The 2010 IEEE International Conference on Information and Automation*, pages 718–722. IEEE, jun 2010.

[265] J. Miltenburg. The effect of breakdowns on U-shaped production lines. *International Journal of Production Research*, 38(2):353–364, jan 2000.

[266] J. Miltenburg. U-shaped production lines: A review of theory and practice. *International Journal of Production Economics*, 70(3):201–214, apr 2001.

[267] V. Minzu, A. Bratcu, and J. M. Henrioud. Construction of the precedence graphs equivalent to a given set of assembly sequences. In *Proceedings of the 1999 IEEE International Symposium on Assembly and Task Planning (ISATP'99)*, number July, pages 14–19. IEEE, 1999.

[268] C. Miralles, J. P. García-Sabater, C. Andrés, and M. Cardós. Branch and bound procedures for solving the Assembly Line Worker Assignment and Balancing Problem: Application to Sheltered Work centres for Disabled. *Discrete Applied Mathematics*, 156(3):352–367, feb 2008.

[269] A. Moghaddam, F. Yalaoui, and L. Amodeo. Lorenz versus Pareto Dominance in a Single Machine Scheduling Problem with Rejection. In R. H. C. Takahashi, K. Deb, E. F. Wanner, and S. Greco, editors, *Evolutionary multi-criterion optimization*, volume 6576 of *Lecture Notes in Computer Science*, pages 520–534. Springer, Berlin, 2011.

[270] A. Moghaddam, F. Yalaoui, and L. Amodeo. Efficient meta-heuristics based on various dominance criteria for a single-machine bi-criteria scheduling problem with rejection. *Journal of Manufacturing Systems*, 34(C):12–22, 2015.

[271] C. K. Mohan and K. G. Mehrotra. Reference set metrics for multi-objective algorithms. In *Lecture Notes in Computer Science (including subseries Lecture Notes in Artificial Intelligence and Lecture Notes in Bioinformatics)*, volume 7076 LNCS, pages 723–730. Springer, 2011.

[272] A. M. Mora, J. J. Merelo, J. L. J. Laredo, C. Millan, and J. Torrecillas. CHAC, A MOACO algorithm for computation of bi-criteria military unit path in the battlefield: Presentation and first results. *International Journal of Intelligent Systems*, 24(7):818–843, jul 2009.

[273] M. C. O. Moreira, M. Ritt, A. M. Costa, and A. A. Chaves. Simple heuristics for the assembly line worker assignment and balancing problem. *Journal of Heuristics*, 18(3):505–524, jun 2012.

[274] H. Mosadegh, M. Zandieh, and S. M. T. F. Ghomi. Simultaneous solving of balancing and sequencing problems with station-dependent assembly times for mixed-model assembly lines. *Applied Soft Computing Journal*, 12(4):1359–1370, 2012.

[275] S. Mostaghim and J. Teich. Strategies for finding good local guides in multi-objective particle swarm optimization (MOPSO). In *Proceedings of the 2003 IEEE Swarm Intelligence Symposium*, volume 2, pages 26–33. IEEE, 2013.

[276] M. M. Mulya Pambudy, S. P. Hadi, and H. R. Ali. Flower pollination algorithm for optimal control in multi-machine system with GUPFC. In *2014 6th International Conference on Information Technology and Electrical Engineering (ICITEE)*, pages 1–6. IEEE, oct 2014.

[277] Ö. Mutlu and E. Özgörmüş. A fuzzy assembly line balancing problem with physical workload constraints. *International Journal of Production Research*, 50(18):5281–5291, 2012.

[278] Ö. Mutlu, O. Polat, and A. A. Supciller. An iterative genetic algorithm for the assembly line worker assignment and balancing problem of type-II. *Computers & Operations Research*, 40(1):418–426, jan 2013.

[279] M. C. Nadeau, A. Kar, R. Roth, and R. E. Kirchain. A dynamic process-based cost modeling approach to understand learning effects in manufacturing. In *International Journal of Production Economics*, volume 128, pages 223–234. Elsevier, 2010.

[280] N. Nahas, M. Nourelfath, and D. Ait-Kadi. Selecting machines and buffers in unreliable series-parallel production lines. In *2006 International Conference on Service Systems and Service Management*, pages 190–196. IEEE, oct 2006.

[281] D. Nam and C. H. Park. Multiobjective Simulated Annealing: A Comparative Study to Evolutionary Algorithms. *International Journal of Fuzzy Systems*, 2(2):87–97, 2000.

[282] A. C. Nearchou. Balancing large assembly lines by a new heuristic based on differential evolution method. *The International Journal of Advanced Manufacturing Technology*, 34(9-10):1016–1029, sep 2007.

[283] A. Niazi, J. S. Dai, S. Balabani, and L. Seneviratne. Product Cost Estimation: Technique Classification and Methodology Review. *Journal of Manufacturing Science and Engineering*, 128(2):563, 2006.

[284] A. Nickabadi, M. M. Ebadzadeh, and R. Safabakhsh. A novel particle swarm optimization algorithm with adaptive inertia weight. *Applied Soft Computing Journal*, 11(4):3658–3670, 2011.

[285] G. Nicosia, D. Pacciarelli, and A. Pacifici. Optimally balancing assembly lines with different workstations. *Discrete Applied Mathematics*, 118(1-2):99–113, 2002.

[286] S. Y. Nof. Robot time and motion system provides means of evaluating alternate robot work methods. *Industrial Engineering*, (4):38–48, 1982.

[287] A. Ochoa-Zezzatti. *Handbook of Research on Military, Aeronautical, and Maritime Logistics and Operations*. Advances in Logistics, Operations, and Management Science. IGI Global, 2016.

[288] J. Oesterle and L. Amodel. Evaluation of the influence of dominance rules on multi-objective algorithms for the Assembly Line Balancing Problem and Equipment Selection Problem under consideration of Product Design Alternatives (In Review). *Engineering Optimization*, 2017.

[289] J. Oesterle and L. Amodeo. Efficient multi-objective optimization method for the mixed-model-line assembly line design problem. In *Procedia CIRP*, volume 17, pages 82–87, 2014.

[290] J. Oesterle and L. Amodeo. Efficient Multi-Objective Optimization Method for the Mixed-Model-Line Assembly Line Design Problem. In *IFORS*, 2014.

[291] J. Oesterle and L. Amodeo. Comparison of Multiobjective Algorithms for the Assembly Line Balancing and Design Problem. *IFAC Proceedings Volumes*, 49(12):313–318, 2016.

[292] J. Oesterle and L. Amodeo. Efficient multi-objective optimization methods for the assembly line design problem under consideration of product design alternatives and buffer sizing (in Review). *Engineering Optimization*, 2017.

[293] J. Oesterle, L. Amodeo, and F. Yalaoui. A comparative study of Multi-Objective Algorithms for the Assembly Line Balancing and Equipment Selection Problem under consideration of Product Design Alternatives (Accepted). *Journal of Intelligent Manufacturing*, 2017.

[294] J. Oesterle, T. Bauernhansl, and L. Amodeo. Hybrid Multi-objective Optimization Method for Solving Simultaneously the line Balancing, Equipment and Buffer Sizing Problems for Hybrid Assembly Systems. *Procedia CIRP*, 57:416–421, 2016.

[295] J. Oesterle, M. S. Maier, P. Holtewert, and M. Lickefett. Rechnergestützte Austaktung einer Mixed-Model Line. Der Weg zur optimalen Aus-taktung. *wt Werkstattstechnik online*, 103:679ff, 2014.

[296] D. Ogan and M. Azizoğlu. A branch and bound method for the line balancing problem in U-shaped assembly lines with equipment requirements. *Journal of Manufacturing Systems*, 36:46–54, 2015.

[297] T. Okabe, Yaochu Jin, and B. Sendhoff. A critical survey of performance indices for multi-objective optimisation. In *The 2003 Congress on Evolutionary Computation, 2003. CEC '03.*, volume 2, pages 878–885. IEEE, 2004.

[298] D. Ortiz-Boyer, C. Hervás-Martínez, and N. García-Pedrajas. CIXL2: A crossover operator for evolutionary algorithms based on population features. *Journal of Artificial Intelligence Research*, 24:1–48, 2005.

[299] E. Osaba, X.-S. Yang, F. Diaz, P. Lopez-Garcia, and R. Carballedo. An improved discrete bat algorithm for symmetric and asymmetric Traveling Salesman Problems. *Engineering Applications of Artificial Intelligence*, 48:59–71, 2016.

[300] A. Otto and A. Scholl. Incorporating ergonomic risks into assembly line balancing. *European Journal of Operational Research*, 212(2):277–286, 2011.

[301] C. Otto and A. Otto. Multiple-source learning precedence graph concept for the automotive industry. *European Journal of Operational Research*, 234(1):253–265, mar 2014.

[302] A. Ouaarab, B. Ahiod, and X.-S. Yang. Discrete cuckoo search algorithm for the travelling salesman problem. *Neural Computing and Applications*, 24(7-8):1659–1669, jun 2014.

[303] A. Ouaarab, B. Ahiod, X.-S. Yang, and M. Abbad. Discrete Cuckoo Search algorithm for job shop scheduling problem. In *2014 IEEE International Symposium on Intelligent Control (ISIC)*, pages 1872–1876. IEEE, oct 2014.

[304] Y. Ouazene, A. Yalaoui, F. Yalaoui, and H. Chehade. Non-linear Programming Method for Buffer Allocation in Unreliable Production Lines. In *Analytical and Stochastic Modeling Techniques and Applications*, pages 80–94. Springer, 2014.

[305] L. Ozbakir, A. Baykasoğlu, B. Gorkemli, and L. Gorkemli. Multiple-colony ant algorithm for parallel assembly line balancing problem. *Applied Soft Computing*, 11(3):3186–3198, 2011.

[306] L. Özbakır and P. Tapkan. Bee colony intelligence in zone constrained two-sided assembly line balancing problem. *Expert Systems with Applications*, 38(9):11947–11957, sep 2011.

[307] U. Özcan, T. Kellegöz, and B. Toklu. A genetic algorithm for the stochastic mixed-model U-line balancing and sequencing problem. *International Journal of Production Research*, 49(6):1605–1626, mar 2011.

[308] U. Özcan and B. Toklu. A tabu search algorithm for two-sided assembly line balancing. *The International Journal of Advanced Manufacturing Technology*, 43(7-8):822–829, aug 2009.

[309] M. Padrón, M. de los A. Irizarry, P. Resto, and H. P. Mejía. A methodology for cost-oriented assembly line balancing problems. *Journal of Manufacturing Technology Management*, 20(8):1147–1165, oct 2009.

[310] Q.-k. Pan, M. Fatih Tasgetiren, and Y.-c. Liang. A discrete particle swarm optimization algorithm for the no-wait flowshop scheduling problem. *Computers & Operations Research*, 35(9):2807–2839, sep 2008.

[311] Q.-K. Pan, M. F. Tasgetiren, P. N. Suganthan, and T. J. Chua. A discrete artificial bee colony algorithm for the lot-streaming flow shop scheduling problem. *Information Sciences*, 181(12):2455–2468, 2011.

[312] W. Pan, K. Li, M. Wang, J. Wang, and B. Jiang. Adaptive Randomness: A New Population Initialization Method. *Mathematical Problems in Engineering*, 2014:1–14, 2014.

[313] H. T. Papadopoulos and M. I. Vidalis. A heuristic algorithm for the buffer allocation in unreliable unbalanced production lines. *Computers & Industrial Engineering*, 41(3):261–277, 2001.

[314] V. Paramasivam and V. Senthil. Analysis and evaluation of product design through design aspects using digraph and matrix approach. *International Journal on Interactive Design and Manufacturing (IJIDeM)*, 3(1):13–23, feb 2009.

[315] K. E. Parsopoulos and M. N. Vrahatis. Multi-Objective Particles Swarm Optimization Approaches. *IGI Global*, pages 20–42, 2008.

[316] R. Pastor and L. Ferrer. An improved mathematical program to solve the simple assembly line balancing problem. *International Journal of Production Research*, 47(11):2943–2959, 2009.

[317] N. Pekin and M. Azizoğlu. Bi criteria flexible assembly line design problem with equipment decisions. *International Journal of Production Research*, 46(22):6323–6343, 2008.

[318] A. Pinnoi and W. E. Wilhelm. Assembly System Design: A Branch and Cut Approach. *Management Science*, 44(1):103–118, 1998.

[319] P. A. Pinto, D. G. Dannenbring, and B. M. Khumawala. A branch and bound algorithm for assembly line balancing with paralleling. *International Journal of Production Research*, 13(2):183–196, jan 1975.

[320] P. A. Pinto, D. G. Dannenbring, and B. M. Khumawala. Branch and bound and heuristic procedures for assembly line balancing with paralleling of stations. *International Journal of Production Research*, 19(5):565–576, sep 1981.

[321] P. A. Pinto, D. G. Dannenbring, and B. M. Khumawala. Assembly Line Balancing with Processing Alternatives: An Application. *Management Science*, 29(7):817–830, jul 1983.

[322] O. Polat, C. B. Kalayci, Ö. Mutlu, and S. M. Gupta. A two-phase variable neighbourhood search algorithm for assembly line worker assignment and balancing problem type-II: an industrial case study. *International Journal of Production Research*, 54(3):722–741, feb 2016.

[323] D. Pollard, S. Chuo, and B. Lee. Strategies For Mass Customization. *Journal of Business & Economics Research (JBER)*, 6(7):77–86, feb 2011.

[324] S. G. Ponnambalam, P. Aravindan, and G. M. Naidu. A comparative evaluation of assembly line balancing Heuristics. *The International Journal of Advanced Manufacturing Technology*, 15(8):577–586, 1999.

[325] K. Popovici and P. J. Mosterman. *Real-Time Simulation Technologies: Principles, Methodologies, and Applications*. Computational Analysis, Synthesis, and Design of Dynamic Systems. CRC Press, 2016.

[326] C. Potti, Subbaraj; Chinnasamy. Strength Pareto Evolutionary Algorithm based Multi-Objective Optimization for Shortest Path Routing Problem in Computer Networks. *Journal of Computer Science*, 7(1):17–26, jan 2011.

[327] P. Preux and E. G. Talbi. Towards hybrid evolutionary algorithms. *International Transactions in Operational Research*, 6(6):557–570, 1999.

[328] C. Qiu, C. Wang, and X. Zuo. A novel multi-objective particle swarm optimization with K -means based global best selection strategy. *International Journal of Computational Intelligence Systems*, 6(5):822–835, sep 2013.

[329] M. Rabbani, S. M. Kazemi, and N. Manavizadeh. Mixed model U-line balancing type-1 problem: A new approach. *Journal of Manufacturing Systems*, 31(2):131–138, 2012.

[330] M. Rabbani, M. Moghaddam, and N. Manavizadeh. Balancing of mixed-Model two-Sided assembly lines with multiple u-Shaped layout. *International Journal of Advanced Manufacturing Technology*, 59(9-12):1191–1210, 2012.

[331] M. Rabbani, Z. Mousavi, and H. Farrokhi-Asl. Multi-objective metaheuristics for solving a type II robotic mixed-model assembly line balancing problem. *Journal of Industrial and Production Engineering*, 1015(February):1–13, feb 2016.

[332] M. Rabbani, A. Ziaeifar, and N. Manavizadeh. Mixed-model assembly line balancing in assemble-to-order environment with considering express parallel line: problem definition and solution procedure. *International Journal of Computer Integrated Manufacturing*, 27(7):690–706, jul 2014.

[333] J. Rada-Vilela, M. Chica, Ó. Cordón, and S. Damas. A comparative study of Multi-Objective Ant Colony Optimization algorithms for the Time and Space Assembly Line Balancing Problem. *Applied Soft Computing*, 13(11):4370–4382, nov 2013.

[334] S. Rahnamayan, H. R. Tizhoosh, and M. M. Salama. A novel population initialization method for accelerating evolutionary algorithms. *Computers & Mathematics with Applications*, 53(10):1605–1614, may 2007.

[335] H. Rajabalipour Cheshmehgaz, H. Haron, F. Kazemipour, and M. I. Desa. Accumulated risk of body postures in assembly line balancing problem and modeling through a multi-criteria fuzzy-genetic algorithm. *Computers & Industrial Engineering*, 63(2):503–512, sep 2012.

[336] R. Ramezanian and A. Ezzatpanah. Modeling and solving multi-objective mixed-model assembly line balancing and worker assignment problem. *Computers & Industrial Engineering*, 87:74–80, 2015.

[337] B. Rekiek and A. Delchambre. Assembly Line Design: The Balancing of Mixed-Model Hybrid Assembly Lines with Genetic Algorithms. In *Assembly Automation*, volume 26, page 252. Springer, 2006.

[338] B. Rekiek, A. Delchambre, A. Dolgui, and A. Bratcu. Assembly Line Design: A Survey. *IFAC Proceedings Volumes*, 35(1):155–166, 2002.

[339] I. Ribeiro, P. Peças, and E. Henriques. Incorporating tool design into a comprehensive life cycle cost framework using the case of injection molding. *Journal of Cleaner Production*, 53:297–309, aug 2013.

[340] M. Ritt and A. M. Costa. Improved integer programming models for simple assembly line balancing and related problems, 2015.

[341] M. Ritt, A. M. Costa, and C. Miralles. The assembly line worker assignment and balancing problem with stochastic worker availability. *International Journal of Production Research*, 00(00):1–16, 2015.

[342] W. G. Rodenacker. *Methodisches Konstruieren*, volume 27 of *Konstruktionsbücher*. Springer Berlin Heidelberg, Berlin, Heidelberg, 1991.

[343] A. Roshani, P. Fattahi, A. Roshani, M. Salehi, and A. Roshani. Cost-oriented two-sided assembly line balancing problem: A simulated annealing approach. *International Journal of Computer Integrated Manufacturing*, 25(8):689–715, aug 2012.

[344] A. Roshani, A. Roshani, A. Roshani, M. Salehi, and A. Esfandyari. A simulated annealing algorithm for multi-manned assembly line balancing problem. *Journal of Manufacturing Systems*, 32(1):238–247, jan 2013.

[345] R. Roy, P. Souchoroukov, and E. Shehab. Detailed cost estimating in the automotive industry: Data and information requirements. *International Journal of Production Economics*, 133(2):694–707, oct 2011.

[346] J. Rubinovitz, J. Bukchin, and E. Lenz. RALB - A Heuristic Algorithm for Design and Balancing of Robotic Assembly Lines. *Annals of the CIRP*, 42(1):497–500, 1993.

[347] I. Sabuncuoglu, E. Erel, and A. Alp. Ant colony optimization for the single model U-type assembly line balancing problem. *International Journal of Production Economics*, 120(2):287–300, 2009.

[348] U. Saif, Z. Guan, W. Liu, B. Wang, and C. Zhang. Multi-objective artificial bee colony algorithm for simultaneous sequencing and balancing of mixed model assembly line. *The International Journal of Advanced Manufacturing Technology*, 75(9-12):1809–1827, dec 2014.

[349] U. Saif, Z. Guan, W. Liu, C. Zhang, and B. Wang. Pareto based artificial bee colony algorithm for multi objective single model assembly line balancing with uncertain task times. *Computers & Industrial Engineering*, 76(1):1–15, 2014.

[350] U. Saif, Z. Guan, B. Wang, J. Mirza, and S. Huang. A survey on assembly lines and its types. *Frontiers of Mechanical Engineering*, 9(2):95–105, jun 2014.

[351] Y. Saji and M. Essaid. A novel discrete bat algorithm for solving the travelling salesman problem. *Neural Computing and Applications*, jun 2015.

[352] Y. Saji, M. E. Riffi, and B. Ahiod. Discrete bat-inspired algorithm for travelling salesman problem. In *2014 Second World Conference on Complex Systems (WCCS)*, pages 28–31. IEEE, nov 2014.

[353] M. E. Salveson. The assembly line balancing problem. *Journal of Industrial Engineering*, 6(3):18–25, 1955.

[354] B. Sankararao and S. K. Gupta. Multi-objective optimization of an industrial fluidized-bed catalytic cracking unit (FCCU) using two jumping gene adaptations of simulated annealing. *Computers & Chemical Engineering*, 31(11):1496–1515, 2007.

[355] H. Sato, H. E. Aguirre, and K. Tanaka. Controlling Dominance Area of Solutions and Its Impact on the Performance of MOEAs. In S. Obayashi, editor, *Evolutionary Multi-Criterion Optimization*, volume 4403 of *Lecture Notes in Computer Science*, pages 5–20. Springer Berlin Heidelberg, Berlin, Heidelberg, 2007.

[356] H. Sato, H. E. Aguirre, and K. Tanaka. Self-Controlling Dominance Area of Solutions in Evolutionary Many-Objective Optimization. In *Lecture Notes in Computer Science (including subseries Lecture Notes in Artificial Intelligence and Lecture Notes in Bioinformatics)*, volume 6457, pages 455–465. Springer Berlin Heidelberg, 2010.

[357] A. Scholl. *Balancing and sequencing of assembly lines*. Production and logistics. Physica-Verlag, 1995.

[358] A. Scholl and C. Becker. State-of-the-art exact and heuristic solution procedures for simple assembly line balancing. *European Journal of Operational Research*, 168(3):666–693, feb 2006.

[359] A. Scholl, N. Boysen, and M. Fliedner. The sequence-dependent assembly line balancing problem. *OR Spectrum*, 30(3):579–609, jun 2008.

[360] A. Scholl, N. Boysen, and M. Fliedner. Optimally solving the alternative subgraphs assembly line balancing problem. *Annals of Operations Research*, 172(1):243–258, nov 2009.

[361] A. Scholl, N. Boysen, and M. Fliedner. The assembly line balancing and scheduling problem with sequence-dependent setup times: Problem extension, model formulation and efficient heuristics. *OR Spectrum*, 35(1):291–320, 2013.

[362] A. Scholl, M. Fliedner, and N. Boysen. Absalom: Balancing assembly lines with assignment restrictions. *European Journal of Operational Research*, 200(3):688–701, feb 2010.

[363] A. Scholl and R. Klein. SALOME: A bidirectional branch-and-bound procedure for assembly line balancing. *INFORMS Journal on Computing*, 9(4):319–334, 1997.

[364] E. Semenkin and M. Semenkina. Self-configuring genetic algorithm with modified uniform crossover operator. *Lecture Notes in Computer Science (including subseries Lecture Notes in Artificial Intelligence and Lecture Notes in Bioinformatics)*, 7331 LNCS(PART 1):414–421, 2012.

[365] E. C. Sewell and S. H. Jacobson. A branch, bound, and remember algorithm for the simple assembly line balancing problem. *INFORMS Journal on Computing*, 24(3):433–442, 2012.

[366] E. Shehab and H. S. Abdalla. An Intelligent Knowledge-Based System for Product Cost Modelling. *International Journal of Advanced Manufacturing Technology*, 19(1):49–65, jan 2002.

[367] C. Shi. *Efficient Buffer Design Algorithms for Production Line Profit Maximization*. PhD thesis, Massachusetts Institute of Technology, 2012.

[368] D. Shin. An efficient heuristic for solving stochastic assembly line balancing problems. *Computers & Industrial Engineering*, 18(3):285–295, 1990.

[369] A. S. Simaria and P. M. Vilarinho. A genetic algorithm based approach to the mixed-model assembly line balancing problem of type II. *Computers & Industrial Engineering*, 47(4):391–407, dec 2004.

[370] P. Sivasankaran and P. Shahabudeen. Literature review of assembly line balancing problems. *The International Journal of Advanced Manufacturing Technology*, 73(9-12):1665–1694, 2014.

[371] L. Smith and P. D. Ball. Steps towards sustainable manufacturing through modelling material, energy and waste flows. *International Journal of Production Economics*, 140(1):227–238, 2012.

[372] K. M. Spens and G. Kovács. A content analysis of research approaches in logistics research. *International Journal of Physical Distribution & Logistics Management*, 36(5):374–390, jun 2006.

[373] A. Sprecher. A competitive branch-and-bound algorithm for the simple assembly line balancing problem. *International Journal of Production Research*, 37(8):1787–1816, 1999.

[374] J. Sternatz. The joint line balancing and material supply problem. *International Journal of Production Economics*, 159:304–318, 2015.

[375] B. Suman and P. Kumar. A survey of simulated annealing as a tool for single and multiobjective optimization. *Journal of the Operational Research Society*, 57(10):1143–1160, 2006.

[376] E. G. Talbi. A taxonomy of hybrid metaheuristics. *Journal of Heuristics*, 8(5):541–564, 2002.

[377] E. G. Talbi. *Metaheuristics: From Design to Implementation*. Wiley, 2009.

[378] E. G. Talbi. A unified taxonomy of hybrid metaheuristics with mathematical programming, constraint programming and machine learning. In *Studies in Computational Intelligence*, volume 434, pages 3–76. Springer, 2013.

[379] F. B. Talbot, J. H. Patterson, and W. V. Gehrlein. A Comparative Evaluation of Heuristic Line Balancing Techniques. *Management Science*, 32(4):430–454, apr 1986.

[380] M. G. C. Tapia and C. A. Coello Coello. Applications of multi-objective evolutionary algorithms in economics and finance: A survey. In *2007 IEEE Congress on Evolutionary Computation*, pages 532–539, 2007.

[381] P. Tapkan, L. Özbakır, and A. Baykasoğlu. Bees Algorithm for constrained fuzzy multi-objective two-sided assembly line balancing problem. *Optimization Letters*, 6(6):1039–1049, aug 2012.

[382] L. Thiele, K. Miettinen, P. J. Korhonen, and J. Molina. A Preference-Based Evolutionary Algorithm for Multi-Objective Optimization. *Evolutionary Computation*, 17(3):411–436, sep 2009.

[383] N. T. Thomopoulos. Line Balancing-Sequencing for Mixed-Model Assembly. *Management Science*, 14(2):B–59–B–75, 1967.

[384] L. Tiacci. Simultaneous balancing and buffer allocation decisions for the design of mixed-model assembly lines with parallel workstations and stochastic task times. *International Journal of Production Economics*, 162:201–215, apr 2015.

[385] V. A. Tipnis, S. J. Mantel, and G. J. Ravignani. Sensitivity Analysis for Macroeconomic and Microeconomic Models of New Manufacturing Processes. *Annals of the CIRP*, 30(1):401–404, 1981.

[386] D. R. Tobergte and S. Curtis. *Montage in der industriellen Produktion*, volume 53. Springer Berlin Heidelberg, Berlin, Heidelberg, 2013.

[387] M. D. Toksarı, S. K. İşleyen, E. Güner, and Ö. F. Baykoç. Assembly line balancing problem with deterioration tasks and learning effect. *Expert Systems with Applications*, 37(2):1223–1228, 2010.

[388] S.-J. (Tony) Hsieh. Hybrid analytic and simulation models for assembly line design and production planning. *Simulation Modelling Practice and Theory*, 10(1-2):87–108, oct 2002.

[389] S. Topaloglu, L. Salum, and A. A. Supciller. Rule-based modeling and constraint programming based solution of the assembly line balancing problem. *Expert Systems with Applications*, 39(3):3484–3493, 2012.

[390] H. Triki, A. Mellouli, and F. Masmoudi. Assembly Line Resource Assignment and Balancing Problem of Type 2. In M. Haddar, L. Romdhane, J. Louati, and A. Ben Amara, editors, *Design and Modeling of Mechanical Systems*, Lecture Notes in Mechanical Engineering, pages 627–634. Springer Berlin Heidelberg, Berlin, Heidelberg, 2013.

[391] H. Triki, A. Mellouli, and F. Masmoudi. A multi-objective genetic algorithm for assembly line resource assignment and balancing problem of type 2 (ALRABP-2). *Journal of Intelligent Manufacturing*, 2, oct 2014.

[392] M. M. Tseng and S. J. Hu. Mass Customization. In *CIRP Encyclopedia of Production Engineering*, pages 836–843. Springer Berlin Heidelberg, Berlin, Heidelberg, 2014.

[393] G. Tuncel and S. Topaloglu. Assembly line balancing with positional constraints, task assignment restrictions and station paralleling: A case in an electronics company. *Computers & Industrial Engineering*, 64(2):602–609, 2013.

[394] S. Ullah, G. Zailin, X. Xianhao, H. Zongdong, and W. Baoxi. Multi Objective Simultaneous Assembly Line Balancing and Buffer Sizing. *International Journal of Mathematical, Computational, Physical, Electrical and Computer Engineering*, 9(1):63–70, 2015.

[395] D. Ullman. *The mechanical design process*. McGraw-Hill, 2010.

[396] E. Ulungu and J. Teghem. The two phases method: An efficient procedure to solve bi-objective combinatorial optimization problems. *Foundations of Computing and Decision Sciences*, 20(2):149–165, 1995.

[397] T. L. Urban and W.-C. Chiang. Designing energy-efficient serial production lines: The unpaced synchronous line-balancing problem. *European Journal of Operational Research*, 248(3):789–801, 2016.

[398] D. a. Van Veldhuizen. Multiobjective Evolutionary Algorithms: Classifications, Analyses and New Innovations. *IRE Transactions on Education*, 1999.

[399] D. a. Van Veldhuizen and G. B. Lamont. Evolutionary Computation and Convergence to a Pareto Front. *Late Breaking Papers at the Genetic Programming 1998 Conference*, pages 221–228, 1998.

[400] D. A. van Veldhuizen and G. B. Lamont. Multiobjective evolutionary algorithm test suites. In *Proceedings of the 1999 ACM symposium on Applied computing - SAC '99*, pages 351–357, New York, New York, USA, 1999. ACM Press.

[401] J. I. van Zante-de Fokkert and T. G. de Kok. The mixed and multi model line balancing problem: a comparison. *European Journal of Operational Research*, 100(3):399–412, 1997.

[402] D. A. V. Veldhuizen and G. B. Lamont. Multiobjective Evolutionary Algorithms: Analyzing the State-of-the-Art. *Evolutionary Computation*, 8(2):125–147, jun 2000.

[403] M. Vilà and J. Pereira. An enumeration procedure for the assembly line balancing problem based on branching by non-decreasing idle time. *European Journal of Operational Research*, 229(1):106–113, 2013.

[404] M. Vilà and J. Pereira. A branch-and-bound algorithm for assembly line worker assignment and balancing problems. *Computers & Operations Research*, 44:105–114, apr 2014.

[405] M. Villalobos-Arias, G. Toscano Pulido, and C. A. Coello Coello. A proposal to use stripes to maintain diversity in a multi-objective particle swarm optimizer. In *Proceedings 2005 IEEE Swarm Intelligence Symposium, 2005. SIS 2005.*, pages 22–29. IEEE, 2005.

[406] C. Voudouris and E. Tsang. Guided local search and its application to the traveling salesman problem. *European Journal of Operational Research*, 113(2):469–499, 1999.

[407] L. Wang, S. Keshavarzmanesh, H. Y. Feng, and R. O. Buchal. Assembly process planning and its future in collaborative manufacturing: A review. *International Journal of Advanced Manufacturing Technology*, 41(1-2):132–144, 2009.

[408] E. Westkämper, K. Drexler, and A. Moisan. *CIRP: Wörterbuch der Fertigungstechnik-Band 3: Produktionssysteme. 1.* Springer, Berlin, Heidelberg, 2004.

[409] W. W. White. Letter to the Editor—Comments on a Paper by Bowman. *Operations Research*, 9(2):274–276, apr 1961.

[410] J. C. Wortmann, D. R. Muntslag, and P. J. M. Timmermans, editors. *Customer-driven Manufacturing.* Springer Netherlands, Dordrecht, 1996.

[411] E.-F. Wu, Y. Jin, J.-S. Bao, and X.-F. Hu. A branch-and-bound algorithm for two-sided assembly line balancing. *The International Journal of Advanced Manufacturing Technology*, 39(9-10):1009–1015, 2008.

[412] B. Xia, L. Xi, and B. Zhou. An improved decomposition method for evaluating the performance of transfer lines with unreliable machines and finite buffers. *International Journal of Production Research*, 50(15):4009–4024, 2012.

[413] Xiufen Zou, Yu Chen, Minzhong Liu, and Lishan Kang. A New Evolutionary Algorithm for Solving Many-Objective Optimization Problems. *IEEE Transactions on Systems, Man, and Cybernetics, Part B (Cybernetics)*, 38(5):1402–1412, oct 2008.

[414] L. Xu, Z. Li, S. Li, and F. Tang. A decision support system for product design in concurrent engineering. *Decision Support Systems*, 42(4):2029–2042, 2007.

[415] L.-Y. Xu, L. Bélec, W. Liu, Q.-F. Gu, and A.-P. Li. Improved Computer Methods for Sequencing Operations for U-Shaped Assembly Lines. In E. Qi, J. Shen, and R. Dou, editors, *Proceedings of the 21st International Conference on Industrial Engineering and Engineering Management*, pages 51–55. Atlantis Press, Paris, 2015.

[416] B. Yagmahan. Mixed-model assembly line balancing using a multi-objective ant colony optimization approach. *Expert Systems with Applications*, 38(10):12453–12461, sep 2011.

[417] A. Yalaoui, H. Chehade, F. Yalaoui, and L. Amodeo. *Optimization of Logistics*. ISTE. Wiley, 2012.

[418] C. Yammani, S. Maheswarapu, and S. K. Matam. A Multi-objective Shuffled Bat algorithm for optimal placement and sizing of multi distributed generations with different load models. *International Journal of Electrical Power & Energy Systems*, 79:120–131, jul 2016.

[419] N.-C. Yang and M.-D. Le. Multi-objective bat algorithm with time-varying inertia weights for optimal design of passive power filters set. *IET Generation, Transmission & Distribution*, 9(7):644–654, 2015.

[420] T. Yang, C.-T. C. Su, and Y. Y.-R. Hsu. Systematic layout planning: a study on semiconductor wafer fabrication facilities. *International Journal of Operations & Production Management*, 20(11):1359–1371, nov 2000.

[421] X.-S. Yang. A New Metaheuristic Bat-Inspired Algorithm. *Nature Inspired Cooperative Strategies for Optimization*, pages 65–74, 2010.

[422] X.-S. Yang. Flower pollination algorithm for global optimization. In *International Conference on Unconventional Computing and Natural Computation*, pages 240–249. Springer, 2012.

[423] X.-S. Yang and S. Deb. Multiobjective cuckoo search for design optimization. *Computers & Operations Research*, 40(6):1616–1624, 2013.

[424] X.-S. Yang and X. He. Swarm Intelligence and Evolutionary Computation: Overview and Analysis. In *Recent Advances in Swarm Intelligence and Evolutionary Computation*, Studies in Computational Intelligence, pages 1–23. Springer International Publishing, Cham, 2015.

[425] X.-S. Yang, M. Karamanoglu, and X. He. Multi-objective Flower Algorithm for Optimization. *Procedia Computer Science*, 18:861–868, 2013.

[426] X.-S. Yang and Suash Deb. Cuckoo Search via Lévy flights. In *2009 World Congress on Nature & Biologically Inspired Computing (NaBIC)*, pages 210–214. IEEE, 2009.

[427] M. F. Yegul, K. Agpak, and M. Yavuz. A new algorithm for U-shaped two-sided assembly line balancing. *Transactions of the Canadian Society for Mechanical Engineering*, 34(2):225–241, 2010.

[428] A. Yolmeh and F. Kianfar. An efficient hybrid genetic algorithm to solve assembly line balancing problem with sequence-dependent setup times. *Computers & Industrial Engineering*, 62(4):936–945, 2012.

[429] A. Yoosefelahi, M. Aminnayeri, H. Mosadegh, and H. D. Ardakani. Type II robotic assembly line balancing problem: An evolution strategies algorithm for a multi-objective model. *Journal of Manufacturing Systems*, 31(2):139–151, 2012.

[430] H. Yu, H. Fang, P. Yao, and Y. Yuan. A combined genetic algorithm/simulated annealing algorithm for large scale system energy integration. *Computers & Chemical Engineering*, 24(8):2023–2035, 2000.

[431] J. Yu and Y. Yin. Assembly line balancing based on an adaptive genetic algorithm. *The International Journal of Advanced Manufacturing Technology*, 48(1-4):347–354, apr 2010.

[432] P. T. Zacharia and A. C. Nearchou. A meta-heuristic algorithm for the fuzzy assembly line balancing type-E problem. *Computers & Operations Research*, 40(12):3033–3044, 2013.

[433] L. Zadeh. Optimality and non-scalar-valued performance criteria. *IEEE Transactions on Automatic Control*, 8(1):59–60, jan 1963.

[434] J. Zha and J. J. Yu. A hybrid ant colony algorithm for U-line balancing and rebalancing in just-in-time production environment. *Journal of Manufacturing Systems*, 33(1):93–102, jan 2014.

[435] X. F. Zha, S. Y. E. Lim, and S. C. Fok. Integrated intelligent design and assembly planning: A survey. *The International Journal of Advanced Manufacturing Technology*, 14(9):664–685, sep 1998.

[436] L. Y. Zhai, L. P. Khoo, and Z. W. Zhong. Design concept evaluation in product development using rough sets and grey relation analysis. *Expert Systems with Applications*, 36(3 PART 2):7072–7079, 2009.

[437] J. Zhang, W. Wang, and X. Xu. A hybrid discrete particle swarm optimization for dual-resource constrained job shop scheduling with resource flexibility. *Journal of Intelligent Manufacturing*, apr 2015.

[438] L. Zhang. System-theoretic properties of production lines. *ProQuest Dissertations and Theses*, page 290, 2009.

[439] W. Zhang and M. Gen. An efficient multiobjective genetic algorithm for mixed-model assembly line balancing problem considering demand ratio-based cycle time. *Journal of Intelligent Manufacturing*, 22(3):367–378, jun 2011.

[440] W. Zhang, W. Xu, and M. Gen. Hybrid Multiobjective Evolutionary Algorithm for Assembly Line Balancing Problem with Stochastic Processing Time. *Procedia Computer Science*, 36(3):587–592, 2014.

[441] Z. Zhang and W. Cheng. An Exact Method for U-Shaped Assembly Line Balancing Problem. In *2010 2nd International Workshop on Intelligent Systems and Applications*, pages 1–4. IEEE, may 2010.

[442] Z. Zhang and W. Cheng. Solving Fuzzy U-Shaped Line Balancing Problem with Exact Method. *Applied Mechanics and Materials*, 26-28(200806131014):1046–1051, 2010.

[443] Z. Zhang and W. Cheng. Teaching Assembly Line Balancing Problem by Using Lingo Software. In *2010 Second International Workshop on Education Technology and Computer Science*, volume 1, pages 663–666. IEEE, 2010.

[444] Z. Zhang and W. Cheng. Improved Heuristic Procedure for Mixed-Model U-line Balancing Problem with Fuzzy Times. In *Lecture Notes in Electrical Engineering*, volume 286 of *Lecture Notes in Electrical Engineering*, pages 395–406. Springer Berlin Heidelberg, Berlin, Heidelberg, 2015.

[445] Q. Zheng, M. Li, Y. Li, and Q. Tang. Station ant colony optimization for the type 2 assembly line balancing problem. *The International Journal of Advanced Manufacturing Technology*, 66(9-12):1859–1870, jun 2013.

[446] Y.-B. Zhong, Y. Xiang, and H.-L. Liu. A multi-objective artificial bee colony algorithm based on division of the searching space. *Applied Intelligence*, 41(4):987–1011, dec 2014.

[447] A. Zhou, B.-y. Qu, H. Li, S.-Z. Zhao, P. N. Suganthan, and Q. Zhang. Multiobjective evolutionary algorithms: A survey of the state of the art. *Swarm and Evolutionary Computation*, 1(1):32–49, 2011.

[448] L. Zhou, J. Li, F. Li, Q. Meng, J. Li, and X. Xu. Energy consumption model and energy efficiency of machine tools: a comprehensive literature review. *Journal of Cleaner Production*, 112(April 2016):3721–3734, jan 2016.

[449] W. Zhou and Z. Lian. A tandem network with a sharing buffer. *Applied Mathematical Modelling*, 35(9):4507–4515, 2011.

[450] X. Zhu, S. J. Hu, Y. Koren, S. P. Marin, and N. Huang. Sequence Planning to Minimize Complexity in Mixed-Model Assembly Lines. In *2007 IEEE International Symposium on Assembly and Manufacturing*, pages 251–258. IEEE, jul 2007.

[451] I. Zidi, K. Mesghouni, K. Zidi, and K. Ghedira. A multi-objective simulated annealing for the multi-criteria dial a ride problem. *Engineering Applications of Artificial Intelligence*, 25(6):1121–1131, 2012.

[452] E. Zitzler. Evolutionary Algorithms for Multiobjective Optimization : Methods and Applications. *English*, no13398(30), 1999.

[453] E. Zitzler, K. Deb, and L. Thiele. Comparison of Multiobjective Evolutionary Algorithms: Empirical Results. *Evolutionary Computation*, 8(2):173–195, 2000.

[454] E. Zitzler, M. Laumanns, and S. Bleuler. A Tutorial on Evolutionary Multiobjective Optimization. In *Evolutionary Computation*, volume 535, pages 3–37. Springer, 2004.

[455] E. Zitzler, M. Laumanns, and L. Thiele. SPEA2: Improving the Strength Pareto Evolutionary Algorithm. *Evolutionary Methods for Design Optimization and Control with Applications to Industrial Problems*, pages 95–100, 2001.

[456] E. Zitzler and L. Thiele. Multiobjective optimization using evolutionary algorithms — A comparative case study. In *Lecture Notes in Computer Science, Parallel Problem Solving from Nature—PPSN V*, volume 1498, pages 292–301, 1998.

[457] E. Zitzler and L. Thiele. Multiobjective evolutionary algorithms: A comparative case study and the strength Pareto approach. *IEEE Transactions on Evolutionary Computation*, 3(4):257–271, 1999.

[458] E. Zitzler, L. Thiele, M. Laumanns, C. M. Fonseca, and V. G. Da Fonseca. Performance assessment of multiobjective optimizers: An analysis and review. *IEEE Transactions on Evolutionary Computation*, 7(2):117–132, 2003.

[459] C. Zopounidis and M. Doumpos. Multi-criteria decision aid in financial decision making: methodologies and literature review. *Journal of Multi-Criteria Decision Analysis*, 11(4-5):167–186, jul 2002.

Jonathan OESTERLE

Doctorat : Optimisation et Sûreté des Systèmes

Année 2017

Approche holistique pour la conception de lignes d'assemblage hybrides

Le travail présenté dans cette thèse concerne la formulation et la résolution de deux problèmes d'optimisation multi-objectifs. Ces problèmes de décision, liés à une approche holistique, ont pour but de sélectionner la meilleure configuration « produit/ligne d'assemblage » à partir d'un ensemble de design produits, et de ressources. Concernant le premier problème, un modèle de coût a été développé afin de traduire les interdépendances complexes entre la sélection d'un design produit et les caractéristiques des ressources. Une étude empirique est proposée et vise à comparer, selon plusieurs indicateurs de qualité multi-objectifs, différentes méthodes de résolution - comprenant des algorithmes génétiques, de colonies de fourmis, d'optimisation par essaims particulaires, des chauves-souris, de recherche du coucou et de pollinisation des fleurs. Plusieurs règles de dominance et une recherche locale spécifique au problème ont été appliquées aux méthodes de résolution les plus prometteuses. Concernant le second problème, qui se penche également sur le dimensionnement des stocks tampons, les méthodes de résolution sont couplées à un modèle de simulation à événements discrets, dont la fonction première est l'évaluation des valeurs des différentes fonctions objectifs. L'approche holistique associée aux deux problèmes a été validée avec deux cas industriels.

Mots clés : conception technique - systèmes de production - production en série - systèmes d'aide à la décision - optimisation combinatoire - simulation, méthodes de.

Holistic Approach to Designing Hybrid Assembly Lines

The work presented in this thesis concerns the formulation and the resolution of two holistic multi-objective optimization problems associated with the selection of the best product and hybrid assembly line configuration out of a set of products, processes and resources alternatives. Regarding the first problem, a cost model was developed in order to translate the complex interdependencies between the selection of specific product designs, processes and resources characteristics. An empirical study is proposed, which aimed at comparing, according to several multi-objective quality indicators, various resolution methods – including variants of evolutionary algorithms, ant colony optimization, particle swarm optimization, bat algorithms, cuckoo search algorithms, and flower-pollination algorithms. Several dominance rules and a problem-specific local search were applied to the most promising resolution methods. Regarding the second problem, which also considers the buffer sizing, the developed algorithms were enhanced with a genetic discrete-event simulation model, whose primary function is to evaluate the value of the various objective functions. The demonstration of the associated resolution frameworks for both problems was validated through two industrial-cases.

Keywords: engineering design - production systems - mass production - decision support systems - combinatorial optimization - simulation methods.